

AMC PAMPHLET

AMCP 706-285

ENGINEERING DESIGN HANDBOOK

ELEMENTS OF AIRCRAFT AND MISSILE PROPULSION

HEADQUARTERS, U.S. ARMY MATERIEL COMMAND

JULY 1969

LIST OF ILLUSTRATIONS

Figure No.	Title	Page
1-1	Essential Elements of an Air-breathing Jet Engine	1-6
1-2	Essential Elements of a Jet Propulsion System	1-8
1-3	Fin-stabilized Rocket Motor	1-8
1-4	Development of Thrust in a Rocket Motor	1-9
1-5	Essential Elements of a Liquid Bipropellant Rocket Engine	1-12
1-6	Principal Elements of an Uncooled Liquid Bipropellant Rocket Engine	1-13
1-7	Essential Elements of an Internal-burning Case-bonded Solid Propellant Rocket Motor	1-14
1-8	Essential Features of a Hybrid Chemical Rocket Engine . . .	1-15
2-1	Control Surface and Control Volume Enclosing a Region of a Flowing Fluid	2-5
2-2	Transport of Momentum by a Flowing Fluid	2-5
2-3	Forces Acting on a Flowing Fluid	2-8
2-4	Air-breathing Jet Engine in a Relative Coordinate System . .	2-8
2-5	Determination of the Thrust Developed by a Jet Propulsion System	2-10
3-1	Control Surface Enclosing a Region in a Flowing Fluid to Which Heat Is Added and Which Does Work on Its Surroundings	3-9
3-2	Element of a Control Surface Which Encloses a Region in a Flowing Fluid	3-10
3-3	Energy Balance for a One-dimensional Steady Flow	3-11
3-4	Comparison of Adiabatic and Isentropic Flow Processes on the h - s -plane	3-16
3-5	Isentropic Flow Expansion of a Gas to the Critical Condition ($u = a^*$)	3-19
3-6	A Fanno Line Plotted in the h - s -plane	3-24
3-7	Comparison of Fanno Lines for Two Different Values of the Flow Density ($G = \dot{m}/A$)	3-25
3-8	Determination of Duct Length To Accomplish a Specified Change in Flow Mach Number (Fanno Line)	3-27
3-9	Flow Parameters for a Fanno Line for a Gas with $\gamma = 1.40$	3-30
3-10	Physical Situation for a Rayleigh Flow	3-31

LIST OF ILLUSTRATIONS (Continued)

Figure No.	Title	Page
3-11	Rayleigh Line Plotted in the Pv -plane	3-33
3-12	Rayleigh Line Plotted in the hs - (or Ts -) plane	3-34
3-13	Flow Parameters for a Rayleigh Flow as a Function of M , for $\gamma = 1.40$	3-36
3-14	Development of Compression Shock	3-38
4-1	Two Basic Types of Nozzles Employed in Jet Propulsion Engines	4-4
4-2	Ideal Nozzle Flow in Converging Nozzles	4-6
4-3	Flow Factor ψ for a Converging Nozzle As a Function of the Expansion Ratio r_t	4-9
4-4	Mass Flow Rate As a Function of the Nozzle Expansion Ratio, for a Fixed Value of γ	4-11
4-5	Enthalpy Converted into Kinetic Energy by Isentropic Expansions in Converging and Converging-diverging Nozzles	4-12
4-6	Flow Characteristics of a Converging-diverging (or De Laval) Nozzle Passing the Critical Mass Flow Rate \dot{m}^*	4-13
4-7	Parameter $(G\sqrt{\gamma RT^0})/P^0$ As a Function of P_t/P^0 for Ideal Nozzle Flow ($\gamma = 1.25$)	4-15
4-8	Area Ratio A_x/A^* for Complete Expansion As a Function of the Nozzle Pressure Ratio P^0/P_x for Different Values of $\gamma = c_p/c_v$	4-17
4-9	Ratio of the Isentropic Exit Velocity u'_x to the Isentropic Throat Velocity u'_t As a Function of the Nozzle Pressure Ratio P^0/P_x for Different Values of $\gamma = c_p/c_v$	4-18
4-10	Expansion Ratio P_e/P^0 and Exit Mach Number M_e As Function of the Area Ratio A^*/A_e for a Converging- diverging Nozzle Passing the Critical Mass Flow Rate \dot{m}^*	4-21
4-11	Pressure Distributions in a Converging-diverging Nozzle Under Different Operating Conditions	4-22
4-12	Conical Converging-diverging Nozzle Operating With Overexpansion	4-23
4-13	Correlation of Data on Jet Separation in Conical Nozzles for Rocket Motors (According to Reference 10)	4-25
4-14	General Characteristics of a Conical Converging- diverging Nozzle	4-30
4-15	Radial Flow in a Conical Nozzle	4-32
4-16	Divergence Loss Coefficient λ as a Function of the Semi- divergence Half-angle α for a Conical Nozzle	4-33

LIST OF ILLUSTRATIONS (Continued)

Figure No.	Title	Page
4-17	General Features of a Contoured or Bell-shaped Nozzle . . .	4-35
4-18	Essential Features of an Annular Nozzle	4-37
4-19	Essential Features of a Plug Nozzle	4-38
4-20	Essential Features of an Expansion-deflection or E-D Nozzle	4-39
5-1	Thermodynamic Conditions for a Chemical Rocket Nozzle Operating Under Steady State Conditions	5-3
5-2	Forces Acting on a Rocket-propelled Body in Rectilinear Motion	5-10
5-3	Drag Coefficient As a Function of the Flight Mach Number for Two Angles of Attack	5-12
5-4	Ideal Burnout Velocity V_{b1} for a Single Stage Vehicle As a Function of Effective Jet Velocity c for Different Values of Vehicle Mass Ratio m_0/m_b	5-15
6-1	Dissociation in Percent as a Function of Gas Temperature for CO_2 , H_2O , H_2 , O_2 , HF , CO , and N_2 at 500 psia	6-7
6-2	Isentropic Exhaust Velocity as a Function of Mixture Ratio \dot{m}_O/\dot{m}_f for Different Values of P_c/P_e ; Propellants: Nitrogen Tetroxide (N_2O_4) Plus 50% Aerozine-50– 50% Hydrazine (N_2H_4) and 50% Unsymmetrical Dimethyl Hydrazine ($(\text{CH}_3)_2\text{N}_2\text{H}_2$, (UDMH)	6-8
6-3	Velocity Parameter $u_e/\phi\sqrt{T_c^0/\bar{m}}$ as a Function of P_c^0/P_e (for a Range of 10 to 50) for Different Values of $\gamma = c_p/c_v$	6-9
6-4	Velocity Parameter $u_e/\phi\sqrt{T_c^0/\bar{m}}$ as a Function of P_c^0/P_e (for a Range of 40 to 200) for Different Values of $\gamma = c_p/c_v$	6-10
6-5	Values of the Parameter $\Gamma = \sqrt{\gamma \left(\frac{2}{\gamma+1} \right)^{\frac{\gamma+1}{\gamma-1}}}$ and $\Gamma_1 = \Gamma\sqrt{\gamma}$ as Functions of γ	6-12
6-6	Parallel Flow Vacuum Thrust Coefficient $(C_F)_0$ as a Function of Nozzle Area Ratio ϵ	6-14
6-7	Parameter $(P_e/P_c)\epsilon$ as a Function of the Nozzle Area Ratio ϵ	6-15
6-8	Nozzle Area Ratio ϵ as a Function of P_c/P_e (0 to 20) for Different Values of γ	6-16

LIST OF ILLUSTRATIONS (Continued)

Figure No.	Title	Page
6-9	Nozzle Area Ratio ϵ as a Function of P_c/P_e (20 to 50) for Different Values of γ	6-17
6-10	Nozzle Area Ratio ϵ as a Function of P_c/P_e (50 to 200) for Different Values of γ	6-18
6-11	Nozzle Area Ratio $\epsilon = A_e/A_t$ as a Function of the Mixture Ratio and Different Values of P_c/P_e for the N_2O_4 - Aerozine-50 Propellant Combination	6-19
6-12	Ideal Characteristic Velocity c^{*} as a Function of Mixture Ratio for Different Combustion Pressures P_c ; Propellants: N_2O_4 Plus Aerozine-50	6-21
6-13	Ideal Specific Impulse I'_{sp} as a Function of the Mixture Ratio (\dot{m}_O/\dot{m}_f) for Several Liquid Propellant Combinations	6-22
6-14	Combustion Temperature as a Function of the Mixture Ratio (\dot{m}_O/\dot{m}_f) for Several Liquid Propellants	6-24
6-15	Density Impulse I_d as a Function of the Mixture Ratio (\dot{m}_O/\dot{m}_f) for Several Liquid Propellant Systems	6-25
7-1	Case-bonded Chamber	7-8
8-1	Piobert's Law of Burning	8-4
8-2	Combustion Schematic for a Double-base Solid Propellant	8-6
8-3	Combustion Schematic for a Composite Solid Propellant...	8-8
8-4	Linear Burning Rate r_0 (at 60°F) for Several Composite Propellants Made With the Same Binder Fuel and Different Kinds and Amounts of Inorganic Oxidizers.	8-10
8-5	Terminology and Phenomena Associated With Unstable Burning in Solid Propellant Rocket Motors	8-15
8-6	Types of Burning Observed in Solid Propellant Rocket Motors	8-16
8-7	Some Typical Propellant Grain Configurations	8-21
8-8	Effect of Variations in the Area of the Burning Surface of a Solid Propellant Grain on the Pressure-time Curve	8-22
8-9	Section Through a Rocket Motor Nozzle	8-29
8-10	Jet Deflection To Achieve Attitude Control	8-30
8-11	Mechanical Means for Effecting Thrust Vector Control ...	8-31
8-12	Movable Nozzles for TVC	8-33
8-13	Secondary Injection for TVC	8-34

LIST OF ILLUSTRATIONS (Continued)

Figure No.	Title	Page
9-1	Comparison of Specific Impulses Obtained With Several Liquid Fuels Reacted With Liquid Fluorine and With Liquid Oxygen	9-16
9-2	Enthalpy of Combustion of Several Fuels With Liquid Oxygen	9-25
10-1	Essential Elements of a Liquid Bipropellant Thrust Chamber	10-4
10-2	Nine Different Injector Patterns for Liquid Bipropellant Thrust Chambers	10-6
10-3	Cooling Systems for Rocket Thrust Chambers	10-12
10-4	Typical Mean Circumferential Heat Flux Distribution Along a Thrust Chamber Wall	10-13
10-5	Application of an Ablating Material to a Liquid Propellant Thrust Chamber.	10-18
10-6	Heat Balances for Ablation Cooling	10-19
10-7	Diagrammatic Arrangement of a Stored Gas Pressurization System	10-21
10-8	Schematic Arrangement of the Components of a Turbo-pump Pressurization System	10-23
11-1	Essential Features of a Hybrid Rocket Engine With Head-end Injection of the Liquid Oxidizer	11-2
11-2	Essential Features of an Afterburning Hybrid Rocket Engine	11-3
11-3	Variations in Instantaneous and System Specific Impulse During the Firing of a Hybrid Rocket Engine	11-10
11-4	Typical Pressure-time Curve for a Hybrid Rocket Engine.	11-11
11-5	Three Types of Injectors That Have Been Utilized in Hybrid Rocket Engines	11-15
12-1	Essential Features of the Ramjet Engine	12-9
12-2	Essential Features of the Turbojet Engine	12-12
12-3	Components of Gas Generator for an Afterburning Turbojet Engine	12-13
12-4	Arrangement of the Components of an Afterburning Turbojet Engine	12-14
12-5	Essential Features of a Turbofan Engine	12-15
12-6	Essential Features of a Turboshaft Engine	12-16
12-7	Essential Features of a Turboprop Engine	12-18
12-8	Historical Trend in the Maximum Allowable Temperatures for Turbine Disk, Blade, and Vane Materials	12-22

LIST OF ILLUSTRATIONS (Continued)

Figure No.	Title	Page
12-9	Increase in Overall Efficiency of Gas-turbine Jet Engines Since 1945	12-25
12-10	Comparison of <u>TSFC</u> 's for Air-breathing and Rocket Engines	12-26
12-11(A)	Specific Output Characteristics As a Function of Cycle Pressures	12-29
12-11(B)	Specific Fuel Consumption Characteristics As a Function of Cycle Pressures	12-30
13-1	Subsonic Inlet With Solely External Compression	13-3
13-2	Subsonic Internal-compression Diffuser	13-4
13-3	Diffusion Processes Plotted on the h -plane	13-6
13-4	Design and Off-design Operation of the Normal Shock Diffuser	13-8
13-5	Schematic Diagram of a Conical Shock (Oswatitsch type) Supersonic Diffuser	13-10
13-6	Three Principal Operating Modes for Supersonic External Compression Diffusers	13-12
13-7	Multiple Conical Shock Supersonic Diffusion System	13-13
13-8	Total and Static Pressure Ratios As a Function of the Free-stream Mach Number for Supersonic Diffusers With Different Numbers of Shocks	13-14
14-1	Schematic Arrangement of an Axially Symmetric Ramjet Engine for Supersonic Flight	14-2
14-2	Flow of Cold Air Through a Shaped Duct	14-3
14-3	Effect of Varying the Exit Area of a Shaped Duct Passing an Internal Flow of Cold Air	14-4
14-4	Variation in the Static Pressure and Gas Velocity Inside a Ramjet Engine ($M_0 = 2.0$)	14-6
14-5	Calculated Values of the Net Thrust of Ramjet Engines As a Function of the Flight Mach Number	14-9
14-6	Gross Thrust Characteristics of a Fixed-geometry Ramjet Engine As a Function of the Flight Mach Number (Constant Fuel-air Ratio f and a Fixed Altitude z)	14-11
14-7	Variation of Gross Thrust Coefficient C_{Fg} for a Fixed-geometry Ramjet Engine With Flight Mach Number M_0 ; (A) With a Constant Combustion Stagnation Temperature T_3^0 at Two Altitudes; and (B) With Two Different Fuel-air Ratios at a Fixed Altitude.	14-12

LIST OF ILLUSTRATIONS (Continued)

Figure No.	Title	Page
14-8	Best Operating Ranges for Supersonic Diffusers for Fixed-geometry Ramjet Engines	14-15
14-9	Diagrammatic Cross-section Through a SCRAMJET Engine	14-17
14-10	SCRAMJET Engine Diffusion Process Plotted in the h -plane	14-19
15-1	Isentropic Diffusion and Air Compression Processes Plotted in the h -plane	15-3
15-2	Diffuser Performance Charts	15-5
15-3	Expansion Processes for Turboshaft, Turboprop, and Turbojet Engines Plotted in the h -plane	15-7
15-4	Ideal Thermodynamic Cycle for a Turboshaft Engine	15-11
15-5	Comparison of Actual and Ideal Turboshaft Engine Cycles	15-14
15-6	Thermal Efficiency of Turboshaft Engine As a Function of the Cycle Pressure Ratio, With the Turbine Inlet Temperature as a Parameter	15-16
15-7	Specific Output of Turboshaft Engine as a Function of the Cycle Pressure Ratio, With the Turbine Inlet Temperature as a Parameter	15-17
15-8	Air-rate of the Turboshaft Engine as a Function of the Cycle Pressure Ratio, With the Turbine Inlet Temperature as a Parameter	15-19
15-9	Work-ratio of Turboshaft Engine as a Function of the Cycle Pressure Ratio, With the Turbine Inlet Temperature as a Parameter	15-20
15-10	Thermal Efficiency of Turboshaft Engine as a Function of the Cycle Pressure Ratio, With η_c and η_t as Parameters	15-21
15-11	Specific Output of Turboshaft Engine as a Function of the Cycle Pressure Ratio for Different Values of Machine Efficiency	15-22
15-12	Turbine Inlet Temperature T_4^0 as a Function of the Optimum Cycle Pressure Ratio for Maximum Specific Output (Turboshaft Engine)	15-23
15-13	Effect of Air Intake Temperature ($T_0 = T_2$) Upon the Designpoint Performance Characteristics of Turboshaft Engine	15-24
15-14	Effect of Pressure Drop on the Specific Output and Thermal Efficiency of Turboshaft Engine	15-25

LIST OF ILLUSTRATIONS (Continued)

Figure No.	Title	Page
15-15	Component Arrangements for a Regenerative Turbo- shaft Engine	15-26
15-16	Thermal Efficiency and Specific Output as Functions of Cycle Pressure Ratio for Regenerative Turbo- shaft Engines	15-31
15-17	Thermal Efficiency for Regenerative Turboshift Engines as a Function of Cycle Pressure Ratio, With e_R as a Parameter, for Three Different Turbine Inlet Temperatures	15-32
15-18	Component Arrangement and Thermodynamic Cycle for the Turboprop Engine	15-33
15-19	<u>SFC</u> as a Function of Compressor Pressure Ratio With Flight Speed as a Parameter (Turboprop Engine)	15-35
15-20	<u>SFC</u> as a Function of the Percent of Energy in Jet, With Flight Speed as a Parameter (Turboprop Engine)	15-36
15-21	Effect of Altitude on the <u>SFC</u> of Turboprop Engines	15-37
15-22	Effect of Turbine and Compressor Isentropic Efficiencies and Turbine Inlet Temperature Upon the Performance Characteristics of Turboprop Engines	15-39
15-23	Operating Characteristics of a Typical Turboprop Engine.	15-40
15-24	Thermodynamic Cycle and Component Arrangement for the Turbojet Engine	15-42
15-25	Dimensionless Enthalpy Change for Propulsive Nozzle as a Function of the Compressor Pressure Ratio, With Flight Mach Number as a Parameter (Turbojet Engine)	15-44
15-26	Dimensionless Thrust Parameter λ and Overall Efficiency η_O as Functions of the Compressor Pressure Ratio (Turbojet Engine)	15-45
15-27	Dimensionless Thrust Parameter λ for Turbojet Engine, and Its Overall Efficiency η_O as Functions of the Cycle Temperature Ratio α , With Flight Mach Number as a Parameter	15-47
15-28	<u>TSFC</u> and Specific Thrust I_a as Functions of the Com- pressor Pressure Ratio, With Flight Speed as a Parameter (Turbojet Engine)	15-48
15-29	Arrangement of Components for a Turbofan Engine	15-50
A-1	Specific Heats of Ideal Gases as Functions of the Specific Heat Ratio	A-11
A-2	Control Surface Enclosing a Control Volume in a Region of Flowing Fluid	A-16

LIST OF ILLUSTRATIONS (Continued)

Figure No.	Title	Page
A-3	Control Volume for a One-dimensional Flow	A-17
A-4	Control Surface Enclosing a Region in a Flowing Fluid to Which Heat is Added and Which Does Work on Its Surroundings	A-21
A-5	Element of a Control Surface Which Encloses a Region in a Flowing Fluid	A-22
A-6	Energy Balance for a Steady One-dimensional Flow	A-23
A-7	Comparison of Isentropic and Adiabatic Flow Processes in the h -plane	A-32
A-8	Isentropic Flow Expansion of a Gas to the Critical Condition	A-40
A-9	Area Configuration for Nozzle or Diffuser Action, for the One-dimensional Flow of an Ideal Gas	A-45
A-10	Converging-diverging Flow Passage	A-45
A-11	Converging-diverging Flow Passage Which Passes the Critical Mass Flow Rate \dot{m}^*	A-47
A-12	Functional Relationship Between dA/dx and x for the Flow of an Ideal Gas in a Converging-diverging Flow Passage	A-48
A-13	One-dimensional Passage With Adiabatic Flow	A-50
A-14	One-dimensional Flow Passage Passing an Adiabatic Flow in the Presence of Wall Friction	A-50
A-15	Adiabatic Flow in a Constant Area Duct in the Presence of Wall Friction (Fanno Flow)	A-53
A-16	A Fanno Line Plotted in the h -plane	A-54
A-17	Two Fanno Lines Plotted in the h -plane	A-55
A-18	Determination of the Duct Length Required for Accomplishing a Specified Change in the Flow Mach Number, for a Fanno Flow	A-58
A-19	Frictionless Flow in a Constant Area Duct With Heat Addition (Rayleigh Flow)	A-65
A-20	Rayleigh Line Plotted in the P - v -plane	A-66
A-21	Conditions for Maximum Enthalpy and for Maximum Entropy for a Rayleigh Line in the P - v -plane	A-68
A-22	Rayleigh Line Plotted in the h - (or T -) plane	A-69
A-23	Development of a Compression Shock	A-72
A-24	Propagation of Sound Waves from a Point Source	A-73
A-25	Pressure Waves Produced by a Body Moving With Sub- sonic Speed (Small Disturbances)	A-74
A-26	Propagation of a Small Disturbance by a Body (A) Moving at Supersonic Speed, and (B) in a Uniform Supersonic Flow Field	A-75

LIST OF ILLUSTRATIONS (Continued)

Figure No.	Title	Page
A-27	Stationary Shock Wave (Normal Shock)	A-77
A-28	The Oblique Shock Wave	A-83
A-29	Coordinate System for an Oblique Shock	A-85
A-30	Maximum Deflection Angle δ_m and Wave Angle ϵ_m for Oblique Shocks as Functions of the Mach Number in Front of the Shock ($\gamma = 1.40$)	A-88
A-31	Illustration of Detachment of an Oblique Shock Due to Flow Deflection Angle δ Exceeding δ_m	A-89
A-32	Deflection Angle δ as a Function of the Wave Angle ϵ , With M_1 as a Parameter	A-90
A-33(A)	Mach Number in Back of Oblique Shock M_2 as a Function of the Mach Number in Front of the Shock M_1 , for Different Values of the Deflection Angle δ ($\gamma = 1.40$)	A-91
A-33(B)	Oblique Shock Wave Angle ϵ as a Function of the Mach Number in Front of the Shock M_1 , for Different Values of the Deflection Angle δ ($\gamma = 1.40$)	A-91
A-34(A)	Static Pressure Ratio P_2/P_1 as a Function of M_1 , the Mach Number in Front of an Oblique Shock, for Different Values of Deflection Angle δ ($\gamma = 1.40$)	A-92
A-34(B)	Stagnation Pressure Ratio P_2^0/P_1^0 as a Function of M_1 , the Mach Number in Front of an Oblique Shock, for Different Values of Deflection Angle δ ($\gamma = 1.40$)	A-92
A-35	Static Density Ratio ρ_2/ρ_1 as a Function of M_1 , the Mach Number in Front of the Oblique Shock, for Different Values of the Deflection Angle δ ($\gamma = 1.40$)	A-93
A-36	Supersonic Flow Over a Symmetrical Wedge	A-95
A-37	Supersonic Flow Over a Symmetrical Cone at Zero Angle of Attack	A-99
A-38	Comparison of Streamlines for the Supersonic Flow Over a Frictionless Infinite (A) Symmetrical Wedge, and (B) Symmetrical Cone, at Zero Angle of Attack	A-100
A-39	Conical Shock Wave Angle ϵ_c as a Function of M_1 , the Mach Number in Front of the Conical Shock, for Different Semi-cone Angles θ_c ($\gamma = 1.40$)	A-101
A-40	Shock Wave Detachment Angles (for Semi-wedge and Semi-cone) as Functions of the Mach Number M_1 in Front of the Shock Wave	A-102
A-41	Mach Number at the Cone Surface M_c , in Back of a Conical Shock, as a Function of the Mach Number M_1 in Front of the Shock, for Different Semi-cone Angles θ_c ($\gamma = 1.40$)	A-103

LIST OF ILLUSTRATIONS (Continued)

Figure No.	Title	Page
A-42	Stagnation Pressure Ratio P_2^0/P_1^0 for a Conical Shock as a Function of M_1 , the Mach Number in Front of the Shock, for Different Semi-cone Angles θ_c ($\gamma = 1.40$)	A-104
A-43	Pressure Ratio P_c/P_1^0 as a Function of M_1 , the Mach Number in Front of a Conical Shock, for Different Semi-cone Angles θ_c ($\gamma = 1.40$).	A-105
A-44	Prandtl-Meyer Expansion Flow Around a Convex Corner . .	A-106
A-45	Prandtl-Meyer Angle δ^* as a Function of M_2 , for Different Values of γ ($M_2 = 1.0$ to 3.0)	A-108
A-46	Prandtl-Meyer Angle δ^* as a Function of M_2 , for Different Values of γ ($M_2 = 3.0$ to 5.0)	A-109
A-47	Maximum Value of the Prandtl-Meyer Angle δ_m^* as a Function of the Specific Heat Ratio γ	A-110

AMCP 706-285

LIST OF TABLES

Table No.	Title	Page
1-1	Classification of Propulsion Engines	1-2
1-2	Rocket-propelled Weapons	1-16
3-1	Flow Processes in Jet Propulsion Engines	3-4
3-2	Integral Equations for Isentropic Flow Functions Applied to Two Arbitrary Cross-sections of Flow Channel	3-22
3-3	Isentropic Functions for the Flow of Ideal Gases	3-22
3-4	Equations for Computing Fanno Flow Functions for Ideal Gases	3-28
7-1	Properties of Double-base Propellants	7-3
7-2	Binders for Composite Propellants	7-4
7-3	Oxidizers for Composite Propellants	7-5
7-4	Typical Composite Propellant Formulations	7-6
8-1	Some Effects Due to Acoustic Instability in a Solid Propellant Rocket Motor	8-17
8-2	Principal Conclusions from Experiments Concerned With Acoustic Instability	8-18
8-3	Methods for Suppressing Acoustic Instability (Solid Propellant Rocket Motors)	8-18
9-1	Calculated Specific Impulses for Several Liquid Propellant Systems	9-5
9-2	Physical Properties of Water Solutions of Hydrogen Peroxide	9-10
9-3	Physical Properties of Several Liquid Oxidizers	9-14
9-4	Physical Properties of Oxides of Nitrogen	9-21
9-5	Physical Properties of Several Oxidizers Containing Fluorine and Oxygen	9-23
9-6	Physical Properties of Liquid Fuels	9-26
9-7	Physical Properties of Light Hydrocarbon Fuels	9-30
11-1	Performance of Hybrid Fuels With Fluorine and Oxygen Oxidizers	11-6
11-2	Performance of Hybrid Fuels With Hydrogen Peroxide Chlorine Trifluoride Oxidizers	11-7

LIST OF TABLES (Continued)

Table, No.	Title	Page
12-1	Classification of Air-breathing Engines	12-8
15-1	Army Aircraft and Their Engines	15-2
15-2	Values of Loss in Specific Output (Δh_{AR}) As a Function of Regenerator Effectiveness (e_R)	15-28
A-I	Critical Pressure P_{cr} and Critical Temperature T_{cr} for Several Gases	A-13
A-II	Relationships Between Dependent Flow Variables and the Friction Parameter	A-61
A-III	Changes in the Flow Variable With Increase in Flow Mach Number	A-61
A-IV	Equations for Conditions Along a Fanno Line	A-62
A-1	Compressible Flow Functions for Isentropic Flow	A-115
A-2	Compressible Flow Functions for Fanno Flow	A-155
A-3	Compressible Flow Functions for Rayleigh Flow	A-195
A-4	Compressible Flow Functions for Normal Shock Waves	A-235
B-1	Abbreviations for Principal Units of Measurement	B-1
B-2	Systems of Dimensions, Their Units and Conversion Factors	B-3
B-3	Conversion Factors (American Engineers System of Units)	B-4
B-4	Dimensional Formulas and Units	B-8
B-5	Functions of the Specific Heat Ratio γ	B-10
B-6	Values of $(P_c^0/P_e)^{1/\gamma}$	B-14
B-7	Values of the Parameter $\theta_t = (P_e/P_c^0)^{\gamma-1/\gamma}$	B-18
B-8	Values of the Parameter $\sqrt{Z_t}$ as a Function of P_c^0/P_e	B-19
B-9	Molar Specific Heats at Constant Pressure for C-H-N-O Compounds	B-20
B-10	Enthalpy of C-H-N-O Compounds above $T_0 = 298.16^\circ\text{K}$	B-21

PREFACE

The Engineering Design Handbook of the Army Materiel Command is a coordinated series of handbooks containing basic information and fundamental data useful in the design and development of Army materiel and systems. The Handbooks are authoritative reference books of practical information and quantitative facts helpful in the design and development of materiel that will meet the needs of the Armed Forces.

This Handbook replaces AMCP 706-282, *Propulsion and Propellants Handbook*; it is not merely a revision to up-date the text material. As suggested by the title, the main emphasis has been placed on propulsion. However, the properties and characteristics of both liquid and solid propellants have been updated and are included in the text.

The Handbook is divided into two parts: Part One "Chemical Rocket Propulsion" and Part Two "Air-breathing Jet Propulsion Engines". Part Two – devoted to air-breathing engines, other than piston engines, employed for propelling winged aircraft, helicopters, and target drones – represents the new addition.

This Handbook was prepared for the U. S. Army Materiel Command. The text was authored by Dr. Maurice J. Zucrow under contract with Duke University. Technical assistance was provided by Mr. J. Swotinsky and Mr. E. Costa, both of Picatinny Arsenal, and Mr. W. D. Guthrie, U. S. Army Missile Command.

The Handbooks are readily available to all elements of AMC including personnel and contractors having a need and/or requirement. The Army Materiel Command policy is to release these Engineering Design Handbooks to other DOD activities and their contractors, and other Government agencies in accordance with current Army Regulation 70-31, dated 9 September 1966. Procedures for acquiring these Handbooks follow:

a. Activities within AMC and other DOD agencies should direct their request on an official form to:

Publications Distribution Branch
Letterkenny Army Depot
ATTN: AMXLE-ATD
Chambersburg, Pennsylvania 17201

PREFACE (Continued)

b. Contractors who have Department of Defense contracts should submit their request, through their contracting officer with proper justification, to the address indicated in par. a above.

c. Government agencies other than DOD having need for the Handbooks may submit their request directly to the Letterkenny Army Depot, as indicated in par. a above, or to:

Commanding General
U. S. Army Materiel Command
ATTN: AMCAD-PP
Washington, D. C. 20315

or

Director
Defense Documentation Center
ATTN: TCA
Cameron Station
Alexandria, Virginia 22314

d. Industry not having a Government contract (this includes Universities) must forward their request to:

Commanding General
U. S. Army Materiel Command
ATTN: AMCRD-TV
Washington, D. C. 20315

e. All foreign requests must be submitted through the Washington, D.C. Embassy to:

Office of the Assistant Chief of Staff
for Intelligence
ATTN: Foreign Liaison Office
Department of the Army
Washington, D. C. 20310

PREFACE (Continued)

All requests, other than those originating within DOD, must be accompanied by a valid justification.

Comments are invited and should be addressed to Commanding Officer,
U. S. Army Research Office—Durham, Box CM, Duke Station, Durham,
North Carolina 27706.

HEADQUARTERS
UNITED STATES ARMY MATERIEL COMMAND
WASHINGTON, D. C. 20315

AMC PAMPHLET
No. 706-285*

ENGINEERING DESIGN HANDBOOK
ELEMENTS OF AIRCRAFT AND MISSILE PROPULSION

29 July 1969

Paragraph		Page
	LIST OF ILLUSTRATIONS	xxiii
	LIST OF TABLES	xxxiv
	PREFACE	xxxvii
	 PART ONE. CHEMICAL ROCKET PROPULSION	
	 CHAPTER 1. CLASSIFICATION AND ESSENTIAL FEATURES OF ROCKET JET PROPULSION SYSTEMS	
1-0	Principal Notation for Chapter 1	1-1
1-1	Purpose and Scope of Handbook	1-1
1-2	Scope of the Field of Propulsion	1-2
1-3	The Reaction Principle	1-3
1-4	The Jet Propulsion Principle	1-3
1-5	Classification of Jet Propulsion Systems	1-3
1-5.1	Air-breathing Jet Engines	1-4
1-5.2	Rocket Jet Propulsion Systems	1-5
1-5.3	Classification of Rocket Propulsion Systems	1-5
1-5.4	Chemical Rocket Propulsion Systems	1-7
1-6	Essential Features of Chemical Rocket Propulsion Systems ..	1-7
1-6.1	Classification of Rocket Propulsion Systems	1-10
1-6.2	Liquid Bipropellant Rocket Engine	1-11
1-6.3	Liquid Monopropellant Rocket Engine	1-11
1-6.4	Solid Propellant Rocket Motor	1-11
1-6.5	Hybrid Rocket Engine	1-11
1-7	Units of Measurement	1-11
	References	1-17
	 CHAPTER 2. MOMENTUM THEORY APPLIED TO PROPULSION	
2-0	Principal Notation for Chapter 2	2-1
2-1	Momentum Theorem of Fluid Mechanics	2-3
2-1.1	Transport of a Fluid Property Across a Control Surface	2-3
2-1.2	Momentum of a Fluid in Steady Flow	2-4
2-1.3	External Forces Acting on a Flowing Fluid	2-6
2-1.4	Steady Flow Momentum Theorem	2-7
2-2	Application of Momentum Theorem to Propulsion Systems	2-7
2-2.1	General Thrust Equation	2-9

*This pamphlet supersedes AMCP 706-282, Propulsion and Propellants, August 1963.

TABLE OF CONTENTS (Continued)

Paragraph		Page
2-2.2	Effective Jet Velocity	2-12
2-2.3	Exit Velocity of the Propulsive Jet	2-13
2-3	Thrust Equations for Rocket Propulsion	2-13
2-4	Power Definitions for Propulsion Systems	2-14
2-4.1	Thrust Power (P_T)	2-14
2-4.2	Propulsive Power (P)	2-14
2-4.3	Exit Loss (P_{KE})	2-14
2-4.4	Jet Power (P_j)	2-15
2-5	Performance Parameters for Jet Propulsion System	2-15
2-5.1	Specific Thrust	2-15
2-5.2.1	Specific Impulse (I_{sp})	2-15
2-5.2.2	Specific Impulse and Jet Power	2-15
2-5.3	Overall Efficiency (η_o)	2-16
2-5.4	Thermal Efficiency (η_{th})	2-16
2-5.5	Propulsive Efficiency (η_p)	2-16
2-5.6	Ideal Propulsive Efficiency (η_p)	2-16
	References	2-18
	CHAPTER 3. ELEMENTARY GAS DYNAMICS	
3-0	Principal Notation for Chapter 3	3-1
3-1	Introduction	3-4
3-2	The Ideal Gas	3-5
3-2.1	The Thermally Perfect Gas	3-5
3-2.2	Specific Heat	3-5
3-2.2.1	Specific Heat at Constant Volume (c_v)	3-6
3-2.2.2	Specific Heat at Constant Pressure (c_p)	3-6
3-2.2.3	Specific Heat Ratio (γ)	3-6
3-2.2.4	Specific Enthalpy and Specific Heat	3-6
3-2.3	Calorically Perfect Gas	3-6
3-2.4	Specific Heat Relationships	3-6
3-2.5	Acoustic or Sonic Speed in an Ideal Gas	3-7
3-2.6	Mach Number	3-7
3-3	General Steady One-dimensional Flow	3-7
3-3.1	Continuity Equation	3-7
3-3.2	Momentum Equation	3-8
3-3.2.1	General Form of Momentum Equation	3-8
3-3.2.2	Momentum Equation for Steady, One-dimensional, Reversible Flow	3-8
3-3.3	Energy Equation for Steady One-dimensional Flow...	3-8
3-4	Steady One-dimensional Flow of an Ideal Gas	3-10
3-4.1	Continuity Equation	3-10

TABLE OF CONTENTS (Continued)

Paragraph		Page
3-4.2.1	Momentum Equations for the Steady One-dimensional Flow of an Ideal Gas	3-12
3-4.2.2	Momentum Equation for a Reversible, Steady, One-dimensional Flow	3-12
3-4.3	Energy Equation	3-12
3-4.3.1	Energy Equation for a Simple Adiabatic Flow . . .	3-12
3-4.3.2	Energy Equation for the Simple Adiabatic Flow of an Ideal Gas	3-13
3-5	Steady One-dimensional Isentropic Flow	3-13
3-5.1	Energy Equation for the Steady One-dimensional Isentropic Flow of an Ideal Gas	3-14
3-5.2	Stagnation (or Total) Conditions	3-15
3-5.2.1	Stagnation (or Total) Enthalpy (h^0)	3-15
3-5.2.2	Stagnation (or Total) Temperature (T^0)	3-15
3-5.2.3	Stagnation (or Total) Pressure (P^0)	3-15
3-5.2.4	Relationship Between Stagnation Pressure and Entropy	3-17
3-5.2.5	Stagnation (or Total) Density (ρ^0)	3-17
3-5.2.6	Stagnation (or Total) Acoustic Speed (a^0)	3-17
3-5.3	Isentropic Exhaust Velocity	3-17
3-5.4	Critical Conditions for the Steady, One-dimensional, Isentropic Flow of an Ideal Gas	3-18
3-5.4.1	Definition of Critical Area and Critical Acoustic Speed	3-18
3-5.4.2	Critical Thermodynamic Properties for the Steady, One-dimensional, Isentropic Flow of an Ideal Gas	3-18
3-5.5	Continuity Equations for Steady, One-dimensional, Isentropic Flow of an Ideal Gas	3-20
3-5.5.1	Critical Area Ratio (A/A^*)	3-20
3-5.5.2	Critical Area Ratio in Terms of the Flow Expansion Ratio (P/P^0)	3-20
3-5.5.3	Critical Area Ratio in Terms of the Flow Mach Number	3-20
3-5.6	Reference Speeds (a^0), (a^*), and (c_0)	3-20
3-5.6.1	Continuity Equations in Terms of Stagnation Conditions	3-21
3-5.6.2	Critical Mass Flow Density (G^*)	3-21
3-5.7	Tables of Isentropic Flow Functions for Ideal Gases . . .	3-21
3-6	Steady One-dimensional Adiabatic Flow in a Constant Area Duct With Wall Friction (Fanno Flow)	3-23
3-6.1	Friction Coefficient (f)	3-23
3-6.2	Principal Equations for Fanno Flow	3-23

TABLE OF CONTENTS (Continued)

Paragraph		Page
3-6.3	Fanno Line Equation	3-23
3-6.4	Fanno Flow With Ideal Gases	3-26
3-6.4.1	Principal Equations	3-26
3-6.4.2	Critical Duct Length for the Fanno Flow of an Ideal Gas	3-27
3-6.4.3	Duct Length for a Specified Change in Mach Number	3-27
3-6.4.4	General Characteristics of the Fanno Flow of an Ideal Gas	3-28
3-6.5	Equations for Compiling Tables for Fanno Flow Functions, for Ideal Gases	3-28
3-7	Steady One-dimensional Frictionless Flow in a Constant Area Duct With Stagnation Temperature Change (Rayleigh Flow)	3-29
3-7.1	Principal Equations for a Rayleigh Flow	3-29
3-7.2	Rayleigh Line	3-32
3-7.2.1	General Characteristics	3-32
3-7.2.2	Characteristics of the Rayleigh Line for the Flow of an Ideal Gas	3-32
3-7.3	Rayleigh Flow Equations for Ideal Gases	3-34
3-7.4	Equations for Tables of Rayleigh Flow Functions for Ideal Gases	3-35
3-7.5	Development of Compression Shock	3-37
	References	3-39
	CHAPTER 4.COMPRESSIBLE FLOW IN NOZZLES	
4-0	Principal Notation for Chapter 4	4-1
4-1	Introduction	4-3
4-2	Ideal Flow in a Converging Nozzle	4-5
4-2.1	Isentropic Exit Velocity for a Converging Nozzle ..	4-5
4-2.2	Isentropic Throat Velocity for the Flow of a Perfect Gas in a Converging Nozzle	4-5
4-2.3	Effect of Varying the Back Pressure Acting on a Converging Nozzle	4-7
4-2.4	Mass Flow Rate for Ideal Nozzle Flow (Converging and Converging-diverging Nozzles)	4-8
4-3	Ideal Flow in a Converging-diverging (or De Laval) Nozzle ..	4-10
4-3.1	Area Ratio for Complete Expansion of the Gas Flowing in a Converging-diverging Nozzle	4-14
4-3.2	Effect of Varying the Back Pressure Acting on a Converging-diverging Nozzle	4-20
4-3.2.1	Underexpansion in a Converging-diverging Nozzle	4-20

TABLE OF CONTENTS (Continued)

Paragraph		Page
4-3.2.2	Overexpansion in a Converging-diverging Nozzle .	4-21
4-3.3	Effect of Varying the Inlet Total Pressure of a Nozzle. . .	4-24
4-4	Flow in Real Nozzles	4-26
4-4.1	Losses in Nozzles	4-26
4-4.2	Area Ratio for an Adiabatic Nozzle	4-26
4-5	Nozzle Performance Coefficients	4-27
4-5.1	Nozzle Efficiency (η_n)	4-27
4-5.2	Nozzle Velocity Coefficient (ϕ)	4-27
4-5.3	Nozzle Discharge Coefficient (C_d)	4-27
4-6	Mass Flow Rate for a Nozzle Operating With Adiabatic Flow and Wall Friction	4-28
4-7	Nozzle Design Principles	4-28
4-8	Nozzle Design Configurations	4-29
4-8.1	Conical Nozzle	4-30
4-8.1.1	Thrust Equation for a Conical Nozzle	4-31
4-8.1.2	Factors for Determining Adequacy of a Conical Nozzle	4-32
4-8.2	Contoured or Bell-shaped Nozzle	4-34
4-8.3	Annular Nozzle	4-36
4-8.4	Plug Nozzle	4-36
4-8.5	Expansion-deflection or E-D Nozzle	4-39
	References	4-40
 CHAPTER 5. PERFORMANCE CRITERIA FOR ROCKET PROPULSION		
5-0	Principal Notation for Chapter 5	5-1
5-1	Introduction	5-2
5-2	Effective Jet (or Exhaust) Velocity (c)	5-2
5-3	Specific Impulse (I_{sp})	5-3
5-3.1	Specific Propellant Consumption (\dot{w}_{sp})	5-4
5-3.2	Weight-flow Coefficient (C_w)	5-4
5-3.3	Mass-flow Coefficient (C_m)	5-4
5-4.1	Thrust Coefficient (C_F)	5-4
5-4.2	Relationship Between I_{sp} , C_w , and C_F	5-5
5-5	Characteristic Velocity (c^*)	5-5
5-6	Jet Power (P_j)	5-5
5-7	Total Impulse (I_T)	5-5
5-8	Weight and Mass Ratios	5-6
5-8.1	Propulsion System Weight (W_{PS})	5-6
5-8.2	Specific Engine Weight (τ)	5-7
5-8.3	Payload Ratio (W_{pay}/W_o)	5-7

TABLE OF CONTENTS (Continued)

Paragraph		Page
5-8.4	Propellant Weight (W_p)	5-7
5-8.5	Propellant Mass Ratio (ξ)	5-7
5-8.6	Vehicle Mass Ratio (Λ)	5-7
5-8.7	Relationship Between the Propellant Mass Ratio (ξ) and the Vehicle Mass Ratio (Λ)	5-8
5-8.8	Propellant Loading Density (δ_p)	5-8
5-8.9	Impulse-weight Ratio for a Rocket Engine	5-8
5-9	Vehicle Performance Criteria	5-8
5-9.1	Linear Motion With Drag and Gravity	5-9
5-9.1.1	Thrust of Rocket Engine With Linear Motion of Vehicle	5-9
5-9.1.2	Aerodynamic Drag	5-11
5-9.1.3	Approximate Solution of Differential Equation for Linear Motion With Drag and Gravity	5-11
5-9.2	Burnout Velocity (V_b)	5-13
5-9.2.1	Burnout Altitude (z_b)	5-14
5-9.2.2	Coasting Altitude After Burnout (z_c)	5-14
5-9.2.3	Maximum Drag-free Altitude (z_{\max})	5-14
5-9.3	Ideal Burnout Velocity (V_{bi})	5-14
	References	5-16
	CHAPTER 6. THERMODYNAMIC RELATIONSHIPS FOR CHEMICAL ROCKET PROPULSION	
6-0	Principal Notation for Chapter 6	6-1
6-1	Introduction	6-3
6-2	Assumptions in Thermochemical and Gas Dynamic Calculations	6-4
6-2.1	Exothermic and Endothermic Chemical Reactions. . .	6-5
6-2.2	Conditions for Thermochemical Equilibrium	6-6
6-2.3	Dissociation and Reassociation Reactions	6-6
6-3	Thermodynamic Equations for Rocket Performance Criteria .	6-6
6-3.1	Isentropic Exit Velocity (u_e')	6-7
6-3.2	Actual or Adiabatic Exit Velocity (u_e)	6-9
6-3.3	Propellant Flow Coefficients	6-11
6-3.3.1	Mass Flow Rate of Propellant Gas (\dot{m})	6-11
6-3.3.2	Weight Flow Coefficient (C_w)	6-11
6-3.4	Thrust (F)	6-11
6-3.4.1	Effective Jet (or Exhaust) Velocity (c)	6-13
6-3.4.2	Thrust Coefficient (C_F)	6-13
6-3.5	Nozzle Area Ratio for Complete Expansion	6-13
6-3.6	Characteristic Velocity (c^*)	6-18

TABLE OF CONTENTS (Continued)

Paragraph		Page
6-3.7	Theoretical Specific Impulse (I'_{sp})	6-20
6-3.7.1	Reduced Specific Impulse	6-20
6-3.7.2	Density Specific Impulse (I_d)	6-23
	References	6-26
CHAPTER 7 .PROPERTIES AND CHARACTERISTICS OF SOLID PROPELLANTS		
7-1	Classification of Solid Propellants	7-1
7-2	Homogeneous Propellants	7-1
7-2.1	Polymers for Homogeneous Propellants	7-2
7-2.2	Oxidizer-plasticizers for Homogeneous Propellants	7-2
7-2.3	Fuel-plasticizers for Homogeneous Propellants	7-2
7-2.4	Additives to Double-base Propellants	7-2
7-2.5	General Characteristics and Applications of Double-base Solid Propellants	7-2
7-3	Heterogeneous or Composite Propellants	7-4
7-3.1	Binders for Composite Propellants	7-4
7-3.2	Oxidizers for Composite Propellants	7-5
7-3.3	Additives to Composite Propellants	7-6
7-4	Factors Governing the Selection of a Solid Propellant	7-7
7-4.1	Specific Impulse (I_{sp})	7-7
7-4.2	Density of Propellant (ρ_p)	7-7
7-4.3	Hygroscopicity	7-7
7-4.4	Controllable Linear Burning Rate (r_0)	7-7
7-4.5	Coefficient of Thermal Expansion	7-7
7-4.6	Thermal Conductivity	7-7
7-4.7	Chemical Stability	7-7
7-4.8	Toxicity	7-8
7-4.9	Shock Sensitivity	7-8
7-4.10	Explosive Hazard	7-8
7-4.11	Smoke in Exhaust	7-8
7-4.12	Attenuation of Electromagnetic Signals	7-8
7-4.13	Availability of Raw Materials	7-9
7-4.14	Fabrication and Process Control	7-9
7-4.15	Cost	7-9
7-5	Mechanical Properties of Solid Propellants	7-9
7-5.1	Ultimate Tensile Strength	7-9
7-5.2	Elongation in Tension	7-10
7-5.3	Modulus in Tension	7-10
7-5.4	Stress Relaxation	7-10
7-5.5	Creep	7-10

TABLE OF CONTENTS (Continued)

Paragraph		Page
7-5.6	Compressive Strength	7-10
7-5.6.1	Deformation At Rupture in Compression	7-10
7-5.6.2	Modulus in Compression	7-10
7-5.7	Shear Properties	7-11
7-5.8	Brittle Temperature	7-11
	References	7-12
	CHAPTER 8 SOLID PROPELLANT ROCKET MOTORS	
8-0	Principal Notation for Chapter 8	8-1
8-1	Internal Ballistics of Solid Propellant Rocket Motors	8-3
8-1.1	Burning of a Solid Propellant (Piobert's Law)	8-3
8-1.2	Combustion Temperature	8-3
8-1.3	General Characteristics of the Combustion Process ...	8-4
8-1.4	Combustion Characteristics of Double-base Solid Propellants	8-5
8-1.5	The Flame Reaction Zone for a Double-base Solid Propellant	8-7
8-1.6	Combustion Characteristics of Composite (Non- homogeneous) Solid Propellants	8-7
8-1.7	Linear Burning Rate (Saint-Robert's Law)	8-7
8-1.8	Weight Rate of Propellant Consumption (\dot{w}_p)	8-9
8-1.9	Volumetric Rate of Propellant Consumption (\dot{Q}_p) ...	8-9
8-1.10	Equilibrium Combustion Pressure and Its Stability ...	8-11
8-1.11	Effect of Propellant Area Ratio (K_n)	8-11
8-1.12	Stability of the Shape of the Burning Surface	8-12
8-1.13	Pressure Deflagration Limit and Pressure Limit	8-12
8-1.14	Effect of the Temperature of a Solid Propellant	8-12
8-1.14.1	General Effects of Temperature	8-12
8-1.14.2	Temperature Sensitivity	8-13
8-1.15	Erosive Burning	8-13
8-2	Combustion Pressure Oscillations in Solid Propellant Rocket Motors (Unstable Burning)	8-14
8-2.1	Terminology Employed in Unstable Burning of Solid Propellant Rocket Motors	8-14
8-2.2	Acoustic Instability in Solid Propellant Rocket Motors	8-14
8-3	Ignition of Propellant Grain	8-19
8-4	Solid Propellant Grain Configurations	8-20
8-5	Port-to-throat Area Ratio ($1/J$)	8-23
8-6	Heat Transfer in Solid Propellant Rocket Motors	8-23
8-6.1	Aerodynamic Heating	8-24

TABLE OF CONTENTS (Continued)

Paragraph		Page
8-6.2	Effect of Aerodynamic Heating on Integrity of Rocket Motor Chambers	8-24
8-7	General Design Considerations	8-25
8-7.1	Selection of Combustion Pressure	8-25
8-7.2	Estimate of the Weight and Volume of the Solid Propellant Grain	8-25
8-7.3	Determination of Nozzle Throat Area	8-26
8-7.3.1	General Considerations	8-26
8-7.3.2	Effect of Propellant Grain Configuration	8-26
8-7.4	Rocket Motor Chamber and Insulation	8-26
8-7.5	Nozzles for Solid Propellant Rocket Motors	8-27
8-7.6	Control of Vehicle Range	8-28
8-7.7	Thrust Vector Control (TVC) of Solid Propellant Rocket-propelled Vehicles	8-28
8-7.7.1	Mechanical Means for Achieving TVC	8-30
8-7.7.2	Movable Nozzles	8-32
8-7.7.3	Secondary Injection for TVC	8-32
	References	8-35

CHAPTER 9. PROPERTIES AND CHARACTERISTICS OF
LIQUID PROPELLANTS

9-1	Factors To Be Considered in Selecting Liquid Propellants ..	9-1
9-2	Principal Physical Properties of Liquid Propellants	9-1
9-2.1	Enthalpy of Combustion	9-1
9-2.2	Chemical Reactivity	9-2
9-2.3	Chemical Structure	9-2
9-2.4	Average Density of Propellant System ($\bar{\rho}_p$)	9-2
9-2.5	Boiling Point and Vapor Pressure	9-2
9-2.6	Freezing Point	9-3
9-2.7	Dynamic or Absolute Viscosity	9-3
9-2.8	Specific Heat	9-3
9-2.9	Chemical Stability	9-3
9-2.10	Corrosivity	9-3
9-2.11	Toxicity	9-4
9-2.12	Availability	9-4
9-2.13	Cost	9-4
9-3	Liquid Monopropellants	9-8
9-3.1	Hydrazine (N_2H_4)	9-9
9-3.2	Hydrogen Peroxide (H_2O_2)	9-10
9-3.3	Ethylene Oxide (C_2H_4O)	9-12
9-3.4	Mixtures of Nitroparaffins	9-12

TABLE OF CONTENTS (Continued)

Paragraph		Page
9-3.5	Mixtures of Nitric Acid, Nitrobenzene and Water (Dithekites)	9-12
9-3.6	Mixtures of Methyl Nitrate and Methanol (Myrols) . . .	9-12
9-4	Oxidizers for Liquid Propellant Systems	9-12
9-4.1	Liquid Fluorine (F_2)	9-13
9-4.2	Liquid Oxygen (LOX)	9-16
9-4.3	Oxidizers Containing Fluorine	9-17
9-4.3.1	General Considerations	9-17
9-4.3.2	Chlorine Trifluoride (ClF_3)	9-17
9-4.4	Oxidizers Containing Oxygen	9-17
9-4.4.1	Liquid Ozone (LOZ)	9-18
9-4.4.2	Hydrogen Peroxide (H_2O_2)	9-18
9-4.4.3	Nitric Acid (HNO_3)	9-18
9-4.4.4	Mixed Oxides of Nitrogen (MON)	9-19
9-4.5	Oxidizers Containing Fluorine and Oxygen	9-20
9-4.5.1	Oxygen Bifluoride (OF_2)	9-22
9-4.5.2	Perchlorylfluoride (ClO_3F)	9-22
9-5	Fuels for Liquid Bipropellant Systems	9-22
9-5.1	Cryogenic Fuels Rich in Hydrogen	9-22
9-5.2	The Borohydrides	9-24
9-5.3	Organic Fuels	9-24
9-5.3.1	Ethyl Alcohol (C_2H_5OH)	9-29
9-5.3.2	Light Hydrocarbon Fuels	9-29
9-5.3.3	Unsymmetrical Dimethylhydrazine (UDMH) . . .	9-29
9-5.3.4	Aerozine-50 ($N_2H_4 + UDMH - 50/50$)	9-30
9-5.3.5	Diethylenetriamine (DETA)	9-30
9-5.4	Nitrogen Hydrides	9-31
9-5.4.1	Anhydrous Ammonia (NH_3)	9-31
9-5.4.2	Hydrazine (N_2H_4)	9-31
9-5.4.3	Mixtures of Hydrazine and Ammonia	9-31
9-6	Gels, Slurries, and Emulsions (Heterogeneous Propellants)	9-32
9-6.1	Thixotropic Gels	9-32
9-6.2	Thixotropic Slurries	9-33
9-6.3	Emulsions	9-33
9-6.4	Summary	9-33
	References	9-34
	 CHAPTER 10. LIQUID PROPELLANT ROCKET ENGINES	
10-0	Principal Notation for Chapter 10	10-1
10-1	Introduction	10-2

TABLE OF CONTENTS (Continued)

Paragraph		Page
10-2	Essential Components of a Liquid Bipropellant	
	Rocket Engine	10-2
10-3	The Thrust Chamber	10-3
10-3.1	The Injector	10-3
10-3.2	The Combustion Chamber	10-5
10-3.2.1	Characteristic Length for a Liquid Propellant	
	Thrust Chamber (L^*)	10-6
10-3.2.2	Gas-side Pressure Drop in a Liquid Propellant	
	Thrust Chamber	10-8
10-3.3	The Exhaust Nozzle	10-9
10-4	Heat Transfer in Liquid Propellant Thrust Chambers	10-9
10-4.1	Classification of Thrust Chamber Cooling Systems	10-10
10-4.2	Nonregenerative Cooling Systems	10-11
10-4.2.1	Heat-sink Cooling of Thrust Chambers	10-11
10-4.2.2	Heat-barrier Cooling of Thrust Chambers	10-11
10-4.2.3	Compound Heat-sink and Heat-barrier Cooling	
	of Thrust Chambers	10-14
10-4.3	Regenerative Cooling Systems	10-14
10-4.4	Internal Cooling Systems	10-16
10-4.4.1	Film Cooling	10-16
10-4.4.2	Transpiration Cooling	10-17
10-4.4.3	Ablation Cooling	10-17
10-5	Feed Systems for Liquid Propellant Rocket Engines	10-20
10-5.1	Stored (Inert) Gas Pressurization	10-20
10-5.2	Chemical Gas Pressurization	10-21
10-5.3	Turbopump Pressurization	10-22
10-6	Thrust Vector Control	10-22
10-7	Variable Thrust Liquid Rocket Engines	10-24
	References	10-25
 CHAPTER 11. COMPOSITE CHEMICAL JET		
PROPULSION ENGINES		
11-1	Introduction	11-1
11-2	Hybrid-type Rocket Engines	11-1
11-2.1	Classification of Hybrid-type Rocket Engines	11-2
11-2.1.1	Head-end Injection Hybrid Rocket Engine	11-2
11-2.1.2	Afterburning (Conventional) Hybrid Rocket	
	Engine	11-3
11-2.1.3	Tribrid Rocket Engines	11-3
11-3	Potential Advantages of the Hybrid Rocket Engine	11-4
11-3.1	Safety in Handling Hybrid Propellants	11-4

TABLE OF CONTENTS (Continued)

Paragraph		Page
11-3.2	Thrust Termination and Restart	11-4
11-3.3	Volume-limited Propulsion Systems	11-4
11-3.4	Variable Thrust Operation	11-5
11-3.5	Mechanical Properties of the Solid Fuel Grain	11-5
11-3.6	Storability of High Energy Propulsion Systems	11-5
11-3.7	Flexibility in Propellant Selection	11-5
11-3.8	Simplicity	11-5
11-4	Theoretical Specific Impulses for Hybrid Rocket Propellant Systems	11-5
11-4.1	Characteristics of the Propulsive Gas of a Hybrid Rocket Engine	11-7
11-4.2	Combustion of Hybrid Propellants	11-8
11-5	Performance Parameters for Hybrid Rocket Engines	11-9
11-5.1	Specific Impulse of a Hybrid Rocket Engine	11-9
11-5.2	Characteristic Velocity for a Hybrid Rocket Engine...	11-9
11-6	Internal Ballistics of the Hybrid Rocket Engine	11-10
11-6.1	Thrust Equation	11-11
11-6.2	Burning Rate of Hybrid Propellants	11-11
11-7	General Design Considerations Pertinent to Hybrid-type Rocket Engines	11-12
11-7.1	Pressurization of the Liquid Oxidizer	11-13
11-7.1.1	Chemical Gas Pressurization	11-13
11-7.1.2	Bladders	11-13
11-7.1.3	Oxidizer Tank Pressure Requirements	11-13
11-8	Design Considerations Pertinent to the Head-end Injection Hybrid Rocket Engine	11-13
11-8.1	The Combustion Chamber	11-14
11-8.2	Exhaust Nozzle Design	11-14
11-8.3	Injectors for the Liquid Oxidizer	11-14
11-8.4	Ignition of Hybrid Rocket Engines	11-14
11-9	Design Considerations Pertinent to the Afterburning (Conventional) Hybrid Rocket Engine	11-16
11-9.1	General Discussion	11-16
11-9.2	Afterburner Chamber	11-16
	References	11-17

PART TWO, AIR-BREATHING JET PROPULSION ENGINES

CHAPTER 12. CLASSIFICATION AND ESSENTIAL
FEATURES OF AIR-BREATHING PROPULSION ENGINES

12-0	Principal Notation for Part Two	12-1
12-1	Classification of Air-breathing Propulsion Engines	12-7

TABLE OF CONTENTS (Continued)

Paragraph		Page
12-1.1	Propulsive Duct Engines	12-8
12-1.2	The Ramjet Engine	12-8
12-1.3	The SCRAMJET Engine	12-10
12-2	Gas-turbine Jet Engines	12-11
12-2.1	The Turbojet Engine	12-11
12-2.2	The Afterburning Turbojet Engine	12-11
12-2.3	The Turbofan Engine	12-14
12-2.4	The Turboramjet or Dual-cycle Engine	12-16
12-2.5	The Turboshift Engine	12-16
12-2.6	The Turboprop Engine	12-17
12-3	General Thrust Equations for Air-breathing Engines	12-18
12-3.1	General Thrust Equations	12-18
12-3.2	General Thrust Equations in Terms of Fuel-air Ratio ..	12-19
12-4	Thrust Equations for Specific Air-breathing Engines	12-20
12-4.1	Thrust Equations and Coefficients for the Ramjet Engine	12-20
12-4.2	Thrust Equation for Simple Turbojet Engine	12-21
12-4.3	Thrust Equation for Afterburning Turbojet Engine ...	12-21
12-4.4	Thrust Equation for Turbofan Engine	12-22
12-5	Efficiency Definitions	12-23
12-5.1	Propulsive Efficiency (η_p)	12-23
12-5.2	Thermal Efficiency (η_{th})	12-24
12-5.3	Overall Efficiency (η_o)	12-24
12-5.3.1	Thrust Specific Fuel Consumption ($TSFC$)	12-24
12-5.3.2	Specific Fuel Consumption (SFC)	12-24
12-6	Performance Parameters for Air-breathing Jet Engines ...	12-27
12-6.1	Air Specific Impulse or Specific Thrust (I_a)	12-27
12-6.2	Fuel Specific Impulse (I_{sp})	12-27
12-6.3	Specific Engine Weight (W_E/F_0)	12-27
12-6.4	Turbine Inlet Temperature (T_4^0)	12-28
12-7	General Comments Regarding Air-breathing Engines	12-28
	References	12-31
	CHAPTER 13. COMPRESSIBLE FLOW IN DIFFUSERS	
13-1	Introduction	13-1
13-2	Subsonic Intake-diffusers	13-2
13-2.1	Subsonic External-compression Diffusers	13-2
13-2.1.1	Static Temperature Ratio for an External- compression Diffuser	13-2
13-2.1.2	Static Pressure Ratio for an External- compression Diffuser	13-3

TABLE OF CONTENTS (Continued)

Paragraph		Page
13-2.2	Subsonic Internal-compression Diffusers	13-3
13-3	Performance Criteria for Diffusers	13-5
13-3.1	Isentropic (Adiabatic) Diffuser Efficiency (η_d)	13-5
13-3.2	Stagnation (or Total) Pressure Ratio (r_D)	13-5
13-3.3	Energy Efficiency of Diffuser (η_{KE})	13-6
13-4	Supersonic Inlet-diffusers	13-7
13-4.1.1	Normal Shock Diffuser	13-7
13-4.1.2	Ram Pressure Ratio for a Normal Shock Diffuser	13-8
13-4.2	The Reversed De Laval Nozzle Supersonic Diffuser	13-9
13-4.3	External Compression Supersonic Diffusers	13-9
13-4.4	Operating Modes for External Shock Diffusers	13-11
13-4.4.1	Critical Operation	13-11
13-4.4.2	Supercritical Operation	13-11
13-4.4.3	Subcritical Operation	13-11
13-5	Diffuser Performance Characteristics and Design Considerations	13-11
	References	13-15
	CHAPTER 14. PROPULSIVE DUCT ENGINES	
14-1	Introduction	14-1
14-2	Thrust Developed by a Propulsive Duct Engine	14-1
14-2.1	Cold Flow Through Shaped Duct	14-1
14-2.2	Methods for Supporting a Static Pressure Higher Than the External Static Pressure Inside a Duct	14-1
14-2.2.1	Restriction of the Exit Area	14-1
14-2.2.2	Heat Addition to the Internal Flow	14-5
14-3	Definitions of Terms Employed in Ramjet Engine Technology	14-5
14-3.1	Gross Thrust (F_g)	14-5
14-3.2	External Drag (D_e)	14-7
14-3.3	Net Thrust (F_n)	14-7
14-3.4	Effective Jet (or Exhaust) Velocity (V_j)	14-7
14-3.5	Net Thrust Coefficient (C_{Fn})	14-8
14-3.6	Gross Thrust Coefficient (C_{Fg})	14-8
14-3.6.1	Effect of Altitude (z) on C_{Fg} ($T_3^0 = \text{const.}$)	14-10
14-3.6.2	Effect of Fuel-air Ratio on C_{Fg} ($z = \text{const.}$)	14-10
14-4	Critical, Supercritical, and Subcritical Operation of the Ramjet Engine	14-10
14-4.1	Critical Operation of the Ramjet Engine	14-13
14-4.2	Supercritical Operation of the Ramjet Engine	14-13

TABLE OF CONTENTS (Continued)

Paragraph		Page
14-4.3	Subcritical Operation of the Ramjet Engine	14-13
14-5	Losses in the Ramjet Engine	14-13
14-6	Diffuser Performance in a Ramjet Engine	14-14
14-7	Burner Efficiency (η_B)	14-16
14-8	Overall Efficiency of the Ramjet Engine (η_o)	14-16
14-9	Gross Thrust Specific Fuel Consumption of the Ramjet Engine ($F_g SFC$)	14-16
14-10	Variable-geometry Ramjet Engine	14-16
14-11	SCRAMJET Engine Performance Parameters	14-17
14-11.1	Gross Thrust (F_g)	14-17
14-11.2	Gross Thrust Specific Impulse (I_{Fg})	14-17
14-11.3	Inlet Kinetic Energy Efficiency (η_{KE})	14-18
14-11.4	Nozzle Thrust Efficiency (η_{nF})	14-18
	References	14-20
	CHAPTER 15. GAS-TURBINE AIR-BREATHING ENGINES	
15-1	Introduction	15-1
15-2	Gas-turbine Powerplant Engines	15-1
15-3	Efficiencies of Components of Gas-turbine Engines	15-2
15-3.1	Diffusion Process	15-2
15-3.1.1	Diffuser Isentropic Efficiency (η_d)	15-2
15-3.1.2	Diffuser Temperature Ratio (a_d)	15-2
15-3.1.3	Diffuser Pressure Ratio Parameter (Θ_d)	15-2
15-3.2	Compression Process	15-4
15-3.2.1	Compressor Isentropic Efficiency (η_c)	15-4
15-3.2.2	Compressor Pressure Ratio Parameter (Θ_c)	15-4
15-3.2.3	Temperature Rise in Air Compressor (ΔT_c)	15-4
15-3.3	Combustion Process	15-6
15-3.3.1	Burner Efficiency (η_B)	15-6
15-3.3.2	Dimensionless Heat Addition Parameter ($Q_i \eta_B / \bar{c}_{pB} T_o$)	15-6
15-3.4	Turbine Expansion Process	15-6
15-3.4.1	Turbine Work for Turboshaft, Turboprop, and Turbojet Engines	15-7
15-3.4.2	Turbine Isentropic Efficiency (η_t)	15-8
15-3.5	Nozzle Expansion Process and Isentropic Efficiency (η_n)	15-8
15-3.6	Machine Efficiency (η_{tc})	15-8
15-4	The Turboshaft Engine	15-8
15-4.1	Design Criteria for Turboshaft Engine	15-9
15-4.1.1	Thermal Efficiency (η_{th})	15-9

TABLE OF CONTENTS (Continued)

Paragraph		Page
15-4.1.2	Specific Output (L)	15-9
15-4.1.3	Air-rate (A)	15-9
15-4.1.4	Work-ratio (U)	15-9
15-4.2	Thermodynamic Cycle for Turboshaft Engine and Thermal Efficiency of Ideal Turboshaft Engine (η_a)..	15-10
15-4.3	Losses in a Turboshaft Engine Cycle	15-12
15-4.4	Simplified Analysis of the Turboshaft Engine Cycle ..	15-12
15-4.4.1	Compression Work (Δh_c)	15-13
15-4.4.2	Turbine Work (Δh_t)	15-13
15-4.4.3	Specific Output (L)	15-13
15-4.4.4	Heat Added (Q_i)	15-13
15-4.4.5	Thermal Efficiency (η_{th})	15-13
15-4.4.6	Air-rate (A)	15-14
15-4.4.7	Work-ratio (U)	15-15
15-4.4.8	Specific Fuel Consumption (SFC)	15-15
15-4.5	Performance Characteristics of the Turboshaft Engine .	15-15
15-4.5.1	Effect of Cycle Pressure Ratio (Θ)	15-15
15-4.5.2	Effect of Cycle Pressure Ratio (Θ) and Turbine Inlet Temperature (T_4^0)	15-15
15-4.5.3	Air-rate (A)	15-18
15-4.5.4	Work-ratio ($U = L/L_t$)	15-18
15-4.5.5	Effect of Machine Efficiency (η_{tc})	15-18
15-4.5.6	Effect of Ambient Air Temperature ($T_0 = T_2$) . . .	15-19
15-4.5.7	Effect of Pressure Drops	15-20
15-4.6	Modifications to Basic Turboshaft Engine to Improve Its Performance	15-21
15-5	Regenerative Turboshaft Engine	15-24
15-5.1	The Regeneration Process	15-25
15-5.1.1	Regenerator Effectiveness (e_R)	15-27
15-5.1.2	Effect of Pressure Drops in the Regenerator ...	15-27
15-5.2	Regenerator Heat Transfer Surface Area and Regenerator Effectiveness	15-28
15-5.3	Cycle Analysis for Regenerative Turboshaft Engine . . .	15-28
15-5.3.1	Temperature of Air Leaving Air Compressor (T_3) .	15-29
15-5.3.2	Temperature of Gas Leaving Turbine (T_5)	15-29
15-5.3.3	Heat Supplied the Regenerative Turboshaft Engine (Q_{iR})	15-29
15-5.3.4	Specific Output of Regenerative Turboshaft Engine ($L/c_p T_0$)	15-29
15-5.3.5	Thermal Efficiency of Regenerative Turboshaft Engine (η_{th})	15-30

TABLE OF CONTENTS (Continued)

Paragraph		Page
15-5.3.6	Work-ratio for Regenerative Turboshaft Engine (U)	15-30
15-5.4	Performance Characteristics of the Regenerative Turboshaft Engine	15-30
15-6	Turboprop Engine	15-30
15-6.1	Thermodynamic Analysis of the Turboprop Engine Cycle	15-32
15-6.1.1	Propeller Thrust Horsepower (P_{prop})	15-34
15-6.1.2	Jet Thrust Power (P_{Tj})	15-34
15-6.1.3	Total Thrust Horsepower for Turboprop Engine ($P_{\text{turboprop}}$)	15-34
15-6.2	Performance Characteristics for the Turboprop Engine	15-34
15-6.2.1	Effect of Altitude and Turbine Inlet Temperature	15-36
15-6.2.2	Effect of Machine Efficiency (η_{tc}) and Turbine Inlet Temperature (T_4^0)	15-38
15-6.3	Operating Characteristics of Turboprop Engine	15-38
15-7	Gas-turbine Jet Engines	15-38
15-8	Turbojet Engine	15-38
15-8.1	Dimensionless Heat Addition for Turbojet Engine ($Q_i \eta_B / c_p B T_0$)	15-41
15-8.2	Turbine Pressure Ratio (P_4^0 / P_5^0)	15-41
15-8.3	Dimensionless Enthalpy Change for the Propulsive Nozzle ($\Delta h_n / c_p T_0$)	15-41
15-8.4	Dimensionless Thrust Parameter (λ)	15-43
15-8.5	Thermal Efficiency of Turbojet Engine (η_{th})	15-43
15-8.6	Overall Efficiency of Turbojet Engine (η_o)	15-43
15-8.7	Performance Characteristics of Turbojet Engine	15-44
15-8.7.1	Effect of Cycle Temperature Ratio (α) and Compressor Pressure Ratio (P_3^0 / P_2^0) for a Constant Flight Speed	15-44
15-8.7.2	Effect of Flight Mach Number (M_0) and Cycle Temperature Ratio (α) on the Dimensionless Thrust Parameter (λ)	15-46
15-8.7.3	Effect of Flight Speed and Compressor Pressure Ratio (P_3^0 / P_2^0) on Performance of Turbojet Engine	15-46
15-9	Turbofan Engine	15-48
15-9.1	Definitions Pertinent to the Turbofan Engine	15-49
15-9.1.1	Bypass Ratio (β)	15-49

TABLE OF CONTENTS (Continued)

Paragraph		Page
15-9.1.2	Fan Isentropic Efficiency (η_F)	15-49
15-9.1.3	Fan Pressure Ratio Parameter (Θ_F)	15-49
15-9.1.4	Fan Power (P_F)	15-51
15-9.2	Analysis of Processes in Turbofan Engine	15-51
15-9.2.1	Diffusion for Hot Gas Generator Circuit	15-51
15-9.2.2	Compressor Power for Turbofan Engine (P_{cTF})	15-51
15-9.2.3	Burner Fuel-air Ratio for Turbofan Engine (f)	15-52
15-9.2.4	Turbine Power for Turbofan Engine (P_{tTF})	15-52
15-9.2.5	Nozzle Expansions for Turbofan Engine	15-53
15-9.2.5.1	Nozzle Expansion Work for Gas Generator Nozzle	15-54
15-9.2.5.2	Nozzle Expansion Work for Cold Air- stream	15-54
15-10	Performance Parameters for Turbofan Engine	15-54
15-10.1	Thrust Equation (F)	15-54
15-10.2	Mean Jet Velocity for Turbofan Engine (\bar{V}_{jTF})	15-54
15-10.3	Air Specific Impulse (or Specific Thrust) (I_a)	15-55
15-10.4	Conclusions	15-55
	References	15-56
APPENDIX A ELEMENTARY GAS DYNAMICS		
A-0	Principal Notation for Appendix A	A-1
A-1	Introduction	A-5
A-2	The Ideal Gas	A-7
A-2.1	The Thermally Perfect Gas	A-7
A-2.2	The Calorically Perfect Gas	A-7
A-2.3	Specific Heat Relationships for the Ideal Gas	A-8
A-2.4	Some Results from the Kinetic Theory of Gases	A-9
A-2.5	Some Characteristics of Real Gases	A-11
A-2.6	Acoustic or Sonic Speed (a)	A-12
A-2.6.1	Isentropic Bulk Modulus (K_g)	A-13
A-2.6.2	Acoustic Speed in an Ideal Gas	A-14
A-2.7	Mach Number	A-14
A-3	Steady One-dimensional Flow	A-14
A-3.1	Continuity Equation	A-15
A-3.2	Momentum Equation	A-18
A-3.2.1	Impulse Function	A-19
A-3.2.2	Rayleigh Line Equation	A-19
A-3.3	Energy Equation for Steady One-dimensional Flow	A-20
A-3.4	Entropy Equation for Steady One-dimensional Flow	A-24
A-4	Steady One-dimensional Flow of an Ideal Gas	A-25

TABLE OF CONTENTS (Continued)

Paragraph		Page
A-4.1	Continuity Equation for an Ideal Gas	A-25
A-4.2	Momentum Equation for the Steady One-dimensional Flow of an Ideal Gas	A-26
A-4.2.1	Reversible Steady One-dimensional Flow of an Incompressible Fluid	A-26
A-4.2.2	Reversible Steady One-dimensional Flow of a Compressible Fluid	A-26
A-4.2.3	Irreversible Steady One-dimensional Flow	A-26
A-4.2.4	Irreversible Steady One-dimensional Flow of an Ideal Gas	A-27
A-4.3	Energy Equation for Steady One-dimensional Flow	A-27
A-4.3.1	Energy Equation for a Simple Adiabatic Flow	A-28
A-4.3.2	Energy Equation for the Simple Adiabatic Flow of an Ideal Gas	A-28
A-4.4	Entropy Equation for the Steady One-dimensional Flow of an Ideal Gas	A-29
A-5	Steady One-dimensional Isentropic Flow	A-29
A-5.1	Energy Equation for the Steady Isentropic One- dimensional Flow of an Ideal Gas	A-30
A-5.2	Stagnation (or Total) Conditions	A-33
A-5.2.1	Stagnation (or Total) Enthalpy (h^0)	A-33
A-5.2.2	Stagnation (or Total) Temperature (T^0)	A-33
A-5.2.3	Stagnation (or Total) Pressure (P^0)	A-34
A-5.2.4	Relationship Between Stagnation Pressure and Entropy	A-34
A-5.2.5	Stagnation (or Total) Density (ρ^0)	A-35
A-5.2.6	Stagnation Acoustic Speed (a^0)	A-35
A-5.2.7	Nondimensional Linear Velocity ($w=u/a^0$)	A-36
A-5.3	Adiabatic Exhaust Velocity (u_e)	A-36
A-5.4	Isentropic Exhaust Velocity (u')	A-36
A-5.4.1	Nozzle Efficiency (η_n)	A-37
A-5.4.2	Nozzle Velocity Coefficient (ϕ)	A-37
A-5.5	Maximum Isentropic Speed (c_0)	A-37
A-5.6	Continuity Equation for Steady One-dimensional Isentropic Flow of an Ideal Gas in Terms of Stagnation Conditions	A-38
A-6	Critical Condition for the Steady One-dimensional Isentropic Flow of an Ideal Gas	A-39
A-6.1	Critical Thermodynamic Properties for the Isentropic Flow of an Ideal Gas	A-40
A-6.1.1	Critical Acoustic Speed (a^*)	A-40

TABLE OF CONTENTS (Continued)

Paragraph		Page
A-6.1.2	Critical Static Temperature (T^*)	A-41
A-6.1.3	Critical Expansion Ratio (P^*/P^0)	A-41
A-6.1.4	Critical Density Ratio (ρ^*/ρ^0)	A-41
A-6.1.5	Dimensionless Velocity ($M^* = u/a^*$)	A-41
A-6.2	Relationships Between the Reference Speeds a^0 , a^* , and c_0	A-42
A-6.2.1	Relative Values of Reference Speeds for a Gas Having $\gamma = 1.40$	A-42
A-6.2.2	Energy Equations in Terms of the Reference Speeds a^0 and c_0	A-42
A-6.3	Critical Area Ratio for the Steady One-dimensional Isentropic Flow of an Ideal Gas	A-42
A-6.3.1	Critical Area Ratio (A/A^*)	A-43
A-6.3.2	Mass Flow Rate (\dot{m}) and Critical Area Ratio (A/A^*)	A-43
A-6.4	Flow Area Changes for Subsonic and Supersonic Isentropic Flow	A-44
A-6.5	Dimensionless Thrust Function (F/F^*)	A-44
A-7	Flow of an Ideal Gas in a Converging-diverging One- dimensional Passage	A-46
A-7.1	Maximum Flow Density	A-47
A-7.2	Critical Flow Density (G^*)	A-49
A-8	Steady One-dimensional Adiabatic Flow With Wall Friction	A-49
A-8.1	Adiabatic Flow With Wall Friction in a Constant Area Duct	A-51
A-8.1.1	Friction Coefficient (f)	A-52
A-8.1.2	Friction Coefficient for Compressible and Incompressible Flows	A-52
A-8.2	Fanno Line Equation for Steady Adiabatic Flow in a Constant Area Duct	A-53
A-8.3	Fanno Line Equation for the Flow of an Ideal Gas in a Constant Area Duct	A-57
A-8.3.1	Friction Parameter for a Fanno Flow	A-57
A-8.3.2	Critical Duct Length for a Fanno Flow	A-57
A-8.3.3	Duct Length and Mach Number Change for Fanno Flow	A-58
A-8.3.4	Entropy Increase Due to Wall Friction for the Fanno Flow of an Ideal Gas	A-59
A-8.3.5	Entropy Gradient for the Fanno Flow of an Ideal Gas	A-59

TABLE OF CONTENTS (Continued)

Paragraph		Page
A-8.3.6	Gradient of the Flow Mach Number for Adiabatic Flow of an Ideal Gas in a Constant Area Duct . . .	A-60
A-8.4	Relationships Between Dependent Flow Variables and Friction Parameter for Adiabatic Flow of an Ideal Gas in a Constant Area Duct	A-60
A-8.5	Equations for Compiling Tables for Conditions Along a Fanno Line	A-61
A-8.5.1	Choking Due to Wall Friction for a Fanno Line in a Constant Area Duct	A-63
A-8.5.2	Subsonic or Supersonic Flow in a Duct	A-63
A-9	One-dimensional Steady Frictionless Flow With Heat Addition (Simple Diabatic or Rayleigh Flow)	A-64
A-9.1	Principal Equations for a Rayleigh Flow	A-65
A-9.2	The Rayleigh Line	A-66
A-9.3	Condition for Maximum Enthalpy on a Rayleigh Line . .	A-67
A-9.4	State of Maximum Entropy on a Rayleigh Line	A-67
A-9.5	Rayleigh Line Equations for an Ideal Gas	A-70
A-9.6	Equations for Compiling Tables of Flow Parameters Along a Rayleigh Line	A-71
A-9.7	The Development of a Compression Shock	A-71
A-10	Disturbances in a Compressible Fluid	A-72
A-10.1	Propagation of Small Disturbances in a Compressible Fluid	A-72
A-10.2	Propagation of Strong Disturbances in a Compressible Fluid	A-76
A-10.2.1	Shock Wave or Shock Front	A-77
A-10.2.2	Examples of Gasdynamic Discontinuities	A-77
A-10.3	The Normal Shock Wave	A-79
A-10.3.1	Basic Equations for the Normal Shock	A-79
A-10.3.2	Rankine-Hugoniot Equations for a Normal Shock .	A-81
A-10.3.3	Parameters for the Normal Shock as Function of the Flow Mach Number in Front of Shock	A-81
A-10.3.4	The Rayleigh Pitot Tube Equation	A-82
A-10.4	The Oblique Shock Wave	A-83
A-10.4.1	Basic Equations for the Oblique Shock	A-84
A-10.4.2	Oblique Shock Parameters as Functions of the Mach Number in Front of the Shock and the Wave Angle (ϵ)	A-86
A-10.4.3	Prandtl Relationship for Oblique Shocks	A-87
A-10.4.4	Charts Presenting Relationships Between the Parameters for Oblique Shocks	A-89

TABLE OF CONTENTS (Continued)

Paragraph		Page
A-10.4.5	Application of Normal Shock Table to Oblique Shocks	A-93
A-11	Supersonic Flow Over an Infinite Wedge	A-94
A-12	Supersonic Flow Over a Cone	A-98
A-13	Prandtl-Meyer Expansion Flow	A-99
	References	A-112
	APPENDIX B, USEFUL TABLES	B-1
	INDEX	I-1

PART ONE

CHEMICAL ROCKET PROPULSION

CHAPTER 1

CLASSIFICATION AND ESSENTIAL FEATURES OF ROCKET JET PROPULSION SYSTEMS

1-0 PRINCIPAL NOTATION FOR CHAPTER 1*

A	cross-sectional area	u_e	velocity of propellant gas at exit cross-section A_e of exhaust nozzle
A_e	cross-sectional area of nozzle exit section	W	weight, lb
A_F	frontal area	W_E	dry weight of rocket engine
D	drag, lb		
F	thrust, lb		
m	mass, slug		
\dot{m}	mass rate of consumption, slug/sec		
\dot{m}_p	mass rate of propellant consumption		
P_c	gas pressure at entrance to exhaust nozzle (combustion pressure)		
P_e	pressure in exit plane of the exhaust nozzle		
<u>TSFC</u>	thrust specific fuel consumption, lb of fuel per hr per lb of thrust		
u_c	velocity of propellant gas at entrance cross-section of exhaust nozzle		

1-1 PURPOSE AND SCOPE OF HANDBOOK

This handbook is intended to provide a general description of the characteristics and design features of the propulsion systems for missiles and aircraft either employed in or being developed for weapon systems of interest to the Department of the Army. The handbook assumes that the reader has a technical background equivalent to the bachelor's degree in either engineering, physics, or chemistry, but no previous experience in either propulsion or propellant technology.

For convenience the handbook is divided into the following two parts:

PART ONE CHEMICAL ROCKET PROPULSION

and

PART TWO AIR-BREATHING JET PROPULSION ENGINES

*Any consistent set of units may be employed; the units presented here are for the American Engineers System (see par. 1-7).

1-2 SCOPE OF THE FIELD OF PROPULSION

Since World War II there has been a tremendous broadening of the field of propulsion particularly as applied to aircraft, missiles, space vehicles, and reaction control devices. An appreciation of the scope of propulsion as a technology can be inferred by examining Table 1-1.

Piston and turboprop engines (see A-(1) and A-(4), Table 1-1) employ propellers for developing the propulsive force, called the *thrust*. In such systems the propeller is the *propulsive element* of the system. A system which utilizes a propeller for producing thrust is termed *propeller propulsion*. The turboshaft engine is employed for powering the rotors of helicopters and as a general gas turbine powerplant.

TABLE 1-1

CLASSIFICATION OF PROPULSION ENGINES

A. AIR-BREATHING CHEMICAL SYSTEMS

- (1) Piston Engine-Propeller Systems
- (2) Turboshaft Engine
- (3) Regenerative Turboshaft Engine
- (4) Turboprop Engines
- (5) Turbojet Engines
- (6) Ramjet Engines
- (7) Turbofan or By-pass Engines
- (8) Turbo-ramjet Engines

B. AIR-BREATHING NUCLEAR ENGINES

- (1) Nuclear Turboprop Engines
- (2) Nuclear Turbojet Engines
- (3) Nuclear Ramjet Engines

C. ROCKET PROPULSION SYSTEMS (NON-AIR-BREATHING SYSTEMS)

- (1) Chemical Rocket Propulsion Systems
- (2) Nuclear (Heat-transfer) Rocket Engines
- (3) Electric Rocket Engines

D. COMPOSITE PROPULSION SYSTEMS

- (1) Hybrid Type Rocket Engines
- (2) Combinations of Chemical Rocket Engines Using Atmospheric Air

All of the propulsion systems listed in Table 1-1, except A-(1), A-(2), and A-(3), utilize the *jet propulsion principle*, discussed in par. 1-3, for developing propulsive thrust. It should be noted, however, that a turboprop engine develops a portion of its thrust by jet propulsion and the balance by propeller propulsion.

1-3 THE REACTION PRINCIPLE²*

The verb *to propel* means to drive or push forward or onward, and the force which propels a body is called the *thrust*, and is denoted by *F*. Experience has demonstrated that every method for propelling a body in either a fluid medium or in space is basically an application of Newton's *reaction principle*. According to that principle, forces always occur in equal and opposite pairs; i.e., *to every action (force) there is an equal, but oppositely directed, reaction (force)*. Thus, swimming in water, rowing a boat, the screw propelling a ship, the propeller causing the flight of an airplane, and *jet propulsion* are examples of the application of the reaction principle to propulsion problems.

In each of the above examples, the application of the reaction principle involves *increasing* the momentum of a flowing mass of fluid in one direction so that the reaction to the action force causing the *time rate of increase in the momentum of the fluid* produces a thrust for propelling the body. Hence, the thrust acts in the direction of the desired motion for the body and is produced by *increasing the momentum of a flowing fluid in the direction opposite to that desired for the body*.

1-4 THE JET PROPULSION PRINCIPLE^{1,3}

Jet propulsion differs from other propulsion methods in that the rate of increase in the momentum of the *propulsive fluid* is achieved by causing that fluid to be ejected from *within* the propelled body in the form of a *high speed*

fluid jet. A characteristic of all other propulsion schemes is that the propulsive fluid is caused to flow around the propelled body as, for example, in the case of an airplane propeller. Hence, the thrust produced by a *jet propulsion engine* is the reaction produced by accelerating a propulsive fluid as it flows from the *inlet* section of the engine through the exist planes of one or more suitable *exhaust nozzles*. The high speed jet of fluid ejected from an exhaust nozzle is termed a *propulsive jet* and the fluid comprising the jet is called a *propellant*.

There is no restriction, at least in the abstract, upon the material which can be used for producing the propulsive jet. It may be a liquid, a vapor, solid particles, the gas produced by a chemical reaction, a plasma, ions, electrons, and combinations thereof^{1,4}. The choice of the most appropriate propellant materials is dictated by the propulsion requirements of the mission.

A common feature of all of the propulsion systems for propelling either missiles or aircraft is that the *propulsive element* of the system is the *exhaust nozzle* (or nozzles), also called the *propulsive nozzle*.

1-5 CLASSIFICATION OF JET PROPULSION SYSTEMS

For propelling either an aircraft or a missile in and through the atmosphere surrounding earth, the most suitable fluid for forming the propulsive jet is a hot gas. Consequently, the jet propulsion engines for propelling such vehicles are basically devices for producing a hot gaseous propellant. They may be grouped into two broad classes depending upon the method employed for producing the hot gaseous propulsive jet^{1,5}.

In general, every jet propulsion system that uses a hot gaseous exhaust jet as its propulsive jet comprises two principal subassemblies: (1) a *hot gas generator* and (2) an exhaust nozzle, the *propulsive element*. Regardless of its complexity, the only function of the hot gas

*Superscript numbers refer to References at the end of the Chapter.

generator is to supply a gas at the desired pressure, temperature, and mass flow rate to the propulsive nozzle.

Because there are different methods and means for producing the hot gaseous propellant, there can be differences in the thermodynamic cycle for producing the hot gas. Consequently, the different types of jet propulsion systems for propelling aircraft and missiles are related to the design of the hot gas generator. In general, the jet propulsion systems employing hot gaseous propulsive jets can be divided into two groups:

- (1) Air-breathing Jet Propulsion Systems
- (2) Rocket Jet Propulsion Systems

Hereafter, the above will be termed *air-breathing jet engines*, and *rocket propulsion systems*, respectively. Obviously, air-breathing jet engines can propel vehicles only within the atmosphere of earth, and have maximum altitudes (or ceilings) above which they are inoperable. Rocket propulsion systems, on the other hand, since they do not use atmospheric air in their functioning, can be employed for propelling vehicles in any environment; i.e., in the atmosphere of earth, in space, and in or on water.

1-5.1 AIR-BREATHING JET ENGINES

A basic characteristic of an air-breathing jet engine is that it inducts atmospheric air continuously so that its propulsive (exhaust) jet contains air as a major ingredient. If the heating of the inducted air is accomplished by burning a fuel with it (a liquid hydro-carbon, a cryogenic fuel such as either liquid hydrogen or liquid methane, or a solid fuel); the propulsion engine is called a *chemical air-breathing jet engine*. The propulsive jet in that case contains a small amount of combustion products admixed with the hot air^{5,7}.

If the inducted atmospheric air is heated by heat-transfer, either direct or indirect, with a

nuclear source of energy the propulsion engine is termed a *nuclear air-breathing jet engine*. The name air-breathing jet engines as employed hereafter will refer to the chemical engines. There will be no discussion hereafter of the nuclear air-breathing engines.

All air-breathing jet engines utilize one or more of the following *gas dynamic* processes in their functioning:

- (1) The induction of atmospheric air.
- (2) Compression of the inducted air by *diffusion*, i.e., by converting the kinetic energy of flowing air into a rise in static pressure.
- (3) Adiabatic flow with friction.
- (4) Compression of the flowing air by transferring energy to it as it flows through some form of *turbo-compressor*, axial flow or radial flow machine.
- (5) Heating of the compressed flowing air by burning it with a fuel, usually a liquid fuel.
- (6) Expansion of the compressed heated air, admixed with combustion products, in some form of turbine which furnishes the power for driving the compressor.
- (7) Expansion of the hot propellant gas in an appropriate exhaust nozzle and its ejection to the surroundings, as a propulsive jet.

In view of its utilization of one or more of the above processes in its functioning, an air-breathing jet engine is frequently referred to as a *gas dynamic* propulsion engine.

Air-breathing jet engines may be grouped into two main groups:

- (1) *Propulsive duct jet engines* which employ no machinery in the hot gas generator.
- (2) *Gas-turbine jet engines* which employ machinery in the hot gas generator.

Fig. 1-1 is a block diagram illustrating the essential elements of an air-breathing jet engine. In a propulsive duct jet engine, the air compression is due entirely to diffusion, the conversion of the kinetic energy associated with a flowing fluid into static pressure rise, and the turbine element is omitted. The components I, II and III coact to form the *hot gas generator*.

In a gas-turbine engine the components I, II, III, and IV coact to form the hot gas generator. The air heating system III for either type of engine is termed either the *burner* or the *combustor*.

Detailed discussions of the different types of air-breathing jet engines are presented in Part Two of this handbook.

1-5.2 ROCKET JET PROPULSION SYSTEMS

By definition, a rocket jet propulsion system is one which does not use any atmospheric air in producing the hot gaseous propulsive jet. Consequently, a rocket propulsion system can propel bodies both within and beyond the atmosphere of earth. Air-breathing jet engines can function only within that atmosphere^{5,6,9}.

Fig. 1-2 illustrates diagrammatically the essential elements of a rocket jet propulsion system. It comprises the following:

- (1) A supply of a *propellant material* (or materials) stored in appropriate tanks carried in the *rocket-propelled* vehicle.
- (2) Means for metering the rate at which the propellant material is forced into the *rocket motor*, wherein energy is added to it.
- (3) One or more rocket motors (also called thrust chambers, thrusters, or accelerators) from which the propulsive high speed jet is ejected to the surroundings.

In every rocket propulsion system, irrespective of its type, means must be provided for adding energy to the propellant material as it moves through the rocket motor.

Refer to Fig. 1-2. Propellant material from the Propellant Supply (A) is metered and fed by the Feed and Metering System (B) to the Rocket Motor (C), wherein energy is added to the propellant material. As a consequence of the energy addition, a propellant gas is ejected from the rocket motor as a propulsive jet. Accordingly, a thrust force, denoted by F , is produced acting in the direction opposite to that for the *jet velocity*, denoted by u_e ; the latter is measured with respect to the walls of the rocket motor.

If one considers rocket jet propulsion from the broadest point of view so that it includes space propulsion engines, then consideration must be given to the feasibility of utilizing one or more of the following forms of energy for propulsion purposes: (a) chemical energy, (b) solar energy, (c) nuclear energy, and (d) electrical energy⁹.

1-5.3 CLASSIFICATION OF ROCKET PROPULSION SYSTEMS

Rocket propulsion systems may be grouped in accordance with the forms of energy they use in their functioning. Thus there are four groups:

- (1) Chemical Rocket Propulsion Systems
- (2) Solar Energy Rocket Engines
- (3) Nuclear (Heat-transfer) Rocket Engines
- (4) Electrical Rocket Engines

The discussions in Part One of this handbook will be limited to chemical rocket propulsion systems; hereafter referred to as *rocket propulsion systems*.

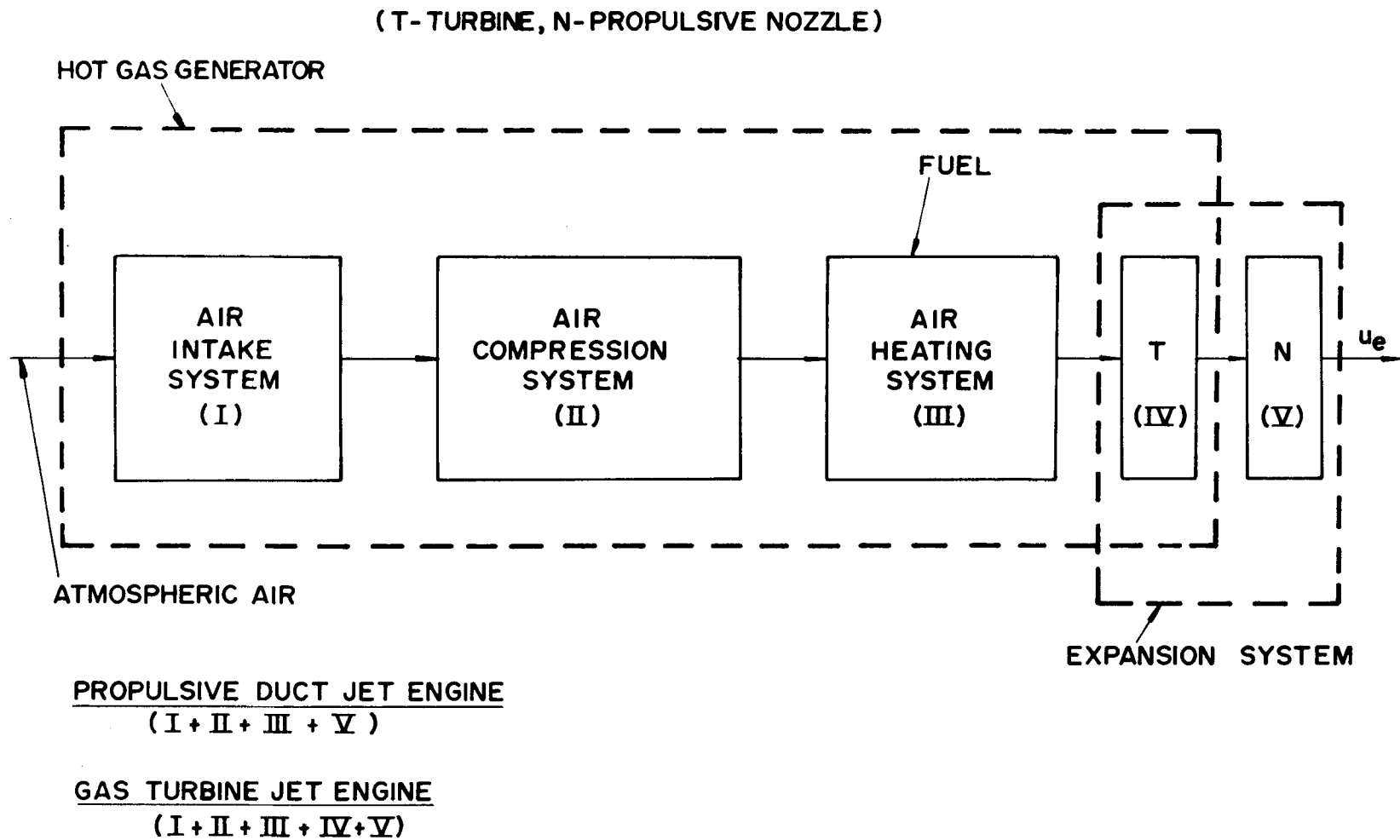


Figure 1-1. Essential Elements of an Air-breathing Jet Engine

1-5.4 CHEMICAL ROCKET PROPULSION SYSTEMS

Only the chemical types of rocket propulsion systems have achieved operational realization and have a broad, well-developed technology. Chemical rocket propulsion systems have the following two characteristics:

- (1) They utilize chemical reactions in the thrust chamber to produce a high pressure high temperature *propellant gas* at the entrance plane of a *converging-diverging* exhaust nozzle.
- (2) The propellant gas is expanded as it flows through the exhaust nozzle and is ejected to the surroundings as a supersonic gaseous propulsive jet.

The expansion in the exhaust nozzle is a thermodynamic process by which approximately one-half of the enthalpy released by the chemical reaction is converted into the kinetic energy associated with the supersonic gaseous propulsive jet. Chemical rocket jet propulsion systems belong to a class of propulsion systems which are frequently termed *thermodynamic jet propulsion systems*.

In a thermodynamic rocket jet propulsion system, as in an air-breathing jet engine, (see par. 1-5.1) all of the components except the exhaust nozzle constitute a hot-gas generator for supplying a high pressure, high temperature gas to a converging-diverging exhaust nozzle (see Fig. 4-6).

The amount of energy that can be added to the propellant gas produced by a chemical reaction is limited by the nature of the chemical bonds of the reactants and products. For that reason chemical rocket propulsion systems are frequently referred to as *energy-limited rocket propulsion systems*⁹. It is because of this energy limitation that consideration must be given, especially for space propulsion engines, to

thrust-producing systems in which larger amounts of energy can be added per unit mass of the consumed propellant. As to be expected, when sources of larger amounts of energy are considered, atomic energy is a prime contender.

1-6. ESSENTIAL FEATURES OF CHEMICAL ROCKET PROPULSION SYSTEMS^{5,6,9}

The general operating principle of a chemical rocket motor can be demonstrated by considering the fin-stabilized solid propellant rocket motor illustrated in Fig. 1-3.

As the solid propellant burns it produces tremendous quantities of hot gas. If the propellant burns in a closed chamber, such as that illustrated in Fig. 1-4(A), the gas pressures inside the chamber are balanced in all directions and no *thrust* is developed. Assume now that a small hole is opened in the chamber, as illustrated in Fig. 1-4(B), and that the propellant burns at a constant rate. Under these conditions the *combustion pressure* inside the chamber, denoted by P_c , remains constant (a short time after the grain is ignited) at a value governed by the area of the hole and the rate, denoted by \dot{m}_p , at which the propellant burns. At the hole in the chamber there is an escape of gas and the latter has no surface against which it can push. Hence, there is an unbalanced force or thrust, denoted by F , acting to the left. In a practical rocket motor the hole (see Fig. 1-4(B)) is replaced by a converging-diverging nozzle, termed a De Laval nozzle, as illustrated in Fig. 1-4(C). Conditions are similar if the hot gas is produced by burning one or more liquids rather than by burning a solid material. In any case the main objective is to produce a propulsive jet having the largest ejection velocity.

Because the gas pressure P_c at the entrance to the exhaust nozzle is normally several times that of the surroundings into which the propellant gas is discharged, the velocity of the propulsive jet is supersonic. Furthermore, the

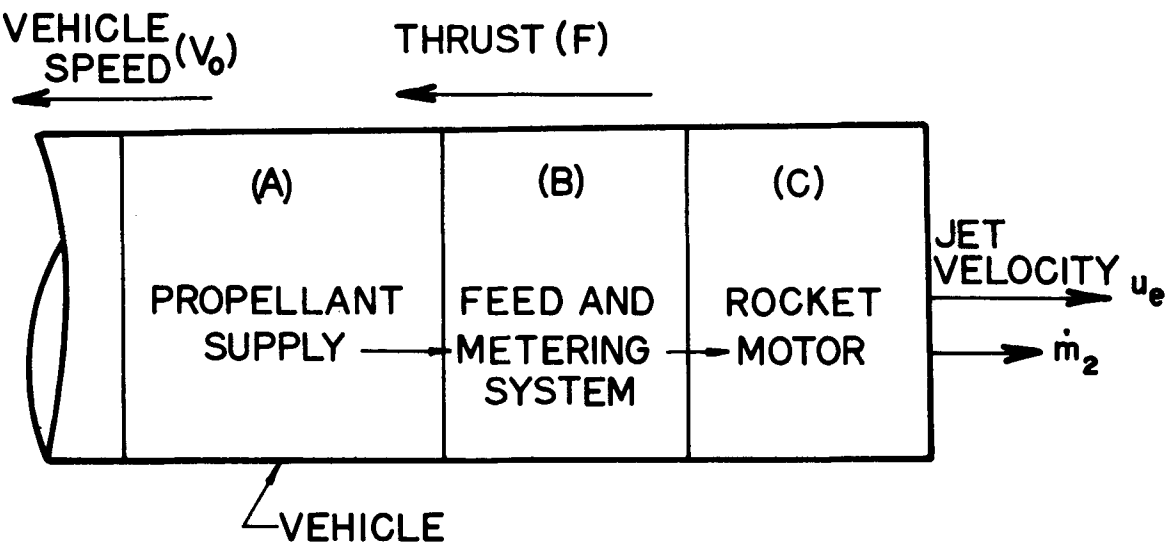


Figure 1-2. Essential Elements of a Jet Propulsion System

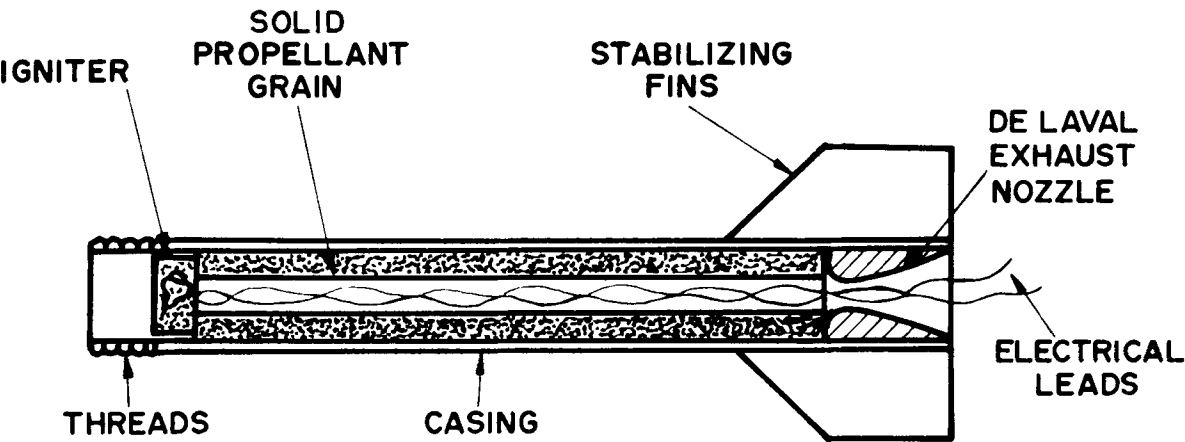
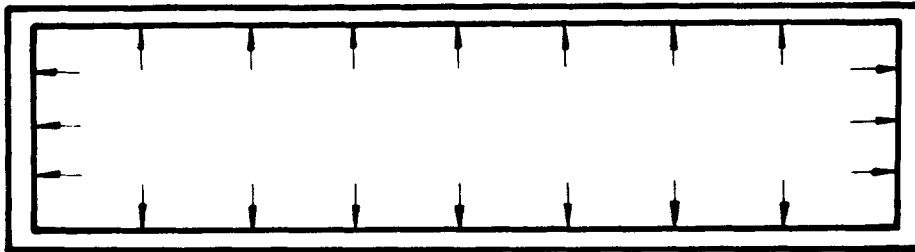


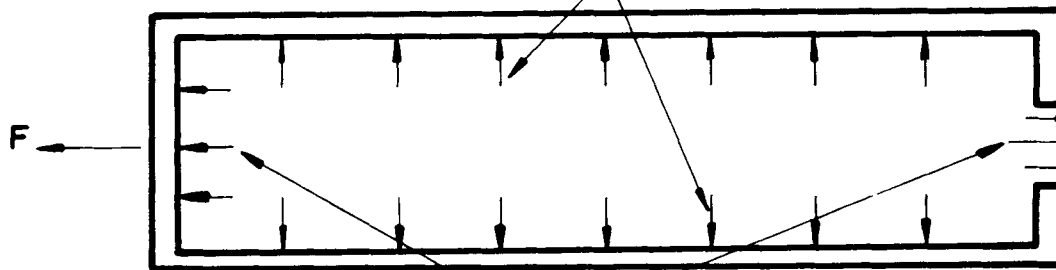
Figure 1-3. Fin-stabilized Rocket Motor

ALL PRESSURES ARE BALANCED



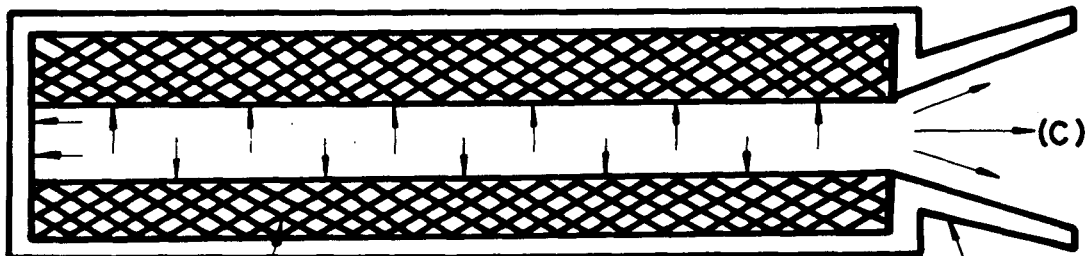
(A)

RADIAL PRESSURES ARE BALANCED



(B)

THIS PRESSURE IS NOT
BALANCED, SO A THRUST
IS DEVELOPED



(C)

PROPELLANT GRAIN

CASE

DE LAVAL
EXHAUST
NOZZLE

Figure 1-4. Development of Thrust in a Rocket Motor

mean velocity of the gas crossing the throat section may be assumed to be equal to the local speed of sound (see Chapter 3).

The following two characteristics of a rocket jet propulsion system are mainly responsible for the fundamental differences in its operation and in that of an air-breathing jet engine^{2,3}.

- (1) A rocket propulsion system consumes no atmospheric air.
- (2) The thrust developed by a rocket jet propulsion system depends almost entirely upon the velocity of the propulsive jet, while the thrust of an air-breathing jet engine depends upon the difference between the momentum of the propellant gas leaving and entering the engine.

Because of the above two characteristics, rocket jet propulsion systems have the following advantages compared with other jet propulsion systems:

- (1) The thrust is essentially independent of flight speed and altitude.
- (2) The thrust per unit of cross-sectional area F/A_F is the largest for all known types of propulsion systems.
- (3) The thrust per unit of engine weight F/W_E is the largest for all known types of propulsion systems.
- (4) A rocket jet propulsion system has no altitude ceiling.

Experience has amply confirmed the predictions of the pioneers in rocketry, that from a propulsion standpoint, all of the space missions so far conceived can be achieved by properly applying the rocket jet *propulsion principle*, hereafter termed *rocket propulsion*.

Because the oxygen for burning with the fuel is not obtained from the surrounding atmosphere, the rate at which a rocket propulsion system consumes its propellant materials

(fuel plus oxidizer) is several times the rate at which an air-breathing jet engine consumes fuel, in developing an equivalent thrust.

The most important parameters governing the flight speed of a propelled vehicle are:

- (1) F/A_F - the thrust per unit of frontal area, and
- (2) F/W_E - the thrust per unit of engine weight.

As mentioned earlier, judged by the above parameters rocket propulsion is unsurpassed.

The range of flight for winged aircraft depends in large measure upon the thrust specific fuel consumption (TSFC) of the propulsion system, measured in pounds of fuel per hour per pound of thrust. To obtain a long range for a rocket-propelled vehicle, such as an intercontinental guided ballistic missile (ICBM), a trajectory must be utilized which takes advantage of its large values of F/A_F and F/W_E , but minimizes the adverse effects of its large TSFC. To achieve a long range, the large thrust of the rocket engine is utilized for propelling the vehicle to a very high altitude (several tens of miles) and for imparting to it a very large velocity (several thousands of feet per second), at the end of the operating period for the rocket engine, termed the *powered flight*. The velocity at the end of the powered flight is called either the *cut-off velocity*, *burnout velocity*, or *burned velocity*. The kinetic energy of the vehicle after it reaches the cut-off velocity is then used for coasting along a ballistic trajectory⁵.

1-6.1 CLASSIFICATION OF ROCKET PROPULSION SYSTEMS

It is convenient to group rocket propulsion systems into four principal categories:

- (1) Liquid bipropellant rocket engines
- (2) Liquid monopropellant rocket engines

- (3) Solid propellant rocket motors
- (4) Hybrid rocket engines

Brief descriptions of the above engines will be presented in this chapter, primarily for identification purposes.

1-6.2 LIQUID BIPROPELLANT ROCKET ENGINE

Fig. 1-5 illustrates the essential elements of a liquid bipropellant rocket engine employing a turbo-pump (a gas turbine driving the propellant pumps) for feeding a liquid fuel and a liquid oxidizer to a rocket motor. Fig. 1-6 illustrates the principal elements of an uncooled liquid bipropellant rocket engine.

1-6.3 LIQUID MONOPROPELLANT ROCKET ENGINE

Fig. 1-5 also illustrates schematically the essential elements of a monopropellant rocket engine, if one removes the oxidizer supply tank, oxidizer pump, oxidizer lines, etc. A monopropellant contains the oxygen for combustion in either its chemical or physical structure, or both. Consequently, an oxidizer supply, metering, and feed system is unnecessary.

1-6.4 SOLID PROPELLANT ROCKET MOTOR

Fig. 1-7 illustrates diagrammatically a solid propellant rocket motor employing an *internal-burning case-bonded* solid propellant grain; the latter burns radially at a substantially constant rate. A solid propellant contains both its fuel and the requisite oxidant for burning it, either in the solid propellant molecule (*double-base propellants*) or as an intimate mechanical mixture (termed either a heterogeneous or composite propellant), (see Chapters 7 and 8 for details). The chemical reaction is initiated by means of an electrically fired igniter.

1-6.5 HYBRID ROCKET ENGINE

Fig. 1-8 illustrates diagrammatically the essential elements of one form of hybrid (chemical) rocket engine. The solid propellant grain, which may or may not contain a small amount of oxidizer, is reacted with a liquid oxidizer and

burns in the radially outward direction at a substantially constant rate. Of course, the reverse of the above is possible.

Of the chemical rocket propulsion systems presented above, only the liquid bipropellant engine and the solid propellant rocket motor have attained an operational state of development for missile propulsion. Thus the ATLAS and TITAN ICBM's employ liquid bipropellant rocket engines; the MINUTEMAN ICBM and POLARIS IRBM utilize solid propellant rocket motors. Monopropellant engines have found application in reaction control devices.

Table 1-2 lists some Army weapons which employ rocket propulsion systems.

1-7 UNITS OF MEASUREMENT

The units of measurement employed in this handbook, unless specifically stated to be otherwise, are listed below:

<u>Dimension</u>	<u>Symbol</u>	<u>Unit of Measurement</u>
MASS	M	1 slug
FORCE	F	1 pound (lb)
LENGTH	L	1 foot (ft)
TIME	T	1 second (sec)

The following tables pertinent to units and measurement are presented in the Appendix B to this handbook:

Table B-1	Abbreviations for Principal Units of Measurement
Table B-2	Systems of Dimensions, Their Units and Conversion Factors
Table B-3	Conversion Factors (American Engineers System of Units)
Table B-4	Dimensional Formulas and Units

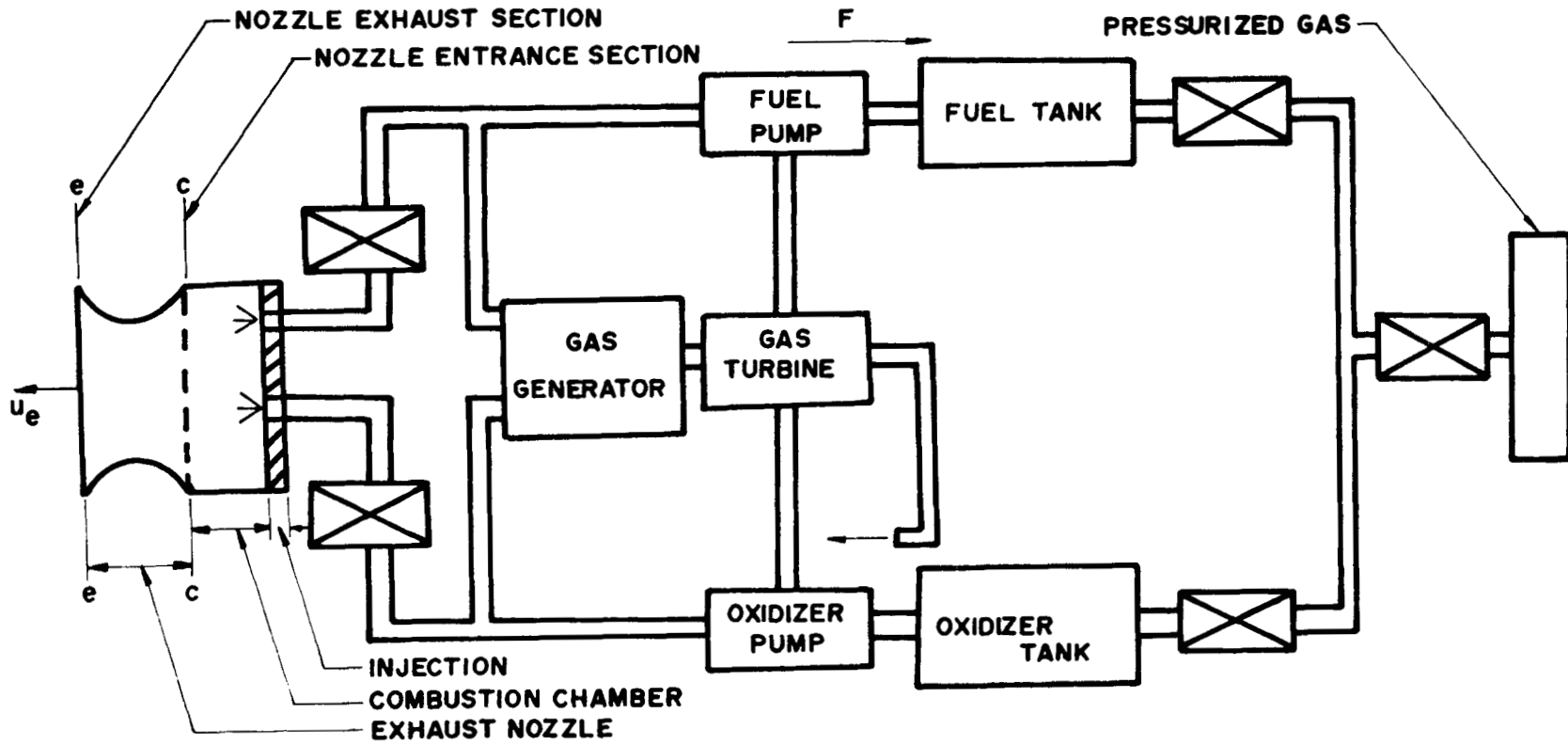


Figure 1-5. Essential Elements of a Liquid Bipropellant Rocket Engine

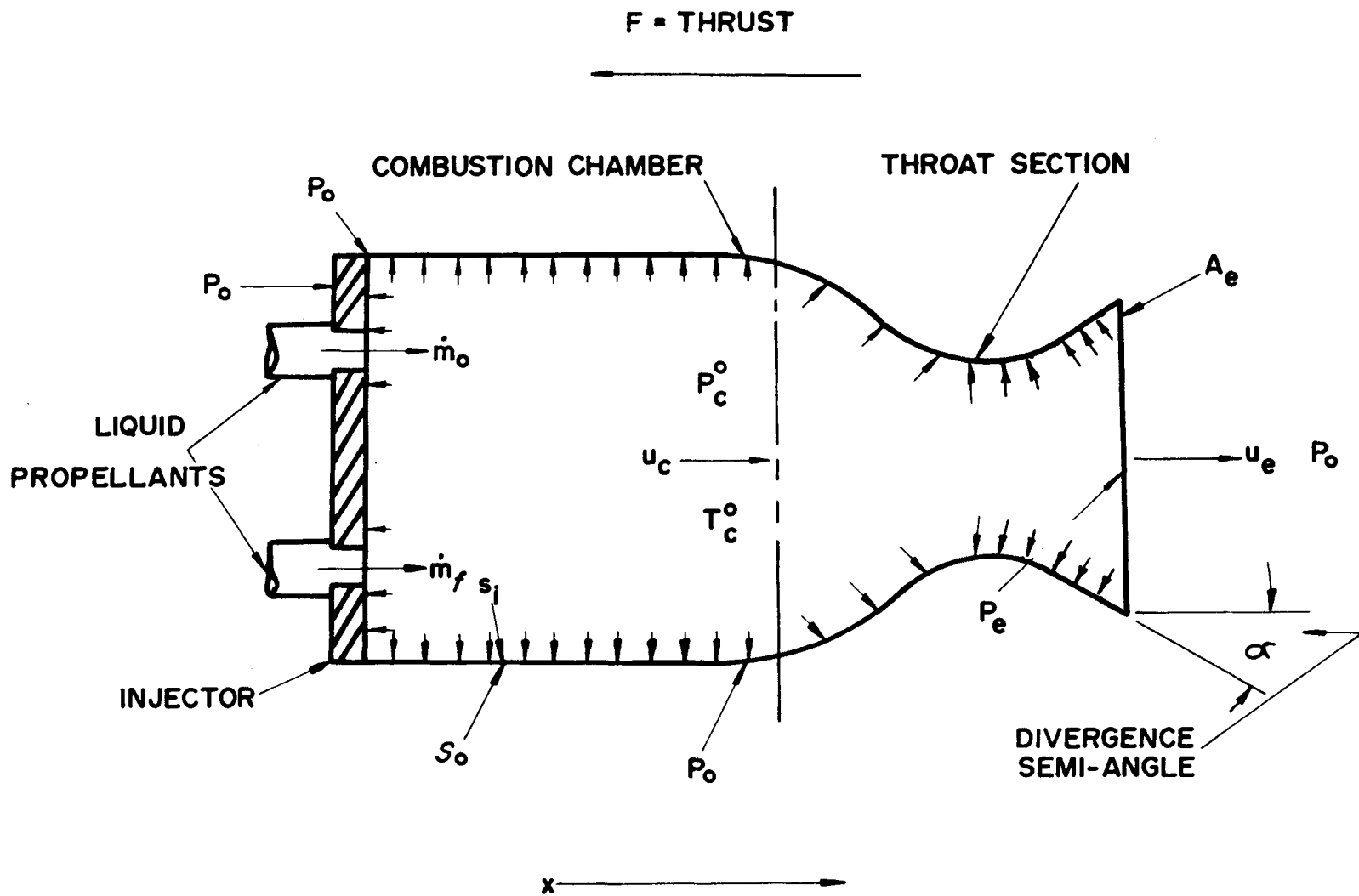
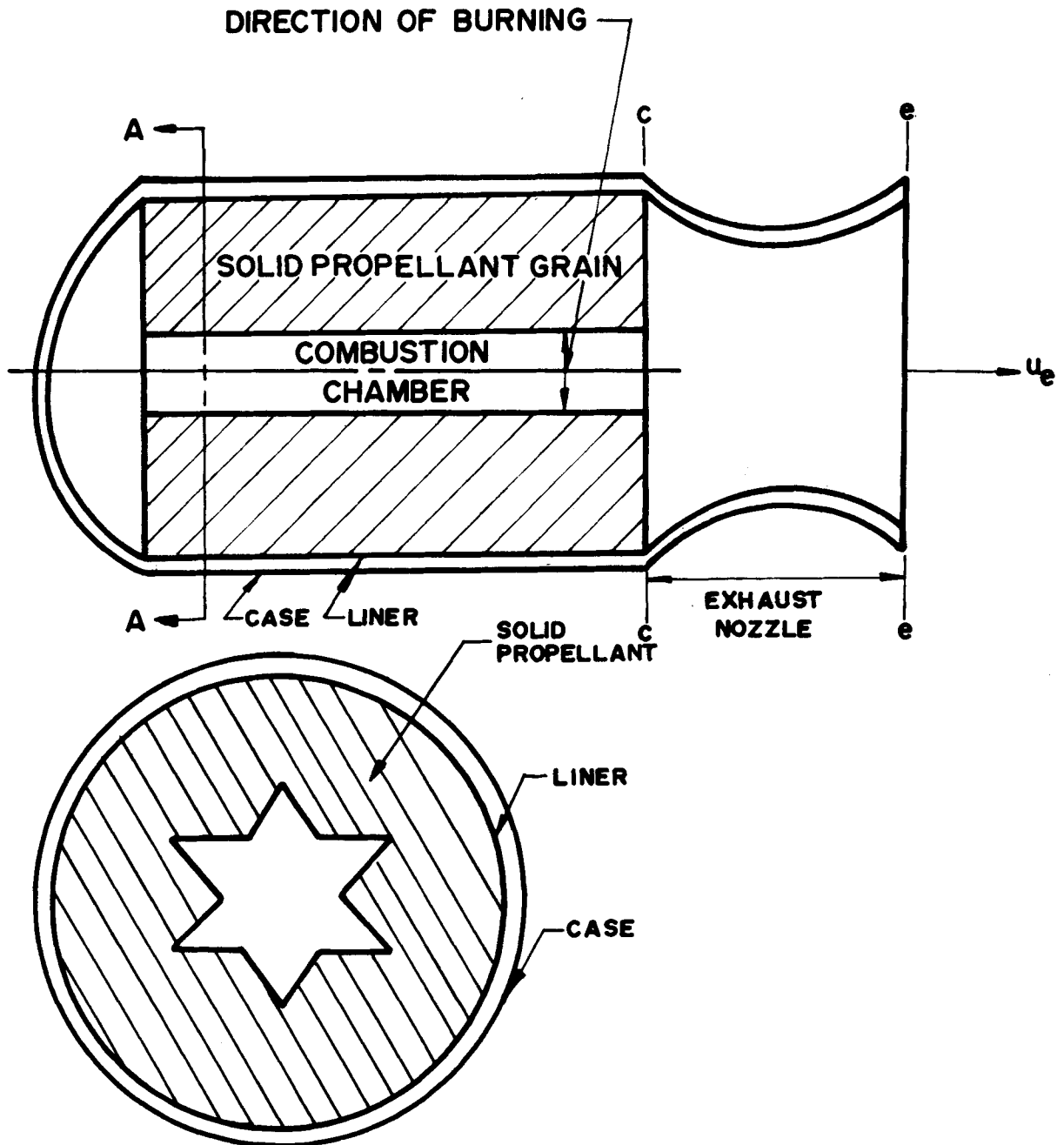


Figure 1-6. Principal Elements of an Uncooled Liquid Bipropellant Rocket Engine



**CROSS-SECTION THROUGH A STAR SHAPED BONDED
SOLID PROPELLANT ROCKET MOTOR**

Figure 1-7. Essential Elements of an Internal-burning Case-bonded Solid Propellant Rocket Motor

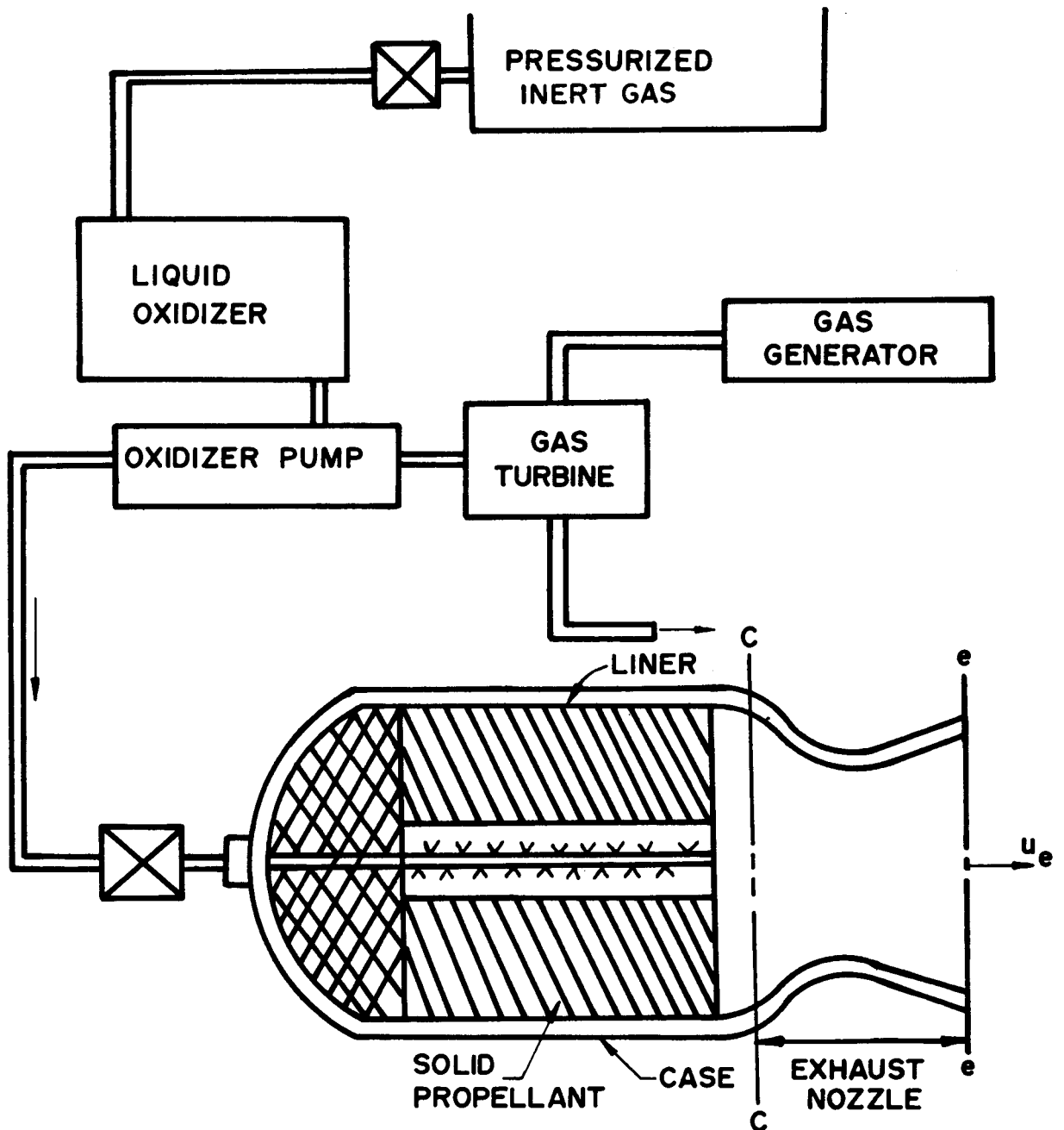


Figure 1-8. Essential Features of a Hybrid Chemical Rocket Engine

TABLE 1-2

ROCKET-PROPELLED WEAPONS

NAME	STATUS	PROPULSION
SURFACE-TO-SURFACE MISSILES		
HONEST JOHN	0	Single Stage SPRM
LITTLE JOHN	0	Single Stage SPRM
PERSHING	0	Two Stage SPRM
SERGEANT	0	Single Stage SPRM
LANCE	ED	Storable LPRE
SURFACE-TO-AIR MISSILES		
REDEYE	0	Dual Stage SPRM
HAWK (MIN-234)	0	Dual Stage SPRM
CHAPPARAL	ED	SPRM
NIKE HERCULES (MIM-14B)	0	Two Stage SPRM
SPRING	ED	Two Stage SPRM
SPARTAN	ED	Three Stage SPRM
ANTITANK MISSILES		
SHILLELAGH	0	SPRM
MAW	ED	SPRM
TOW	ED	SPRM
M72 ROCKET GRENADE	0	SPRM
ENTAC	0	SPRM

0 - Operational; SPRM - Solid Propellant Rocket Motor; LPRE - Liquid Propellant Rocket Engine;
 ED - Engineering Development

REFERENCES

1. M.J. Zucrow, *Panel on Science and Technology Fourth Meeting, Committee on Science and Astronautics*, U.S. House of Representatives, 87th Congress, Second Session, March 21 and 22, 1962, p. 19.
2. M.J. Zucrow, *Jet Propulsion and Gas Turbines*, John Wiley and Sons, Inc., 1948, p. 38.
3. M.J. Zucrow, *Aircraft and Missile Propulsion*, John Wiley and Sons, Inc., Vol. 1, 1958, Ch. 2.
4. W.J. Hesse and N.V. Mumford, *Jet Propulsion for Aerospace Applications*, Pitman Publishing Corporation, 2nd Ed., 1964, Ch. 2.
5. M.J. Zucrow, *Aircraft and Missile Propulsion*, John Wiley and Sons, Inc., Vol. 2, 2nd Printing, 1964.
6. G.P. Sutton, *Rocket Propulsion Elements*, John Wiley and Sons, Inc., 1963, Ch. 1.
7. C.W. Smith, *Aircraft Gas Turbines*, John Wiley and Sons, Inc., 1956, Ch. 1 and 2.
8. D. Kuchermann and J. Weber, *Aerodynamics of Propulsion*, McGraw-Hill Book Company, Inc., 1953.
9. M.J. Zucrow, *Science in Progress*, Fourteenth Series, Yale University Press, 1964, p. 241.

CHAPTER 2

MOMENTUM THEORY APPLIED TO PROPULSION

2-0 PRINCIPAL NOTATION FOR CHAPTER 2*

A	cross-sectional area	h^o	total or stagnation specific enthalpy
A_1	cross-sectional area of inlet to a propulsion system	ΔH_c	lower heating value of a fuel, B/slug
A_e	cross-sectional area of exit section of exhaust nozzle	ΔH_p	calorific value of propellant material, B/slug
c	effective jet velocity, fps	\underline{i}	unit vector along x-axis
d	diameter	I_a	$F/g_c \dot{m}_a$ = specific thrust or air specific impulse, sec
D	drag force, lb	I_f	$F/g_c \dot{m}_f$ = fuel specific impulse, sec
f	fuel-air ratio	I_{sp}	$F/\dot{w} = F/(\dot{w}_o + \dot{w}_f)$ = specific impulse, sec
\underline{F}	thrust or net external force acting on a body of fluid enclosed by a control surface S , lb	\underline{j}	unit vector along y-axis
F	magnitude of the force vector \underline{F} , or thrust developed by a propulsion system, lb	\underline{k}	unit vector along z-axis
F_A	available thrust, lb	m	mass, slug
F_{ext}	net external force, lb	\dot{m}	mass rate of flow of propellants, slug/sec
g	local acceleration due to the gravitational attraction of earth, ft/sec ²	\dot{m}_f	mass rate of flow of fuel, slug/sec
g_c	gravitational correction factor = 32.174 slug-ft/lb-sec ²	\dot{m}_a	mass rate of flow of air, slug/sec
h	static specific enthalpy, B/slug	\dot{m}_o	mass rate of flow of oxidizer, slug/sec
		\underline{M}	momentum vector
		$\dot{\underline{M}}$	$d\underline{M}/dt$ = rate of change of momentum, slug ft/sec ²
		\underline{n}	unit vector along normal to a surface; positive direction is outward from surface
		p	static pressure intensity, psia

*Any consistent set of units may be employed; the units presented here are for the American Engineers System (see par. 1-7).

p_e	static pressure intensity in exit area A_e of exhaust nozzle, psia	u_e	velocity of jet crossing area A_e of exhaust nozzle, fps
p_o	static pressure of the surroundings	V	control volume, i.e., volume inclosed by S
P	static pressure intensity, psf	V_o	flight speed, fps
P_e	static pressure in area A_e , psf	V_j	effective jet velocity
P	propulsive power, ft-lb/sec	v	velocity of a fluid parallel to y-axis, fps
P_E	required power output	w	velocity of a fluid parallel to z-axis, fps
P_T	thrust power, ft-lb/sec	\tilde{W}	body force = mg
P_{KE}	exit loss associated with propulsive jet, ft-lb/sec	\dot{w}	weight rate of flow, lb/sec
P_λ	power loss, ft-lb/sec	\dot{w}_a	weight rate of flow of atmospheric air, lb/sec
\underline{q}	velocity vector	\dot{w}_f	weight rate of flow of fuel, lb/sec
q	magnitude of velocity vector, fps	\dot{w}_o	weight rate of flow of oxidizer, lb/sec
q_n	normal velocity, normal to a flow area, fps	X	net external force in direction of x-axis, lb
\dot{Q}_v	volumetric rate of flow, cfs	Y	net external force in direction of y-axis, lb
r	\dot{m}_o/\dot{m}_f = mixture ratio of a propellant material combination	Z	net external force in direction of z-axis, lb
\tilde{R}	resultant force vector due to the interaction of the internal flow with surfaces of the propulsion system, lb	z	altitude or elevation, ft
R	magnitude of \tilde{R} , lb	<u>GREEK LETTERS</u>	
s	static specific entropy	α	angle between velocity vector and normal to flow cross-section
S	area of a control surface, or a projected area, sq ft	β	\dot{m}_{aE}/\dot{m}_a = the bypass ratio
t	time, sec	η	efficiency
u	velocity component parallel to x-axis, fps	η_E	energy conversion efficiency

η_o	overall efficiency of propulsion system
η_p	propulsive efficiency
η_P	ideal propulsive efficiency
η_{th}	thermal efficiency
ν	V_o/V_j = effective speed ratio
ρ	density, slug/ft ³
Ψ	characteristic property of a flowing fluid inside control volume, per unit volume

SUBSCRIPTS

a	air
amb	ambient or air, as specified in test
e	exit area of exhaust nozzle
f	fuel
o	oxidizer
i	internal
o	undisturbed atmosphere

2-1 MOMENTUM THEOREM OF FLUID MECHANICS

Fig. 2-1 illustrates diagrammatically a region of a fluid flow field that is enclosed, at the instant $t = t_o$, by a fictitious *stationary control surface* S . The volume of the fluid instantaneously enclosed by S is termed the *control volume* and is denoted by V . At some later instant of time, $t = t_o + dt$, the same mass of fluid is no longer enclosed by S , due to fluid entering and leaving the control volume V , as illustrated in

Fig. 2-2. Consequently, at the instant $t = t_o + dt$ the mass of fluid enclosed by S at $t = t_o$ is now enclosed by the fictitious surface S' .

When a fluid flows into or out of a control volume it can transport, in addition to its mass, other characteristics or properties associated with its mass; such as momentum, energy, enthalpy, entropy, etc. It is assumed in all of the discussions which follow that the fluid is a continuum¹.

2-1.1 TRANSPORT OF A FLUID PROPERTY ACROSS A CONTROL SURFACE. If Ψ denotes a characteristic property of a flowing fluid *per unit volume*, that is transported across a control surface S (see Fig. 2-1) then

$$\frac{D}{dt}(\Psi V) = \frac{\partial}{\partial t} \int_V \Psi dV + \int_S \Psi \underline{\underline{q}} \cdot \underline{\underline{n}} dS \quad (2-1)$$

where

$\frac{D}{dt}(\Psi V)$ = the flow or particle derivative of ΨV

$\frac{\partial}{\partial t} \int_V \Psi dV$ = the local rate of change of Ψ ; i.e., the rate at which Ψ , fluid property per unit volume, changes inside the control volume V

$\Psi \underline{\underline{q}} \cdot \underline{\underline{n}} dS$ = the convective rate of change of Ψ due to fluid crossing the control surface S ; i.e., leaving and entering V

$\underline{\underline{q}} = \underline{\underline{i}} u + \underline{\underline{j}} v + \underline{\underline{k}} w$ = the velocity vector at the point under consideration

$\underline{\underline{i}}, \underline{\underline{j}}, \underline{\underline{k}}$ = unit vectors along the Cartesian coordinate axis; x,y,z, respectively

u, v, w = rectangular components of \underline{q} parallel to the x, y, z -axis, respectively

\underline{n} = unit normal vector at dS , its positive direction is outward from V (see Figs. 2-1 and 2-2)

$\underline{q} \cdot \underline{n}$ = scalar product of \underline{q} and \underline{n} = $q \cos \alpha$

q_n = the normal velocity = $q \cos \alpha$

In Eq. 2-1 there is no restriction upon Ψ —it may be either a vector or a scalar. In general, the right-hand side is the sum of a *nonstationary term* and a *convective term*.

The nonstationary term arises from the fact that in an *unsteady flow* the density of the fluid inside the control volume V varies with the time t .

The convective term expresses the condition that the mass of fluid entering and leaving the control volume also transports Ψ , the characteristic or property of the fluid.

Eq. 2-1 is the general form of the *integral equation* for determining the rate of change of Ψ for a flowing fluid; it applies to both unsteady and steady flows. To obtain the corresponding *differential equation*, the surface integral in Eq. 2-1 is transformed into a volume integral by applying the divergence theorem^{2,3}. Thus

$$\int_S \Psi \underline{q} \cdot \underline{n} dS = \int_V \text{div} (\Psi \underline{q}) dV \quad (2-2)$$

Substituting Eq. 2-2 into Eq. 2-1, yields

$$\frac{D}{Dt} (\Psi V) = \frac{\partial}{\partial t} \int_V \Psi dV + \int_V \text{div} (\Psi \underline{q}) dV \quad (2-3)$$

In Eq. 2-3, the differential dV has the same value in both of the integral terms. Hence

$$\frac{D}{Dt} (\Psi V) = \left(\frac{\partial \Psi}{\partial t} \right)_V + \text{div} (\Psi \underline{q}) \quad (2-4)$$

In Cartesian coordinates³

$$\text{div} (\Psi \underline{q}) = \nabla \cdot (\Psi \underline{q}) \quad (2-5)$$

The operator ∇ , called *del* or *nabla*, is defined by

$$\nabla () = \underline{i} \frac{\partial}{\partial x} () + \underline{j} \frac{\partial}{\partial y} () + \underline{k} \frac{\partial}{\partial z} () \quad (2-6)$$

In the case of *steady flow*, the nonstationary terms in Eqs. 2-1 and 2-4 vanish, so that

$$\frac{D}{Dt} (\Psi V) = \int_S \Psi \underline{q} \cdot \underline{n} dS \quad (2-7)$$

and

$$\frac{D}{Dt} (\Psi V) = \text{div} (\Psi \underline{q}) = \nabla \cdot (\Psi \underline{q}) \quad (2-8)$$

2-1.2 MOMENTUM OF A FLUID IN STEADY FLOW. By definition, the momentum of a flowing fluid of density ρ , occupying instantaneously the control volume V , see Fig. 2-2, is given by

$$\underline{M} \equiv (\rho V) \underline{q} \quad (2-9)$$

In the subject case, Ψ is given by

$$\Psi = \frac{\underline{M}}{V} = \rho \underline{q} = \text{momentum per unit volume} \quad (2-10)$$

By analogy with Eq. 2-1

$$\frac{D\underline{M}}{Dt} = \frac{\partial}{\partial t} \int_V (\rho \underline{q}) dV + \int_S (\rho \underline{q}) \underline{q} \cdot \underline{n} dS \quad (2-11)$$

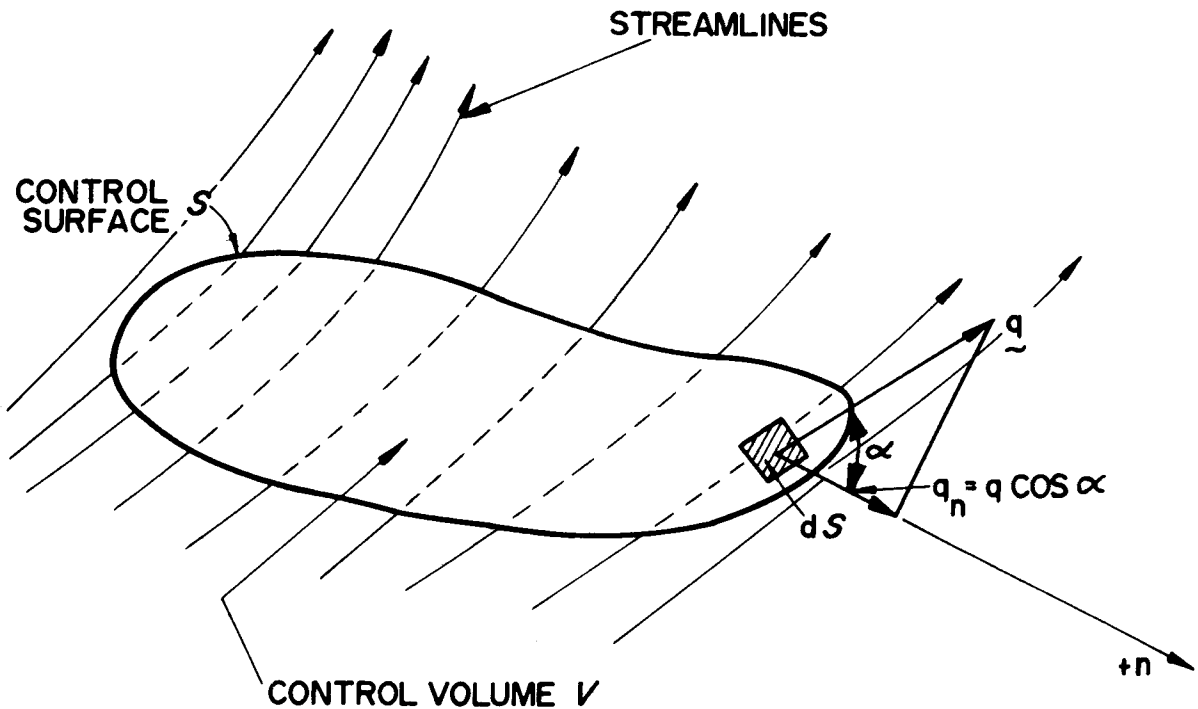


Figure 2-1. Control Surface and Control Volume Enclosing a Region of a Flowing Fluid

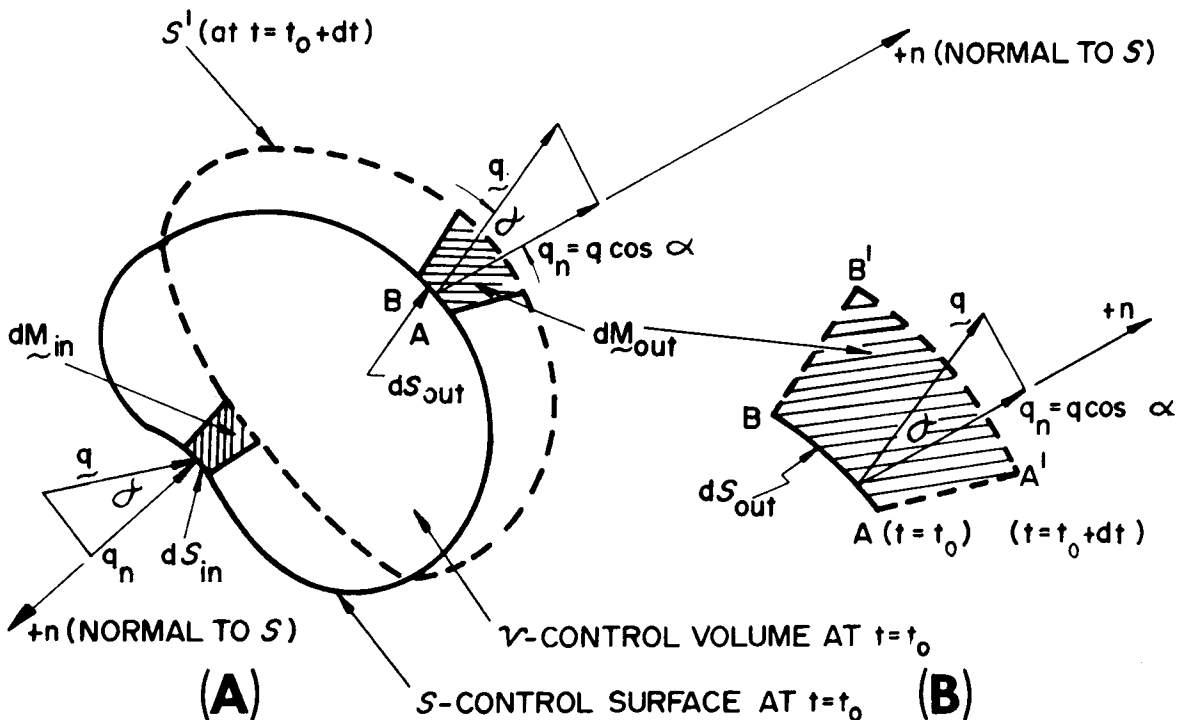


Figure 2-2. Transport of Momentum by a Flowing Fluid

By analogy with Eq. 2-4, one obtains the following differential equation:

$$\frac{d\mathbf{M}}{dt} = \left(\frac{\partial \mathbf{M}}{\partial t} \right)_V + \text{div} (\rho \mathbf{q}) \mathbf{q} \quad (2-12)$$

If the flow is *steady*, then

$$\frac{\partial}{\partial t} \int_V (\rho \mathbf{q}) dV = \left(\frac{\partial \mathbf{M}}{\partial t} \right)_V = 0$$

For a steady flow—the type of flow assumed in all of the future discussions unless it is specifically stated to be otherwise—the integral equation for the rate of change of momentum is given by

$$\frac{d\mathbf{M}}{dt} = \int_S (\rho \mathbf{q}) \mathbf{q} \cdot \mathbf{n} dS \quad (2-13)$$

The corresponding differential equation is

$$\frac{d\mathbf{M}}{dt} = \text{div} (\rho \mathbf{q}) \mathbf{q} \quad (2-14)$$

By Newton's second law of motion, the net external force acting upon a mass of fluid instantaneously enclosed by a stationary control surface S is equal to the rate of change in the momentum of the fluid.

Let \mathbf{F}_{ext} denote the net external force, and

$$\dot{\mathbf{M}} = \frac{d\mathbf{M}}{dt} = \text{the rate of change in the momentum of the fluid.}$$

Then

$$\mathbf{F}_{\text{ext}} = \dot{\mathbf{M}} = \int_S (\rho \mathbf{q}) \mathbf{q} \cdot \mathbf{n} dS \quad (2-15)$$

Eq. 2-15 is a *vector equation*. It applies to either a steady or a mean steady flow, and to steady viscous and nonviscous flows.

Let X denote the external force acting in the direction of the x -coordinate axis, and u denote the fluid velocity in the same direction, then

$$X = \dot{M}_x = \int_S (\rho q_n) u dS = \int_S \rho u (q \cos \alpha) dS \quad (2-16)$$

Similar equations can be written for the forces Y and Z acting in the directions of the y - and z -coordinate axes, respectively.

Accordingly, the magnitude of the net external force \mathbf{F}_{ext} is given by

$$F_{\text{ext}} = \sqrt{X^2 + Y^2 + Z^2} \quad (2-17)$$

The magnitude of the velocity vector \mathbf{q}

$$q = |\mathbf{q}| = \sqrt{u^2 + v^2 + w^2} \quad (2-18)$$

2-1.3 EXTERNAL FORCES ACTING ON A FLOWING FLUID. In general, the external forces acting on a body of fluid can be divided into two types: (1) *surface forces*, and (2) *body forces*.

Surface forces are those which are distributed over the surface of a body, such as the *pressure* exerted by one body on another; as for example, the *hydrostatic pressure* in a body of liquid. The component of a surface force acting perpendicular to the surface of a body is termed a *normal force*, and the component parallel to the surface of a body is called either a *tangential* or a *shearing force*.

A *body force* is one which is distributed over the entire volume of a body of material; for example, the forces due to the gravitational attraction of earth, magnetic fields, electrostatic fields, and the like. In the absence of all fields of force except the gravitational field of earth, the net external force \mathbf{F}_{ext} acting on the fluid instantaneously enclosed by the control surface S (see Fig. 2-3) has the following components:

- (1) The body force $\mathbf{W} = m\mathbf{g}$ acting toward the center of earth, due to gravitational attraction.

(2) The following two surface forces:

(a) The pressure force \underline{F}_p where

$$\underline{F}_p = - \int_S \underline{p} \underline{n} \, dS = \int_S (p_0 - p_i) \, dS \quad (2-19)$$

where

$(p_0 - p_i)$ = the *excess pressure*.

(b) The net force \underline{R} due to contact between the body of flowing fluid and solid surfaces.

Hence, the net external force \underline{F}_{ext} is the *vector sum* of the body and surface forces. Thus

$$\underline{F}_{ext} = \underline{W} + \underline{F}_p + \underline{R} \quad (2-20)$$

2-1.4 STEADY FLOW MOMENTUM THEOREM. Combining Eqs. 2-13 and 2-19, one obtains

$$\underline{W} - \int_S \underline{p} \underline{n} \, dS + \underline{R} = \int (\rho \underline{q}) \underline{q}_n \, dS \quad (2-21)$$

If the propulsive fluid is a gas $\underline{W} \approx 0$.

Eq. 2-21 is known as the *momentum theorem of fluid mechanics* for a *steady flow*⁴.

If X denotes the component of force R in the x -direction, then from Eqs. 2-16 and 2-21

$$X = \int_S \rho \underline{q}_n \cdot \underline{u} \, dS + \int_S p_x \, dS \quad (2-22)$$

If no solid bodies are wetted by the flowing fluid and the gravitational attraction of earth is negligible, the Eq. 2-22 reduces to

$$\int_S \rho \underline{q}_n \cdot \underline{u} \, dS = - \int p_x \, dS \quad (2-23)$$

where \underline{u} is the velocity of the fluid parallel to the x -direction.

The application of Eq. 2-21 for determining the thrust of a jet propulsion system is illustrated in par. 2-2.1.

2-2 APPLICATION OF THE MOMENTUM THEOREM TO PROPULSION SYSTEMS. The application of Eq. 2-21 to determine the thrust of a jet propulsion system will now be illustrated.

Fig. 2-4 illustrates diagrammatically some form of air-breathing engine which is held stationary while atmospheric air flows toward it with the *free stream velocity* V_0 . The stream of air that enters the engine and wets its internal surfaces will be called the *internal flow*. Similarly, the air stream flowing past the external surfaces or *housing* of the engine will be termed the *external flow*.

The interactions of the internal flow with the internal surfaces of the engine produce a *net component of force* parallel to the longitudinal axis of the engine, termed the *net internal axial force*, and is denoted by F_i . In the relative coordinate system (see Fig. 2-4), if an axial force acts in the direction opposite to that for the *free stream velocity*, it is called a *thrust*.

On the other hand, an axial force which acts in the same direction as the free stream velocity, in the relative coordinate system, is called an *internal drag* and is denoted by D_i .

For the external flow, the net force acting parallel to the longitudinal axis of the engine – due to the interaction of external flow with the *engine housing* – is termed the *external drag* D_e . Hence, the force available for accelerating the vehicle to be propelled by the air-breathing jet engine, termed the *available thrust* F_A , is given by

$$F_A = F_i - (D_e - D_i) \quad (2-24)$$

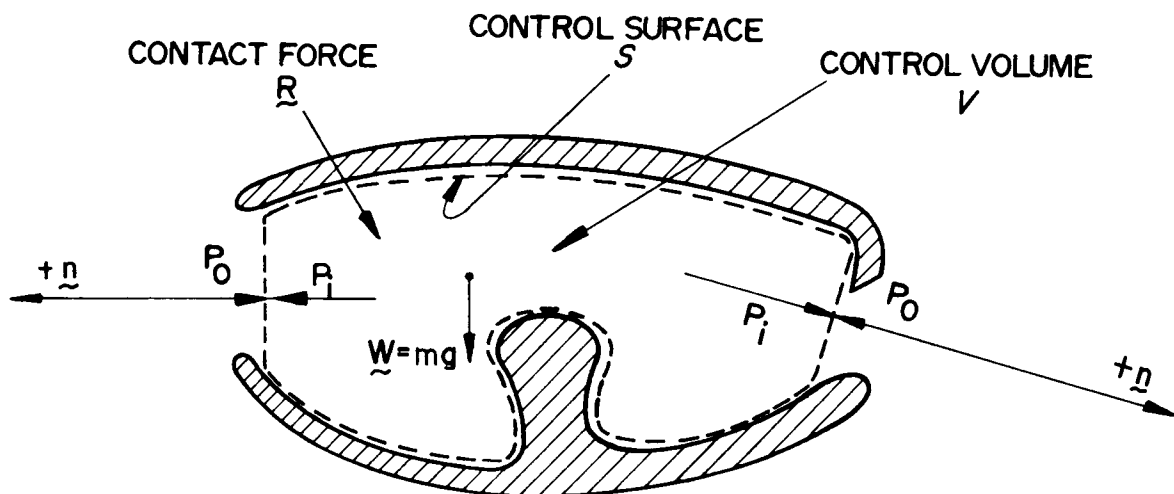


Figure 2-3. Forces Acting on a Flowing Fluid

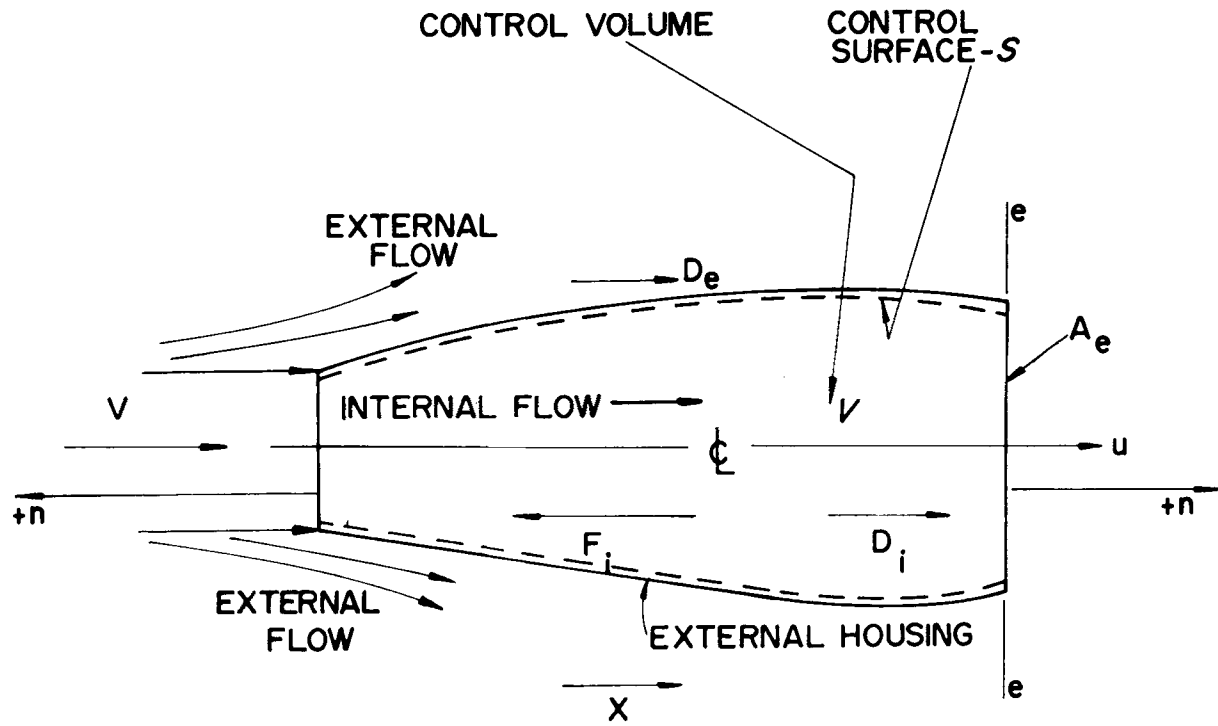


Figure 2-4. Air-breathing Jet Engine in a Relative Coordinate System

The available thrust F_A depends not only upon the interactions between the internal flow and the internal surfaces of the engine, but also upon the configuration of the engine housing, as dictated by the installation requirements of the propelled vehicle. It is not a direct measure of the thrust-producing capability of the engine ($F_i - D_i$), but involves the design features of the engine housing.

In a jet propulsion engine the rate at which *propulsive work* is performed, termed the *propulsive power*, is denoted by P . It is a consequence of causing the internal flow to undergo suitable energy transformations as it moves along its flow path. In the case of an air-breathing jet engine, heat is added to the atmospheric air flowing through the engine. In a rocket propulsion system, on the other hand, no atmospheric air is inducted into the propulsion system.

2-2.1 GENERAL THRUST EQUATION. It is desirable that the thrust-producing capability of a jet propulsion system be expressed in a manner which is independent of the configuration of the engine and its installation in the propelled vehicle. In general terms, the thrust produced by a jet propulsion system is the resultant axial component of the static pressure acting upon the surfaces of the engine wetted by the internal flow. In determining the thrust it is convenient to employ a *relative coordinate system*.

Fig. 2-5 illustrates diagrammatically an arbitrary jet propulsion system held stationary in a uniform stream of atmospheric air having the velocity V_0 relative to the propulsion system. The jet propulsion system is shown as a hollow body of arbitrary shape; it has an inlet area A_i and an exit area A_e , both areas are measured perpendicular to the velocity V_0 . The ducted body may enclose struts, burners, rotating machinery, and may be unsymmetrical. For simplicity, however, it is assumed to be symmetrical with respect to its longitudinal axis; the

latter is parallel to the x-axis. The positive direction of the x-axis is in the same direction as the thrust F . It should be noted that F points in the same direction as the *line-of-flight* when the engine is propelling a vehicle in the atmosphere.

The thrust due to the internal flow, denoted by F_i , is given by

$$F_i = \int_{S_i} p_i \cdot \underline{n} \, dS_i \quad (2-25)$$

where

S_i = area of internal surfaces wetted by the internal flow

p_i = the internal static pressure

$p_i \cdot \underline{n}$ = axial component of p_i

\underline{n} = unit normal vector in the axial direction

Because it is extremely difficult, if not impossible, to evaluate the integral in Eq. 2-25, the thrust F_i will be determined by applying the momentum theorem.

EXAMPLE 2-1.

Determine the thrust of a jet propulsion system by applying the momentum theorem of fluid mechanics (Eq. 2-21).

SOLUTION.

To apply Eq. 2-21, a control surface must be established. Since the location and configuration of the control surface is arbitrary, it can be arranged so that it is convenient for the analysis.

Let S_1 and S_2 be two infinite planes drawn perpendicular to the longitudinal axis of the propulsion system. Plane S_1 is located sufficiently far upstream from the propulsion system so that the static pressure p_0 acting on S_1 is identical with the value it has when there is no propulsion system between S_1 and S_2 .

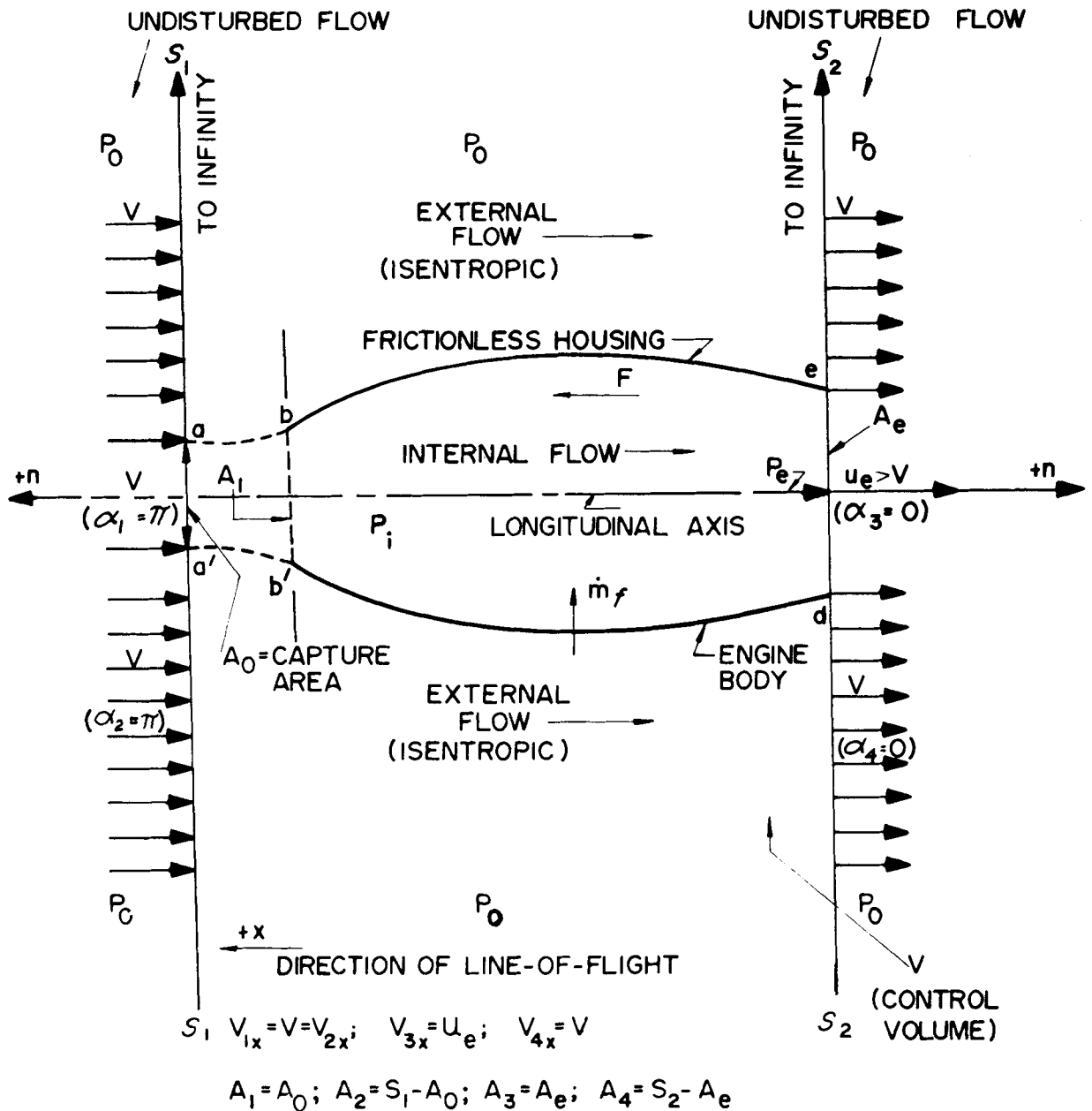


Figure 2-5. Determination of the Thrust Developed by a Jet Propulsion System

The infinite plane S_2 is located where, except for the area affected by the propulsive jet, the static pressure over S_2 is equal to that over S_1 .

The following *assumptions* are introduced:

- (1) The atmospheric pressure acting on the housing of the propulsion system is uniform.
- (2) The internal flow is one-dimensional and steady.
- (3) The body forces are negligible, so that $\tilde{W} \approx 0$; this is substantially correct when the flowing fluid is a gas of low density.
- (4) All of the internal flow undergoes identical thermodynamic transformations and the addition of energy is uniformly distributed over its mass flow rate.
- (5) All of the openings through which the internal flow enters the engine can be replaced by a *single equivalent inlet area*, denoted by A_1 .
- (6) All of the openings through which the internal flow is ejected from the propulsion system can be replaced by a *single exit area*, denoted by A_e .
- (7) The areas A_1 and A_e are normal to the *free stream velocity* V_0 ; the latter is the relative velocity of the atmospheric air at the inlet section of the engine.
- (8) The engine body is at rest, or moving with the constant velocity V_0 , at a fixed altitude.
- (9) The relative velocity of the gases ejected through the exit area A_e , denoted by u_e , is normal to and uniformly distributed over A_e . Moreover, $u_e > V_0$.

- (10) The external flow is adiabatic and frictionless; i.e., *isentropic*.
- (11) The line-of-flight is coincident with the free-stream velocity V_0 , but oppositely directed.
- (12) The static pressure of the fluid crossing the exit plane of area A_e , denoted by p_e , either exceeds or is equal to the undisturbed atmospheric pressure p_0 .

The *internal flow* crosses the capture area A_0 , located in plane S_1 , and flows through the *bounding streamtube* $aa' bb'$ into the jet propulsion system. The internal flow is ejected through the *exit area* A_e , located in S_2 ; the *ejection velocity* u_e is perpendicular to A_e .

The rate of change in the momentum of the internal flow is given by

$$\dot{M}_x = \int_A (\rho u) V_0 \cos \alpha \, dA \quad (a)$$

where A denotes flow area.

The flow areas, the velocities crossing them, and the corresponding values of the angle α are presented in Fig. 2-5. Hence, Eq. (a) above can be rewritten in the form

$$\begin{aligned} \dot{M}_x = & \int_{A_1} \rho_1 V_{1x} V_1 \cos \alpha \, dA \\ & + \int_{A_2} \rho_2 V_{2x} V_2 \cos \alpha_2 \, dA \\ & + \int_{A_3} \rho_3 V_{3x} V_3 \cos \alpha_3 \, dA \\ & + \int_{A_4} \rho_4 V_{4x} V_4 \cos \alpha_4 \, dA \end{aligned} \quad (b)$$

In Eq. (b)

$$a_1 = a_2 = \pi; a_3 = a_4 = 0$$

$$\cos a_1 = \cos a_2 = -1; \cos a_3 = \cos a_4 = 1$$

$$\rho_1 = \rho_2 = \rho_0; \rho_3 = \rho_e; \rho_4 = \rho_0$$

$$V_{1x} = V_{2x} = V_{4x} = V_0; V_{3x} = u_e$$

The expressions under the integral signs are constant and uniformly distributed over their respective flow areas. Hence, Eq. (b) becomes

$$\begin{aligned} \dot{M}_x = & A_e \rho_e u_e^2 - A_0 \rho_0 V_0^2 + (S_2 - A_e) \rho_0 V_0^2 \\ & - (S_1 - A_0) \rho_0 V_0^2 \end{aligned} \quad (c)$$

In Eq. (c)

$$(A_e \rho_e u_e^2 - A_0 \rho_0 V_0^2) = \text{rate of change in the x-momentum for the internal flow} \quad (d)$$

$$(S_2 - A_e) \rho_0 V_0^2 - (S_1 - A_0) \rho_0 V_0^2 = \text{rate of change in x-momentum for the external flow} \quad (e)$$

Because the external flow is isentropic (Assumption 9), no external force arises from its interaction with the external housing. Hence, Eq. (e) is equal to zero and Eq. (c) reduces to

$$\dot{M}_x = \rho_e u_e^2 A_e - \rho_0 V_0^2 A_0 \quad (f)$$

But

$$\rho_e u_e A_e = \dot{m}_e = \text{mass rate of flow crossing } A_e \quad (g)$$

and

$$\rho_0 A_0 V_0 = \dot{m}_1 = \text{mass rate of fluid into the jet propulsion system} \quad (h)$$

Hence

$$\dot{M}_x = \dot{M}_{2x} - \dot{M}_{1x} = \dot{m}_e u_e - \dot{m}_1 V_0 \quad (2-26)$$

Since it is assumed that the body forces are negligible ($\tilde{W} = 0$), the x-component of the external of the external force acting on the internal flow is given by

$$\begin{aligned} X = R_x - \int_S p_x dS = R_x - \left[- \int_{A_1} p_0 dA \right. \\ \left. - \int_{A_2} p_0 dA + \int_{A_3} p_e dA + \int_{A_4} p_0 dA \right] \quad (i) \end{aligned}$$

where, as before

$$A_1 = A_0; A_2 = S_1 - A_0; A_3 = A_e; A_4 = S_2 - A_e$$

Hence

$$X = R_x - (p_e - p_0) A_e \quad (j)$$

Combining Eqs. 2-26 and (j), yields

$$R_x = \dot{m}_e u_e - \dot{m}_1 V_0 + (p_e - p_0) A_e \quad (2-27)$$

where R_x is the action force causing the rate of change in the momentum of the internal flow.

By the reaction principle (see par. 1-3), the thrust $F = -R_x$, and acts in the opposite direction to u_e , as shown in Fig. 2-5. Hence, the equation for calculating the thrust produced by a jet propulsion system is

$$F = \dot{m}_e u_e - \dot{m}_1 V_0 + (p_e - p_0) A_e \quad (2-28)$$

The thrust equations for rocket propulsion systems are discussed in par. 2-3 and for air-breathing engines in par. 12-3.

2-2.2 EFFECTIVE JET VELOCITY

It is convenient to eliminate the pressure thrust from Eq. 2-28. In order to do this, a

fictitious velocity, called the *effective jet velocity* c is introduced. It is defined by

$$F = \dot{m}_e c - \dot{m}_0 V_0 = \dot{m}_e u_e - \dot{m}_0 V_0 + (p_e - p_0) A_e \quad (2-29)$$

Hence, the effective jet velocity c is given by*

$$c = u_e + (p_e - p_0) \frac{A_e}{\dot{m}_e} = V_j \quad (2-30)$$

In the special case where the static pressure p_e of the propellant gas crossing A_e is equal to the atmospheric pressure p_0 (into which the jet is ejected), so that $p_e = p_0$, the pressure thrust is equal to zero and $c = V_j = u_e$.

2-2.3 EXIT VELOCITY OF THE PROPULSIVE JET

The flow through the exhaust nozzle of a jet propulsion system, the propulsive element of the system (see par. 1-5), may be assumed to be adiabatic. If h^0 denotes the stagnation (or total) enthalpy of the propellant gas at the entrance section of the exhaust nozzle, then

$$u_e = \sqrt{2\Delta h_n} = \sqrt{2(h^0 - h_e)} \quad (2-31)$$

where

h^0 = stagnation specific enthalpy of the propellant gas at the entrance cross-section of the exhaust nozzle.

2-3 THRUST EQUATIONS FOR ROCKET PROPULSION

In a rocket propulsion system the hot gas generator is the combustion chamber of the rocket motor (see par. 1-6.1 and Fig. 1-6). For a rocket engine $\dot{M}_{1X} = 0$ (see Eq. 2-26). Hence,

the axial thrust of a rocket propulsion engine is given by

$$F = \dot{M}_{2X} = \dot{m}_e u_e + (p_e - p_0) A_e \quad (\text{lb}) \quad (2-32)$$

where u_e is the velocity of the propulsive jet perpendicular to A_e , and $p_0 = p_{\text{amb}}$ = the static pressure of the ambient atmosphere. Let

\dot{m}_0 = the mass rate of consumption of oxidizer

\dot{m}_f = the mass rate of consumption of fuel

$\dot{m} = \dot{m}_0 + \dot{m}_f$ = the mass rate of consumption of propellant materials

Introducing the effective jet velocity c , one obtains the following equation for the thrust of a rocket propulsion system:

$$F = \dot{m} c \quad (\text{lb}) \quad (2-33)$$

The ratio \dot{m}_0/\dot{m}_f is termed the *mixture ratio* and is denoted by r . Thus

$$r = \frac{\dot{m}_0}{\dot{m}_f} = \text{mixture ratio} \quad (2-34)$$

EXAMPLE 2-2.

A rocket propulsion system is to develop 15,000 lb thrust and burns red fuming nitric acid (RFNA) and aniline (AN), at the rate of 78 lb/sec at a mixture ratio of 3.0. The propulsive gas is to enter the exhaust nozzle at a combustion pressure of 500 psi and expand so the $p_e = 16$ psia at sea level; the ambient atmospheric pressure is $p_{\text{amb}} = 14.7$ psia. The exit area of the exhaust nozzle is $A_e = 106$ sq in. Calculate the effective jet velocity for the propulsive jet, and its exit velocity u_e .

SOLUTION.

$$\begin{aligned} \text{Eq. 2-33; } F &= 15,000 \text{ lb; } \dot{m} = 78/32.17 \\ &= 2.42 \text{ slug/sec;} \end{aligned}$$

*Both c and V_j are employed interchangeably for the effective jet velocity in the literature on jet propulsion engines. The symbol c is employed mainly for rocket jet propulsion.

$$c = \frac{F}{\dot{m}} = 15,000 \frac{32.17}{78} = 6190 \text{ fps}$$

$$\begin{aligned} u_e &= c - \frac{1}{\dot{m}} (p_e - p_0) A_e \\ &= 6190 - \frac{(16-14.7)}{2.42} 106 \\ &= 6190 - 57 = 6133 \text{ fps} \end{aligned}$$

The aniline flow rate (\dot{m}_f)

$$\frac{\dot{m}}{\dot{m}_f} = r + 1 = 4$$

Hence

$$\dot{m}_f = \frac{78}{4} = 19.5 \text{ lb/sec} = 0.608 \text{ slug/sec}$$

The RFNA flow rate

$$\dot{m}_O = 3\dot{m}_f = 1.824 \text{ slug/sec}$$

Thrust at 100,000 ft altitude

$$p_{amb} = 14.7 (0.0106) = 0.1558 \text{ psia}$$

$$\begin{aligned} F &= \frac{78(6133)}{32.17} + (16 - 0.1558) 106 \\ &= 16,520 \text{ lb} \end{aligned}$$

2-4 POWER DEFINITIONS FOR PROPULSION SYSTEMS

The power definitions which follow are useful in studies of propulsion systems.

2-4.1 THRUST POWER (P_T). The rate at which useful work is done on a vehicle propelled at a constant speed V_0 is termed the thrust power. Hence, for a vehicle in uniform flight

$$P_T = FV_0 = DV_0 \quad (2-35)$$

where D is the drag of the vehicle.

2-4.2 PROPULSIVE POWER (P). By definition, the rate at which energy is *supplied* to the *propulsive element* of a propulsion system is called the *propulsive power*.

In the case of a *piston-engine propeller system*, the propulsive power is the power delivered to the propeller shaft. In the case of a turboprop engine, the propulsive power is the sum of the power supplied to the propeller shaft and that supplied to the exhaust nozzle.

In a jet propulsion system, the propulsive power is the rate at which energy is supplied to the exhaust nozzle, the propulsive element.

In general

$$P = P_T + P_\lambda \quad (2-36)$$

where P_λ denotes the sum of the power losses in the propulsion system. Thus

$$P_\lambda = P_{KE} + P_{L1} + P_{L2} + \dots \quad (2-37)$$

where P_{KE} denotes the kinetic energy associated with the propulsive jet and is called the *exit loss*; P_{L1} , P_{L2} --- refer to the other losses associated with the system⁴.

2-4.3 EXIT LOSS (P_{KE})

An *ideal propulsion system*, by definition, is one in which all of the extraneous power losses P_{L1} , P_{L2} --- are zero; i.e., the only loss is the exit loss.

The *exit loss* P_{KE} is given by

$$P_{KE} = \frac{\dot{m}v^2}{2} = \frac{\dot{m}}{2} (c - V_0)^2 \quad (2-38)$$

where $v = c - V_0$ = the *effective absolute velocity* of the propulsive jet.

If it is assumed that there are no extraneous power losses and that all linear

momentum changes are in the direction of motion of the vehicle, then the propulsive power P is given by

$$P = P_T + P_{KE} \quad (2-39)$$

2-4.4 JET POWER (P_j). The power associated with the propulsive jet of a jet propulsion system is termed the *jet power*. By definition

$$P_j = \frac{\dot{m}c^2}{2} = \frac{\dot{m}}{2} V_j^2 \quad (2-40)$$

For *power limited systems*, such as electric rocket engines, the power output of the source of electric power P_E carried in the propelled vehicle is related to the jet power P_j . Thus, by definition

$$P_E = \frac{P_j}{\eta_E} \quad (2-41)$$

where η_E is the energy conversion efficiency.

It will be shown in par. 2-5 that the jet power can be related to the thrust F and the specific impulse I_{sp} ; the latter is defined in that paragraph.

2-5 PERFORMANCE PARAMETERS FOR JET PROPULSION SYSTEM

The performance parameters discussed in this paragraph are based on the assumption that the propulsion system operates under steady conditions.

2-5.1 SPECIFIC THRUST. In the case of an air-breathing jet engine, the specific thrust is defined by the following equation:

$$I_a = \frac{F}{\dot{m}_a/g_c} = \frac{F}{\dot{w}_a} \quad (\text{sec}) \quad (2-42)$$

where $g_c = 32.174 \text{ slug-ft/lb-sec}^2$, and \dot{w}_a is the weight rate of air induction per sec.

I_a is frequently termed the *air specific impulse*.

2-5.2.1 SPECIFIC IMPULSE. In the case of rocket propulsion, the specific impulse, denoted by I_{sp} , is defined by

$$I_{sp} = \frac{F}{\dot{m}/g_c} = \frac{F}{\dot{w}} = \frac{c}{32.17} \quad (\text{sec}) \quad (2-43)$$

where

$\dot{m} = \dot{m}_o + \dot{m}_f$ = the mass rate of consumption of propellant material, slug/sec

$\dot{w} = \dot{w}_o + \dot{w}_f$ = the weight rate of consumption of propellant material, lb/sec

In the case of an air-breathing jet engine the *fuel specific impulse*, denoted by I_f , is defined by

$$I_f = \frac{F}{\dot{m}_f/g_c} = \frac{F}{\dot{w}_f} \quad (\text{sec}) \quad (2-44)$$

where

\dot{w}_f = the rate of fuel consumption for the air-breathing jet engine, lb/sec

2-5.2.2 SPECIFIC IMPULSE AND JET POWER. The jet power P_j (see par. 2-4.4) is related to the specific impulse I_{sp} by the following equation:

$$P_j = \frac{\dot{m}c^2}{2} = \frac{g_c F I_{sp}}{2} \quad (2-45)$$

For electric rocket engines it is convenient to express P_j in kilowatts. Thus

$$P_j = \frac{F I_{sp}}{45.8} \quad (\text{kw}) \quad (2-46)$$

Hence, the required power output from the electric power source installed in the propelled vehicle is accordingly (see par. 2-4.4).

$$P_E = \frac{F I_{sp}}{2\eta_E} \quad (2-47)$$

2-5.3 OVERALL EFFICIENCY (η_o). By definition, the *overall efficiency* of a propulsion system is given by

$$\eta_o = \frac{P_T}{E_{in}} = \eta_{th} \eta_p \quad (2-48)$$

where

$$P_T = FV = \text{thrust power}$$

E_{in} = rate at which energy is supplied the system

η_{th} = thermal efficiency of the system

η_p = propulsive efficiency of the system

2-5.4 THERMAL EFFICIENCY (η_{th}). By definition, the thermal efficiency η_{th} is given by

$$\eta_{th} \equiv \frac{P}{E_{in}} \quad (2-49)$$

The thermal efficiency measures the effectiveness with which the energy E_{in} supplied the propulsion system is converted into propulsive power P . In a jet propulsion system the thermal efficiency is a criterion of the effectiveness with which the energy supplied to the system is utilized for *increasing the kinetic energy* of the propulsive fluid as it flows through the system.

In the case of an *air-breathing jet engine* the rate at which energy is supplied the engine is given by

$$E_{in} = \dot{m}_f \left(\Delta H_c + \frac{V_o^2}{2} \right) \quad (2-50)$$

where

ΔH_c = the calorific value of the fuel, B/slug

$V_o^2/2$ = the kinetic energy associated with the fuel due to the flight speed of the vehicle, B/slug

\dot{m}_f = the rate at which fuel is consumed, slug/sec

The energy flow $\dot{m}_f V_o^2/2$ was supplied by fuel that was consumed previously.

In the case of a rocket propulsion system, E_{in} is given by

$$E_{in} = \dot{m} \left(\Delta H_p + \frac{V_o^2}{2} \right) \quad (2-51)$$

where

ΔH_p = the calorific value of the propellant material burned in the rocket motor, B/slug

$\dot{m} = \dot{m}_o + \dot{m}_f$ = the mass rate of consumption of propellant material, slug/sec

2-5.5 PROPULSIVE EFFICIENCY (η_p). The propulsive efficiency is defined by the relationship

$$\eta_p \equiv \frac{P_T}{P} = \frac{P_T}{P_T + P_\lambda} \quad (2-52)$$

The propulsive efficiency η_p measures the effectiveness with which the propulsive power P is converted into the thrust power P_T .

2-5.6 IDEAL PROPULSIVE EFFICIENCY (η_p). The propulsive efficiency defined by Eq. 2-51 makes no assumption regarding the power losses in the propulsion system.

In the ideal case where the only power loss is P_{KE} (see par. 2-4.2), the ideal propulsive efficiency, denoted by η_P , is defined by

$$\eta_P \equiv \frac{P_T}{P_T + P_{KE}} \quad (2-53)$$

It is readily shown that for⁵

(a) *Air-breathing jet engines*

$$\eta_P = \frac{2\nu(f + 1 - \nu)}{2\nu(f + 1 - \nu) + (f + 1)(1 - \nu)^2} \quad (2-54)$$

For a *simple turbojet engine* $f \approx 0$ so that

$$\eta_P = \frac{2\nu}{1 + \nu} \quad (2-55)$$

where $\nu = V_0/c$.

(b) *Rocket propulsion systems*

$$\eta_P = \frac{2\nu}{1 + \nu^2} \quad (2-56)$$

Eqs. 2-53 and 2-54 demonstrate that for any propulsion system the ideal propulsive efficiency is primarily a function of the effective speed ratio $\nu = V_0/c$.

REFERENCES

1. A.H. Shapiro, *Handbook of Fluid Mechanics*, V.L. Streeter, Editor-In-Chief, McGraw-Hill Book Company, Inc., 1961, Section 2.
2. I.S. Sokolnikoff and R.M. Redheffer, *Mathematics of Physics and Modern Engineering*, McGraw-Hill Book Company, Inc., 1958, p. 388.
3. H. Wayland, *Differential Equations Applied in Science and Engineering*, D. Van Nostrand Company, 1957, Ch. 2.
4. M.H. Zucrow, *Aircraft and Missile Propulsion*, John Wiley and Sons, Inc., 1958, Vol. 1, Ch. 2.
5. M.J. Zucrow, *Aircraft and Missile Propulsion*, John Wiley and Sons, Inc., 1958, Vol. 2.

CHAPTER 3

ELEMENTARY GAS DYNAMICS

3-0 PRINCIPAL NOTATION FOR CHAPTER 3*

a	acoustic or sonic speed, fps	d	diameter, ft or in., as specified in text
a*	critical acoustic speed, where $M=1$, fps	D	drag force, lb
a^o	stagnation or total acoustic speed, fps	D	hydraulic diameter = $4R$, where R is the hydraulic radius
A	flow cross-sectional area, sq ft or sq in., as specified in text	e	stored energy per unit mass of fluid
A*	critical cross-sectional area where $u=a^*$	E	total amount of stored energy associated with a system
A_m	maximum cross-sectional area	f	friction coefficient in the Fanning equation for pressure loss
B	British thermal unit	F	thrust, lb
c	effective jet or exhaust velocity	F	impulse function, lb
c_o	maximum isentropic speed = $\sqrt{2c_p T^o}$	g_c	gravitational conversion factor = $32.174 \text{ slug-ft/lb-sec}^2$
c_p	instantaneous specific heat constant pressure, B/slug-°R	G	flow density or mass velocity = \dot{m}/A
\bar{c}_p	mean value of c_p for a specified temperature range	G*	critical flow density, value of G where $M=1$
\bar{c}_v	instantaneous value of the specific heat at constant volume	h	static specific enthalpy, B/slug
C_c	contraction coefficient	h^o	stagnation or total specific enthalpy, B/slug
C_d	discharge coefficient	Δh	finite change in specific enthalpy
		Δh_c	finite change in specific enthalpy for a compression, B/slug

*Any consistent set of units may be employed; the units presented here are for the American Engineers System (see par. 1-7).

$\Delta h'_c$	finite change in specific enthalpy for an isentropic compression, B/slug	q'_{\max}	maximum isentropic speed = $c_o = \sqrt{2c_p T^o}$
Δh_t	finite change in specific enthalpy for an expansion, B/slug	\dot{Q}	volumetric rate of flow, cfs
$\Delta h'_t$	finite change in specific enthalpy for an isentropic expansion, B/slug	r	pressure ratio
J	mechanical equivalent of heat ≈ 778 ft-lb/B	r_c	pressure ratio for a compression process = P_2/P_1 (or p_2/p_1), where $P_2 > P_1$
L	length, unit as specified in text	r_t	expansion ratio for an expansion process = P_2/P_1 , where $P_1 > P_2$
m	mass, slug	r_t^*	expansion ratio which makes $u = a^*$
\bar{m}	molecular weight, slug/mole	R	gas constant = R_u/\bar{m}
M	Mach number (q/a or u/a) or magnitude of momentum vector, as specified in text	R	hydraulic radius, in ft or in., as specified in text
M^*	dimensionless velocity (u/a^* or q/a^*)	R_u	universal gas constant = 49,717 ft-lb/slug-mole $^{\circ}R$ = 63.936 B/slug-mole- $^{\circ}R$
\underline{M}	momentum vector	$^{\circ}R$	degrees Rankine
$\dot{\underline{M}}$	rate of change in momentum = $d\underline{M}/dt$	s	static specific entropy, B/slug- $^{\circ}R$
p	absolute static pressure, psia	s^*	critical value of s , where $u = a^*$
p_a	ambient static pressure, psia	t	time, sec
p^*	critical static pressure, where $u=a^*$, psia	T	absolute static temperature ($^{\circ}F + 460$), $^{\circ}R$
P	absolute static pressure, psf	T^*	critical static temperature, value of T where $u = a^*$
P^*	critical static pressure, where $u=a^*$, psf	T^o	stagnation or total temperature, $^{\circ}R$
\underline{q}	velocity vector	u	velocity parallel to the x-axis, fps
q	magnitude of \underline{q} or the dynamic pressure, as specified in text	u_e	adiabatic exhaust velocity
q'	isentropic velocity, fps		

u^* critical value of u , where $u=a^*$

u' isentropic exhaust velocity =

$$a^o \sqrt{\frac{2}{\gamma - 1}} (Z_t)$$

v specific volume = $1/\rho$ = cu ft/slug

v^o stagnation value of specific volume
= $1/\rho^o$

V control volume in a region of a flowing fluid

w weight = mg_c , lb

W shaft work

${}_1W_2$ shaft work done by system in going from state 1 to state 2

w weight rate of flow = $\dot{m}g_c$, lb/sec

Z_c compression factor = $(r_c)^{\frac{\gamma-1}{\gamma}} - 1$

Z_t expansion factor = $1 - (r_t)^{\frac{\gamma-1}{\gamma}}$

GREEK LETTERS

α angle between velocity vector and normal to flow cross-sectional area

γ specific heat ratio = c_p/c_v

η efficiency

ρ density, slug/ft³

ρ^* critical density = $1/v^*$, value of ρ where $u=a^*$

ρ^o stagnation or total density

τ shear stress (friction force per unit area)

SUBSCRIPTS

Numerals

0 free stream

1 initial state, or reference state 1

2 final state, or reference state 2

Letters

a ambient or atmospheric

c compression or entrance section of a nozzle

e exit cross-sectional area normal to flow direction

ext external

f friction

int internal

max maximum value

min minimum value

n nozzle

t expansion or turbine, as specified in text

th thermal

SUPERSCRIPTS

' (prime) denotes the value is obtained by means of an isentropic process

* critical value, where $u=a^*$, and $M=1$

o stagnation or total value

3-1 INTRODUCTION*

Gas dynamics, which is the theory of the flow of a compressible fluid, is of fundamental importance to the analysis and design of the chemical rocket and air-breathing engines described in Chapter 1. By applying the principles of gas dynamics to such engines one can determine the parameters which characterize the motion of the compressible fluid and its thermodynamic state at pertinent stations in its

flow path through a jet propulsion engine or a turboshaft engine. In most cases it may be assumed the flow of fluid through the engine is *steady* and *one-dimensional*. Consequently, the basic principles of steady one-dimensional flow are of great importance to the studies concerned with the engines discussed in this handbook.

Table 3-1 presents the flow processes of major importance to the engines to be studied.

TABLE 3-1

FLOW PROCESSES IN JET PROPULSION ENGINES

FLOW PROCESS	TYPE OF ENGINE
1. Compression by diffusion	Ramjet, turbojet, turboprop
2. Compression by mechanical means	Turbojet, turboprop, turbomachinery
3. Flow expansion	Ramjet, turbojet, turboprop, chemical rocket, nuclear rocket, electrothermal rocket
4. Flow with friction	Ramjet, turbojet, turboprop, nuclear rocket
5. Flow with heat transfer	Ramjet, turbojet, turboprop, chemical rocket, nuclear rocket, electrothermal rocket
6. Flow with mass addition	Solid propellant rocket, hybrid rocket

*Appendix A presents more detailed information on elementary gas dynamics.

For analyzing the flow processes listed in Table 3-1, the following physical principles are available:

- (a) The principle of the conservation of matter for a flowing fluid.
- (b) The principle of the conservation of momentum which is expressed by the momentum theorem of fluid mechanics.
- (c) The principle of the conservation of energy which was first demonstrated for an *isolated mechanical system* by Liebnitz (1693). For a flowing fluid the energy principle leads to the so-called *energy equation*.
- (d) The second law of thermodynamics from which one obtains the entropy equation for a flowing fluid.
- (e) The thermodynamic properties of the flowing compressible medium under consideration; these lead to some form of defining equation (*equation of state*) relating the static pressure, density, and temperature of the flowing fluid.

Flows which are steady and one-dimensional are those for which the variables— P , ρ , q or their equivalents—at a point in the fluid are *invariant* with time and change appreciably in a single direction. Unless it is specifically stated to be otherwise, it is assumed in all of the subsequent discussions in this chapter that the flow is steady and one-dimensional.

3-2 THE IDEAL GAS

The ideal gas is the simplest thermodynamic working fluid; the propulsive gas ejected from the exhaust nozzle of a jet propulsion engine approximates the ideal gas.

3-2.1 THE THERMALLY PERFECT GAS

A gas is said to be thermally perfect if it satisfies the following equation. Thus

$$P = \rho RT = \rho R_u T / \bar{m} \quad (3-1)$$

where in the American Engineers System of units (see par. 1-7)

T = absolute temperature of the gas, °R

P = absolute pressure of the gas, psf

ρ = density of gas, slug/ft³

R_u = universal gas constant = 49,717
ft-lb/slug-mole°R = 63.936
B/slug-mole°R

$R = R_u / \bar{m}$ = gas constant

\bar{m} = molecular weight of the gas,
slug/mole

Hence, for a thermally perfect gas

$$\frac{P}{\rho RT} = 1 \quad (3-2)$$

For a *real* gas, the deviations of the ratio $P/\rho RT$ from unity become significant at very high pressures, such as those occurring in guns, and at very low temperatures. The deviations arise from the fact that *every real gas can be liquefied*, while an ideal gas cannot.

3-2.2 SPECIFIC HEAT

By definition, the *specific heat* c of a medium is given by

$$c = \delta Q / dT \quad (\text{B/slug-}^\circ\text{R}) \quad (3-3)$$

The magnitude of the specific heat c depends upon the manner in which the heat increment δQ is added to the medium. Two

specific heats are of importance; c_v the specific heat at constant volume, and c_p the specific heat at constant pressure.

3-2.2.1 SPECIFIC HEAT AT CONSTANT VOLUME (c_v)

If δQ is added to a mass of gas while its volume is held constant, then

$$c_v = \frac{\delta Q}{dT} = \left(\frac{\partial u}{\partial T} \right)_v \quad (\text{B/slug-}^\circ\text{R}) \quad (3-4)$$

where

∂u = the specific internal energy of the gas, B/slug

From Eq. 3-4 the specific internal energy of a gas is given by

$$u = \int_{T_0}^T c_v dT + u_0 \quad (\text{B/slug}) \quad (3-5)$$

3-2.2.2 SPECIFIC HEAT AT CONSTANT PRESSURE (c_p)

If heat is added to a mass of gas under isobaric conditions ($dP = 0$), then

$$c_p = \left(\frac{\delta Q}{dT} \right) = \left(\frac{du}{dT} \right)_v + \left[\left(\frac{\partial u}{\partial v} \right)_T + P \right] \left(\frac{\partial v}{\partial T} \right)_P \quad (\text{B/slug-}^\circ\text{R}) \quad (3-6)$$

It follows from Eqs. 3-4 and 3-6 that $c_p > c_v$.

3-2.2.3 SPECIFIC HEAT RATIO (γ)

By definition

$$\gamma \equiv \frac{c_p}{c_v} = \text{the specific heat ratio} \quad (3-7)$$

3-6

3-2.2.4 SPECIFIC ENTHALPY AND SPECIFIC HEAT

By definition, the *specific enthalpy* h , which is a property of the gas, is defined by

$$h \equiv u + P/\rho \quad (\text{B/slug-}^\circ\text{R}) \quad (3-8)$$

and

$$c_p = dh/dt \quad (\text{B/slug-}^\circ\text{R}) \quad (3-9)$$

3-2.3 CALORICALLY PERFECT GAS

A gas is said to be *calorically perfect* if the specific heat c_v is independent of the gas temperature. If a gas is thermally perfect but *calorically imperfect*, then

$$P = \rho RT \quad \text{and} \quad c_v = f(T) \quad (3-10)$$

A gas which is both thermally and calorically perfect is called an *ideal gas*; frequently such a gas is termed a polytropic gas⁴.

3-2.4 SPECIFIC HEAT RELATIONSHIPS

For an ideal gas c_v , c_p , and γ are constants independent of the gas temperature. These constants are related by the equations which follow.

Thus

$$c_p - c_v = R \quad (\text{Regnault Relationship}) \quad (3-11)$$

and

$$c_v = R \left(\frac{1}{\gamma - 1} \right) \quad \text{and} \quad c_p = R \left(\frac{\gamma}{\gamma - 1} \right) \quad (3-12)$$

3-2.5 ACOUSTIC OR SONIC SPEED IN AN IDEAL GAS

The speed with which a sound wave (or a very small pressure disturbance) is propagated in a medium is termed either the *acoustic* or *sonic speed*, and is denoted by a . If the medium is an ideal gas, then

$$a = \sqrt{\gamma \frac{P}{\rho}} = \sqrt{\gamma RT} = \sqrt{\gamma R_u} \sqrt{\frac{T}{\bar{m}}} \quad (3-13)$$

where \bar{m} is the molecular weight of the gas.

3-2.6 MACH NUMBER

When there is a large relative speed between a body and the compressible fluid in which it is immersed, the *compressibility* of the fluid, which is the variation of its density with speed, affects the drag of the body. The ratio of the local speed of the body u , to its acoustic speed a , is called the local Mach number, which is denoted by M . For an ideal gas

$$M = \frac{u}{a} = \frac{u}{\sqrt{\gamma RT}}; \quad (3-14)$$

or

$$M^2 = \frac{u^2}{a^2} = \frac{u^2}{\gamma RT} \quad (3-15)$$

The speed u measures the directed motion of the gas molecules, and u^2 is a measure of the kinetic energy of the directed flow. According to the kinetic theory of gases the temperature T is a measure of the random kinetic energy of the gas molecules. Hence, $M^2 = u^2/a^2$ is a measure of the ratio of the kinetic energies of the directed and random flows of the gas molecules.

3-3 GENERAL STEADY ONE-DIMENSIONAL FLOW

The steady one-dimensional flow approximation gives the simplest solutions to flow

problems. The assumptions underlying the approximation are presented in par. A-3; the A denotes Appendix A.*

3-3.1 CONTINUITY EQUATION

For a steady one-dimensional flow, the continuity equation is given by (see par. A-3.1, Eq. A-45)

$$\rho \frac{\partial u}{\partial x} + u \frac{\partial \rho}{\partial x} = 0 \quad (3-16)$$

The corresponding integral equation is

$$\int_A (\rho u) dA = d(\rho u A) = 0 \quad (3-17)$$

Hence

$$\dot{m} = \frac{dm}{dt} = \rho u A = \text{constant} \quad (3-18)$$

Eq. 3-18 states that if the flow is steady, the same mass rate of flow crosses every cross-section of a one-dimensional flow passage.

By definition, the *mass velocity*, also called the *flow density*, denoted by G , is given by

$$G \equiv \rho u = \dot{m}/A \text{ (slug/sec-sq ft)} \quad (3-19)$$

Logarithmic differentiation of Eq. 3-18, yields the following differential equation for a steady one-dimensional flow:

$$\frac{dA}{A} + \frac{d\rho}{\rho} + \frac{du}{u} = 0 \quad (3-20)$$

*The letter A preceding a paragraph, equation, table, or figure number indicates that the paragraph, equation, etc., are located in Appendix A.

The values of u and ρ in the equations for a steady one-dimensional flow are the *effective mean values* for the cross-sectional area A .

3-3.2 MOMENTUM EQUATION

3-3.2.1 GENERAL FORM OF MOMENTUM EQUATION

The general form of the momentum equation is given by Eq. 3-11 which for a steady flow and fluids of small density—such as a gas—reduces to

$$\tilde{R} = \int_S \rho q_n \tilde{q} dS - \int_S P \tilde{n} dS \quad (\rho \text{ small}) \quad (3-21)$$

If there are no solid bodies immersed in the fluid, no body forces, and no friction, then

$$\int_S P \tilde{n} dS + \int_S \rho q_n \tilde{q} dS = 0 \quad (\tilde{W} = \tilde{R} = 0) \quad (3-22)$$

where

\tilde{q} = fluid velocity

q_n = velocity normal to the element dS of the control surface S

P = static pressure

\tilde{n} = unit normal to dS

3-3.2.2 MOMENTUM EQUATION FOR STEADY, ONE-DIMENSIONAL, REVERSIBLE FLOW

It is readily shown that for a steady, one-dimensional frictionless flow the momentum equation reduces to^{1,2}

$$u du + \frac{dP}{\rho} = 0 \quad (3-23)$$

or

$$u du + v dP = 0 \quad (3-24)$$

Eq. 3-23 is a form of *Euler's equation of motion* and applies only to a *reversible flow*. To integrate Eq. 3-23 requires a relationship between P and ρ . In integral form, Eq. 3-23 is

$$\frac{u^2}{2} + \frac{dP}{\rho} = \text{constant} \quad (3-25)$$

3-3.3 ENERGY EQUATION FOR STEADY ONE-DIMENSIONAL FLOW

Figure 3-1 illustrates diagrammatically a stationary control surface S enclosing the control volume V in a region of a flowing fluid. According to the first law of thermodynamics, if δQ denotes the amount of heat *added* to the mass of fluid instantaneously enclosed by S , and δW^* denotes the amount of work done by the same mass of fluid on the surroundings in time dt , then

$$dE = \delta Q - \delta W^* \quad (3-26)$$

By convention δQ is positive if heat is transferred to the system, and δW^* is positive if the system does work on its surroundings. The notation signifies that δQ and δW^* are *inexact differentials* because Q and W are *not properties* of the system. The stored energy E is a property, and dE is an exact differential^{1,6}.

Figure 3-2 illustrates schematically the conditions at an arbitrary element dS of the control surface S if the flow is *steady*. In that case the stored energy associated with the fluid occupying the control volume V does not change with time. For a *steady flow* the integral form of the energy equation is^{1,2}

$$\frac{\delta Q}{dt} - \frac{\delta W}{dt} = \int_S \left(h + \frac{u^2}{2} + gz \right) q_n dS \quad (B/\text{slug-sec}) \quad (3-27)$$

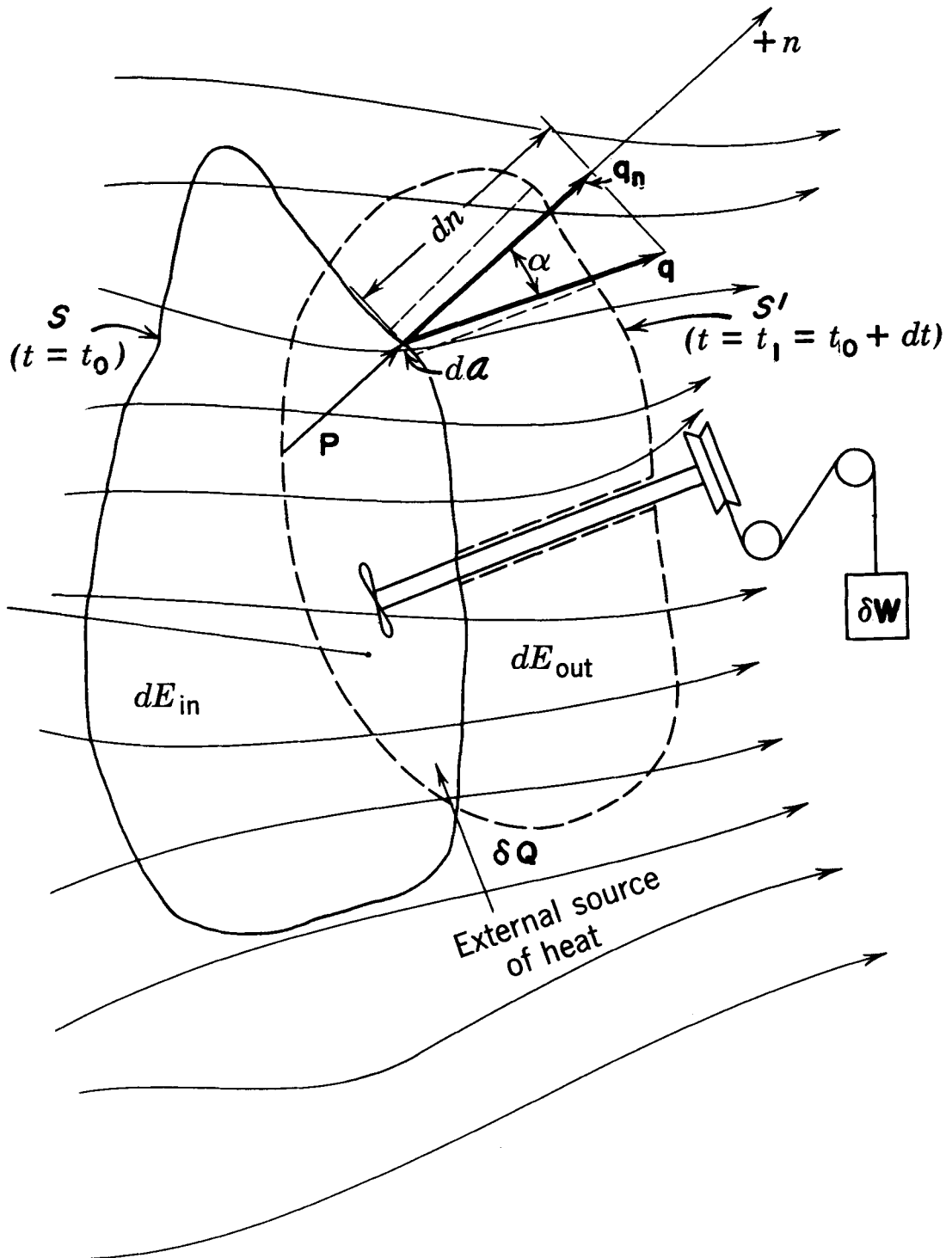


Figure 3-1. Control Surface Enclosing a Region in a Flowing Fluid to Which Heat Is Added and Which Does Work on Its Surroundings

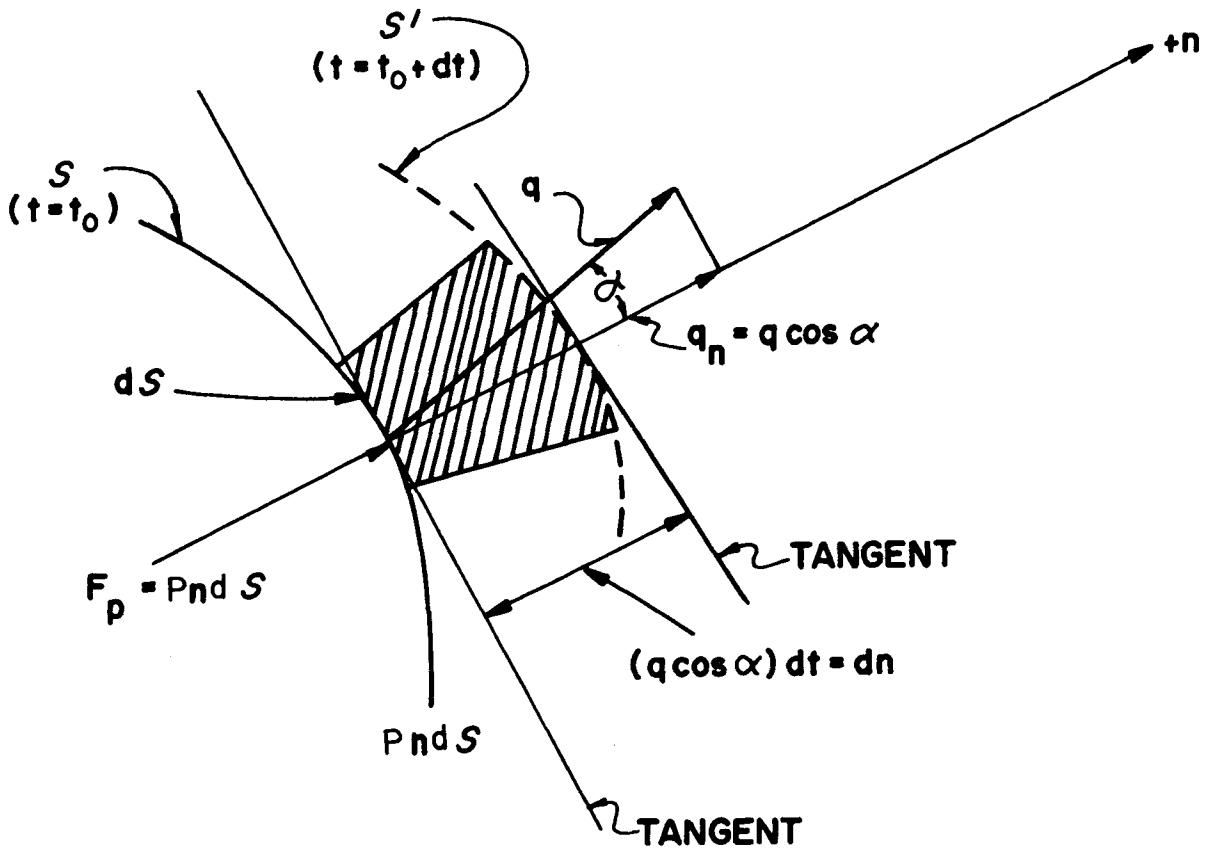


Figure 3-2. Element of a Control Surface Which Encloses a Region in a Flowing Fluid

where

δQ = the heat added to the fluid, B/slug

δW = the shaft work done by the fluid, B/slug

$h = u + P/\rho$ = specific enthalpy of the fluid, B/slug

u = specific internal energy of the fluid, B/slug

$q_n = q \cos \alpha$ = velocity of fluid normal to flow area dS , fps

q = magnitude of velocity vector q , fps

α = angle between normal to dS and the velocity vector

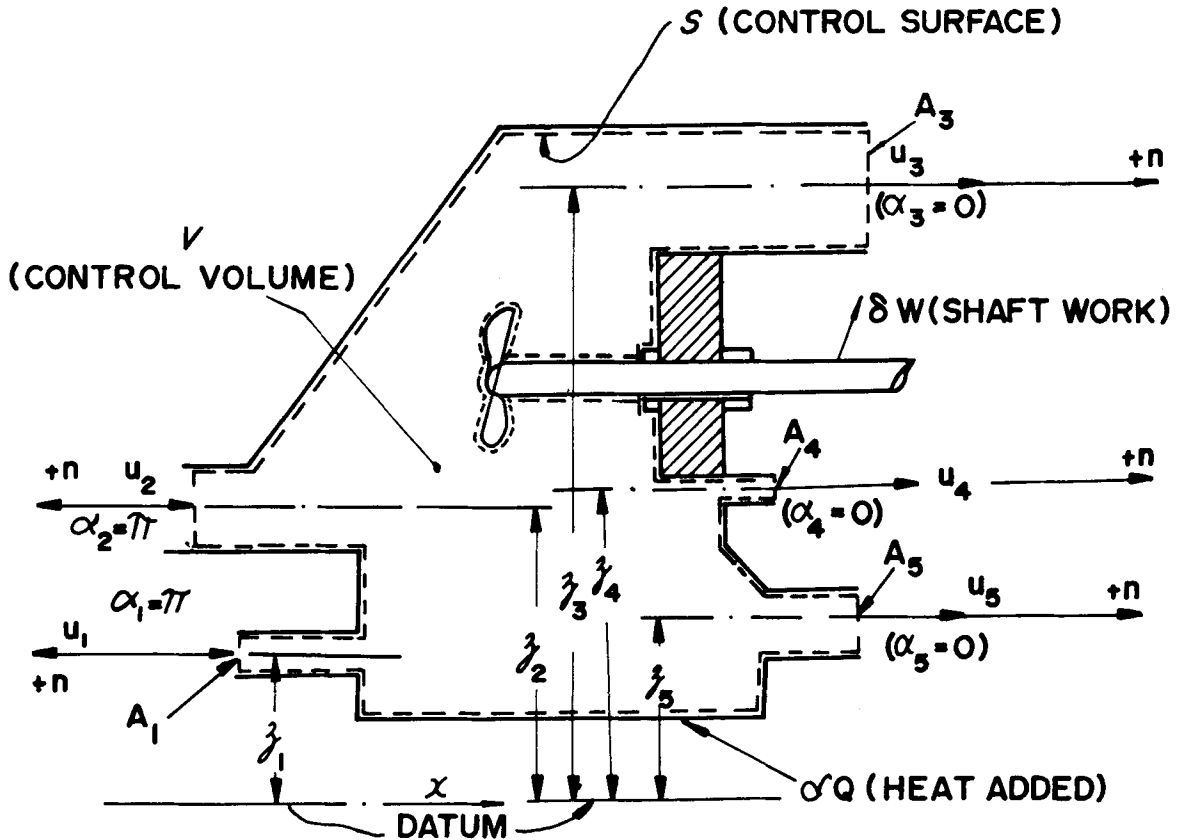
Fig. 3-3 illustrates the application of Eq. 3-27 to a one-dimensional flow (see Example A-3).

3-4 STEADY ONE-DIMENSIONAL FLOW OF AN IDEAL GAS

If the flowing medium is an ideal gas, the mathematical analysis of compressible media is greatly simplified. (see par. 3-2).

3-4.1 CONTINUITY EQUATION

The steady one-dimensional flow of a compressible medium is given by Eq. 3-18. For an



$$\begin{aligned}
 \frac{\delta Q}{dt} - \frac{\delta W}{dt} &= \int_{A_{out}} \left(h + \frac{u^2}{2} + gz \right) \rho u \cos \alpha dA - \int_{A_{in}} \left(h + \frac{u^2}{2} + gz \right) \rho u \cos \alpha dA \\
 &= \left(h_3 + \frac{u_3^2}{2} + z_3 \right) \dot{m}_3 + \left(h_4 + \frac{u_4^2}{2} + z_4 \right) \dot{m}_4 + \left(h_5 + \frac{u_5^2}{2} + z_5 \right) \dot{m}_5 \\
 &\quad - \left(h_1 + \frac{u_1^2}{2} + z_1 \right) \dot{m}_1 - \left(h_2 + \frac{u_2^2}{2} + z_2 \right) \dot{m}_2
 \end{aligned}$$

Figure 3-3. Energy Balance for a One-dimensional Steady Flow

ideal gas, the density ρ can be expressed in terms of the local flow Mach number M . Thus

$$\rho = \gamma P \left(\frac{M}{u} \right)^2 \quad (3-28)$$

where $\gamma = c_p/c_v$ = the specific heat ratio = constant. Combining Eqs. 3-18 and 3-28 yields the continuity equation for the *steady one-dimensional flow of an ideal gas*. Thus

$$\dot{m} = APM \sqrt{\frac{\gamma}{RT}} = APM \sqrt{\frac{\gamma \bar{m}}{R_u T}} \text{ (slug/sec)} \quad (3-29)$$

where A is the flow area, sq ft; P is the absolute static pressure, psf; and \bar{m} is the molecular weight of the gas.

Eq. 3-29 gives the mass flow rate of an ideal gas crossing the area A with a flow Mach number equal to M .

3-4.2.1 MOMENTUM EQUATIONS FOR THE STEADY ONE-DIMENSIONAL FLOW OF AN IDEAL GAS

The general momentum equation for the *steady one-dimensional flow of a compressible fluid* is Eq. 3-25.

3-4.2.2 MOMENTUM EQUATION FOR A REVERSIBLE, STEADY, ONE-DIMENSIONAL FLOW

From Eq. 3-23 one obtains

$$u du + \left(\frac{dP}{d\rho} \right)_s \frac{d\rho}{\rho} = 0 \quad (3-30)$$

But

$$\left(\frac{dP}{d\rho} \right)_s = a^2 = (\text{acoustic speed})^2 \quad (3-31)$$

Hence

$$\frac{dP}{\rho} + M^2 \frac{du}{u} = 0 \quad (3-32)$$

The subscript s indicates an isentropic process ($ds = 0$).

3-4.3 ENERGY EQUATION

It is shown in par. A-4.3 that the energy equation for the *steady one-dimensional flow of a gas* is given by

$$\delta Q - \delta W = dh + d \left(\frac{u}{2} \right)^2 \quad (3-33)$$

In Eq. 3-33 the heat added to the fluid δQ includes the heat transferred through the walls to the fluid plus that transferred to the fluid by bodies immersed within it.

3-4.3.1 ENERGY EQUATION FOR A SIMPLE ADIABATIC FLOW

A *simple adiabatic flow* is characterized by the following:

$$\delta Q = 0; \delta W = 0; dz = 0; ds > 0 \quad (3-34)$$

The flow of a gas through such passages of a jet propulsion engine as a diffuser, duct, nozzle, etc., may be assumed to be a simple adiabatic flow, and the corresponding energy equation is

$$dh + d \left(\frac{u^2}{2} \right) = 0 \quad (3-35)$$

Eq. 3-35 applies to both reversible ($ds=0$) and irreversible flows ($ds>0$). Integrating between any two cross-sections of a flow passage, denoted by the subscripts 1 and 2, yields

$$h_1 + \frac{u_1^2}{2} = h_2 + \frac{u_2^2}{2} = \text{constant} \quad (3-36)$$

3-4.3.2 ENERGY EQUATION FOR THE SIMPLE ADIABATIC FLOW OF AN IDEAL GAS

The simple adiabatic flow of an ideal gas is characterized by the following:

$$\delta Q = 0; \delta W = 0; g dz = 0; c_p = \gamma R / (\gamma - 1);$$

$$c_v = R / (\gamma - 1); dh = c_p dT; a^2 = \gamma P / \rho = \gamma RT;$$

$$\text{and } \gamma = c_p / c_v \quad (3-37)$$

For an ideal gas Eq. 3-35 becomes

$$c_p dT + d\left(\frac{u^2}{2}\right) = 0 \quad (3-38)$$

Similarly, Eq. 3-36 becomes

$$c_p T_1 + \frac{u_1^2}{2} = c_p T_2 + \frac{u_2^2}{2} = \text{constant} \quad (3-39)$$

Let $M_1 = u_1 / a_1$ and $M_2 = u_2 / a_2$, and substituting for c_p from Eq. 3-37 into Eq. 3-39, yields the following equations:

$$a_1^2 \left(1 + \frac{\gamma - 1}{2} M_1^2\right) = a_2^2 \left(1 + \frac{\gamma - 1}{2} M_2^2\right) = \text{constant} \quad (3-40)$$

or

$$\frac{u_1^2}{2} + \frac{a_1^2}{\gamma - 1} = \frac{u_2^2}{2} + \frac{a_2^2}{\gamma - 1} = \text{constant} \quad (3-41)$$

and

$$T_2 = T_1 \left\{ 1 + \left(\frac{\gamma - 1}{2}\right) M_1^2 \left[1 - \left(\frac{u_2}{u_1}\right)^2 \right] \right\} \quad (3-42)$$

Eqs. 3-38 through 3-42 are different forms of the energy equation for the steady one-dimensional flow of an ideal gas.

Refer to Eq. 3-42. A flow process for which the gas velocity $u_2 > u_1$ is called a *flow expansion* and the flow passage for achieving the expansion is termed either a *nozzle* or an *effuser*. Conversely, a passage which causes a *flow compression*, one in which the velocity $u_2 < u_1$, is called a *diffuser*.

3-5 STEADY ONE-DIMENSIONAL ISENTROPIC FLOW

In general, a steady one-dimensional isentropic flow is characterized by the following:

$$\delta Q = \delta W = d\dot{m} = dz = ds = 0 \text{ (i.e., no friction)} \quad (3-43)$$

The assumption of isentropicity is valid in those regions of a flow field where the velocity gradients perpendicular to the direction of flow are negligible, i.e., to the regions of an adiabatic flow field that are external to *boundary layers*. According to boundary layer theory all frictional effects in a flowing fluid are confined to the boundary layers adjacent to the surfaces wetted by the flowing fluid, wherein the velocity gradients are large. Consequently, the fluid in the regions external to the boundary layers may be assumed to be a *perfect fluid*, i.e., a fluid characterized by the following two properties:

- (a) It possesses bulk elasticity so that $K \neq 0$.
- (b) It has no rigidity so that the *shear modulus* N is equal to zero; i.e., it is inviscid.

If an ideal gas undergoes an isentropic change of state, then

$$Pv^\gamma = \text{constant} \quad (3-44)$$

Furthermore

$$\frac{T'_2}{T_1} = \left(\frac{P_2}{P_1} \right)^{c_p/R} = \left(\frac{P_2}{P_1} \right)^{(\gamma-1)/\gamma} \quad (3-45)$$

where the *superscript prime* ' attached to T_2 indicates that the change of state from state 1 to state 2 is accomplished by an isentropic process.

The assumption of isentropicity is realistic for subsonic and supersonic flows when the isentropic conditions are closely approximated. It should be noted, however, an adiabatic diffusion of a compressible fluid may be assumed to be isentropic—when $\delta Q \simeq 0$ and friction is negligible—only if the flow is *subsonic* throughout.

If a *supersonic* compressible fluid is being diffused the flow may be assumed to be isentropic—when $\delta Q = 0$ and friction is negligible—only if no *shock waves* are produced in the flow field. Shock waves increase the entropy of the flowing fluid. Consequently, even though the flow is adiabatic and frictionless in front of and in back of a *shock wave*, which is a discontinuity in the flow, a flow in which shock waves are present cannot be an isentropic flow.

3-5.1 ENERGY EQUATION FOR THE STEADY ONE-DIMENSIONAL ISENTROPIC FLOW OF AN IDEAL GAS

The differential forms of the energy equation—i.e., Eqs. 3-35 and 3-38—apply to either a simple adiabatic or an isentropic steady one-dimensional flow. The latter equations do not indicate explicitly the effect of any irreversibility which may be present upon the flow parameters. To distinguish an isentropic flow from a simple adiabatic flow, the upper limit of the integration of Eq. 3-35 (and Eq. 3-38) will

be denoted by $2'$ for an isentropic flow, and by 2 for an adiabatic flow. Hence

(a) *Simple adiabatic flow*

$$(\delta Q = \delta W = d\dot{m} = dz = 0; ds > 0)$$

In general

$$\int_1^2 dh + \int_1^2 u du = \text{constant}$$

so that

$$h_2 + \frac{u_2^2}{2} = h_1 + \frac{u_1^2}{2} = \text{constant} \quad (3-46)$$

If $h_2 < h_1$, then $u_2 > u_1$ and the processes is a flow expansion. Hence, the specific enthalpy change for a *simple adiabatic flow expansion*, denoted by $\Delta h_t = h_1 - h_2$, is given by

$$\Delta h_t = \frac{1}{2}(u_2^2 - u_1^2) \quad (\text{B/slug})$$

For a simple adiabatic *flow compression*, $h_2 > h_1$ and $u_2 < u_1$, the corresponding change in the specific enthalpy of the fluid is denoted by $\Delta h_c = h_2 - h_1$, so that

$$\Delta h_c = \frac{1}{2}(u_1^2 - u_2^2) \quad (\text{B/slug}) \quad (3-47)$$

The corresponding equations for an isentropic flow are presented below.

(b) *Isentropic flow*

$$(\delta Q = \delta W = d\dot{m} = dz = ds = 0)$$

$$h'_2 + \frac{(u'_2)^2}{2} = h_1 + \frac{u_1^2}{2} = \text{constant} \quad (3-48)$$

$$\Delta h'_t = h_1 - h'_2 = \frac{1}{2} [(u'_2)^2 - u_1^2] \quad (3-49)$$

$$\Delta h'_c = h'_2 - h_1 = \frac{1}{2} [u_1^2 - (u'_2)^2] \quad (3-50)$$

Figs. 3-4(A) and 3-4(B) compare the simple adiabatic and the isentropic flow expansion and compression processes on the h - s -plane.

3-5.2 STAGNATION (OR TOTAL) CONDITIONS

Consider the integrated form of the energy equation for the steady, one-dimensional, adiabatic flow between sections 1 and 2 of a flow passage i.e., Eq. 3-46

$$h_1 + \frac{u_1^2}{2} = h_2 + \frac{u_2^2}{2} = \text{constant}$$

The above equation applies to both isentropic and irreversible adiabatic flows.

3-5.2.1 STAGNATION (OR TOTAL) ENTHALPY (h^0)

Assume that the flowing fluid is decelerated isentropically to zero flow velocity (i.e., $u_2 = 0$). By definition

$$h^0 \equiv h + \frac{u^2}{2} = \text{constant} = \text{stagnation enthalpy} \quad (3-51)$$

Eq. 3-51 applies to both reversible (isentropic) and irreversible steady one-dimensional adiabatic flows.

3-5.2.2 STAGNATION (OR TOTAL) TEMPERATURE (T^0)

If the flowing fluid is an ideal gas (see par. 3-2.3), then from Eqs. 3-9 and 3-51 one obtains

$$\frac{T^0}{T} = 1 + \frac{u^2}{2c_p T} \quad (3-52)$$

Eq. 3-52 is the energy equation for the steady one-dimensional flow of an ideal gas under either adiabatic or isentropic conditions.

According to Eq. 3-52 the total or stagnation temperature of an ideal gas remains constant along its flow path for either a simple adiabatic or an isentropic flow. Such a flow is said to be *isoenergetic*.

From Eq. 3-42, if $u_2 = 0$ the corresponding value of T_2 is the stagnation or total temperature T^0 . Hence

$$\frac{T^0}{T} = 1 + \frac{\gamma-1}{2} M^2 \quad (3-53)$$

The total temperature T^0 may be conceived to be the temperature of the gas contained by an *infinite reservoir* from which it flows adiabatically to the actual gas velocity u . The corresponding value of the static pressure inside that infinite reservoir is termed either the *stagnation pressure* or the *total pressure*, and is denoted by P^0 .

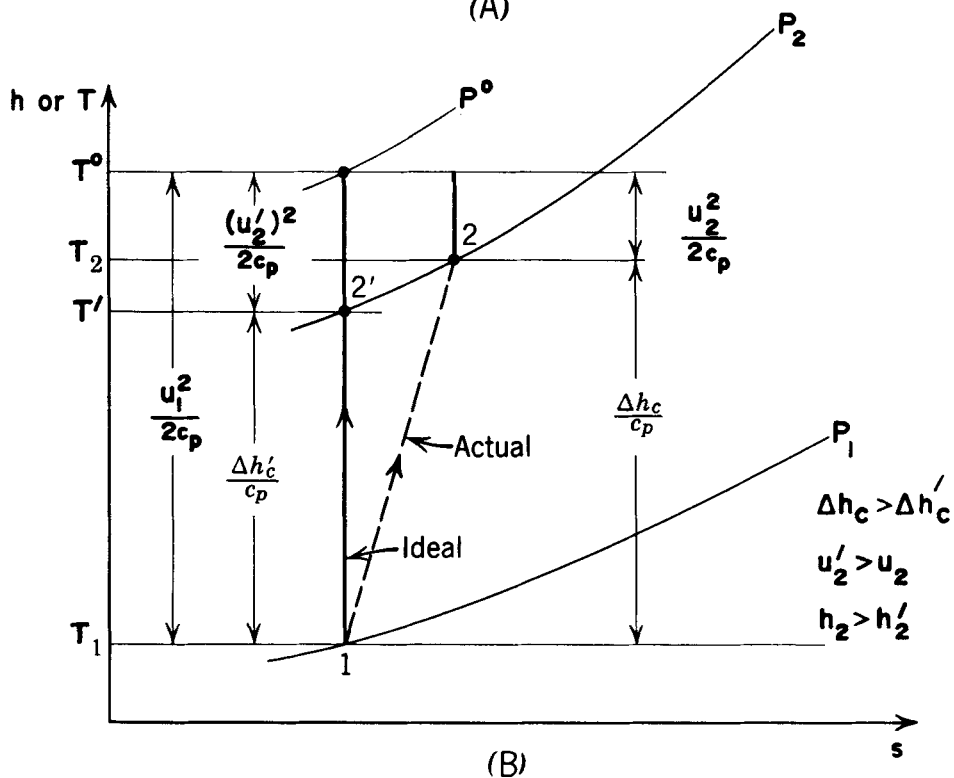
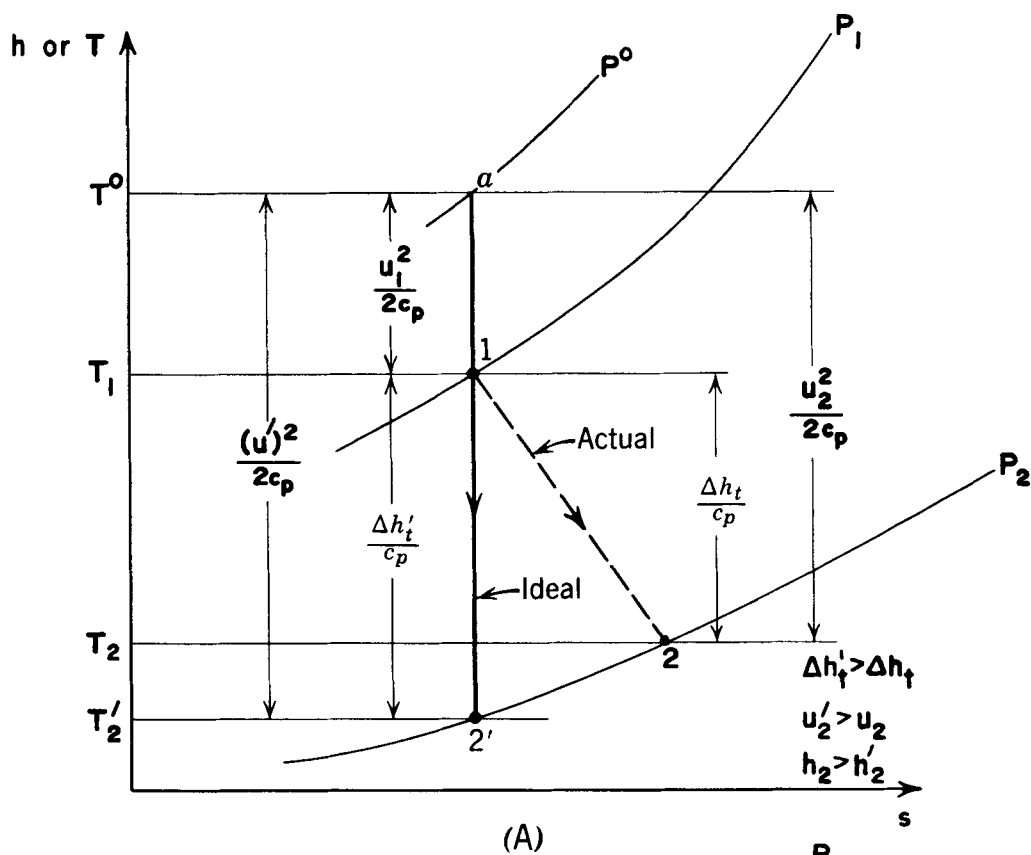
3-5.2.3 STAGNATION (OR TOTAL) PRESSURE (P^0)

The density of the gas in the aforementioned infinite reservoir is termed the *stagnation* or *total density*, and is denoted by ρ^0 . For a thermally perfect gas

$$P^0 = \rho^0 T^0 R \quad (3-54)$$

For the isentropic flow of an ideal gas, one obtains from Eq. 3-44

$$\frac{P^0}{P} = \left(\frac{T^0}{T} \right)^{\frac{\gamma}{\gamma-1}} \quad (3-55)$$

Figure 3-4. Comparison of Adiabatic and Isentropic Flow Processes on the hs -plane

Combining Eqs. 3-53 and 3-55, yields

$$\frac{P^O}{P} = \left[1 + \left(\frac{\gamma-1}{2} \right) M^2 \right]^{\frac{\gamma}{\gamma-1}} \quad (\text{isentropic}) \quad (3-56)$$

It should be noted that the total pressure P^O for a flow can always be calculated by merely assuming that it is accelerated isentropically from an infinite reservoir to the actual values of P and M .

3-5.2.4 RELATIONSHIP BETWEEN STAGNATION PRESSURE AND ENTROPY

It is shown in par. A-5.2.4 that the entropy change for an ideal gas is related to T^O and P^O by

$$ds = c_p d \left\{ \ln \left[\frac{T^O}{P^O (\gamma-1)/\gamma} \right] \right\} > 0 \quad (3-57)$$

For a real isoenergetic flow ($T^O = \text{constant}$), since $ds > 0$, the total pressure P^O must decrease in the direction of flow. If the flow is isentropic, however, $ds = 0$ and Eq. 3-57 shows that P^O remains constant. In other words, the decrease in the stagnation pressure of the gas may be regarded as a measure of the increase in the specific entropy of the gas.

For an irreversible simple adiabatic flow process (see par. A-5.2.4)

$$\Delta s = s_2 - s_1 = R \ln (P_1^O / P_2^O) > 0 \quad (3-58)$$

or

$$\frac{P_2^O}{P_1^O} = e^{-\Delta s/R} \quad (3-59)$$

If heat is transferred to a flowing gas or if the gas performs external work, there *cannot* be a conservation of the total pressure. The heat

added to a compressible fluid causes the total pressure to decrease even if the heating process is reversible. If the heating process is *irreversible* the decrease in the total pressure is larger than it would be for a corresponding reversible heat-exchange process.

3-5.2.5 STAGNATION (OR TOTAL) DENSITY (ρ^O)

From Eqs. 3-53 and 3-54 one obtains the following relationship between the *total density*, denoted by ρ^O , and the flow Mach number M . Thus

$$\frac{\rho^O}{\rho} = \left[1 + \left(\frac{\gamma-1}{2} \right) M^2 \right]^{\frac{\gamma}{\gamma-1}} \quad (3-60)$$

3-5.2.6 STAGNATION (OR TOTAL) ACOUSTIC SPEED (a^O)

From par. A-5.2.6, the stagnation acoustic speed in an ideal gas, denoted by a^O , is given by

$$a^O = \sqrt{\gamma P^O / \rho} = \sqrt{\gamma R T^O} \quad (3-61)$$

where, as before, the gas constant $R = R_u / \bar{m}$. Hence

$$\left(\frac{a^O}{a} \right)^2 = \frac{T^O}{T} = 1 + \left(\frac{\gamma-1}{2} \right) M^2 \quad (3-62)$$

3-5.3 ISENTROPIC EXHAUST VELOCITY

Let a flowing gas, having the stagnation enthalpy h^O , expand isentropically to the static specific enthalpy h' . The velocity of the gas corresponding to that expansion is termed the *isentropic exhaust velocity* and is denoted by u . Thus

$$u = \sqrt{2(h^O - h')} = \sqrt{2\Delta h'_t} \quad (3-63)$$

Let

$$Z_t = 1 - \left(\frac{P}{P^0} \right)^{\frac{\gamma-1}{\gamma}} = \text{expansion factor} \quad (3-64)$$

$$a^0 = \sqrt{\gamma R_u T^0 / \bar{m}} = \text{total acoustic speed} \quad (3-65)$$

Then, the isentropic exhaust velocity is given by

$$u = a^0 \sqrt{\left(\frac{2}{\gamma-1} \right) Z_t} \quad (3-66)$$

In terms of the flow Mach number M (combining Eqs. 3-13, 3-14, and 3-53) one obtains

$$u = M \sqrt{\frac{\gamma R T^0}{1 + \left(\frac{\gamma-1}{2} \right) M^2}} \quad (3-67)$$

3-5.4 CRITICAL CONDITIONS FOR THE STEADY, ONE-DIMENSIONAL ISENTROPIC FLOW OF AN IDEAL GAS

3-5.4.1 DEFINITION OF CRITICAL AREA AND CRITICAL ACOUSTIC SPEED

Assume an ideal gas flows isentropically out of an infinite reservoir wherein $u = 0$, $T = T^0$, $P = P^0$, and $\rho = \rho^0$. The gas flows in a variable area one-dimensional adiabatic frictionless duct as illustrated schematically in Fig. 3-5. At a particular cross-sectional area of the duct, the gas velocity u is equal to the local acoustic speed a ; i.e., $M = u/a = 1$ (see par. A-6).

The cross-sectional area where $M=1$, called the *critical area*, is denoted by A^* . The value of the acoustic speed a in A^* , called the *critical acoustic speed*, is denoted by a^* ; i.e., $u = u^* = a^*$.

3-5.4.2 CRITICAL THERMODYNAMIC PROPERTIES FOR THE STEADY, ONE-DIMENSIONAL, ISENTROPIC FLOW OF AN IDEAL GAS

From par. A-6.1 one obtains the following relationships for the critical flow parameters:

(a) Critical speed of sound (a^*)

$$a^* = \sqrt{\gamma P^* / \rho^*} = \sqrt{\gamma R T^*} \quad (3-68)$$

(b) Critical static temperature ratio (T^* / T^0)

$$\frac{T^*}{T^0} = \frac{a^*}{a^0} = \frac{2}{\gamma+1} \quad (3-69)$$

(c) Critical expansion ratio (P^* / P^0)

$$\frac{P^*}{P^0} = \left(\frac{T^*}{T^0} \right)^{\frac{\gamma}{\gamma-1}} = \left(\frac{2}{\gamma+1} \right)^{\frac{\gamma}{\gamma-1}} \quad (3-70)$$

(d) Critical density ratio (ρ^* / ρ^0)

$$\frac{\rho^*}{\rho^0} = \frac{v^0}{v^*} = \frac{P^*}{P^0} = \left(\frac{2}{\gamma+1} \right)^{\frac{\gamma}{\gamma-1}} \quad (3-71)$$

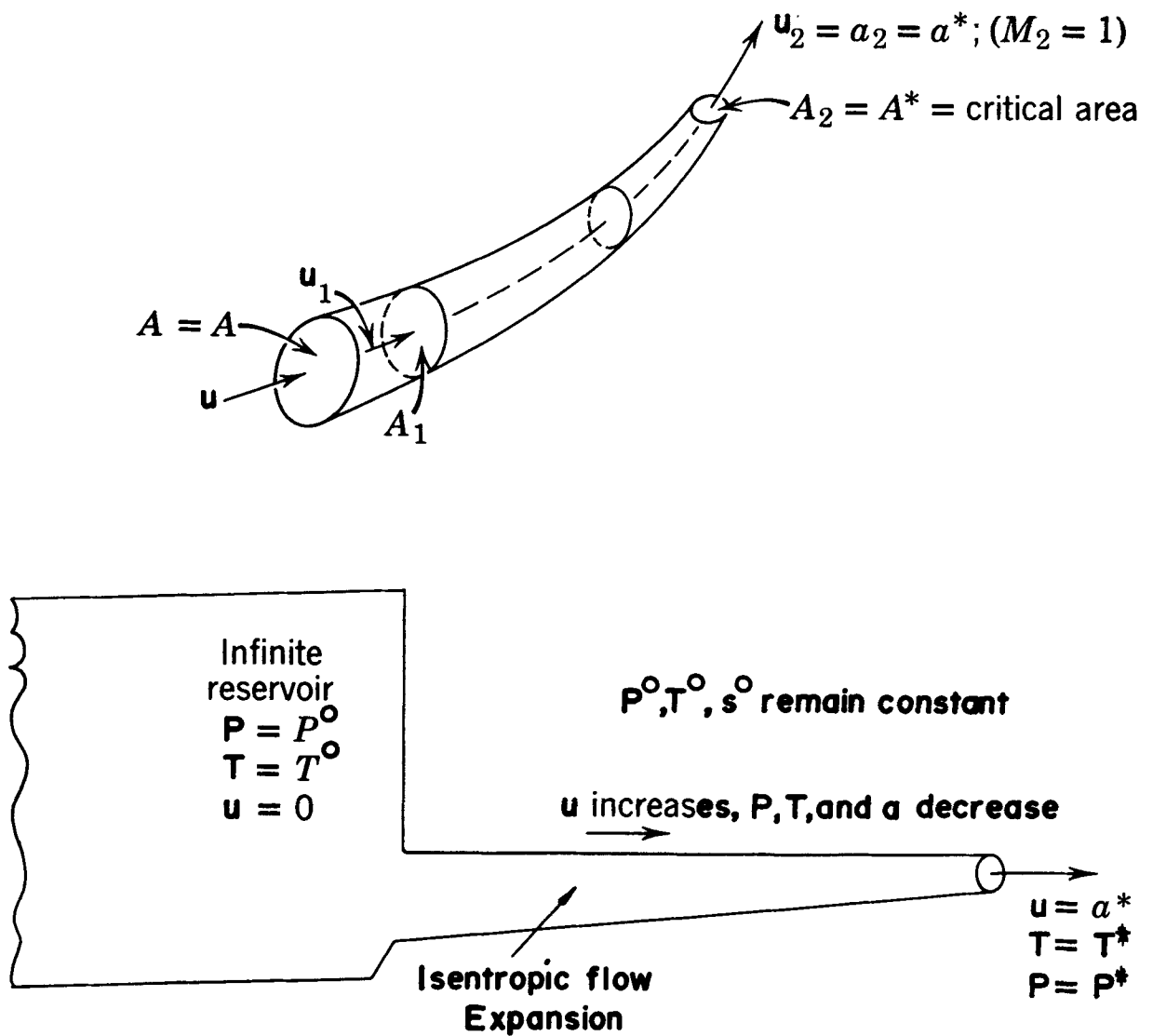
where v denotes the specific volume of the gas, cu ft/slug

(e) Dimensionless velocity (M^{*2})

It is readily shown that (see par. A-6.1.5)

$$M^{*2} = \left(\frac{u}{a^*} \right)^2 = \frac{\left(\frac{\gamma+1}{2} \right) M^2}{1 + \left(\frac{\gamma-1}{2} \right) M^2} \quad (3-72)$$

where a^* is given by Eq. 3-68.

Figure 3-5. Isentropic Flow Expansion of a Gas to the Critical Condition ($u = a^*$)

3-5.5 CONTINUITY EQUATIONS FOR STEADY ONE-DIMENSIONAL, ISENTROPIC FLOW OF AN IDEAL GAS

In general, the continuity equation for a steady one-dimensional flow is given by Eq. 3-18, which is repeated here for convenience. Thus

$$\dot{m} = \rho u A = \text{constant}$$

If the flowing fluid is an *ideal gas* and the flow is isentropic, the last equation may be rewritten as follows:

$$\dot{m} = \rho u A = \rho^* u^* A^* \quad (3-73)$$

where A^* denotes the *critical flow area* (where $u = a^*$). By definition

$$G \equiv \dot{m}/A = \text{flow density or mass velocity} \quad (3-74)$$

3-5.5.1 CRITICAL AREA RATIO (A/A^*)

From Eqs. 3-73 and 3-74, for a given flow passage, the critical area ratio A/A^* is given by

$$\frac{A}{A^*} = \frac{G^*}{G} \quad (3-75)$$

where G^* denotes the *critical flow density*; i.e., $G^* = \dot{m}^*/A^*$, $\dot{m} = \dot{m}^*$ where $A = A^*$.

3-5.5.2 CRITICAL AREA RATIO IN TERMS OF THE FLOW EXPANSION RATIO (P/P^0)

For a given stagnation pressure P^0 and static pressure P , the ratio P/P^0 is termed the *expansion ratio*. From par. A-6.3

$$\frac{A}{A^*} = \left[\frac{\left(\frac{2}{\gamma+1} \right)^{\frac{\gamma+1}{\gamma-1}}}{\frac{2}{\gamma-1} \left[\left(\frac{P}{P^0} \right)^{2/\gamma} - \left(\frac{P}{P^0} \right)^{\frac{\gamma+1}{\gamma}} \right]} \right]^{\frac{1}{2}} \quad (3-76)$$

or

$$\frac{A}{A^*} = \frac{\left(\frac{2}{\gamma+1} \right)^{\frac{1}{\gamma-1}}}{\left(\frac{P}{P^0} \right)^{1/\gamma} \sqrt{\frac{\gamma+1}{\gamma-1} \left[1 - \left(\frac{P}{P^0} \right)^{\frac{\gamma-1}{\gamma}} \right]}} \quad (3-76a)$$

3-5.5.3 CRITICAL AREA RATIO IN TERMS OF THE FLOW MACH NUMBER

$$\frac{A}{A^*} = \frac{1}{M} \left[\frac{1 + \left(\frac{\gamma-1}{2} \right) M^2}{\frac{\gamma+1}{2}} \right]^{\frac{\gamma+1}{2(\gamma-1)}} \quad (3-77)$$

and

$$M^2 = \frac{\left(\frac{2}{\gamma+1} \right) M^2}{1 - \left(\frac{\gamma-1}{\gamma+1} \right) M^2} \quad (3-78)$$

The dimensionless velocity M^* is proportional to the flow speed u of the ideal gas, while the Mach number M is not; $a^* = f(\gamma) = \text{constant}$, while $a = f(T)$.

3-5.6 REFERENCE SPEEDS (a^0), (a^*), AND (c_0)

The following reference speeds are characteristics for a given flow of an ideal gas:

(a) Stagnation acoustic speed (a^0)

$$a^0 = \sqrt{\gamma RT^0} = a^* \sqrt{\frac{\gamma+1}{2}} = c_0 \sqrt{\frac{2}{\gamma-1}} \quad (3-79)$$

(b) Maximum isentropic speed (c_0)

The maximum isentropic speed is defined in par. A-5.5, it is related to a^0 and a^* . Thus

$$c_0 = a^0 \sqrt{\frac{2}{\gamma-1}} = a^* \sqrt{\frac{\gamma+1}{\gamma-1}} \quad (3-80)$$

3-5.6.1 CONTINUITY EQUATIONS IN TERMS OF STAGNATION CONDITIONS

Eq. 3-29 gives the mass rate of flow of gas for a steady one-dimensional flow, where A is the cross-sectional area where the flow is measured, and M is the Mach number in A . Thus

$$\dot{m} = APM \sqrt{\frac{\gamma}{RT}}$$

In terms of the stagnation temperature T^0 and stagnation pressure P^0 , the last equation (see par. A-5.6) becomes

$$G = \frac{\dot{m}}{A} = \rho u = \frac{MP^0}{\sqrt{T^0}} \sqrt{\frac{\gamma}{R}} \left[\frac{1}{1 + \left(\frac{\gamma-1}{2}\right)M^2} \right]^{\frac{\gamma+1}{2(\gamma-1)}} \quad (3-81)$$

The last equation can be transformed to read (see par. A-5.6)

$$G = \frac{\dot{m}}{A} = \frac{P^0 \gamma}{a^0 \sqrt{\gamma-1}} \sqrt{\frac{2}{\left(\frac{P}{P^0}\right)^{\frac{2}{\gamma}} - \left(\frac{P}{P^0}\right)^{\frac{\gamma+1}{\gamma}}}} \quad (3-82)$$

where

$$a^0 \sqrt{\gamma RT^0}$$

3-5.6.2 CRITICAL MASS FLOW DENSITY (G^*)

For a given ideal gas and stagnation conditions the flow density becomes a maximum where $M=1$, that flow density is called the *critical flow density* and is denoted by G^* (see par. A-7). Thus

$$G^* = \dot{m}^*/A^* = \frac{P^0}{a^0} \left(\frac{2}{\gamma+1} \right)^{\frac{\gamma+1}{2(\gamma-1)}} \quad (3-83)$$

where, as before,

$$a^0 = \sqrt{\gamma RT^0}$$

Eq. 3-83 applies to the steady one-dimensional isentropic flow of an ideal gas.

3-5.7 TABLES OF ISENTROPIC FLOW FUNCTIONS FOR IDEAL GASES

Table 3-2 is a summary table giving the equations for calculating u_2/u_1 , P_2/P_1 , ρ_2/ρ_1 , T_2/T_1 , and A_2/A_1 for the steady, one-dimensional isentropic flow of an ideal gas between stations 1 and 2 of a flow channel.*

Table 3-3 lists the equations employed for calculating the values of M^* , P/P^0 , ρ/ρ^0 , T/T^0 , A/A^* , and F/F^* presented in Table A-1. The latter table presents the values of those isentropic flow functions as functions of M , with γ as a parameter.

*Since $T^0 = T \left[1 + \left(\frac{\gamma-1}{2}\right)M^2 \right]$ applies to all energetic flows, the equation for T/T^0 in Table A-1 applies to both isentropic and adiabatic steady one-dimensional flows.

TABLE 3-2
INTEGRAL EQUATIONS FOR ISENTROPIC
FLOW FUNCTIONS APPLIED TO TWO
ARBITRARY CROSS-SECTIONS OF
FLOW CHANNEL

$$\frac{u_2}{u_1} = \frac{M_2}{M_1} \sqrt{\frac{1 + \left(\frac{\gamma-1}{2}\right) M_1^2}{1 + \left(\frac{\gamma-1}{2}\right) M_2^2}}$$

$$\frac{P_2}{P_1} = \left[\frac{1 + \left(\frac{\gamma-1}{2}\right) M_1^2}{1 + \left(\frac{\gamma-1}{2}\right) M_2^2} \right]^{\frac{\gamma}{\gamma-1}}$$

$$\frac{\rho_2}{\rho_1} = \frac{v_1}{v_2} = \left[\frac{1 + \left(\frac{\gamma-1}{2}\right) M_1^2}{1 + \left(\frac{\gamma-1}{2}\right) M_2^2} \right]^{\frac{1}{\gamma-1}}$$

$$\frac{T_2}{T_1} = \left(\frac{a_2}{a_1} \right)^2 = \frac{1 + \left(\frac{\gamma-1}{2}\right) M_1^2}{1 + \left(\frac{\gamma-1}{2}\right) M_2^2}$$

$$\frac{A_2}{A_1} = \frac{M_1}{M_2} \left[\frac{1 + \left(\frac{\gamma-1}{2}\right) M_2^2}{1 + \left(\frac{\gamma-1}{2}\right) M_1^2} \right]^{\frac{\gamma+1}{2(\gamma-1)}}$$

TABLE 3-3
ISENTROPIC FUNCTIONS FOR THE
FLOW OF IDEAL GASES

$$M^* = u/a^* = \frac{\sqrt{\left(\frac{\gamma+1}{2}\right) M^2}}{\sqrt{1 + \left(\frac{\gamma-1}{2}\right) M^2}}$$

$$\frac{P}{P^0} = \left[\frac{1}{1 + \left(\frac{\gamma-1}{2}\right) M^2} \right]^{\frac{\gamma}{\gamma-1}}$$

$$\frac{\rho}{\rho^0} = \left[\frac{1}{1 + \left(\frac{\gamma-1}{2}\right) M^2} \right]^{\frac{1}{\gamma-1}}$$

$$\frac{T}{T^0} = \frac{1}{1 + \left(\frac{\gamma-1}{2}\right) M^2}$$

$$\frac{A}{A^*} = \frac{1}{M} \left[\frac{1 + \left(\frac{\gamma-1}{2}\right) M^2}{\frac{\gamma+1}{2}} \right]^{\frac{\gamma+1}{2(\gamma-1)}}$$

$$F/F^* = \frac{1 + \gamma M^2}{M \sqrt{2(\gamma+1) \left[1 + \left(\frac{\gamma-1}{2}\right) M^2 \right]}}$$

The impulse function is discussed in pars. A-3.2.1 and A-6.5. For a perfect gas

$$F = PA(1 + \gamma M^2)$$

3-6 STEADY ONE-DIMENSIONAL ADIABATIC FLOW IN A CONSTANT AREA DUCT WITH WALL FRICTION (FANNO FLOW)

The adiabatic flow of a compressible fluid in a constant area duct is characterized by the following conditions:

$$\delta Q = \delta W = d\dot{m} = d\gamma = d\bar{m} = \delta D/A = dA/A = 0$$

$$ds \neq 0, \text{ and } f \frac{u^2 4dx}{2D} \neq 0 \quad (3-84)$$

where D the hydraulic diameter of the duct, dx is an element of the duct length, A is the area of the duct, D is the drag of bodies immersed in the fluid, and f is the friction coefficient for the duct.

3-6.1 FRICTION COEFFICIENT (f)

If τ denotes the wall shearing stress, then (see par A-8.1.1)

$$f = \frac{\tau}{\frac{1}{2}\rho u^2} \quad (3-85)$$

Experiments show that

$$f = f(\text{Re}, \epsilon/D) \quad (3-86)$$

where ϵ denotes the roughness of the wall surface.

3-6.2 PRINCIPAL EQUATIONS FOR FANNO FLOW

The continuity, momentum, and energy equations are as follows:

(a) Continuity

$$G = \dot{m}/A = \rho u \quad (3-87)$$

(b) Momentum

$$\frac{dp}{p} + \frac{du^2}{2} + f \frac{u^2 4dx}{2D} = 0 \quad (3-88)$$

(c) Energy

$$h^0 = h + \frac{u^2}{2} = \text{constant} \quad (3-89)$$

3-6.3 FANNO LINE EQUATION

From Eqs. 3-84 and 3-86 one obtains

$$h_1 + \frac{1}{2}(Gv_1)^2 = h + \frac{1}{2}(Gv)^2 = \text{constant} \quad (3-90)$$

Eq. 3-90 is called the Fanno line equation. It relates the local values of h and $\rho = 1/v$ for different specified initial values of h_1 and $\rho_1 = 1/v_1$. Figure 3-6 illustrates schematically a Fanno line, for a specified $G = \dot{m}/A$, plotted in the h - s -plane.

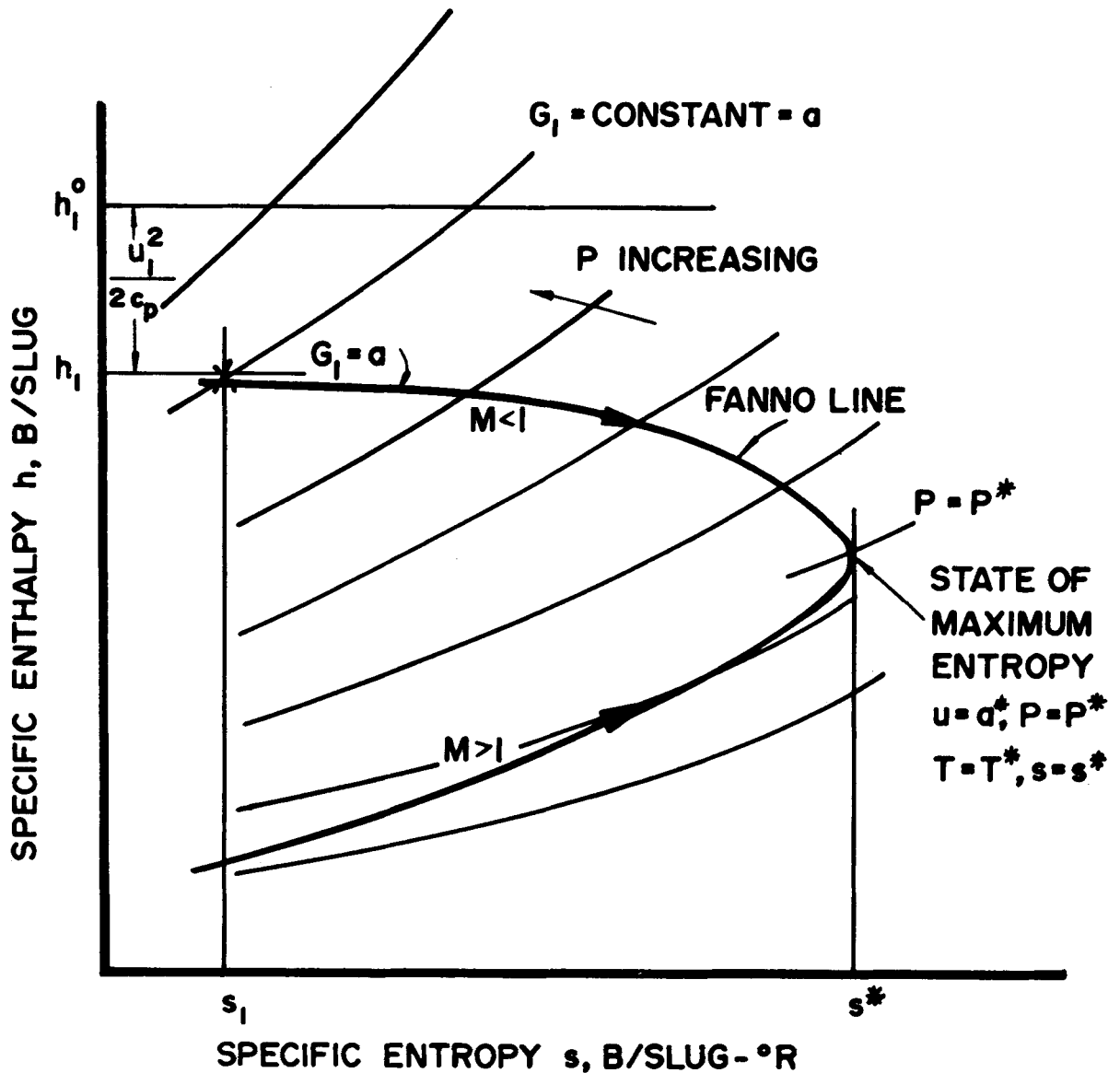
A Fanno line is the locus of the thermodynamic states for a compressible fluid flowing adiabatically ($h^0 = \text{constant}$) in a constant area duct in the presence of wall friction alone. A Fanno flow has the following characteristics:

(a) The stagnation enthalpy h^0 remains constant.

(b) Each value of $G = \dot{m}/A$ —for the same initial values of h_1 and $\rho_1 = 1/v_1$ —gives rise to a separate Fanno line, as illustrated in Fig. 3-7.

(c) If the initial conditions ($h_1, \rho_1 = 1/v_1$) are held constant, all Fanno lines for those initial conditions intersect at h_1, ρ_1 .

(d) The length of constant area duct, denoted by L , for accomplishing a specified change in the thermodynamic state of the fluid depends upon

Figure 3-6. A Fanno Line Plotted in the hs -plane

- (i) the friction coefficient f , and
- (ii) the entropy gradient ds/dx .
- (e) The path of a compressible fluid along a Fanno line is always in the direction of *increasing entropy*, so that the second law of thermodynamics will be satisfied.
- (f) The lower branch of a Fanno line, that lying to the left of the state corresponding to $s = s_{\max}$ (see Fig. 3-6), cannot be reached by a continuous flow process starting from the upper branch. The lower branch represents the locus of the thermodynamic states for the flowing compressible fluid starting at

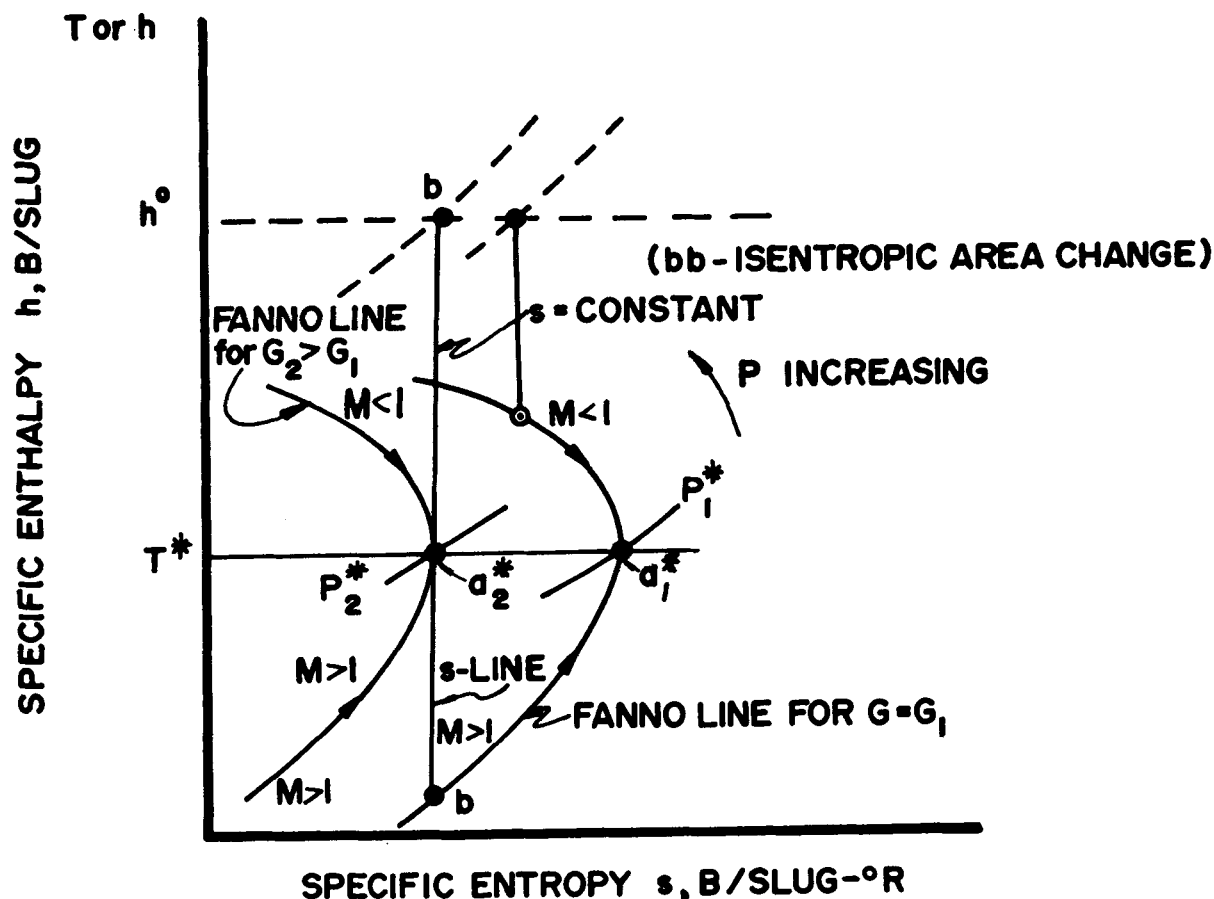


Figure 3-7. Comparison of Fanno Lines for Two Different Values of the Flow Density ($G = \dot{m}/A$)

values of h , s , and P which are smaller than those corresponding to $s = s_{\max}$. Such a process is a *supersonic flow compression* (diffusion).

Friction and drag effects alone are responsible for the change in the thermodynamic state of the fluid as it flows through the constant area duct. Because the adiabatic is irreversible, the entropy of the fluid must increase in the direction of flow. Consequently the direction of flow along a Fanno line must always be that which leads to $s = s_{\max}$. The velocity of the

fluid when $s = s_{\max}$ is equal to the local acoustic speed, i.e., $u = u^* = a^*$. Hence, $s_{\max} = s^*$.

The acoustic speed a^* for a Fanno line should not be confused with the *critical acoustic speed* a^* for an isentropic flow (see par. A-6.1.1). The asterisk attached to a symbol — such as a , u , P , T , etc. — merely denotes the value of the pertinent quantity when $M = 1$ for the flow process under consideration.

The following conclusions are applicable to a Fanno flow:

- (1) If the flow is subsonic ($M < 1$), then:
 - (a) u and M increase in the direction of flow, and
 - (b) simultaneously h and P decrease.
- (2) If the flow is supersonic ($M > 1$), then:
 - (a) u and M decrease in the direction of flow, and
 - (b) simultaneously h and P increase.
- (3) A subsonic Fanno flow cannot be transformed into a supersonic flow; it can only approach a sonic flow ($M=1$), as a limit.
- (4) A supersonic Fanno flow cannot be transformed by a continuous process into a subsonic flow; it can only be reduced to a sonic flow ($M=1$) as a limit. For a supersonic flow to be transformed into a subsonic flow some form of discontinuity in the flow, such as a compression shock, must occur.
- (5) There is a definite length of the duct, denoted by L^* , that causes the flow Mach number to become unity. When $M=1$ the flow is said to be *choked*.
- (6) Reducing the static pressure of the surroundings, denoted by P^0 , into which the flow from the duct is discharged to a value $P^0 < P^*$ has no effect upon the fluid flowing inside the duct when $u_{\text{exit}} = u^* = a^*$; a small pressure disturbance cannot be propagated into the core of the flow.
- (7) When $P_{\text{exit}} = P^*$, the expansion of the fluid from P^* to P_a takes place beyond the exit section of the duct.

- (8) Because the entropy of the fluid increases in the direction of flow, due to the wall friction, the stagnation pressure P^0 decreases in the direction of flow.

3-6.4 FANNO FLOW WITH IDEAL GASES

3-6.4.1 PRINCIPAL EQUATIONS

The following principal equations govern the Fanno flow of an ideal gas (see par. A-8.3)

(a) Continuity

$$G = \dot{m}/A = \rho u = PM\sqrt{\gamma/RT} = \text{constant} \quad (3-91)$$

(b) Momentum

$$\frac{dP}{P} + \gamma M^2 \left[\frac{1 + (\gamma - 1) M^2}{2(1 - M^2)} \right] \left(4f \frac{dx}{D} \right) = 0 \quad (3-92)$$

(c) Energy

$$c_p dT^0 = c_p dT + d\left(\frac{u^2}{2}\right) = 0 \quad (3-93)$$

(d) Equation of state

$$P = \rho RT \text{ or } \frac{dP}{P} = \frac{d\rho}{\rho} + \frac{dT}{T} \quad (3-94)$$

(e) Mach number

$$\frac{dM^2}{M^2} = \frac{du^2}{u^2} - \frac{dT}{T} = 2u \frac{du}{u} - \frac{dT}{T} \quad (3-95)$$

(f) Impulse function

$$\frac{dF}{F} = \frac{dP}{P} + \left(\frac{\gamma M^2}{1 + \gamma M^2} \right) \frac{dM^2}{M^2} \quad (3-96)$$

Eqs. 3-91 through 3-96 form a system of linear equations relating the *dependent variables*

dM^2/M^2 , du/u , etc., with the flow Mach number M and the friction parameter $4f dx/D$.

3-6.4.2 CRITICAL DUCT LENGTH FOR THE FANNO FLOW OF AN IDEAL GAS

Let f denote the mean value of the friction coefficient for the duct length $\Delta x = L^* - L$; $x=L$ where $M=M$ and $x=L^*$ where $M=1$. From par. A-8.3.2, the critical length L^* is given by

$$4f \frac{L^*}{D} = \frac{1-M^2}{2\gamma M^2} + \left(\frac{\gamma+1}{2\gamma} \right) \ln \left[\frac{\left(\frac{\gamma+1}{2} \right) M^2}{1 + \left(\frac{\gamma-1}{2} \right) M^2} \right] \quad (3-97)$$

3-6.4.3 DUCT LENGTH FOR A SPECIFIED CHANGE IN MACH NUMBER

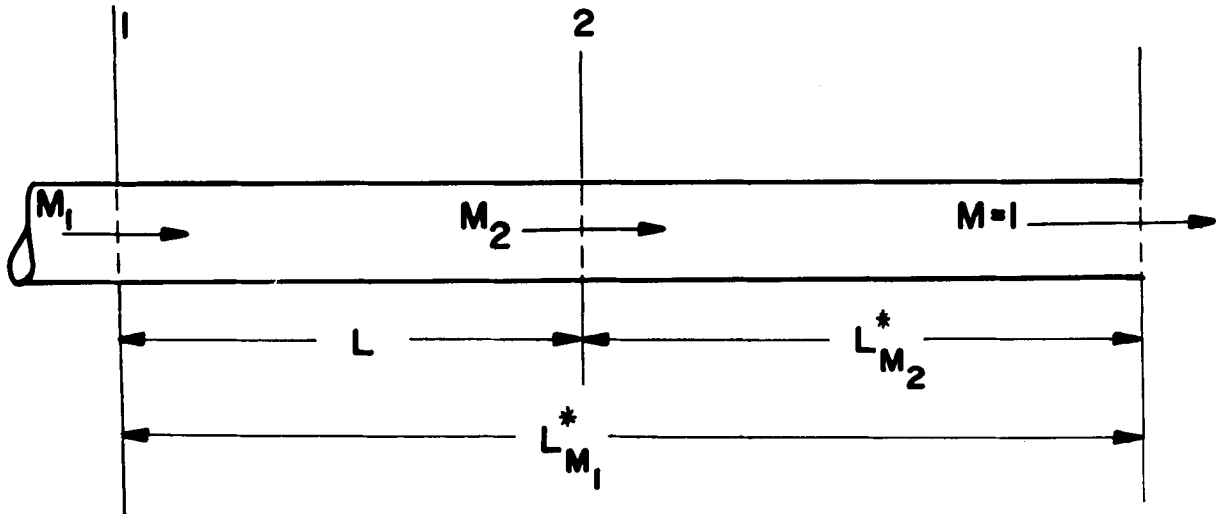
Fig. 3-8 illustrates schematically the physical situation for determining the duct length

required to change the flow Mach number from M_1 to M_2 (see par. A-8.3.3).

It can be shown that

$$4f \frac{L}{D} = \frac{1}{\gamma M_1^2} \left(\frac{M_2^2 - M_1^2}{M_2^2} \right) + \left(\frac{\gamma-1}{\gamma} \right) \ln \left\{ \frac{M_1 \left[1 + \left(\frac{\gamma-1}{2} \right) M_2^2 \right]}{M_2 \left[1 + \left(\frac{\gamma-1}{2} \right) M_1^2 \right]} \right\} \quad (3-98)$$

By means of Eq. 3-98 one can compute the length of duct L , of hydraulic diameter D , having the mean friction coefficient f , for changing M_1 to M_2 when the flowing gas has a specific heat ratio of γ .



$$4f \gamma L / D = \left(4f \gamma \frac{L^*}{D} \right)_{M_1} - \left(4f \gamma \frac{L^*}{D} \right)_{M_2}$$

Figure 3-8. Determination of Duct Length To Accomplish a Specified Change in Flow Mach Number (Fanno Line)

From the equations of the entropy gradient ds/dx and the Mach number gradient dM/dx for the Fanno flow of an ideal gas (see pars. A-8.3.5 and A-8.3.6) one obtains the characteristics of the Fanno flow.

3-6.4.4 GENERAL CHARACTERISTICS OF THE FANNO FLOW OF AN IDEAL GAS

- (1) If the flow is initially subsonic ($M < 1$), the effect of wall friction is to *increase* the Mach number in the direction of flow.
- (2) If the flow is initially supersonic ($M > 1$), the effect of wall friction is to *decrease* the Mach number in the direction of flow.
- (3) Regardless of whether the initial flow is either subsonic or supersonic at a given cross-section of the constant area duct, the flow Mach number approaches the value $M=1$ as a *limiting value*. When the flow Mach number attains the value $M=1$ the flow is said to be *choked*, and that the condition ($M=1$) corresponds to the thermodynamic state where the specific entropy of the fluid is a maximum (see par. A-8.3.6).

3-6.5 EQUATIONS FOR COMPILING TABLES FOR FANNO FLOW FUNCTIONS, FOR IDEAL GASES

For calculation purposes it is convenient to employ the flow condition where $M = 1$ as a *reference condition*, which condition is denoted by attaching a superscript asterisk (*) to the pertinent variables. Since the variables P/P^* , P^0/P^{0*} , T/T^* , etc., are functions of M and γ , tables for the preceding variables as functions of M for different values of γ are readily computed.

Table 3-4 presents the equations employed for calculating Table A-2 (Compressible Flow Functions for Fanno Flow).

TABLE 3-4
EQUATIONS FOR COMPUTING FANNO FLOW FUNCTIONS FOR IDEAL GASES

(Conditions: Adiabatic flow in a constant area duct in the presence of only wall friction.)

$$\frac{T}{T^*} = \frac{\gamma+1}{2 \left[1 + \left(\frac{\gamma-1}{2} \right) M^2 \right]}$$

$$\frac{P}{P^*} = \frac{1}{M} \left[\frac{(\gamma+1)/2}{1 + \left(\frac{\gamma-1}{2} \right) M^2} \right]^{\frac{1}{2}}$$

$$\frac{\rho}{\rho^*} = \frac{u^*}{u} = \frac{1}{M^*} = \frac{1}{M} \left[\frac{1 + \left(\frac{\gamma-1}{2} \right) M^2}{\frac{\gamma-1}{2}} \right]^{\frac{1}{2}}$$

$$\frac{P^0}{P^{0*}} = \frac{1}{M} \left[\frac{1 + \left(\frac{\gamma-1}{2} \right) M^2}{\frac{\gamma+1}{2}} \right]^{\frac{\gamma+1}{2(\gamma-1)}}$$

$$\frac{F}{F^*} = \frac{1 + \gamma M^2}{M \sqrt{2(\gamma+1) \left[1 + \left(\frac{\gamma-1}{2} \right) M^2 \right]}}$$

$$\frac{4fL^*}{D} = \frac{1-M^2}{\gamma M^2} + \frac{\gamma+1}{2\gamma} \ln \left\{ \frac{\left(\frac{\gamma+1}{2} \right) M^2}{1 + \left(\frac{\gamma-1}{2} \right) M^2} \right\}$$

EXAMPLE 3-1.

Compute L/D as a function of the initial Mach number M_1 for air ($\gamma = 1.40$), to cause choking in a smooth constant area duct. Assume air is an ideal gas, and that the average value of the friction coefficient is $f = 0.0025$.

SOLUTION.

From Table A-2, for $M_1 = 0.2$, $4fL^*/D = 14.553$

$$\text{Hence } L/D = \frac{14.53}{4(0.0025)} = 1453$$

In a similar manner one obtains the results presented below

M_1	$4fL^*/D$	L/D	P^0/P^0^*	P^0^*/P^0
0	∞	∞	∞	0
0.2	14.53	1,453	2.96	0.338
0.4	2.31	231	1.59	0.629
0.6	0.491	49.1	1.19	0.840
0.8	0.072	7.2	1.038	0.963
1.0	0	0	1.00	1.000
1.5	0.136	13.6	1.176	0.850
2.0	0.305	30.5	1.688	0.592
4.0	0.633	63.3	10.72	0.924
10.0	0.787	78.7	535.9	.0018
∞	0.821	82.1	∞	∞

The results tabulated in Example 3-1 show that for a purely supersonic flow ($M > 1$) the maximum value of L/D is limited by choking to $L/D = 82.1$ irrespective of the value of M_1 (based on $\gamma = 1.4$ and $f = 0.0025$).

3-7 STEADY ONE-DIMENSIONAL FRICTIONLESS FLOW IN A CONSTANT AREA DUCT WITH STAGNATION TEMPERATURE CHANGE (RAYLEIGH FLOW)

A *Rayleigh flow* is defined as one which is steady, one-dimensional, frictionless, takes place in a duct of constant area, and is accompanied by a change in stagnation enthalpy ($dh^0 \neq 0$). Such a flow is characterized by the following:

$$\delta W = \delta F_f = d\dot{m}/\dot{m} = dA/A = 0 \quad (\delta Q \neq 0) \quad (3-99)$$

In general, a flow which is accompanied by heat transfer to (or from) the flowing fluid is called a *diabatic flow*. A flow characterized by Eq. 3-99 is termed either a *Rayleigh flow* or a *simple diabatic flow* (see par. A-9).

For a Rayleigh flow, all changes in the stagnation enthalpy of the flowing fluid are due to heat transfer to (or from) the fluid. Consequently, the analytical results pertinent to a Rayleigh flow are limited to the following:

- simple diabatic flows for which the effect of heat transfer overwhelms any effects due to fluid frictions, and
- flows where the heat transfer process is confined to such a short length of the duct that the effects of friction may be ignored.

Fig. 3-9 illustrates the manner in which the flow parameters for a Fanno flow vary with the initial flow Mach number, for an ideal gas with $\gamma = 1.40$.

3-7.1 PRINCIPAL EQUATIONS FOR A RAYLEIGH FLOW

Fig. 3-10 illustrates schematically the physical situation governing a Rayleigh flow. The

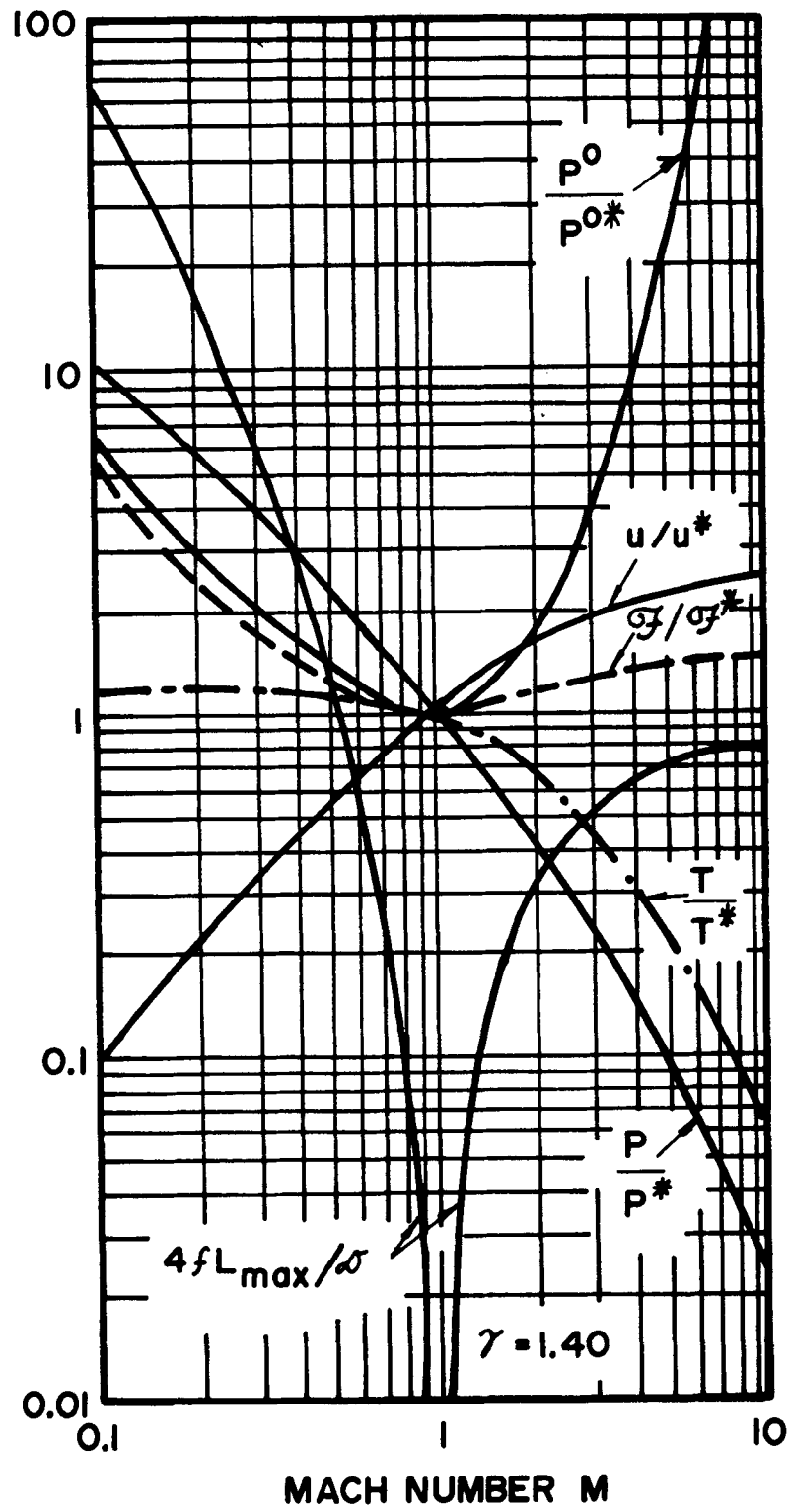


Figure 3-9. Flow Parameters for a Fanno Line for a Gas with $\gamma = 1.40$

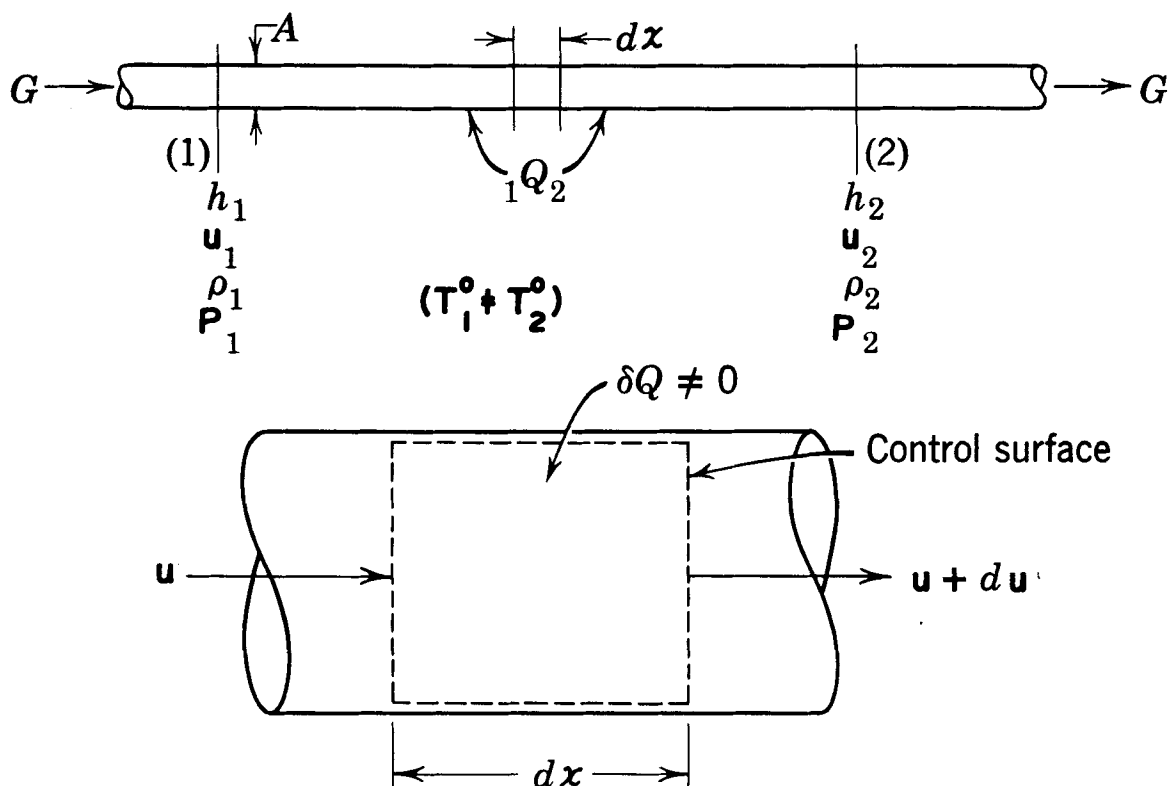


Figure 3-10. Physical Situation for a Rayleigh Flow

following principal equations apply (see par. A-9):

(a) *Continuity*

$$u = G/\rho$$

(b) *Momentum*

$$\frac{dP}{P} + u du = 0$$

(c) *Energy*

$$h_1 + \frac{u_1^2}{2} + {}_1Q_2 = h_2 + \frac{u_2^2}{2}$$

where ${}_1Q_2$ is the heat added per unit mass of fluid between Station 1 and 2.

(d) *Rayleigh line equation*

Combining Eqs. 3-100 and 3-101, one obtains

$$P_2 + Gu_2 = P_1 + Gu_1 = \text{constant} \quad (3-103)$$

Introducing the impulse function F (see Eq. A-56), one obtains

$$F = PA + \dot{m}u = P + Gu \quad (3-104)$$

Combining Eqs. 3-100 and 3-102, yields

$$P_2 - P_1 = G^2 \left(\frac{1}{\rho_1} - \frac{1}{\rho_2} \right) = G^2 (v_1 - v_2) \quad (3-105)$$

where $v = 1/\rho$ = the specific volume of the fluid.

Since G is a constant, Eq. 3-105 is the equation of a straight line drawn in the Pv -plane, and that line is the locus of the thermodynamic states for the fluid for a constant value of the flow density G , as illustrated in Fig. 3-11.

A curve which is the locus of the thermodynamic states of a fluid, for a Rayleigh flow, is called a *Rayleigh line*.

3-7.2 RAYLEIGH LINE

3-7.2.1 GENERAL CHARACTERISTICS

Fig. 3-11 illustrates a Rayleigh line plotted in the Pv -plane, and Fig. 3-12 illustrates a Rayleigh line plotted in the hs -(or Ts)-plane.

Refer to Fig. 3-11. A Rayleigh line in the Pv -plane is a straight line having a negative slope. Thus

$$-\left(\frac{\partial P}{\partial v}\right)_G = \tan \alpha = G^2 \quad (3-106)$$

Each value of G corresponds to a different Rayleigh line. Lines of constant enthalpy are also illustrated schematically in Fig. 3-11, and one may conclude from Fig. 3-11 as follows:

- (a) Increasing h for the fluid, from h_1 to h_2 , causes its density ρ and its static pressure P to decrease.
- (b) Decreasing h , from h_2 to $h_1 < h_2$ by cooling the fluid, increases both ρ and P .

Refer to Fig. 3-12. It is evident that a Rayleigh line plotted in the hs -plane has two branches. As in the case of the Fanno line, each branch corresponds to a different type of flow. The *upper branch* is the locus of the thermodynamic states attainable by a *subsonic* flow ($M < 1$) by heating the fluid from an initial state (such as state 1) having a value of specific

entropy smaller than $s_{\max} = s^*$; the state corresponding to s^* is termed the *thermal choking state*.

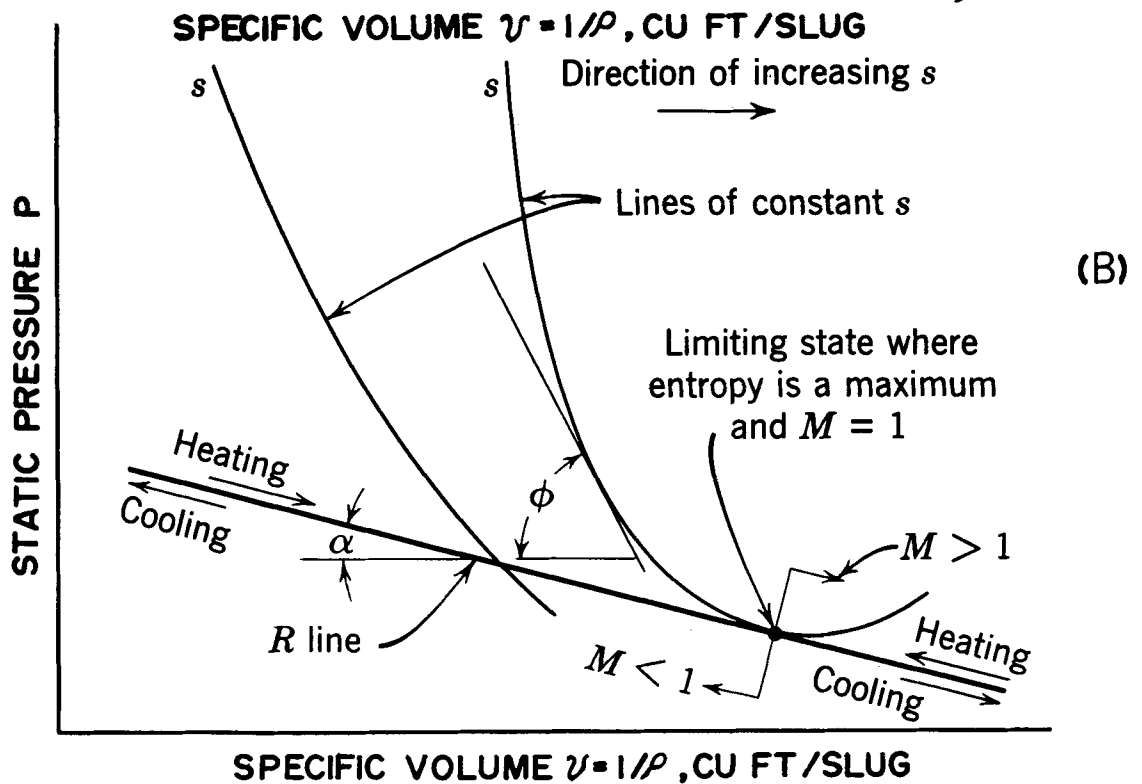
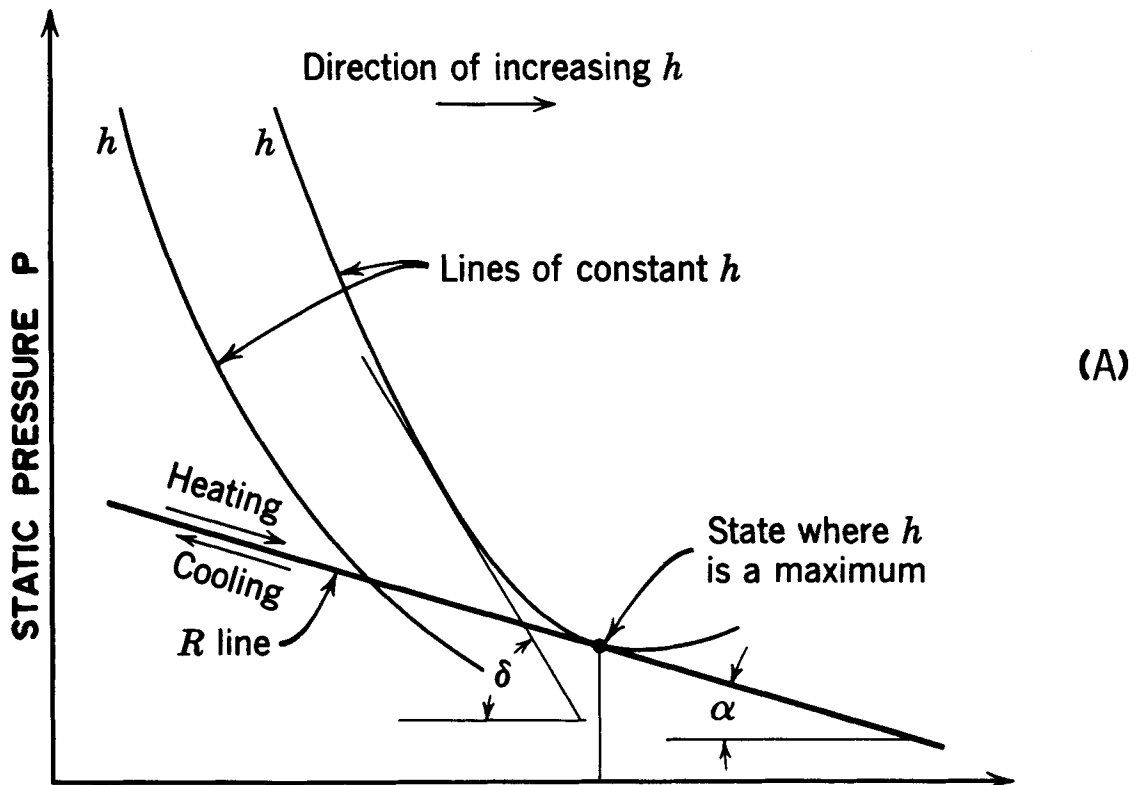
The *lower branch* of the Rayleigh line (see Fig. 3-12) is the locus of the thermodynamic states which are attainable by heating a *supersonic* flow ($M > 1$) from an initial state, such as state 2, where $s < s^*$ to s^* .

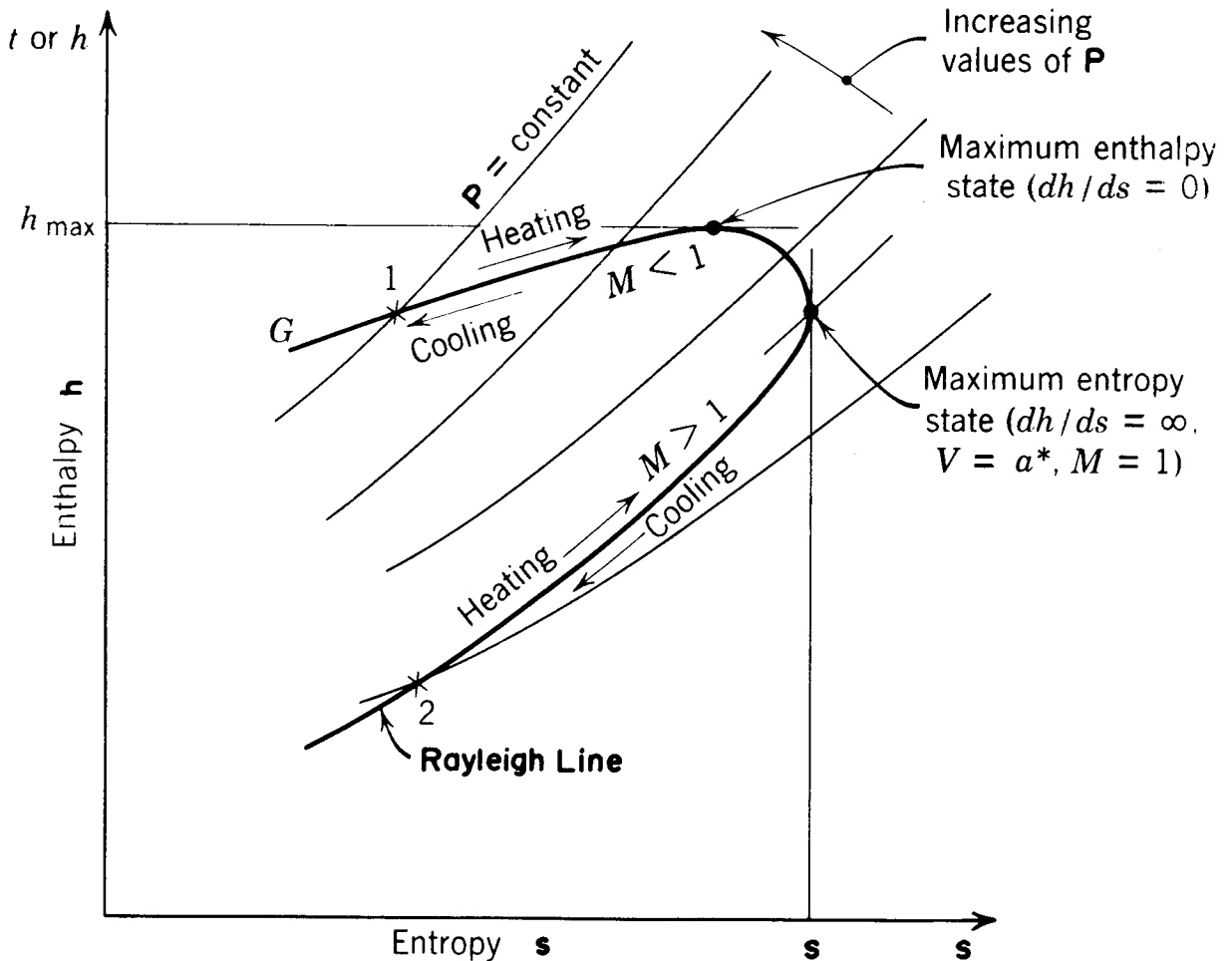
Hence, *heating* a compressible fluid flowing in a frictionless constant area duct accelerates the fluid toward $M=1$, as a limit, if the flow is subsonic, but decelerates to $M=1$, as a limit, if the initial flow is supersonic.

3-7.2.2 CHARACTERISTICS OF THE RAYLEIGH LINE FOR THE FLOW OF AN IDEAL GAS

If the flowing fluid is an ideal gas, the Rayleigh line has the following characteristics:

- (a) If the initial flow is subsonic, heating it results in an increase in the Mach number and a decrease in the static of the fluid; the drop in the static pressure is due to the rate of change in the momentum of the fluid, and it is called the *momentum pressure loss*.
- (b) Heating the gas in the subsonic flow range causes its temperature to increase until a maximum value of T is reached when $M = 1/\sqrt{\gamma}$.
- (c) Heating the gas in the subsonic flow range will cause the flow to become *thermally choked*, when $M=1$, unless the initial conditions are altered.
- (d) Increasing the initial Mach number of the gas, in the subsonic flow range, reduces the amount of static enthalpy which can be added to the flowing gas.

Figure 3-11. Rayleigh Line Plotted in the Pv -plane

Figure 3-12. Rayleigh Line Plotted in the hs -(or Ts)-plane

- (e) Heating the flowing gas in the supersonic flow range causes the Mach number to decrease and the static pressure to increase. The flow becomes thermally choked when $M=1$ if the initial conditions are not altered.

3-7.3 RAYLEIGH FLOW EQUATIONS FOR IDEAL GASES

Let the subscripts 1 and 2 refer to two stations in a frictionless constant area duct.

Then for the Rayleigh flow of an ideal gas

- (a) *Impulse function per unit area (F/A)*

$$F/A = P(1 + \gamma M^2) = \text{constant} \quad (3-107)$$

- (b) *Static pressure ratio (P_2/P_1)*

$$P_2/P_1 = (1 + \gamma M_1^2) / (1 + \gamma M_2^2) \quad (3-108)$$

(c) *Density ratio* (ρ_2/ρ_1)

$$\begin{aligned}\rho_2/\rho_1 &= u_1/u_2 \\ &= M_1^2 (1 + \gamma M_2^2) / \left[M_2^2 (1 + \gamma M_1^2) \right] \quad (3-109)\end{aligned}$$

(d) *Static temperature ratio* (T_2/T_1)

$$\begin{aligned}T_2/T_1 &= (P_2 M_2)^2 / (P_1 M_1^2) \\ &= (M_2/M_1)^2 (1 + \gamma M_1^2)^2 / (1 + \gamma M_2^2)^2 \quad (3-110)\end{aligned}$$

(e) *Stagnation temperature ratio* (T_2^O/T_1^O)

$$\frac{T_2^O}{T_1^O} = \left[\frac{M_2 (1 + \gamma M_1^2)}{M_1 (1 + \gamma M_2^2)} \right]^2 \left[\frac{1 + \left(\frac{\gamma-1}{2}\right) M_2^2}{1 + \left(\frac{\gamma-1}{2}\right) M_1^2} \right] \quad (3-111)$$

(f) *Stagnation pressure ratio* (P_2^O/P_1^O)

$$\begin{aligned}\frac{P_2^O}{P_1^O} &= \frac{P_1}{P_2} \left(\frac{T_2^O}{T_1^O} \right)^{\frac{\gamma}{\gamma-1}} \\ &= \left(\frac{1 + \gamma M_1^2}{1 + \gamma M_2^2} \right) \left[\frac{1 + \left(\frac{\gamma-1}{2}\right) M_2^2}{1 + \left(\frac{\gamma-1}{2}\right) M_1^2} \right]^{\frac{\gamma}{\gamma-1}} \quad (3-112)\end{aligned}$$

(g) *Entropy change* ($\Delta s/R$)

$$\begin{aligned}\frac{\Delta s}{R} &= \ln \left(\frac{T_2}{T_1} \right)^{\frac{\gamma}{\gamma-1}} \frac{P_1}{P_2} \\ &= \left[\ln \left(\frac{M_2}{M_1} \right)^{\frac{2\gamma}{\gamma-1}} \right] \left(\frac{1 + \gamma M_1^2}{1 + \gamma M_2^2} \right)^{\frac{\gamma+1}{\gamma-1}} \quad (3-113)\end{aligned}$$

It is seen from Eq. 3-111 that the Mach number M_2 for the Rayleigh flow of an ideal gas

depends upon the initial flow Mach number M_1 and the stagnation temperature ratio T_2^O/T_1^O . Eq. 3-112 shows that the stagnation pressure ratio P_2^O/P_1^O depends upon the change in Mach number from M_1 to M_2 .

3-7.4 EQUATIONS FOR TABLES OF RAYLEIGH FLOW FUNCTIONS FOR IDEAL GASES

For calculation purposes it is desirable to relate the flow parameters for the Rayleigh flow of an ideal gas to a reference state. As was done for Fanno flow, the reference state for a Rayleigh flow is that corresponding to $M=1$. Employing an asterisk superscript (*) to denote the reference state where $M=1$, one obtains the following equations¹ (see par. A-9):

$$\frac{T^O}{T^O*} = \frac{2(\gamma+1)M^2 \left[1 + \left(\frac{\gamma-1}{2}\right) M^2 \right]}{(1 + \gamma M^2)^2} \quad (3-114)$$

$$\frac{T}{T^*} = \left(\frac{1 + \gamma}{1 + \gamma M^2} \right)^2 M^2 \quad (3-115)$$

$$\frac{P}{P^*} = \frac{1 + \gamma}{1 + \gamma M^2}$$

$$\frac{P^O}{P^O*} = \left(\frac{2}{\gamma+1} \right)^{\frac{\gamma}{\gamma-1}} \left(\frac{1 + \gamma}{1 + \gamma M_2^2} \right) \left[1 + \left(\frac{\gamma-1}{2}\right) M^2 \right]^{\frac{\gamma}{\gamma-1}}$$

$$\frac{\rho}{\rho^*} = \frac{u^*}{u} = \frac{1}{M^*} = \frac{1 + \gamma M^2}{(\gamma+1) M^2}$$

Table A-3 presents the variables T^O/T^O* , T/T^* , P/P^* , P^O/P^O* , and u/u^* as functions of M , for different values of γ . Fig. 3-13 presents the

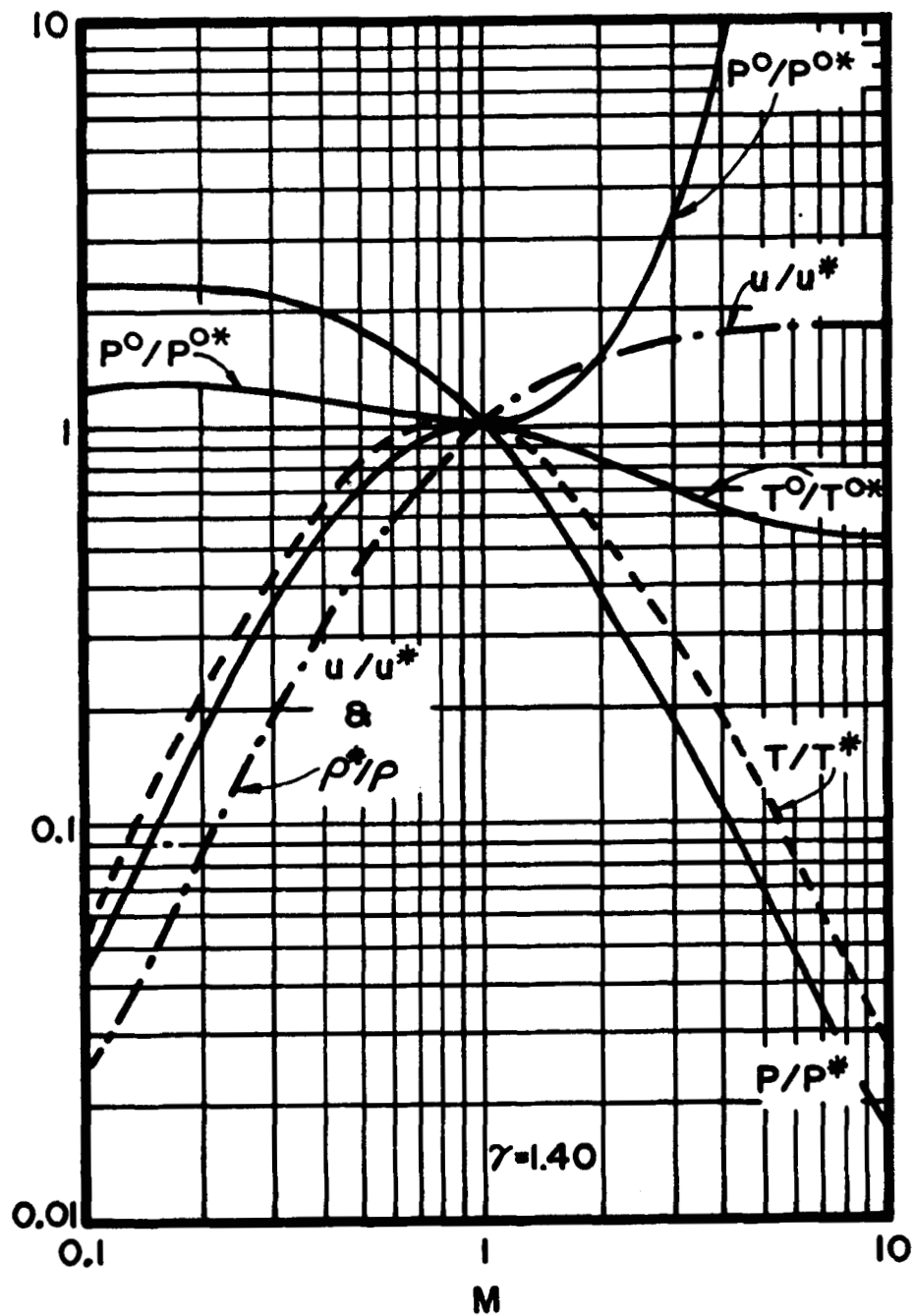


Figure 3-13. Flow Parameters for a Rayleigh Flow As a Function of M , for $\gamma = 1.40$

flow parameters for a Rayleigh flow as a function of the Mach number M for $\gamma=1.40$.

3-7.5 DEVELOPMENT OF COMPRESSION SHOCK

If a Fanno and a Rayleigh line for the same value of the flow density G are plotted on the Ts -plane, they will intersect at two states, such as **a** and **b** illustrated in Fig. 3-14. Because all of the states on the same Fanno line have the same stagnation temperature T_1^0 , and because F/A has the same value for all states on the same Rayleigh line, the states **a** and **b** have identical values of G , T , and F/A . It can be shown (see par. A-10) that the flow through a normal compression shock wave satisfies the continuity and energy equations for a Fanno line and also the momentum equation for a Rayleigh line. Consequently, a spontaneous change from state **a** to state **b** can be accomplished by a *shock*

wave. Since state **b** is at a larger value of entropy than state **a**, a spontaneous change from state **a** to state **b** *does not* violate the second law of thermodynamics.

It is seen from Fig. 3-14 that the static pressure at state **b** is larger than that at state **a**. Hence, the spontaneous change of state (**a**→**b**) is termed a *compression shock*. In view of the second law, a change of state from **b** to **a** is impossible; i.e., a spontaneous change from a subsonic to a supersonic flow is *impossible*. Only the reverse can occur. The abrupt compression of the gas by the compression shock increases the static pressure and temperature, and the entropy of the gas. Its velocity after flowing through the shock wave, however, is reduced to a subsonic value ($M < 1$).

For a detailed discussion of shock waves and supersonic flow see Appendix A.

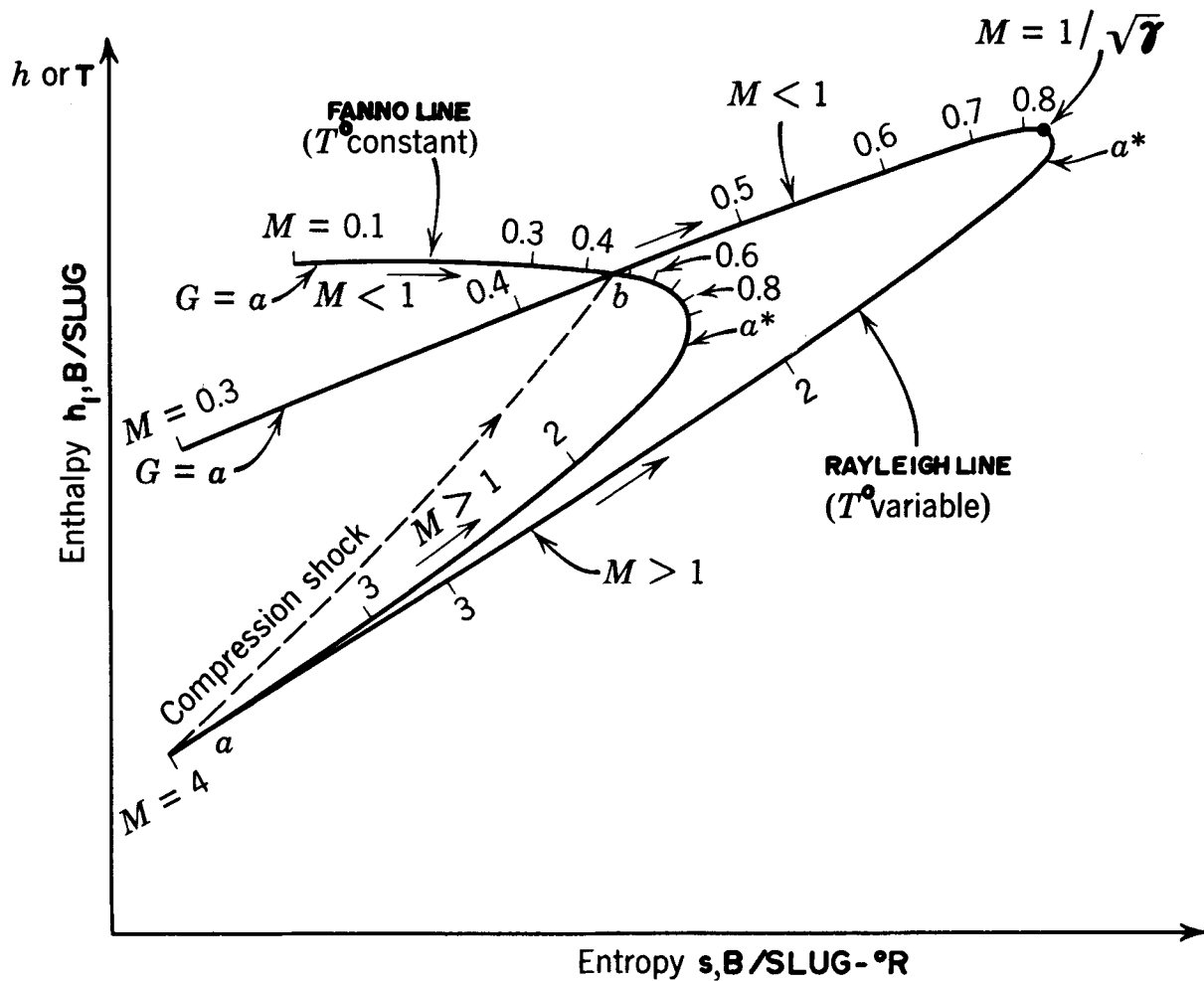


Figure 3-14. Development of Compression Shock

REFERENCES

1. M.J. Zucrow, *Aircraft and Missile Propulsion*, John Wiley and Sons, Inc., Vol. 1, 1958, Ch. 3.
2. K. Brenkert, *Elementary Theoretical Fluid Mechanics*, John Wiley and Sons, Inc., 1960, Ch. 3.
3. H.W. Liepmann and A. Roshko, *Elements of Gas Dynamics*, John Wiley and Sons, Inc., 1957, Ch. 2.
4. R. Von Mises, *Mathematical Theory of Compressible Fluid Flow*, Academic Press, 1958, Ch. 1 & 2.
5. E.R.C. Miles, *Supersonic Aerodynamics*, McGraw-Hill Book Co., Inc., 1950, Ch. 1 & 2.
6. A. H. Shapiro, *The Dynamics and Thermodynamics of Compressible Fluid Flow*, The Ronald Press Company, Vol. 1, 1953.
7. V. L. Streeter (Editor-in-Chief), *Handbook of Fluid Mechanics*, McGraw-Hill Book Co., Inc., 1961.
8. L. Crocco, "Fundamentals of Gas Dynamics", Vol. III, *High Speed Aerodynamics and Jet Propulsion*, Section B, Princeton University Press, 1958.
9. J. H. Keenan and J. Kaye, *Gas Tables*, John Wiley and Sons, Inc., 1945.

CHAPTER 4

COMPRESSIBLE FLOW IN NOZZLES

4-0 PRINCIPAL NOTATION FOR CHAPTER 4*

a	acoustic speed = $\sqrt{\gamma RT}$	E	energy, in general
a^*	critical acoustic speed, in cross-section A^* where $M=1$	δE_f	energy expended in overcoming friction
a^0	stagnation acoustic speed = $\sqrt{\gamma RT^0}$ = $a^* \sqrt{(\gamma+1)/2}$	E_{KE}	kinetic energy
A	flow cross-sectional area, in general	E_{PE}	potential energy
A^*	critical cross-section area, where $M=1$ for a steady one-dimensional isentropic flow	f	friction coefficient in the Fanning equation
A_t	cross-sectional area of throat of nozzle	F	thrust, lb
B	British thermal unit	g	acceleration due to gravitational attraction of earth, ft/sec ²
c_o	maximum isentropic speed = $a^0 \sqrt{\frac{2}{\gamma-1}}$	g_c	gravitational correction factor = 32.174 slug-ft/lb-sec ²
c_p	specific heat at constant pressure	G	flow density = \dot{m}/A
c_v	specific heat at constant volume	h	static specific enthalpy, B/slug
C_c	contraction coefficient for a fluid jet	h^0	stagnation specific enthalpy, B/slug
C_d	discharge coefficient for a nozzle (or orifice) = ψC_c	Δh	a finite change in static specific enthalpy
d	diameter	Δh_c	increase in static specific enthalpy due to a compression of the fluid, B/slug
D	drag	Δh_n	change in the static specific enthalpy of a compressible fluid due to its expansion in a nozzle, B/slug
D	hydraulic diameter	Δh_t	decrease in the static specific enthalpy of a compressible fluid due to an expansion process, B/slug

*Any consistent set of units may be employed; the units presented here are for the American Engineers System (see par. 1-7).

J	mechanical equivalent of heat ≈ 778 ft-lb/B	v	velocity of fluid parallel to the y-axis, fps, or specific volume ($v=1/\rho$), as specified in text
L	length, unit as specified in text	w	velocity of fluid parallel to the z-axis, fps, or weight, as specified in text
\bar{m}	molecular weight	\dot{w}	weight rate of flow, lb/sec
\dot{m}	mass flow rate	z	elevation or altitude
\dot{m}^*	critical mass flow rate	Z_c	compression factor $= r_c^{\frac{\gamma-1}{\gamma}} - 1$
M	local Mach number	Z_t	expansion factor $= 1 - (P_e/P^O)^{\frac{\gamma-1}{\gamma}}$
p	static pressure, psia	<u>GREEK LETTERS</u>	
P	static pressure, psfa		
P^O	total or stagnation pressure	a	semi-angle of diverging portion of a nozzle
P_t	static pressure in throat of nozzle	β	semi-angle of cone for an annular nozzle (Fig. 4-18)
r_c	pressure ratio for a compression process, $r_c = P_2/P_1$, where $P_2 > P_1$	γ	specific heat ratio $= c_p/c_v$
r_t	expansion ratio for an expansion in a nozzle ($r_t = P_t/P^O$)	Δ	finite change in the parameter
R	gas constant $= R_u/\bar{m}$	ϵ	area ratio (A_e/A_t) for a nozzle
R_u	universal gas constant $= 49,717$ ft-lb/slug-mole $^{\circ}R$ $= 63.936$ B/slug-mole $^{\circ}R$	η	efficiency
s	static specific entropy, B/slug $^{\circ}R$	λ	flow divergence loss coefficient for a nozzle
s^O	stagnation specific entropy	ρ	density
S	surface area	ϕ	velocity coefficient for a nozzle; $\phi = \sqrt{\eta_n}$
t	time, sec	ψ	flow factor for a nozzle (see Eq. 4-11)
T	static temperature, $^{\circ}R$	ψ^*	critical flow factor corresponding to maximum mass rate for ideal nozzle flow (see Eq. 4-16)
T^O	total or stagnation temperature, $^{\circ}R$		
u	velocity of fluid parallel to the x-axis fps, or specific internal energy, as specified in text		

SUBSCRIPTS

a	ambient or environment
c	compression or combustion, as specified in text
e	exit cross-section of nozzle
f	friction
g	gas
max	maximum
n	nozzle
t	throat section

SUPERSCRIPTS

- * critical condition where $M=1$, for an isentropic flow
- ' value to which prime is attached is reached by an isentropic process
- o stagnation value

4-1 INTRODUCTION

The present chapter is concerned with the application of the gas dynamic theory, presented in Chapter 3 and Appendix A, to the flow of compressible fluids in nozzles. It will be recalled from Chapter 1 that some form of nozzle serves as the propulsive element in every type of jet propulsion system. In paragraph 3-4.3.2 a nozzle was defined as a flow passage which causes an expansion ($dP < 0$) of the compressible fluid flowing through it.

The nozzles employed in current jet propulsion engines can be grouped into two broad classes: (1) converging nozzles, and (2) converging-diverging or *De Laval* nozzle. Figure

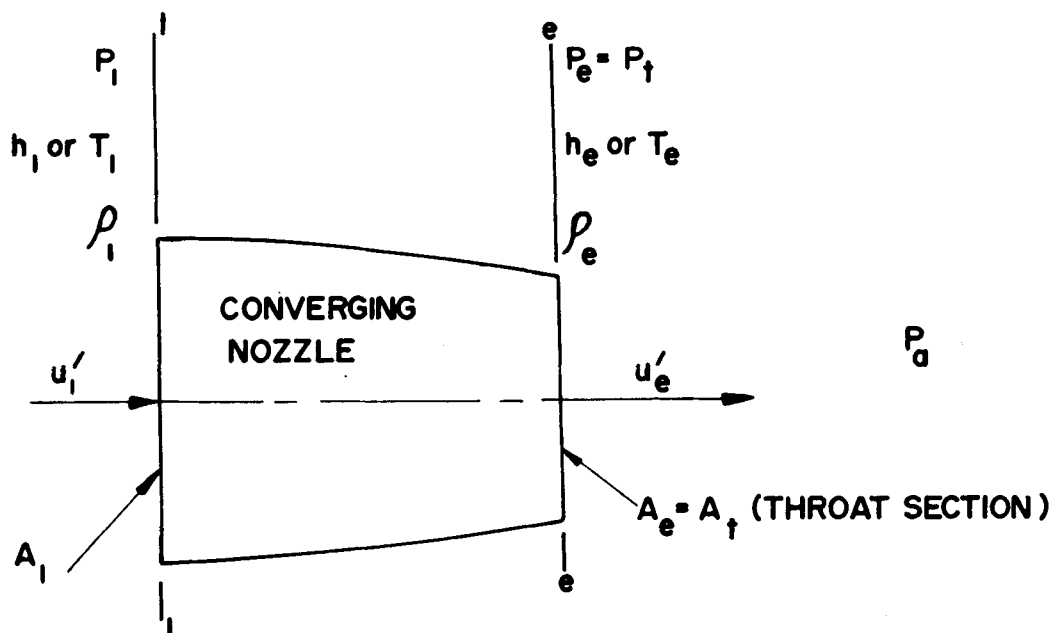
4-1 illustrates schematically the manner in which the flow area varies in the two general classes of nozzles. It should be pointed out, however, that the longitudinal axis of a nozzle need not be a straight line, as is shown in Fig. 4-1.

In the analytic treatment of the flow of a compressible fluid in a nozzle, regardless of type, it will be assumed unless it is specifically stated to be otherwise that the flow is steady, one-dimensional, and isentropic. Such a flow will be termed *ideal nozzle flow*.

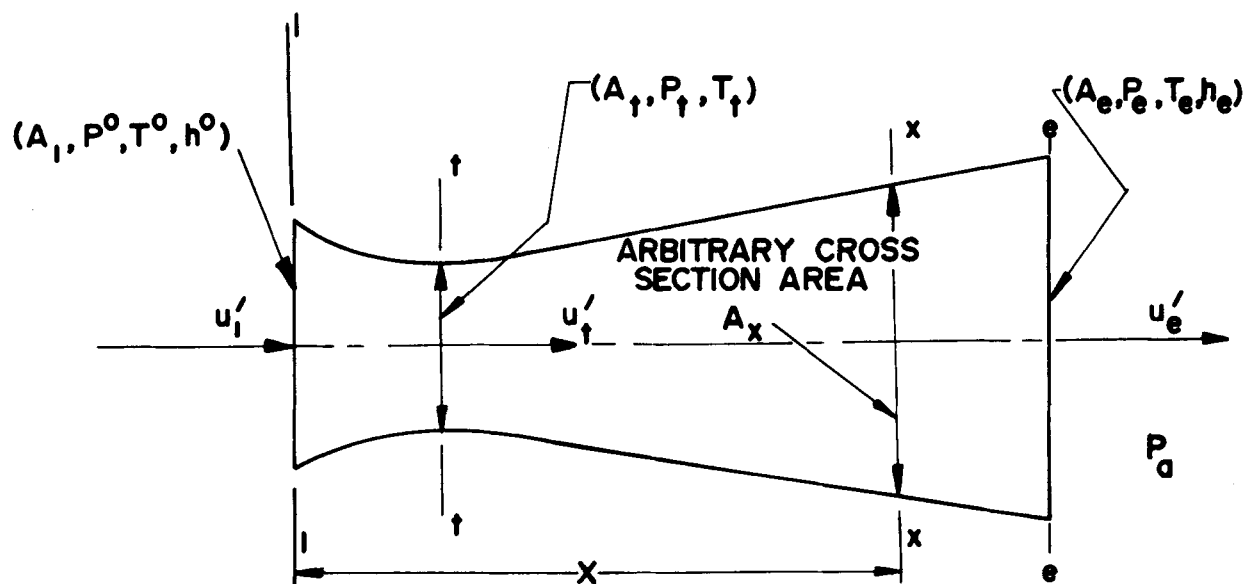
Experiments have demonstrated that the effects of friction upon the changes in the thermodynamic properties of the compressible fluid and its pertinent flow parameters, in the case of nozzle flow, are considerably smaller than the effects produced by the changes in the cross-sectional area of the nozzle. It is customary to account for the effects of friction in actual nozzle flow by applying pertinent empirical coefficients to the results obtained from analyses based on ideal nozzle flow. One may, therefore, regard the results obtained by assuming ideal nozzle flow as a close approximation to the actual flow in a nozzle.

A basic characteristic of nozzle flow is that the compressible fluid moves in the direction of a negative *pressure gradient* which enables the fluid layers adjacent to the walls of the nozzle to follow the contour of the nozzle quite readily, despite the *decelerating influence* of wall friction upon the flowing fluid. Consequently, wall friction exerts only a minor influence upon the flow of a compressible fluid in a well-designed nozzle.

Since the results obtained by analyzing ideal nozzle flow in a converging nozzle can be readily applied to a converging-diverging (*De Laval*) nozzle, the converging nozzle will be discussed first.



(A) IDEAL NOZZLE FLOW IN A CONVERGING NOZZLE



(B) IDEAL NOZZLE FLOW IN A CONVERGING-DIVERGING OR DE LAVAL NOZZLE

Figure 4-1. Two Basic Types of Nozzles Employed in Jet Propulsion Engines

4-2 IDEAL FLOW IN A CONVERGING NOZZLE

The converging nozzle, see Fig. 4-1, is suitable for applications where the pressure ratio P_1/P_e is small. It is the type of nozzle employed in gas-turbine jet engines for propelling aircraft at subsonic flight speeds (see Part Two, Chapters 12 and 15).

Figure 4-2(A) illustrates schematically the flow through a converging nozzle attached to a large storage tank (*infinite reservoir*), and Fig. 4-2(B) illustrates a converging nozzle attached to a pipe. Ideal nozzle flow is assumed (see par. 4-1).

Let subscripts 1 and 3 refer to the entrance and exit cross-sections of the converging nozzle, respectively, and the subscript a to the environment into which the nozzle discharges. The assumed ideal nozzle flow is characterized by the conditions (see pars. A-5.1 and A-5.2)

$$h^0 = \text{a constant and } P^0 = \text{a constant}$$

4-2.1 ISENTROPIC EXIT VELOCITY FOR A CONVERGING NOZZLE

If h denotes the static specific enthalpy of the flowing compressible fluid at an arbitrary cross-sectional area of a converging nozzle, denoted by A_x , and h^0 denotes its stagnation specific enthalpy, then the velocity of the fluid crossing A_x is given by (see par. A-5.3)

$$u_x = \sqrt{2(h^0 - h_x)} \quad (4-1)$$

Eq. 4-1 applies to any isoenergetic flow (reversible or irreversible) and comes directly from the energy equation. The isentropic velocity of the fluid crossing the nozzle exit cross-sectional area A_e is obtained by setting $A_e = A_x$, $h'_e = h_x$, and $u'_e = u_x$, in Eq. 4-1.

Hence

$$u'_e = u'_t = \sqrt{2(h^0 - h'_e)} = \text{isentropic exit velocity} \quad (4-2)$$

In the case of a converging nozzle, however, the exit area A_e is the smallest cross-sectional area of the nozzle, i.e.,

$$A_e = A_t = \text{nozzle throat area}$$

Hence, for a converging nozzle

$$u'_e = u'_t = \text{the isentropic throat velocity} \quad (4-3)$$

Hereafter, in discussing converging nozzles the subscript e will be replaced by the subscript t.

4-2.2 ISENTROPIC THROAT VELOCITY FOR THE FLOW OF A PERFECT GAS IN A CONVERGING NOZZLE

From par. 3-5.3 it follows that if the flowing fluid is an *ideal gas*, then – for ideal nozzle flow in a converging nozzle – the isentropic throat velocity u'_t is given by Eq. A-130 which is repeated and renumbered here for convenience. Thus

$$\begin{aligned} u'_t &= a^0 \sqrt{\left(\frac{2}{\gamma-1}\right) Z_t} = c_o \sqrt{Z_t} \\ &= a^* \sqrt{\left(\frac{\gamma+1}{\gamma-1}\right) Z_t} \end{aligned} \quad (4-4)$$

where (see par. A-6.2)

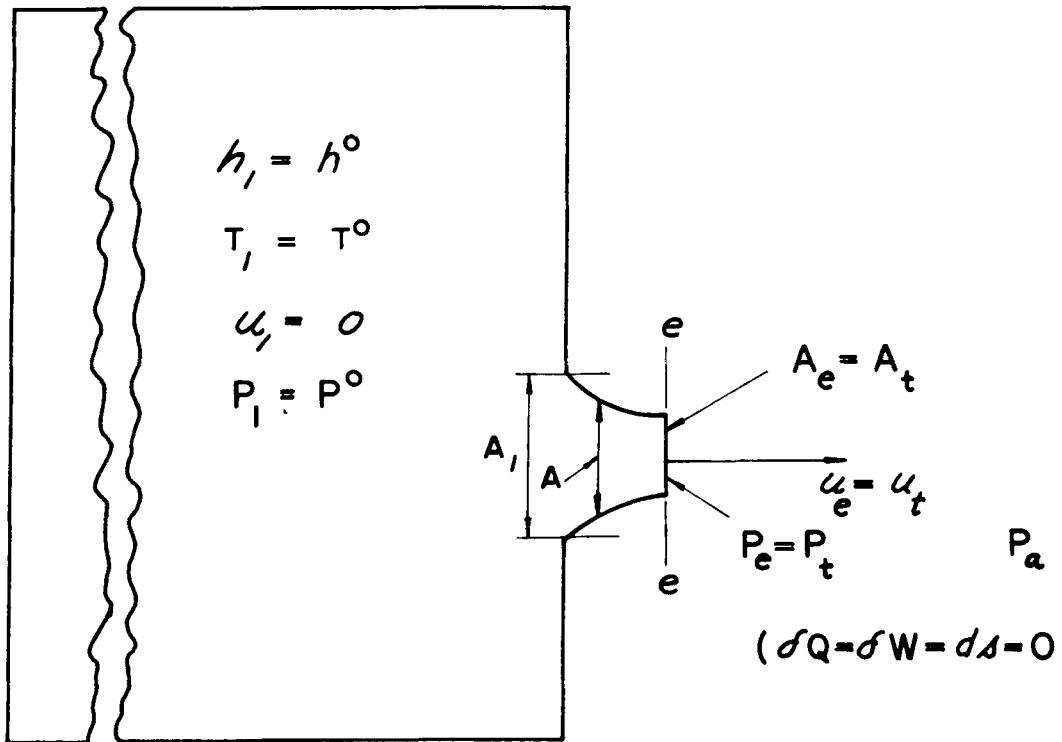
$$a^0 = \sqrt{\gamma R T^0} = \text{stagnation acoustic speed}$$

$$c_o = \sqrt{2 \left(\frac{\gamma}{\gamma-1}\right) R T^0} = \text{maximum isentropic speed}$$

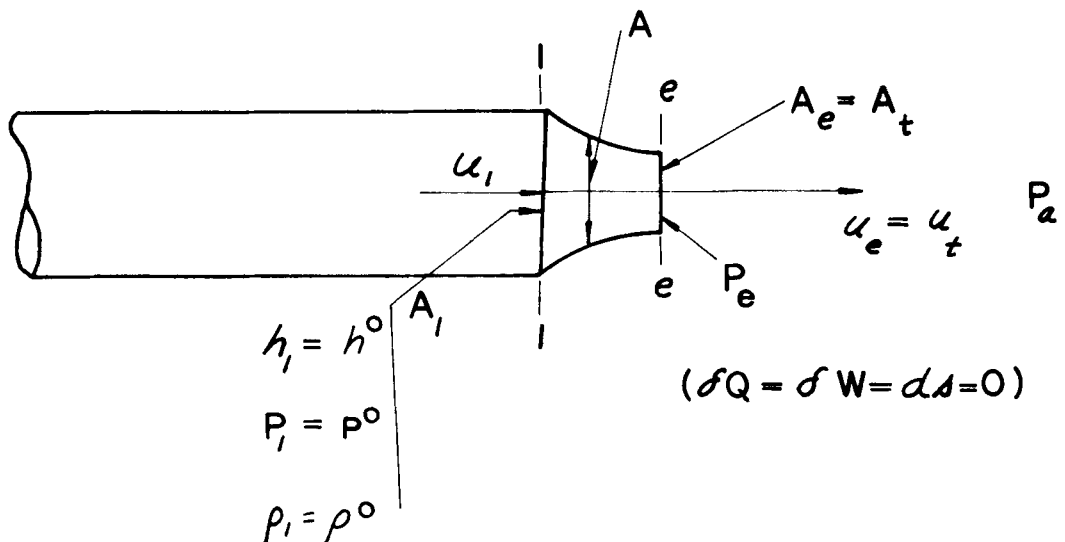
$$a^* = \sqrt{\gamma R T^*} = \text{critical speed of sound}$$

$$Z_t = 1 - r_t^{\frac{\gamma-1}{\gamma}} = \text{expansion factor}$$

$$r_t = P_t/P^0 = P_e/P^0 = \text{nozzle expansion ratio} \\ \text{(for a converging nozzle)}$$



(A) CONVERGING NOZZLE ATTACHED TO A LARGE STORAGE TANK



(B) CONVERGING NOZZLE ATTACHED TO A PIPE

Figure 4-2. Ideal Nozzle Flow in Converging Nozzles

In most cases the initial flow conditions for the gas flowing in the nozzle (T^0 and P^0) are known, so that the reference speeds a^0 , c^0 , and a^* are constants.

It is frequently useful to express u'_t in dimensionless form by introducing the *dimensionless isentropic throat velocity* $w'_t = w'_e$, for a converging nozzle. Combining Eqs. A-124 and A-125, one obtains the following equations for the dimensionless isentropic throat velocity for a converging nozzle:

$$\begin{aligned} w'_t &= \frac{u'_t}{\sqrt{\gamma R T^0}} = \left(\frac{2}{\gamma-1} \right) Z_t \\ &= \frac{M_t}{\sqrt{1 + \left(\frac{\gamma-1}{2} \right) M_t^2}} \end{aligned} \quad (4-5)$$

4-2.3 EFFECT OF VARYING THE BACK PRESSURE ACTING ON A CONVERGING NOZZLE

Consider a converging nozzle which operates with constant values of h^0 and P^0 at its entrance cross-section A_1 (see Fig. 4-2(A)) but with a varying *back pressure* P_a ; where P_a is the static pressure of the surroundings into which the nozzle discharges a compressible fluid. The effect of P_a will now be studied by considering four different operating modes or cases.

Case I. ($P_a = P^0$). In this case, since $P = P^0$ at all cross-sections of the nozzle, there is no flow of fluid through the nozzle, i.e., the mass flow rate $\dot{m} = 0$.

Case II. ($P_t = P_a < P^*$). In this case, termed *subcritical operation*, the pressure in the exit cross-section of the nozzle $P_t = P_a$.

Case III. ($P_t = P_a = P^*$). This mode is termed *critical operation*. The isentropic exit or throat velocity $u'_t = a^* =$ the critical speed of sound.

Furthermore, the throat (or exit) area is identical with the critical flow area A^* (see par. A-6.3.1). Accordingly, when $A_t = A^*$, the nozzle passes the *critical mass flow rate* \dot{m}^* and the corresponding value of the flow density is the *critical flow density* $G^* = \dot{m}^*/A^*$. If the flowing fluid is an *ideal gas*, then it follows from Eq. A-164 that for a converging nozzle

$$G^* = \dot{m}^*/A^* = \frac{P^0}{a^0} \left(\frac{2}{\gamma+1} \right)^{\frac{\gamma+1}{2(\gamma-1)}} \quad (4-6)$$

Hence

$$\frac{G^* a^0}{P^0} = \sqrt{\left(\frac{2}{\gamma+1} \right)^{\frac{\gamma+1}{\gamma-1}}} \quad (4-6a)$$

Case IV. ($P_t = P^* > P_a$). This mode of operation is termed *supercritical operation*. Decreasing the static pressure P_a from $P_a = P^*$ to $P_a = 0$ has no influence upon the throat pressure P_t ; the latter remains constant the critical value P^* , where

$$P^* = \left(\frac{2}{\gamma+1} \right)^{\frac{\gamma}{\gamma-1}} P^0 \quad (4-7)$$

Because the upstream conditions are assumed constant, the throat velocity also remains constant at the value (see Eq. 4-4)

$$u'_t = a^* = a^0 \sqrt{\frac{2}{\gamma+1}} = \sqrt{\frac{2\gamma R T^0}{\gamma+1}} \quad (4-8)$$

Hence, when a converging nozzle is operated under *super-critical* conditions, reducing P_a causes the rarefaction wave to be propagated toward the converging nozzle with a wave speed a^* which is equal to the speed with which the

flowing ideal gas is ejected from the nozzle. Consequently, the flow in the nozzle is unaffected by the reduction in P_a even if it is reduced to zero. As a result the mass flow rate remains constant at the value \dot{m}^* . If a larger flow is desired the upstream conditions (see Eq. 4-6) must be altered or the throat area increased.

Since the static pressure of the gas in the exit cross-sectional area of the converging nozzle ($A_t = A_e$) is $P^* > P_a$, the adjustment of the static pressure of the gas discharged by the nozzle to the back pressure P_a takes place in the environment external to the nozzle. The finite differences in the radial pressure in the exhaust jet produce transverse accelerations of the gas molecules and nonuniformities in the flow that cannot be analyzed on the basis of one-dimensional flow, which is a major assumption of ideal nozzle flow.

4-2.4 MASS FLOW RATE FOR IDEAL NOZZLE FLOW (CONVERGING AND CONVERGING-DIVERGING NOZZLES)

The mass flow rate through either a converging or a converging-diverging nozzle (see Fig. 4-1) is obtained by applying the one-dimensional continuity equation (Eq. 3-18) to the throat area of the nozzle, denoted by A_t . Thus, for an ideal nozzle flow

$$\dot{m}' = \dot{m}'_t = \dot{m}'_e = A_t \rho_t u'_t \quad (4-9)$$

If the flowing fluid is an *ideal gas* (see pars. 3-2 and 3-4), then Eq. 4-9 can be written in the following form¹:

$$\dot{m}' = \psi \left(\frac{P^0 A_t}{\sqrt{RT^0}} \right) \quad (4-10)$$

where

$$\psi = \sqrt{\frac{2\gamma}{\gamma-1} \left[r_t^{\frac{2}{\gamma}} - r_t^{\frac{\gamma+1}{\gamma}} \right]} = \text{flow factor} \quad (4-11)$$

where

$$r_t = P_t/P^0.$$

Eq. 4-10 presents the *isentropic mass flow rate* \dot{m}' for ideal nozzle flow in either a converging or converging-diverging (De Laval) nozzle.

It is apparent from Eq. 4-11 that for fixed initial conditions (P^0 and T^0) and a given value of $r_t = P_t/P^0$ the flow factor ψ is a function only of the specific heat ratio γ . For fixed values of r_t , A_t , and P^0 the mass flow rate \dot{m}' for a given ideal gas depends only upon its total temperature T^0 ; increasing T^0 reduces \dot{m}' .

Figure 4-3 presents the flow factor ψ as a function of P_t/P^0 for γ equal to 1.135, 1.3, and 1.4. For a given value of P_t/P^0 the flow factor ψ decreases slightly as γ is reduced. For all values of γ , the flow factor $\psi=0$ when P_t/P^0 is equal to either zero or unity; between those limiting values of r_t the flow factor ψ has a maximum value.

By differentiating Eq. 4-11, it is readily shown that the expansion ratio P_t/P^0 which makes ψ a *maximum* is given by (see Eq. 4-7)

$$\left(\frac{P_t}{P^0} \right)_{cr} = \left(\frac{2}{\gamma+1} \right)^{\frac{\gamma}{\gamma-1}} = \frac{P^*}{P^0} \quad (4-12)$$

From par. A-6.1, when P_t/P^0 is equal to the *critical expansion ratio* P^*/P^0 , then $A_t=A^*$, the *critical flow area*, and the following conditions obtain in the nozzle throat:

$$u'_t = a^* = \sqrt{\gamma RT^*} \quad (4-13)$$

$$\frac{T_t}{T^0} = \frac{T^*}{T^0} = \frac{2}{\gamma+1} \quad (4-14)$$

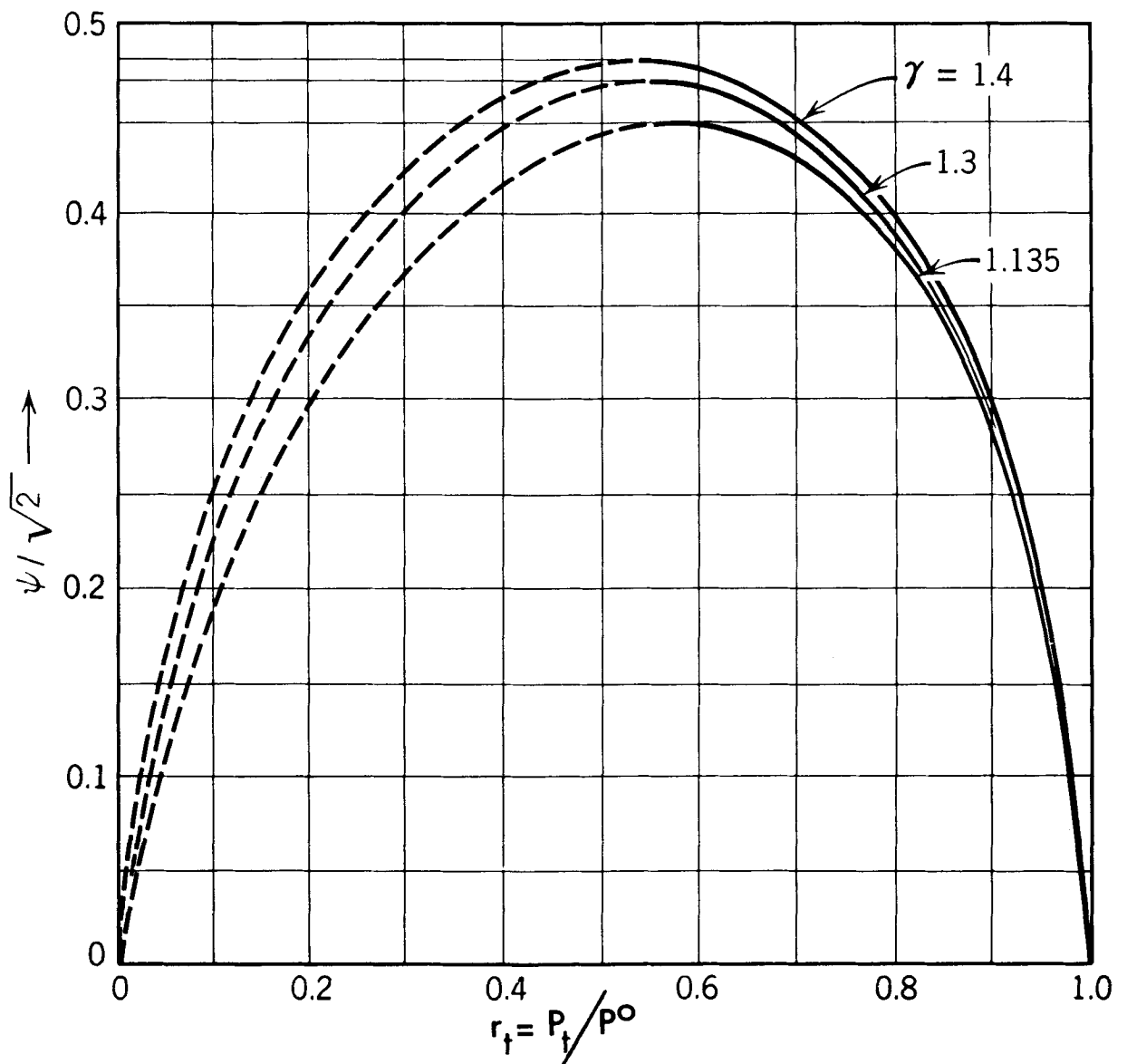


Figure 4-3. Flow Factor ψ for a Converging Nozzle As a Function of the Expansion Ratio r_t

$$\frac{\rho_t}{\rho^0} = \frac{\rho^*}{\rho^0} = \left(\frac{2}{\gamma+1} \right)^{\frac{1}{\gamma-1}} \quad (4-15)$$

Combining Eqs. 4-11 and 4-12 gives the following equation for $\psi_{\max} = \psi^*$:

$$\psi^* = \psi_{\max} = \left(\frac{2}{\gamma+1} \right)^{\frac{1}{\gamma-1}} \sqrt{\frac{2\gamma}{\gamma+1}} \quad (4-16)$$

Hence, the equation for the *maximum isentropic mass flow rate* \dot{m}'_{\max} can be written in the form

$$\dot{m}^* = \dot{m}'_{\max} = \psi^* A^* \frac{P^0}{\sqrt{RT^0}} \quad (4-17)$$

Figure 4-4 illustrates the functional relationship between \dot{m}' and $r_t = P_t/P^0$, as calculated from Eqs. 4-10 and 4-11, for a given value of γ . As one might expect its characteristics are similar to those for the functional relationship between ψ and r_t (see Fig. 4-3).

It is seen in Fig. 4-4 that the critical mass flow rate \dot{m}^* is attained when $P_t/P^0 = P^*/P^0$. Experiments demonstrate that the calculated curve for \dot{m}' vs r_t is correct for the range $r_t = P_t/P^0 = 1.0$ to P^*/P^0 . For that range of expansion ratios the static pressure $P_t = P_e$, for a converging nozzle is always equal to the *back pressure* P_a (see Fig. 4-1(A)). If either P^0 is increased or P_a reduced so that $P_a/P^0 < P^*/P^0$ the pressure P_e no longer equals P_a but remains constant at the value which gives $P_t = P_e = P^*$. Consequently, the calculated broken line segment of the curve in Fig. 4-4 *does not exist* physically. Reducing P_a/P^0 below the value which yields $P_t/P^0 = P^*/P^0 = P_e/P^0$ for a converging nozzle has no effect upon the isentropic mass flow rate. It remains constant at the value $\dot{m}' = \dot{m}^*$.

It should be noted here, that although the equations for the critical mass flow rate \dot{m}^* were derived for a converging nozzle, they apply also to the converging portion of a converging-diverging (De Laval) nozzle.

4-3 IDEAL FLOW IN A CONVERGING-DIVERGING (OR DE LAVAL) NOZZLE

The discussions of ideal nozzle flow in a converging nozzle indicate that such a nozzle can expand a gas only through the pressure range (P^0/P^*) , as illustrated in Fig. 4-5. Consequently, the transformation of the static specific enthalpy of the gas into kinetic energy is limited to the area lying above the line or curve corresponding to $P^* = \text{constant}$. The enthalpy corresponding to the area below the line $P^* = \text{constant}$ cannot be converted into kinetic energy by expanding the gas in a converging nozzle.

The Swedish engineer, De Laval (1883), showed that the enthalpy transformation into kinetic energy corresponding to an isentropic expansion of the fluid from P^* to P_a could be effected by adding a diverging portion to a converging nozzle, as illustrated in Fig. 4-1(B). Figure 4-6 illustrates the characteristics.

Converging-diverging nozzles are employed for nozzles which must operate with large values of the pressure ratio P^0/P_a . In general, the propulsive nozzles for chemical rocket engines are converging-diverging nozzles and they operate with inlet total pressures ranging from 150 to 3000 psia, the back pressure P_a being that of the surroundings into which the nozzle ejects its propellant gas.

Converging-diverging nozzles have not been used widely for turbojet engines until more

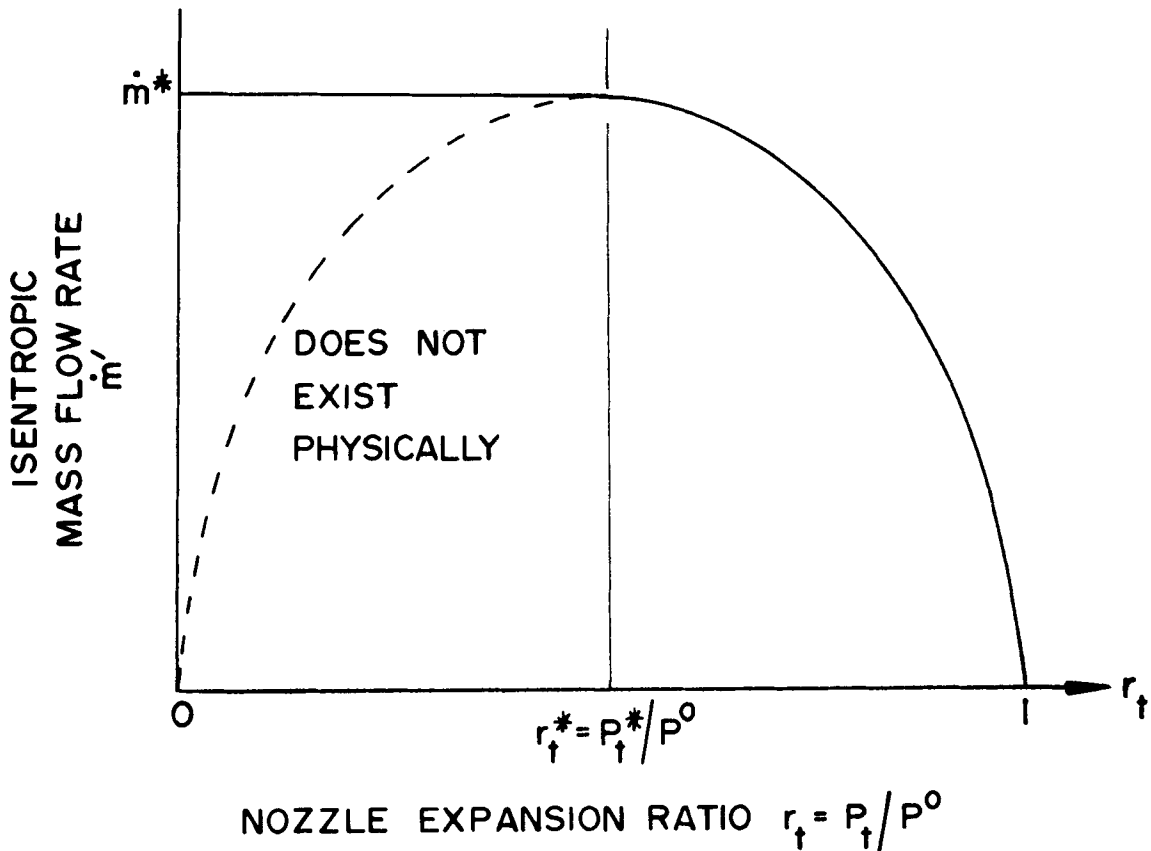


Figure 4-4. Mass Flow Rate As a Function of the Nozzle Expansion Ratio, for a Fixed Value of γ

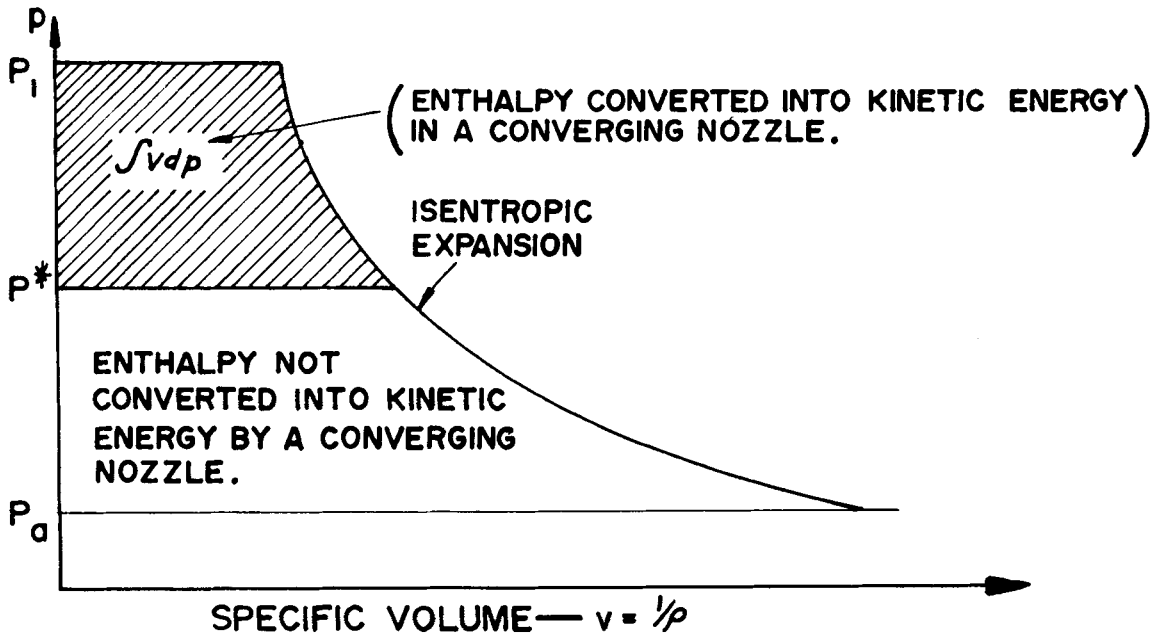
recent years, when supersonic aircraft were developed. Because of the high ram pressure of the air entering the engine, the pressure ratio of the nozzle became large enough to warrant employing the converging-diverging type of nozzle.

Fig. 4-6 illustrates the characteristics of the flow in a converging-diverging nozzle when it is passing the critical mass flow rate $\dot{m}'_{\max} = \dot{m}^*$, and the entrance velocity u_1 is subsonic. In general, the upstream operating conditions at the cross-sectional area A_1 and the exit cross-sectional area A_e may be assumed to be given, and also the area of the throat A_t of the

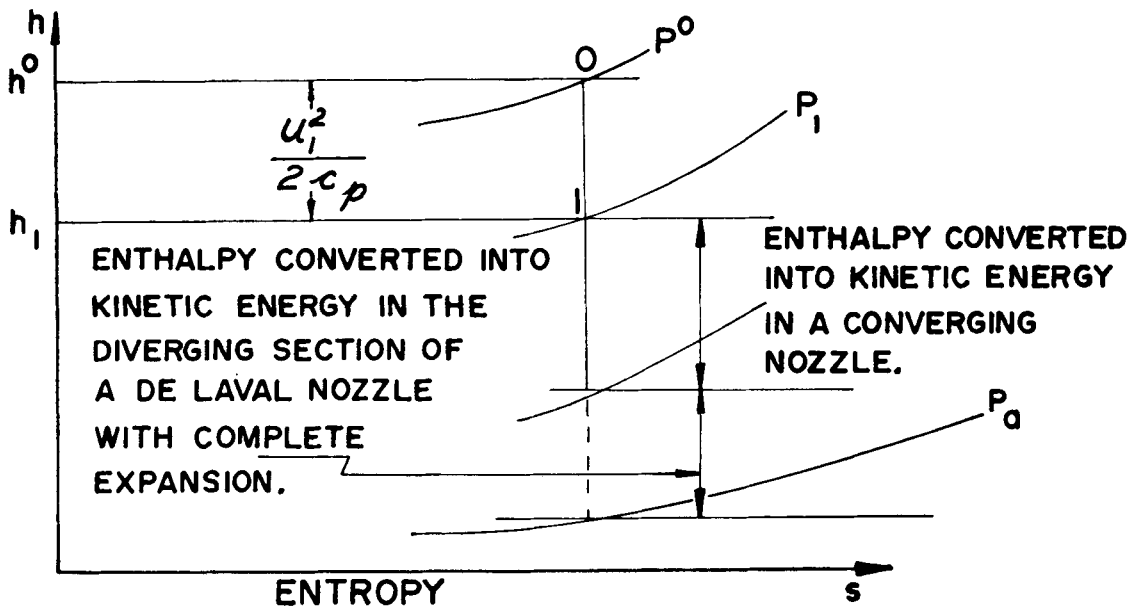
converging-diverging nozzle. It is assumed that the flow is an *ideal nozzle flow* (see par. 4-1) and the flowing fluid is an *ideal gas*.

The gas velocity increases as it flows from the entrance cross-section A_1 to the exit cross-section A_e , due to the decrease in pressure $P^0 - P_e$; the ratio P^0/P_e is called the *nozzle pressure ratio* and is larger than unity. As before, the ratio P_e/P^0 is called the *nozzle expansion ratio* and is denoted by r_n .

If a converging-diverging nozzle is operated so that the gas velocity at every cross-section is *subsonic*, the maximum gas velocity occurs in



(A) P-v DIAGRAM



(B) h-s DIAGRAM

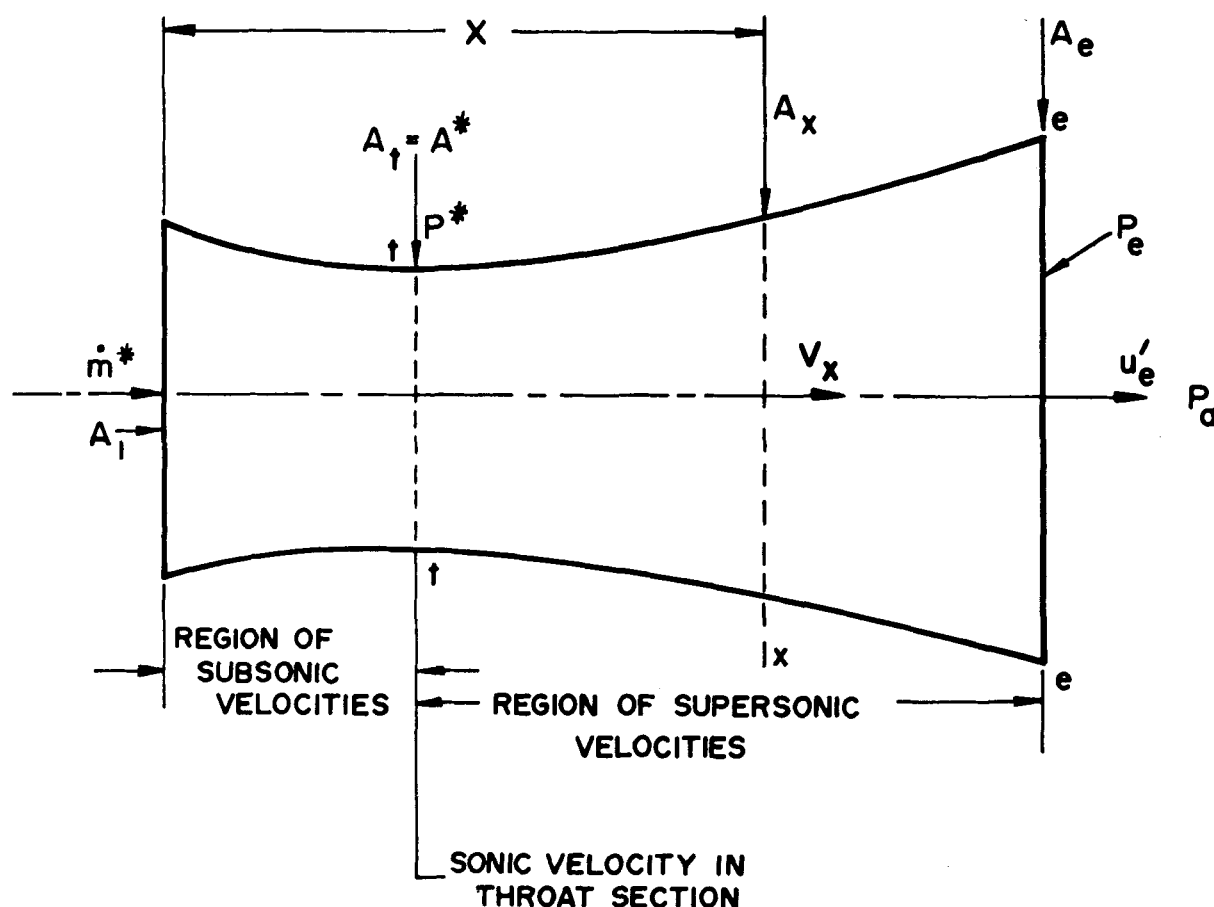
Figure 4-5. Enthalpy Converted Into Kinetic Energy by Isentropic Expansions in Converging and Converging-Diverging Nozzles

the throat area A_t . Decreasing the exit pressure P_e , by reducing the ambient pressure P_a , causes the gas velocities at every cross-section to increase, but the largest gas velocity will be the *throat velocity* u'_t in the area A_t .

Once the throat velocity u'_t , however, becomes equal to the local acoustic speed a^* , then $A_t = A^*$, $P_t = P^*$, and the isentropic mass flow rate $\dot{m}' = \dot{m}^*$ = the critical mass flow rate. It is

then impossible to increase the throat velocity above a^* by reducing P_e , assuming fixed values for P^0 and T^0 .

Assume now that with the entrance conditions for the nozzle held constant, the static pressure in the exit section P_e is reduced so that the flow in the diverging portion of the nozzle becomes *supersonic*. The flow in the nozzle is then unsymmetrical with respect to the throat,



(IDEAL NOZZLE FLOW)

Figure 4-6. Flow Characteristics of a Converging-Diverging (or DeLaval) Nozzle Passing the Critical Mass Flow Rate \dot{m}^*

wherein the gas velocity remains constant at the value $u_t' = a^*$. The latter conditions are illustrated schematically in Fig. 4-6.

The operating characteristics of the converging-diverging nozzle can be explained by the equations presented earlier for ideal nozzle flow of an ideal gas in a converging nozzle. Thus, the *isentropic exit velocity* u_e' is given by Eq. 4-4, which is repeated here for convenience. Thus

$$u_e' = \sqrt{2(h^0 - h_e')} = c_o \sqrt{Z_t} \quad (4-18)$$

the velocity u_e' is the velocity crossing the exit cross-section of the converging-diverging nozzle in Eq. 4-18

$$Z_t = 1 - \left(\frac{P_e}{P^0} \right)^{\frac{\gamma-1}{\gamma}}$$

The isentropic mass flow rate \dot{m}' for a converging-diverging nozzle is given by Eq. 4-10 and its critical flow rate is given by Eq. 4-17. Hence

$$\begin{aligned} \dot{m}^* &= \psi^* A^* \frac{P^0}{\sqrt{RT^0}} \\ &= A^* P^0 \sqrt{\frac{2}{RT^0}} \sqrt{\frac{\gamma}{\gamma+1}} \left(\frac{2}{\gamma+1} \right)^{\frac{1}{\gamma-1}} \end{aligned} \quad (4-19)$$

It is convenient to express the mass flow rate \dot{m}' in terms of the flow density $G = \dot{m}'/A_t$. Eq. 4-10 can be transformed to read

$$\frac{G \sqrt{\gamma RT^0}}{P^0} = \gamma \sqrt{\frac{2}{\gamma-1}} \sqrt{\left(\frac{P_t}{P^0} \right)^{\frac{2}{\gamma}} - \left(\frac{P_t}{P^0} \right)^{\frac{\gamma+1}{\gamma}}} \quad (4-20)$$

Fig. 4-7 presents the dimensionless parameter $(G \sqrt{\gamma RT^0})/P^0$ as a function of P_t/P^0 , for $\gamma = 1.25$.

4.3.1 AREA RATIO FOR COMPLETE EXPANSION OF THE GAS FLOWING IN A CONVERGING-DIVERGING NOZZLE

For a converging-diverging nozzle, the ratio of its exit area A_e to its throat area A_t is called the nozzle area ratio and is denoted by ϵ . Thus

$$\epsilon = A_e/A_t = \text{nozzle area ratio} \quad (4-20a)$$

Fig. 4-6 illustrates a converging-diverging nozzle which passes the critical mass flow rate \dot{m}^* ; ideal nozzle flow is assumed. Let A_x denote an arbitrary cross-sectional area of the nozzle located a distance x from the entrance cross-section A_1 . From continuity and Eq. 4-10 one obtains

$$\dot{m}^* = A^* \rho^* a^* = A_x \rho_x u_x' = \psi A^* \frac{P^0}{\sqrt{RT^0}} \quad (4-21)$$

Hence, for an ideal nozzle flow

$$\frac{A_x}{A^*} = \frac{\psi^*}{\psi_x} = \frac{\rho^* a^*}{\rho_x u_x'} \quad (4-22)$$

Substituting for ψ and ψ^* from Eqs. 4-11 and 4-16, respectively, yields

$$\frac{A_x}{A^*} = \frac{A_x}{A_t} = \frac{\left(\frac{2}{\gamma+1} \right)^{\frac{1}{\gamma-1}} \sqrt{\frac{\gamma-1}{\gamma+1}}}{\left(\frac{P_x}{P^0} \right)^{\frac{1}{\gamma}} \sqrt{1 - \left(\frac{P_x}{P^0} \right)^{\frac{\gamma-1}{\gamma}}}} \quad (4-23)$$

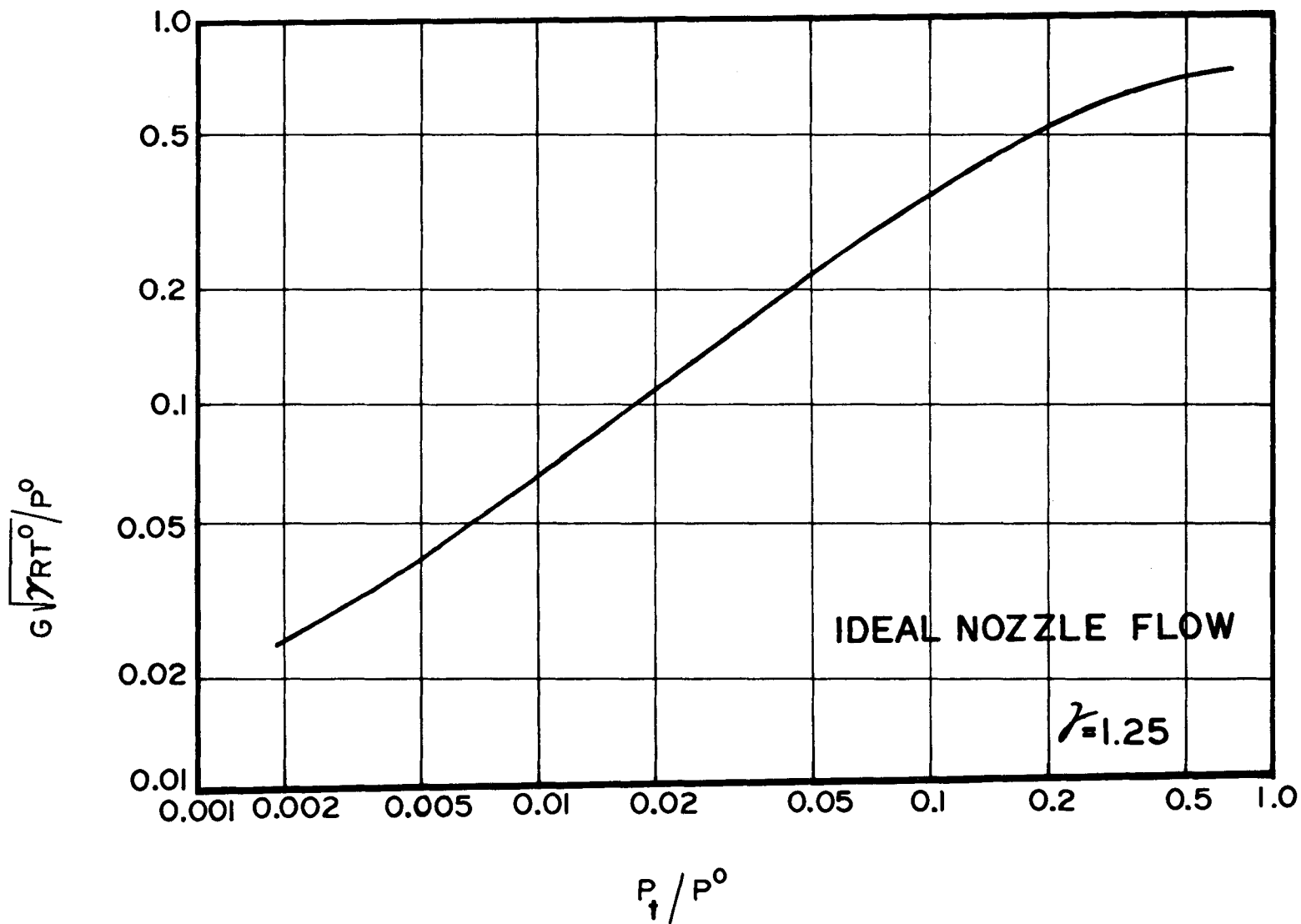


Figure 4-7. Parameter $\left(G\sqrt{\gamma RT^0}\right)/P^0$ As a Function of P_t/P^0 for Ideal Nozzle Flow ($\gamma = 1.25$)

Figure 4-8 presents the area ratio $A_x/A_t = A_x/A^*$ as a function of P^0/P_x for different values of γ . The curves give the required area ratio A_x/A_t for expanding an ideal gas isentropically from the stagnation conditions P^0 and T^0 to the static pressure P_x in the cross-sectional area A_x , when the nozzle passes the critical flow \dot{m}^* .

Fig. 4-9 presents the velocity ratio u'_x/u'_t as a function of P^0/P_x for gases having different values of γ . The curves apply to the isentropic flow of ideal gases. The gas velocities u'_x and u'_t apply to the cross-sectional areas A_x and A_t , respectively.

For some purposes it is convenient to express A_x/A_t as a function of M_x , the Mach number in A_x . Rewriting Eq. A-153 yields¹

$$\begin{aligned} \frac{A_x}{A_t} &= \frac{A_x}{A^*} \\ &= \frac{1}{M_x} \left[\frac{2}{\gamma+1} \left(1 + \frac{\gamma-1}{2} M_x^2 \right) \right]^{\frac{\gamma+1}{2(\gamma-1)}} \quad (4-23) \end{aligned}$$

The dimensionless velocity M_x^* (see par. A-6.1.5), is given by

$$M_x^* = \frac{u'_x}{a^*} = \sqrt{\frac{\gamma+1}{\gamma-1} \left[1 - \left(\frac{P_x}{P^0} \right)^{\frac{\gamma-1}{\gamma}} \right]} \quad (4-24)$$

When $\dot{m}' < \dot{m}^*$, the area of the nozzle throat $A_t > A^*$, and $u'_t < a^*$; i.e., the flow is subsonic throughout the converging-diverging nozzle, as explained in par. 4-3. In that case, the static pressure of the flowing gas decreases between A_1 and A_t (see Fig. 4-6), attains its smallest value in A_t , and then increases between A_t and A_e .

When A_x coincides with exit cross-sectional area A_e , then $P_x = P_e$ and $M_x = M_e$. Furthermore, the ratio u'_e/a^* is obtained from Eq. 4-24 by setting $P_x = P_e$.

The maximum value of the exit velocity u'_e is obtained when the nozzle is designed so that $\epsilon = A_e/A_t = A_e/A^*$ gives a static pressure P_e , in the exit cross-sectional area A_e , exactly equal to the back pressure P_a . Such a nozzle is said to operate with either the *optimum area ratio* or the *area ratio for complete expansion*, denoted by ϵ_{opt} .

When a nozzle operates with ϵ_{opt} , $P_e = P_a$ and all of the available enthalpy for the ideal nozzle flow is transformed into jet kinetic energy. Hence, for such a nozzle

$$u'_e = \sqrt{2(h^0 - h'_e)} \quad (\text{for } \epsilon_{opt}) \quad (4-25)$$

EXAMPLE 4-1.

A converging-diverging nozzle discharges air, assumed to be an ideal gas, into a receiver where the static pressure $P_a = 15$ psia. The nozzle is designed so that the nozzle passes the maximum mass flow rate under conditions of ideal nozzle flow. The nozzle is attached to a pipe and at the entrance cross-sectional area of the nozzle the following conditions obtain; $p_1 = 100$ psia, $T_1 = 800^\circ$ R, $M_1 = 0.3$, and $A_1 = 1$ sq ft. Calculate:

- the stagnation values of the properties of the air (T^0 , P^0 , ρ^0 , and a^0);
- the weight rate of air flow in lb per sec;
- the values of P , T , ρ , and u'_t in the throat;
- the throat area A_t ;
- The area of the exit cross-section A_e , to give complete expansion of the flowing air, and the corresponding values of P_e , ρ_e , u'_e , M_e , and T_e .

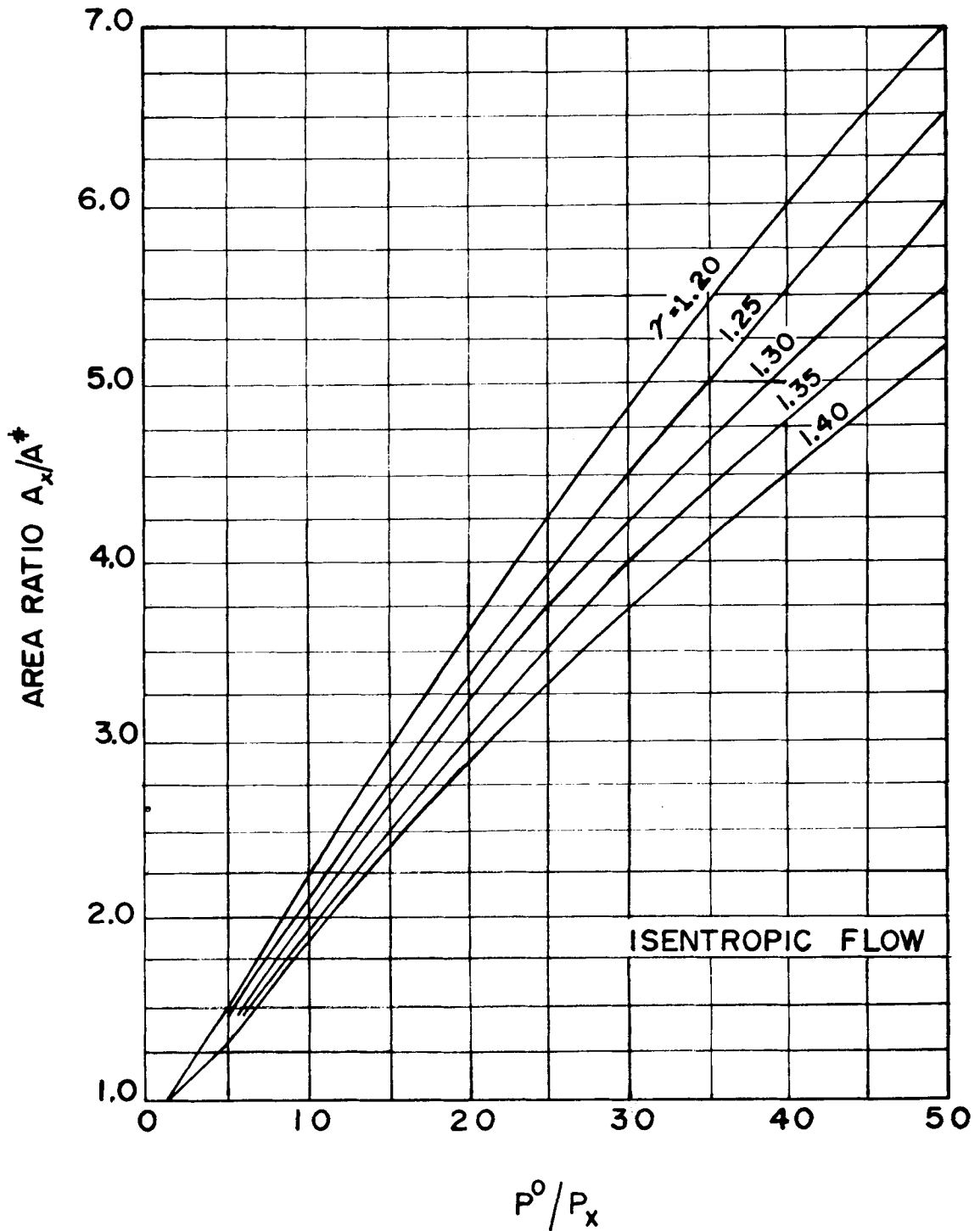


Figure 4-8. Area Ratio A_x/A^* for Complete Expansion As a Function of the Nozzle Pressure Ratio P^0/P_x for Different Values of $\gamma = c_p/c_v$

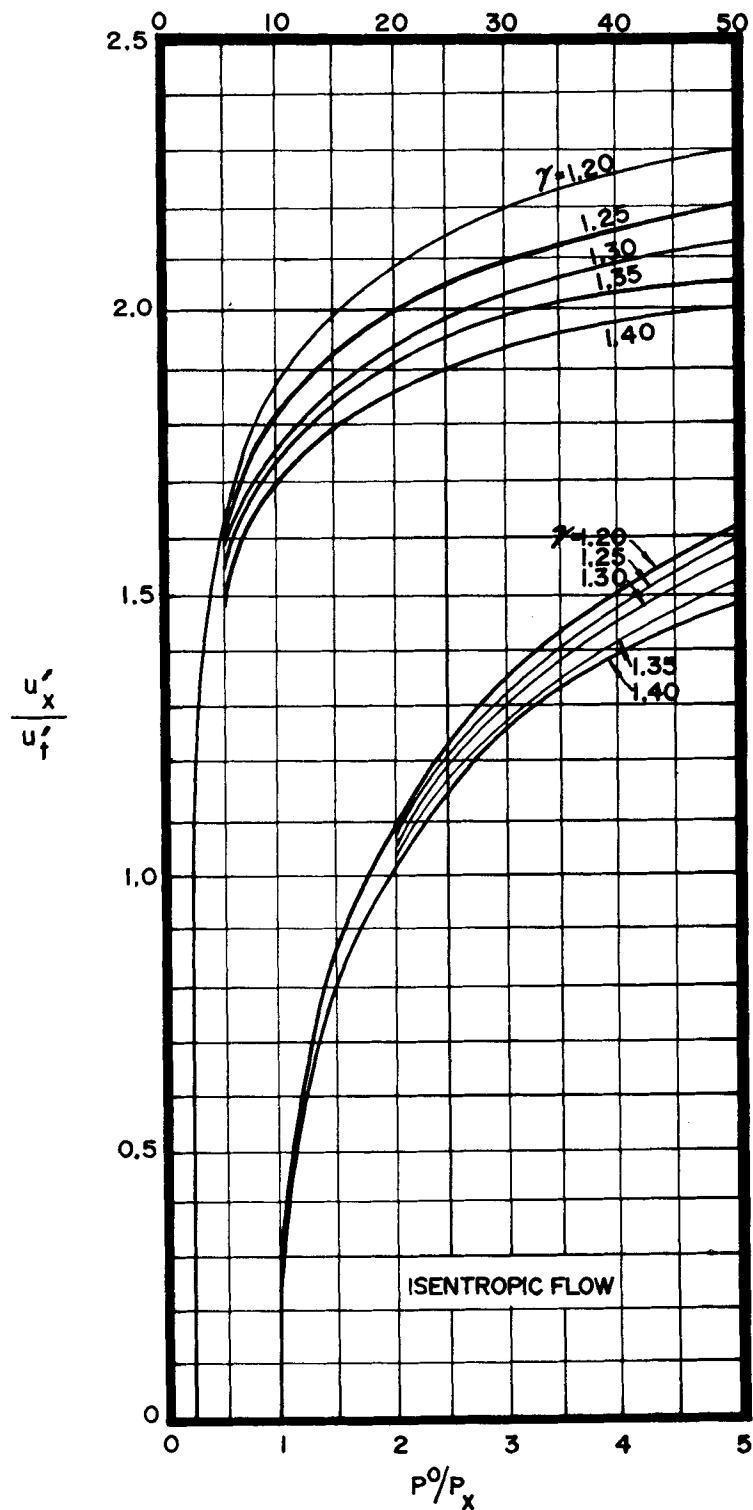


Figure 4-9. Ratio of the Isentropic Exit Velocity u'_x to the Isentropic Throat Velocity u'_t As a Function of the Nozzle Pressure Ratio P^0/P_x for Different Values of $\gamma = c_p/c_v$

SOLUTION.

(a) Stagnation values of the flowing air

Assume

$$\gamma = 1.40; a_1 = 49.02 \sqrt{800} = 1390 \text{ fps};$$

$$M_1^2 = 0.09$$

$$u_1 = M_1 a_1 = 0.3 (1390) = 417 \text{ fps};$$

$$R_{\text{air}} = 1712 \text{ ft-lb/slug}^\circ \text{R}$$

$$\rho_1 = P_1 / (RT_1) = \frac{100 (144)}{1712 (800)} = 0.01052 \text{ slug/ft}^3$$

$$T^0 = T_1 (1 + 0.2 \times 0.09) = 814^\circ \text{R}$$

$$P^0 = 14400 (1.018)^{3.5} = 15,420 \text{ psf} = 107 \text{ psia}$$

$$\rho^0 = P^0 / (RT^0) = 15,420 / [(1712)(814)] \\ = 0.01106 \text{ slug/ft}^3$$

$$a^0 = \sqrt{\gamma RT^0} = 49.02 \sqrt{814} = 1400 \text{ fps}$$

(b) Weight rate of flow

$$\dot{m}' = \dot{m}^* = \dot{w}' / g_c = \rho_1 A_1 u_1 / g_c$$

$$\dot{w}' = 32.174 (\dot{m}^*) = 32.174 (0.01052)(1) (417) \\ = 141 \text{ lb/sec}$$

$$\dot{m}^* = 4.38 \text{ slug/sec}$$

(c) Throat conditions

Since the nozzle passes the critical flow rate \dot{m}^* , from Eqs. 4-12 to 4-15:

$$P_t = P^* = \left(\frac{2}{2.4} \right)^{3.5} P^0 = 0.5283(15,420) \\ = 8,150 \text{ psf} = 56.50 \text{ psia}$$

$$T_t = T^* = (2/2.4)814 = 678^\circ \text{R}$$

$$\rho_t = \rho^* = \left(\frac{2}{2.4} \right)^{2.5} (0.01106) = 0.01106/1.577 \\ = 0.00698 \text{ slug/ft}^3$$

$$u_t' = a^* = a^0 \sqrt{2/2.4} = 1400(0.912) = 1277 \text{ fps}$$

(d) Throat area

Since $\dot{m}' = \dot{m}^*$, from Eqs. 4-16 and 4-17:

$$A_t = A^* = \dot{m}^* \frac{\sqrt{RT^0}}{\psi^* P^0}$$

$$\psi^* = \left(\frac{2}{2.4} \right)^{2.5} \sqrt{\frac{2.8}{2.4}} = (0.634) 1.08 = 0.686$$

Hence

$$A^* = 4.38 \frac{\sqrt{1712 (814)}}{0.686 (15420)} = 0.492 \text{ sq ft} \\ = 70.7 \text{ sq in.}$$

Check

$$\dot{m}^* = 0.00698 (0.492) 1277 = 4.38 \text{ slug/sec}$$

(e) Area of exit cross-section (A_e)

When

$$\epsilon = \epsilon_{\text{opt}}, P_e = P_a = 15(144) = 2160 \text{ psf}$$

$$\left(\frac{P_a}{P^0} \right)^{\frac{\gamma-1}{\gamma}} = \left(\frac{2160}{15,420} \right)^{0.286} = (0.140)^{0.286} = 0.5702$$

$$\sqrt{1 - 0.5702} = 0.6556$$

From Eq. 4-24:

$$M_e^* = \frac{u_e'}{a^*} = 0.6556 \sqrt{6} = 1.608$$

Hence

$$u' = a^* M_e^* = 1277 (1.608) = 2050 \text{ fps}$$

Since flow is isentropic:

$$T_e = T^* \left(\frac{P_e}{P^*} \right)^{0.286} = 680 \left(\frac{2160}{8150} \right)^{0.286} \\ = 680(0.696) = 472^\circ \text{R}$$

$$a_e = 49.02 \sqrt{472} = 1063 \text{ fps}$$

$$M_e = \frac{u'_e}{a_e} = \frac{2050}{1063} = 1.93$$

From Eq. 4-20a:

$$\epsilon_{\text{opt}} = \frac{A_e}{A^*} = \frac{1}{1.93} \sqrt{\frac{5}{6}} (1.756)^6 = 1.616$$

$$A_e = 1.616 (0.492) = 0.796 \text{ sq ft} = 114.5 \text{ sq in.}$$

$$\rho_e = 0.01052 \left(\frac{800}{472} \right) \frac{2160}{14,400} \\ = 0.00267 \text{ slug/ft}^3$$

4-3.2 EFFECT OF VARYING THE BACK PRESSURE ACTING ON A CONVERGING-DIVERGING NOZZLE

Fig. 4-10 presents the expansion ratio P_e/P_a and the exit Mach number M_e as functions of the area ratio A_e/A^* . It is evident from the figure that for each value of A_e/A^* there are two values of M_e , one is subsonic and the other supersonic. The back pressure P_a determines which value of M_e will occur.

If a converging-diverging nozzle passes an isentropic mass flow rate $\dot{m}' < \dot{m}^*$, the flow is subsonic throughout the nozzle, and there is a small range of exit pressures which can be attained with a subsonic isentropic flow, as indicated in Fig. 4-11.

When the nozzle passes the critical mass flow rate \dot{m}^* , only two exit pressures satisfy the requirements for an isentropic flow throughout the converging-diverging nozzle, as illustrated schematically in Fig. 4-11. The gas can expand isentropically to the throat pressure $P_t = P^*$; then it may either continue to expand isentropically, along curve a, to the lower exit pressure $P_{e1} < P^*$ or it may diffuse isentropically, along curve b, to a higher exit pressure $P_{e2} > P^*$. If the gas expands isentropically to P_{e1} , the exit velocity u'_e will be supersonic ($M_e > 1$). On the other hand, if the gas undergoes an isentropic diffusion along curve b, then $M_e < 1$. None of the exit pressures between P_{e1} and P_{e2} can be reached by an ideal nozzle flow.

A converging-diverging nozzle having a fixed area ratio A_e/A^* and operating with fixed inlet conditions gives complete expansion of the flowing gas, only when $P_e = P_a$ = back pressure. Consequently, such a nozzle can be designed to operate with the optimum area ratio at *only one altitude or back pressure*. Consequently, at all but one back pressure P_a , the nozzle operates with either $P_e > P_a$ or $P_e < P_a$.

4-3.2.1 UNDEREXPANSION IN A CONVERGING - DIVERGING NOZZLE

When $P_e > P_a$, the gas expansion from P_e to P_a takes place beyond the nozzle exit area A_e . A nozzle operating with $P_e > P_a$ is said to operate with *underexpansion*. Conversely, if the fixed area nozzle operates with $P_e < P_a$, it is said to operate with *overexpansion*.

As long as a converging-nozzle is operated with *underexpansion* ($P_e > P_a$), the flow conditions inside the nozzle are unaffected by any variations in the back pressure. The supersonic gas jet ejected from the nozzle expands in

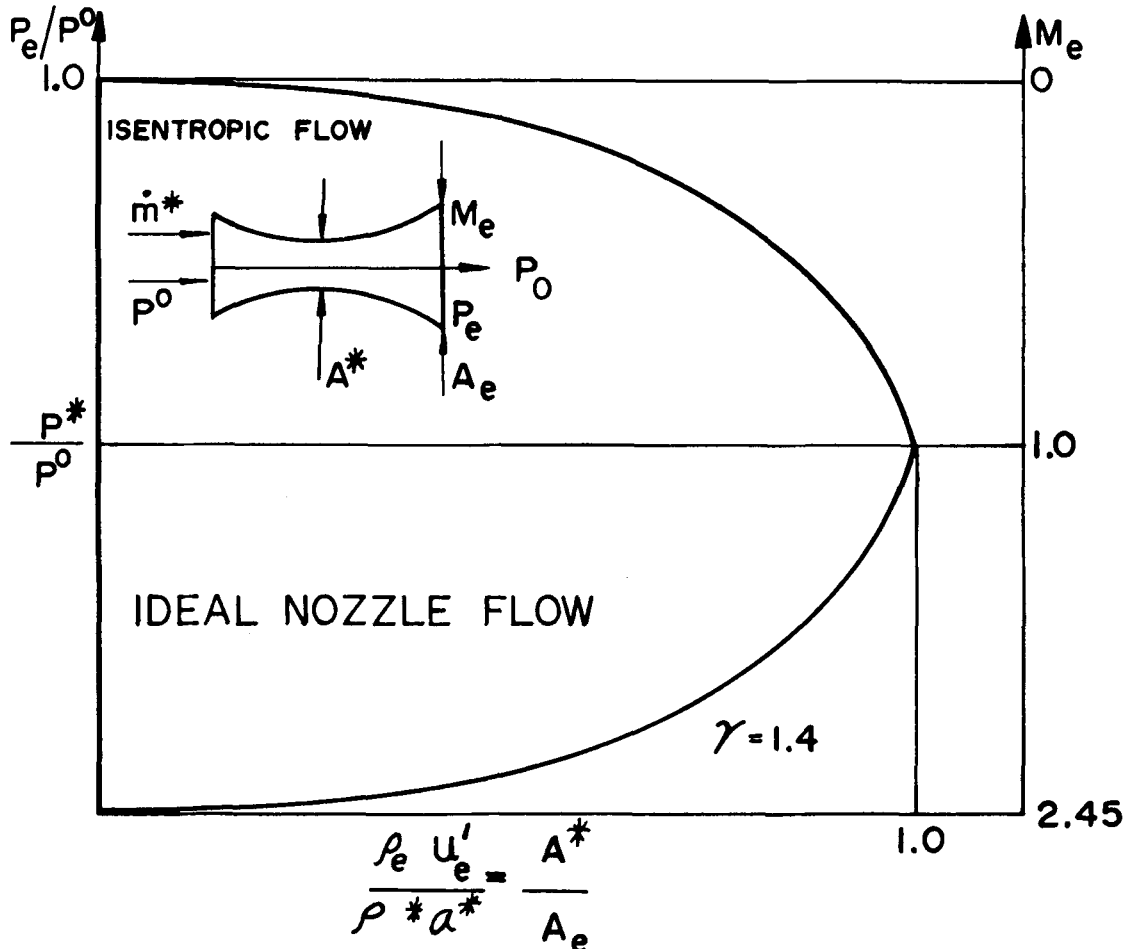


Figure 4-10. Expansion Ratio P_e/P^0 and Exit Mach Number M_e As Function of the Area Ratio A^*/A_e for a Converging-Diverging Nozzle Passing the Critical Mass Flow Rate \dot{m}^*

much the same manner as that discharged by a converging nozzle operated supercritically. Consequently, the thrust produced by an underexpanded jet is less than that obtained from a nozzle operating with complete expansion ($P_e = P_a$), and a pressure thrust term equal to $(P_e - P_a)A_e$ enters into the thrust equation for a propulsive nozzle (see pars. 2-3 and 2-4).

4-3.2.2 OVEREXPANSION IN A CONVERGING-DIVERGING NOZZLE

If a converging-diverging nozzle is operated with *overexpansion*, the gas flowing inside the

nozzle may expand to a static pressure P_e lower than that corresponding to the back pressure P_a . The gas is compressed to the back pressure by flowing through one or more oblique shock waves, as illustrated schematically in Fig. 4-12. The problem of overexpansion has been studied by several investigators, but a general and accurate procedure for predicting separation in all types of nozzles is lacking^{10,11,12,13}.

Consider a converging-diverging nozzle having a fixed area ratio A_e/A_t and assume it is

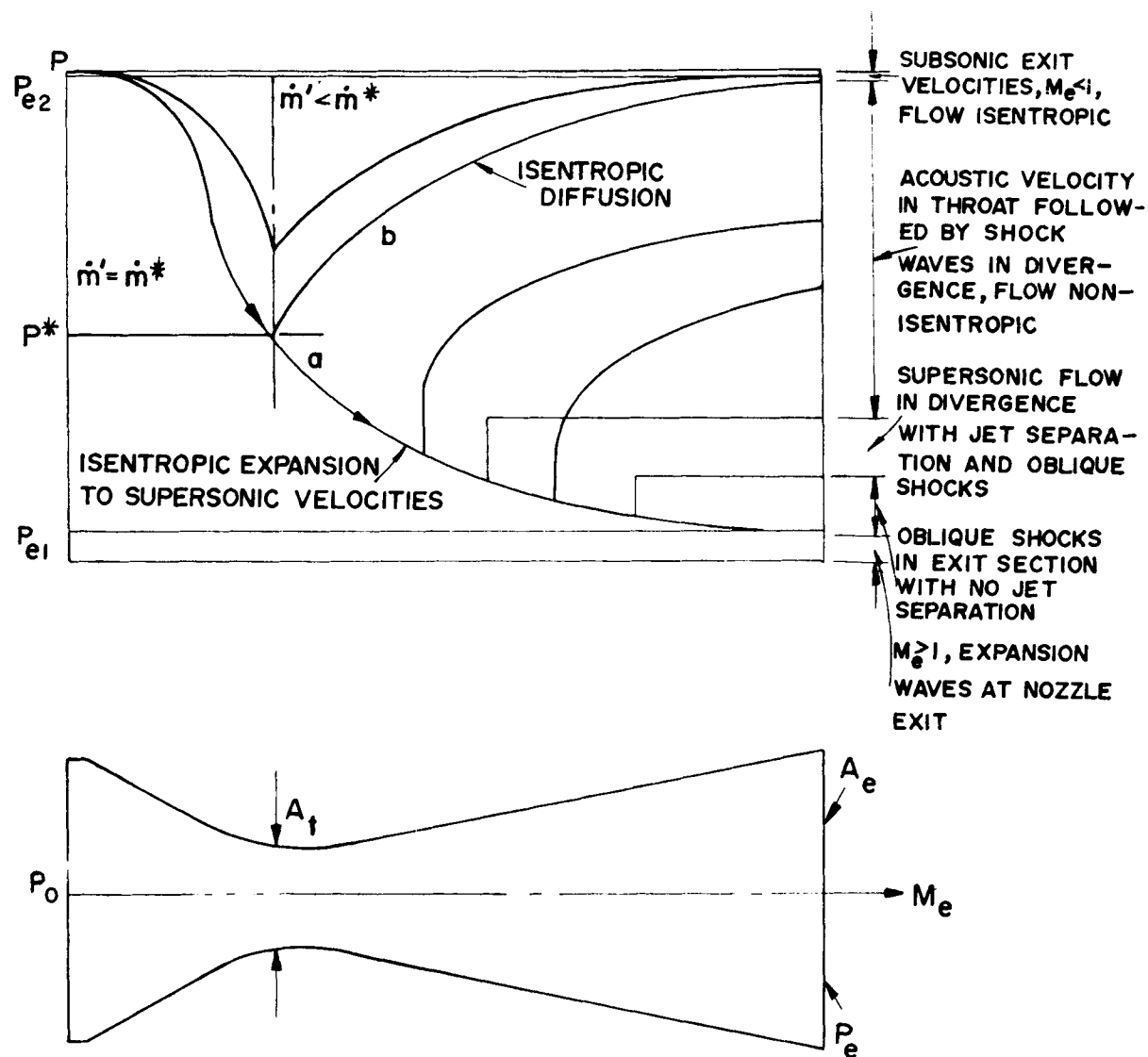


Figure 4-11. Pressure Distributions in a Converging-Diverging Nozzle Under Different Operating Conditions

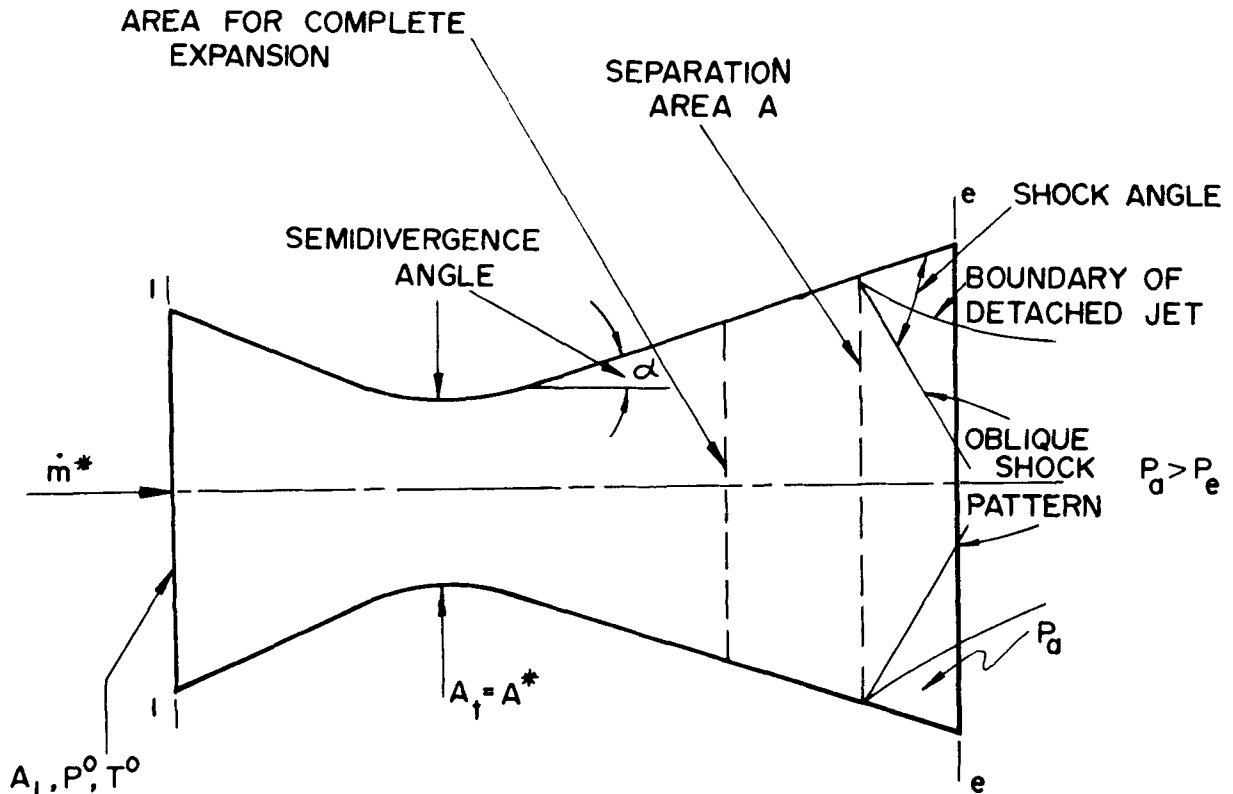


Figure 4-12. Conical Converging-Diverging Nozzle Operating With Overexpansion

designed so that $P_e = P_a$. The flow in the divergence is isentropic and supersonic. Assume now that the back pressure is raised slightly above the design value for the exit pressure P_e , i.e., A_e is larger than that required for expanding the gas to $P_a > P_e$.

When P_a is only slightly larger than P_e , oblique shocks are formed in exit corner of the diverging portion of the nozzle, and the shock angle depends on the pressure ratio P_a/P_e and M_e . Increasing P_a causes the oblique shocks to steepen and become stronger. The range of

values of P_a that cause oblique shocks without jet separation is indicated schematically in Fig. 4-11.

It should be noted that in an actual nozzle the back pressure P_a can propagate upstream through the boundary layer adjacent to the walls of the nozzle; within the boundary layer the gas velocities decrease from supersonic at its interface with the main gas stream to subsonic velocities and to zero at the walls. When P_a is only slightly larger than P_e , as mentioned earlier, weak oblique shocks are formed in the exit

corner of the diverging section of the nozzle and the gas is compressed by the shocks to the back pressure P_a , a nonisentropic process which results in a reduction of the exit velocity of the jet.

If the back pressure P_a is raised further, the oblique shocks steepen which gives rise to shock-boundary layer interactions; if the shock-induced compression of the gas is high enough, the boundary layer will separate from the wall slightly upstream from the shock. If the back pressure is increased further, the shock moves upstream steepens and its propagation speed increases. The shock will become substantially normal to the flow and locate itself in the diverging portion of the nozzle where the pressure rise of the shock-induced compression of the gas is insufficient to cause boundary layer separation. The gas leaves the shock front with a subsonic velocity (see Fig. 4-11).

Fig. 4-13 presents a correlation of the data obtained by several experimenters with conical rocket motor nozzles having a semidivergence angle of $\alpha = 15^\circ$. The parameter $(P_a - P_s)/P^0$ is plotted as a function of P^0/P_a .

Experiments indicate that for a given value of α , the separation pressure ratio P_s/P_a is a function of the nozzle pressure ratio P^0/P_a .

It is desirable to have some control of the separation phenomena especially for the nozzles of jet propulsion engines which must operate over a wide range of altitudes as, for example, the nozzles of rocket motors for propelling launch vehicles. Efforts to reduce the thrust loss resulting from operating a nozzle with over-expansion have led to the development of nozzles having different configurations than the conventional *internal flow* converging-diverging nozzle. Such nozzles are the plug nozzle, the expansion-deflection nozzle, and the ejector nozzle. They are discussed briefly in par. 4-8.

4.3.3 EFFECT OF VARYING THE INLET TOTAL PRESSURE OF A NOZZLE

Assume ideal nozzle flow and the operation of a nozzle with a constant back pressure P_a . Let the inlet total pressure P^0 be varied with T^0 held constant. As P^0 is increased from the value $P^0 = P_a$, the flow of gas through the nozzle increases. At some value of P^0 the ratio $P_t/P^0 = P^*/P^0$ and the nozzle passes the critical mass flow rate \dot{m}^* which is given by Eq. 4-17. Further increase in P^0 has no effect upon the critical pressure ratio P^*/P^0 , because it is a function of γ alone (see Eq. 4-7). Consequently, P^*/P^0 remains constant for all values of P^0 larger than

$$P^0 = \left(\frac{\gamma+1}{2} \right)^{\frac{\gamma}{\gamma-1}} P_a \quad (4-26)$$

When the nozzle passes the critical mass flow rate \dot{m}^* , the isentropic throat velocity u_t' is given by Eq. 4-8, which is repeated here for convenience

$$u_t' = a^* = a^0 \sqrt{2/(\gamma+1)} \quad (4-27)$$

Eq. 4-27 shows that for a given gas, the gas velocity in the throat of the nozzle depends only upon its inlet total temperature T^0 , it is independent of the total pressure P^0 , because a^0 is a constant. Hence, when the critical condition prevails in the throat of a nozzle, increasing the total pressure has no effect upon $u_t' = a^*$.

The static pressure in the throat is given by

$$P_t = P^* = \left(\frac{2}{\gamma+1} \right)^{\frac{\gamma}{\gamma-1}} P^0 \quad (4-28)$$

Hence, if P_a is held constant, and P^0 is increased, and the nozzle is operated *supercritically*, so that $P^* > P_a$; then the following conditions are realized:

- (a) The static pressure in the nozzle throat increases linearly with P^0 .

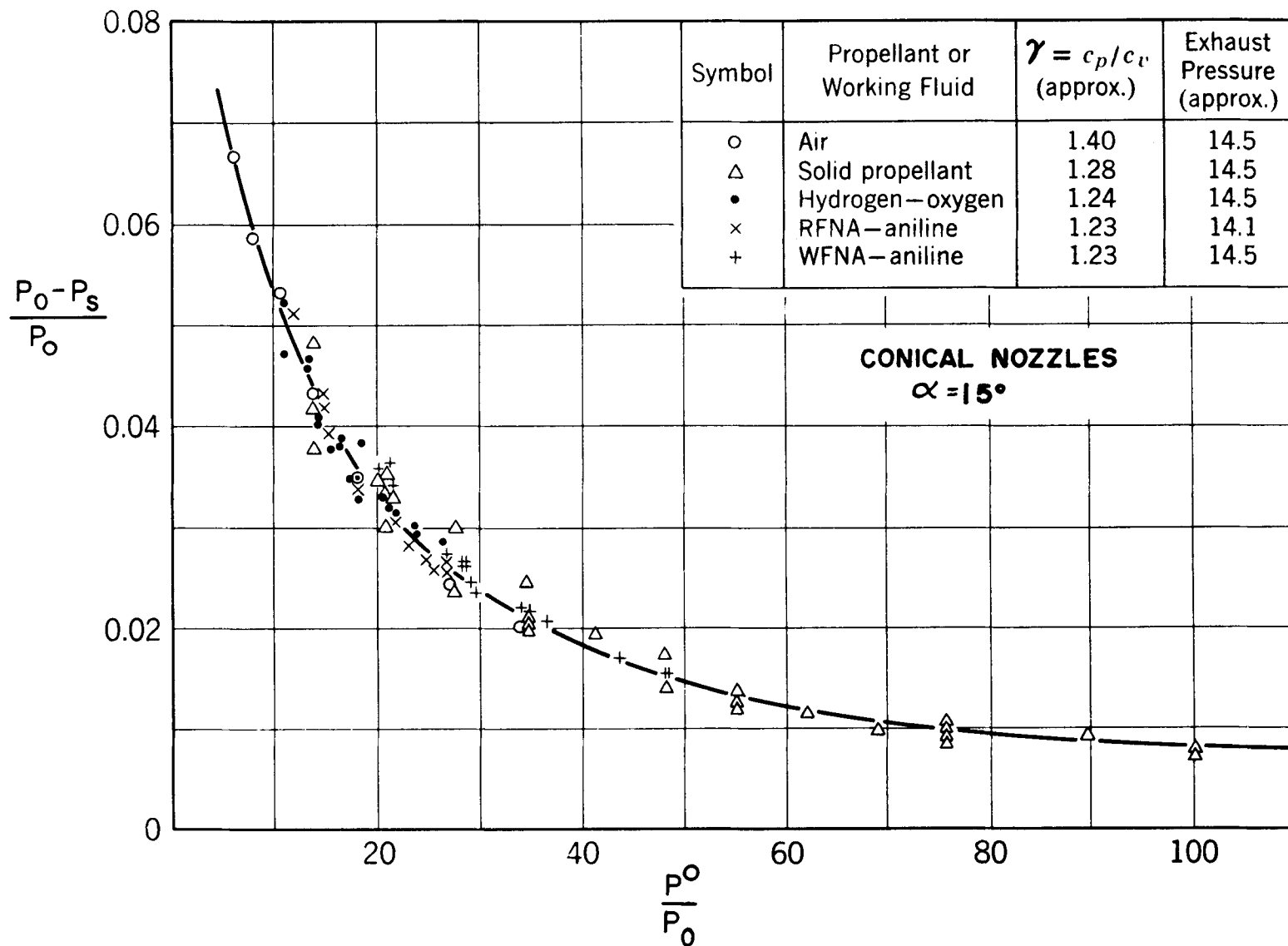


Figure 4-13. Correlation of Data on Jet Separation in Conical Nozzles for Rocket Motors (According to Reference 10)

- (b) The static temperature of the gas in the throat remains constant at the value

$$T_t = T^* = \left(\frac{2}{\gamma+1} \right) T^0$$

- (c) The gas density in the throat is given by

$$\rho_t = \rho^* = \frac{P_t}{RT}$$

or

$$\rho_t = \left(\frac{\gamma+1}{2} \right) \left(\frac{2}{\gamma+1} \right)^{\frac{\gamma}{\gamma-1}} \frac{P^0}{R}$$

Hence, $\rho_t = \rho^*$ increases linearly with P^0 .

- (d) Since T^0 , R , and γ are constants—so that the critical flow factor ψ^* is a constant—the mass flow rate for the nozzle is given by

$$\dot{m}' = \dot{m}^* = A^* \psi^* \frac{P^0}{\sqrt{RT^0}} = (\text{constant})(P^0) \quad (4-29)$$

In the last equation all terms except P^0 are constants. Hence, if a nozzle is operated with a constant back pressure, once $P_t = P^*$ an increase in P^0 causes the mass flow rate of gas to increase linearly with P^0 .

4-4 FLOW IN REAL NOZZLES

4-4.1 LOSSES IN NOZZLES

Up to this point the discussions have been concerned with nozzles operating with ideal nozzle flow. Although it is reasonable to assume in most cases that in an actual well-designed nozzle the flow is steady and one-dimensional, the expansion process in the nozzle may be assumed *adiabatic* but not *isentropic*. The loss of available energy in a well designed nozzle operating at its design point is quite small and is due primarily to wall friction. Other losses can arise due to operating the nozzle with either underexpansion or overexpansion. As pointed out in par.

4-3.2.1 when a nozzle is operated with underexpansion, there is a loss due to the expansion from the exit pressure P_e to the back pressure P_a taking place in the free jet. The loss due to underexpansion is not serious if the difference between the actual and operating pressure for the nozzle is not too large because the variations in back pressure have negligible effect upon the flow conditions in a nozzle. For example, if a converging nozzle for a subsonic turbojet engine is designed to operate with a pressure ratio $P_t/P^0 = 1.89$ it can be operated supercritically at $P_t/P^0 = 6$ with a thrust loss of approximately 5 percent^{5,13}. In par 4-3.2.2 it was explained why serious thrust loss can be encountered if a converging-diverging nozzle operates with serious overexpansion.

The discussions in this paragraph are concerned with the loss due to wall friction.

4-4.2 AREA RATIO FOR AN ADIABATIC NOZZLE

In general, the conditions at the inlet to a jet propulsion nozzle are known and the usual problem is to determine the flow area for passing a specified mass flow rate. Because of the wall friction, Eq. 3-74, which applies to an isentropic flow, must be modified.

Let the subscripts 1 and 2 denote any two stations in a nozzle, and assume the flowing fluid is an ideal gas. Applying Eq. 3-29 to Stations 1 and 2, and solving for the area ratio A_2/A_1 , yields

$$\frac{A_2}{A_1} = \frac{M_1}{M_2} \frac{P_1}{P_2} \sqrt{\frac{T_2}{T_1}} \quad (4-30)$$

For an adiabatic flow $T^0 = \text{constant}$, but $P_1^0 > P_2^0$. It is readily shown, that

$$\frac{A_2}{A_1} = \frac{M_1}{M_2} \left[\frac{1 + \left(\frac{\gamma-1}{2} \right) M_2^2}{1 + \left(\frac{\gamma-1}{2} \right) M_1^2} \right]^{\frac{\gamma+1}{2(\gamma-1)}} \frac{P_1^0}{P_2^0} \quad (4-31)$$

Let $s(A/A^*)_{M_1}$ denote the area ratio corresponding to an isentropic flow from $M = M_1$ to $M = 1$. Then¹

$$\frac{A_2}{A_1} = \frac{P_1^O}{P_2^O} \left[\frac{s\left(\frac{A_2}{A^*}\right)_{M_2}}{s\left(\frac{A_1}{A^*}\right)_{M_1}} \right] \quad (4-32)$$

Eq. 4-32 shows that because of friction the throat area of a real nozzle must be larger than that for a comparable isentropic nozzle; Eq. 4-35 applies to any one-dimensional flow channel in which an ideal gas flows adiabatically.

4-5 NOZZLE PERFORMANCE COEFFICIENTS

To correct the results obtained by assuming ideal nozzle flow, certain empirical coefficients are employed. These are discussed below.

4-5.1 NOZZLE EFFICIENCY (η_n)

If u_e denotes the actual exit velocity of the gas crossing the exit cross-section A_e of a nozzle and u'_e is the corresponding isentropic exit velocity, then by definition (see par. A-5.4.1) the nozzle efficiency η_n is given by

$$\eta_n \equiv \frac{h^O - h_e}{h^O - h'_e} = \left(\frac{u}{u'_e} \right)^2 \quad (4-33)$$

The nozzle efficiency is the ratio of the kinetic energy of the jet ejected from the nozzle to that for an isentropic expansion between the same values of P^O and P_e .

4-5.2 NOZZLE VELOCITY COEFFICIENT(ϕ)

By definition the nozzle velocity coefficient is given by

$$\phi \equiv \frac{u_e}{u'_e} \quad \text{or} \quad u_e = \phi u'_e \quad (4-34)$$

If the flowing fluid is an ideal gas, then Eq. 4-34 can be transformed to read

$$u_e = \phi u'_e = \phi c_o \sqrt{Z_t} \quad (4-35)$$

where

$$c_o = a^O \sqrt{\frac{2}{\gamma-1}} \quad \text{and} \quad a^O = \sqrt{\gamma R T^O}$$

$$Z_t = 1 - \left(\frac{P_e}{P^O} \right)^{\frac{\gamma-1}{\gamma}}$$

The effects of friction may be assumed to be confined to the boundary layer adjacent to the walls of the nozzle, and the core flow may be assumed to be isentropic. The choking of the flow occurs in the core flow when the local Mach number is unity. The flow cross-sectional area where $M=1$ based on isentropic flow can then be increased by the thickness of the boundary layer to obtain the required throat area for a real nozzle. The result would, of course, be approximate because the isentropic flow is assumed to be one-dimensional^{1,7,20}.

4-5.3 NOZZLE DISCHARGE COEFFICIENT (C_d)

By definition, the discharge coefficient, denoted by C_d , for either a nozzle or an orifice is

$$C_d = \frac{\text{actual mass flow rate } (\dot{m})}{\text{isentropic mass flow rate } (\dot{m}')} \quad (4-36)$$

In those cases where the fluid jet contracts beyond the exit section A_e , a *contraction coefficient* ($C_c < 1$) can be introduced so that

$$C_d = C_c \phi = \text{discharge coefficient} \quad (4-37)$$

The value of C_d for a given nozzle must be determined experimentally. Data on converging

nozzles are presented in Reference 14. If there is no jet contraction $C_c = 1$, and $C_d = \phi^{1/2}$.

In general, the discharge coefficient depends upon the configuration of the nozzle, the roughness of its walls, its dimensions, the kind of gas, and the expansion ratio for the nozzle. If the nozzle passes the critical mass flow rate then C_d depends only upon the conditions upstream to the throat section. For large nozzles the discharge coefficient is usually close to unity, while for small nozzles C_d can be smaller than unity.

If there is little or no *reassociation* of combustion products as a gas flows through a nozzle, the values of C_d will range from 0.93 to 1.0 depending upon the configuration of the nozzle and the density of the flowing gas. If there occurs significant reassociation of the *dissociated* combustion products, C_d may be appreciably larger than unity, approximately 1.15^{2,21}.

4-6 MASS FLOW RATE FOR A NOZZLE OPERATING WITH ADIABATIC FLOW AND WALL FRICTION

It is convenient to express the mass flow rate through a real nozzle, denoted by \dot{m} , in terms of the stagnation conditions at the entrance cross-section of the nozzle, the discharge coefficient C_d , and the throat area A_t . Thus

$$\dot{m} = C_d A_t \rho_t u_t' \quad (4-38)$$

Hence

$$\dot{m} = C_d A_t \sqrt{2(h^0 - h_t')} \quad (4-39)$$

If the flowing fluid is an ideal gas, then Eq. 4-39 transforms into (see Eq. 4-10)

$$\dot{m} = C_d \frac{P^0 A_t}{\sqrt{RT^0}} \psi \quad (4-40)$$

The maximum flow rate, denoted by \dot{m}_{\max} , for a real nozzle occurs when $\psi = \psi^*$ (see Eqs. 4-16 and 4-19). Hence

$$\dot{m}_{\max} = C_d A_t P^0 \sqrt{\frac{2}{RT^0}} \sqrt{\frac{\gamma}{\gamma+1}} \left(\frac{2}{\gamma+1}\right)^{\frac{1}{\gamma-1}} \quad (4-41)$$

The above equations—since they involve only the stagnation conditions P^0 and T^0 , the throat area A_t , the gas constant R , and its specific heat ratio γ —apply to both converging and converging-diverging nozzles.

4-7 NOZZLE DESIGN PRINCIPLES

Propulsive nozzles for rocket engines and air-breathing engines are usually axisymmetric and have circular cross-sections. The nozzles for rocket engines—and also for ramjet and turbojet engines for propelling vehicles at supersonic speeds—are of the converging-diverging type. For the purpose of studying the flow in such a nozzle it is convenient to divide a converging-diverging nozzle into the following three portions:

- (a) the converging portion wherein the flow is subsonic ($M < 1$).
- (b) the throat section, wherein the flow is sonic ($M_t = 1$).
- (c) the diverging portion, wherein the flow is supersonic ($M > 1$).

It is assumed in the discussions which follow that the nozzle operates with *complete nozzleing*; i.e., the expansion ratio r_t is less than the critical value (see Eq. 4-12). Although the remarks will be concerned primarily with converging-diverging nozzles for rocket engines, they also apply to such converging-diverging nozzles for air-breathing engines.

4-8 NOZZLE DESIGN CONFIGURATIONS

The objective in a nozzle design problem is to determine the physical dimensions of the nozzle in terms of prescribed quantities. In general, the following are prescribed:

- (a) The thermodynamic properties of the flowing gas; these include its specific heat at constant pressure c_p , its specific heat ratio $\gamma = c_p/c_v$, its molecular weight \bar{m} , and the pertinent chemical equilibrium constants.
- (b) The total temperature T^0 and the total pressure P^0 of the gas entering the nozzle.
- (c) The equation of state for the gas; for rocket motor nozzle design the perfect gas law $P/\rho = RT$ gives satisfactory results in most cases.
- (d) The ambient pressure P_a into which the nozzle discharges the propellant gas. For a rocket nozzle which is to operate over a range of altitudes, the *design value* for the back pressure is usually determined as a separate problem which is related to optimizing some operating conditions; e.g., the "burnout velocity" of a rocket-propelled missile (see par. 5-9.2).
- (e) Physical operating conditions; e.g., one or more of the following may be prescribed:
 - (1) Total thrust of the nozzle
 - (2) Overall weight of the nozzle
 - (3) Overall length of the nozzle
 - (4) Exit area of nozzle
 - (5) Parallel flow at nozzle exit cross-section

- (6) The throat area or mass flow rate

- (7) The nozzle contour for maximizing the thrust, for either a given nozzle length or weight.

In the initial design of a nozzle the effects of heat loss due to radiation, incomplete combustion, changes in the chemical properties of the flowing gas as it expands, and wall friction are neglected. The nozzle contour so determined is corrected subsequently for those secondary effects. In other words, the initial design is based on the assumption of potential flow, and the contour based on that assumption is called the *potential wall contour*.

The design of a converging-diverging propulsive nozzle involves the determination of the following:

- (a) The shape of the converging portion
- (b) The shape and dimensions of the throat section
- (c) The configuration of the diverging portion
- (d) The corrections for boundary layer and other effects to the potential wall contour.

The flow in the converging portion is an accelerating flow and is subsonic ($M < 1$) until the throat section, the minimum flow area, is reached. Because the subsonic flow in the converging portion is governed by *elliptic* type partial differential equations, its contour is not a solution of those equations that is uniquely dependent upon the initial flow conditions.

The exact geometry of the converging portion of either a converging or a converging-diverging nozzle is not too critical because of the favorable (negative) pressure gradient. All that is

required is that the contour and the transition to the throat be smooth¹. For a correctly designed nozzle having a well-polished interior surface the velocity coefficient will range from $\phi = 0.96$ to 0.98 . A well-rounded converging portion, though not essential, decreases the length of that part of the nozzle. The throat section can be quite short.

Major differences in nozzle configurations are concerned with the design of the diverging or supersonic flow portion of the nozzle. The different nozzle configurations which have either been applied or considered for propulsive nozzles are:

- (a) Conical Nozzle
- (b) Contoured or Bell-shaped Nozzle
- (c) Annular Nozzle
- (d) Plug Nozzle
- (e) Expansion Deflection or E-D Nozzle.

4-8.1 CONICAL NOZZLE

Until a few years ago the problem of designing a rocket motor nozzle was based on the one-dimensional conical flow approximation. Investigations indicated that an *optimum* divergence angle could be specified for a conical nozzle that would minimize pressure losses and achieve satisfactory performance over an anticipated range of exit pressures.

Fig. 4-14 illustrates the general features of a conical nozzle employed in rocket jet propulsion. The semiangle of the convergence,

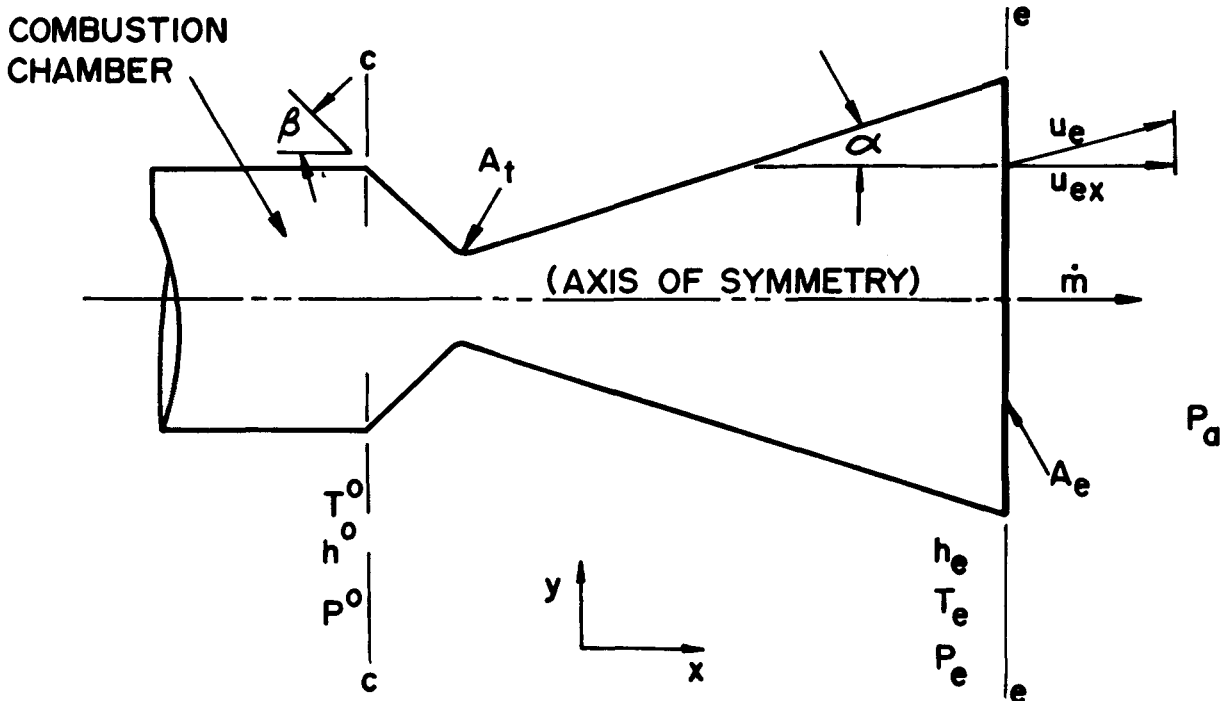


Figure 4-14. General Characteristics of a Conical Converging-diverging Nozzle

denoted by β , is usually between 12° and 35° . The semiangle of the divergence, denoted by α , should not exceed 18° to avoid the jet separating from the wall of the diverging (supersonic) portion of the nozzle. From the viewpoints of nozzle weight and heat losses, the semi-divergence angle should be as large as is permissible. Experiments indicate that the most favorable value of α for a rocket motor nozzle is between 12° and 15° ²².

The conical nozzle finds a wide application in rocket engines employed in Army weapons, particularly, where low fabrication cost is important and the nozzle area ratio (A_e/A_t) is relatively small.

The design of a conical nozzle is based on one-dimensional gas dynamic theory. For the initial expansion from the throat, where $M=1$, to the diverging portion, where $M>1$, almost any smooth curve is satisfactory. Two widely used designs are employed for the throat: (1) a circular arc having a radius equal to approximately $R_t/2$, where R_t is the *throat radius*, and (2) a sharp corner.

The design of the supersonic diverging conical portion can be done nondimensionally and scaled to any desired value of thrust. Only two geometric parameters are involved: the semidivergence angle α and the nozzle length. To minimize the nozzle weight and reduce the friction losses, a short nozzle having a large divergence angle would appear desirable. The larger the divergence angle, however, the larger is the thrust loss due to *nonaxial* flow in the exit plane A_e (see Fig. 4-16). A nozzle having $\alpha=15^\circ$ is commonly termed a 15° nozzle and has become almost a standard for propulsive nozzles because it achieves a good compromise between the effects discussed above.

4-8.1.1 THRUST EQUATION FOR A CONICAL NOZZLE

The *axial thrust* F obtainable from a conical nozzle can be determined by integrating the rate

at which momentum crosses a control surface at the nozzle exit, as illustrated in Fig. 4-15. Let

\dot{m} = mass rate of flow of gas through the nozzle

A_s = area of the spherical exit surface

u_e = adiabatic velocity of the gas crossing A_s

Hence

$$F = \int_A^0 [(\dot{m}_s u_e)_x + (P_s - P_a)] dA_s \quad (4-42)$$

It is evident from Eq. 4-42 that, because of the radial flow in the diverging portion of the nozzle (see Fig. 4-15), the velocity u_e and the static pressure P_s are referred to the spherical control surface A_s and not to the nozzle exit planar area A_e .

It is convenient to express the thrust in terms of the adiabatic exit velocity u_e (see Eq. 4-34), the exit area A_e , and the static pressure P_e . To do this, we introduce the *divergence loss coefficient* λ ^{23, 24}

Hence*

$$F = \lambda [\dot{m} u_e + (P_e - P_a) A_e] \quad (4-43)$$

where

$$\lambda = \frac{1}{2} (1 + \cos \alpha) \quad (4-44)$$

and

$$u_e = \phi u'_e = \phi 2 (h^0 - h_e) \quad (4-45)$$

*When the divergence loss coefficient was first derived, see Reference 23, it was applied only to $\dot{m} u_e$ and not to $(P_e - P_a) A_e$. The resulting thrust equation is $F = \lambda \dot{m} u_e + (P_e - P_a) A_e$. The latter equation is still widely used.

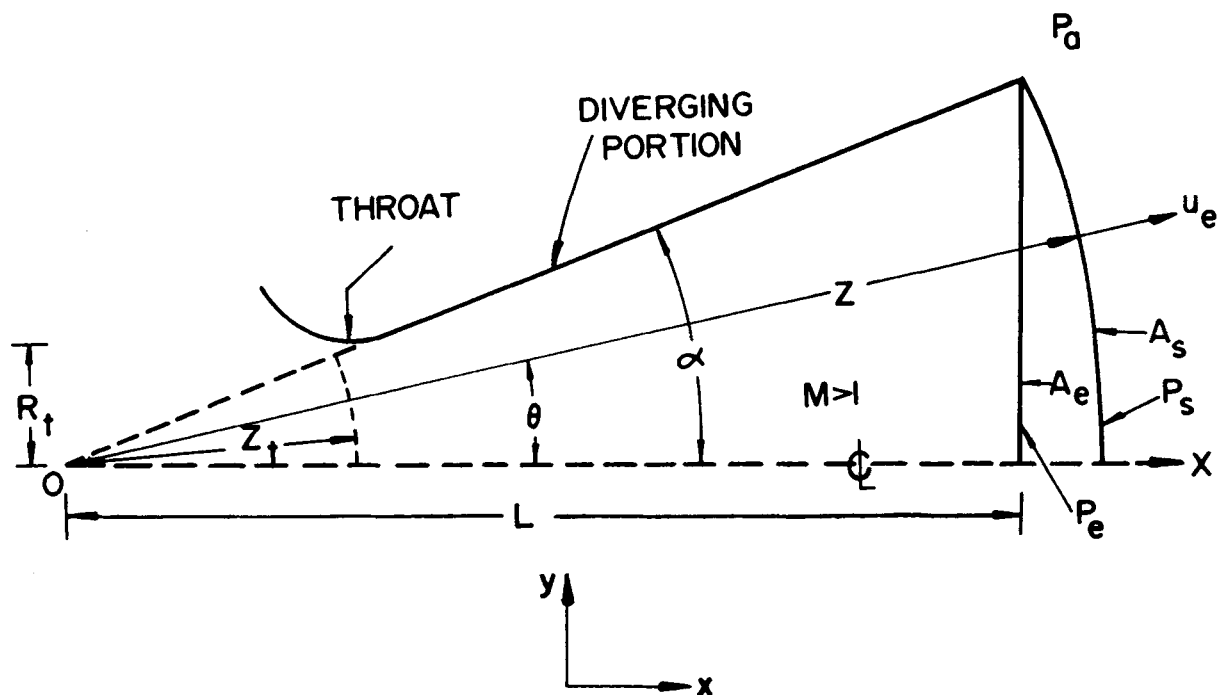


Figure 4-15. Radial Flow in a Conical Nozzle

Fig. 4-16 presents λ as a function of α .

When $P_e > P_a$, the nozzle is said to be *underexpanded* and develops less than the maximum possible thrust. If $P_e < P_a$, the nozzle is *overexpanded* and there are losses in thrust due to oblique shock waves forming in the exit section. Maximum thrust is obtained only when $P_e = P_a$.

If the nozzle must be operated over a range of altitudes (or back pressures), the design point altitude is selected so that the thrust is close to the maximum for the widest anticipated operating range.

The optimum semidivergence angle for a conical nozzle is approximately 15° . If such a nozzle is to expand air ($\gamma=1.40$) from $P^0=300$ psia to $P_a=14.7$ psia, the required dimensionless length for the diverging portion of $L/R_t=2.5$,

where R_t is the throat radius. For an expansion from 300 psia to 0.5 psia, the required dimensionless length increases to $L/R_t=15.7$. Conical nozzles are not well suited to large expansion ratios.

4-8.1.2 FACTORS FOR DETERMINING ADEQUACY OF A CONICAL NOZZLE

The following factors should be considered in determining the adequacy of a conical propulsive nozzle:

- (a) *The design altitude.* For operation at close to sea level altitudes, the performance characteristics of a 15° conical nozzle are not significantly different from those obtainable with more elaborate and expensive designs. For high altitude operations other designs yield significant reductions in size and weight, and may yield an increased thrust.

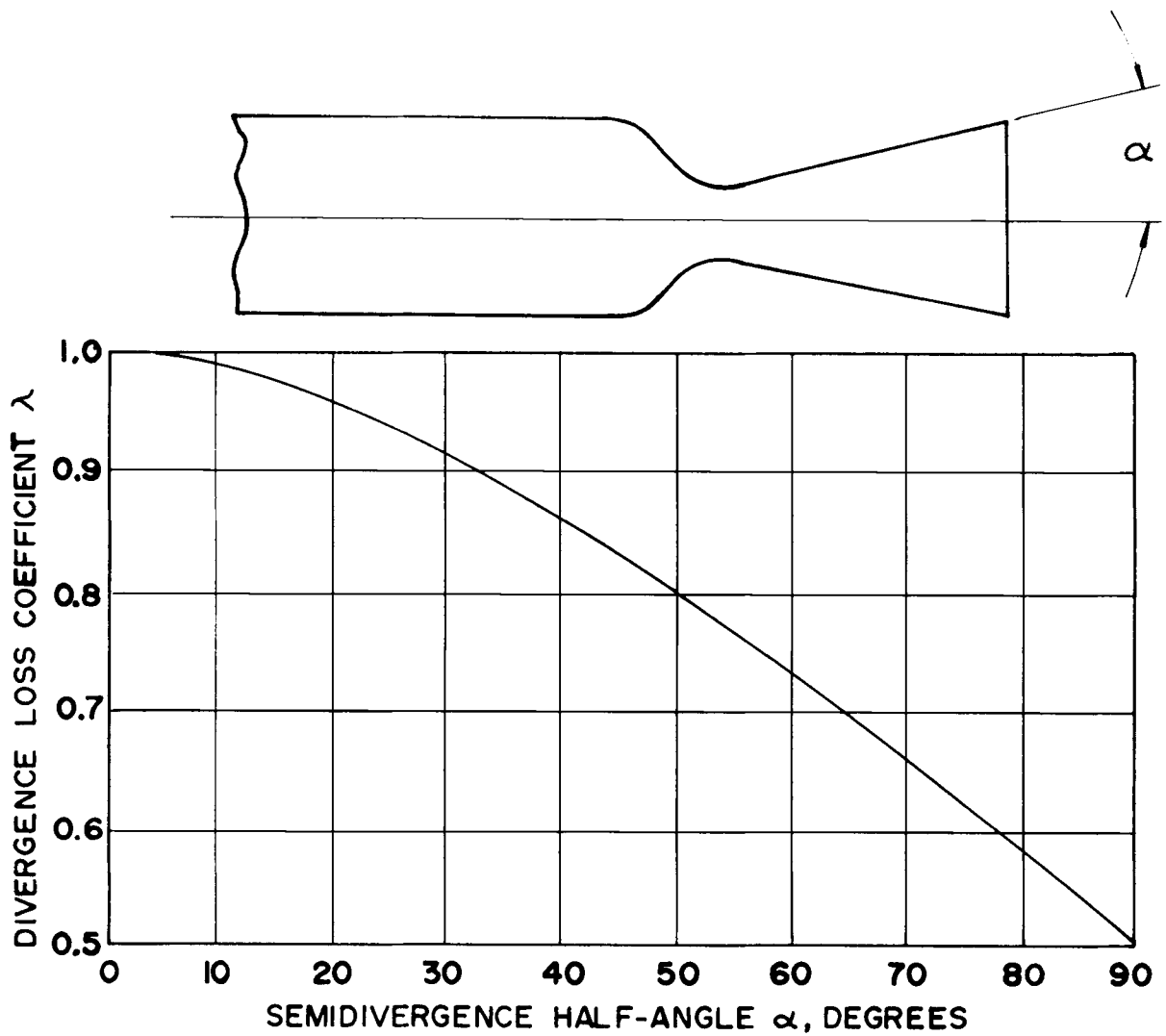


Figure 4-16. Divergence Loss Coefficient λ as a Function of the Semidivergence Half-angle α for a Conical Nozzle

(b) *Effects due to changes in the properties of the propellants.* The main difficulty encountered in determining the effects due to the properties of the propellant gas changing as it expands in the nozzle arises from the lack of knowledge of the chemical reaction rate equations. Consequently, it is customary to consider the following two limiting cases.

- (1) *Frozen flow*, which assumes the composition of the gas to be identical at all sections of the nozzle.
- (2) *Equilibrium flow*, which assumes that the gas is in equilibrium at the calculated values of pressure and temperature at every point in the flow.

The actual condition is between the above limiting cases^{2,4}. The effect of the changing properties of the gas can be taken into account if equations for the change are available. The algebraic work is complicated but computer solutions can be readily obtained.

(c) *Effect of heat transfer.* The accurate determination of the optimum wall contour should take into consideration the effect of heat transfer upon the properties of the propellant gas. In many cases, however, the flow may be assumed to be adiabatic without introducing a serious error.

(d) *Effect of wall friction.* Current methods for calculating the effect of wall friction are empirical^{2,6}. The application of the techniques of boundary layer theory appears to be the most successful of the analytical methods for predicting the effects of friction. It permits separate solutions of the potential and wall friction problems. The potential flow

solution is employed as a boundary condition in analyzing the wall friction.

(e) *Cost and ease of fabrication.* Any gains in performance obtainable from more complicated and expensive nozzle configurations must be justified economically.

Although the above factors apply specifically to conical nozzles they apply in a general way to all nozzles.

4-8.2 CONTOURED OR BELL-SHAPED NOZZLE

Fig. 4-17 illustrates schematically the general features of a *contoured*, also called *bell-shaped*, nozzle. The nozzle wall is contoured in such a manner that the exit flow is nearly axial thereby reducing the thrust loss due to radial flow that is inherent to a conical nozzle. Fig. 4-16 illustrates one-half of such an axisymmetric nozzle. The throat radius is denoted by R_t and the radius of the exit section A_e is R_e ^{2,7}.

From the viewpoint of flow analysis the contour nozzle comprises a *subsonic flow* converging portion, a *transonic flow* portion in the vicinity of the throat, and a *supersonic expansion* portion.

The converging portion is designed so that it produces an *irrotational* subsonic flow that can be expanded in the supersonic portion in a prescribed manner^{2,8,29,30}. The transition from the subsonic flow into a supersonic flow must be smooth and depends upon: (1) the design of the *throat section*, which is a region of *transonic flow*, and (2) a mixture of subsonic and supersonic flows that has no exact mathematical solution. The design of the supersonic expansion portion depends, however, upon the solution of the transonic flow or *initial expansion section*, denoted by I in Fig. 4-17. Several approximate methods have been developed for obtaining

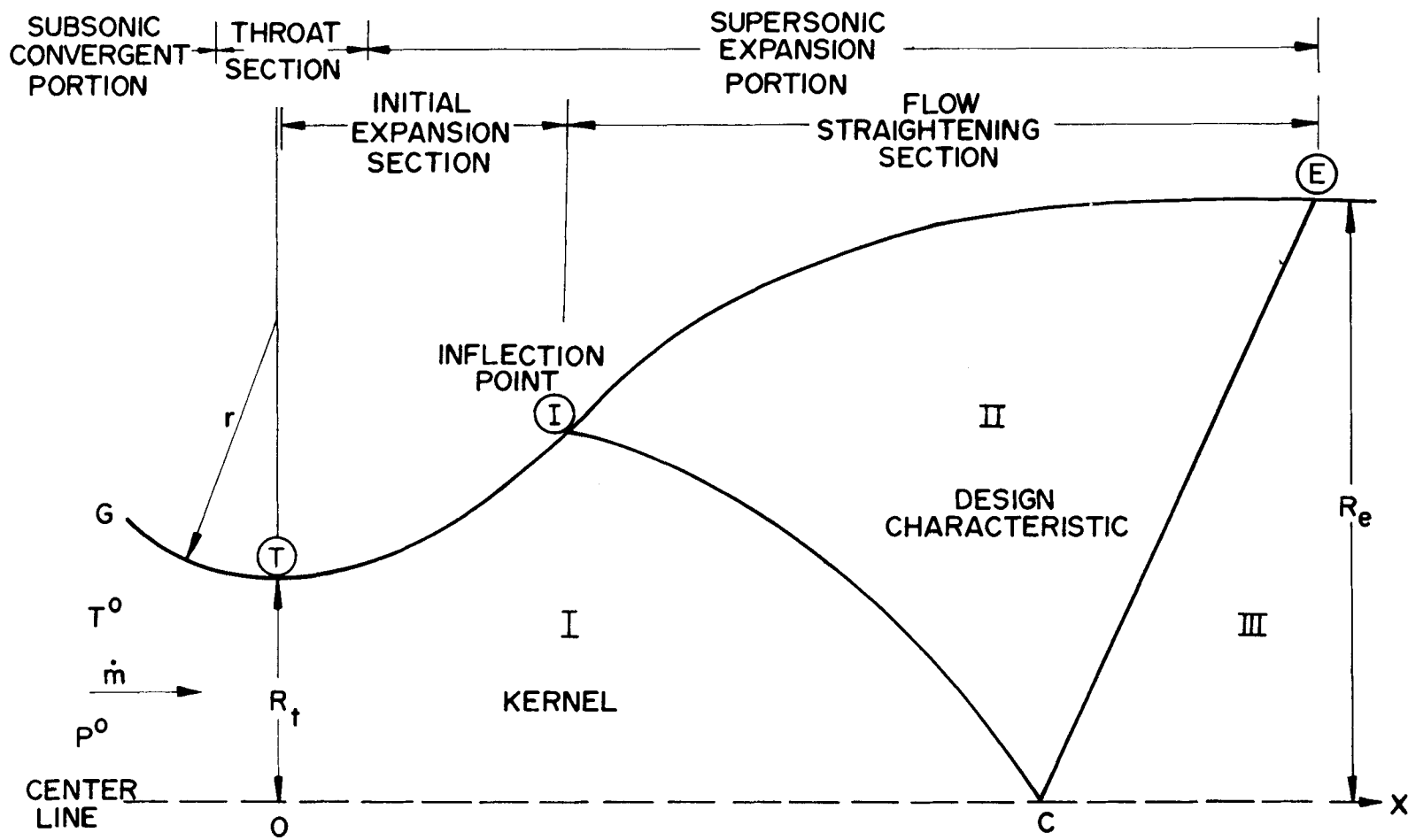


Figure 4-17. General Features of a Contoured or Bell-shaped Nozzle

either an approximate solution to the transonic flow problem^{31,32,33} or for circumventing the transonic flow problem in the design of the supersonic flow portion of the nozzle³⁴.

It is apparent from Fig. 4-17 that the design of the wall contour of the supersonic portion involves the design of the initial expansion section TI and the design of the flow straightening section IE. The details of the nozzle design are based on the application of the *method of characteristics* to the flow and is beyond the scope of this handbook; for detailed information on the method of characteristics see References 27, 37, 39, 40, 41.

The problem of determining the nozzle wall contour for an axisymmetric nozzle that will maximize the thrust for a nozzle of given length has been solved by Reference 35. The results indicate that the wall contour for the initial expansion section TI in Fig. 4-17 should be designed to cause as rapid as possible shock-free expansion of the gas. The contour TI has a wall angle of 28° to 30° that turns the gas away from the *nozzle axis*³⁶. The contour IE of the flow straightening section redirects the flow toward the nozzle axis and, in the nozzle exit plane, the wall makes an angle of 10° to 14° with the nozzle axis depending upon the *nozzle length* and its area ratio A_e/A_t .

The step-by-step determination of the supersonic flow field is widely employed in propulsive nozzle design. Several Government agencies and industrial companies have developed computer programs for designing contour type converging-diverging nozzles. In general, such nozzles are used in large thrust chemical rocket engines.

4-8.3 ANNULAR NOZZLE

Fig. 4-18 illustrates schematically the essential features of an annular nozzle. In this nozzle the throat section is an annulus formed

between an external diverging housing and a central converging conical plug. The gases expand in the diverging annular passage formed between the diverging external housing and the converging conical plug. The assembly is assumed to be axisymmetric.

If the vertex of the conical plug lies in the exit plane A_e , the *divergence loss coefficient* for the annular nozzle illustrated in Fig. 4-18 is given by

$$\lambda = \frac{\frac{1}{2} (\sin \alpha + \sin \beta)^2}{(a + \beta) \sin \beta + \cos \beta - \cos \alpha} \quad (4-46)$$

For the area ratios A_e/A_t and nozzle length, the thrust loss due to radial flow is smaller than for the equivalent conical nozzle.

By contouring the nozzle walls the thrust loss due to flow divergence can be further reduced and the nozzle length decreased somewhat. The mathematical procedure for optimizing a contoured annular nozzle is more complicated than it is for a conventional bell-mouth nozzle because the inner and outer wall contours have to be optimized simultaneously.

4-8.4 PLUG NOZZLE

The nozzles discussed up to this point have the common feature that the expansion of the flowing gas is regulated entirely by the configuration of the walls wetted by that gas; the ambient static pressure P_a has no effect upon the flow inside the nozzle. As the ambient pressure is reduced, by operating the nozzle above the *design altitudes* the propellant gas can be *overexpanded*, and if P_a is sufficiently small the overexpansion phenomena (see par. 4-3.2.2) could cause the flow to separate from the walls of the nozzle with an attendant loss in thrust.

In recent years, considerable effort has been expended upon developing propulsive nozzle

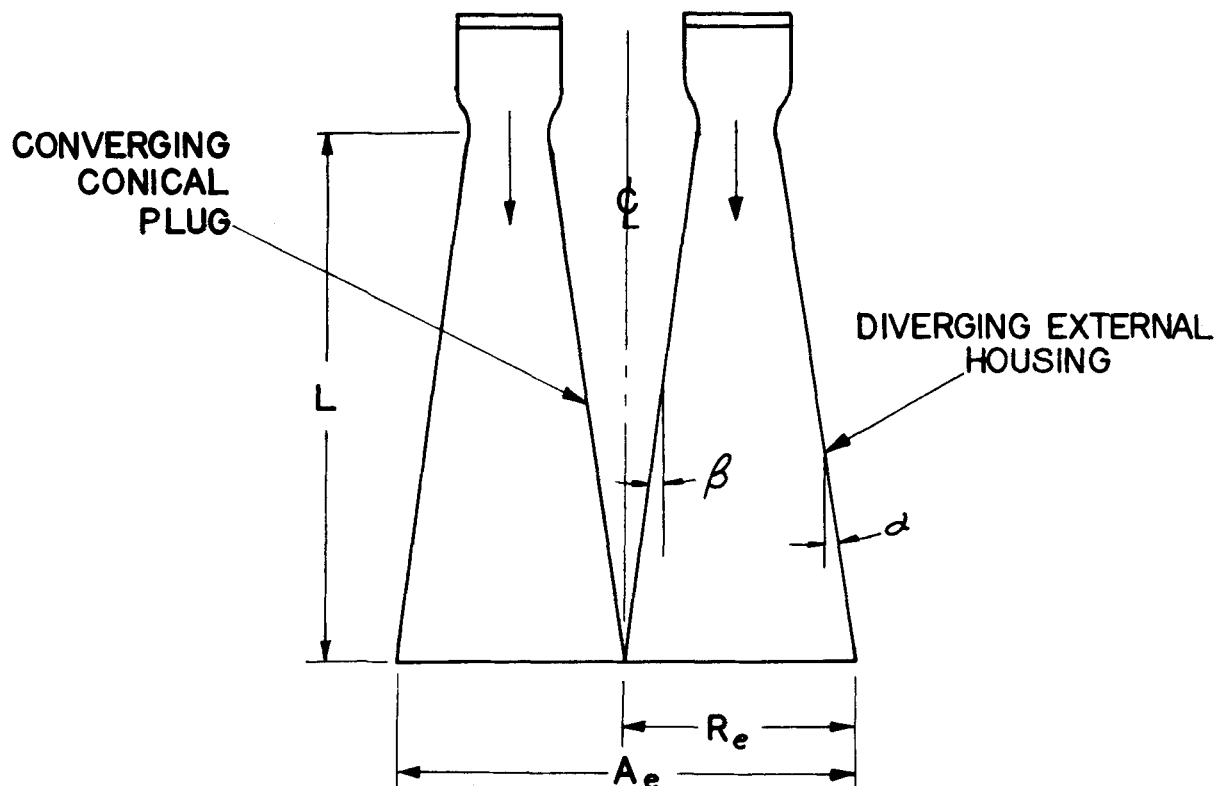


Figure 4-18. Essential Features of an Annular Nozzle

designs which utilize the ambient static pressure P_a for regulating the flow so that it adjusts itself automatically to the prevailing ambient pressure. Such nozzles are frequently called *self-adjusting* nozzles and there are two principal types: (1) the plug nozzle, and (2) the *expansion-deflection* nozzle³⁶. The plug nozzle is discussed in this paragraph and the expansion-deflection nozzle is discussed in par. 4-8.5.

The design of a plug nozzle is based upon the application of the Prandtl-Meyer type of expansion to an expanding flow (see par. A-13); the details of plug nozzle design are discussed in Reference 42. Fig. 4-19 illustrates schematically the basic features of a plug nozzle design giving *full external expansion* of the gas. There are

several variations of the basic concept. The throat of the nozzle is the annulus between the plug and the outer diameter. The propellant gas is discharged in an inward direction. The flow of the exhaust gas stream is controlled by the expansion waves emanating at the cowl-lip in much the same manner as in a Prandtl-Meyer expansion over a corner. In the plug nozzle, however, the flow is three-dimensional instead of two-dimensional and the turning of the gas is effected by the plug.

The contour of the plug can be designed so that the gas flows parallel to the axis of the plug after it has been expanded to the ambient pressure P_a . In that case external diameter of the nozzle ($2R_e$) would be the same as that for a

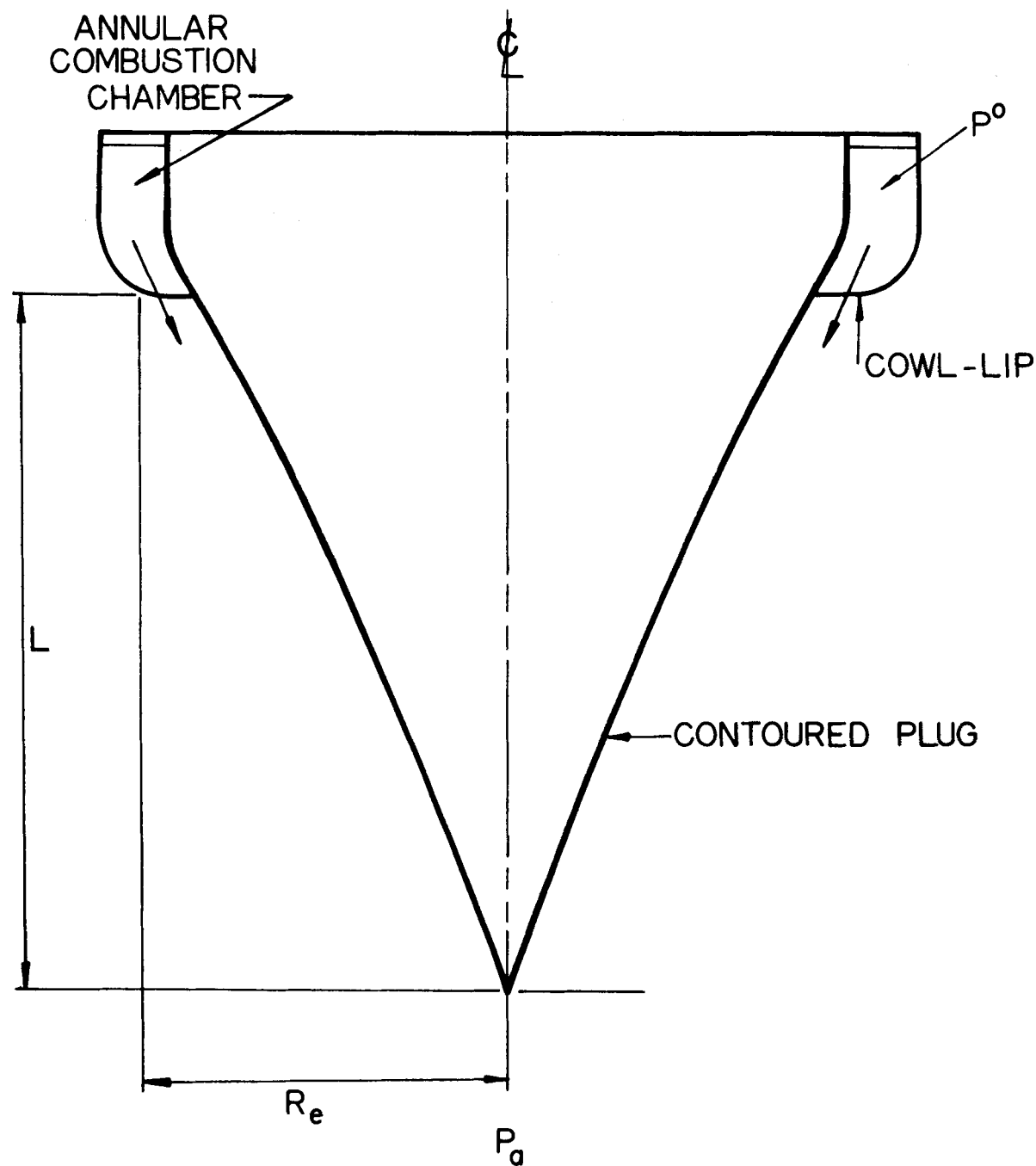


Figure 4-19. Essential Features of a Plug Nozzle

bell-type nozzle giving uniform axial flow at its exit plane. The plug nozzle, however, would be shorter. Furthermore, because of the *free jet* flow there is a self-adjustment of the flow to variations in the ambient pressure P_a . Consequently, a plug nozzle, when operated at less than the design pressure ratio, gives better thrust performance than the corresponding conventional nozzle⁴³

Studies of the effect of the contour of the plug and the plug length are reported in References 44, 45, and 46. The results indicate that no serious penalty in thrust performance is incurred if the contoured plug is replaced by a simple conical plug. Conical plugs having included angles of 60° to 80° give performances close to 99 percent of that for a contoured plug and have the same insensitivity to variations in the ambient pressure P_a .

4-8.5 EXPANSION-DEFLECTION OR E-D NOZZLE

Fig. 4-20 illustrates schematically the essential features of the E-D nozzle⁴⁷. In this nozzle design the annular throat is formed by a contoured nozzle wall and a short internal plug. The propellant gas is discharged from the throat in a radially outward direction and expands around the shoulder of the central plug. The contoured nozzle wall turns the expanding gases so that they cross the exit plane A_e in a substantially axial direction.

The flow in an E-D nozzle, like that in the plug nozzle, is insensitive to variations in the ambient static pressure P_a . The base pressure at the base of the central plug limits the amount of expansion of the exhaust gas of the shoulder of the plug, thereby causing self-adjustment of the flow. For detailed discussion of the flow inside an E-D nozzle the reader is referred to Reference 47.

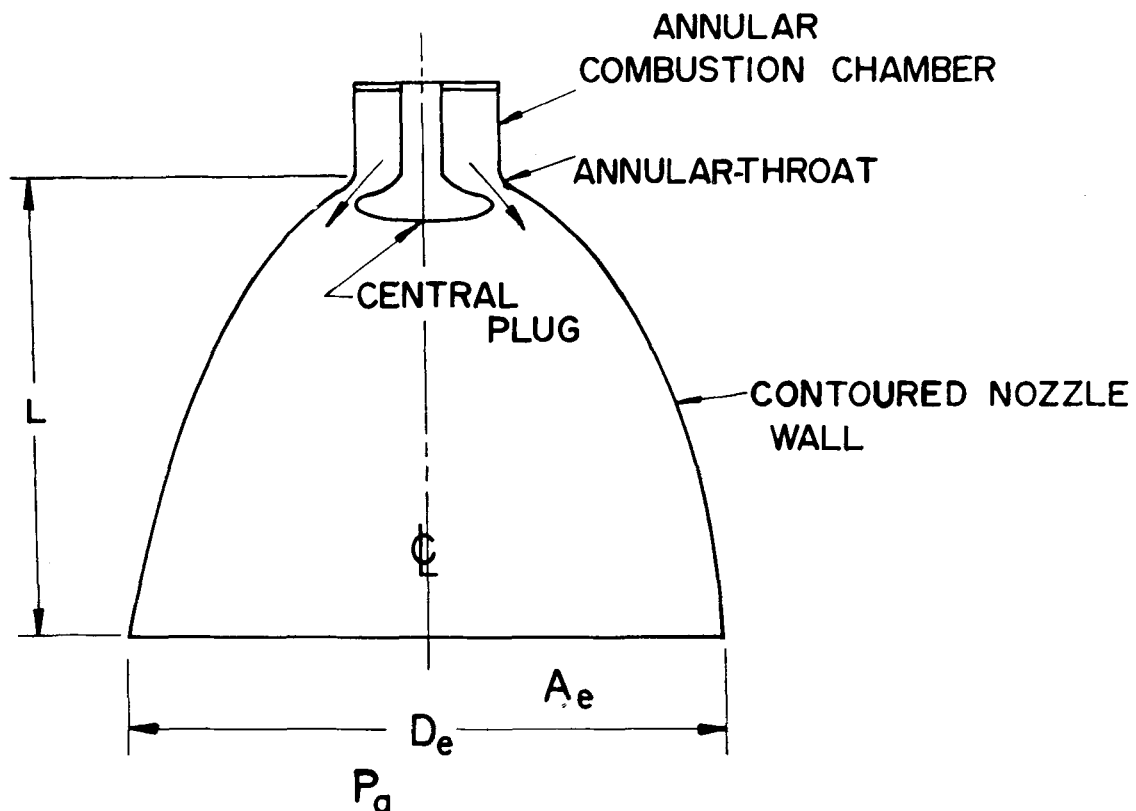


Figure 4-20. Essential Features of an Expansion-deflection or E-D Nozzle

REFERENCES

1. M.J.Zucrow, *Aircraft and Missile Propulsion*, John Wiley and Sons, Inc. 1958.
2. L. Crocco, "One-Dimensional Treatment of Steady Gas Dynamics", Section B, "Fundamentals of Gas Dynamics", *High Speed Aerodynamics and Jet Propulsion*, Princeton University Press, 1958.
3. H. W. Liepmann, *Elements of Gas Dynamics*, John Wiley and Sons, Inc., 1957.
4. R. von Mises, *Mathematical Theory of Fluid Flow*, Academic Press, Inc., 1958.
5. W. J. Hesse and N.V.S. Mumford, *Jet Propulsion for Aerospace Application*, Pitman Publishing Corporation, 2nd Ed., 1964, Chapters 3 and 5.
6. G. P. Sutton, *Rocket Propulsion Elements*, John Wiley and Sons, Inc., 3rd Ed., 1963.
7. M. Summerfield, C. R. Foster and W. G. Swan, "Flow Separation in Overexpanded Supersonic Nozzles," *Jet Propulsion*, September-October 1954, p. 319.
8. A. Stodola, *Steam and Gas Turbines*, McGraw-Hill Book Co., Inc., 1927.
9. C. R. Foster and F. B. Cowles, *Experimental Determination of a Static Pressure Distribution in an Overexpanded Rocket Motor Exhaust Nozzle*, JPL-CIT Prog. Report 4-125, March 21, 1951.
10. L. Green, "Flow Separation in Rocket Nozzle," *ARS Jour.*, January-February 1953, p. 34.
11. D. Altman, J. M. Carter, S. S. Penner and M. Summerfield, *Liquid Propellant Rockets*, (Princeton Aeronautical Paperbacks), Princeton University Press, 1960.
12. C. E. Campbell and J. M. Farley, *Performance of Several Conical Convergent-Divergent Rocket-Type Exhaust Nozzles*, NASA TN D467, September 1960.
13. C. W. Smith, *Aircraft Gas Turbines*, John Wiley and Sons, Inc., 1956.
14. R. E. Gray and H. D. Wilsted, *Performance of Conical Jet Nozzles in Terms of Flow*, NACA TN 1757, November 1948.
15. W. O. Meckley, "Jet Nozzles for Aircraft Turbines" *Aero. Eng. Rev.*, October 1950, p. 696.
16. R. P. Fraser, P. N. Rowe and M. O. Coulter, "Efficiency of Supersonic Nozzles for Rockets and Some Unusual Designs", *Inst. Mech. Eng'rs.*, 1957.
17. W. T. Snyder, "Nonisentropic Nozzle Flow," *ARS Jour.*, March 1960, p. 270.
18. G. V. R. Rao, "Recent Developments in Rocket Nozzle Configurations," *ARS Jour.*, November 1961, pp. 1488-1494.
19. E. L. Knuth, "Optimum Contours for Propulsion Nozzles," *ARS Jour.*, October 1960, p. 983.
20. R. A. A. Bryant, "Adiabatic Nozzle Flows," *ARS Jour.*, June 1961, p. 828.
21. M. J. Zucrow, *Aircraft and Missile Propulsion*, John Wiley and Sons, Inc., Vol. 2, 1964, Ch. 10.

REFERENCES (Continued)

22. M. Barrere, A. Jaumatte, B. F. DeVeubeke and J. Vanderherckhave, *Rocket Propulsion*, Elsevier, New York, 1960.
23. F. Malina, "Characteristics of the Rocket Motor Unit Based on the Theory of Perfect Gases," *J. Franklin Inst.*, Vol. 230, 1940, p. 433.
24. E. M. Landsbaum, "Thrust of a Conical Nozzle" *ARS Jour.*, March 1959, p. 212.
25. F. J. Krieger, *Chemical Kinetics and Rocket Nozzle Design*, USAF, Project Rand, R-203, August 15, 1960.
26. J. H. Ahlberg, S. Hamilton D. Migdal and E. N. Nilson, "Truncated Perfect Nozzles in Optimum Design," *ARS Jour.*, Vol. 31, May 1961, p. 614.
27. H. D. Thompson, *Design Procedure for Optimization of Rocket Motor Nozzles*, Report No. TM-63-6, Jet Propulsion Center, Purdue University, May 1963.
28. K. O. Friedrichs, *Theoretical Studies on the Flow through Nozzles and Related Problems*, NRDC, 82.1R, Applied Math. Group, New York University, April 1944.
29. K. O. Friedrichs, *On Supersonic Compressors and Nozzles*, AMP Report 82.2R, Supplement to AMP Report 82.1R, AMG, New York University, October 1944.
30. R. J. Baron, *Analytical Design of a Family of Supersonic Nozzles by the Friedrichs Method*, WADC Tech. Report 54-279, Naval Supersonic Laboratory, MIT, June 1954.
31. R. Sauer, *General Characteristics of the Flow Through Nozzles at Near Critical Speeds*, NACA TM No. 1147, June 1947, pp. 1-18.
32. K. Ostwatitsch and W. Rothstein, *Flow Pattern in a Converging-Diverging Nozzle*, NACA TM No. 1215, March 1949, pp. 1-43.
33. S. G. Hooker, *Flow of a Compressible Fluid in the Neighborhood of the Throat of a Constriction in a Circular Wind Channel*, ACR REM 1429, 1931.
34. K. Foelsch, "The Analytical Design of an Axially Symmetric Laval Nozzle for a Parallel and Uniform Jet," *Jour. IAS*, Vol. 16, March 1949, p. 161.
35. G. V. R. Rao, "Exhaust Nozzle Contour for Optimum Thrust," *Jet Propulsion*, Vol. 28, June 1958, p. 377.
36. G. V. R. Rao, "Recent Developments in Rocket Nozzle Configurations," *ARS Jour.*, November 1961, p. 1488.
37. A. H. Shapiro, *The Dynamics and Thermodynamics of Compressible Fluid Flow*, Vols. 1 and II, Ronald Press, 1958.

REFERENCES (Continued)

38. R. Courant and K. O. Friedrichs, *Supersonic Flow and Shock Waves*, Interscience Publishers, Inc., Vol. 1, 1948.
39. J. D. Hoffman, *An Analysis of the Effects of Gas-Particle Mixtures on the Performance of Rocket Nozzles*, Report No. TM-63-1, Jet Propulsion Center, Purdue University, Jan. 1963.
40. R. von Mises, *Mathematical Theory of Compressible Fluid Flow*, Academic Press, Inc., 1958.
41. A. R. Graham, *NASA Plug Nozzle Handbook*, General Electric Company, Contract NAS 9-3748, New York State Atomic and Space Development Authority.
42. K. Berman, "The Plug Nozzle: A New Approach to Engine Design," *Astronautics*, April 1960.
43. H. G. Krull and W. T. Beale, *Effect of Plug Design on Performance Characteristics of Convergent-Plug Exhaust Nozzles*, NACA RME 54 Ho5, October 1954.
44. H. G. Krull, W. T. Beale and R. F. Schmiedlen, *Effect of Several Design Variables on Internal Performance of Convergent-Plug Exhaust Nozzles*, NACA RME 56, October 1956.
45. G. V. R. Rao, "Spike Nozzle Contour for Optimum Thrust," *Ballistic Missile and Space Technology*, Vol. 2, C. W. Morrow, Editor, Pergamon Press, N. Y., 1961.
46. G. V. R. Rao, "Analysis of a New Concept Rocket Nozzle," *Progress in Astronautics and Rocketry*, Vol. 2, 1960, p. 669.
47. G. V. R. Rao, "The E-D Nozzle," *Astronautics*, September 1960.

CHAPTER 5

PERFORMANCE CRITERIA FOR ROCKET PROPULSION

5-0 PRINCIPAL NOTATION FOR CHAPTER 5*

a	acoustic speed
A	cross-sectional area perpendicular to the flow
A_e	area of exit cross-section of the exhaust nozzle
A_t	area of the cross-section of the throat of the exhaust nozzle
c	effective jet or exhaust velocity for the gas ejected from the exhaust nozzle
c*	characteristic velocity for a chemical rocket motor
C_D	drag coefficient
C_F	thrust coefficient = $F/A_t P_c$
C_m	mass flow coefficient = $m/A_t P_c$
D	aerodynamic drag
F	thrust
g	local acceleration of gravity, ft/sec ²
g_c	gravitational conversion factor = 32.174 slug-ft/lb-sec ²
I_{sp}	specific impulse, sec
I	total impulse of a rocket system
L	aerodynamic lift force
m	mass, slug
\bar{m}	molecular weight

m_p	mass of propellants prior to initiation of burning
\dot{m}	mass rate of flow, slug/sec
m₀	mass of rocket-propelled vehicle at take-off
m_b	mass of rocket-propelled vehicle at instant when all propellants are consumed
M	Mach number
p	static pressure, psia
P	static pressure, psfa
P_a	ambient static pressure
P_c	static pressure in the inlet cross-section of the rocket nozzle (the combustion pressure)
P_e	static pressure in the exit cross-section A _e of a rocket nozzle
P_j	jet power, ft-lb/sec
P⁰	stagnation pressure of the gas in the inlet cross-section of the rocket nozzle
t	time
t_B	burning time for a rocket motor or engine
T	static temperature, °R
T_c	combustion temperature measured in the inlet cross-section of the rocket nozzle
T_e	static temperature of the gas in the exit cross-section A _e of the rocket nozzle

*Any consistent set of units may be employed; the units presented here are for the American Engineers System (see par. 1-7).

T_t	static temperature of the gas in the throat cross-section A_t of the rocket nozzle
T^*	static temperature in cross-section A^*
T^0	stagnation or total temperature
u	velocity parallel to the x-axis
u_e	velocity of gas crossing exit cross-section A_e of the rocket nozzle
V	linear velocity of a rocket-propelled vehicle
V_{bi}	ideal burnout velocity
w	weight, lb
\tilde{W}	gravitational force, lb
\dot{w}	weight rate of flow, lb/sec
W_E	engine weight
W_p	propellant weight

GREEK LETTERS

α	semidivergence angle for a conical rocket nozzle
α	angle of attack
β	semiconvergence angle for a conical rocket nozzle
δ_p	propellant loading density
λ	flow divergence loss coefficient
Λ	vehicle mass ratio = m_0/m_b
ξ	propellant mass ratio = m_p/m_0
τ	specific engine weight for chemical or nuclear (heat-transfer) rocket engines
τ_e	specific engine weight for electric rocket engine

5-1 INTRODUCTION

In most applications of chemical rocket propulsion the objective is to produce a large thrust for a specified time, called the *burning time*. Consequently, the criteria of performance for a rocket engine are related to its thrust and burning time rather than to its thermal efficiency and thrust power (see par. 2-5.1). In most applications the rocket engine is operated under steady state conditions so that the combustion parameters at the entrance section of the rocket nozzle may be assumed to be constant; i.e., the values of P_c , T_c , ρ_c , and u_c do not change with the burning time t_B .

Fig. 5-1 illustrates the thermodynamic conditions at the inlet and exit sections of a conical rocket nozzle. Unless it is specifically stated to be otherwise, steady state operating conditions are assumed.

5-2 EFFECTIVE JET (OR EXHAUST) VELOCITY (c)

When a rocket engine (liquid or solid propellant) is fired statically, the thrust F is readily measured. Furthermore, the average rate at which the propellants are consumed (m_p/t_B) can be determined with good accuracy. It is unfeasible, however, to measure the exit pressure P_e with accuracy (see Fig. 5-1). From Eq. 4-43, the thrust of the rocket engine is given by (see par. 4-8.1.1)

$$F = \lambda \left[\dot{m} u_e + (P_e - P_a) A_e \right] \quad (5-1)$$

where \dot{m} is the rate at which propellants are consumed, and $u_e = \lambda u_c$.

Introducing the *effective jet velocity* c (see par. 2-4), one can write

$$F = \dot{m} c = \frac{\dot{w}}{g_c} c \quad (5-2)$$

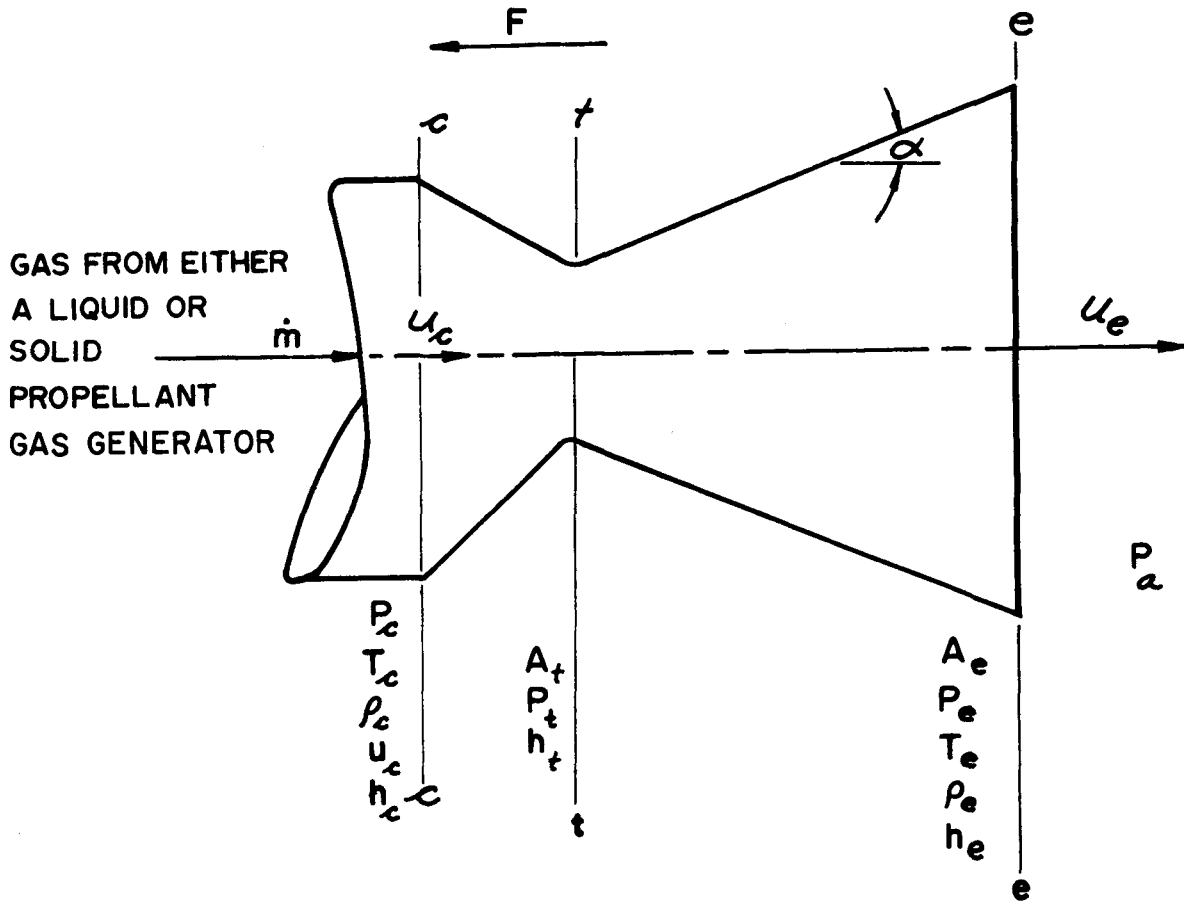


Figure 5-1. Thermodynamic Conditions for a Chemical Rocket Nozzle Operating Under Steady State Conditions

where \dot{w} is the weight rate of propellant consumption. Hence

$$c = \frac{F}{\dot{m}} = \frac{\lambda g_c}{\dot{w}} \left[\dot{m} u_e + (P_e - P_a) A_e \right] \quad (5-3)$$

It should be noted that from the firing test of a rocket engine or motor one computes the effective jet velocity c and not the exit velocity u_e .

5-3 SPECIFIC IMPULSE (I_{sp})

By definition, the specific impulse I_{sp} is the thrust developed in burning one pound (weight) of propellants. Hence

$$I_{sp} = \frac{F}{\dot{w}} = \frac{1}{W_p} \int_0^t F dt \quad (\text{sec}) \quad (5-4)$$

where W_p is the total weight of propellants consumed (assuming constant gravitational attraction) in the burning time $t_B = \int dt$ and $\dot{w} = dw/dt$, is the corresponding weight rate of propellant consumption.

The specific impulse and the effective jet velocity are related by (see Eqs. 5-3 and 5-4)

$$I_{sp} = c/g_c = F/\dot{w} \quad (\text{fps}) \quad (5-5)$$

The specific impulse I_{sp} — like the effective jet velocity c — is basically a property of the propellants burned in the rocket motor. For a given propellant combination — fuel plus its oxidizer — the theoretical value of I_{sp} , denoted by I'_{sp} , can be calculated by the methods of thermochemistry⁹. Because of heat losses, imperfect combustion of the propellants, frictional losses in the exhaust nozzle, and variations in back pressure, the measured values of I_{sp} are somewhat smaller than I'_{sp} ; the latter assumes that the gases are expanded isentropically and completely to the atmospheric back pressure. Well-designed rocket motors give values of I_{sp} ranging from 0.92 to more than 0.98 of I'_{sp} .

In the case of a solid propellant rocket motor the instantaneous rate of propellant consumption \dot{w} cannot be measured. Consequently, the measured specific impulse is an average value calculated from the curve of thrust as a function of the burning time, called the *thrust-time curve*, and the weight of the solid propellant consumed during the burning time.

5-3.1 SPECIFIC PROPELLANT CONSUMPTION (\dot{w}_{sp})

By definition \dot{w}_{sp} is the weight of propellants (fuel plus oxidizer) consumed in producing an impulse of 1 lb-sec. Hence

$$\dot{w}_{sp} = \frac{\dot{w}}{F} = \frac{1}{I_{sp}} = \frac{g_c}{c} \quad (5-6)$$

5-3.2 WEIGHT-FLOW COEFFICIENT (C_w)

It is convenient to express the weight rate of propellant consumption \dot{w} in terms of the combustion pressure P_c , the throat area of the nozzle A_t , and an *experimentally* determined *weight-flow coefficient* C_w . By definition

$$C_w = \dot{w} / (P_c A_t) \quad (5-7)$$

Curves of C_w as a function of P_c for a given propellant combination give the information for determining the required weight rate of propellant consumption for an application of that propellant combination. The curves of $C_w = f(P_c)$ are obtained from firings of small rocket motors.

If the Mach number for the combustion gas entering the exhaust nozzle is larger than $M=0.3$, then the static values P_c and T_c should be replaced by their stagnation values (see pars. A-5.2.2 and A-5.2.3).

5-3.3 MASS-FLOW COEFFICIENT (C_m)

By analogy with Eq. 5-6, one obtains

$$C_m = \dot{m} / (P_c A_t) = C_w / g_c \quad (5-8)$$

5-4.1 THRUST COEFFICIENT (C_F)

In conducting a static firing of a rocket engine the following parameters can be measured accurately with relative ease: the combustion pressure at the nozzle inlet P_c , the thrust F , the area of the nozzle throat A_t before and after the firing test, and the weight rate of propellant consumption $\dot{w} = F/I_{sp}$. It is convenient, therefore, to relate F , P_c , and A_t . Introducing the *thrust coefficient* C_F , defined by an equation analogous to Eq. 5-7, one obtains

$$C_F = F / (P_c A_t) \quad (5-9)$$

Strictly speaking, the value of A_t that should be used in Eq. 5-9 is the throat area during the firing run. Since that area cannot be measured, the value of A_t used in the equation is one that is estimated from the value of A_t measured prior to the firing run and the temperature of the nozzle material.

Curves of C_F as a function of P_c obtained experimentally for several different mixture ratios $r = \dot{w}_o / \dot{w}_f$ and for different propellant

combinations, comprise the basic data for establishing the throat area of the exhaust nozzle. When experimental data are unavailable, theoretical values of C_F , denoted by C'_F , can be calculated by thermodynamic methods, see Chapter 6.

5-4.2 RELATIONSHIP BETWEEN I_{sp} , C_w , AND C_F

From Eqs. 5-4, 5-7, and 5-9 it is seen that

$$F = \dot{w} I_{sp} = C_w A_t P_c I_{sp} = C_F A_t P_c \quad (5-10)$$

Hence

$$I_{sp} = C_F / C_w \quad (5-11)$$

5-5 CHARACTERISTIC VELOCITY (c^*)

The characteristic velocity, denoted by c^* , is frequently employed for comparing the performance of different rocket engines. This parameter measures the effectiveness with which the chemical reaction is accomplished in the combustion chamber. c^* is defined by

$$c^* = c / C_F \quad (5-12)$$

One of the advantages of employing c^* as a performance criterion is that its experimental determination does not require measuring the thrust F . Substituting for $C_F = F / (P_c A_t)$ into Eq. 5-12, yields

$$c^* = P_c A_t g_c / \dot{w} = P_c A_t / \dot{m} \quad (5-13)$$

Basically, c^* measures the effectiveness of the combustion process in the gas generator which supplies the propellant gas to the exhaust nozzle (see par. 1-6). Consequently, c^* is related to the specific impulse I_{sp} . Thus

$$c^* = \frac{c}{C_F} = \frac{g_c I_{sp}}{C_F} = \frac{g_c}{C_w} = \frac{g_c}{\dot{w}_{sp} C_F} \quad (5-14)$$

5-6 JET POWER (P_j)

The power associated with the propulsive jet ejected from a rocket engine is

termed the *jet power* and is denoted by P_j . Thus

$$P_j = \frac{1}{2} \dot{m} c^2 \quad (\text{ft-lb/sec}) \quad (5-15)$$

In the case of electric rocket engines for space propulsion it is useful to express P_j in kilowatts, the thrust F , and the specific impulse I_{sp} . Thus

$$P_j = F I_{sp} / 45.8 \quad (\text{kw}) \quad (5-16)$$

where F is in pounds and I_{sp} in seconds.

It is seen from Eq. 5-16 that for a fixed value of the jet power P_j the specific impulse I_{sp} varies inversely with the thrust F .

5-7 TOTAL IMPULSE (I_T)

From Eq. 5-4 the *total impulse* I_T , also called the *impulse*, is the integral of the thrust over the burning time t_B . Hence, by integrating the thrust-time curve for a firing test over the burning time, one obtains

$$I_T = \int_0^{t_B} F dt = \int_0^{t_B} I_{sp} \dot{w} dt = W_p I_{sp} \quad (5-17)$$

It follows from Eq. 5-17 that if all other factors remain unchanged for a given rocket engine, the same total impulse can result from either a small thrust over a long time or from a large thrust over a short time.

EXAMPLE 5-1.

A liquid propellant rocket motor is to be designed to burn RFNA and JP-4 at a mixture ratio of 4.1 to 1. The motor is to develop 50,000 lb thrust at standard sea level, when the combustion total pressure is 500 psia. Two small rocket motors are tested with the same propellants, and the data tabulated below are obtained.

P_c , psia	F , lb	A_t , in. ²	\dot{w} , lb/sec	\dot{w}_o / \dot{w}_f
548	543	0.660	2.375	4.1
478	512	0.712	2.255	4.1

Determine the required propellant flow rate for the 50,000-lb-thrust rocket motor, the throat diameter of its exhaust nozzle, the characteristic velocity, the effective jet velocity, and the specific impulse.

SOLUTION.

From data obtained with small rocket motors:

$$C_{F1} = \frac{F}{P_c A_t} = \frac{543}{548(0.660)} = 1.495 ;$$

$$C_{F2} = \frac{512}{478(0.712)} = 1.505$$

Value of C_F at $P_c = 500$ psia: by interpolation, $C_F = 1.50$.

Weight flow coefficients:

$$C_{w1} = \frac{\dot{w}}{A_t P_c} = \frac{2.375}{0.66(548)} = 0.00655$$

$$C_{w2} = \frac{2.255}{478(0.712)} = 0.0066$$

Value of C_w , by interpolation, is $C_w = 0.00658$.

Required throat area for exhaust nozzle:

$$A_t = \frac{F}{C_F P_c} = \frac{50,000}{1.5(500)} = 66.6 \text{ in.}^2$$

Required propellant flow rate:

$$\dot{w} = C_w P_c A_t = 0.00658(500)66.6 = 218 \text{ lb/sec}$$

Characteristic velocity:

$$c^* = \frac{g_c}{C_w} = \frac{32.174}{0.00658} = 4885 \text{ fps}$$

Effective jet velocity:

$$c = \frac{32.174(25,000)}{109} = 7350 \text{ fps}$$

Check: Eq. 5-14

$$c^* = \frac{c}{C_F} = \frac{7350}{1.50} = 4880 \text{ fps}$$

5-8 WEIGHT AND MASS RATIOS

Certain weight and/or mass ratios are employed for evaluating the performance of a rocket-propelled vehicle. The gross weight or *take-off weight* of a fully loaded rocket-propelled vehicle, denoted by W_o , is given by

$$W_o = W_{\text{str}} + W_{\text{pay}} + W_E + W_p \quad (5-18)$$

where

W_{str} = structural weight of the vehicle (including the control systems)

W_{pay} = the payload carried in the vehicle

W_E = dry weight of the rocket engine

W_p = weight of propellant

For a liquid propellant rocket engine, W_E includes the weight of the propellant tankage, gas generator equipment, inert gas storage system, turbopump, valves, plumbing, rocket engine controls, and rocket motors. The propellant weight W_p includes the weight of all the auxiliary fluids, if any are used, in the operation of the liquid propellant rocket engine.

In the case of a solid propellant rocket engine, the engine weight W_E includes the weights of the cylindrical casing, fore and aft caps, exhaust nozzles, restriction (inhibiting) liner, insulation of the fore and aft cap, thrust termination equipment, and the means for achieving thrust vector control.

In the case of an *electric rocket engine* the engine weight includes the weights of the power source, energy conversion equipment, accelerator or thrust chamber, propellant tankage, and engine control systems.

5-8.1 PROPULSION SYSTEM WEIGHT (W_{PS})

The propulsion system weight is defined by

$$W_{PS} = W_E + W_p \quad (5-19)$$

5-8.2 SPECIFIC ENGINE WEIGHT (τ)

For either a *chemical* or a *nuclear* (heat-transfer) *rocket engine*, the specific engine weight is denoted by τ which is defined by

$$\tau \equiv W_E/F \quad (5-20)$$

In the case of an electric rocket engine which is equipped with nuclear electric power plant, the specific engine weight is denoted by τ_e , where

$$\tau_e = W_E/P_j \quad (5-21)$$

5-8.3 PAYLOAD RATIO (W_{pay}/W_0)

By definition

$$\frac{W_{\text{pay}}}{W_0} = 1 + \frac{W_{\text{str}}}{W_0} + \frac{W_{\text{PS}}}{W_0} \quad (5-22)$$

In general, it is desirable that the payload ratio be as large as possible.

5-8.4 PROPELLANT WEIGHT (W_p)

The propellant weight W_p is the weight of the fuel plus oxidizer required to achieve a given flight objective in the *powered flight* or *burning time* t_B . Hence

$$W_p = Ft_B/I_{sp} \quad (5-23)$$

Eq. 5-23 shows that if the value of F and of t_B are fixed, then W_p varies inversely with the specific impulse I_{sp} . Consequently, a large value for I_{sp} is desirable.

5-8.5 PROPELLANT MASS RATIO (ξ)

Consider a rocket-propelled vehicle, such as a missile, at any instant $t=t$ during its *powered flight* i.e., when $t < t_B$, where t_B is the time during which propellant is being burned. Assuming steady state operating conditions, the mass rate of propellant consumption \dot{m} is a constant. Hence, if g denotes the local value of gravity,

$$\dot{m} = \dot{w}/g = m_p/t_B \quad (5-24)$$

Furthermore, the thrust F may be assumed constant so that

$$F = \dot{m}c = m_p c/t_B \quad (5-25)$$

where m_p is the mass of propellants (fuel plus oxidizer) consumed in time t_B .

The consumption of propellants reduces the total mass of the propelled vehicle. If m_0 denotes the mass of the vehicle at take-off ($t=0$), then its *instantaneous mass*, denoted by m , at any time $t < t_B$ is given by

$$m = m_0 - \dot{m}t = m_0 \left(1 - \frac{m_p}{m_0} \cdot \frac{t}{t_B} \right) \quad (5-26)$$

At the instant when all of the propellants are consumed, the instantaneous mass m is denoted by m_b , where

$$m_b = m_0 (1 - m_p/m_0) \quad (5-27)$$

The ratio m_p/m_0 is called the *propellant mass ratio* and is denoted by ξ . Thus

$$\xi = \frac{m_p}{m_0} = \frac{\text{effective propellant mass}}{\text{initial mass of vehicle}} \quad (5-28)$$

From the point of view of achieving a long range, the propellant mass ratio should be as large as possible.

5-8.6 VEHICLE MASS RATIO (Λ)

The ratio $m_0/(m_0 - m_p)$ is called the *vehicle mass ratio* and is denoted by Λ . Thus

$$\Lambda = \frac{m_0}{m_b} = \frac{\text{initial mass of vehicle}}{\text{(mass of vehicle after consuming propellants)}} \quad (5-29)$$

where

$$m_b = m_0 - m_p = \text{mass of vehicle at burnout}$$

5-8.7 RELATIONSHIP BETWEEN THE PROPELLANT MASS RATIO (ξ) AND THE VEHICLE MASS RATIO (Λ)

From Eqs. 5-28 and 5-29 it is seen that the propellant mass ratio ξ and the vehicle mass ratio Λ are related by the equation

$$\xi = 1 - 1/\Lambda \quad (5-30)$$

5-8.8 PROPELLANT LOADING DENSITY (δ_p)

The ratio of total weight of the propellant in a rocket-propelled vehicle, denoted by W_p , to the weight of the rocket engine, denoted by W_E , is termed the *propellant loading density*, or *engine weight efficiency*, and is denoted by δ_p

$$\delta_p = \frac{W_p}{W_E} = \left(\frac{I_t}{I_{sp}} \right) \left(\frac{1}{W_E} \right) \quad (5-31)$$

It is usually desirable that the propellant loading density have a large value.

5-8.9 IMPULSE-WEIGHT RATIO FOR A ROCKET ENGINE

If a rocket engine operating under steady state conditions develops a thrust F for a burning time t_B , then the *impulse-weight ratio* for the rocket engine denoted by $R_{I/W}$, is given by

$$R_{I/W} = \frac{I_t}{W_p + W_E} \quad (5-32)$$

where, as before,

$$I_t = \int_0^{t_B} F dt.$$

If F is constant, then $I_t = Ft_B$. The impulse-weight ratio is a criterion of the overall design of the rocket jet propulsion system, and a large value is desirable. The items to be included

in W_E for liquid and solid propellant engines are discussed in par. 5-8.

5-9 VEHICLE PERFORMANCE CRITERIA

In general, the analysis of the flight of a rocket-propelled vehicle, such as a missile, is a particular application of the dynamics of a rigid body in three dimensions; actually the vehicle is usually elastic and its design must take that into account. In applying rigid body dynamics to a rocket-propelled vehicle it is convenient to divide the study into the following two parts.

- (a) The determination of the motion of the *center of mass* or *centroid* of the vehicle.
- (b) The determination of the motion of the vehicle about its center of mass.

The studies concerned with the motion of the centroid of the vehicle comprise the theory of its *flight performance*. On the other hand, the studies concerned with the motion of the vehicle around its centroid comprise the theory of *flight stability and control*^{1 0, 1 1, 1 2, 1 3}.

A recurring problem in rocketry is the rapid determination of the overall design parameters affecting the flight of a rocket-propelled vehicle, as for example, a ballistic missile. An accurate analysis of the flight of a rocket-propelled body involves the application of rigid body dynamics in three dimensions. To obtain an understanding of the parameters influencing the flight of a rocket-propelled vehicle, however, a simple two-dimensional analysis is sufficient. It is assumed, therefore, that

- (a) The motion of the vehicle is determined from the motion of its centroid.
- (b) The motion is planar.
- (c) The flight path is a straight line.

It is desired to obtain relationships between the specific impulse I_{sp} , the mass ratio $\Lambda = m_0/m_p$, and the *burnout velocity* V_b which is the velocity attained by a rocket-propelled body at the instant $t=t_b$; i.e., the instant when the rocket engine consumes the propellant load m_p .

5-9.1 LINEAR MOTION WITH DRAG AND GRAVITY

Fig. 5-2 illustrates schematically a rocket-propelled body at an instant t during its powered flight, i.e., $t < t_b$. It is assumed that the vehicle moves along the linear path $S-S$, and that the motion is planar. It is seen from Fig. 5-2 that the following forces act on the vehicle:

- (a) Aerodynamic drag \underline{D} .
- (b) Thrust \underline{F} produced by the rocket engine.
- (c) Gravitational force $\underline{W} = m \underline{g}_c$.

The general differential equation of motion, in vector form, for the position of the centroid of the vehicle along the linear path $S-S$, is given by

$$m \frac{d^2 s}{dt^2} = m \frac{dV}{dt} = \underline{F} - \underline{D} - \underline{W} \quad (5-33)$$

Let γ denote the angle made by the linear trajectory of the centroid G of the vehicle, denoted by $S-S$ in Fig. 5-2, and the line of action of the weight $\underline{W} = m \underline{g}_c$. Further, assume that the line of action of the thrust \underline{F} is coincident with the longitudinal axis of the vehicle. Since \underline{F} , \underline{D} , \underline{W} and path $S-S$ are coplanar, the equation of motion for the vehicle is given by

$$m \frac{d^2 s}{dt^2} = m \frac{dV}{dt} = F - D - mg_c \cos \gamma \quad (5-34)$$

At any instant $t < t_b$, the instantaneous mass of the vehicle, denoted by m , is given by

$$m = m_0 - \dot{m}t \quad (5-35)$$

where m_0 is the launch mass of the vehicle, and \dot{m} the propellant consumption which is assumed constant. Hence, Eq. 5-34 can be transformed to read

$$(m_0 - \dot{m}t) \frac{d^2 s}{dt^2} = F - D - g (m_0 - \dot{m}t) \cos \gamma \quad (5-36)$$

Eq. 5-36 is a nonlinear second order differential equation with *variable* coefficients. It can only be integrated by numerical methods.

5-9.1.1 THRUST OF ROCKET ENGINE WITH LINEAR MOTION OF VEHICLE

If the propellant consumption rate \dot{m} is maintained *constant* during the powered flight, then from Eq. 5-1

$$F = \dot{m}c = \lambda [\dot{m}u_e + (P_e - P_a) A_e] \quad (5-37)$$

Let x denote the fraction of the propellant load m_p consumed per unit time. The thrust F is accordingly given by

$$F = (xm_p) c \quad (5-38)$$

The effective jet velocity c , and hence the thrust F is influenced by the variations in the ambient atmospheric pressure P_a as the altitude of the vehicle changes. Thus, if F_∞ denotes the thrust in the vacuum space above the atmosphere, then the thrust F at any lower altitude z in the atmosphere, *assuming* no flow separation occurs in the exhaust nozzle, is given by

$$F = F_\infty - P_a A_e \quad (5-39)$$

The analysis is simplified, without sensible loss in accuracy, if the variable effective jet velocity c in Eq. 5-38 is replaced by an appropriate constant mean value, denoted by \bar{c} . Hence

$$F = (xm_p) \bar{c} \quad (5-40)$$

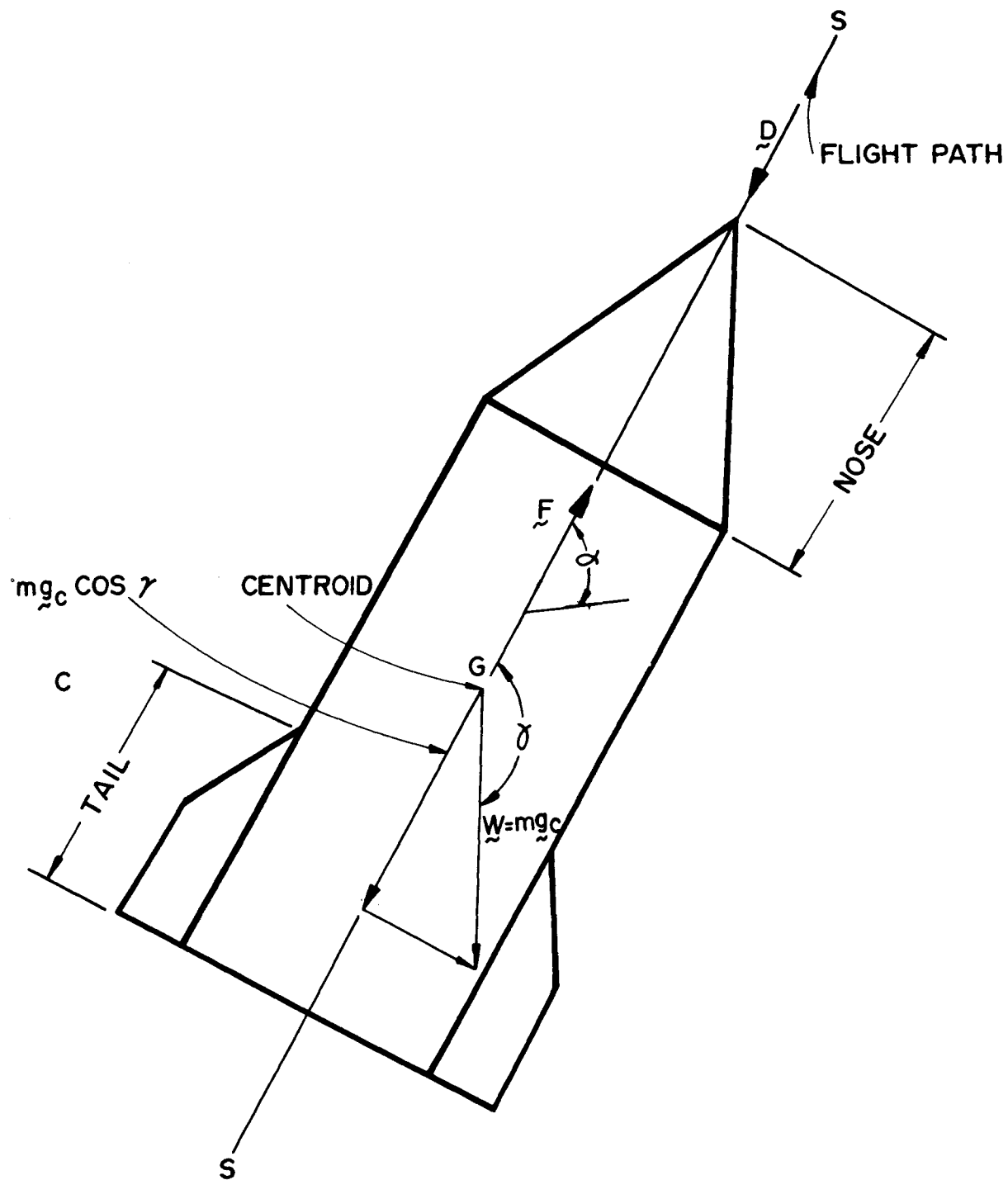


Figure 5-2. Forces Acting on a Rocket-Propelled Body in Rectilinear Motion

5-9.1.2 AERODYNAMIC DRAG

In general, the drag force acting on a missile is composed of the following:

- (a) Nose drag
- (b) Skin friction drag
- (c) Tail drag

The *nose drag* is due to high pressure regions in the vicinity of the nose where, due to the deceleration of the vehicle, the static pressure becomes higher than that of the undisturbed air, because of the shock waves formed in front of the nose.

The *tail drag* arises as a result of the air in the vicinity of the tail separating from the propelled body, thereby causing a *suction effect* in the vicinity of the tail of the propelled body.

It is difficult to assess the influence of the gaseous propulsive jet ejected from the rocket motor on the nose and skin friction drags. The action of the exhaust jet does, however, exert a large influence on the *tail drag* because it overcomes the suction effect which is present when there is no exhaust jet¹⁵.

At high supersonic speeds the nose drag, owing to the formation of shock waves, is considerably larger than the sum of the skin friction and the tail drag. Consequently, the effect of the exhaust jet upon the total drag of the vehicle is much reduced at high supersonic flight speeds.

If A_m denotes the *maximum cross-sectional area* of the propelled body and C_D is an experimentally determined *drag coefficient*, then

$$D = C_D A_m \left(\frac{1}{2} \rho V^2 \right) \quad (\text{lb}) \quad (5-41)$$

where

A_m = maximum cross-sectional (frontal) area of the vehicle

C_D = the drag coefficient

V = the velocity of the vehicle

ρ = the density of the atmospheric air

The drag coefficient is a function of the Mach number M and the angle of attack α of the vehicle. Fig. 5-3 illustrates schematically the manner in which C_D varies with the flight Mach number of a ballistic missile.

Combining Eqs. 5-36, 5-40, and 5-41 yields¹

$$(m_0 - \dot{m}t) \frac{dV}{dt} = x m_p c - \frac{1}{2} \rho V^2 A_m C_D - g (m_0 - \dot{m}t) \cos \gamma \quad (5-42)$$

or

$$\frac{dV}{dt} = \frac{x m_p c}{m_0 - x m_p t} - g \cos \gamma - \frac{\rho V^2 A_m C_D}{2(m_0 - x m_p t)} \quad (5-43)$$

5-9.1.3 APPROXIMATE SOLUTION OF DIFFERENTIAL EQUATION FOR LINEAR MOTION WITH DRAG AND GRAVITY¹

Let \bar{C}_D denote a *constant mean value* for the drag coefficient C_D . Also, $x = 1/t$, and $m_p = \Delta m_0$ (see par. 5-8.5), then Eq. 5-43 can be transformed to give the following equation for the vehicle velocity at any instant $t < t_B$:

$$V = \frac{ds}{dt} = \int_0^t \frac{\Lambda \bar{c}}{t_B - \Lambda t} dt - \int_0^t g \cos \gamma dt - \int_0^t \left(\frac{1}{2} \rho V^2 \right) \frac{C_D A_m / m_0}{1 - \Lambda t / t_B} dt + V_0 \quad (5-44)$$

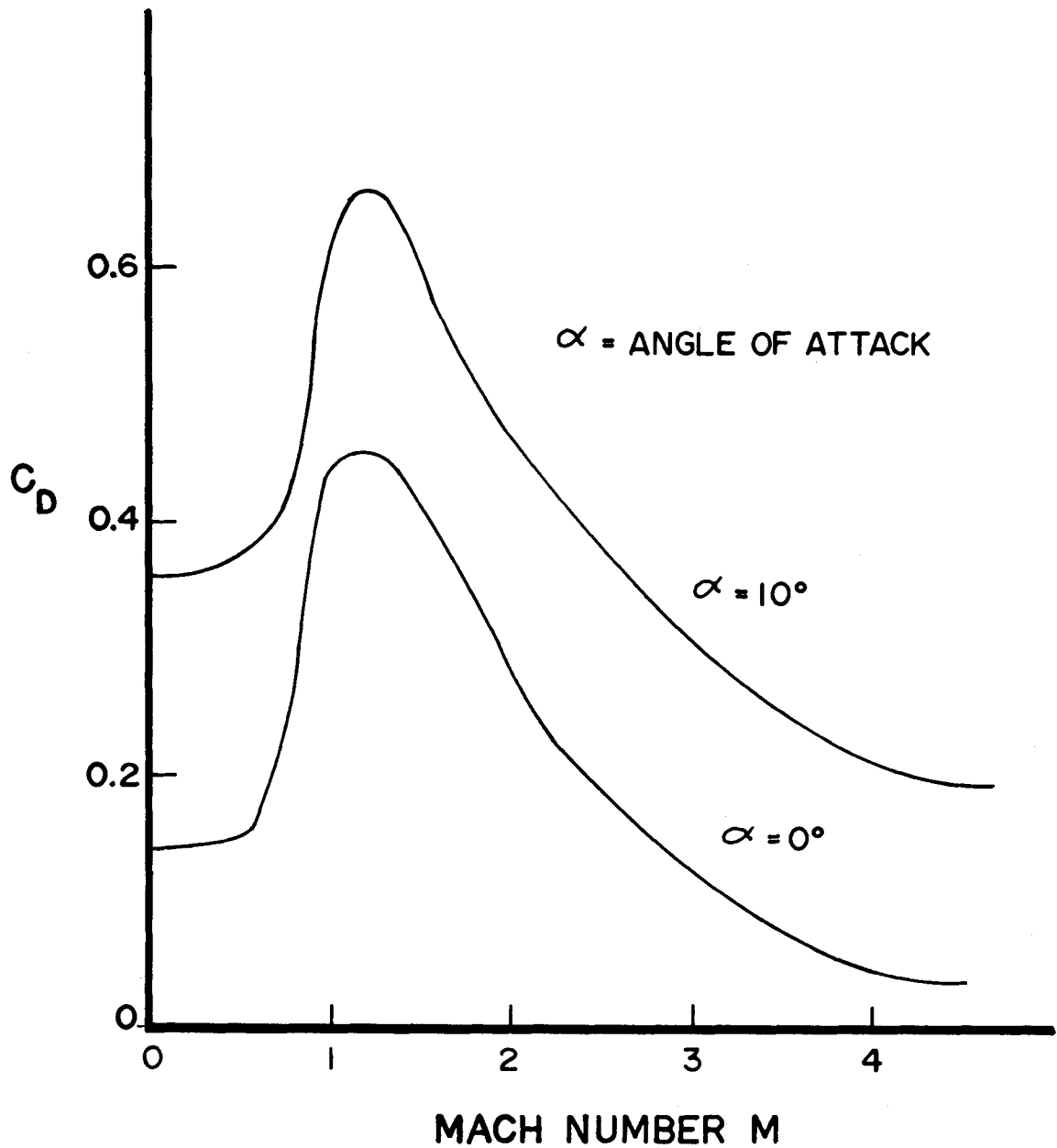


Figure 5-3. Drag Coefficient As a Function of the Flight Mach Number for Two Angles of Attack

where V_0 denotes the initial or *launching velocity* of the rocket-propelled vehicle.

The ratio m_0/A_m , the *take-off mass per unit of frontal area*, is a measure of the relative importance of the drag term in Eq. 5-44. The *larger* value of m_0/A_m the *less influential* is the drag term, as can be seen from the qualitative analysis below. Thus, if one considers a family of similar vehicles which have the same ballistic properties, then

(a) the drag $D \propto A_m \propto L^2$, where L is a typical dimension of the vehicle

(b) the launch mass of the vehicle $m_0 \propto L^3$.

Hence

$$D/m_0 \propto L^2/L^3 \propto 1/L \quad (5-45)$$

The last expression demonstrates that lengthening a rocket-propelled vehicle decreases $\bar{C}_D A_m/m_0$; i.e., reduces the effect of the drag term in Eq. 5-44.

For a ballistic missile having a launch weight of approximately 100,000 lb, the aerodynamic drag reduces the *burnout velocity* of the vehicle, the value of V when $t=t_B$, by approximately 5 percent. Consequently, the effect of aerodynamic drag on the burnout velocity for larger missiles, such as IRBM's and ICBM's, is so small that it may be neglected in studies concerned with determining the effect of vehicle and engine parameters upon the burnout velocity. It should be noted that the assumed constant effective jet velocity actually increases somewhat during the powered flight since P_a decreases with the altitude.

For small missiles, however, the neglect of aerodynamic drag introduces a serious error.

Consider now the *gravity term* in Eq. 5-44, i.e.,

$$\int_0^t g \cos \gamma dt$$

As the altitude of the vehicle above the surface of the earth increases, the local value of g changes in accordance with the following relationship

$$\frac{g}{g_0} = \left(\frac{R_E}{R_E + z} \right)^2 \quad (5-46)$$

where g_0 is the gravitational acceleration at standard sea level, R_E is the radius of the earth, and z the altitude of the body.

One can assume, therefore, a *mean constant value* of $g = \bar{g}$ corresponding to the altitude z at the time t . Hence, the gravitational term can be transformed to read

$$\int_0^t \bar{g} \cos \gamma dt \quad (5-47)$$

Hence, Eq. 5-44 can be rewritten in the following form:

$$\begin{aligned} \frac{dV}{dt} = & \int_0^t \frac{\Lambda \bar{c}}{t_B - \Lambda t} dt - \int_0^t \bar{g} dt \\ & - \int_0^t \left[\frac{\bar{C}_D A_m}{m_0} \left(\frac{1}{2} \rho V^2 \right) \right] dt + V_0 \end{aligned} \quad (5-48)$$

5-9.2 BURNOUT VELOCITY (V_b)

The burnout velocity V_b is obtained by setting $t=t_B$ in Eq. 5-48. The result is

$$\begin{aligned} V_b = & -\bar{c} \ln \left(\frac{m_0 - m_p}{m_0} \right) - \bar{g} t_B \\ & - \Pi_1 \bar{C}_D A_m / m_0 + V_0 \end{aligned} \quad (5-49)$$

where

$$\Pi_1 = \int_0^{t_B} \frac{\frac{1}{2} \rho V^2}{1 - \Lambda t / t_B} dt \quad (5-50)$$

5-9.2.1 BURNOUT ALTITUDE (z_b)

Let z_b denote the altitude of the vehicle at the instant $t = t_B$, then

$$z_b = \bar{c} t_B \left[1 + \left(\frac{m_0 - m_p}{m_p} \right) \ln \left(\frac{m_0 - m_p}{m_0} \right) \right] - \frac{1}{2} \bar{g} t_B^2 \cos \gamma + V_0 t_B + z_0 - \Pi_2 \bar{C}_D A_m / m_0 \quad (5-51)$$

where

$$\Pi_2 = \int_0^{t_B} \Pi_1 dt \quad (5-52)$$

5-9.2.2 COASTING ALTITUDE AFTER BURN-OUT (z_c)

At the end of the powered flight the vehicle coasts to a vertical distance z_c above the *burnout altitude* z_b . If it is assumed that at all altitudes above z_b the density of the atmosphere is negligibly small, then the drag force opposing the motion of the *coasting vehicle* may be neglected during the coasting period. In that case the *coasting altitude* z_c is given by

$$z_c = \frac{V_b^2}{2g_c} \quad (5-53)$$

5-9.2.3 MAXIMUM DRAG-FREE ALTITUDE (z_{\max})

If it is assumed that there is no drag during the coasting period, the *maximum altitude* denoted by z_{\max} attained by the vehicle is given by

$$z_{\max} = z_b + z_c \quad (5-54)$$

5-9.3 IDEAL BURNOUT VELOCITY (V_{bi})

The *ideal burnout velocity* denoted by V_{bi} is the maximum velocity a rocket-propelled vehicle would attain if it were propelled in a

frictionless medium without doing work against gravity, i.e., the vehicle moves in a vacuum space where there is no force field. Although the equations obtained for the above hypothetical conditions cannot be applied directly to a practical case, they are useful for determining the relative performances obtainable from different rocket engines when propelling a single stage vehicle. The ideal burnout velocity V_{bi} is often termed the *vacuum burnout velocity*.

Assume that the rocket engine operates under steady state conditions so that it consumes propellants at the constant rate \dot{m} and that its effective jet velocity c remains constant.

For the case in question the drag and gravity terms in Eq. 5-49 vanish, and the ideal burnout velocity V_{bi} is given by

$$\begin{aligned} V_{bi} &= c \ln \left(\frac{m_0}{m_0 - m_p} \right) + V_0 \\ &= g_0 I_{sp} \ln \left(\frac{m_0}{m_0 - m_p} \right) + V_0 \end{aligned} \quad (5-55)$$

The velocity difference $V_{bi} - V_0$ is termed the *ideal burnout velocity increment* and is denoted by ΔV_{bi} . Thus

$$\Delta V_{bi} = V_{bi} - V_0 \quad (5-56)$$

If $V_0 = 0$, then the ideal burnout velocity is given by

$$V_{bi} = g_0 I_{sp} \ln \Lambda \quad (5-57)$$

where

$\Lambda = m_0 / m_b$ = vehicle mass ratio

$m_b = m_0 - m_p$ = vehicle mass at burnout

Eqs. 5-56 and 5-57 indicate that the ideal burnout velocity (increment) depends on the specific impulse obtainable from the propellants and the vehicle mass ratio $\Lambda = m_0 / m_b$.

Fig. 5-4 presents V_{bi} as a function of $c = g_0 I_{sp}$ for different values of vehicle mass ratio m_0 / m_b , for a single stage rocket-propelled vehicle.

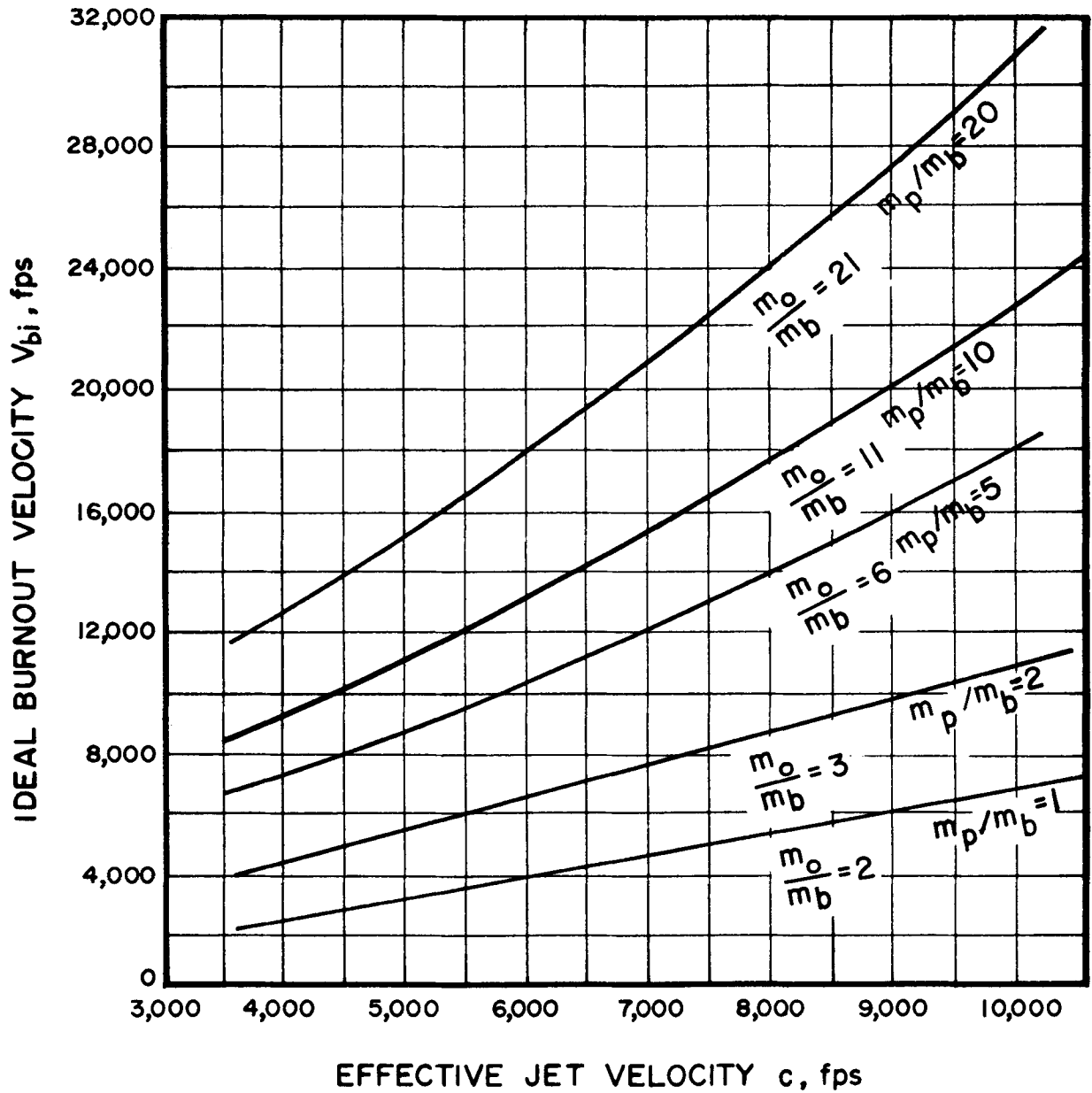


Figure 5-4. Ideal Burnout Velocity V_{bi} for a Single Stage Vehicle As a Function of Effective Jet Velocity c for Different Values of Vehicle Mass Ratio m_o/m_b

REFERENCES

1. M.J. Zucrow, *Aircraft and Missile Propulsion*, John Wiley and Sons, Inc., New York, 2nd Printing, Vol. 2, 1964, Ch. 10.
2. F.J. Malina, "Characteristics of a Rocket Motor Unit Based on the Theory of Perfect Gases," *Jour. Franklin Inst.*, Vol. 230, No. 4, October 1940, pp. 433-454.
3. CPIA Publication No. 80, *Solid Propulsion Nomenclature*, Chemical Propulsion Information Agency, The Johns Hopkins University, Applied Physics Laboratory, Silver Spring, Md., May 1965.
4. G.P. Sutton, *Rocket Propulsion Elements*, John Wiley and Sons, Inc., 3rd Ed., 1963.
5. W.J. Hesse and N.V.S. Mumford, *Jet Propulsion*, Pitman Publishing Company, 2nd Ed., 1964.
6. H.S. Tsien, "A Method for Comparing the Performance of Power Plants for Vertical Flight," *ARS Jour.* Vol. 22, No. 4, July-Aug., 1952.
7. J.W. Wiggins, "The Use of Solid Propellant Engines for Achievement of Super Velocities," *Jet Propulsion*, Vol. 26, No. 12, December 1956, pp. 1084-7.
8. S.S. Penner, *Chemistry Problems in Jet Propulsion*, Pergamon Press, New York, 1957.
9. R.B. Dow, *Fundamentals of Advanced Missiles*, John Wiley and Sons, Inc., 1958, Ch. 3.
10. E. A. Bonney, M. J. Zucrow and C. W. Besserer, "Aerodynamics, Propulsion, and Structures," *Principles of Guided Missile Design*, G. Merrill, Editor, D. Van Nostrand Company, Inc., 1956.
11. A.E. Puckett and S. Ramo, *Guided Missile Engineering*, McGraw-Hill Book Company, Inc., 1959, Ch. 3.
12. B.Etkin, *Dynamics of Flight - Stability and Control*, John Wiley and Sons, Inc., 1959.
13. R.A. Struble and H.D. Black, "A Generalized Closed Form for the Burnt Velocity," *Jet Propulsion*, Vol. 27, No. 151, 1957.
14. P.H. Blatz, "Kinematics of a Vertical Booster," *Jet Propulsion*, Vol. 24, No. 37, 1954.
15. J.B. Rosser, R.R. Newton, and G.L. Gross, *Mathematical Theory of Rocket Flight*, McGraw-Hill Book Company, Inc., 1947.

CHAPTER 6

THERMODYNAMIC RELATIONSHIPS FOR CHEMICAL ROCKET PROPULSION

6-0 PRINCIPAL NOTATION FOR CHAPTER 6*

a	acoustic speed	$(C_F)_0$	parallel-flow vacuum thrust coefficient
a^0	stagnation acoustic speed	C_w	weight flow coefficient = $\dot{w}/A_t P_c$
a^*	critical acoustic speed (where $M = 1$)	d	diameter
A_c	area of the inlet cross-section of a rocket nozzle	D	drag
A_e	area of exit cross-section of a rocket nozzle	F	thrust
A_t	area of throat cross-section of rocket nozzle	g_c	gravitational conversion factor = 32.174 slug-ft/lb-sec ²
A^*	cross-section of nozzle where $M = 1$	h	static specific enthalpy, B/slug
B	British thermal unit	h_c	static specific enthalpy at inlet cross-section A_c of the rocket nozzle
c	effective jet (or exhaust) velocity	h_e	static specific enthalpy at exit cross-section A_e of the rocket nozzle
c^*	characteristic velocity for a rocket motor	h^0	stagnation specific enthalpy
$c^{*'} $	ideal characteristic velocity	h_c^0	stagnation specific enthalpy at cross-section A_c
c_p	specific heat at constant pressure	I_{sp}	specific impulse = $F g_c / \dot{m}$, sec
c_v	specific heat at constant volume	I'_{sp}	theoretical specific impulse
\bar{c}_p	mean value of the specific heat at constant pressure		$= 6.94 \sqrt{T_c / \bar{m}} \sqrt{2\gamma Z_t / (\gamma - 1)}$
C_d	discharge coefficient for a rocket nozzle	I_d	density impulse
C_F	thrust coefficient = $F/A_t P_c$	J	mechanical equivalent of heat ≈ 778 ft-lb/B
		m	mass, slug

*Any consistent set of units may be employed; the units presented here are for the American Engineers System (see par. 1-7).

\bar{m}	molecular weight	T_c^o	stagnation temperature of the combustion gas
\dot{m}	mass rate of flow of propellants = $\dot{m}_f + \dot{m}_o$, slug/sec	u_e	adiabatic exhaust velocity
\dot{m}_f	mass rate of fuel consumption	\dot{w}	weight rate of propellant consumption
\dot{m}_o	mass rate of oxidizer consumption	Z_t	expansion factor = $1 - (P_e/P_c)^{\frac{\gamma-1}{\gamma}}$
p	static pressure, in psia	<u>GREEK LETTERS</u>	
P	static pressure, in psf	a	semiangle of diverging section of nozzle
P_a	ambient static pressure	γ	specific heat ratio = c_p/c_v
P_c	static pressure in A_c , the combustion pressure	Γ_1	$\Gamma\sqrt{\gamma}$
P_e	static pressure in nozzle exit cross-section A_e	Γ	(see Eq. 6-16)
P^o	stagnation (or total) pressure	η_n	nozzle efficiency
P_c^o	combustion stagnation pressure	κ	see Eq. 6-39b
R	gas constant = R_u/\bar{m}	λ	divergence loss coefficient
R_u	universal gas constant = 49,717 ft-lb/slug-mole-°R	ρ	density
t	time	ϕ	nozzle velocity coefficient = $\sqrt{\eta_n}$
T	static temperature, °R	<u>SUPERSCRIPTS</u>	
T_c	static temperature of gas in the inlet cross-section A_c of the rocket nozzle; the combustion temperature	*	critical conditions where $M = 1$ for an isentropic flow
T^o	stagnation or total temperature	'	value to which prime is attached is reached by an isentropic process
		o	stagnation value

6-1 INTRODUCTION

In the preliminary design of a rocket engine good estimates are required of the engine performance parameters, discussed in Chapter 5, over the anticipated range of operating conditions. In most cases the prediction of the performance of a rocket engine is desired with more than one propellant combination. Good estimates of the important design parameters should be available before any of the engine components are designed or manufactured.

It has been pointed out (see Chapter 1) that a rocket engine comprises a propulsive nozzle, the thrust-producing element, and a gas generator; the latter comprises the combustion chamber wherein the propellants are burned and its appurtenances. The foregoing remarks apply to chemical, nuclear heat-transfer, electrothermal, and solar-heating rocket engines. In fact, to any rocket engine which utilizes the thermodynamic process of expanding a compressible fluid by ejecting it through a nozzle for the production of a propulsive exhaust jet.

The discussions in the subject chapter are concerned specifically with chemical rocket engines but they apply equally well to the prediction of the performance of an exhaust nozzle for a nuclear heat-transfer, electrothermal, and solar-heating rocket engine.

Fig. 5-1 illustrates schematically the thermodynamic states of a propulsive gas as it expands in a propulsive nozzle. All of the subsequent discussions assume steady state operating conditions.

For preliminary design purposes it is desirable to predict the adiabatic exhaust velocity u_e with a high degree of accuracy. Since u_e is given by (see par. A-3)

$$u_e = \sqrt{2(h_c^O - h_e)} \quad (6-1)$$

where

h_c^O = the stagnation specific enthalpy of the inlet cross-section of the nozzle

h_e = static specific enthalpy at the exit cross-section of the nozzle, after an adiabatic expansion from the inlet cross-section

In Eq. 6-1, h_c^O is given by

$$h_c^O = h_c + \frac{u_c^2}{2} \quad (6-2)$$

It is apparent from Eq. 6-1, that two kinds of information are needed for calculating u_e .

- (a) The nature and chemical composition of the propellant gas at A_c , the inlet cross-section of the nozzle, and the *thermodynamic properties* of the propellant gas (h, P, T , etc.) at Stations c , t , and e in Fig. 5-1.
- (b) The heat added to the working fluid prior to its arrival at plane A_c (see Fig. 5-1). In a chemical rocket engine the heat is supplied by the *enthalpy of combustion* or *chemical reaction* for the specific chemical *reactants* involved. In a nuclear-transfer, electrothermal, or solar heating rocket engine it is the heat transferred to the working fluid by nuclear, electric, or solar energy, respectively. All of the aforementioned rocket engines, including the chemical rocket engines, employ the same type thermodynamic process for producing thrust. Hence, they are called *thermodynamic rocket engines* (see par. 1-5.4).

The working fluid entering the exhaust nozzle of a thermodynamic rocket engine is in the

gaseous state. In the *nonchemical engines* the working fluid is ordinarily a single-component gas; e.g., hydrogen, ammonia, helium, etc. In a chemical rocket motor the gas is composed of the gaseous products due to the combustion of a fuel (liquid or solid) with an oxidizer (liquid or solid). For example, the fuel used in a liquid bipropellant rocket engine (see par. 1-6.2) may be hydrocarbon, such as octane C_8H_{18} , and the oxidizer could be liquid oxygen (*LOX*). The thermochemical energy released by the combustion reaction raises the temperature of the *combustion products* to quite high values. Depending upon the propellant combination and their *mixture ratio* (\dot{m}_O/\dot{m}_F), the static temperature T_c of the gas entering the exhaust nozzle will range from $5,000^\circ R$ to approximately $8,500^\circ R$. For a nuclear-heat transfer rocket engine equipped with a carbon solid core nuclear reactor the corresponding temperature will be approximately $4,500^\circ R$ and for an arc-jet electrothermal rocket engine it may be higher than $15,000^\circ R^1$. The aforementioned temperatures are well above the critical temperatures T_{cr} for the gaseous constituents forming the propellant gas of a rocket engine (see par. A-2 and Table A-I). In those cases where the propellant gas contains condensable products – such as vaporized light metals – and the static pressure P_c at the entrance to the exhaust nozzle is high, the pressure P_c may approach the critical pressure for that constituent³.

In view of the foregoing, no sensible error is introduced in the large majority of cases if it is assumed that the equation of state for each gaseous constituent of the propellant gas at the inlet cross-section A_c (see Fig. 5-1) of the rocket nozzle is given by (see par. A-2.1)

$$P/\rho = RT \quad (6-3)$$

It is further assumed that the specific heats c_p and c_v , and their ratio $\gamma = c_p/c_v$ are functions only of the gas temperature.

To obtain the thermodynamic properties of the propellant gas, the methods of thermochemistry are employed^{2,5,6}.

6-2 ASSUMPTIONS IN THERMOCHEMICAL AND GAS DYNAMIC CALCULATIONS

The calculation of the composition and the thermodynamic properties of the propellant gas are based on the following simplifying assumptions.

- (a) The propellants react chemically and burn under steady state conditions.
- (b) The walls of the combustion chamber do not influence the combustion process.
- (c) The dimensions of the combustion chamber are sufficiently large so that *thermochemical equilibrium conditions* prevail at the inlet cross-section of the exhaust nozzle.
- (d) The equation of state of each constituent gas entering the exhaust nozzle is given by Eq. 6-3.
- (e) The combustion process is adiabatic and is also isobaric ($dP = 0$).
- (f) One of the two following assumptions is generally introduced:
 - (1) The equilibrium composition of the gases in the combustion chamber is unaltered during the expansion process in the nozzle. Calculations employing that assumption are said to be based on *frozen equilibrium*, or *frozen flow*.
 - (2) Chemical equilibrium is maintained throughout the expansion process; the composition and molecular weight of the gas changing because

of the chemical reactions occurring during the expansion process. Calculations employing this assumption are said to be based on either *equilibrium flow, shifting, mobile, or maintained equilibrium*.

In addition to the foregoing thermodynamic assumptions the following gas dynamic assumptions are introduced.

- (a) The flow through the nozzles is steady and one-dimensional, and the velocity u_e of the gas crossing the exit section (Area A_e) is parallel to the axis of the exhaust nozzle (see Fig. 5-1).
- (b) The velocity of the gases in the combustion chamber is negligibly small compared to the velocity of the gases crossing the exit section of the exhaust nozzle.
- (c) The flow through the nozzles is isentropic ($ds = 0$).
- (d) The gases are expanded completely to the surrounding atmospheric pressure P_a , i.e., the pressure P_e in the exit section of the nozzles is equal to P_a .

In view of the above assumptions, the *equilibrium composition* of the propellant gas entering the exhaust nozzle and its *thermodynamic properties* are determined *uniquely* by the *equilibrium combustion temperature* T_c and the *equilibrium combustion pressure* P_c ; hereafter T_c and P_c will be termed the combustion temperature and the combustion pressure, respectively.

In view of *gas dynamic assumption* (b) ($u_c \approx 0$) the stagnation specific enthalpy h_c^0 in Eq. 6-1 may be replaced by its corresponding static specific enthalpy h_c . Hence

$$u_e = \sqrt{2(h_c - h_e)} = 6.96\sqrt{h_c - h_e} \text{ (fps)} \quad (6-4)$$

where h_c and h_e are in B/slug. If h_e and h_c are in B/lb_m, then the 6.96 in Eq. 6-4 is replaced by 223.7.

When the Mach number $M_c < 0.3$, the static values T_c and P_c may be employed instead of the corresponding stagnation values T_c^0 and P_c^0 without introducing a significant error. The static and stagnation values are related by (see par. A-5.2)

$$h_c^0 = h_c + u_c^2/2 \quad (6-5)$$

$$T_c^0 = T_c \left[1 + \left(\frac{\gamma-1}{2} \right) M_c^2 \right] \quad (6-6)$$

$$P_c^0 = P_c \left(T_c^0/T_c \right)^{\gamma/(\gamma-1)} \quad (6-7)$$

where $M_c = u_c/a_c$ = Mach number for the gas at the inlet cross-section A_c of the exhaust nozzle

and $a_c = \sqrt{\gamma RT_c}$ = the acoustic speed in the gas at the combustion temperature T_c .

For a chemical rocket engine the combustion temperature depends primarily upon the kind of propellants, their mixture ratio (\dot{m}_o/\dot{m}_f), and to a small extent upon P_c the combustion pressure. The magnitude of P_c is governed by the propellant consumption rate \dot{m} and the throat area A_t of the nozzle; the latter statement is applicable to nonchemical as well as chemical thermodynamic rocket engines.

6-2.1 EXOTHERMIC AND ENDOTHERMIC CHEMICAL REACTIONS

A chemical reaction between the reactants aA and bB that yields the products mM and nN , may be represented by the following equation:



where ΔH_r is the *enthalpy of reaction*.

If the sign preceding ΔH_r is *negative* (–) the reaction is said to be *exothermic*; if the sign is positive (+), the reaction is said to be *endothermic*.

6-2.2 CONDITIONS FOR THERMOCHEMICAL EQUILIBRIUM

Thermochemical equilibrium for the propellant gas is attained when the rate at which products are formed equals the rate at which reactants are produced by the reversible chemical reaction. At equilibrium there is no change in the free-energy function, i.e., $\Delta F_{TP} = 0$ (see Reference 2, pp. 529-535). The conditions which must be satisfied for chemical equilibrium to be attained at a given T_c and P_c determine the composition of the propellant gas.

6-2.3 DISSOCIATION AND REASSOCIATION REACTIONS

Dissociation reactions may be considered to be the decomposition of a chemical compound due to exposing it to a high temperature. Because of the dissociation phenomena a portion of the thermochemical energy associated with a propellant combination becomes unavailable for producing jet kinetic energy when the propellant gas is expanded in the exhaust nozzle. As the gas expands in flowing through the nozzle it cools and its pressure falls, conditions which favor *reassociation reactions*. Any reassociation reactions that might occur are governed by reaction kinetics, and take place at a lower temperature than their corresponding dissociation reactions. Consequently, reassociation reactions can recover only a portion of the energy used in producing dissociation. The effect of the reassociation reactions that do occur is to reduce the decrease in temperature due to the expansion process which results in an apparent increase in the specific heat ratio γ .

Very large values of T_c favor dissociation reactions. Moreover, if T_c is sufficiently high

(above approximately 10,000°R) as in an arc-jet thermoelectric rocket motor, all of the molecular species are decomposed into atoms and ions. As a consequence of the dissociation reactions the maximum realizable value of T_c , at a given P_c , is limited. In general, the higher the gas temperature, the greater is the dissociation of the products. Increasing the static pressure P_c tends to reduce the amount of the dissociation.

Fig. 6-1 presents the percent dissociation for CO_2 , H_2O , H_2 , O_2 , HF , CO , and N_2 as functions of the gas temperature at 500 psia. It is seen that N_2 , CO , and HF do not dissociate appreciably at temperatures below 9,000°F. On the other hand, H_2O , H_2 , and O_2 are dissociated appreciably at 8,000°F.

The occurrence of dissociation and reassociation reactions is not related to rocket motor design, as is the occurrence of incomplete combustion; in the case of incomplete combustion, burning occurs during the expansion process in the rocket nozzle. The occurrence of dissociation and reassociation reactions is related to the specific propellant combination, the combustion temperature T_c , and the combustion pressure P_c . The effect of reassociation reactions upon the jet velocity of the exhaust gas may be as large as 10 percent for the LH-LOX* and LH-LF* propellant systems. For systems in which the fuel component is a hydrocarbon, the effect of reassociations upon the jet velocity is usually less than 5 percent.

6-3 THERMODYNAMIC EQUATIONS FOR ROCKET PERFORMANCE CRITERIA

In the preliminary design of a rocket motor for developing a specified thrust, the specific impulse I_{sp} of the suitable propellant systems (oxidizer plus fuel) must be known for a range

*LH - liquid hydrogen; LOX - liquid oxygen
LF - liquid fluorine

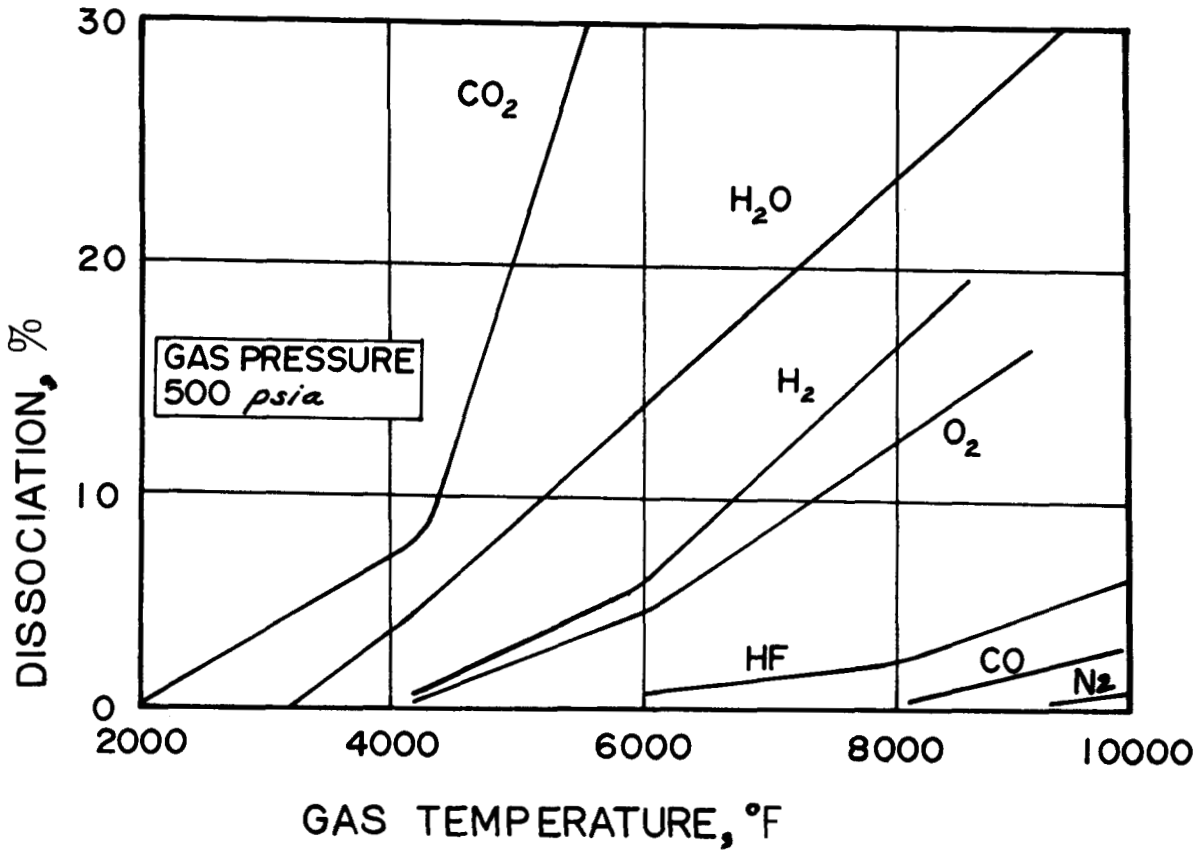


Figure 6-1. Dissociation in Percent as a Function of Gas Temperature for CO_2 , H_2O , H_2 , O_2 , HF , CO , and N_2 at 500 psia

of mixture ratios (\dot{m}_o/\dot{m}_f) and different values of combustion temperature T_c and combustion pressure P_c , respectively. It will be assumed that the aforementioned data are available either from experimental data or from thermochemical calculations. The design is then concerned with determining the dimensions of the main components, and predicting the performance criteria (see Chapter 5).

The subject paragraph is concerned with the basic gas dynamic equations for calculating the performance parameters. It combines the gas dynamic equations based on steady isentropic flow with the practical performance parameters discussed in Chapter 5.

6-3.1 ISENTROPIC EXIT VELOCITY (u'_e)

Since the flow in the exhaust nozzle is assumed isentropic, the isentropic exit velocity u'_e is given by (see par. A-5.4)

$$u'_e = \sqrt{2(h_c - h'_e)} = \sqrt{2\bar{c}_p T_c Z_t} \quad (6-9)$$

where \bar{c}_p is the mean value of c_p for the expansion process (from P_c , T_c to P_e , T'_e), and

$$Z_t = 1 - \left(\frac{P_e}{P_c} \right)^{(\gamma-1)/\gamma} \quad (6-10)$$

Eq. 6-9 can be rewritten to read

$$u'_e = \sqrt{2 \left(\frac{\gamma}{\gamma-1} \right) R_u \left(\frac{T_c}{\bar{m}} \right) Z_t} \quad (6-11)$$

If the Mach number $M_c = u_c/a_c > 0.3$, measured at A_c in Fig. 5-1, then h_c , T_c and P_c in the preceding equations should be replaced by

h_c^0 , T_c^0 , and P_c^0 . Fig. 6-2 presents the u'_e as a function of the mixture ratio (\dot{m}_o/\dot{m}_f), for different values of P_c/P_e , for the propellant combination nitrogen tetroxide (N_2O_4) and Aerozine-50 (50% Hydrazine + 50% UDMH).

In Eq. 6-11 the values of γ and \bar{m} are suitable average values for the expansion of the propellant gas from the state (P_c, T_c) to the state

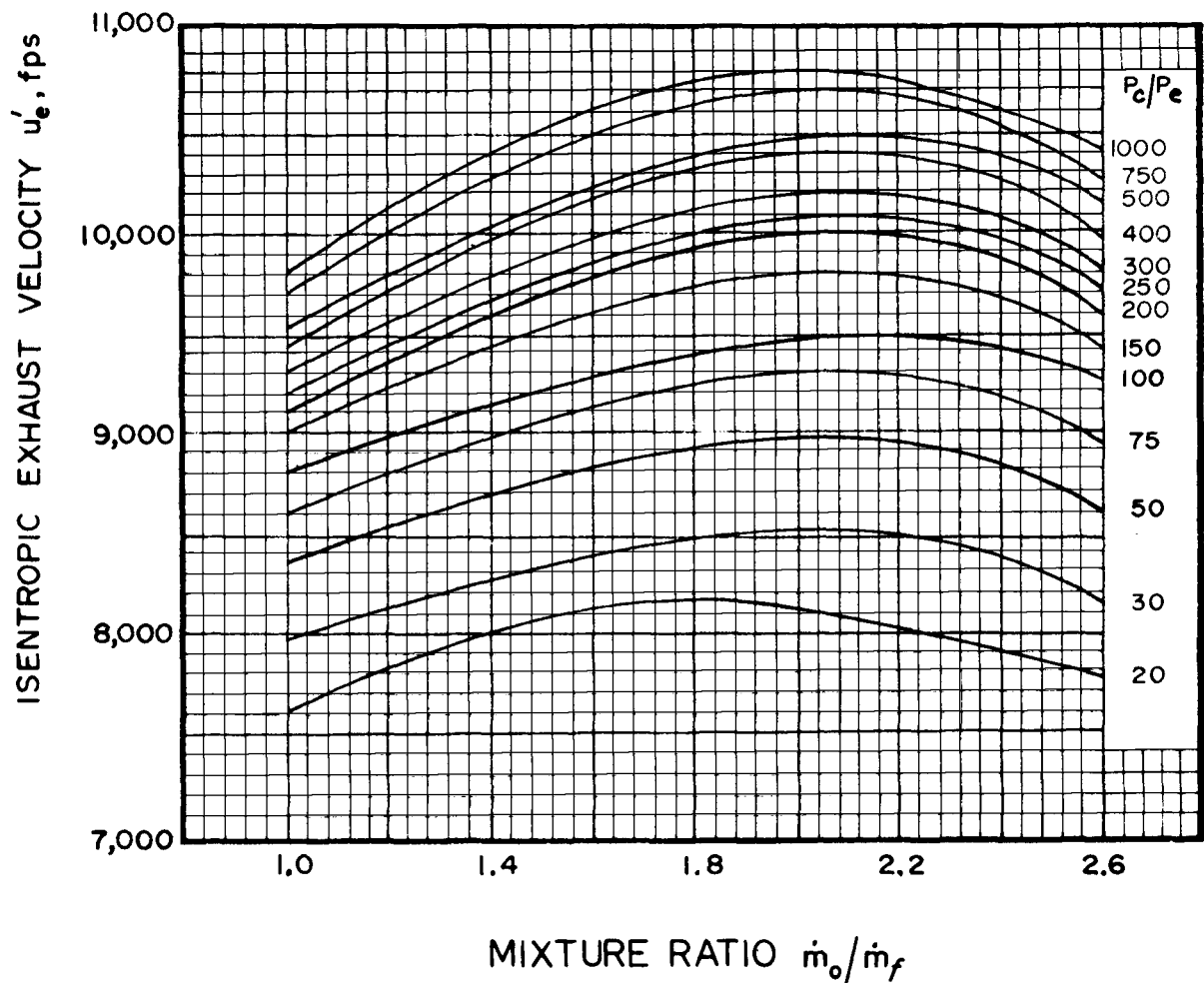


Figure 6-2. Isentropic Exhaust Velocity as a Function of Mixture Ratio \dot{m}_o/\dot{m}_f for Different Values of P_c/P_e ; Propellants: Nitrogen Tetroxide (N_2O_4) plus 50% Aerozine-50–50% Hydrazine (N_2H_4) and 50% Unsymmetrical Dimethyl Hydrazine ($(CH_3)_2N_2H_2$, (UDMH))

(P_e , T_e). Careful consideration must be given to the selection of the values of γ and \bar{m} . The selection of the appropriate value for γ is basically the determination of the appropriate value for $\bar{m}\bar{c}_p$.

Substituting for $R_u = 49.717$ ft-lb per slug mole °R into Eq. 6-11, yields

$$u'_e = 315.3 \sqrt{T_c / \bar{m}} \sqrt{\frac{\gamma}{\gamma-1}} Z_t \text{ (fps)} \quad (6-12)$$

It is evident from Eq. 6-12 that for a given expansion ratio P_e/P_c the main parameter affecting u'_e is $\sqrt{T_c / \bar{m}}$.

6-3.2 ACTUAL OR ADIABATIC EXIT VELOCITY (u_e)

In real nozzle flow, the actual or adiabatic exit velocity, denoted by u_e , is given by

$$u_e = \phi u'_e \quad (6-13)$$

where $\phi = \sqrt{\eta_n}$ = the nozzle velocity coefficient (see par. 4-5.2). The value of ϕ ranges from 0.95 to 0.98 for well-designed rocket nozzles.

Figs. 6-3 and 6-4 present the *velocity parameter* $u_e / \phi \sqrt{T_c^0 / \bar{m}}$ as a function of the pressure ratio P_c^0 / P_e for different values of $\gamma = c_p / c_v$.

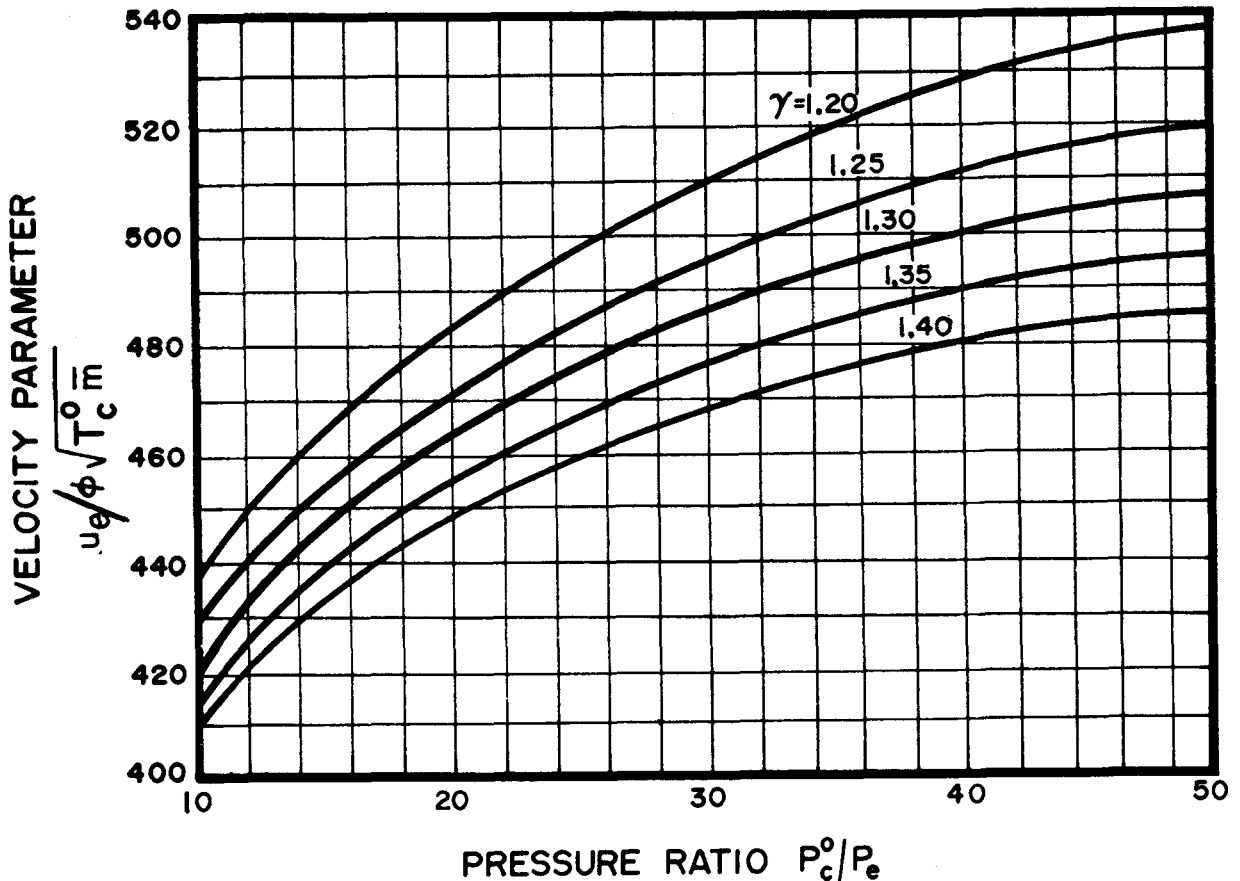


Figure 6-3. Velocity Parameter $u_e / \phi \sqrt{T_c^0 / \bar{m}}$ as a Function of P_c^0 / P_e (for a Range of 10 to 50) for Different Values of $\gamma = c_p / c_v$

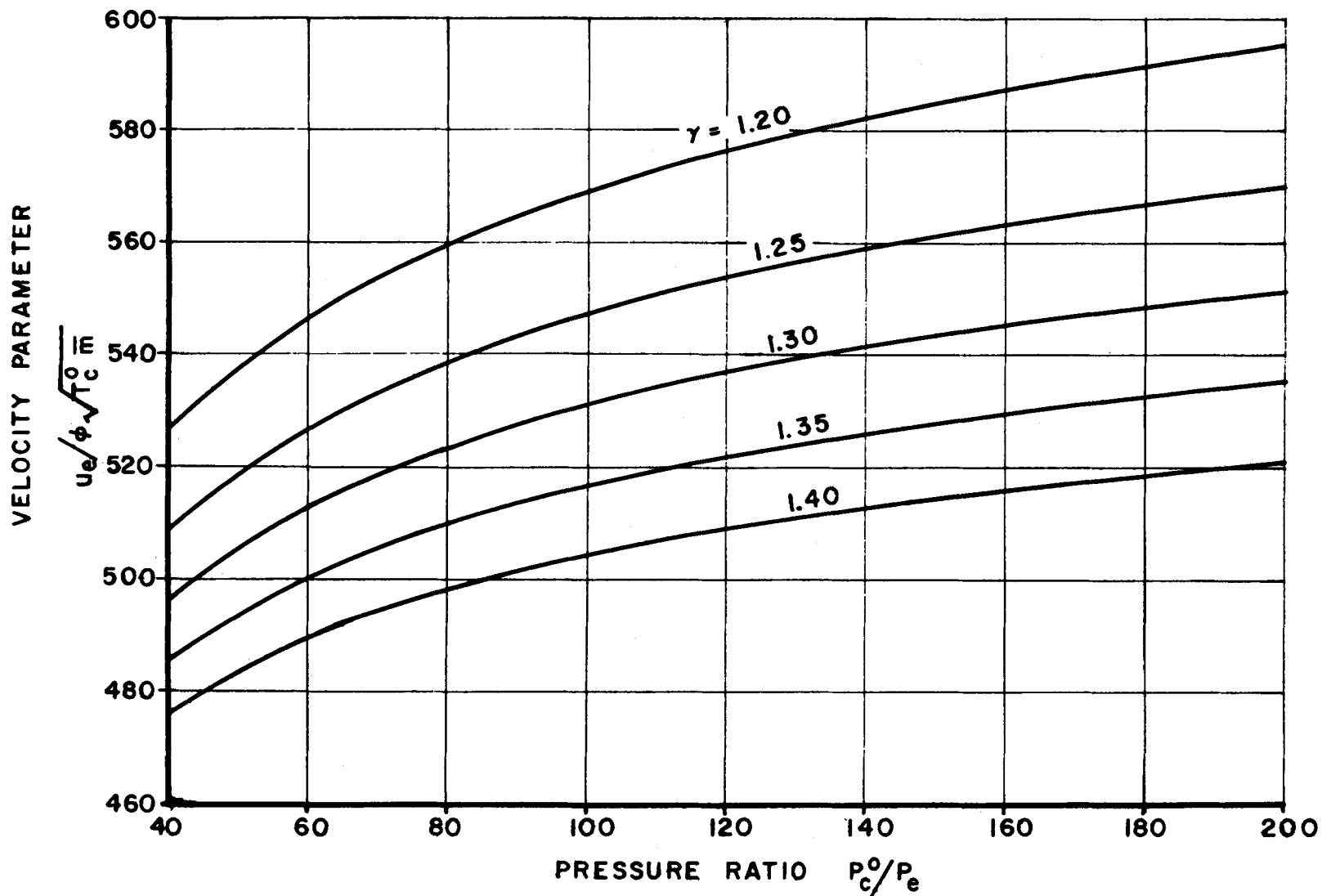


Figure 6-4. Velocity Parameter $u_e / \phi \sqrt{T_c^0 / m}$ as a Function of P_c^0 / P_e (for a Range of 40 to 200) for Different Values of $\gamma = c_p / c_v$

It is preferable to estimate the parameter $\sqrt{T_c^0/\bar{m}}$ from experimental data when they are available.

6-3.3 PROPELLANT FLOW COEFFICIENTS

6-3.3.1 MASS FLOW RATE OF PROPELLANT GAS (\dot{m})

Since the *nozzle pressure ratio* P_c^0/P_a for a rocket nozzle is always *supercritical* (see par. 4-3.3), a rocket motor nozzle is said to operate with either *complete nozzling* or with *choked flow*, i.e., critical conditions prevail in the throat (see par. A-6) and $P_t = P^*$, $T_t = T^*$, and $u_t' = u^*$. Hence

$$u_t' = 315.3 \sqrt{\frac{\gamma}{\gamma+1}} \sqrt{\frac{T_c}{\bar{m}}} \quad (6-14)$$

From Eq. 4-41 it follows that the mass rate of gas flow through the nozzles of a rocket engine is given by

$$\dot{m} = C_d A_t P_c \sqrt{\frac{\gamma}{RT_c} \left(\frac{2}{\gamma+1} \right)^{(\gamma+1)/(\gamma-1)}} \quad (6-15)$$

where C_d is the discharge coefficient for the nozzle (see par. 4-5.2) and its value ranges from approximately 0.93 to 1.15.

Let

$$\Gamma = \sqrt{\gamma} \left(\frac{2}{\gamma+1} \right)^{\frac{\gamma+1}{2(\gamma-1)}} \quad (6-16)$$

Then

$$\dot{m} = \frac{\dot{w}}{g_c} = 4.48(10)^{-3} C_d A_t P_c \frac{\Gamma}{\sqrt{T_c/\bar{m}}} \quad (6-17)$$

(slug/sec)

where

$$g_c = 32.174 \text{ slug-ft/lb-sec}^2$$

\dot{w} = weight flow rate of propellants, lb/sec

Values of Γ as a function of γ are presented in Fig. 6-5 and are tabulated in Appendix B, Table B-4.

6-3.3.2 WEIGHT FLOW COEFFICIENT (C_w)

The weight rate of propellant flow, from Eq. 6-17, is given by

$$\dot{w} = g_c \dot{m} = 144.3(10)^{-3} C_d A_t P_c \frac{\Gamma}{\sqrt{T_c/\bar{m}}} \quad (6-18)$$

(lb/sec)

The weight flow coefficient C_w (see Eq. 5-7) is accordingly given by

$$C_w = 144.3(10)^{-3} C_d \frac{\Gamma}{\sqrt{T_c/\bar{m}}} \quad (6-19)$$

Eq. 6-19 is employed for estimating the value of $\sqrt{T_c/\bar{m}}$ from measured values of C_w . A small error in the calculated value of γ , from thermochemical calculations, exerts an insignificant effect on the value of $\sqrt{T_c/\bar{m}}$ calculated from

$$\sqrt{T_c/\bar{m}} = 144.3(10)^{-3} \frac{C_d}{C_w} \Gamma \quad (6-20)$$

6-3.4 THRUST (F)

It is shown in par. 4-8.1.1 that if the exit flow from a propulsive nozzle diverges, as in a conical nozzle, then there is a reduction in thrust termed the *divergence loss*. In general, therefore, the thrust is given by Eq. 4-43 which is repeated here for convenience. Thus

$$F = \lambda \left[\dot{m} u_e + (P_e - P_a) A_e \right] \quad (6-21)$$

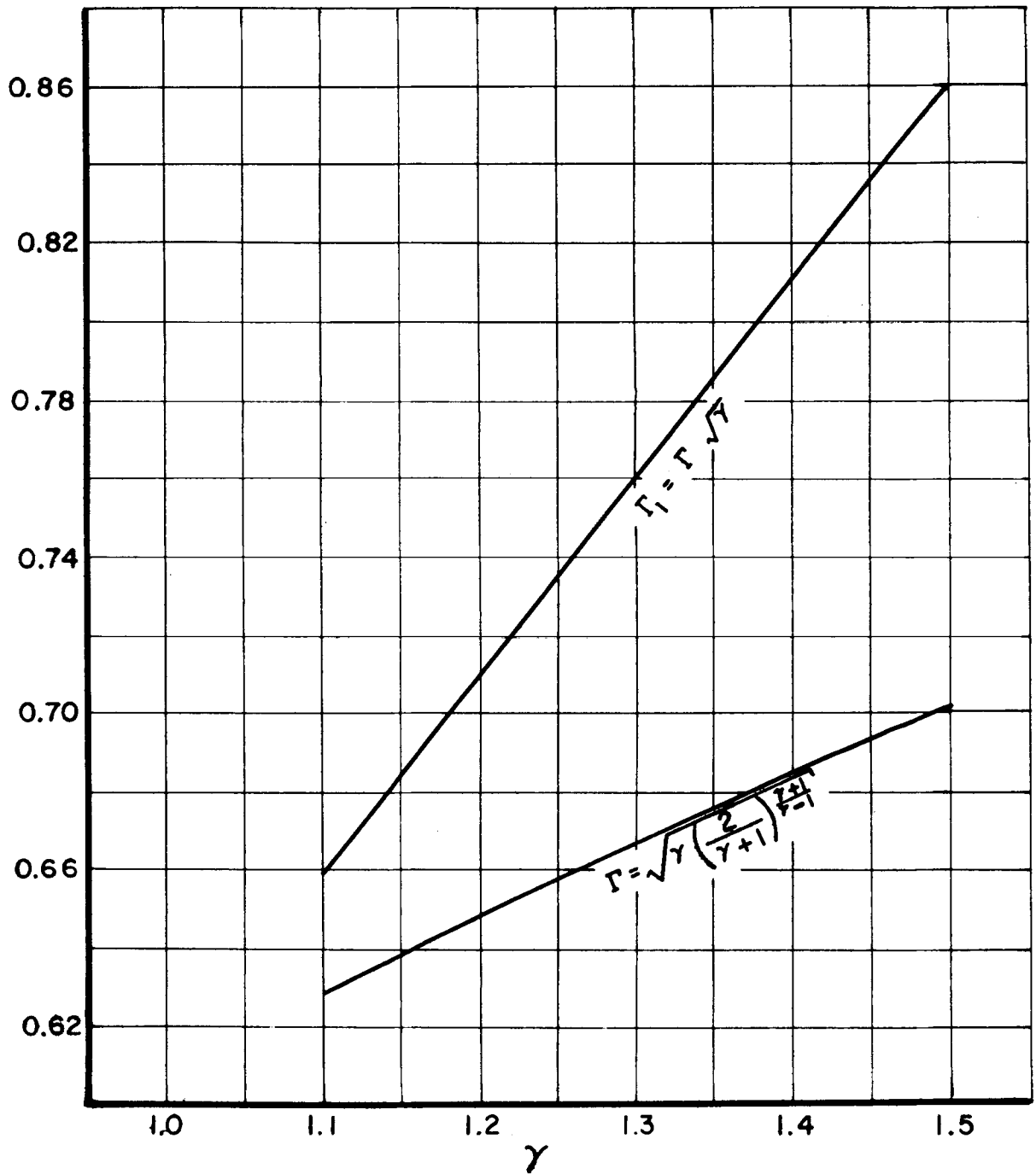


Figure 6-5. Values of the Parameter $\Gamma = \sqrt{\gamma} \left(\frac{2}{\gamma+1} \right)^{\frac{\gamma+1}{\gamma-1}}$ and $\Gamma_1 = \Gamma\sqrt{\gamma}$ as Functions of γ

The divergence loss coefficient λ is given by

$$\lambda = \frac{1}{2} (1 + \cos a) \quad (6-22)$$

where a is the semidivergence angle for the conical nozzle (see Fig. 5-1).

Combining Eqs. 6-14, 6-18, and 6-21 one can have the following equation for thrust F :

$$F = \lambda \left[\phi C_d A_t P_c \Gamma \sqrt{\frac{2}{\gamma-1}} Z_t + A_e (P_e - P_a) \right] \quad (6-23)$$

where Z_t is given by Eq. 6-10, P_a denotes the ambient static pressure, and P_e is the static pressure in exit cross section of the nozzle A_e (see Fig. 5-1).

6-3.4.1 EFFECTIVE JET (OR EXHAUST) VELOCITY (c)

The effective jet velocity c is defined by Eq. 5-3, which is repeated here for convenience.

$$c = F/\dot{m}$$

Combining Eqs. 6-17, 6-23, and 5-3 one obtains the following thermodynamic equation for c :

$$c = \lambda \frac{\sqrt{\gamma R T_c}}{\Gamma_1} \left[\Gamma_1 \sqrt{\frac{2}{\gamma-1}} Z_t + \left(\frac{P_e}{P_c} - \frac{P_a}{P_c} \right) \epsilon \right] \quad (6-24)$$

where

$$\Gamma_1 = \Gamma \sqrt{\gamma} = \gamma \left(\frac{2}{\gamma+1} \right)^{\frac{\gamma+1}{2(\gamma-1)}} \quad (6-25)$$

$$\epsilon = A_e/A_t = \text{area ratio of the nozzle}$$

6-3.4.2 THRUST COEFFICIENT (C_F)

The thrust coefficient C_F is defined by Eq. 5-9, and can be written in the form

$$C_F = \dot{m} c / (P_c A_t) \quad (6-26)$$

Hence

$$C_F = \lambda \left[\Gamma_1 \sqrt{\frac{2}{\gamma-1}} Z_t + \frac{P_e}{P_c} \epsilon - \frac{P_a}{P_c} \epsilon \right] \quad (6-27)$$

For a given value of γ the thrust coefficient depends only on P_a/P_c and λ ; the effect of the ambient pressure P_a is to decrease C_F by the quantity $(P_a/P_c)\epsilon$. When $P_a = 0$, as in space, C_F attains its maximum value. It can be shown that for a fixed value of P_a/P_c there is a value of ϵ which yields a maximum value of C_F . That value of ϵ is called the *optimum nozzle area ratio* and occurs when $P_e/P_c = P_a/P_c$; i.e., when the pressure thrust $(P_e - P_a)A_e = 0$.

Let $(C_F)_0$ denote the so-called *parallel flow vacuum thrust coefficient*, which assumes that $\lambda=1$ and $P_a/P_c = 0$; then the thrust coefficient C_F is given by

$$C_F = \lambda \left[\left(C_F \right)_0 - \left(\frac{P_e}{P_c} \right) \epsilon \right] \quad (6-28)$$

Fig. 6-6 presents $(C_F)_0$ as a function of ϵ and Fig. 6-7 presents $(P_e/P_c)\epsilon$ as a function of ϵ . Detailed tables for those parameters are presented in Reference 13.

6-3.5 NOZZLE AREA RATIO FOR COMPLETE EXPANSION

The thrust F attains its maximum value when the nozzle is designed so that the propellant gas is expanded completely to the ambient pressure P_a ; i.e., when $P_e = P_a$. The area ratio is ϵ is given by (see par. 4-3.1)

$$\epsilon = \left(\frac{A_e}{A_t} \right) \frac{\frac{2}{\gamma+1}}{\left(\frac{P_e}{P_c} \right)^{\frac{1}{\gamma}} \sqrt{\frac{\gamma+1}{\gamma-1}} Z_t} \quad (6-29)$$

Figs. 6-8, 6-9, and 6-10 present ϵ as a function of P_c/P_e for values ranging up to $P_c/P_e = 200$, for different values of γ .

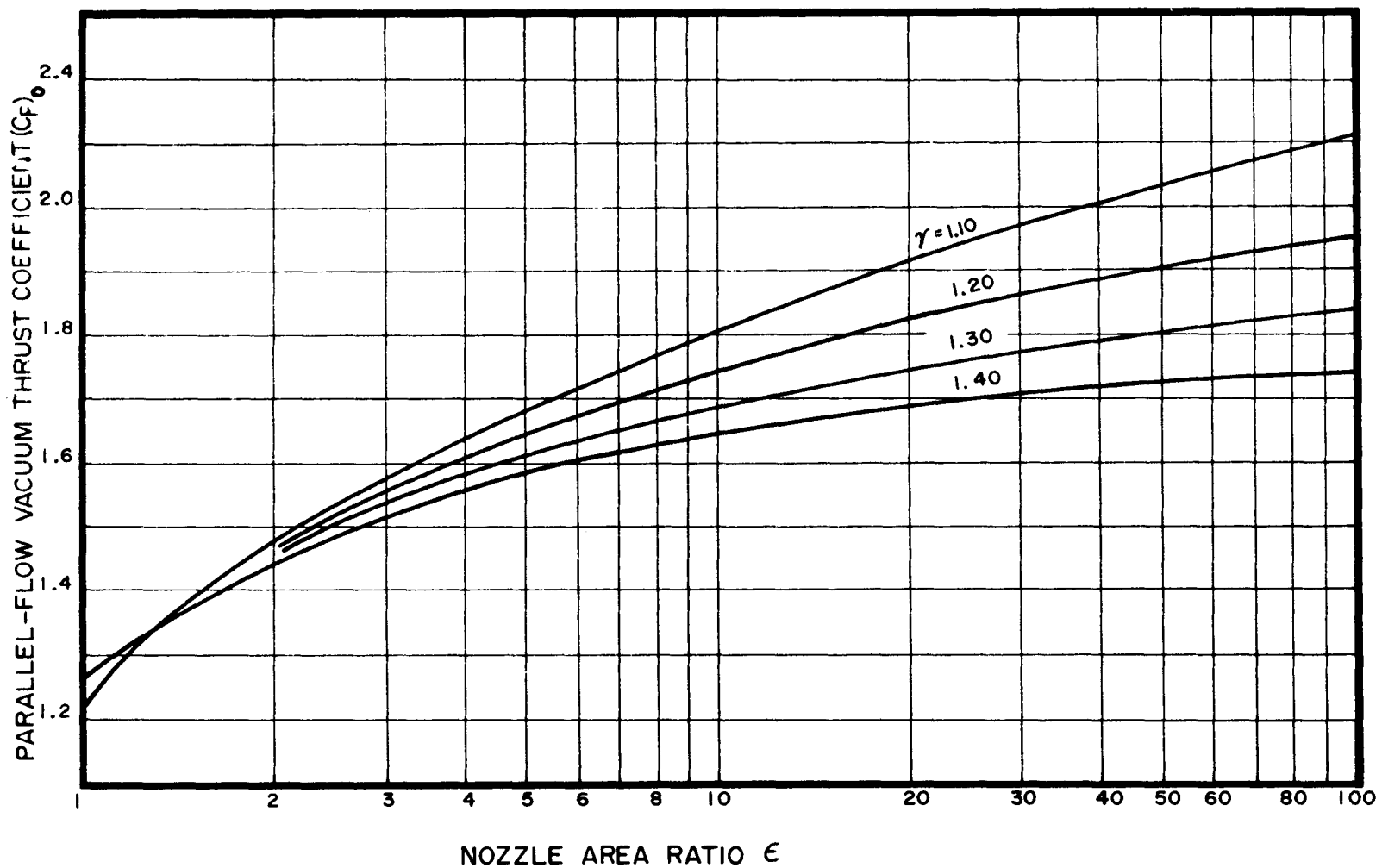


Figure 6-6. Parallel Flow Vacuum Thrust Coefficient $(C_F)_0$ as a Function of Nozzle Area Ratio ϵ

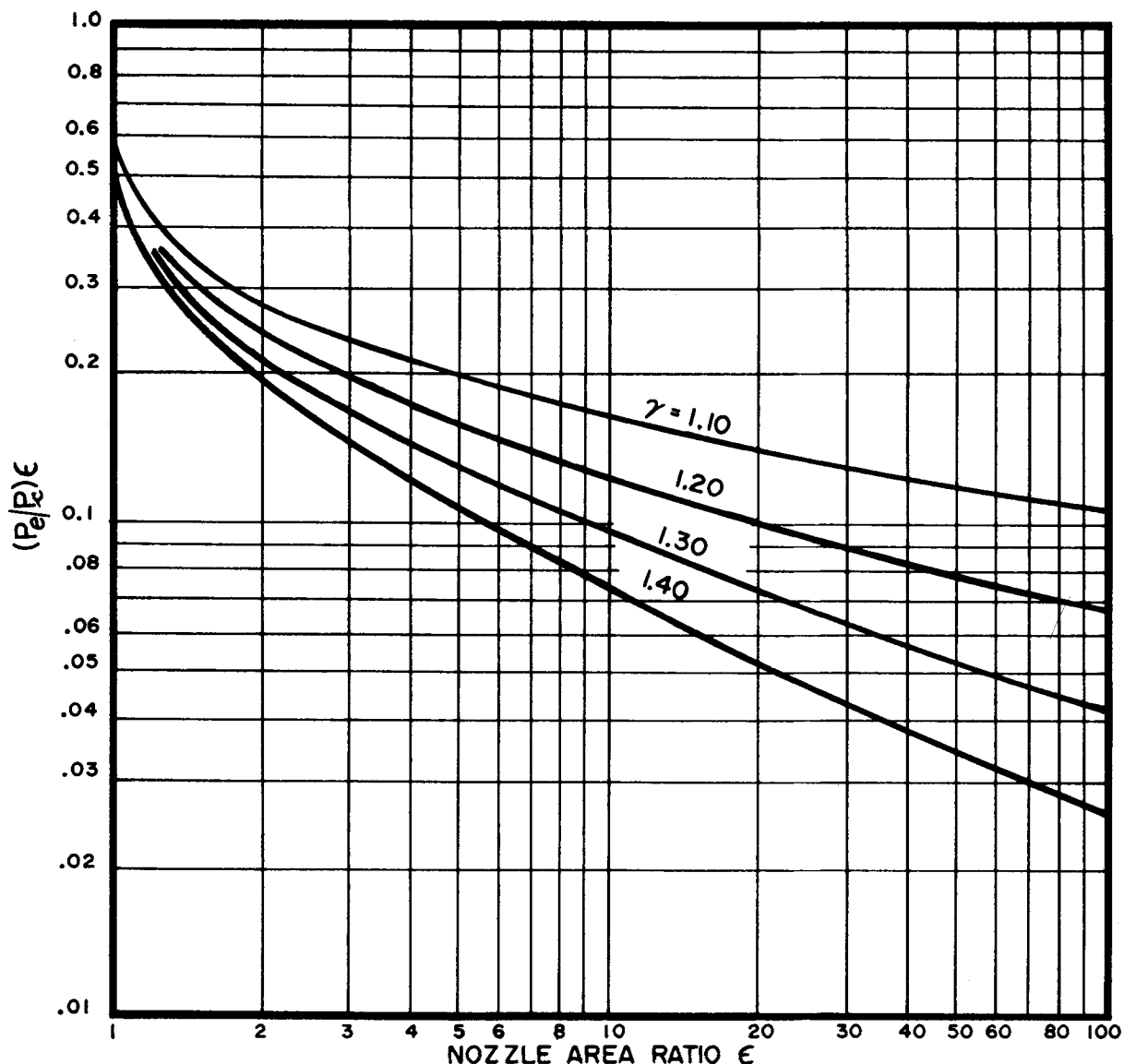


Figure 6-7. Parameter $(P_e/P_c)\epsilon$ as a Function of the Nozzle Area Ratio ϵ

Since the flow through the rocket nozzle is assumed to be one-dimensional, the area ratio ϵ is given by

$$\epsilon = \frac{A_e}{A_t} = \frac{\rho_t u_t'}{\rho_e u_e'} \quad (6-30)$$

The maximum flow density occurs at the throat of the nozzle, and is determined in the

computer program for calculating the thermodynamic equilibrium properties of the propellant gas¹⁴. Fig. 6-11 presents ϵ as a function of the mixture ratio (\dot{m}_O/\dot{m}_F) for different values of P_c/P_e for the propellant combination nitrogen tetroxide and Aerozine-50.

For rocket engines which must operate over a wide range of altitudes it may be advisable to

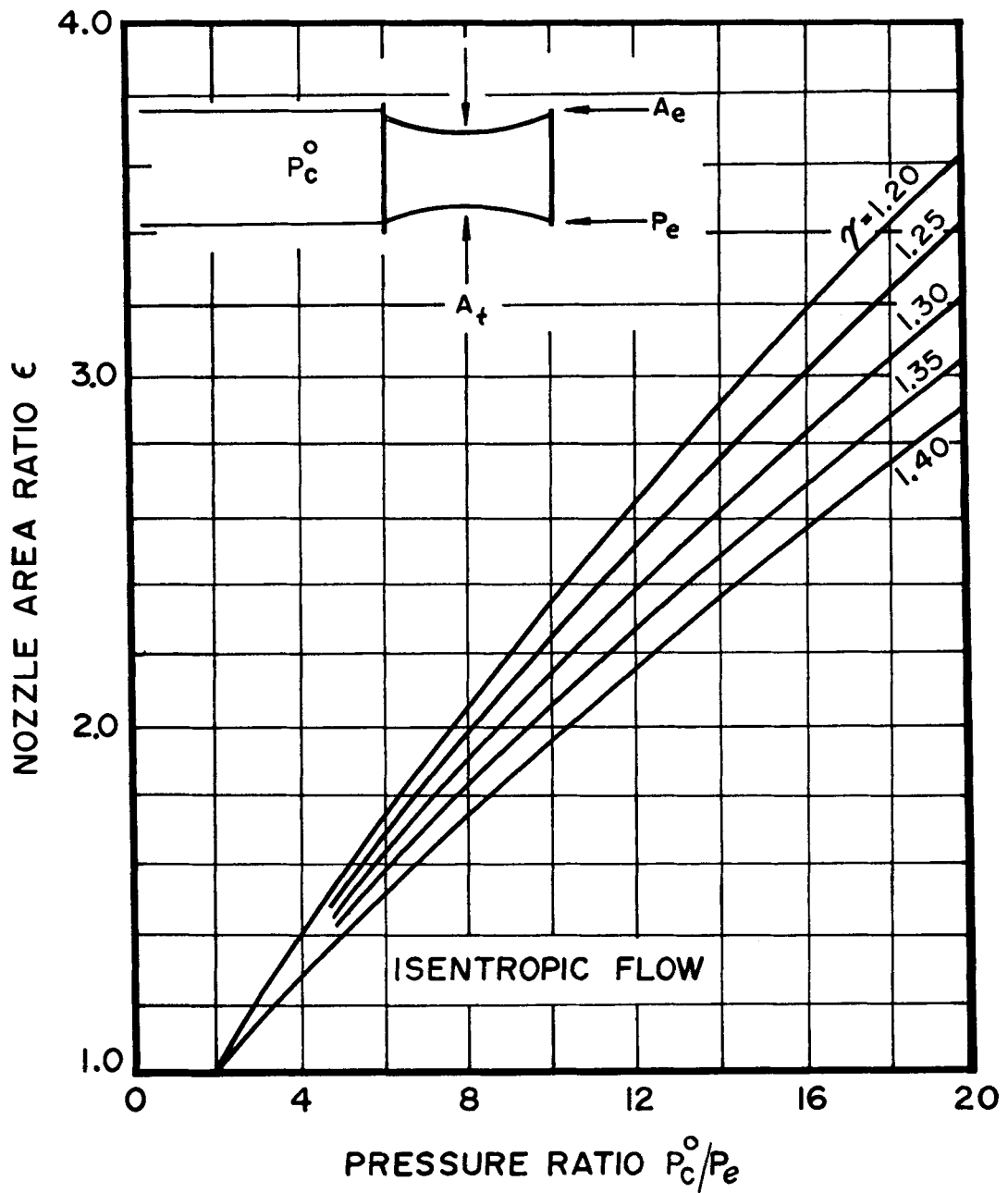


Figure 6-8. Nozzle Area Ratio ϵ as a Function of P_c^o/P_e (0 to 20) for Different Values of γ

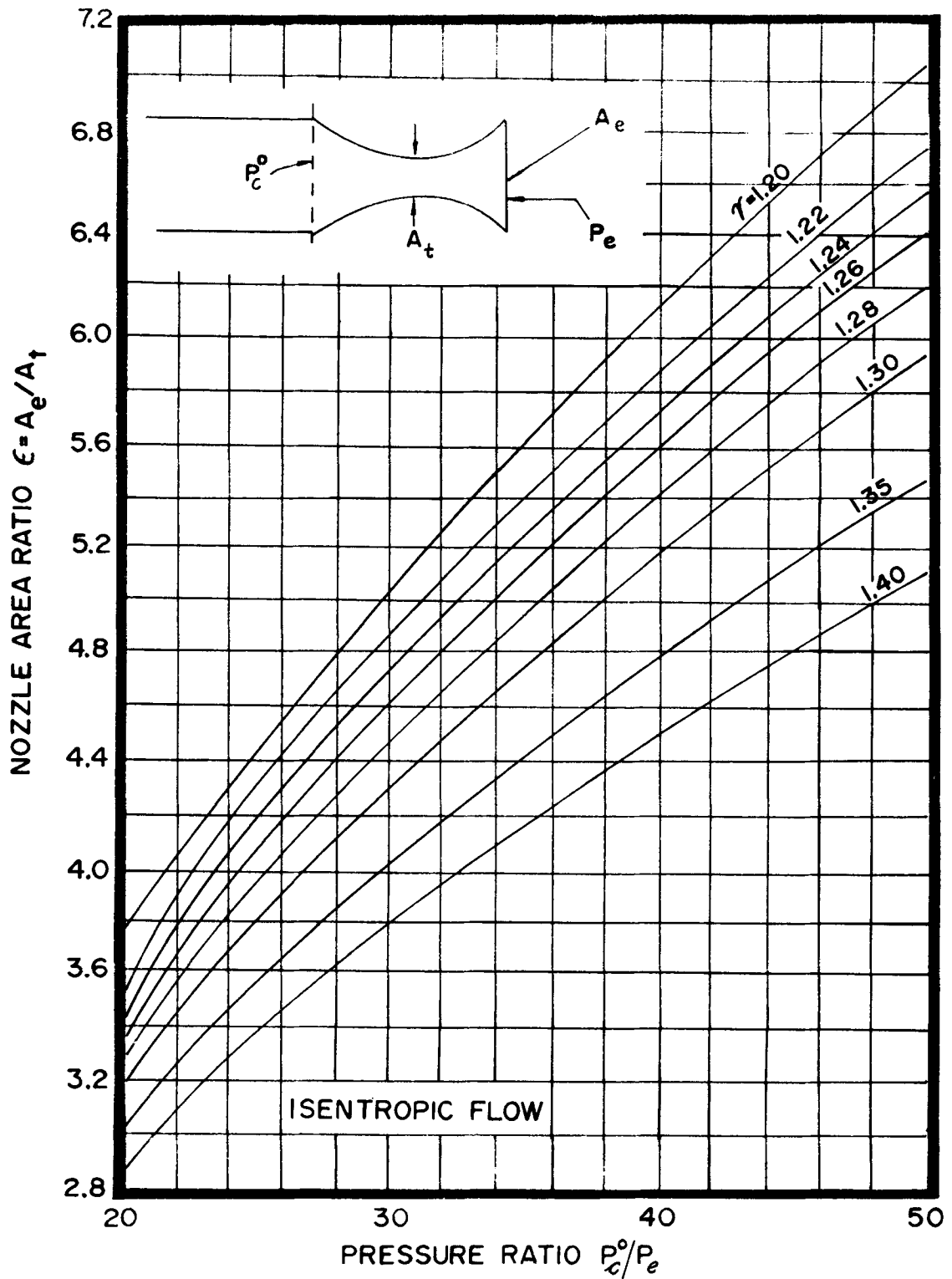


Figure 6-9. Nozzle Area Ratio ϵ as a Function of P_c^0/P_e (20 to 50) for Different Values of γ

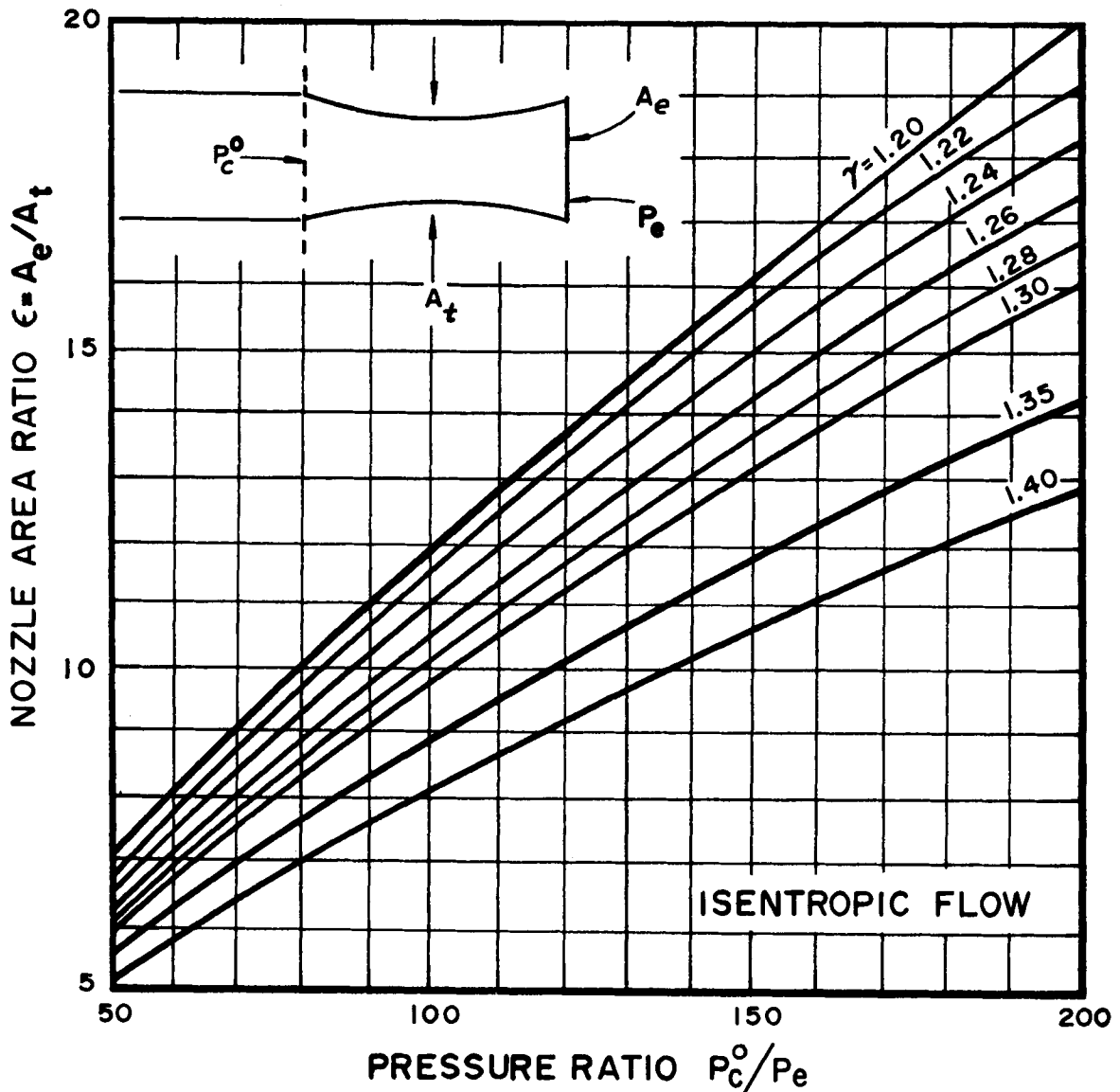


Figure 6-10. Nozzle Area Ratio ϵ as a Function of P_c^0/P_e (50 to 200) for Different Values of γ

operate with underexpansion to avoid the large nozzle weight accompanying large expansion ratios (see par. 4-8).

6-3.6 CHARACTERISTIC VELOCITY (c^*)

When experimental data for determining c^* are lacking, its value can be calculated with satisfactory accuracy from the thermodynamic properties for the propellant gas obtained by

applying thermochemical calculations to the chemical reaction equation for the propellants^{7,8,11}. From Eq. 5-13, which is repeated here for convenience, c^* is given by

$$c^* = \frac{g_c}{C_w} \quad (6-31)$$

where $g_c = 32.174 \text{ slug-ft/lb-sec}^2$

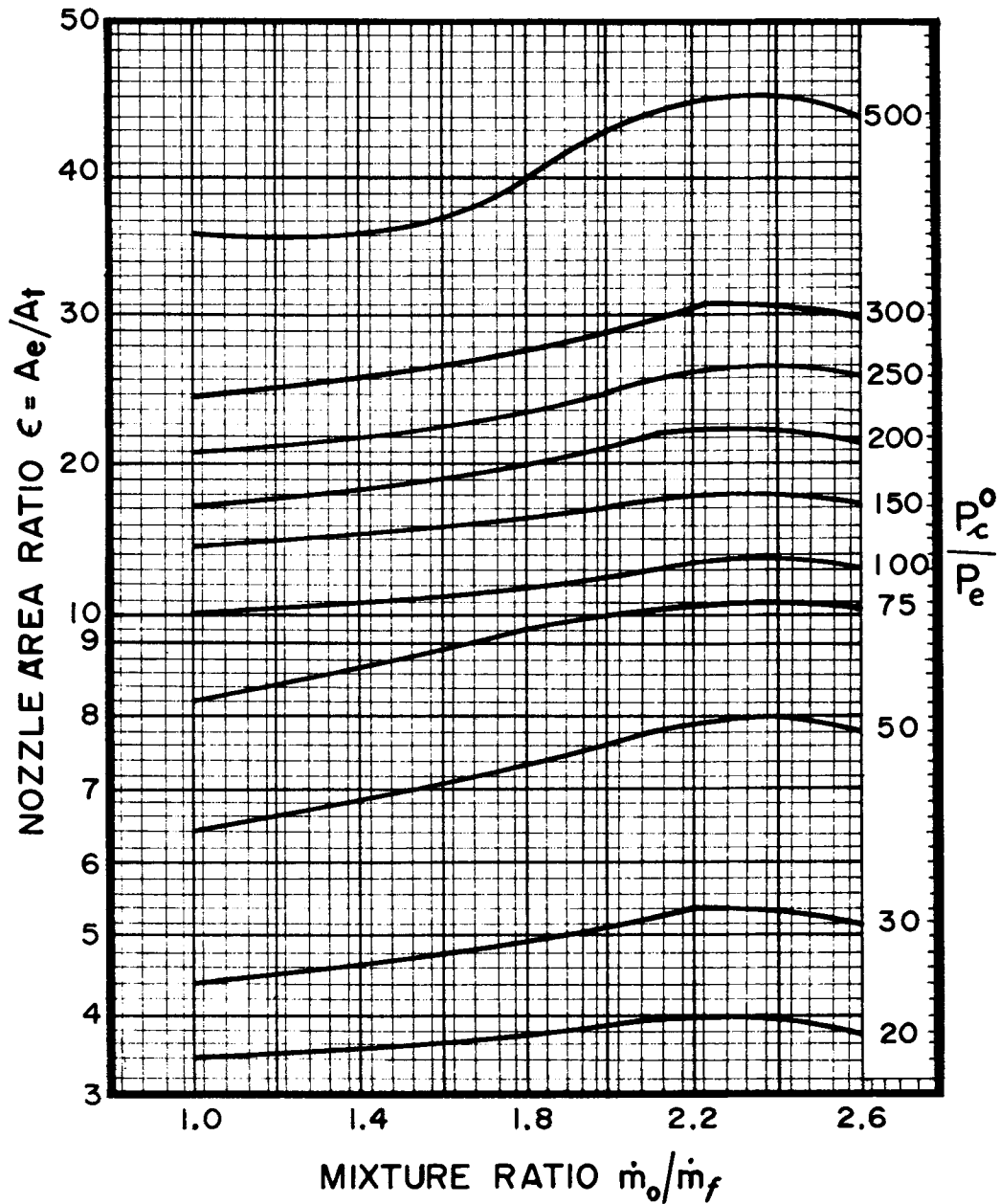


Figure 6-11. Nozzle Area Ratio $\epsilon = A_e/A_t$ as a Function of the Mixture Ratio and Different Values of P_c/P_e for the N_2O_4 -Aerozine-50 Propellant Combination

Combining Eqs. 6-19 and 6-31 one obtains the following thermodynamic equation for c^* :

$$c^* = \frac{1}{C_d} \left(\frac{a_c}{\Gamma_1} \right) = 223.0 \frac{\sqrt{T_c/\bar{m}}}{C_d \Gamma} \text{ (fps)} \quad (6-32)$$

where the acoustic speed in the propellant gas at the temperature T_c is given by

$$a_c = \sqrt{\gamma R T_c} \quad (6-33)$$

The parameters Γ and Γ_1 are given by Eqs. 6-14 and 6-24. Their values as functions of γ are presented graphically in Fig. 6-4 and in tabular form in Appendix B, Table B-4.

If it is assumed that $C_d = 1.0$, the corresponding value of c^* is termed the *ideal characteristic velocity* and is denoted by $c^{*'}$. Thus

$$c^{*'} = 223.0 \frac{\sqrt{T_c/\bar{m}}}{\Gamma_1} \quad (6-34)$$

Eqs. 6-32 and 6-34 show that c^* and $c^{*'}$ depend only upon γ and T_c/\bar{m} , i.e., primarily upon the propellant combination (fuel + oxidizer) and the mixture ratio (\dot{m}_o/\dot{m}_f). The combustion pressure has less influence because of its much smaller effect upon T_c , \bar{m} , and γ . Fig. 6-12 illustrates the effect of mixture ratio (\dot{m}_o/\dot{m}_f) and combustion pressure P_c upon the $c^{*'}$ for the propellant combination nitrogen tetroxide and Aerozine-50.

6-3.7 THEORETICAL SPECIFIC IMPULSE (I'_{sp})

From Eqs. 5-3 and 5-5 it follows that the thrust F and the specific impulse I_{sp} are related by

$$F = \dot{w} I_{sp} \quad (6-35)$$

Hence

$$I_{sp} = \lambda \left[\frac{u_e}{g_c} + \left(P_e - P_a \right) A_e / \dot{w} \right] = c/g_c \quad (6-36)$$

It is readily shown that¹

$$I_{sp} = \lambda \phi \sqrt{\frac{2R_u}{g_c}} \sqrt{\frac{T_c}{\bar{m}}} \sqrt{\left(\frac{\gamma}{\gamma-1} \right)} Z_t \quad (6-37)$$

where

$$\sqrt{\frac{2R_u}{g_c}} = 9.797$$

If $\lambda = \phi = 1$ then the flow is isentropic with no divergence and the corresponding value of the specific impulse is denoted by I'_{sp} which is the *theoretical specific impulse*. Fig. 6-13 presents the I'_{sp} as a function of the mixture ratio (\dot{m}_o/\dot{m}_f) for several liquid propellant combinations reacted at $P_c = 300$ psia.

6.3.7.1 REDUCED SPECIFIC IMPULSE

The calculated specific impulse based on one-dimensional flow is denoted by I_{sp} , where

$$I_{sp} = \lambda \phi I'_{sp}$$

Hence

$$\frac{I_{sp}}{\lambda \phi \sqrt{T_c/\bar{m}}} = 9.797 \sqrt{\frac{\gamma}{\gamma-1}} \sqrt{1 - \left(\frac{P_e}{P_c} \right)^{(\gamma-1)/\gamma}} \quad (6-38)$$

The ratio $I_{sp}/\lambda \phi \sqrt{T_c/\bar{m}}$ is sometimes called the *reduced specific impulse*. Its magnitude is a function of the specific heat ratio for the combustion gas mixture.

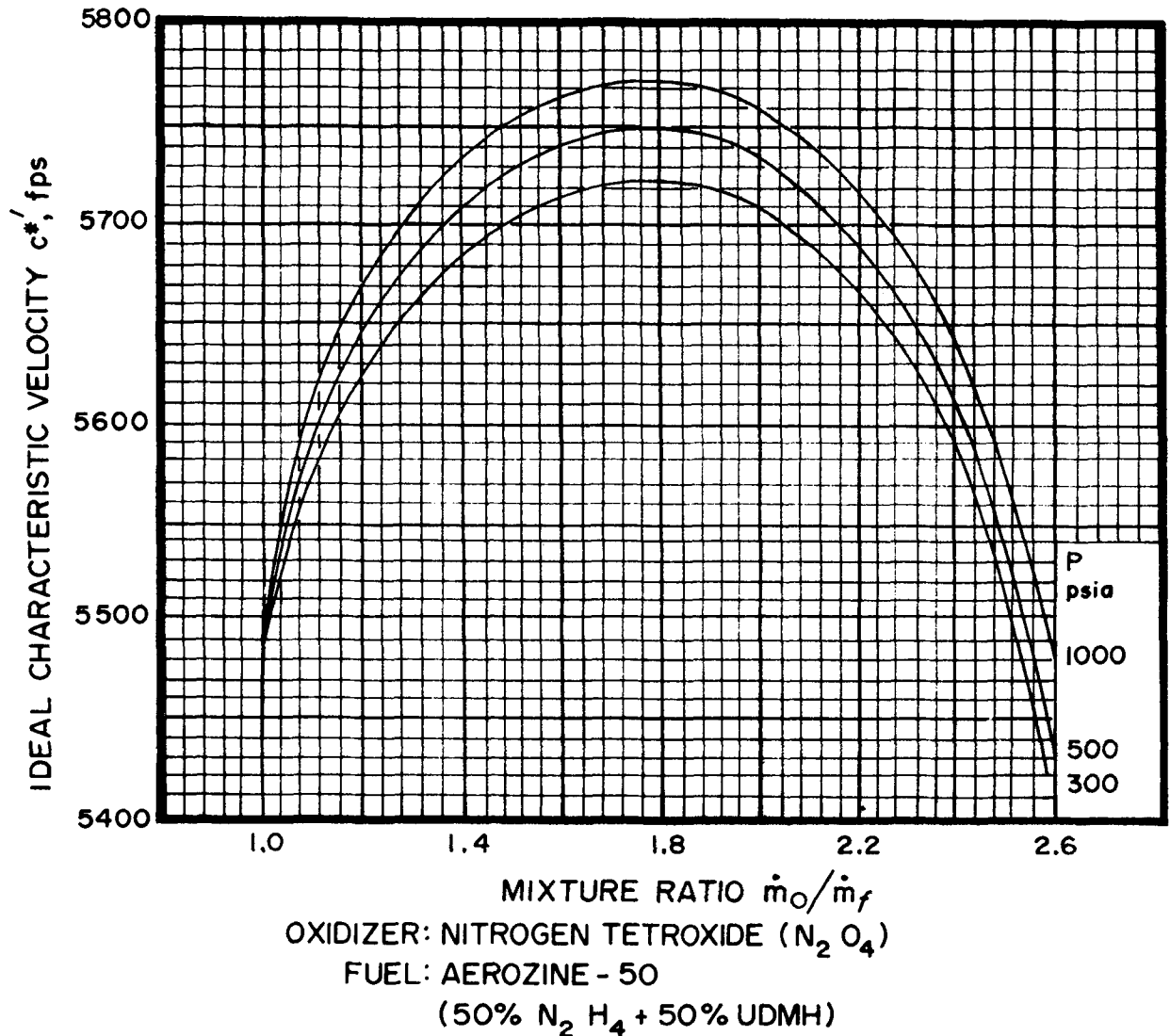


Figure 6-12. Ideal Characteristic Velocity c^* as a Function of Mixture Ratio for Different Combustion Pressures P_c ; Propellants: N_2O_4 Plus Aerozine-50

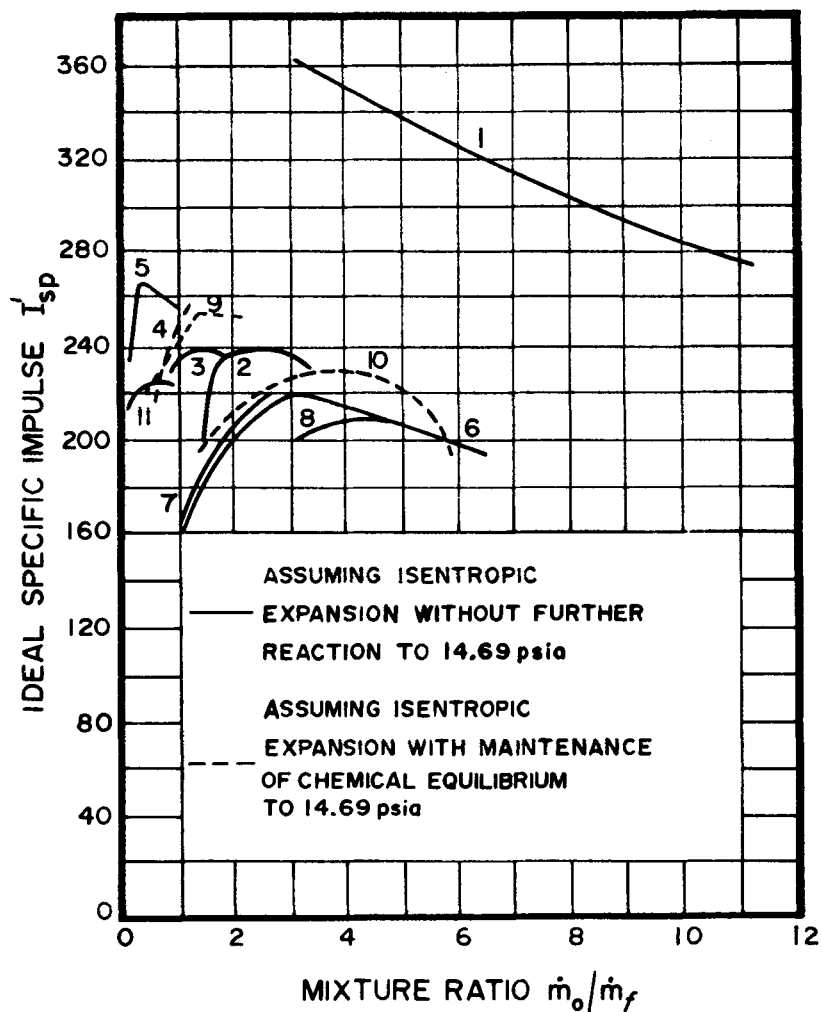
It is seen from Eq. 6-37 that I'_{sp} depends upon two factors

$$(a) Z_t = 1 - \left(\frac{P_e}{P_c} \right)^{(\gamma-1)/\gamma} = \text{expansion factor} \quad (6-39a)$$

$$(b) \kappa = \left[\frac{1}{g_c} \left(\frac{2\gamma}{\gamma-1} \right) \frac{R_u T_c}{\bar{m}} \right]^{1/2} \quad (6-39b)$$

The magnitude of the expansion factor Z_t depends mainly upon the expansion ratio P_e/P_c and it is only slightly influenced by variations in γ . The value of κ depends primarily upon $\sqrt{T_c/\bar{m}}$. Hence, raising T_c , lowering \bar{m} , or doing both, are helpful in increasing the specific impulse.

In general, for any propellant combination the combustion temperature depends primarily



NO.	SYSTEM	P_c psia
1	LIQUID OXYGEN-LIQUID HYDROGEN	340
2	LIQUID OXYGEN-GASOLINE *	300
3	LIQUID OXYGEN-ETHANOL	300
4	LIQUID OXYGEN-LIQUID AMMONIA	300
5	LIQUID OXYGEN-HYDRAZINE	300
6	RFNA† - ANILINE	300
7	RFNA† - ORTHOTOLUIDINE	300
8	MIXED ACID-MONOETHYL ANILINE	340
9	HYDROGEN PEROXIDE‡ - HYDRAZINE	300
10	HYDROGEN PEROXIDE§ - METHANOL	300
11	HYDROGEN PEROXIDE§ - NITROMETHANE	300
12	HYDROGEN PEROXIDE-NITROMETHANE§, WITH METHANOL, 30%	300

* 0.15 WT. FRAC. HYDROGEN, 0.85 WT. FRAC. CARBON. ‡ 100 WT. % CONCENTRATION.
 † 0.15 WT. FRAC. N_2O_4 . § 87 WT. % CONCENTRATION.

Figure 6-13. Ideal Specific Impulse I'_{sp} as a Function of the Mixture Ratio (\dot{m}_o/\dot{m}_f) for Several Liquid Propellant Combinations²

upon the mixture ratio (\dot{m}_O/\dot{m}_F) as can be seen from Fig. 6-14. The maximum combustion temperature is, however, limited by dissociation reactions (see par. 6-3.3). From an engine design standpoint, however, the maximum permissible combustion temperature is limited by the available construction materials and the ability to cool them.

The possibility of increasing the specific impulse by using fuels rich in hydrogen suffers from certain restrictions due to their low density. Furthermore, many of them are *cryogenic* and their storage becomes a problem in Army applications.

6-3.7.2 DENSITY IMPULSE (I_d)

A criterion which must be considered in selecting a propellant combination for a specific

rocket jet propulsion application is the so-called density impulse, denoted by I_d , which is defined as the product of I'_{sp} and the specific gravity of the propellant system. Hence

$$I_d \equiv I'_{sp} \times (\text{sp. gr.}) \quad (6-40)$$

where *sp.gr.* denotes the specific gravity of the propellant system, and I'_{sp} is the theoretical specific impulse.

A high value I_d is desirable, especially for single stage rocket propelled vehicles. Fig. 6-15 presents the values of I_d as a function of \dot{m}_O/\dot{m}_F for the same propellants for which the I'_{sp} is presented in Fig. 6-13.

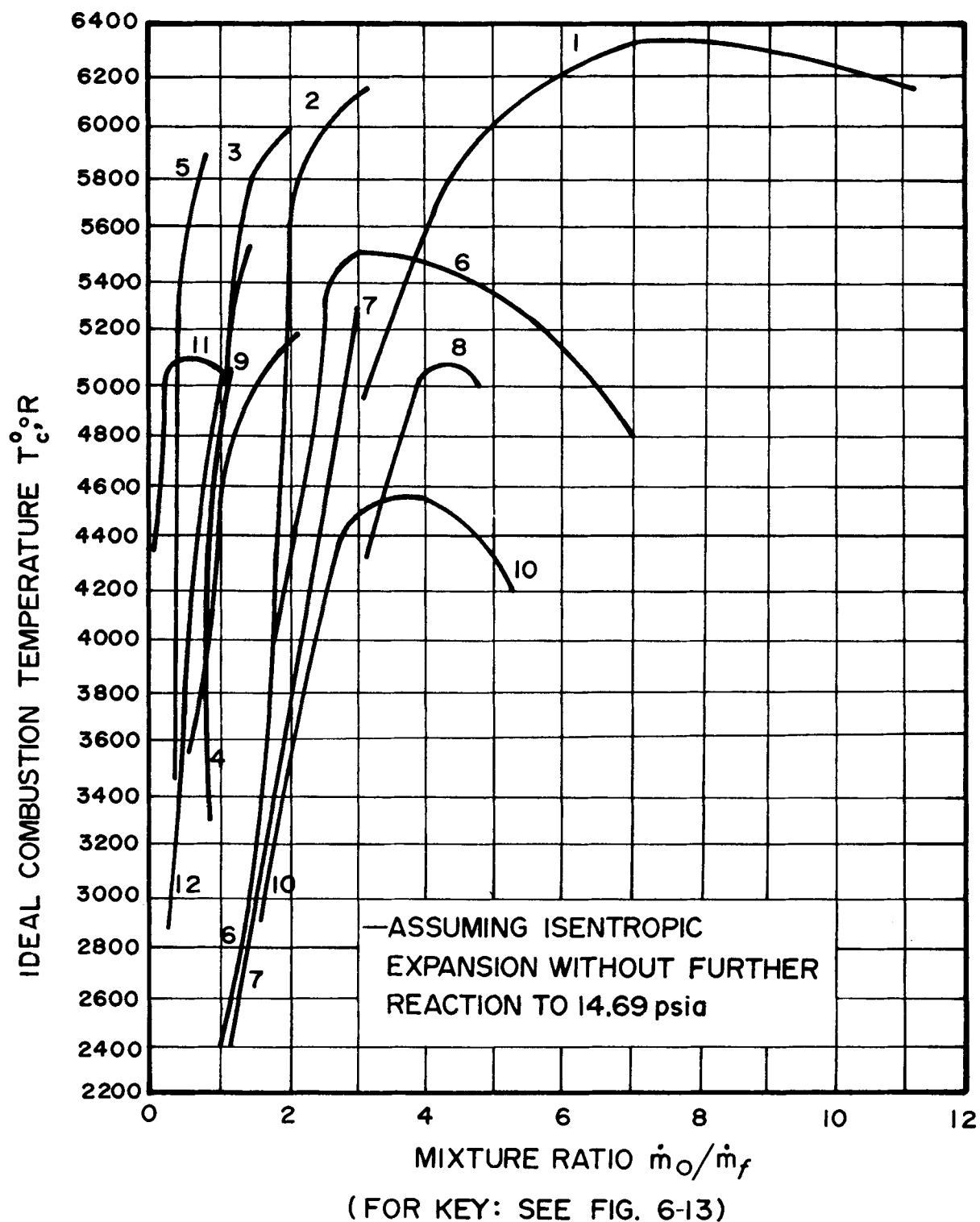


Figure 6-14. Combustion Temperature as a Function of the Mixture Ratio (\dot{m}_O/\dot{m}_f) for Several Liquid Propellants²

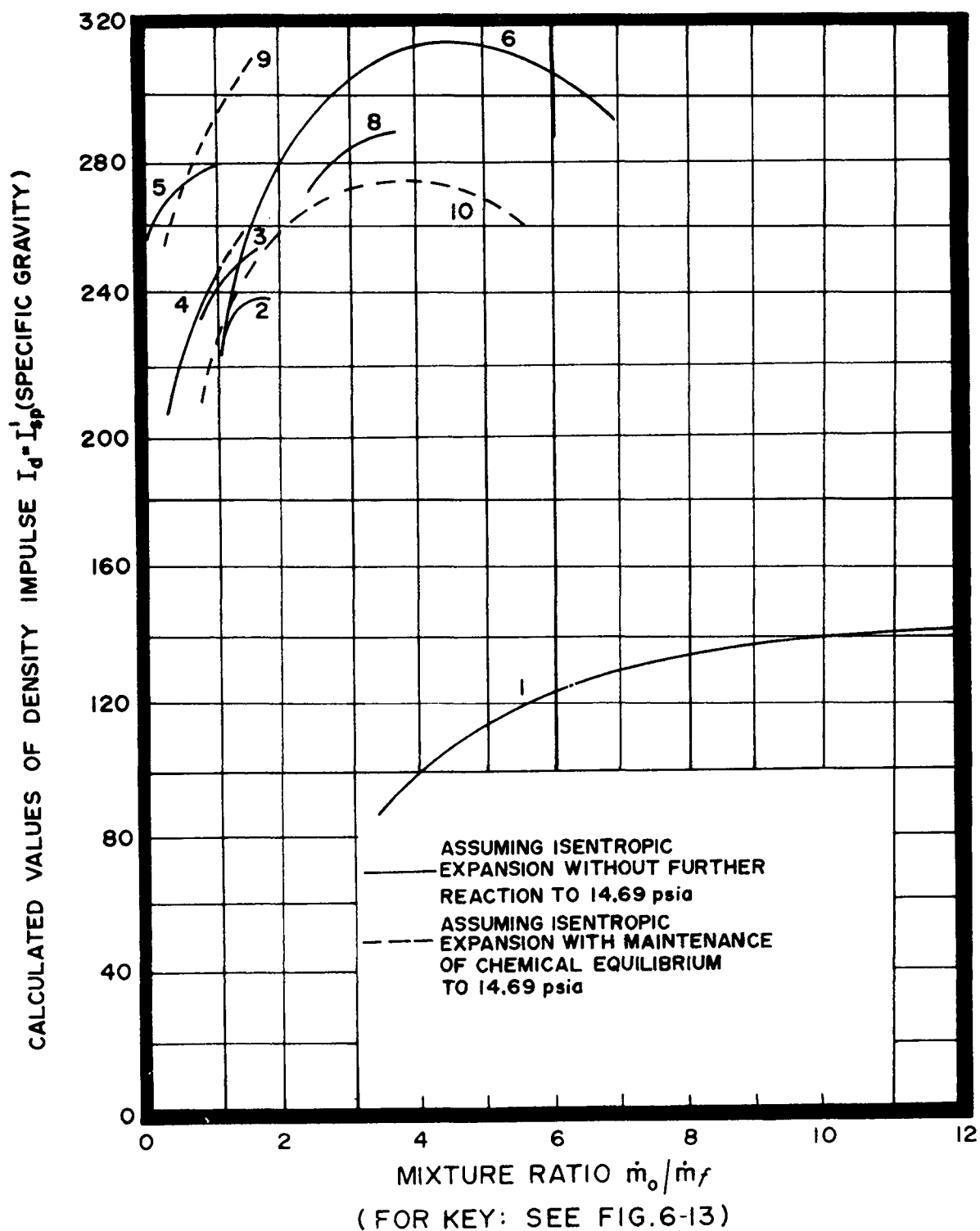


Figure 6-15. Density Impulse I_d as a Function of the Mixture Ratio (\dot{m}_o / \dot{m}_f) for Several Liquid Propellant Systems²

REFERENCES

1. M.J. Zucrow, *Space Propulsion Engines: Their Characteristics and Problems*, 14th Series, Science in Progress, Edited by W.R. Brode, Yale University Press, 1964.
2. M.J. Zucrow, *Aircraft and Missile Propulsion*, John Wiley and Sons, Inc., 2nd Printing, 1964, Ch. 10.
3. J.D. Hoffman, *An Analysis of the Effects of Gas-Particle Mixtures on the Performance of Rocket Nozzles*, Rept. No. TM-63.1, JPC 348, Jet Propulsion Center, Purdue University, Jan. 1963.
4. D.W. Netzer, *Calculation of Flow Characteristics for Two-Phase Flow in Annular Converging-Diverging Nozzles*, Rept. No. TM-62.3, JPC 305, Jet Propulsion Center, Purdue University, June 1962.
5. S.S. Penner, *Chemistry Problems in Jet Propulsion*, Peragamon Press, New York, 1957.
6. L.E. Steiner, *Introduction to Chemical Thermodynamics*, McGraw-Hill Book Company, Inc., 1941.
7. V.N. Huff, S. Gordon, and V.E. Morrell, *General Method and Thermodynamic Tables for Computation of Equilibrium Composition and Temperature of Chemical Reactions*, NACA Report No. 1037, 1951.
8. T.O. Dobbins, *Thermodynamics of Rocket Propulsion and Theoretical Evaluation of Some Prototype Propellant Combinations*, Wright Air Development Center, ARDC, WPAFB, WADC TR-59-757, December 1959.
9. H.N. Browne, M.M. Williams and D.R. Cruise, *The Theoretical Computation of Equilibrium Compositions, Thermodynamic Properties and Performance Characteristics of Propellant Systems*, U.S. NOTS, China Lake, Calif. NOTS-TR2434, NAVWEPS Report 7043, June 1960.
10. S. Gordon, F.J. Zeleznik and V.N. Huff, *A General Method for Automatic Computation of Equilibrium Compositions and Theoretical Performance of Propellants*, NASA, TN D-132, October 1959.
11. S.R. Goldwasser, *Calculation of Equilibrium Gas Temperature*, Aerojet-General Corporation, Tech. Memo. No. 126 LRP, 29 April 1957.
12. J.S. Martinez and G.W. Elverum, *A Method of Calculating the Performance of Liquid-Propellant Systems Containing the Species $C_1H_1O_1N_1F_1$ and One Other Halogen with Tables of Required Thermochemical Properties to 6000°K*, JPL Memo 20-121, 6 December 1955.
13. H.S. Seifert and J. Crum, *Thrust Coefficient and Expansion Ratio Tables*, Ramo-Wooldridge Corporation, Los Angeles, Cal., 29 February 1956.
14. *Performance and Properties of Liquid Propellants*, Aerojet-General Corporation, LRP, 7 March 1961.

CHAPTER 7

PROPERTIES AND CHARACTERISTICS OF SOLID PROPELLANTS

7-1 CLASSIFICATION OF SOLID PROPELLANTS

The performance criteria and thermodynamic equations presented in Chapters 5 and 6, respectively, are applicable to rocket engines burning either solid or liquid propellants. The attractiveness of solid propellants for many Army applications arises from the following considerations:

- (a) The greater simplicity of solid propellant rocket motors
- (b) The greater ease with which they can be handled in the field
- (c) Their instant readiness for use
- (d) Their good storage properties
- (e) Their lower first cost
- (f) Their lower susceptibility to malfunctioning because of fewer moving parts

In general, once the characteristics of a specific solid propellant have been established, the development of solid propellant rocket motors using that propellant for widely different thrusts and burning times t_B is a relatively straightforward, though often expensive, engineering development problem. Furthermore, if a solid propellant rocket motor application takes full cognizance of its characteristics and handling requirements, excellent rocket motor reliability should be obtained.

A solid propellant is a material which contains both a fuel and an oxidizer; the fuel and

oxidizer, however, do not react chemically below some fixed temperature, called the ignition temperature. When ignited, the solid propellant burns but does not require atmospheric oxygen for its ignition or combustion. A characteristic feature of a solid propellant is that the exothermic conversion of the solid phase to the gas phase, when conducted under appropriate conditions, does not produce explosions or detonations. The production of the propulsive gas proceeds at a controlled rate^{1,2}.

Since a solid propellant is a single phase containing both its fuel and oxidizer, it is also termed a *solid monopropellant* (see par. 1-6.4).

It is convenient to divide solid propellants into two principal types based on their physical structure:

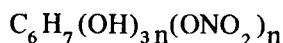
- (a) Homogeneous propellants which are solid solutions of organic substances containing the fuel and oxidizer elements in their chemical structure.
- (b) Heterogeneous propellants, also called composite propellants; these are mechanical mixtures of a combustible (the fuel) and a solid oxidizer.

7-2 HOMOGENEOUS PROPELLANTS

A homogeneous propellant, more commonly called a *double-base propellant* is a plastic solid monopropellant comprising three principal ingredients: a *polymer*, an *oxidizer-plasticizer*, and a *fuel plasticizer*².

7-2.1 POLYMERS FOR HOMOGENEOUS PROPELLANTS

The most widely used polymer is nitrocellulose (NC) but others can be and have been used. The common formula for nitrocellulose is



where $n = 1, 2, 3$ indicates the number of (ONO_2) groups corresponding to the completeness of the nitration of the cellulose.

Nitrocellulose is characterized by its nitrogen content and viscosity as independent variables. If the cellulose is completely nitrated, its nitrogen content is 14.15 percent². The higher the nitrogen content, the larger is the contribution of the nitrocellulose to the calorific value of the propellant.

7-2.2 OXIDIZER-PLASTICIZERS FOR HOMOGENEOUS PROPELLANTS

The oxidizer-plasticizer must be compatible physically with the polymer. Furthermore, it must add *fuel elements* to the solid propellant formulation. In this country, the most widely used oxidizer-plasticizer is nitroglycerin (NG); its chemical formula is



In Germany, probably because of the shortage of glycerin, propellants were developed that used diethylene glycol dinitrate, DEGN $(\text{NO}_2)(\text{OC}_2\text{H}_4)_2\text{ONO}_2$ instead of nitroglycerin as the oxidizer-plasticizer. The feasibility of using nitrocompounds other than nitroglycerin has been established².

Originally, only those propellants which contained nitroglycerin as a colloidal plasticizer for nitrocellulose were called *double-base propellants*, i.e., propellants containing two explosive ingredients (NC and NG). Today all

colloidal propellant systems of nitro-groups with NC are called double-base propellants.

7-2.3 FUEL-PLASTICIZERS FOR HOMOGENEOUS PROPELLANTS

The fuel-plasticizer must be compatible physically with the nitrocellulose. Because they contribute little or no oxidizing elements to the propellant formulation they tend to reduce the combustion temperature. Frequently, the fuel-type plasticizer is some form of plastic.

7-2.4 ADDITIVES TO DOUBLE-BASE PROPELLANTS

Both NC and NG tend to deteriorate in storage due to thermal decomposition. It is essential, therefore, that additives called *stabilizers* be incorporated in the propellant formulations. Common stabilizers are ethyl centralite, diphenylamine, and others (see Reference 2).

7-2.5 GENERAL CHARACTERISTICS AND APPLICATIONS OF DOUBLE-BASE SOLID PROPELLANTS

The ballistic properties of a double-base solid propellant are determined primarily by its calorific value. Its physical properties, however, are related to its polymer content. The best known double-base propellants are the *ballistites* (low nitrogen content) and the *cordites* (high nitrogen content).

Double-base propellants find their widest applications in weaponry; e.g., artillery and aircraft rockets, antitank missiles, surface-to-air missiles, ICBM's, etc. Table 7-1 presents data on three different double-base propellants.

Until a few years after World War II, double-base *propellant grains* were made by extrusion, which limited the size of the grain which could be fabricated. Since that time, a *castable* process has been developed which

TABLE 7-1
PROPERTIES OF DOUBLE-BASE PROPELLANTS*

	JPN	JP	RUSSIAN CORDITE
Weight, %			
Nitrocellulose	51.50	52.2	56.5
Nitroglycerin	43.00	43.0	28.0
Diethyl Phthalate	3.25	3.0	—
Ethyl Centralite	1.00	—	4.5
Other Additives	1.25	1.8	11.0
Manufacturing method	Extruded	Extruded	Extruded
Specific gravity	1.61	1.60	—
Safe storage temperature, °F	120	120	120
Storage stability	Good	—	—
Ignition temperature, °F	300	300	—
Firing temperature limits, °F	-20, +140	—	—
Lower pressure limit, psi	500	500	—
Smoke and toxicity	Smokeless	Smokeless	Smokeless
Specific impulse at 1000 psi, sec	230	230	—
Burning rate at 1000 psi and 70°F, in./sec	0.65	0.67	0.29
Pressure exponent n	0.69	0.71	0.80
Temperature coefficient Π_K , %/°F	0.7	0.9	0.7
Adiabatic flame temperature, °F	5300	5300	3750
Molecular weight of combustion gases	27.8	28	—
Composition of combustion gases at 1000 psi, mole %			
CO ₂	25.1	—	—
CO	26.0	—	—
H ₂ O	28.6	—	—
H ₂	5.0	—	—
N ₂	15.1	—	—
OH	0.5	—	—
Ratio of specific heats	1.21	1.22	—
Characteristic velocity c^* , fps	5000	5000	—
Approximate cost, \$/lb	5	5	—

*Taken from Reference 1.

makes it possible to manufacture cast double-base grains of any desired size and shape. The cast grains are homogeneous and can be case-bonded and may have the same range of compositions as the extruded propellants².

7-3 HETEROGENEOUS OR COMPOSITE PROPELLANTS

The development of composite propellants started during World War II with the development of aircraft JATO's (Jet Assisted Take-Off). The solid propellant used in a JATO unit was basically a mechanical mixture of an asphalt, the fuel, with finely powdered potassium perchlorate (KClO_4), the oxidizer. The asphalt was the *binder* for the KClO_4 .

Modern composite propellants have three principal ingredients: (1) a fuel which is an organic polymer, called the *binder*, (2) a finely powdered oxidizer, and (3) additives for catalyzing the combustion process, increasing the density, increasing the specific impulse, improving physical properties, increasing storage life, etc. After the ingredients have been thoroughly mixed, the resulting viscous fluid is poured—usually under a vacuum to eliminate voids—into the rocket chamber which contains a suitable mandrel for obtaining the desired grain configuration.

The propellant is then cured by polymerization—at a controlled temperature—to a firm, rubbery material; the polymerization is usually an exothermic process. Consequently, there is a shrinkage of the grain, which must be allowed for, when the propellant is cooled slowly from the curing temperature to the ambient temperature. There are new formulations which can be cured at room temperature, thereby eliminating the grain shrinkage phenomena.

The important characteristic of a solid propellant is its calorific value because that determines the combustion temperature and the

composition of the propulsive gas at the entrance cross-section of the rocket nozzle. From the chemical composition of the propellant, the combustion temperatures and the composition of the propulsive gas—for different combustion pressures—are determined by thermochemical calculations, usually conducted on a computer.

The ballistic properties of a composite propellant are determined by the weight fraction of oxidizer in the formulation. Its physical properties depend not only upon the binder material and its weight fraction, but also on the particle size and particle size distribution of the oxidizer.

7-3.1 BINDERS FOR COMPOSITE PROPELLANTS

Several organic materials have been investigated as possible binders (fuels). Those used in modern formulations are *elastomeric monomers*. Of the large number of organic binders which have been investigated, those listed in Table 7-2 have either received the most development effort or the widest application.

TABLE 7-2

BINDERS FOR COMPOSITE PROPELLANTS

Polysulfides

Polyurethanes

Butadiene Pyridine Copolymers

Butadiene Acrylic Acid Copolymers (PBAA)

Polyvinyl Chloride

Petrinacrylate

For a detailed discussion of the binders for composite propellants, see Reference 2.

All of the binders listed in Table 7-2 have been used in making castable propellants except the butadiene pyridine copolymers; these have been used for making molded propellants principally with ammonium nitrate (NH_4NO_3) as the oxidizer.

It is desirable that the binder contain a small amount of oxygen so that a close approach to the stoichiometric oxygen balance can be achieved without having such a large fraction of solid oxidizer that the propellant has either poor mechanical or rheological (plastic) properties.

7-3.2 OXIDIZERS FOR COMPOSITE PROPELLANTS

Only a few solid oxidizers are available for use in solid propellant formulations. Table 7-3 lists the oxidizers with which a substantial background of experience has been obtained, excepting lithium perchlorate (LiClO_4).

All perchlorate oxidizers produce hydrochloric acid (HCl) in the exhaust gas which

condenses into a fog on a moist day. The propulsive gas from a propellant based on KClO_4 is smoky because it contains condensed potassium chloride (KCl) which is a white powder. Practically all of the high performance castable composite propellants are based on using ammonium perchlorate as the oxidizer.

Composite propellants based on metallic nitrate oxidizers such as KNO_3 and sodium nitrate NaNO_3 produce smoky exhausts. Considerable effort has been expended on developing propellants based on NH_4NO_3 as the oxidizer, because of its abundance. Due to its small available oxygen content, 20 percent, and the effect of temperature on its crystalline structure, it is difficult to make a high performance castable propellant having good rheological properties with NH_4NO_3 as the oxidizer.

For detailed information on the oxidizers listed in Table 7-3, see Reference 2.

TABLE 7-3
OXIDIZERS FOR COMPOSITE PROPELLANTS

NAME	FORMULA	\bar{m}	DENSITY, lb/cu in.	% O_2 AVAILABLE
Ammonium Nitrate	NH_4NO_3	80.05	0.061	20.0
Ammonium Perchlorate	NH_4ClO_4	117.49	0.070	34.0
Potassium Nitrate	KNO_3	101.10	0.076	39.5
Potassium Perchlorate	KClO_4	138.55	0.090	46.5
Lithium Perchlorate	LiClO_4	106.40	0.087	60.0

7-3.3 ADDITIVES TO COMPOSITE PROPELLANTS

The energy content of a solid propellant can be increased by including certain light metals in the propellant formulation. Currently the most widely used light metal additive is aluminum in finely powdered form. The addition of the aluminum increases the combustion temperature T_c , and thus thereby the specific impulse $I_{sp} \propto \sqrt{T_c/\bar{m}}$ (see par. 6-3.7). In addition, it increases the propellant loading density δ_p (see par. 5-8.8). Another important advantage of adding powdered aluminum is that it is effective in suppressing high frequency combustion pressure oscillations^{1,2}.

Considerable research effort is being directed to investigating additives which will reduce the molecular weight of the propulsive gas without increasing the combustion temperature to unmanageable values.

The use of metal additives introduces problems. At high temperatures the aluminum incorporated in a solid propellant burns to the oxide AlO which is extremely active chemically. The

AlO reacts with the oxidizable structural materials which come in contact with it. Moreover, as the aluminum oxide cools it forms a higher oxide Al_2O_3 which condenses at 3800°F. Consequently, as the propulsive gas expands and cools, as it flows through the exhaust nozzle, condensed particles of Al_2O_3 impinge upon the nozzle walls, producing severe erosion of the walls. Furthermore, the Al_2O_3 particles exert drag upon the gas molecules surrounding them; therefore, since the particles pass through the nozzle rapidly, a considerable portion of the thermal energy of the particles is lost in the exhaust gases. Consequently, there is a significant reduction in the specific impulse compared to isentropic thermochemical predictions^{5,6,7}.

Table 7-4 presents some typical castable, composite propellant formulations³. It is important for such propellants that the binder-oxidizer slurry flow readily into the chamber or mold wherein it is to be cast and cured. The fluidity of the slurry depends upon the oxidizer/binder ratio, the particle size, and the particle size distribution of the oxidizer and any solid additives. The above consideration limits the useful oxidizer/ binder ratio.

TABLE 7-4
TYPICAL COMPOSITE PROPELLANT FORMULATIONS
(Taken from Reference 3)

INGREDIENT	POLYSULFIDE %	POLYURETHANE %	POLYBUTADIENE %
NH_4ClO_4	71.00	62.00	68.00
Binder	26.00	21.40	16.00
Catalysts	2.00	---	---
Additives	1.00	1.10	---
Aluminum	---	15.50	16.00

7-4 FACTORS GOVERNING THE SELECTION OF A SOLID PROPELLANT

The factors to be considered in judging the merit of a solid propellant for a given application are presented below^{1,2,3}.

7-4.1 SPECIFIC IMPULSE (I_{sp})

The specific impulse of the solid propellant should have the largest possible value because the ideal burnout velocity V_{bi} (see par. 5-9.3) is directly proportional to the I_{sp} .

For modern composite propellant formulations the basic ingredients are such that the combustion gases are compounds of the following elements: carbon (C), hydrogen (H), nitrogen (N), oxygen (O), and chlorine (Cl). For C-H-N-O-Cl systems the maximum obtainable specific impulses are in the range 240 to 250 sec. For a given composite propellant the specific impulse increases with the ratio of oxidizer to binder. There is a limit, however, to the quantity of oxidizer which can be incorporated into a given binder². Various light metals are added to both composite and double-base propellant formulations for increasing the specific impulse.

7-4.2 DENSITY OF PROPELLANT (ρ_p)

It is desirable that the density of the propellant be high, so that a large value can be achieved for the propellant loading density, $\delta_p = W_p/W_E$ (see para. 5-8.8). For most composite solid propellants² the propellant density ρ_p will range from approximately 1.65 to 1.70 g/cc.

→ 7-4.3 HYGROSCOPICITY

Most solid propellants have ingredients which are hygroscopic and it is necessary to protect such ingredients from moisture. The effect of moisture absorbed by a propellant is tantamount to adding the amount of that moisture to the propellant formulation. The

absorption of moisture can be prevented by hermetically sealing the rocket engine in its storage container. For a fuller discussion of hygroscopicity see Reference 2.

7-4.4 CONTROLLABLE LINEAR BURNING RATE (r_0)

It is desirable to have the capability of varying the linear burning rate r_0 over a wide range. Currently, solid propellant formulations have been developed having linear burning rates ranging from approximately 0.1 in./sec to approximately 4.0 in./sec. A wide range of available burning rates increases the design flexibility of solid propellant rocket motors. Also, it is desirable that the linear burning rate be rather insensitive to the small variations in combustion pressure and ambient pressure.

7-4.5 COEFFICIENT OF THERMAL EXPANSION

If a grain is to be case-bonded to the chamber, see Fig. 7-1, it is not usually feasible to match the thermal expansion coefficients of the chamber, the liner, and the propellant. It is essential, therefore, that the propellant grain be formulated so that it can withstand the stresses due to differential expansion.

7-4.6 THERMAL CONDUCTIVITY

Solid propellants are poor conductors of heat. For that reason it can be assumed without sensible error that the unburned portion of a propellant grain is at the initial temperature of the propellant prior to its ignition. Because of its low thermal conductivity, it takes several hours and even days to bring a large propellant grain to a uniform temperature following a change in its environmental temperature (see Reference 2).

7-4.7 CHEMICAL STABILITY

High chemical stability is desirable so that the solid propellant will have good aging characteristics, i.e., performance should not deteriorate with long time storage.

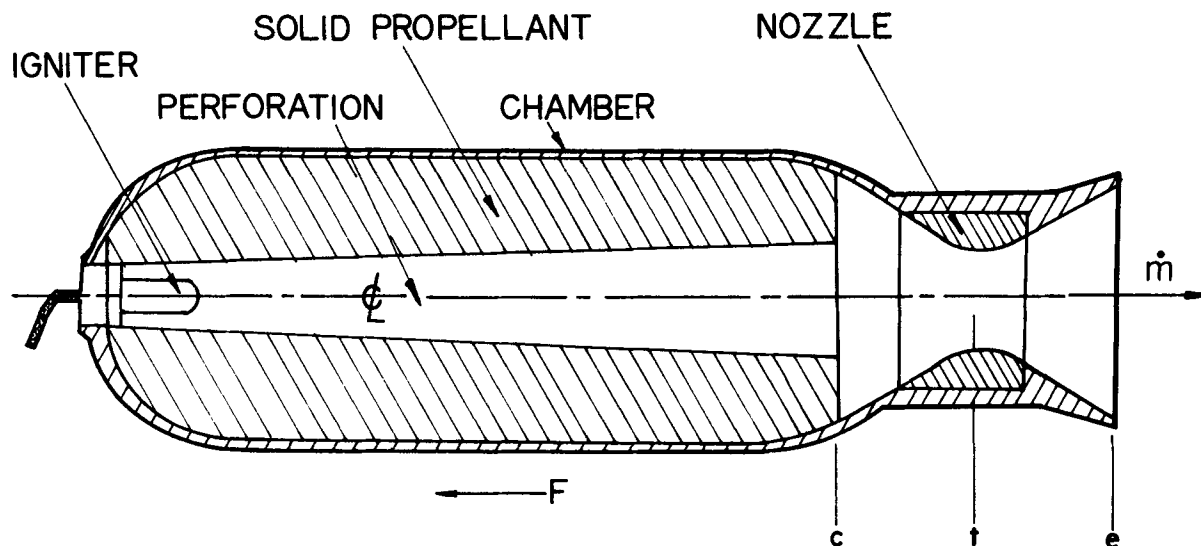


Figure 7-1. Case-Bonded Chamber

7-4.8 TOXICITY

It is desirable that the propellant be safe to handle and, in the case of Army weapons in particular, the propellant gas should be nontoxic and not linger around the launching site.

7-4.9 SHOCK SENSITIVITY

It is desirable that the propellant should not detonate due to either mechanical or thermal shock. Shock studies should be conducted on both composite and double-base propellants, particularly the latter since they contain ingredients which can be detonated by shock^{1 2}.

7-4.10 EXPLOSIVE HAZARD

The propellant should be safe to ship and handle by well-known more or less conventional procedures. Its ignition temperature should be relatively high and the propellant should not burn readily at low pressures. The propellant should, however, readily ignite when fired by the igniter.

7-4.11 SMOKE IN EXHAUST

For many applications smoke in the exhaust gases is highly undesirable because it leaves a *signature* detectable by the enemy. Formulations containing light metals are apt to give smoky exhausts.

7-4.12 ATTENUATION OF ELECTROMAGNETIC SIGNALS

For such missiles as ground-to-air missiles, it is important that good communications via electromagnetic waves be maintained between the ground station and the flying missile. In transmitting information from the ground control station to the flying missile, the propulsive gas jet may be in or near the path between the ground station antenna and the missile antenna. The ion content of the propulsive gas jet can cause severe attenuation of the electromagnetic waves and make communication with the missile difficult. Metallic additives in the solid propellant formulation can increase the communication and tracking difficulties. It appears that higher energy fuels aggravate the attenuation problem.

If possible the antenna on the missile should be located so that the gaseous exhaust jet from the rocket motor is not directly in the path between it and the ground antenna^{9,10,11}.

7-4.13 AVAILABILITY OF RAW MATERIALS

If the propellant will be used in large quantities during an emergency the raw materials from which the binder and oxidizer are made should be available in abundant quantities.

7-4.14 FABRICATION AND PROCESS CONTROL

The propellant should be compatible with the usual construction materials and should lend itself to process control methods for assuring product uniformity in all respects when produced in large quantities.

The propellant should have a low shrinkage during cure and its curing exotherm should be low. A low curing temperature enhances safety in the manufacturing process.

7-4.15 COST

It is desirable, of course, that the propellant be relatively inexpensive.

7-5 MECHANICAL PROPERTIES OF SOLID PROPELLANTS

The mechanical properties of a solid propellant refer to its stress-strain relationship, Poisson's ratio, and its resistance to rupture characteristics. It is essential that the propellant grain withstand the loads imposed upon it during storage under different ambient temperatures, shipping, handling, and firing. The actual loads, of course, will depend upon the application and design of the rocket engine. For many Army applications it is desirable that the solid propellant have good mechanical properties over the temperature range -60° to $+165^{\circ}\text{F}$, and be capable of withstanding temperature cycling between those temperatures.

In general a solid propellant grain is subject to three types of loads: (1) thermal loads due to temperature difference within the grain, (2) pressure loads due to the ignition and combustion processes, and (3) inertial loads due to its acceleration.

A solid propellant is not an elastic solid but a viscoelastic material, therefore, its stress-strain behavior is not elastic but depends upon the *rate of strain* and the type of load. Consequently, it is difficult to predict with accuracy the effect of different types of loads upon the stress-strain relationships of a solid propellant.

The JANAF Panel on Physical Properties of Solid Propellants in its publications describes standard tests for solid propellants. The results of such tests are significant only in that they compare the behavior of different propellants under the same test conditions. Whether or not the comparison is valid under actual operating conditions is open to question.

The results obtained by standard JANAF tests show that the results depend upon the *rate of loading*, and that the faster the rate of loading the stronger the propellant. In the actual operation of a rocket motor the rate of loading varies from slow rates due to temperature changes in storage, to very fast rates during the ignition period.

7-5.1 ULTIMATE TENSILE STRENGTH

A large ultimate tensile strength is important for propellant grains which are supported at the head end and are subject to appreciable accelerations. Otherwise, it is useful as an index of the adequacy of the quality control in manufacturing the propellant; uniform values of ultimate tensile strength are interpreted as uniformity in the manufacture of the propellant².

7-5.2 ELONGATION IN TENSION

In general, the propellant grain and the chamber (see Fig. 7-1) have different coefficients of thermal expansion. Consequently, a case-bonded grain must be capable of deforming to accommodate changes in dimensions of the chamber due to changes in environmental temperature. Otherwise, the case-bonded propellant would pull away from the chamber thereby exposing additional burning surface which could be disastrous. Although the requirements vary with different rocket motor designs, a minimum of 15 percent elongation at rupture in tension at low temperature is a typical requirement for large case-bonded propellant grains.

7-5.3 MODULUS IN TENSION

For case-bonded propellant grains it is desirable that the modulus in tension be relatively low, 300 to 600 psi, to avoid rupture of the adhesive bond or distorting the case when the rocket motor is cooled. The same test determines the tensile strength of the propellant, its elongation, and its modulus in tension².

7-5.4 STRESS RELAXATION

A case-bonded propellant grain, if it is not of the *cigarette-burning* type, contains an internal perforation, as illustrated in Fig. 7-1. The geometrical configuration of the perforation can be a cylinder, a star, a gear, or some other. In perforations where there are sharp turns, points, or grooves, stress concentrations are apt to occur. When the propellant grain is stressed by either pressure or thermal loads, cracks may occur at the sites of the stress concentrations. The effect of such cracks is to expose additional burning surface causing large unanticipated increases in the combustion pressure that may destroy the rocket motor.

It is advantageous, therefore, if the stresses due to distortion can be relaxed as the propellant grain accommodates itself to its new environment so that the residual stress does not cause cracking in the areas of stress concentration.

The relaxation under tension of a propellant is determined by measuring the tensile stress at fixed elongation as a function of time².

7-5.5 CREEP

It is essential that a propellant grain does not change its dimensions appreciably under its own weight. This requirement imposes a lower limit upon the modulus in tension. Such a deformation is termed *creep*. As pointed out in Reference 2, experience is still the best criterion for assessing the tendency of a propellant to creep.

7-5.6 COMPRESSIVE STRENGTH

Ordinarily the compressive strength of a propellant is of the same order of magnitude as its tensile strength; it is readily measured².

7-5.6.1 DEFORMATION AT RUPTURE IN COMPRESSION

The propellant should not be so brittle that its deformation under the gas pressure generated by firing the igniter will cause rupture. Usually, a minimum deformation of 30 percent at rupture is specified for a solid propellant².

7-5.6.2 MODULUS IN COMPRESSION

The deformation of the propellant grain under compressive loads must not cause

significant changes from its design geometry. This requirement imposes a lower limit on the modulus in compression.

7-5.7 SHEAR PROPERTIES

When a case-bonded grain attains its operating combustion pressure, the chamber to which it is bonded will stretch a small amount. Under accelerating conditions the weight of the

propellant grain must be supported by the shear strength of the bond between the propellant grain and the chamber.

7-5.8 BRITTLE TEMPERATURE

Plastic materials exhibit a so-called *brittle temperature* below which their mechanical properties decrease.

REFERENCES

1. M.J. Zucrow, *Aircraft and Missile Propulsion*, John Wiley and Sons, Inc., Vol. 2, 2nd Printing, Ch. 10.
2. AMCP 706-175, Engineering Design Handbook, Explosives Series, *Solid Propellants, Part One*.
3. R.D. Geckler and K. Klager, "Solid Propellant Rocket Engines", *Handbook of Astronautic Engineering*, McGraw-Hill Book Company, Inc., Edited by It. Koelle, Ch. 19, 1961.
4. J.I. Shafer, *Solid Rocket Propulsion Space Technology*, John Wiley and Sons, Inc., Edited by H.S. Seifert, Ch. 16, 1959.
5. R.F. Hoaglund, "Recent Advances in Gas-Particle Nozzle Flows", *ARS Journal*, Vol. 32, No. 5, May 1962, pp. 662-671.
6. J.D. Hoffman, *An Analysis of the Effects of Gas-Particle Mixtures on the Performance of Rocket Nozzles*, Report No. TM-63-1, Jet Propulsion Center, Purdue University, Jan. 1963.
7. J.D. Hoffman and S.A. Lorenc, "A Parametric Study of Gas-Particle Flows in Conical Nozzles", *AIAA Jour*, Vol., 3, No. 1, Jan. 1965.
8. G.P. Sutton, *Rocket Propulsion Elements*, John Wiley and Sons, Inc., 3rd Edition, 1963.
9. D.J. Povejsil, R.S. Raven and P. Waterman, "Airborne Radar", *Principles of Guided Missile Design*, Edited by G. Merrill, D. Van Nostrand Company, Inc., 1960, p. 230.
10. E.I. Capener, J.B. Chown, L.A. Dickenson and J.E. Nanevicz, "Studies on Ionization Phenomena Association with Solid Propellant Rockets", *AIAA Jour.*, Vol. 4, No. 8, August 1966, p. 1349.
11. D.E. Rosner, "Correlation of Radar Attenuation with Rocket Exhaust Temperature", *Jour. of Spacecraft*, July-August 1965, p. 601.
12. N.L. Coleburn, "Sensitivity of Composite and Double-Base Propellants to Shock Waves", *AIA Jour.*, Vol. 4, No. 3, March 1966, p. 521.
13. G.M. Dicken and J.H. Thatcher, "Shear-Strain Measurement in Solid-Propellant Rocket Motors", *Jour. of Spacecraft*, Vol. 2, No. 5, Sept.-Oct. 1965, p. 765.
14. R.D. Geckler, "Thermal Stresses in Solid Propellant Grains", *Jet Propulsion*, Vol. 26, No. 2, February 1956, p. 93.
15. D.D. Ordhal and M.L. Williams, "Preliminary Photoelastic Design Data for Stresses in Rocket Grains", *Jet Propulsion*, Vol. 27, No. 6, June 1957, p. 657.

CHAPTER 8

SOLID PROPELLANT ROCKET MOTORS

8-0 PRINCIPAL NOTATION FOR CHAPTER 8*

a	coefficient of pressure in the burning rate equation, $r = ap^n$	C_d	nozzle discharge coefficient
a_c	acoustic speed for propulsive gas at entrance section of the exhaust nozzle, fps	C_F	nozzle thrust coefficient = $F/P_c A_t$
a_i	moles of ith species of reactants	c_p	specific heat at constant pressure
A	cross-sectional area	c_v	specific heat at constant volume
A_b	area of burning surface for a solid propellant	C_w	weight flow coefficient = $\dot{w}_p/p_c A_t$
A_c	cross-sectional area of entrance section of nozzle	d_i	inner diameter of a tubular grain
A_{ch}	cross-sectional area of chamber enclosing the solid propellant	d_o	outer diameter of a tubular grain
A_G	cross-sectional area of solid propellant grain	F	thrust
A_m	maximum cross-sectional area	g_c	gravitational conversion factor = 32.174 slug-ft/lb-sec ²
A_p	port area for a solid propellant rocket motor	G	\dot{m}/A = flow density
A_t	area of nozzle throat	I	impulse
B	British thermal unit	I_{sp}	specific impulse, sec
c	effective exhaust velocity = Fg_c/\dot{m}_p	I_{tot}	total impulse, sec
c*	characteristic (exhaust) velocity = $P_c A_t g_c / \dot{m}_p$	J	mechanical equivalent of heat ≈ 778 ft-lb/B
		1/J	port-to-throat area ratio = A_p/A_t
		K_n	propellant area ratio = A_b/A_t
		L*	ratio of the chamber volume to the nozzle throat area
		m	mass

*Any consistent set of units may be employed; the units presented here are for the American Engineers System (see par. 1-7).

m_{bo}	mass at burnout; mass of motor, including unburned propellant, at completion of propellant burning	r_0	linear burning rate for $V_g = 0$ and T_0 held constant
\dot{m}	mass rate of flow	\bar{r}_b	average regression rate for burning surface of a solid propellant = $w/t_{b/p}$
\dot{m}_p	mass rate of flow of propulsive gas = mass rate of propellant consumption	t	time
m_m	motor gross mass; includes mass of propellant, liner, case, nozzle, and igniter (if attached)	t_0	zero time; application of firing voltage to the igniter squib
\bar{m}	molecular weight	t_{ap}	pressure action time; the time between the initial 10% maximum pressure level and the final 10% maximum pressure level
M	Mach number	$t_{b/p}$	100 psia burning time; the time between the initial 100 psia level and the web burnout point of maximum rate of change of curvature on the pressure-time record
n	pressure exponent in the linear burning rate equation (see Eq. 8-3)	t_{dp}	pressure delay time; the time between t_0 and the initial 10% maximum pressure level
p	static pressure in psia	t_{if}	thrust ignition interval; time between t_0 and the initial 75% maximum thrust level
P_c	static pressure at the entrance cross-section of the exhaust nozzle, the chamber pressure	T	temperature
P	static pressure in psf	T_p	propellant temperature
P_{amb}	ambient barometric pressure	T_0	motor firing temperature; temperature of the propellant and motor just before ignition and firing
P_c	chamber pressure in psf	T_c	chamber temperature
P_e	exit plane pressure; the static pressure in the flowing gas in the exit plane of the exhaust nozzle	T_t	temperature of gases in nozzle throat
P_{max}	maximum chamber pressure	T_e	exhaust gas static temperature at the exit plane of nozzle
P_{imax}	maximum ignition chamber pressure	w	web thickness
r	linear burning rate or regression rate of burning surface of a solid propellant		

\dot{w} weight rate of flow = \dot{m}/g_c

\dot{w}_p weight rate of propellant consumption = \dot{m}_p/g_c

GREEK LETTERS

α semiangle of diverging portion of exhaust nozzle

γ specific heat ratio = c_p/c_v

γ_p specific weight of propellant, lb/cu in.

ϵ nozzle expansion ratio = A_e/A_t

Π_K temperature sensitivity of pressure at a particular value of K_n

ρ density, slug/ft³

ρ_c density of gas at entrance section of exhaust nozzle

ρ_p density of propellant = γ_p/g_c

σ_p temperature sensitivity of propellant burning rate at a particular value of pressure

$$\sigma_p = \left(\frac{\partial \ln r}{\partial T} \right)_p$$

8-1 INTERNAL BALLISTICS OF SOLID PROPELLANT ROCKET MOTORS

The flight characteristics of a rocket-propelled vehicle depend (among other things) on the performance of the propellant. Important flight performance (ballistic)

properties are described in the paragraphs which follow^{1,13,14}

8-1.1 BURNING OF A SOLID PROPELLANT (PIOBERT'S LAW)

The combustion process for a solid propellant involves a series of chemical and physical processes that convert the solid propellant into a propulsive gas; the overall combustion process is *exothermic*. For a combustible material to be a satisfactory solid propellant, its burning characteristics must be such that the operating combustion pressure P_c is *self-regulating*, i.e., the design value for P_c is maintained solely by the mechanisms governing the combustion process.

A solid propellant, double-base or a composite, burns at the surface and as the burning proceeds the *burning surface* recedes in layers which are parallel to each other. In other words, the burning surface *recedes* into the solid propellant grain in the direction of its *negative*, or inwardly drawn, *normal* (see Fig. 8-1). The burning characteristic just described is known as Piobert's law⁶; the validity of Piobert's law has been confirmed by experience. Because a solid propellant grain burns in parallel layers, the general geometric configuration of the burning surface maintains itself until the web of the grain has burned through.

8-1.2 COMBUSTION TEMPERATURE

The propulsive gas formed by burning a solid propellant under pressure is in *thermodynamic equilibrium* at the prevailing *combustion temperature* T_c . The thermodynamic properties of the propulsive gas are determined by applying thermochemical calculations, as pointed out in par. 6-3. Significant deviations from thermochemical equilibrium may occur if any of the following conditions prevail during the combustion

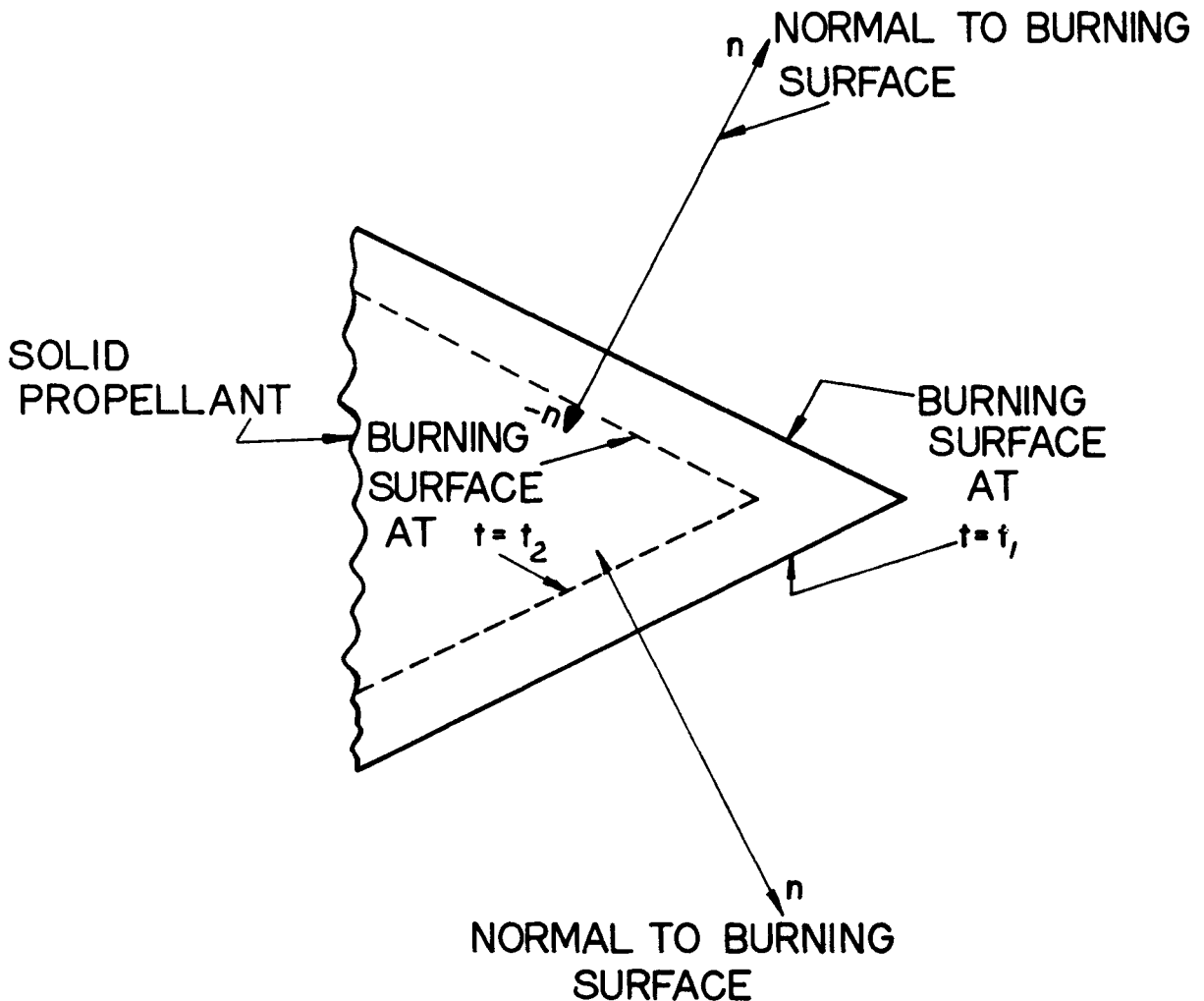


Figure 8-1. Piobert's Law of Burning

process: (1) very low pressures, (2) an atmosphere, different from the propellant combustion gas, that tends to quench the combustion reactions, and (3) when the *residence* or *stay time* for the chemical reactions of the gases inside the *combustion space*, also called the *free volume*, is too short for attaining chemical equilibrium.

8-1.3 GENERAL CHARACTERISTICS OF THE COMBUSTION PROCESS

Since the burning of a solid propellant is in accordance with *Piobert's law*, the burning

process may be assumed to be *one-dimensional* along the negative (inward) normal to the burning surface (see par. 8-1.1). All double-base and composite solid propellants have low thermal conductivities (see par. 7-4.6). Consequently, of the heat liberated at the burning surface only a small portion is conducted a short distance into the propellant grain immediately behind the burning surface. It is in this *subsurface zone* that the chemical reactions for the combustion process are initiated. Artificial means can, of course, be employed for conducting heat to regions behind the subsurface

zone, for example, it is possible to incorporate metal wires or staples in the propellant grain with the object of increasing the *burning rate*.

Because of the chemical reactions in the subsurface zone the local temperature of the propellant is increased, so that liquefaction may occur in the case of some propellants or the propellant may be *decomposed* into volatile reactive fragments at the burning surface. The products of the decomposition of the propellant react in the gas phase and are ultimately converted into the propulsive gas arriving at the entrance cross-section A_c of the exhaust nozzle.

The actual combustion process for a solid propellant is extremely complex and has been the subject of many investigations. Despite its complexity some rather simple concepts have been established that are helpful in giving an insight into the characteristics of the combustion of a solid propellant^{2,6,7,8}.

8-1.4 COMBUSTION CHARACTERISTICS OF DOUBLE-BASE SOLID PROPELLANTS

Observations of the combustion characteristics of double-base propellants have been conducted for many years. They indicate that when a double-base solid propellant burns at the usual combustion pressures employed in rocket motors, the *gas-phase reaction zone* has a definite but complicated structure. Because a double-base propellant is a homogeneous propellant it may be assumed that the gas-phase reaction zone is likewise homogeneous in every plane parallel to the burning surface.

Several theories have been proposed for explaining the combustion of a double-base propellant. Fig. 8-2 illustrates schematically the combustion scheme employed in most of those theories. In general, the theories assume the following:

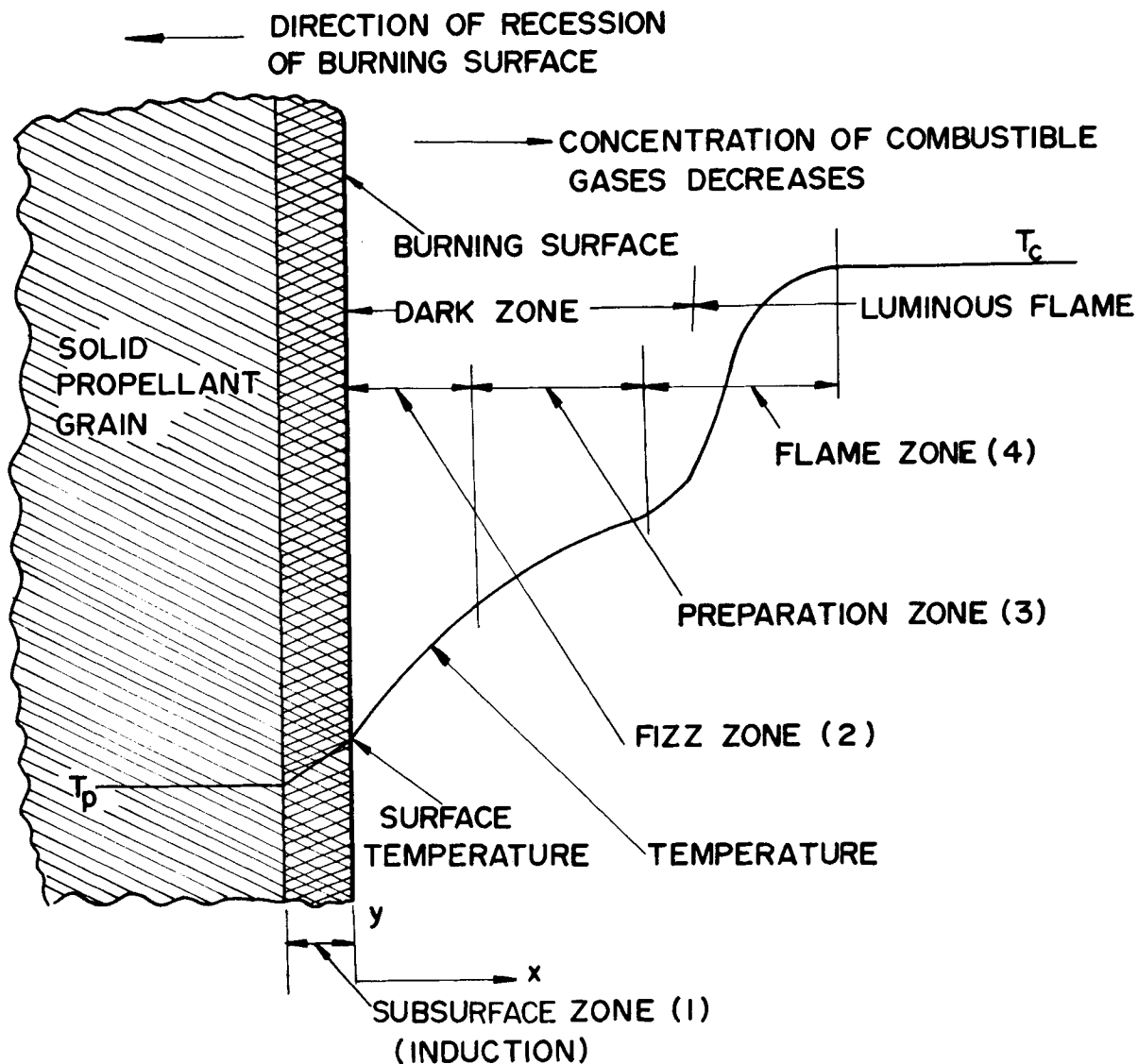
- (a) All of the heat is evolved in the *fizz* and *flame zones* (see Fig. 8-2); the fizz

zone is very thin; it extends only a few hundredths of a centimeter beyond the burning surface.

- (b) The temperature of the products at the end of the *preparation zone* is higher than at the end of the fizz zone.
- (c) The increased temperature of the products is attributed to heat conducted back from the *flame zone* into the preparation zone.
- (d) It is in the flame zone that the *final* chemical reaction occurs; the heat liberated by that chemical reaction raises the temperature of the combustion gases to the final (*isobaric*) combustion temperature, denoted by T_c .
- (e) The reactants formed at the burning surface *diffuse outward* from that surface toward the flame zone. Consequently, the *concentration* of combustible gases decreases as they proceed from the fizz zone through the flame zone.

The propellant layers in the *subsurface zone* (see par. 8-1.3) are heated by thermal conduction from the hot burning surface of the propellant grain. The resulting temperature rise initiates the decomposition of the nitroglycerin and nitrocellulose immediately behind the burning surface. The temperature of the burning surface, termed the *surface temperature*, is difficult to either define or to measure. There is, however, a steep temperature gradient in the subsurface zone.

The exact location of the burning surface is also difficult to determine because of liquefaction and foaming phenomena. Nevertheless, because of the great utility of the *concept* of a surface temperature in studying the combustion process, at least an approximate value must be



NOTES:

1. PROPERTIES ARE CONSTANT ON ANY PLANE PARALLEL TO y-AXIS.
2. AT SURFACE PROPELLANT IS COMPLETELY DECOMPOSED INTO VOLATILE PRODUCTS WHICH REACT FURTHER IN THE GAS PHASE.
3. FIZZ ZONE IS A FEW HUNDREDTHS OF A CENTIMETER THICK AND IS NON - LUMINOUS .

Figure 8-2. Combustion Schematic for a Double-Base Solid Propellant

established for the temperature in the vicinity of the burning surface. Although there is no completely satisfactory method for predicting or measuring the surface temperature, it appears probable that the surface temperature of a double-base solid propellant burning at a moderate pressure is approximately 300°C (Ref. 2).

8-1.5 THE FLAME REACTION ZONE FOR A DOUBLE-BASE SOLID PROPELLANT

If an end-burning strand of a double-base solid propellant is burned in an inert atmosphere, at pressures less than 200 psia, the *flame is nonluminous*. As the inert gas pressure is raised a luminous flame region appears at some distance in front of the burning surface. Further increases in the inert gas pressure cause the luminous flame to approach the burning surface and reduce the thickness of the dark region. When the inert gas pressure is approximately 1000 psia, it becomes difficult to detect the dark region between the burning surface and the luminous flame. It is estimated that the heat produced by the dark region is less than one-half of that produced by the complete reaction, including that in the luminous flame zone.

8-1.6 COMBUSTION CHARACTERISTICS OF COMPOSITE (NONHOMOGENEOUS) SOLID PROPELLANTS

Upon ignition, the binder (fuel) and the solid oxidizer particles exposed on the burning surface of the composite solid propellant grain decompose (pyrolyze) separately and recede at slightly different rates. In a few milliseconds, however, a quasi-steady state is attained. Because of the difference in the recession rates of the binder and oxidizer, the surface of the propellant is rough and dry. The gaseous decomposition products are mixed by molecular diffusion, and the ensuing chemical reactions complete themselves within a thin *flame zone* extending approximately 0.1 mm from the burning surface. If the propellant contains metallic additives

in its formulation, it appears that the vaporized metal also burns in that flame zone. The combustion process is sustained by heat being transferred from the flame zone back to the propellant burning surface that maintains the induction and decomposition processes.

Fig. 8-3 illustrates schematically a combustion model frequently employed in studying the combustion of composite solid propellants.

Heat is transferred to Regions I and II, from Regions III to VI, primarily by conduction, but radiation may also be important. Under normal operation a uniform burning rate is obtained.

8-1.7 LINEAR BURNING RATE (SAINT-ROBERT'S LAW)

The rate at which the burning surface of a solid propellant recedes normal to itself is termed the *linear burning rate*, and is denoted by r ; it is usually measured in in. per sec and its dimension (L/T) is that of velocity. The linear burning rate is a characteristic property of a given solid propellant. For constant values of the propellant temperature T_0 and the *combustion or chamber pressure* P_c the linear burning rate is independent of the dimensions and geometric configuration of the solid propellant grain. *By definition*, the propellant temperature T_0 , also called the motor *firing temperature*, is the temperature of the propellant and motor chamber just before ignition and firing⁹.

If the propellant grain is designed so that it can burn in only one direction, it is termed a *restricted-burning grain*. A propellant grain which can burn simultaneously on all of its surfaces is called an *unrestricted-burning grain*.

For a given propellant, the linear burning rate is a function of the combustion pressure P_c , the propellant temperature T_0 , the velocity of the propellant gas parallel to the burning surface V_g (for an end-burning grain $V_g = 0$), and the

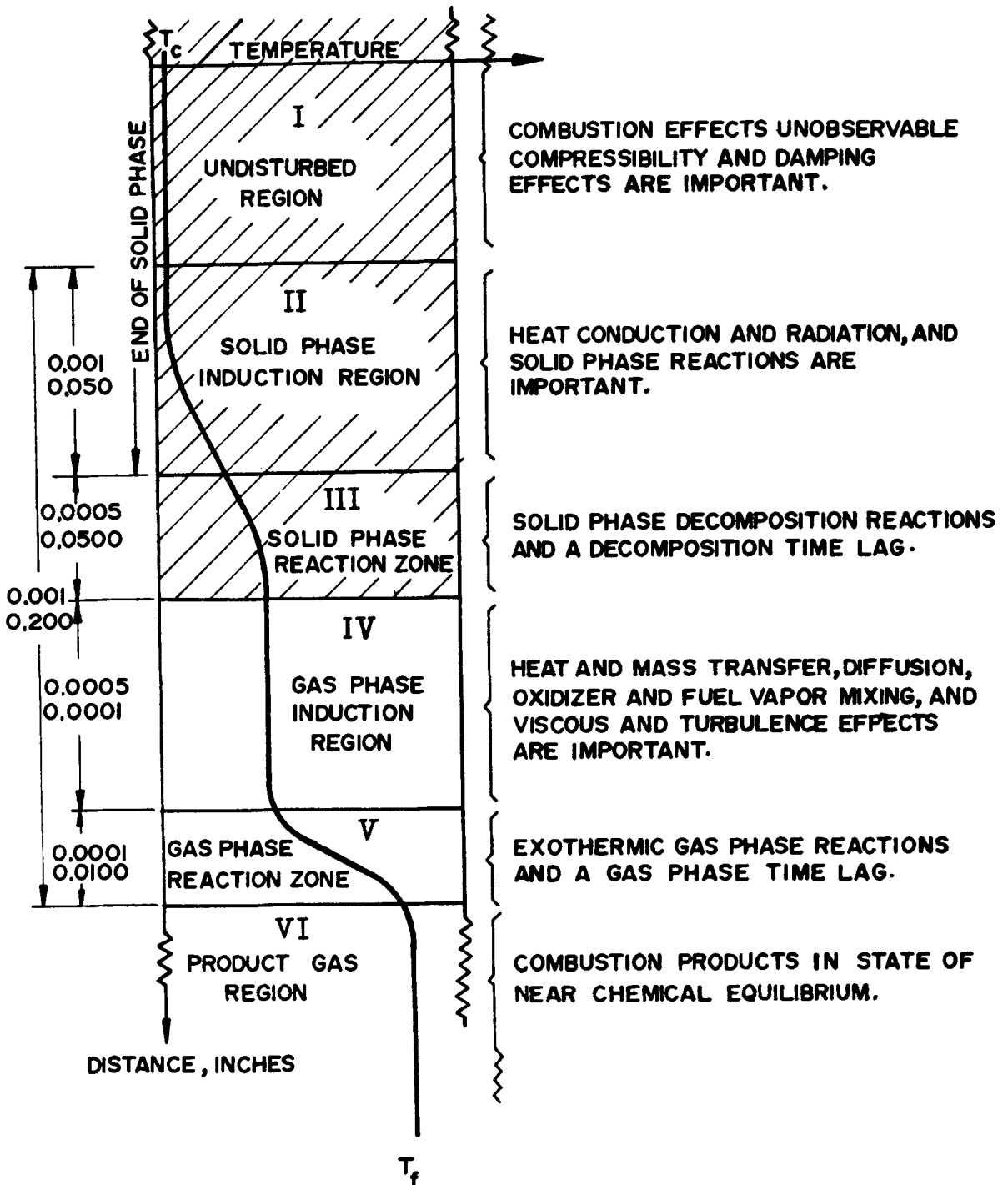


Figure 8-3. Combustion Schematic for a Composite Solid Propellant

elapsed time t after the grain is ignited. It has been pointed out, however, that the burning rate of a combustible material must be independent of the time t if it is to be a satisfactory solid propellant. Hence, one may write, in general, for a solid propellant

$$r = F(p_c, T_0, V_g) \quad (\text{in./sec}) \quad (8-1)$$

where p_c is the combustion pressure in psia.

The effect of the velocity V_g of the propellant gases past the surface of a given propellant is a secondary effect which causes *erosive burning*, this effect is discussed in par. 8-1.14. Because the instantaneous linear burning rate r cannot be determined, it is not possible to measure the instantaneous effect of V_g upon the value of r . In view of the foregoing, the experiments for determining the linear burning rate of a solid propellant are conducted under conditions where $V_g = 0$. The linear burning rate with $V_g = 0$ is denoted by r_0 . Hence

$$r_0 = F(p_c, T_0) \quad (8-2)$$

where $r_0 = r =$ linear burning rate when $V_g = 0$.

The form of the functional relationship expressed by Eq. 8-2 is determined experimentally; in the experiments T_0 is held constant. The results of such experiments indicated that

$$r_0 = ap_c^n \quad (8-3)$$

where a and n are termed the *pressure coefficient* and *pressure exponent* (or *index*), respectively.

Eq. 8-3 is known as *Saint-Robert's law*, and in applying that law it is assumed that the coefficient a depends on T_0 and is independent of p_c while the pressure exponent n is independent of both T_0 and p_c . For the different solid propellants the value of the pressure exponent varies from approximately 0.1 to 0.85. There are some double-base propellant

formulations, termed *mesa* propellants, for which $n = 0$ and n may even be negative, for a usable pressure range.

The burning rates of modern solid propellants can be varied over a wide range from less than 0.1 in./sec to more than 4.0 in./sec. For a large solid propellant rocket motor developing several hundreds of thousands of pounds of thrust a low burning rate with a small pressure exponent is desirable. For several Army weapons, such as antimissile missiles, a fast burning rate is highly desirable.

8-1.8 WEIGHT RATE OF PROPELLANT CONSUMPTION (\dot{w}_p)

From Eq. 5-6 it follows that

$$\dot{w}_p = C_w p_c A_t \quad (\text{lb/sec}) \quad (8-4)$$

In terms of the linear burning rate r_0

$$\dot{w}_p = r_0 A_b \gamma_p \quad (8-5)$$

where

A_t = area of the nozzle throat, sq in.

A_b = area of burning surface for the solid propellant, sq in.

γ_p = specific weight of the solid propellant, lb/cu in.

Fig. 8-4 presents r_0 , at $T_0 = 60^\circ\text{F}$, for several composite propellants made by compounding the same binder (fuel) with different amounts and kinds of inorganic oxidizers.

8-1.9 VOLUMETRIC RATE OF PROPELLANT CONSUMPTION (\dot{Q}_p)

Let V_{ch} denote the internal volume of the rocket motor chamber before the propellant grain is inserted therein, and V_p the volume of the propellant grain. By definition

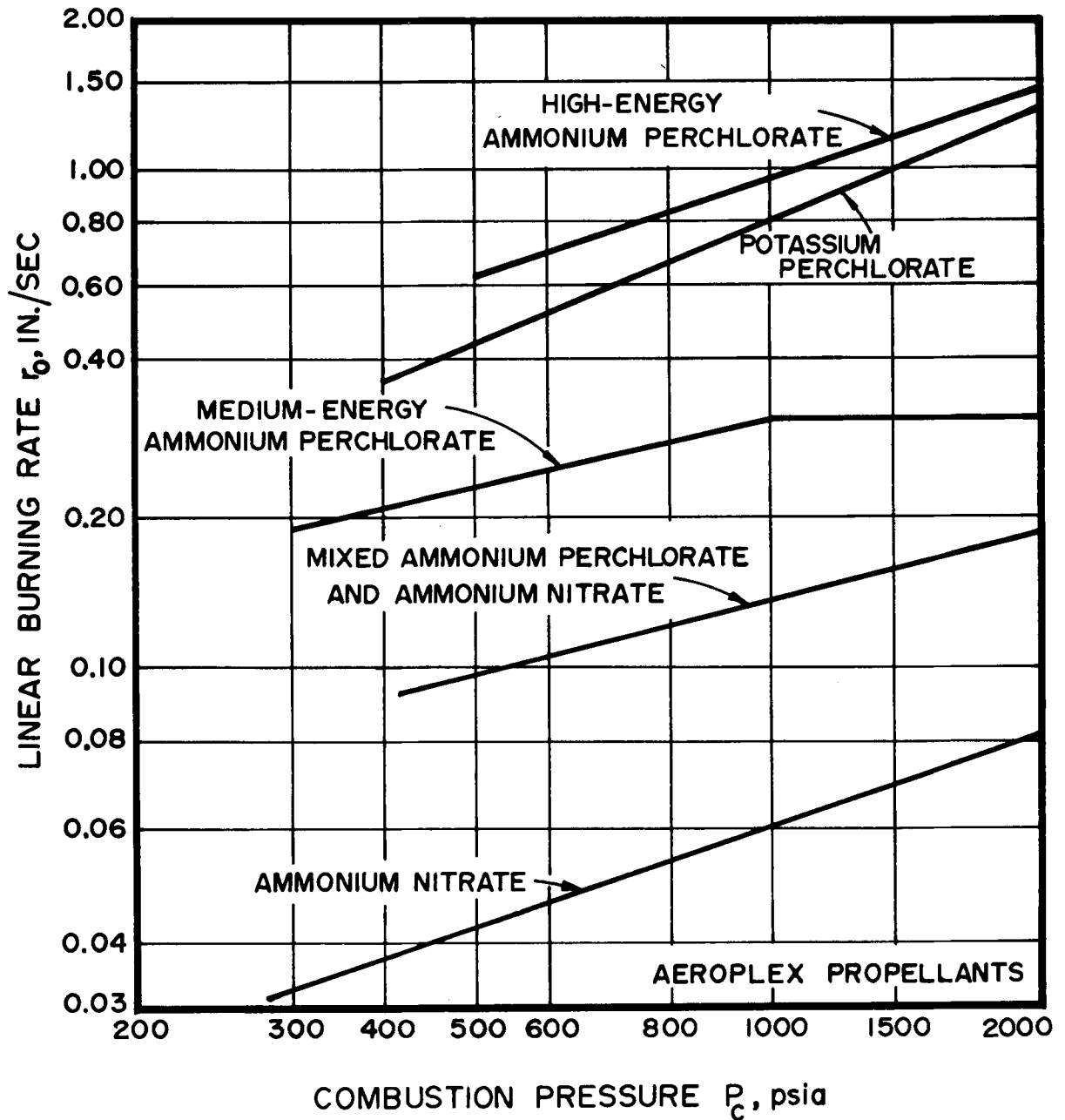


Figure 8-4. Linear Burning Rate r_0 (at 60°F) for Several Composite Propellants Made With the Same Binder Fuel and Different Kinds and Amounts of Inorganic Oxidizers

$$V_f = V_{ch} - V_p = \text{the free volume} \quad (8-6)$$

As the propellant burns, the combustion gas flows into the free volume V_f . Simultaneously, V_p decreases and V_f increases. The volumetric rate of propellant consumption, denoted by \dot{Q}_p , is accordingly

$$\dot{Q}_p = \dot{V}_f = r_0 A_b \quad (8-7)$$

8-1.10 EQUILIBRIUM COMBUSTION PRESSURE AND ITS STABILITY

When a solid propellant burns, the law of the conservation of matter yields¹

$$\begin{bmatrix} \text{mass rate} \\ \text{of} \\ \text{propellant} \\ \text{consumption} \end{bmatrix} = \begin{bmatrix} \text{mass rate} \\ \text{of} \\ \text{increase of} \\ \text{gas occupying} \\ \text{the free volume} \end{bmatrix} + \begin{bmatrix} \text{mass rate} \\ \text{of} \\ \text{flow of gas} \\ \text{through ex-} \\ \text{haust nozzle} \end{bmatrix} \quad (8-8)$$

By applying Eq. 8-8 it is found that if the pressure exponent n for a solid propellant is less than unity, then the equilibrium pressure for steady state operation is inherently self-regulating as far as small perturbations of the burning rate are concerned¹. The larger the value of n , the more sensitive is the combustion pressure p_c to minor irregularities in the combustion process. Such irregularities may arise from slight variations in the homogeneity of the propellant grain and small variations in the area of the burning surface due to small fissures or cracks in the grain, etc. Since $n < 1$ for the solid propellants used in rocket motors, the equilibrium combustion pressure is stable.

8-1.11 EFFECT OF PROPELLANT AREA RATIO (K_n)

When a solid propellant burns under steady-state conditions, the combustion pressure p_c equals the equilibrium combustion pressure¹. Let

$$K_n = \frac{A_b}{A_t} = \text{the propellant area ratio} \quad (8-9)$$

where A_b is the area of the burning surface.

The combustion pressure can be expressed in terms of K_n , the weight flow coefficient C_w , $\Delta\gamma_{pg}$, and the pressure coefficient a . Thus

$$p_c = p_{cE} \left[\frac{a K_n \Delta\gamma_{pg}}{C_w} \right]^{\frac{1}{1-n}} \quad (8-10)$$

where

$$\Delta\gamma_{pg} = \gamma_p - \gamma_g \quad (8-11)$$

γ_p = specific weight of the propellant, lb/cu in.

γ_g = specific weight of the combustion gas, lb/cu in.

p_{cE} = equilibrium combustion pressure, psia

Eq. 8-11 shows that the propellant area ratio K_n exerts a predominant influence upon the combustion pressure p_c . Since n is less than unity, the exponent $1/(1-n)$ is always larger than unity. Consequently, an increase in K_n from any cause results in a much larger increase in p_c . It is important, therefore, that the value of K_n be held within close limits if the design value for p_c is to be realized.

Because of the strong dependence of p_c upon K_n it is important that the propellant grain be free of cracks, fissures, and porous material. Also the propellant grain should not become

separated from the materials employed for inhibiting it from burning.

For a fixed value of propellant temperature experiments demonstrate that the propellant area ratio K_n and the combustion pressure p_c can be related by¹

$$K_n = b p_c^m \quad (8-12)$$

In Eq. 8-12 it is generally assumed that the coefficient b varies with T_0 , the propellant temperature, and the exponent m is independent of T_0 .

8-1.12 STABILITY OF THE SHAPE OF THE BURNING SURFACE

Because the linear burning rate of a solid propellant is substantially the same at all points in the burning surface and also because the combustion pressure is uniform over that surface, the burning surfaces recede parallel to themselves. As a result the geometry of the burning surface does not change during the combustion process.

8-1.13 PRESSURE DEFLAGRATION LIMIT AND PRESSURE LIMIT

For practically every solid propellant there is a minimum combustion pressure, termed the *pressure deflagration limit*, below which the burning of the propellant is erratic. Depending upon the propellant formulation, the pressure deflagration limit ranges from 100 to 500 psia, approximately.

Experiments indicate that if the combustion pressure of a solid propellant is raised to higher and higher values, a combustion pressure may be eventually attained where only a small increase in the propellant area ratio K_n causes the propellant to burn in a more or less uncontrollable manner. The aforementioned limiting combustion pressure is termed the *pressure limit*.

8-1.14 EFFECT OF THE TEMPERATURE OF A SOLID PROPELLANT

The temperature of a solid propellant affects its physical characteristics and behavior, and also its linear burning rate. It is important, therefore, to have a knowledge of the effect of temperature over the anticipated range to be expected in the application of the solid propellant rocket motor.

8-1.14.1 GENERAL EFFECTS OF TEMPERATURE

At low propellant temperatures the elastic properties of practically all solid propellants become poor, and in some cases the grain may become so brittle that it may crack when subjected to either shock or temperature cycling. Differences in the thermal expansion of the motor case, the liner of a case-bonded grain, and of the propellant may cause the grain to crack. When the flame reaches the crack, there is a large increase in the burning surface with a corresponding increase in K_n . As a result the combustion pressure may reach prohibitive values.

Certain propellants become more difficult to ignite as the propellant temperature is lowered, thereby increasing the ignition delay (time elapsed between firing the igniter and complete ignition of the burning surface).

At high propellant temperatures above 140°F many solid propellants tend to soften and become plastic. They may not be able to withstand the sudden pressure application during ignition without appreciable deformation of the grain.

Some propellants are subject to cold flow or slump when stored at the higher ambient temperatures, changing the configuration of the grain and hence the performance of the rocket motor.

Because of the influence of the propellant temperature upon the physical characteristics of a solid propellant, it is important that serious attention be given to the recommendations for storing, handling, and shipping solid propellant rocket motors.

8-1.14.2 TEMPERATURE SENSITIVITY

The linear burning rate for a given propellant burning in a rocket motor having a fixed value of K_n is affected by the propellant temperature T_0 . In general r_0 increases if T_0 is increased and vice versa. The effect of T_0 on r_0 for a given solid propellant is termed its *temperature sensitivity*^{1,16}

It is customary to express the temperature sensitivity of the ballistic parameters (r_0 , p_c , F), in percent change per degree Fahrenheit from their values at some standard firing temperature $T_0 = T_{std}$ (usually $T_{std} = 60^\circ\text{F}$), under a constant condition of K_n . When $T_0 > T_{std}$, the parameters have values larger than those corresponding to $T_0 = T_{std}$, and vice versa.

Thus the temperature sensitivity coefficient for the linear burning rate, denoted by Π_{r_0} is defined by

$$\Pi_{r_0} = \frac{1}{r_0} \left[\frac{\partial r_0}{\partial T_0} \right] K_n \quad (8-13)$$

where $(\partial r_0 / \partial T_0) K_n$ is the rate of change for the linear burning rate with temperature for a constant value of K_n .

For thrust F and combustion pressure p_c , one can write

$$\Pi_F = \frac{1}{F} \left[\frac{\partial F}{\partial T_0} \right] K_n = \begin{array}{l} \text{thrust} \\ \text{temperature} \\ \text{sensitivity} \\ \text{coefficient} \end{array} \quad (8-14)$$

and

$$\Pi_{p_c} = \frac{1}{p_c} \left[\frac{\partial p_c}{\partial T_0} \right] K_n = \begin{array}{l} \text{combustion pressure} \\ \text{temperature} \\ \text{sensitivity} \\ \text{coefficient} \end{array} \quad (8-15)$$

The temperature sensitivity of a solid propellant is an undesirable property. In those applications where the rocket-propelled vehicle can be stored under controlled temperature conditions, as in the case of ABM's and ICBM's, no problems are introduced by temperature sensitivity. It can cause serious problems in systems which must operate over a wide temperature range (-40° to $+160^\circ\text{F}$). Consequently, the effect of the temperature sensitivity upon the performance of a rocket-propelled vehicle must be studied and means for overcoming its adverse effect incorporated in the system design.

For some applications the cold weather problems introduced by the temperature sensitivity of the propellant can be circumvented by employing heating blankets for keeping the solid propellant at a specified temperature.

Many additives to the solid propellant formulation for either reducing or eliminating its temperature sensitivity have been investigated, but no satisfactory solution of the problem has been achieved. Because it is highly desirable to have some method for controlling the temperature sensitivity of solid propellants, research for attaining that objective should receive strong support.

8-1.15 EROSION BURNING

The velocity of combustion gases parallel to the burning surface has an effect upon the linear burning rate called erosive burning. Although the exact mechanism whereby the burning rate increases as the combustion gas velocity is increased is only incompletely understood, its

occurrence has been observed. Since erosive burning increases with increased gas velocity, the effect is more pronounced in a restricted flow cross-section such as the nozzle end of an internal-burning case-bonded grain during the initial phases of combustion. Erosive burning is evidenced by peaks in the combustion pressure during the early phase of the combustion of the propellant grain^{1,10,11,12,13,14,15}

No completely satisfactory relationship has been developed for correlating data on the erosive burning of solid propellants. It is customary, however, to express the erosive burning of a solid propellant in terms of the erosion ratio ϵ as a function of the gas velocity V_g , where

$$\epsilon = r/r_0 \quad (8-16)$$

and r is the linear burning rate with erosive burning.

From the limited data available it appears that ϵ increases with the gas velocity V_g when the latter is above some minimum value. Furthermore, it appears that ϵ is larger for the slower-burning propellants, and is independent of T_p . More research is required to obtain a better understanding of, and more reliable data on, erosive burning. When it becomes available this lacking information will be of great value to the designers and developers of solid propellant grains.

8-2 COMBUSTION PRESSURE OSCILLATIONS IN SOLID PROPELLANT ROCKET MOTORS (UNSTABLE BURNING)

Under certain operating conditions the combustion pressure, and hence the thrust, of a solid propellant rocket motor equipped with an internal-burning grain may increase practically instantaneously to several times its design value for no apparent reason. Experiments indicate that the phenomenon is always accompanied by

dangerous, large-amplitude, high frequency oscillations in the combustion pressure. The aforementioned type of burning has been termed combustion pressure oscillations, resonant burning, sonant burning, unstable combustion, combustion instability, and others; it has been a subject of study since World War II^{16,27}. Consequently, a voluminous literature pertinent to combustion pressure oscillations in solid propellant rocket motors has been developed, and References 16 to 34 inclusive are illustrative of the types of investigations which have been and are being conducted.

8-2.1 TERMINOLOGY EMPLOYED IN UNSTABLE BURNING OF SOLID PROPELLANT ROCKET MOTORS

In general, *unstable burning* in a solid propellant rocket motor is characterized by undesirable irregularities in the combustion pressure and in the linear burning rate. Fig. 8-5 presents the terminology pertinent to the different types of burning that have been observed together with brief descriptions of the principal phenomena associated with the principal types of unstable burning. Although both low and high frequency combustion pressure oscillations have been observed the discussion will be restricted to high frequency oscillations, generally termed *acoustic instability*, because they are the most damaging. The frequencies of such oscillations correspond to one or more of the acoustical modes pertinent to the geometry of the cavity wherein the combustion occurs, hence the term *resonant burning*.

8-2.2 ACOUSTIC INSTABILITY IN SOLID PROPELLANT ROCKET MOTORS

Fig. 8-6 illustrates the pressure-time curves for the different types of burning noted in the figure. Table 8-1 summarizes the harmful effect due to oscillatory burning in a solid propellant rocket motor.

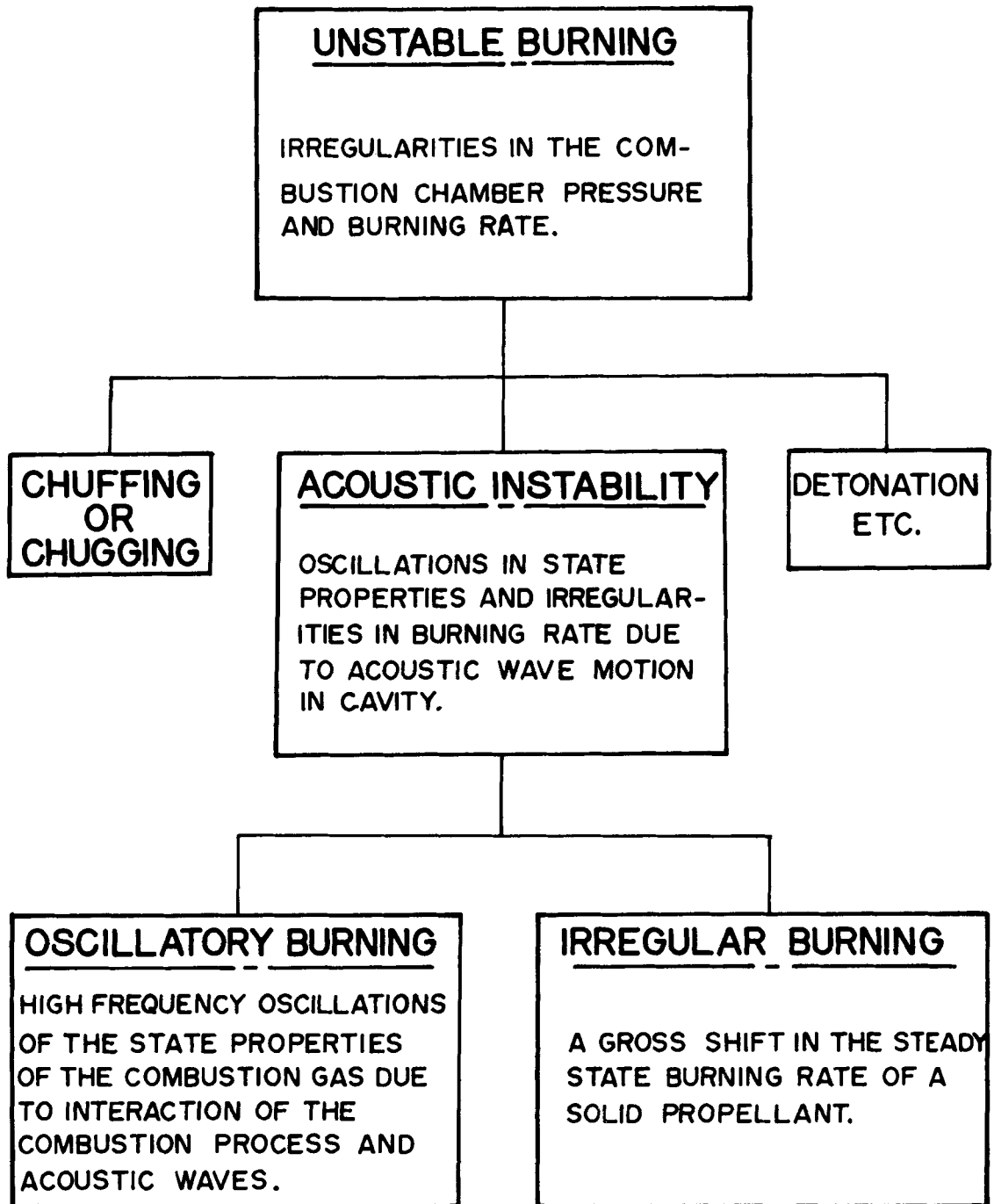


Figure 8-5. Terminology and Phenomena Associated With Unstable Burning in Solid Propellant Rocket Motors

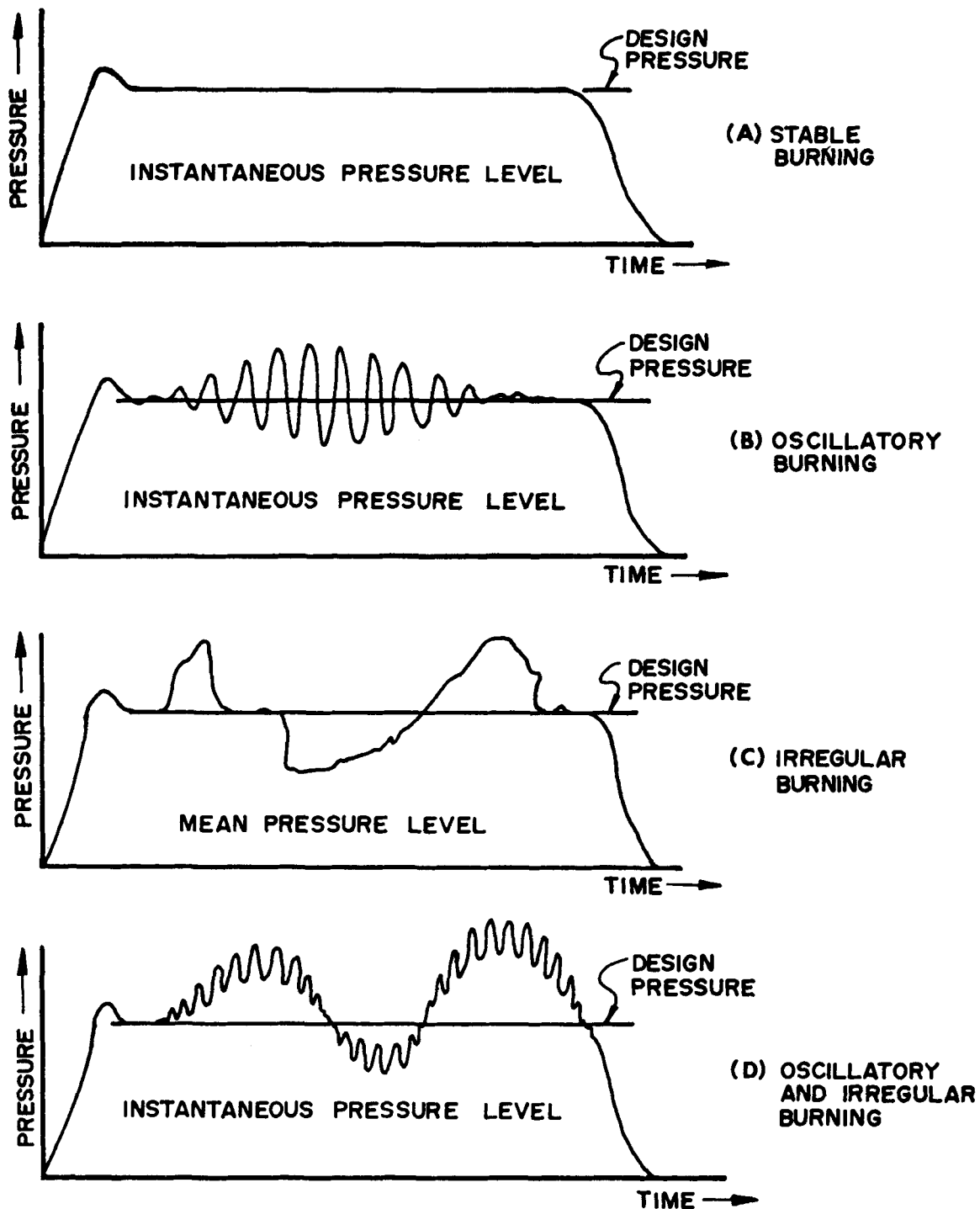


Figure 8-6. Types of Burning Observed in Solid Propellant Rocket Motors

TABLE 8-1

**SOME EFFECTS DUE TO ACOUSTIC
INSTABILITY IN A SOLID
PROPELLANT ROCKET MOTOR**

- (1) Initiation of irregular burning.
- (2) Several-fold increase in the normal heat transfer rates.
- (3) Vibrations of the vehicle structure and, unless they are vibration isolated, the components of guidance, electronics, and other subsystems.
- (4) Fatigue failure of the metal components of the rocket motor and vehicle structure.
- (5) Changes in the physical and chemical properties of the propellant due to oscillations in the heat transfer rates and vibrations.
- (6) Variations in specific impulse due to incomplete combustion.
- (7) Overexpansion or underexpansion of the propellant gas due to oscillations in the combustion pressure, thus affecting the flight program of the vehicle.

It is evident from Table 8-1 that for the satisfactory operation of a vehicle propelled by a solid propellant rocket motor, oscillatory burning and irregular burning of the solid propellant should be avoided.

Oscillatory burning has been observed at almost any time during the burning of a solid propellant grain. It has occurred almost immediately after the onset of burning, and continued through the duration of burning, or

ceased at some time during the burning process. Obviously, no generalizations can be drawn regarding when in the burning period oscillatory burning may occur.

Experimental observations indicate that oscillatory burning "triggers" irregular burning. Consequently, an understanding of the factors causing oscillatory burning and the development of means for either avoiding or suppressing it should be helpful in preventing the occurrence of irregular burning. Because of our ignorance of the precise effects and the relative importance of the different pertinent physical and chemical parameters, the current methods for suppressing oscillatory burning are of necessity based on experience combined with "cut-and-try" experiments on full-scale rocket motors. Although the solutions obtained in that manner are expensive and very time consuming, that method of solution will remain the only sound approach until the much needed information that is lacking has been obtained from well-planned experimental investigations. Without such information for guidance, it is less than realistic to expect a solution to the oscillatory burning problem by mathematical reasoning alone. Moreover, with the increasing application of larger and larger thrust solid rocket engines to the solution of propulsion problems it is essential that strong support be given to research concerned with obtaining a better understanding of the cause and effect processes leading to acoustic instability.

Table 8-2 presents some general conclusions which can be derived from the experimental programs concerned with acoustic instability^{1 7}.

Table 8-3 summarizes the principal methods investigated for suppressing acoustic instability. Of course, the most desirable method is Method 3.

It should be noted that there is considerable variation among the experimental results

TABLE 8-2

**PRINCIPAL CONCLUSIONS FROM
EXPERIMENTS CONCERNED WITH
ACOUSTIC INSTABILITY**

(1) Stability decreases with increasing energy release rate ($r\Delta H_c\rho_p$).
(2) Oscillatory burning is responsive to oscillation of pressure at the burning surface of the propellant.
(3) Irregular burning is responsive to the oscillations in gas velocity at the burning surface, and not to changes in mean gas velocity.
r – linear burning rate.
ΔH_c – enthalpy of combustion.
ρ_p – density of the propellant.

reported in the literature, and much of the work is still uncorrelated. Nevertheless, the experimental effort which has been expended together with that in progress is gradually establishing a basic understanding of the pertinent concepts that should be helpful in developing a sound theoretical approach in the problem of acoustic instability.

In summary, there is still no completely satisfactory theory for explaining the cause of acoustic instability or for predicting whether or not it will occur in a specific design of a solid propellant rocket motor. It has been demonstrated by experiment and firings of large solid propellant rocket motors that the addition of small amounts of either powdered aluminum or aluminum oxide to either composite or double-base propellant formulations effectively reduces or completely eliminates acoustic instability^{3 5}.

TABLE 8-3

**METHODS FOR SUPPRESSING ACOUSTIC INSTABILITY
(Solid Propellant Rocket Motors)**

DESIGNATION	DESCRIPTION	EXAMPLES
(1) Acoustic Interference	Arrangement of geometric factors to make excitation of the acoustic modes difficult.	Resonance rods; baffles; fore-end free-volume; elimination of aft-end irregularities.
(2) Damping of Acoustic Energy	Utilization of viscous effects and heat transfer to dampen the acoustic energy in the flow field. Damping in the solid propellant and bulk damping in the gases to rob the acoustic field of energy.	Turbulence generators in regions of high stream velocity; bare metal wall heat sinks in regions of large temperature oscillation; solid or liquid particles in the gas flow.
(3) Acoustic Uncoupling	Making the propellant unresponsive to pressure oscillations.	Proper location of burning surface; metallic powders in propellant formulation.

8-3 IGNITION OF PROPELLANT GRAIN

A solid propellant will not ignite until the temperature of its burning surface is brought above some minimum temperature called the *ignition temperature*. Furthermore, the burning surface must be held at a sufficiently high temperature for a sufficient period of time. In other words, the rate at which heat is transferred uniformly to the burning surface of the propellant grain must exceed the rate at which it is conducted from that surface to the interior of the grain, i.e., until the required *activation energy* for self-sustaining combustion has been transferred to the burning surface. The *igniter* for achieving the ignition process must produce a sufficient quantity of high temperature gas for raising the *chamber pressure* to an adequate level; the latter is particularly important in those cases where the propellant grain is to be ignited at high altitude, as in the last stage of an ICBM. In some cases it may be necessary to seal the *hot ignition gas* in the motor chamber by incorporating a rupture disc in the nozzle construction.

The igniter charge, usually a pyrotechnic mixture, is located in the fore-end of a small internal-burning combustible grain. Many different igniter materials have been used either in the form of pellets, or as a single slug. Small rocket motors are frequently used as the igniters for large solid propellant rocket motors.

An electrical signal which acts on a heat sensitive material, called the squib, initiates the ignition process. The ignition *train* proceeds through a series of *boosters* which cause hot igniter particles to be sprayed over the burning surface of the propellant grain, in addition to the heat transferred to that surface by convection and radiation from the igniter gases. It is helpful to the ignition process if the igniter gases

are rich in oxygen. If the binder (fuel) does not produce volatile gases readily under the ignition conditions, ignition will be difficult to accomplish.

The time interval from signal t_0 (zero time) to 75% of the maximum pressure level on the pressure-time record is called the *pressure ignition interval* and is denoted by t_{ip} , and is usually of the order of 200 milliseconds. The initial maximum pressure, due to ignition, is termed the *ignition peak* and it should not exceed the design value of the combustion pressure by more than approximately 10 percent.

Fig. 8-5 presents chuffing or chugging as a form of unstable burning which may occur if the igniter does not have sufficient capacity to give complete ignition of the burning surface of the solid propellant grain, i.e., the surface actually ignited is smaller than A_b , the design value of the burning surface. Consequently, the propellant area ratio K_n is also smaller than the design value. Consequently, the combustion pressure becomes abnormally low. The aforementioned situation can occur either when the propellant temperature is low or if the igniter releases insufficient energy for igniting the entire burning surface. Either condition is apt to give rise to chuffing or chugging. The combustion process becomes periodic with a low frequency, and there are large amplitude changes in the combustion pressure. Moreover, the average value of p_c is generally low. The propellant grain usually burns in a pulsating manner until it is consumed or burning ceases. In some cases, the propellant grain may be fractured by the pulsations, especially if the propellant temperature T_p is very low and the propellant is brittle, with the result that there is an inordinately large increase in the actual value of K_n . The combustion pressure may then become so large that the chamber is damaged. Because of the dangers associated with improper ignition of the propellant grain, the igniter employed for initiating burning of the propellant should furnish

sufficient heat to the burning surface so that the propellant ignites properly under all operating conditions. In some motors a thin blow-out diaphragm is installed in the throat of the exhaust nozzle to confine the gases produced by the igniter, thus aiding in building up the igniter combustion gas pressure. In other designs the igniter is designed to scatter burning particles over a sufficiently large area of the propellant burning surface to assure positive ignition of the grain ¹.

The igniter capacity should not be such that the high pressure generated by its explosion will crack the propellant grain, fail the chamber, damage the nozzle or the hardware associated with the *thrust vector control* system.

Some experiments have been conducted wherein a solid propellant grain is ignited by injecting a liquid which reacts spontaneously with the solid propellant. In general, however, the results have been unsatisfactory because of the intolerably large values of the pressure ignition interval t_{ip} .

8-4 SOLID PROPELLANT GRAIN CONFIGURATIONS

Fig. 8-7 illustrates schematically six commonly used solid propellant grain configurations, namely:

- (1) The *end-burning* (also called *cigarette-burning*) grain illustrated in Fig. 8-7(A) is a *restricted-burning grain* and gives a substantially constant chamber pressure, or thrust, with burning time. This burning characteristic is termed *neutral burning* and is illustrated in Fig. 8-8(A).
- (2) Fig. 8-7(B) illustrates the *internal-burning star grain* which can be designed to give neutral burning. The burning takes place on the surface of the star-shaped perforation. The grain is usually

bonded to the chamber (*case-bonded*) which reduces the heat transferred to the chamber during the burning process. By changing the geometry of the star the grain can be made either *regressive-burning* (see Fig. 8-8(B)) or *progressive-burning* (see Fig. 8-8(C)) instead of neutral burning.

- (3) Fig. 8-7(C) illustrates schematically a *single-perforated* or *tubular* solid propellant grain which is a commonly used unrestricted-burning grain. Its geometry is defined by its length L_p , which is assumed to remain constant during the burning period, and the propellant grain cross-sectional area $A_b = \pi (d_o^2 - d_i^2)/4$, and the *web thickness* $w = (d_o - d_i)/2$. The tubular grain suffers from the disadvantage that the combustion pressures acting upon its inner and outer surfaces may be different. Consequently, the differential pressure acting on the grain may cause it to fracture at some instant in the burning period when the web is thin. If it is necessary to equalize the pressures on the two sides of the web, small radial holes may be drilled through it at regular intervals along the grain.

- (4) Fig. 8-7(D) illustrates the *cruciform grain*, a design for eliminating the unequal pressure distribution of the aforementioned tubular grain (Fig. 8-7(C)). A cruciform grain with the outer surface of only two of its legs inhibited against burning yields a *neutral-burning* curve (Fig. 8-8(A)). If all of the outer surfaces are inhibited the area of the burning surface increases with time yielding a *progressive-burning* curve (Fig. 8-8(C)). If none of the outer surfaces are inhibited, then the area of the burning surface decreases with time and a *regressive-burning* curve is obtained (see Fig. 8-8(B)).

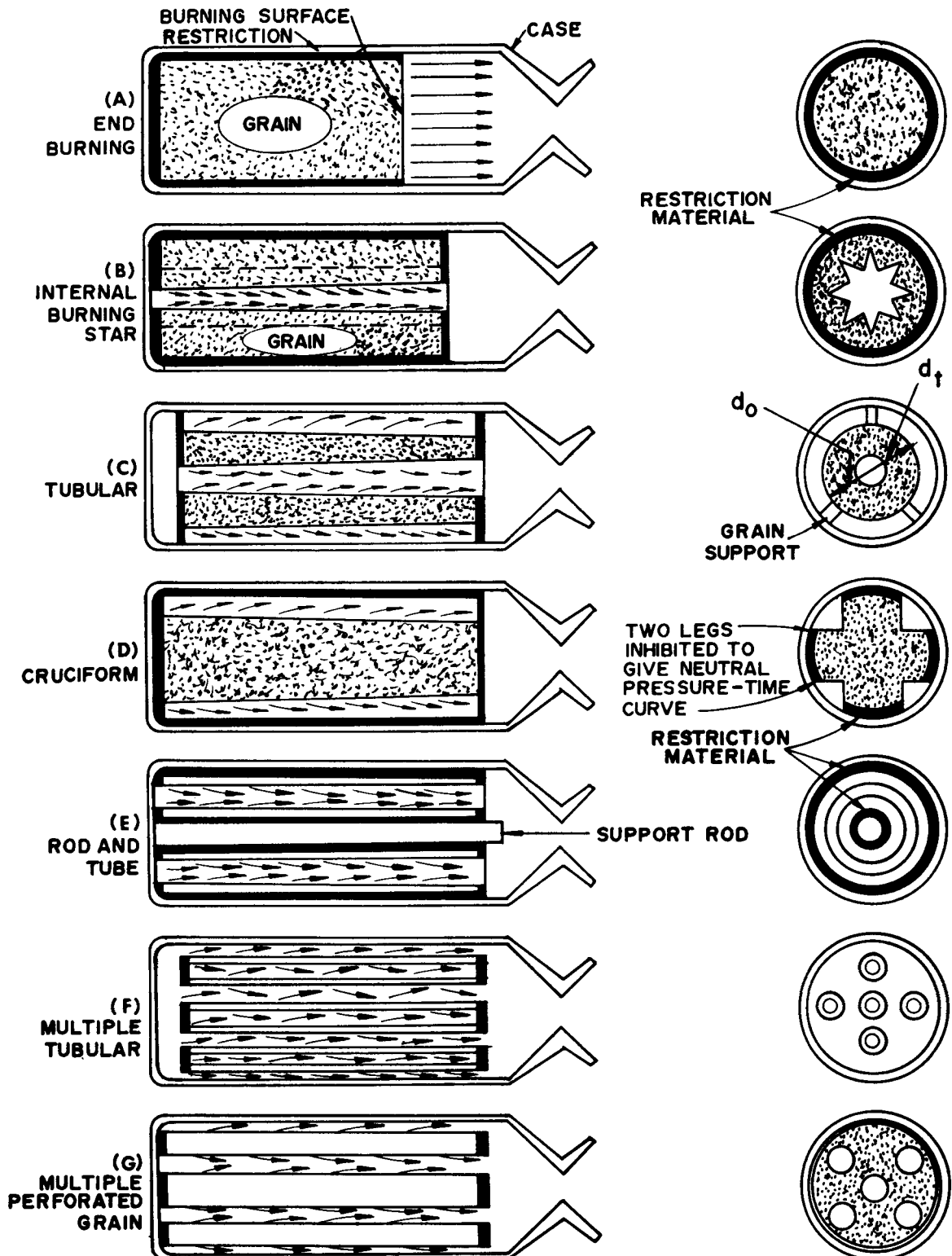
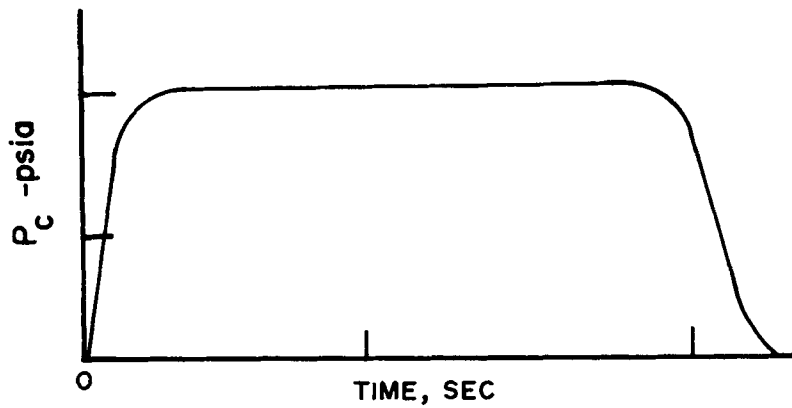
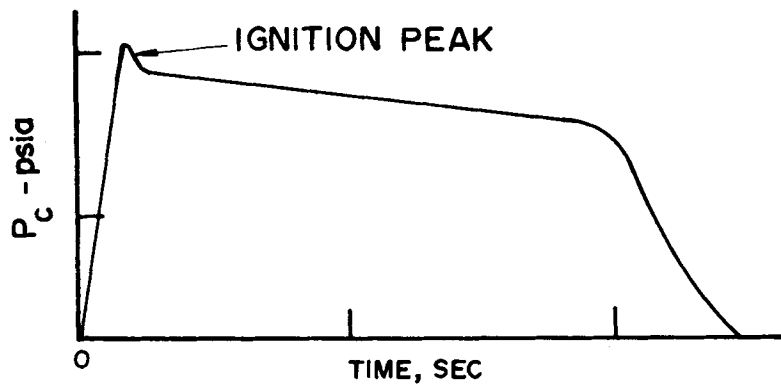


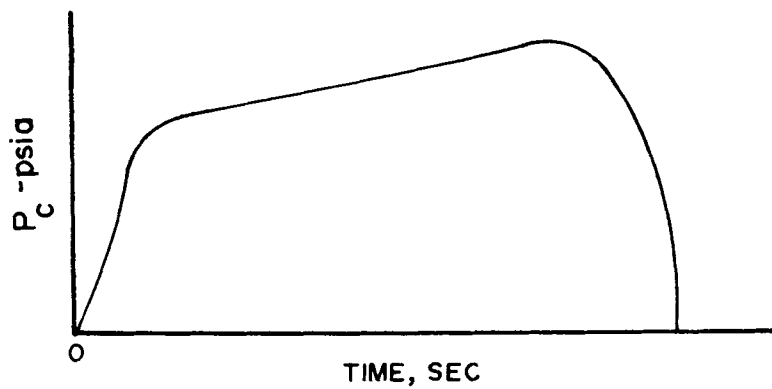
Figure 8-7. Some Typical Propellant Grain Configurations



(A) NEUTRAL BURNING



(B) REGRESSIVE BURNING



(C) PROGRESSIVE BURNING

Figure 8-8. Effect of Variations in the Area of the Burning Surface of a Solid Propellant Grain on the Pressure-Time Curve

The cruciform grain is strong and free of erosive burning.

- (5) Fig. 8-7(E) illustrates schematically a *rod and tube grain design*. The burning surface is the sum of the internal surface of the tube and the external surface of the rod; one of these surfaces increases (the tube) while the other decreases. If the linear burning rates of the tube and the rod are equal, a *neutral-burning curve* can be obtained. By using different propellants for the tube and the rod, the shape of the thrust-time curve can be varied to give a desired variation of thrust as a function of time, within practical limits. Problems are frequently encountered in supporting the rod in applications where the motor is subjected to large accelerations. Fig. 8-7(F) illustrates a *multiple-tubular grain design*.

- (6) Fig. 8-7(G) illustrates schematically a *multiple-perforated grain design*. In such designs the perforations are disposed so that all of the burning surfaces are approximately equal distances apart. Such an arrangement can be designed so that the burning surface will be only slightly progressive.

8-5 PORT-TO-THROAT AREA RATIO ($1/J$)

Consider the tubular grain illustrated schematically in Fig. 8-7(C). Assume that the inner and outer surfaces of the tube have the same linear burning rate, then d_i increases at the same rate that d_o decreases. Consequently, the area of the burning surface A_b remains constant, and if there is no erosion of the nozzle throat, then

$$K_n = \frac{A_b}{A_t} = \text{propellant area ratio} = \text{constant}$$

The duration of the *burning time* t_b depends on the web thickness $w = (d_o - d_i)/2$.

If A_{ch} denotes the cross-sectional area of the chamber housing the tubular grain, then the ratio A_w/A_{ch} is termed the *loading density*, where

$$A_w = \frac{\pi}{4} (d_o^2 - d_i^2)$$

The cross-sectional area through which the combustion gas can flow, adjacent to the propellant grain, is termed the *port area* and is denoted by A_p . Hence

$$A_p = A_{ch} - A_G = \text{port area} \quad (8-17)$$

By definition, the *port-to-throat area ratio*, denoted by $1/J$, is given by

$$1/J = \frac{A_p}{A_t} = \frac{A_{ch} - A_G}{A_t} \quad (8-18)$$

In general, rocket motors are designed so that the port-to-throat area ratio is approximately $1/J \approx 2.0$. Because of demand for higher loading density, values of $1/J < 2$ are used where the resulting erosive burning can be tolerated (see par. 8-1.15).

8-6 HEAT TRANSFER IN SOLID PROPELLANT ROCKET MOTORS

Heat is transferred from the hot combustion gases to those surfaces in contact with them by convection, radiation, and conduction. Of those modes of heat transfer, convection is the dominant one. The quantity of heat transferred to the surfaces in contact with the combustion gases is a complex function of several variables such as the flame temperature, the physical properties of the combustion gases, the grain design, the combustion pressure, and the configuration of the motor case and exhaust nozzle. Since the total weight of the inert metal parts must be held to a minimum, the internal-burning case-bonded grain design is favored since only

the fore-cap and nozzle are exposed to the hot gases. In general, for short burning durations, less than approximately 5 sec, the problems due to heat transfer are not serious. For applications such as ballistic missiles where the duration of burning is relatively long, as much as 90 sec, the problems arising from heat transfer are difficult and challenging.

Because of the extremely high mass velocity of the combustion gases and their high temperature (4500° to 5500°F for high performance propellants), the heat transfer rates to the aft-cap and nozzle are large, but those in the nozzle throat are several-fold those for the aft-cap. The aft-cap is protected from reaching dangerously high temperatures by protecting it with layers of a suitable insulating material. In general, the exhaust nozzle is equipped with a ceramic or carbon liner for protecting the outer metal case surrounding the liner. Propellants which contain metals in their formulation may introduce problems because of the tendency of their exhaust gases to erode the throat of the exhaust nozzle. Considerable research and development effort is required for developing satisfactory temperature resisting materials for protecting the inert parts of solid propellant rocket motors.

Of importance is the fact that the heat transferred to the burning surface of a solid propellant grain by the hot combustion gases flowing past the surface does not penetrate far below that surface, because of the rapid rate with which the surface recedes. Consequently, the changes in temperature of the propellant grain due to the heat transfer need not be considered in internal ballistic studies.

Under transportation and short time storage conditions the temperature of the propellant grain in a solid propellant rocket motor will generally be different from that of the ambient atmosphere. The heat transfer from the atmosphere to the propellant takes place at a slow rate and, when the temperature difference is

substantial, significant temperature gradients can arise in the grain that cause severe thermal stresses. If the grain is being cooled by the ambient temperature, assuming a case-bonded internal-burning grain, the grain tries to pull away from the case and there are large tensile stresses at its inner and outer surfaces.

8-6.1 AERODYNAMIC HEATING^{36, 38, 39, 40}

If a rocket-propelled vehicle moves through the air with very large velocities, as for example an antissile missile, the thin layer of air adjacent to the surfaces of the vehicle cannot be assumed to be a perfect gas; this thin layer of air is characterized by its steep velocity gradient. Because of this velocity gradient, very high local temperatures are produced by the friction (viscosity) resulting from the adjacent layers of air moving at different velocities. Moreover, at stagnation points there are high stagnation temperatures due to bringing the air to stagnation from a high velocity relative to the moving vehicle (see par. A-5.2). For air assumed to be a perfect gas, the stagnation temperature T^0 is

$$T^0 = T_{\text{amb}} (1 + 0.2 M^2)$$

where

$M = V/a$ = the Mach number, V the flight speed, and

$a = \sqrt{\gamma RT_{\text{amb}}}$ = the local acoustic speed

8-6.2 EFFECT OF AERODYNAMIC HEATING ON INTEGRITY OF ROCKET MOTOR CHAMBERS

It is apparent from the last equation that the aerodynamic heating increases with the square of the flight Mach number. Aerodynamic heating affects the structural integrity of both steel and glass-filament wound rocket motor chambers; the former loses strength by annealing and the latter due to charring of the resin or plastic.

The problem is particularly critical on the leading edges of aerodynamic control surfaces

employed for steering the vehicle, as in low altitude intercept missions of incoming ICBM's.

8-7 GENERAL DESIGN CONSIDERATIONS

The design details of a solid propellant rocket motor will depend upon the mission it must fulfill, the storage temperatures and temperature cycling it will encounter, and the conditions it will be subjected to under field handling conditions. By and large most of the requirements to be satisfied are of a practical nature and are not subject to an accurate analytical study. Once the specific propellant formulation has been decided upon, the designer has considerable latitude in selecting such parameters as the combustion pressure, burning rate, grain configuration, and the design of the chamber.

The problems which must be solved in developing solid propellant motors are primarily those pertinent to obtaining precise thrust termination, accurate thrust vector control, and means for taking into account the temperature sensitivity of the propellant.

8-7.1 SELECTION OF COMBUSTION PRESSURE

For a rocket motor equipped with a conventional type of exhaust nozzle having fixed geometry, the following design criteria apply:

- (1) The combustion pressure p_c should be at least 100 psia above the deflagration pressure limit (see par. 8-1.13) corresponding to the lowest value of propellant temperature T_p which is to be encountered.
- (2) The combustion pressure should be well below the pressure limit corresponding to the highest value of T_p to be encountered (see par. 8-1.13). In general,

higher combustion pressures are employed for short duration boost applications where a large but brief thrust is desired, and moderate combustion pressures for long duration applications where the weight of the inert parts of the rocket motor must be kept as light as possible.

- (3) The combustion pressure depends upon the selection of the linear burning rate r_0 obtainable from the propellant formulation. Note that the relation between p_c and r_0 is exponential (see Eq. 8-3).

8-7.2 ESTIMATE OF THE WEIGHT AND VOLUME OF THE SOLID PROPELLANT GRAIN

The total weight of a solid propellant grain, denoted by W_p , depends upon the total impulse required for satisfying the requirements of the mission. If F denotes the thrust required (assumed to remain constant during the burning time t_b) and I_{sp} is the specific impulse of the propellant, then

$$W_p = Ft_b / I_{sp} \quad (8-19)$$

Eq. 8-19 gives the minimum weight of solid propellant for the required total impulse. This weight should be increased by 1 to 3 percent, depending upon the uniformity of the product and the closeness with which it meets the design specifications, to allow for slivers of the propellant that are not consumed. It cannot be overemphasized that the development and application of reliable process control procedures are as much a part of the development of a satisfactory solid propellant as is the chemical research which enters into determining the most satisfactory propellant formulation.

If γ_p denotes the specific weight of the propellant and V_p the volume of the grain, then

$$V_p = W_p / \gamma_p \quad (8-20)$$

8-7.3 DETERMINATION OF NOZZLE THROAT AREA

8-7.3.1 GENERAL CONSIDERATIONS

The exact dimensions of the propellant grain depend upon the configuration which is selected: internal-burning star, rod and tube, etc.^{1,3}. In general, the shape of the grain must be such that its burning area A_b has the correct value for producing the required thrust throughout the burning period.

The throat area of the exhaust nozzle A_t may be determined from any one of the following three relationships¹: Thus

$$A_t = A_b / K_n \quad (8-21)$$

$$A_t = \dot{W}_p / C_w p_c \quad (8-22)$$

$$A_t = F / C_w p_c \quad (8-23)$$

where the weight flow coefficient C_w (see Eq. 5-7) is obtained from experimental data pertinent to the propellant.

The exit area for the nozzle depends on the expansion ratio for the exhaust nozzle (p_e/p_c) and the specific heat ratio γ , for the combustion gases (see Chapter 4).

8-7.3.2 EFFECT OF PROPELLANT GRAIN CONFIGURATION

The thrust of a solid propellant rocket motor, like the combustion pressure, varies with the area of the burning surface A_b . Consequently, variation in the area of the burning surface can be utilized for programming the thrust as a function of the burning time. The programming is accomplished by shaping the grain in such a manner that the desired amount of burning surface is provided

at each instant during the burning period.

With case-bonded, internal-burning, star-shaped, or cruciform grain, it is possible by proper arrangement of the geometric proportions between the number of points of the star, the angle between those points, and web thickness, to obtain either neutral, progressive, or regressive burning characteristics.

In addition to the aforementioned geometric type of control, the area of the burning surface can also be varied by employing inhibiting coatings so that certain areas of the grain are prevented from burning.

A third method of thrust program control which may be preferable for certain applications can be accomplished by constructing the grain from propellants having different burning rates.

8-7.4 ROCKET MOTOR CHAMBER AND INSULATION^{3,9,41,42}

The chamber (see Fig. 7-1) must support the solid propellant grain and also contain the propulsive gas at the design chamber pressure P_c . Such items as the igniter, the nozzle, etc., are attached to or mounted on the chamber. If the rocket motor propels either the first or an intermediate stage of a multistage vehicle, means must be provided for attaching the other stage. If the rocket motor propels either the last stage of a multistage vehicle or propels a single-stage vehicle, means must be provided for attaching the payload to it.

The chamber is designed as a pressure vessel, and its weight must be as small as feasible because of the effect of its empty weight on the burnout velocity (see par. 5-9.2). Care must be exercised to avoid large stress concentrations, due to discontinuities, at such locations as the igniter boss and the nozzle attachment section.

Because of the demand for chambers having high strength and low weight, the criterion for selecting materials for chambers is the *strength-to-weight ratio* of the material. In other words, a light material having a moderate allowable design stress may be more suitable to a heavier material which can carry higher design stresses. Because of its high strength-to-weight ratio, glass-filament wound cases have found favor particularly for the larger rocket motors.

The cylindrical portion of the chamber requires only light lateral heat insulation, but heavy insulation is needed on the aft and forward domes particularly on the aft dome. As the perforation in the grain—considering a case-bonded internal-burning grain (see Fig. 7-1)—increases during burning, the aforementioned domes become exposed to the hot combustion gases.

The gas velocities are highest at the aft end of the perforation and they generally experience somewhat sudden changes in direction as they leave the perforation and impinge upon the aft dome insulation, with considerable turbulence. Consequently, there is severe erosion of that insulation. It is difficult, however, to predict where the most severe erosion will occur. Because the flow conditions are not amenable to mathematical analysis, the development of the proper shape, kind, and amount of insulation needed at the aft dome is determined primarily by experience.

At the temperatures of the combustion products of modern solid propellant no heat insulating material is completely stable. Most of the heat insulating materials are high temperature plastic materials containing carbon, silicon, and others. Some thermal decomposition of the insulating material occurs and is utilized as a part of the mechanism of insulation, termed *ablation*³⁸. The exposed surface of the insulation decomposes thereby absorbing heat, and the flow of the gaseous decomposition products

away from the surface cause a slight thickening of the thermal boundary with a consequent reduction in the rate of heat transfer to the insulating material.

Another cause of serious erosion of the insulation arises from condensed phases in the propellant gas from propellants containing metallic additives. The relative large density of the condensed products prevents them from changing their direction as rapidly as the gaseous products, consequently they are ejected from the gas stream by their inertia and impinge on certain areas of the insulation. Some of the high temperature gaseous components such as carbon dioxide (CO_2) and water vapor cause oxidation of the materials lining the exhaust nozzle, thereby aggravating erosion.

8-7.5 NOZZLES FOR SOLID PROPELLANT ROCKET MOTORS

The gas dynamic considerations affecting the design of the rocket motor (propulsive) nozzle are presented in par. 4-8. Regardless of the nozzle configuration, it is desirable that the throat area of the nozzle A_t remain constant during the burning period for the rocket motor. Unfortunately, two influences cause the throat area to change during the burning period: (1) the temperatures of the propulsive gas exceed the melting temperatures of all but a few materials, and (2) the converging portion and the throat are subject to severe erosion.

With modern propellants, the throat of the nozzle—the region of maximum heat flux—will reach the melting temperature of steel in approximately 5 sec. If the burning time t_B exceeds approximately 5 sec, materials having higher melting temperatures than steel must be employed. Although graphite withstands high temperature per se, it oxidizes readily and because of its softness is susceptible to both mechanical and chemical (oxidation) erosion. Hard, refractory metals such as hot

molybdenum and tungsten have good thermal and erosion resistance, and can be employed in a hot reducing atmosphere; for example, the melting temperature of tungsten is approximately 6100°F. Unfortunately such materials have low thermal conductivities, are brittle, and have low resistance to thermal stress, due to large temperature gradients in the material. Experience indicates that the maximum thermal stress occurs in approximately 0.09 sec, almost coincident with the *ignition peak*; thereafter the thermal stress decreases.

The thermal stress problem can be alleviated by using thin sections of the refractory metal, thus avoiding large temperature gradients in the material. In practice—because some erosion always occurs, and in the interest of reducing the cost and weight of the nozzle—the refractory metal is usually surrounded by an insulating material and then assembled in either a steel or titanium shell.

The portion of the nozzle downstream from the throat is a region of decreasing heat flux, decreasing density of the propulsive gas, and has little or no impact of the condensed phases upon the walls. For those reasons a refractory liner is unnecessary; the diverging portion ordinarily is a steel shell protected by a high temperature plastic liner. Fig. 8-9 illustrates schematically a cross-section through a rocket motor nozzle of the type discussed above.

For short duration rocket motors, t_B less than approximately 3 sec, the heating and erosion problems are greatly reduced and much simpler nozzle constructions can be employed.

8-7.6 CONTROL OF VEHICLE RANGE

A solid propellant rocket motor produces propulsive thrust as long as the burning propellant produces a supply of propulsive gas. At *tail-off*, where the grain finally *completes burning*, the chamber pressure and thrust

decrease to zero. The consumption of the propellant cannot be used as a parameter for controlling the range of a rocket-propelled vehicle because of its inadequate precision for that purpose and also a shorter range may be desired than that corresponding to the complete consumption of the propellant grain. Range control is, therefore, based on either eliminating or neutralizing the propulsive thrust, and the time for actuating the range control must be predicted accurately.

One scheme is to provide the rocket motor with one or more ports through which a gas flow, in the direction opposite to that of the propulsive (nozzle) jet, produces a thrust opposing the main propulsive thrust. The ports are closed until the reversed thrust is desired at which time the ports are opened explosively by an electrical signal. Opening the ports increases the area for the discharging propulsive gas, consequently, the chamber pressure decreases. As a result, the linear burning rate decreases, and there may be irregular burning.

Another scheme is to equip the vehicle with suitable *drag brakes*.

Experiments have shown that positive termination of thrust and some thrust modulation can be achieved by injecting water into an operating solid propellant rocket motor⁴⁷. Thrust termination and payload separation are discussed in Reference 48.

8-7.7 THRUST VECTOR CONTROL (TVC) OF SOLID PROPELLANT ROCKET-PROPELLED VEHICLES

In many applications of solid propellant rocket motors means must be provided for steering the rocket-propelled vehicle, particularly for the larger vehicles which are required to maneuver at very high altitudes where aerodynamic surfaces are ineffective. Even at low altitudes, disturbances during the launch phase

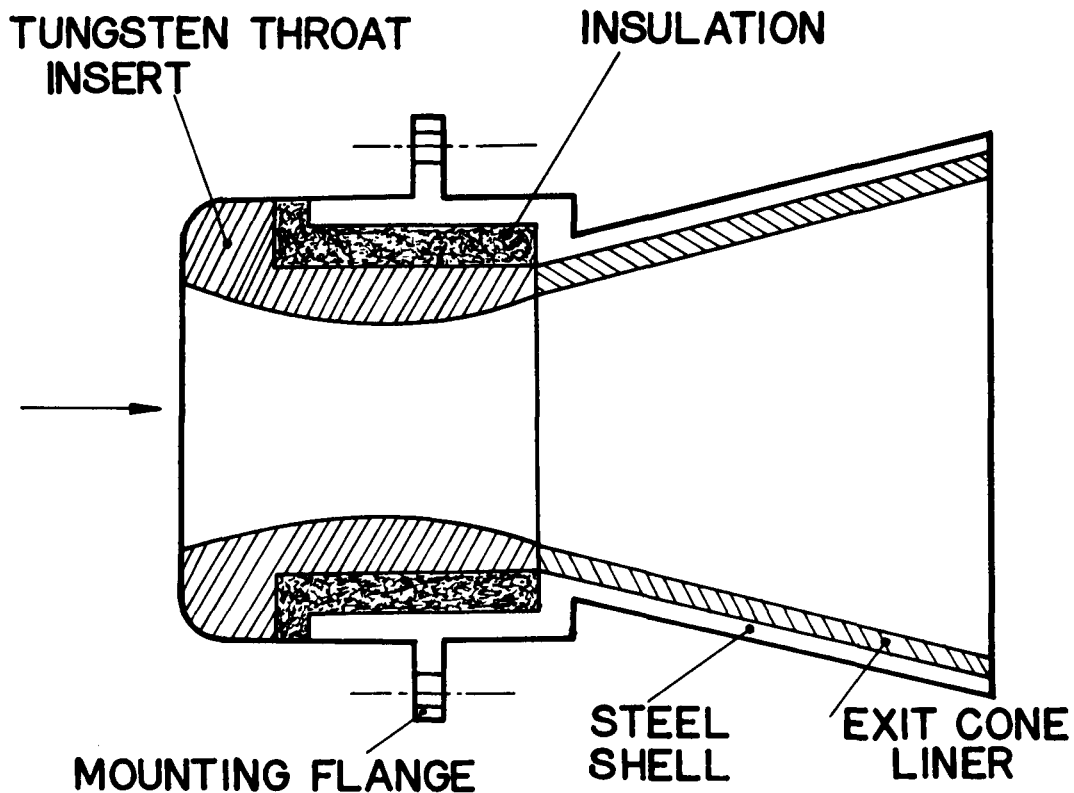


Figure 8-9. Section Through a Rocket Motor Nozzle

of the flight path and cross-winds may cause unacceptable deviations in the flight path which must be corrected. Where efficient aerodynamic forces are inadequate, the propulsive jet ejected by the exhaust nozzle can be utilized for furnishing the forces for changing the attitude of the vehicle.

The thrust F acting on a rocket-propelled vehicle is, of course, due to the reaction to the momentum flux of the propulsive (exhaust) jet. If the *line-of-action* of F coincides with the longitudinal axis of the rocket-propelled vehicle and if that axis passes through the centroid of the vehicle, the thrust F acts in the axial direction and produces no moment on the vehicle. Suppose now that a means is provided which deflects the propulsive jet laterally, as illustrated in Fig. 8-10. Because of the lateral deflection of the propulsive jet, the thrust force

F makes an angle α with the longitudinal axis of the vehicle and the resulting lateral force component produces a turning moment which changes the attitude of the vehicle. The deflection of the propulsive jet for achieving attitude control of the rocket-propelled vehicle is termed *thrust vector control*, or briefly TVC.

There are several means for achieving TVC. In the case of liquid propellant systems, TVC is achieved by *gimballing* the *thrust chamber* (rocket motor plus nozzle). That form of TVC is usually inapplicable to solid propellant rocket motors because of their size and weight. Consequently, other means of TVC had to be developed for solid propellant rocket motors, and these may be divided into three main groups: (1) mechanical means, based on inserting an adjustable obstruction in the supersonic exhaust gas stream; (2) movable nozzles, which are

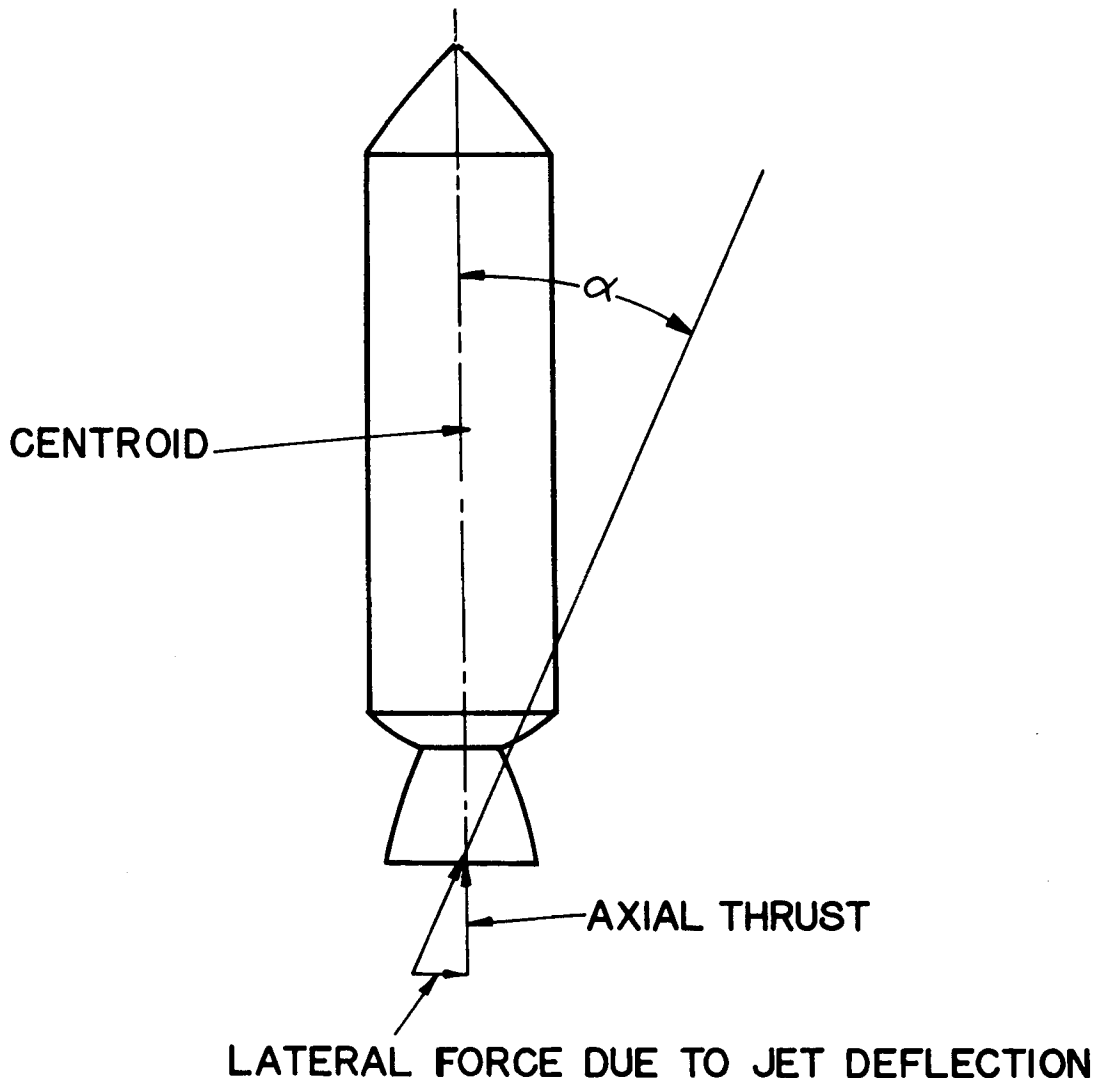


Figure 8-10. Jet Deflection To Achieve Attitude Control

analogous to *gimballing* the thrust chamber of a liquid propellant rocket engine; and (3) fluid mechanical means, termed *secondary injection*, wherein a fluid (a liquid or a gas) is injected laterally into the supersonic stream flowing in the diverging portion of the rocket motor nozzle.

8-7.7.1 MECHANICAL MEANS FOR ACHIEVING TVC

Fig. 8-11 illustrates schematically four different mechanical means for achieving TVC. The

oldest is the jet-vane (Fig. 8-11(A)). Its major disadvantages are its weight and the fact that the jet-vanes are immersed in the hot gas stream during the entire burning period for the rocket motor. With the higher flame temperatures of modern solid propellants with their condensable exhaust products, the problem of finding a material capable of withstanding the higher temperature gases with their increased erosive effect has become insurmountable from an engineering viewpoint.

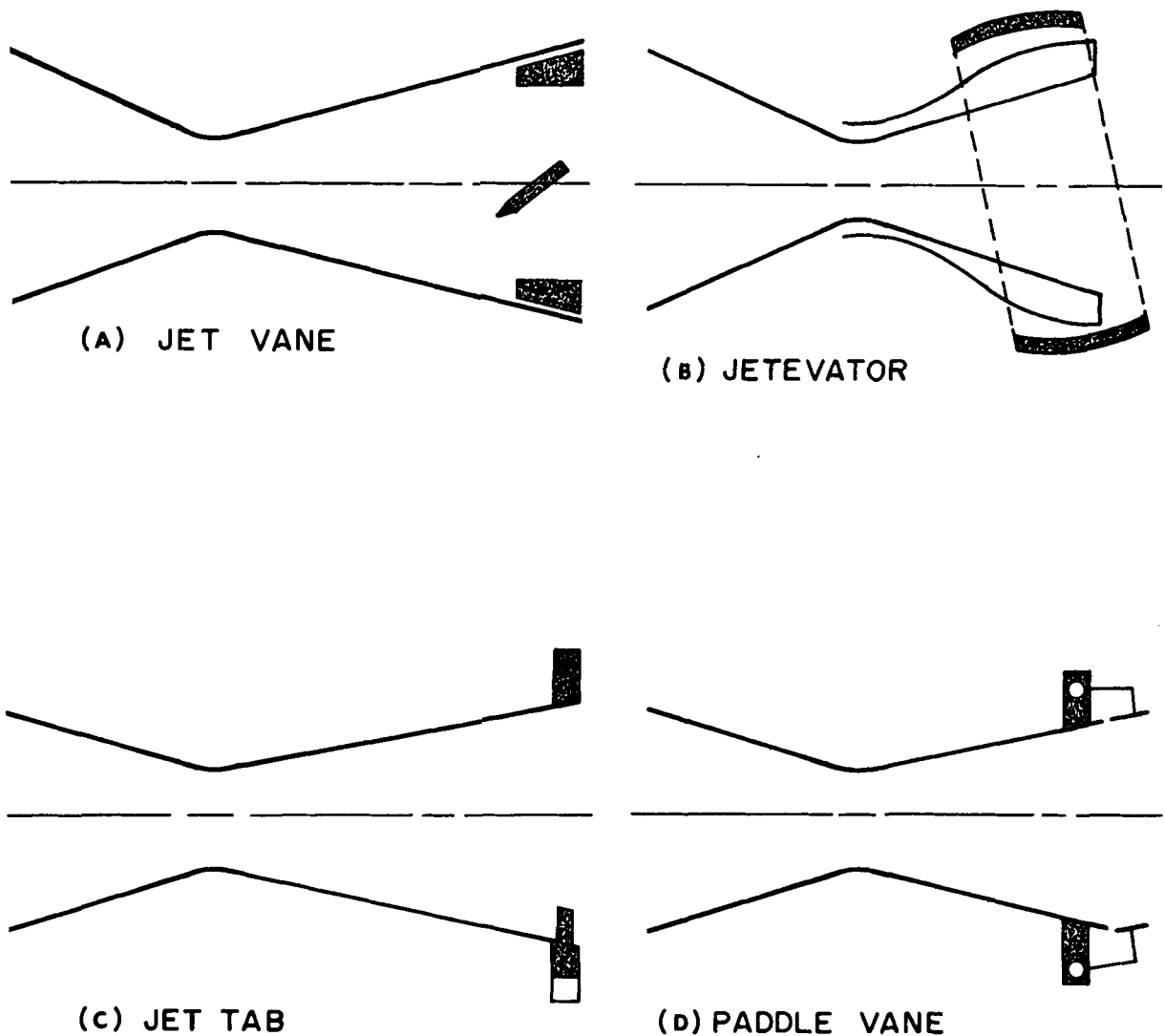


Figure 8-11. Mechanical Means for Effecting Thrust Vector Control

Since there are periods in the burning period t_B when no attitude control is required, it is reasonable to provide a TVC means which removes the jet deflection means from the hot gas stream during such periods. Fig. 8-11(B) illustrates such a TVC means known as a *jetelevator*. When it is rotated into the propulsive jet, the supersonic gas stream is disturbed so that it separates from the nozzle wall. A high pressure is developed in the separated region which is not balanced by the stable flow on the opposite wall, hence a lateral force component is

produced. An additional force component is produced by the deflection of the propulsive jet as it flows through the oblique shock wave, as illustrated in Fig. 8-11(B).

Figs. 8-11(C) and 8-11(D) illustrate schematically how the *jet tab* or *spoiler*^{5,2} and the *paddle vane* achieve jet deflection to accomplish TVC.

All of the mechanical TVC systems illustrated schematically in Fig. 8-11 cause losses

in axial thrust due to the thermodynamic irreversibilities they introduce into the flow field. To eliminate such losses, movable nozzles were introduced.

8-7.7.2 MOVABLE NOZZLES

Fig. 8-12(A) illustrates schematically the essential features and operating principle of the *swivel nozzle*. In this system there is no loss in the magnitude of the thrust vector, only its direction is changed as the diverging portion of the nozzle is rotated, and the control is limited to a direction perpendicular to the axis of rotation. By employing a ball-and-socket type of joint, a lateral force can be developed in any desired direction.

Fig. 8-11(B) illustrates schematically the essential features and operating principle of the *rotatable nozzle* which is a modification of the swivel nozzle. The nozzle can be rotated about a plane which is inclined to the nozzle axis. Control is obtainable in all directions.

The movable nozzles which have been built are bulky, heavy, and complicated. It is essential that the joint be sealed against the high temperature, high pressure propellant gas which is a difficult design problem. Moreover, the control forces required for actuating the movable portion of a large nozzle can become so large that they cause a severe drain upon the electric power source (battery, etc.) installed in the vehicle.

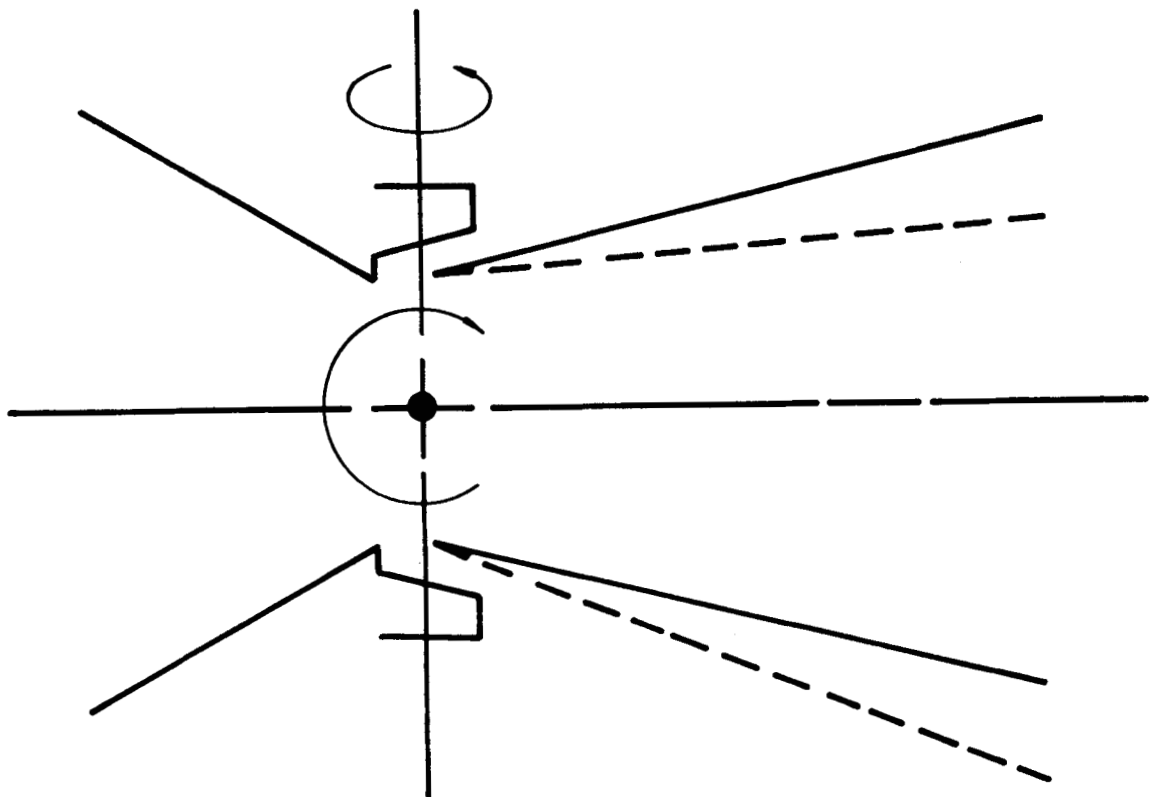
Because of the higher flame temperatures and large amounts of solid particles or liquid droplets in the propulsive gas formed by burning modern high performance solid propellants, the TVC systems illustrated in Figs. 8-11 and 8-12 have become inadequate, especially for long burning times or large thrust solid propellant rocket motors.

8-7.7.3 SECONDARY INJECTION FOR TVC

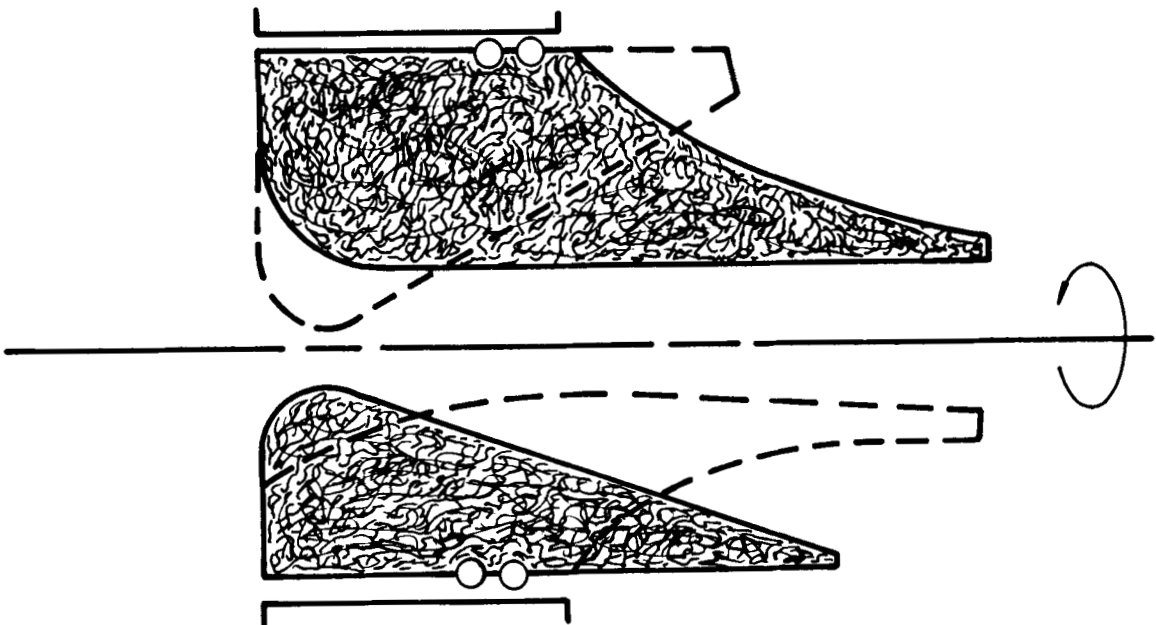
Secondary injection appears to be ideally suited for TVC in the case of rocket motors burning modern solid propellants. Fig. 8-13 illustrates schematically the principle of employing secondary injection for TVC. A fluid, called the *injectant* is injected into the nozzle, downstream from the throat where the *primary flow* is supersonic. The disturbance of the primary flow by the injectant causes a shock wave to form a region of flow separation, as illustrated in Fig. 8-13. The local high pressures associated with the shock wave can yield large lateral forces which are not balanced on the opposite wall of the nozzle. Hence, a net lateral force is produced which is the sum due to the momentum force of the injectant and that due to the induced shock. In general, the total lateral force, also called the *side force* is approximately 1.5 times that due to the momentum flux of the injectant.

In theory, the best injectant would be hot propellant gas drawn from the rocket motor chamber, but two major problems are encountered. First, to obtain side force modulation, which is a requirement, a suitable hot-gas flow-control valve which will maintain its integrity in a high temperature gas containing condensed phases is needed. Second, the opening and closing of the hot-gas valve causes variations in the chamber pressure that may be intolerable. It is, of course, possible to use a separate hot-gas generator for producing the flow of injectant if its dimensions and weight can be tolerated ^{5 3, 5 4, 5 5, 5 6, 5 8}.

To avoid the aforementioned problems, the current secondary injection TVC systems are based on using a liquid injectant; a liquid having a high vapor pressure is desirable. The ideal liquid injectant is one which evaporates almost immediately upon its exposure to the hot primary gas flow. Since the temperature of the



(A) SWIVEL NOZZLE



(B) ROTATABLE NOZZLE

Figure 8-12. Movable Nozzles for TVC

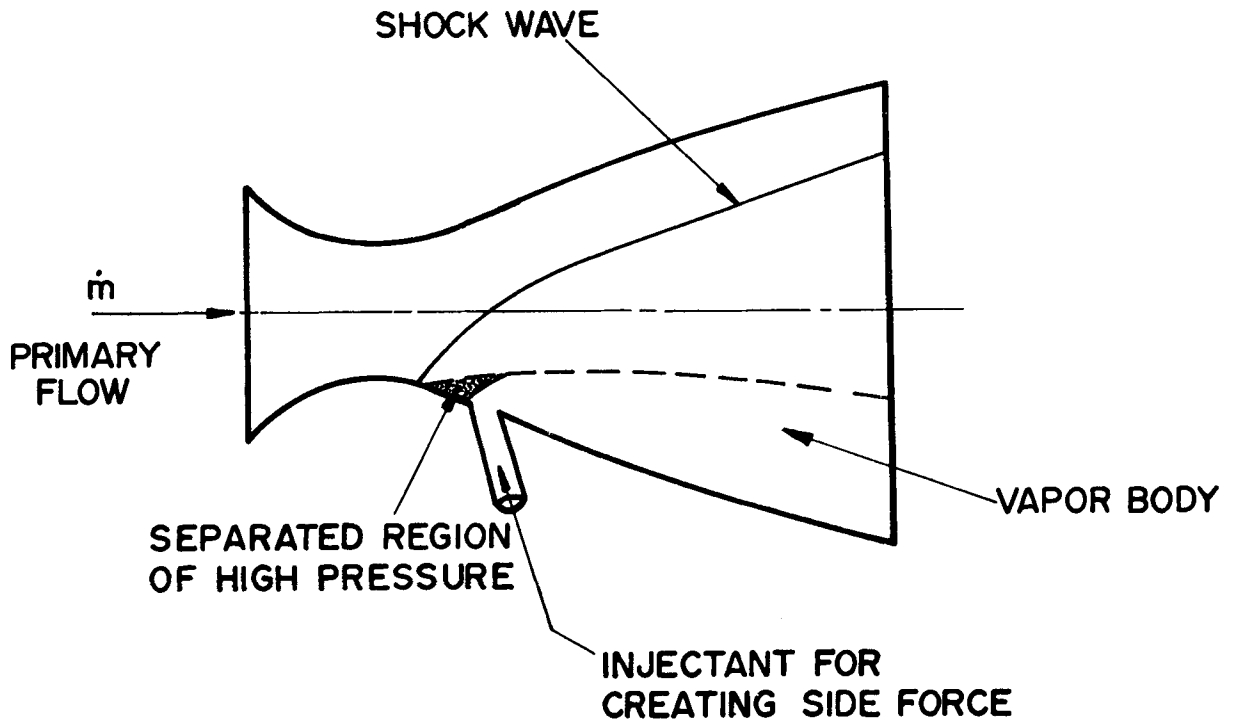


Figure 8-13. Secondary Injection for TVC

liquid injectant is low, its specific impulse will likewise be low so that large amounts of injectant are required.

The quantity of injectant (liquid or gas) per pound of desired side force can be reduced if the injected fluid reacts chemically with the primary

gas flow. Since the propellant gas forming the primary flow is usually rich in fuel components, a fluid containing oxidizing materials should be helpful. Many problems have to be studied before the appropriate domain for the application of secondary injection TVC systems can be established.

REFERENCES

1. M. J. Zucrow, *Aircraft and Missile Propulsion*, John Wiley and Sons, Inc., 2nd Printing, Vol 2, 1964, Ch. 10.
2. C. Huggett, C. E. Bartly, and M. M. Mills, *Solid Propellant Rockets*, Princeton Aeronautical Paperbacks, No. 2, Princeton University Press, 1960.
3. R. N. Wimpres, *Internal Ballistics of Solid Fuel Rocket*, McGraw-Hill Book Company, Inc., 1950.
4. M. Barrere, A. Jaumotte, B. F. de Veubeke and J. Vandekerckhove, *Rocket Propulsion*, Elsevier Publishing Company, Amsterdam, 1960.
5. R. D. Geckler and D. F. Sprenger, "The Correlation of Interior Ballistic Data for Solid Propellants", *ARS Jour.*, Vol. 24, No. 1, Jan.-Feb. 1954, p. 22.
6. R. D. Geckler, *The Mechanism of Combustion of Solid Propellants*, Selected Combustion Papers, AGARD 1954, p. 289.
7. M. Summerfield, G. S. Sutherland, M. J. Webb, H. J. Taback and K. P. Hall, *Burning Mechanism of Ammonium Perchlorate Propellants*, *Progress in Astronautics and Rocketry*, Vol. 1, Academic Press 1960, p. 141.
8. D. W. Blair, E. K. Bastress, C. E. Hermance, K. P. Hall and M. Summerfield, *Some Research Problems in the Steady State Burning of Composite Solid Propellants*, *Progress in Astronautics and Rocketry*, Vol. 1, Academic Press, 1960, p. 183.
9. CPIA Publication No. 80, *Solid Propellant Nomenclature*, Chemical Propulsion Information Agency, The Johns Hopkins University, Applied Physics Laboratory, Silver Spring, Md., May 1965.
10. L. Green, *Erosive Burning of Some Composite Solid Propellants*, ARS, Preprint 441-57, Semi-Annual Mtg., June 10-13, 1957.
11. J. A. Vandekerckhove, "Erosive Burning of a Colloidal Solid Propellant", *Jet Propulsion*, Vol. 28, No. 9, Sept. 1958, p. 599.
12. M. J. Zucrow, J. R. Osborn, and J. M. Murphy, "Propellant Erosive Burning", *Chemical Engineering Progress*, Vol. 60, No. 2, Feb. 1964, p. 43.
13. M. J. Zucrow, J. R. Osborn, and J. M. Murphy, *An Experimental Investigation of the Erosive Burning Characteristics of Non-Homogeneous Solid Propellant*, AIAA Solid Propellant Rocket Conference, Palo Alto, Calif., Preprint No. 64-107, January 29-31, 1964.
14. T. Markland and A. Lake, "Experimental Investigation of Propellant Erosion", *ARS Jour.*, Vol. 30, No. 2, February 1960.
15. T. Markland, *Erosion Studies of Propellants*, Research Inst. of National Defense, Sweden, November 1962.
16. F. T. McClure, et al., *A General Review of Our State of Knowledge, Report of the Working Group on Solid Propellant Combustion Instability*, Applied Physics Laboratory, Johns Hopkins University TG 371-1, July 1960.
17. M. J. Zucrow and J. R. Osborn, *Unstable Burning in Liquid and Solid Propellant Rocket Motors*, Symposium on Missiles and Rockets, Naval Ammunition Depot, Concord, Calif., 18-21 April 1961.
18. E. W. Price, "Terminology in Rocket Combustion Instability", *Jet Propulsion*, Vol. 28, No. 3, March 1958, p. 197.

REFERENCES (Continued)

19. R. D. Geckler, *Unsolved Problems in Solid-Propellant Combustion*, Fifth Symposium on Combustion, Reinhold Publishing Corp., New York, 1955, p. 29.
20. F. T. McClure, R. W. Hart, and J. R. Bird, "Acoustic Instability in Solid Fuel Rocket", *ARS Jour.*, Vol. 30, No. 9, Sept. 1960, p. 908.
21. R. H. Wall, *Resonant Burning of Solid Propellants: Review of Causes, Cures, and Effects, Solid Propellant Rocket Research, Progress in Astronautics and Rocketry*, Vol. 1, Academic Press, 1960, p. 603.
22. R. W. Hart and F. T. McClure, "Combustion Instability: Acoustic Interaction with a Burning Propellant", *The Journal of Chemical Physics*, Vol. 30, No. 6, June 1959, p. 1501.
23. F. T. McClure, R. W. Hart and J. F. Bird, "Acoustic Resonance in Solid Propellant Rockets", *The Journal of Chemical Physics*, Vol. 31, No. 5, May 1960, p. 884.
24. H. Grad, "Resonance Burning in Rocket Motors", *Comm. on Pure and Applied Mathematics*, Vol. II, No. 1, 1949, p. 79.
25. T. Angelus, *Unstable Burning Phenomena in Double-Base Propellants, Progress in Astronautics*, Vol. 1, Academic Press, New York, 1960, p. 527. Also ARS Preprint No. 1066-60, ARS, 1960.
26. Sin-I Cheng, "High Frequency Combustion Instability in Solid Propellant Rockets", Part I, *Jet Propulsion*, Vol. 24, No. 1, Jan.-Feb. 1954, p. 27; Part II, *Jet Propulsion*, Vol. 24, No. 2, March-April 1954, p. 102.
27. J. E. Crump and E. W. Price, "Catastrophic Changes in Burning Rate of Solid Propellants During Combustion Instability", *ARS Jour.*, Vol. 30, No. 7, July 1960, p. 705.
28. R. P. Smith and D. F. Sprenger, *Combustion Instability in Solid Propellant Rockets*, Fourth Symposium on Combustion, The Williams and Wilkins Company, Baltimore, Md., 1953, p. 893.
29. R. W. Hart, J. R. Bird and F. T. McClure, *The Influence of Erosive Burning on Acoustic Instability in Solid Propellant Rocket Motors, Solid Propellant Research, Progress in Astronautics and Rocketry*, Vol. 1, Academic Press, New York, 1960, p. 423.
30. M. J. Zucrow and J. R. Osborn, "An Experimental Study of High-Frequency Combustion Pressure Oscillations", *Jet Propulsion*, Vol. 28, No. 10, October 1958, p. 654.
31. M. J. Zucrow, J. R. Osborn and A. C. Pinchak, "Luminosity and Pressure Oscillations Observed with Longitudinal and Transverse Modes of Combustion Instability", *ARS Jour.*, Vol. 30, No. 8, August 1960, p. 758.
32. *Aviation Age*, Vol. II, 1958-1959, *Research and Development Technical Handbook*, Section D: "Propulsion".
33. H. J. Allen, "Hypersonic Flight and the Re-Entry Problem", *Journal IAS*, Vol. 25, No. 4, April 1958, p. 217.
34. J. W. Bond, K. M. Watson and J. A. Welch, *Atomic Theory of Gas Dynamics* Addison-Wesley, 1965.
35. W. H. Dorrance, *Viscous Hypersonic Flow*, McGraw-Hill Book Company, 1962.

REFERENCES (Continued)

36. J. M. Kelble and J. E. Bernardos, "High-Temperature Nonmetallic Materials", *Aerospace Engineering*, January 1963, p. 56.
37. S. W. Scala, "The Hypersonic Environment", *Aerospace Engineering*, January 1963, p. 10.
38. R. M. Bushong, "Graphite as an Aerospace Material", *Aerospace Engineering*, January 1963, p. 40.
39. T. D. Cooper and O. O. Srp, "Refractory Metals and Their Protection", *Aerospace Engineering*, January 1963, p. 46.
40. G. Kraus, *Uncooled Rocket Nozzles for Ultra-High Temperature Propellants*, SAE National Aerospace Engineering and Manufacturing Meeting, Los Angeles, Calif., SAE 595 J, October 8-12, 1962.
41. T. E. Chappell and J. I. Gonzalez, "Analyzing the Temperature Gradients in Super-Speed Vehicles", *Space/Aeronautics*, May 1962, p. 105.
42. E. V. Stupochenko et al., "Thermodynamic Properties of Air in the Temperature Interval From 1000°K to 12,000°K and the Pressure Intervals from 0.001 to 1000 atm", Translated from "Physical Gasdynamics," USSR Acad. Sci., *ARS Journal Supplement*, January 1960, p. 98.
43. M. L. Hill, "Materials for Structural Use Above 3000°F", *APL Technical Digest*, The Johns Hopkins University, Silver Spring, Md., March-April 1964, p. 2.
44. R. Jaroudi and A. J. McDonald, "Inject Thrust Termination and Modulation in Solid Rockets", *AIAA Jour.*, Vol. 2, No. 11, November 1964, p. 2036.
45. C. J. Green and F. McCullough, "Liquid Injection Thrust Vector Control", *AIAA Jour.*, Vol. 1, No. 3, March 1963, p. 573.
46. G. F. Hausman, *Thrust Axis Control of Supersonic Nozzles by Airjet Shock Interference*, United Aircraft Corporation, R-63143-24, May 1952.
47. H. J. Hollstein, "Jet Tab Thrust Vector Control", *Journal of Spacecraft*, Vol. 2, No. 6, Nov.-Dec. 1965, p. 927.
48. R. Sehgal, "Payload Separation and Thrust Termination in a Solid-Propellant Rocket Motor," *Aerospace Engineering*, May 1962, p. 6.
49. S. N. B. Murthy, *The Upstream Effects Due to Injecting a Jet of Gas Through the Wall of an Axi-Symmetric Nozzle*, Jet Propulsion Center, Purdue University, Report No. TM-63-3, January 1963.
50. H. D. Thompson, J. D. Hoffman and S. N. B. Murthy, *Note on a Parametric Analysis of Thrust Vector Control by Secondary Gas Injection*, Jet Propulsion Center, Purdue University, Report No. TM-63-5, February 1963.
51. R. D. Guhse, *An Experimental Investigation of Thrust Vector Control by Secondary Injection*, NASA CR-297, September 1965.
52. Robert Sehgal and Jai-Ming Wu, "Thrust Vector Control by Liquid Injection in Rocket Nozzles", *Journal of Spacecraft*, Vol. 1, No. 5, Sept.-Oct. 1964, p. 545.
53. G. W. Hawk and L. H. Geyer, "Secondary-Injection Thrust-Vector Control Systems", *Aerospace Engineering*, May 1962, p. 31.

REFERENCES (Continued)

54. M. Shandor, A. R. Stone and R. E. Walker, "Secondary Gas Injection Thrust Vector Control", *APL Technical Digest*, Johns Hopkins University, Silver Spring, Md., March-April 1963, p. 2.
55. T. Inouye and H. B. Nottage, "Experiments on Rocket Thrust Control by Hot Gas Injection", *Journal of Spacecraft*, Vol. 3, No. 5, May 1966, p. 737.
56. B. M. Dunn and A. F. Emery, "Thrust Vectoring Produced by a Supersonic Nozzle With an Oblique Exit Plane", *Journal of Spacecraft*, Vol. 3, No. 10, October 1966, p. 1500.
57. A. I. Ormsbee, R. E. Gardner, N. Rott and R. H. Nunn, "Thrust Magnitude Control for a Solid Rocket by Injection at the Throat", *AIAA Jour.*, Vol. 4, No. 8, August 1966, p. 1424.

CHAPTER 9

PROPERTIES AND CHARACTERISTICS OF LIQUID PROPELLANTS

9-1 FACTORS TO BE CONSIDERED IN SELECTING LIQUID PROPELLANTS

From a broad viewpoint the term liquid propellant refers to any liquid which is injected into the combustion chamber of a liquid rocket motor. By convention, however, the term is applied to any liquid chemical which is an essential component of the liquid chemical reactants, called the *liquid propellant system*, for producing the high temperature *propellant gas* which is expanded in the rocket exhaust nozzle.

Considerable research and development effort has been expended on synthesizing new propellants and improving the properties of the older ones. As a result there is a large number of liquid propellant systems (oxidizer + fuel) to choose from. There is no shortcut, however, for selecting the most suitable propellant system for a given application. The selection is greatly influenced by the operating requirements imposed upon the rocket engine¹.

For example, many military applications of liquid rocket engines require that the performance of the engines be unaffected by variations in the temperatures of the liquid over the range -65° to $+165^{\circ}\text{F}$. These operating specifications impose stringent limitations upon the number of liquid chemicals that can be considered as propellants for such applications. For ground-based ballistic missiles, as the IRBM and ICBM types, the operating temperature specifications can be relaxed materially so that there is a broader choice of liquid propellants for those applications.

In general, there are no liquid propellants which are ideal from all viewpoints—such as

performance, handling, storage, etc. Consequently, one must assess the relative importance of the advantages and disadvantages of the specific liquid propellant with regard to the particular application being considered.

From a strictly technical viewpoint the selection of a propellant system (fuel + oxidizer) should be governed by the factors pertinent to achieving the largest value of impulse-to-weight ratio for the liquid rocket-propelled vehicle. Sound engineering—combined with military needs—dictates that the selection consider the logistics, handling, storage, transportation, availability, toxicity, the use of strategic materials, and other practical factors. Consequently, the selection of a propellant system always involves a compromise between the technical and the practical factors pertaining to the application¹.

9-2 PRINCIPAL PHYSICAL PROPERTIES OF LIQUID PROPELLANTS^{1,2,3}

The properties to be considered in selecting a liquid propellant are discussed in this chapter. Detailed information on liquid propellants can be found in *Liquid Propellant Handbook*, Battelle Memorial Institute (Confidential), or obtained from Chemical Propellant Information Agency, Applied Physics Laboratory, Johns Hopkins University, Silver Spring, Maryland.

9-2.1 ENTHALPY OF COMBUSTION

It is desirable that the calorific value per unit weight of a bipropellant system be as large as possible.

9-2.2 CHEMICAL REACTIVITY

The bipropellants should react rapidly so that the required residence time for complete combustion is short. Otherwise, large values of the characteristics length L^* will be necessary (see par. 10-3.2.1).

If the propellants are hypergolic the engine design is simplified by not requiring an ignition system.

High chemical reactivity is desirable in that there is less danger of explosions from unburned propellants accumulating in the combustion chamber. Furthermore, there is evidence that combustion pressure oscillations are related to chemical reactivity and the susceptibility to them decreases with increased reactivity⁵.

9-2.3 CHEMICAL STRUCTURE

The chemical structures of the liquid propellants are important because they determine the composition of the propellant gas. From Eq. 6-3 it is apparent that the specific impulse I_{sp} is proportional $\sqrt{T_c/\bar{m}}$. Table 9-1 presents calculated values of specific impulse for several liquid propellant systems, based on shifting equilibrium, assuming isentropic expansion of the propellant gas from the nozzle inlet pressure $P_c = 1000$ psia to the nozzle exit pressure $P_e = 14.7$ psia. It is seen from Table 9-1 that values of I_{sp} as large as 411 sec are possible in the ideal case⁴.

To obtain large values of specific impulse the liquid propellants must be selected from those chemicals formed from the atoms listed in the first two rows of the periodic table; i.e., molecules containing one or more of the following elements: H, O, N, F, B, C, and Cl.

9-2.4 AVERAGE DENSITY OF PROPELLANT SYSTEM ($\bar{\rho}_p$)

The average density of the propellant system (fuel plus oxidizer), denoted by $\bar{\rho}_p$, should be high so that the dimensions and weights of the propellant tanks, the propellant pressurizing system, and the associated plumbing are minimized. In general, liquid fuels have smaller densities than liquid oxidizers; hence, those propellant systems giving satisfactory values of specific impulse with large values of mixture ratio r (where $r = \dot{m}_O/\dot{m}_F$) yield large values of average propellant density $\bar{\rho}_p$, and in most cases large values of density impulse I_d (see Eq. 6-34).

The density of a liquid propellant system is a function of its temperature. In the case of a petroleum fuel—such as JP-4, JP-5 or RP-1—the density also varies with the fuel chemical composition. Ordinarily, it is desirable to maintain a constant mixture ratio r for the propellants burned during the powered flight of the rocket-propelled vehicle, so that both fuel and oxidizer tanks will be emptied practically simultaneously. To achieve that objective, some form of automatic propellant utilization system must be provided for maintaining r at the required value.

In the case of a long-range ballistic missile, such as an ICBM, the variations in the density of the propellants due to aerodynamic heating are generally quite small because such a missile reaches a very low density atmosphere (high altitude) in less than one minute of the powered flight.

9-2.5 BOILING POINT AND VAPOR PRESSURE

A high boiling point, preferably above 100°F, is desirable so that the liquid propellants can be stored in lightweight tanks without incurring excessive loss by evaporation. For Army applications it is desirable for the vapor

pressure to be small at temperatures up to approximately 160°F. Otherwise, the evaporation of the propellant in storage will be excessive.

The boiling point and vapor pressure characteristics of a propellant exert a major influence upon the design and operating characteristics of the pressurizing system, particularly in the case of a turbopump system. Because of their low weight, high speed centrifugal pumps are employed exclusively in the turbopumps of large liquid propellant ballistic missiles. Propellants having low boiling points and high vapor pressures tend to induce cavitation phenomena in the pumps and supply lines. To prevent the occurrence of cavitation and vapor lock problems, the propellant tanks have to be pressurized with an inert gas, usually nitrogen or helium, so that pressures at all points in the feed system are above that inducing cavitation⁶. Propellants having large vapor pressures increase the required gas pressures and may necessitate increasing the thickness, and consequently the weights, of the propellant tanks.

9-2.6 FREEZING POINT

It is desirable that the propellant remain liquid at the lowest temperature to be encountered in storage on the ground and in flight. For certain applications some liquid chemicals cannot be considered for use as rocket propellants if their freezing points are above -65°F.

9-2.7 DYNAMIC OR ABSOLUTE VISCOSITY

A low dynamic viscosity is desirable at all operating temperatures; preferably less than 10 centipoises at -65°F. Otherwise, the pressure drop required for transferring the liquid propellant from the supply tank and injecting it into the rocket motor becomes excessive.

9-2.8 SPECIFIC HEAT

If the liquid propellant is utilized for cooling the rocket engine by forced convection, as in a regeneratively cooled rocket motor (see par. 10-4.3), a high specific heat is advantageous. The total amount of heat a regenerative coolant can absorb is equal to the product of its flow rate, specific heat, and the temperature rise between its inlet and saturation temperatures. From a cooling standpoint a high saturation temperature is also desirable. The saturation temperature should be at least 300°F but should not exceed approximately 700°F if the wall temperatures are to be kept from becoming dangerously high⁷.

9-2.9 CHEMICAL STABILITY

The liquid propellant should be stable chemically when stored within the desired temperature range for reasonable periods of time. It must also be stable at the temperatures it will encounter in the operation of the rocket engine. In that connection liquid chemicals which decompose and deposit salts when utilized as a regenerative coolant may not be usable for certain applications¹.

It is preferable that the liquid propellant not decompose violently when heated, nor be sensitive to shock.

9-2.10 CORROSIVITY

It is desirable that the liquid propellant have a low chemical reactivity with the materials employed for storage containers, valves, piping, rocket motors, bearings, pumps, gaskets, etc. Otherwise, problems arise concerned with the storage and handling of the propellant, and the design of the engine components.

Ordinarily, the fuel component of a bipropellant combination introduces fewer material

selection problems than the oxidizer. Nevertheless, the compatibility of the fuel with the available construction materials should be considered since several of the possible fuels do attack the more common metals and plastics.

The selection of the most appropriate materials for all of the components of a liquid propellant rocket engine is one of the major problems entering into the design and construction of a satisfactory engine⁸.

9-2.11 TOXICITY

It is desirable that the toxicity of the liquid propellant be low so that it can be handled with conventional equipment and procedures.

9-2.12 AVAILABILITY

Rocket propellants which would be used in large quantities during an emergency must either be readily available or their production potential must be ample to meet the anticipated demand.

9-2.13 COST

In determining the cost of the propellants for powering a liquid rocket-propelled vehicle, the total amount of propellants supplied to the vehicle from the time it is placed in service readiness to the completion of its firing must be taken into account. It is the total impulse of the missile divided by the cost of all of the propellant consumed that determines the impulse per unit of cost. Obviously, a large value of impulse per unit of cost is desirable.

It was pointed out earlier that the energy for propulsive purposes, in the case of a chemical rocket engine, is derived from a chemical reaction which produces gaseous products and liberates heat; the heat of the reaction raises the temperature of the reaction products to between 5000°F and 8500°F depending upon the

specific propellants involved. Only a portion, ordinarily between 50 and 60 percent of the heat of reaction, can be used for achieving a large exhaust jet velocity. Consequently, the specific impulse obtainable from a chemical rocket engine, regardless of type, is limited by the heat of reaction of the propellants burned in the rocket motor.

Propellant systems are generally compared at the same combustion pressure (usually 1000 psia for liquid propellants) assuming complete (isentropic) expansion of the combustion gases to standard sea level pressure (14.7 psia).

For any thermodynamic rocket engine—chemical, nuclear, electrothermal—the specific impulse, therefore, increases with the square root of the fraction of the available enthalpy converted into jet kinetic energy and the available enthalpy change is, of course, limited by the heat of reaction for the propellants. As mentioned earlier only 50 to 60 percent of the enthalpy can be converted into jet kinetic energy. There are substantial differences, however, in the percent of the enthalpy of the different propulsive gases that can be converted into jet kinetic energy.

Currently, the specific impulses obtainable with typical liquid bipropellant systems exceed those obtainable with solid propellant systems. For liquid systems it will be shown later that the maximum obtainable specific impulse is approximately 400 sec, compared with a *possibility* that specific impulses approaching 300 sec may be obtainable with solid propellants in perhaps a decade.

As can be inferred from par. 9-2, high specific impulse by itself is insufficient as a criterion for selecting a chemical propellant system. One must also consider—and this applies also to the propellants for electric rocket engines—the stability of the propellants under storage

TABLE 9-1
CALCULATED SPECIFIC IMPULSES FOR SEVERAL LIQUID
PROPELLANT SYSTEMS*

(Shifting Equilibrium, Isentropic Expansion; Adiabatic Combustion; One-dimensional Flow;
 $P_c = 1000 \text{ psia} \rightarrow P_e = 14.7 \text{ psia}$)

Oxidizer	Fuel	r^1	$\bar{\rho}_p^2$	T_c^3	c^{*4}	$I_{sp}^{5 \dagger}$
Chlorine Trifluoride (ClF_3)	($\text{N}_2 \text{H}_4$) Hydrazine	2.80	1.50	6553	5961	293.1
	($\text{N}_2 \text{H}_3 \text{CH}_3$) MMH ⁶	2.70	1.41	5858	5670	286.0
	($\text{B}_5 \text{H}_9$) Pentaborane	7.05	1.47	7466	5724	289.0
Fluorine (F_2)	(NH_3) Ammonia	3.30	1.12	7797	7183	359.5
	$\text{N}_2 \text{H}_4$	2.30	1.31	8004	7257	364.0
	(H_2) Hydrogen	7.70	0.45	6902	8380	411.1
	(CH_4) Methane	4.32	1.02	7000	6652	343.8
	$\text{N}_2 \text{H}_3 \text{CH}_3$	2.50	1.25	7612	6825	346.2
	$\text{B}_5 \text{H}_9$	4.45	1.20	8584	7135	360.8
	RP-1	2.62	1.21	6839	6153	318.0
Oxygen Bifluoride OF_2	($\text{B}_2 \text{H}_6$) Diborane	3.73	1.00	7764	7209	365.1
	$\text{N}_2 \text{H}_4$	1.54	1.27	6689	6736	339.0
	Aerozine-50 ⁷	2.15	1.25	7093	6795	341.8
	H_2	6.04	0.39	5880	8188	401.1
	CH_4	5.10	1.07	7334	6917	347.3
	$\text{N}_2 \text{H}_3 \text{CH}_3$	2.32	1.24	7202	6819	342.8
	$\text{B}_5 \text{H}_9$	3.88	1.18	8357	6969	354.4
	RP-1	3.82	1.28	7766	6838	340.7

* Based on *Theoretical Performance of Rocket Propellant Combinations*, Rocketdyne, a Division of North American Aviation, Inc.

TABLE 9-1 (Continued)

Oxidizer	Fuel	r^1	$\bar{\rho}_p^2$	T_c^3	c^{*4}	$I_{sp}^{5†}$
Hydrazine (N_2H_4)	B_2H_6	1.16	0.63	4080	6788	338.6
	B_5H_9	1.28	0.80	4661	6503	328.2
Hydrogen Peroxide (100%) (H_2O_2)	N_2H_4	2.00	1.26	4814	5765	287.4
	$N_2H_3CH_3$	3.44	1.26	4928	5665	284.8
	B_5H_9	2.42	1.04	5000	5990	307.6
IRFNA ⁹	Hydine ¹⁰	3.17	1.26	5198	5367	270.3
	$CH_3N_2H_3$	2.57	1.24	5192	5479	275.5
Nitrogen Tetroxide (N_2O_4)	N_2H_4	1.30	1.22	5406	5871	292.2
	Aerozine-50 ⁷	2.00	1.21	5610	5740	289.2
	$N_2H_3CH_3$	2.15	1.20	5653	5730	288.7
	B_5H_9	3.40	1.12	6866	5862	299.0
Liquid Oxygen (LOX) (O_2)	N_2H_4	0.91	1.07	5667	6208	312.8
	H_2	4.00	0.28	4910	7982	291.2
	CH_4	3.35	0.82	6002	6080	310.8
	B_5H_9	2.21	0.91	7136	6194	318.1
	RP-1	2.60	1.02	6164	5895	300.0

¹ r = mixture ratio = \dot{m}_O/\dot{m}_f

² ρ_p = mean density of propellant system, g/cc

³ T_c = chamber temperature, °F

TABLE 9-1 (Continued)

⁴	c^* = characteristic velocity, ft/sec								
⁵	I_{sp} = theoretical maximum specific impulse, sec								
[†]	To obtain I_{sp} for values of nozzle inlet pressure P_c other than $P_c = 1000$ psia: if $P_c =$ 300 400 500 600 700 800 900 1000, multiply values in Table 9-1 by 0.88 0.91 0.93 0.95 0.97 0.98 0.99 1.00								
⁶	MMH: Monomethyl Hydrazine - $N_2H_3CH_3$								
⁷	Aerozine-50: 50% Hydrazine + 50% UDMH ⁸								
⁸	UDMH: Unsymmetrical Dimethylhydrazine - $(CH_3)_2N_2H_2$								
⁹	IRFNA: Inhibited Red Fuming Nitric Acid: HNO_3 -84.4%; N_2O_4 -14%; H_2O -1%; HF -0.6%								
¹⁰	Hydine: UDMH ⁸ (60%), DETA ¹¹ (40%)								
¹¹	DETA: Diethylene Triamine - $C_2H_{13}N_3$								

conditions, its density, the safety and ease of handling, the combustion characteristics, the flame temperature, the compatibility with materials of construction, the physical and mechanical properties, etc. The propulsion system giving the highest specific impulse is not necessarily the best when all of the technological application factors are considered. The most appropriate system is that which satisfies the propulsion requirements with the lowest overall cost and also gives an engine having the required reliability. Hence, in judging the merits of different systems for a given mission it is the cost of placing a unit weight of payload in the desired location that is the main criterion, assuming equal reliabilities. In military applications the "instant readiness" of the propulsion system may be an overriding criterion, and there is no assurance that "instant readiness" will not become in the future an important criterion for certain space missions.

In a multistage space vehicle, such as an ICBM, the propulsion engine for each stage must impart a specified "burnout" velocity increment to the stages it propels. The "burnout" velocity increment depends on the specific impulse of the engine and the mass ratio (see par. 5-9.2), i.e., the ratio of the mass of the vehicle at "lift-off" to its mass after the propulsion engine has consumed its propellants.

In a multistage vehicle each stage is designed to furnish a specified burnout velocity increment and, because of the small aerodynamic resistance encountered by the upper stages, calculations show that it is desirable that the upper stages contribute larger speed increments than the lower stages. Hence, the propellants with larger values of specific impulse, if they can be used, should be burned in the later stages; it should be noted that each succeeding stage forms a part of the payload for the stage

preceding it. The importance of the specific impulse of the propellants depends primarily upon the incremental speed required from a given stage; the larger the required increment of speed, the more important is a high specific impulse. For a space vehicle the most important parameters are the payload and the speed of the final stage after all of the propellants have been consumed.

For the foreseeable future all spacecraft will be multistage vehicles, requiring large thrust chemical rocket engines for the *first* or *booster* stage. Until the nuclear heat-transfer rocket engine becomes operational, the upper stages will use high-energy propellants such as LOX-Liquid H_2 . As payloads increase—and as our knowledge of space increases, the desired missions will become more ambitious—it is reasonable to expect that the booster thrust requirements will continue to increase.

9-3 LIQUID MONOPROPELLANTS

A liquid monopropellant is a liquid chemical which requires no auxiliary liquid (oxidizer) to cause it to decompose and release its thermochemical energy. Liquid monopropellants may be grouped into three classes^{1,2,1}:

1. *Class A.* Materials which contain both the fuel and oxidizer in the same molecule. Some of the compounds in this group which have been considered as monopropellants are listed below.

<u>Compound</u>	<u>Chemical Formula</u>
Hydrogen Peroxide	H_2O_2
Ethylene Oxide	C_2H_4O
Nitromethane	CH_3NO_2
Ethyl Nitrate	$C_2H_5NO_3$
Methyl Nitrate	CH_3NO_3

Nitroethane	$C_2H_5NO_2$
Nitroethanol	$HOC_2H_4NO_2$
Diethylene Glycol Dinitrate (DEGN)	$(C_2H_4ONO_2)_2O$
Nitroglycerin	$C_3H_5(ONO_2)_3$
Picric Acid	$C_6H_2(NO_2)_3OH$

2. *Class B.* Liquids which contain either the oxidizer or the fuel constituents in an unstable molecular arrangement. Their decomposition releases thermal energy. Compounds in Class B have positive enthalpies of formation. Typical compounds are listed below.

<u>Compound</u>	<u>Chemical Formula</u>
Hydrazine	N_2H_4
Acetylene	C_2H_2
Ethylene	C_2H_4
Nitric Oxide	NO
Hydrogen Peroxide	H_2O_2

3. *Class C.* This class of compounds comprises synthetic mixtures of liquid fuels and oxidizers. To this class belong such materials as Diver's solution, NH_3 (liq.) = NH_4NO_3 , Myrol, CH_3NO_3 - CH_3OH , mixtures of hydrogen peroxide and methanol, ammonium nitrate mixtures, etc.

Since the beginning of World War II a large number of monopropellants have been investigated in the United States and other countries. Only the principal ones, those listed below, will be discussed.

1. Hydrazine
2. Concentrated hydrogen peroxide
3. Ethylene oxide

4. Mixtures of nitroparaffins
5. Mixtures of nitric acid, nitrobenzene and water, called *dithekites*
6. Mixtures of methyl nitrate and methanol, called *myrols*

In general, it appears that liquid monopropellants combine a high energy content with a high shock sensitivity, and yield specific impulse values smaller than those obtainable from liquid bipropellant systems. Of the monopropellants listed above only hydrazine (N_2H_4) and concentrated hydrogen peroxide have found applications as monopropellants—and also as the fuel and oxidizer component, respectively—in liquid bipropellant systems.

The gaseous decomposition products of hydrazine and of hydrogen peroxide are used for the *reaction controls* for space vehicles, such as Gemini and Apollo, for vernier rocket motors for adjusting the cut-off velocity of an ICBM to the desired value, for man-maneuvering space units, and for the high temperature gas for driving the turbines of turbopumps, and of auxiliary power units (APU's) for long-range ballistic missiles.

9-3.1 HYDRAZINE (N_2H_4)

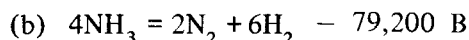
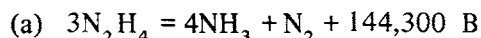
Hydrazine is a toxic colorless liquid having the following physical properties: molecular weight 32.048, density 1.01 g/cc, freezing point $35.1^\circ F$, normal boiling point $236.3^\circ F$, and heat of vaporization 540 B/lb_m. Its vapor pressure at $100^\circ F$ is approximately 7 psia, and its specific heat c_p ranges from 0.76 B/lb_m $^\circ F$ at $80^\circ F$ to 0.853 at $400^\circ F$ ^{9,10}.

Hydrazine can be used either as a monopropellant or as the fuel in a liquid bipropellant system. It is readily soluble in water, alcohol, and certain organic liquids. The water solution,

hydrazine hydrate ($N_2H_4 \cdot H_2O$), was used as the fuel with concentrated hydrogen peroxide as the oxidizer in the Walter rocket engine which propelled the German ME 163 airplane in World War II. It is hypergolic with hydrogen peroxide and also with nitric acid. The propellant system for the TITAN II missile is composed of a 50/50 mixture of hydrazine and unsymmetrical dimethylhydrazine as the fuel, and nitrogen tetroxide as the oxidizer.

Hydrazine and its hydrates are toxic; inhalation of their vapors and prolonged contact of the skin to the liquid are harmful¹¹.

Because it is thermally unstable, hydrazine can be caused to undergo an exothermic decomposition which apparently takes place in the following two steps:



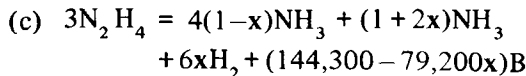
Consequently, the specific impulse obtained from the thermal decomposition of hydrazine depends upon which reaction products are formed. Because reaction (b) is endothermic the decomposition according to reaction (a) gives the higher specific impulse. The decomposition of ammonia (NH_3), reaction (b), is generally a slow process. Hence, if the reaction time is limited as is usually the case, only a small portion of the ammonia formed by reaction (a) will become dissociated. Consequently, the decomposition of hydrazine gives a larger specific impulse if the characteristic length L^* , which is a measure of the time available for decomposing the hydrazine, is short enough to prevent any substantial decomposition of the ammonia formed by reaction (a).

Experiments have demonstrated that the decomposition reaction for hydrazine is influenced by temperature and the presence of

TABLE 9-2
PHYSICAL PROPERTIES OF WATER SOLUTIONS OF HYDROGEN PEROXIDE

Property	Concentration in Percent by Weight			
	70	80	90	100
Freezing Point, °F	−38.2	−10.8	12.6	30.4
Boiling Point, °F	254	269	288	312
Specific Gravity (at 64.4°F)	1.291	1.341	1.394	1.450
Viscosity, centipoise (at 64.4°F)	1.287	1.297	1.301	1.307
Vapor Pressure, psia (at 100°F)	0.023	0.016	0.012	0.007
Heat of Vaporization, B/lb _m	682	634	588	540

catalysts. Accordingly, it is difficult to specify the exact stoichiometry in a given case. Hence, if x denotes the fraction of the ammonia which is decomposed, reactions (a) and (b) can be combined to give²³



If the performance parameters for hydrazine are plotted as a function of the percent of ammonia dissociated, it is found that when $x = 0$, $I_{sp} = 192$ sec and when $x = 100$, $I_{sp} = 168$ sec.

Several materials, such as metallic iron, nickel, and cobalt supported on porous aluminum oxide, catalyze the decomposition of hydrazine. A relatively new catalyst which causes a spontaneous decomposition of hydrazine has made the latter an attractive mono-

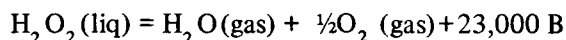
propellant, particularly for reaction control systems. The gaseous decomposition products, using the new catalyst, are at a temperature of approximately 1800°F and yield a vacuum specific impulse of approximately 235 sec, for an area ratio of 50¹³.

The principal disadvantage encountered in the application of hydrazine is its high freezing point of 35°F. Experiments have shown that the freezing point can be depressed by adding nitric acid (HNO₃) and water to the hydrazine. Solutions containing more than 17 percent nitric acid by weight tend to become unstable and shock sensitive.

9-3.2 HYDROGEN PEROXIDE (H₂O₂)

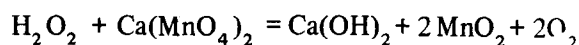
Hydrogen peroxide is used as a rocket propellant in concentrations ranging from 70 to 98 percent. Table 9-2 presents the physical properties of hydrogen peroxide solutions as a function of H₂O₂ concentration.

Hydrogen peroxide can be readily decomposed either thermally or with suitable catalysts according to the following equation:



The heat of decomposition of 98% H_2O_2 (at 77°F and 1 atm) is 1215 B/lb_m, and the adiabatic decomposition temperature (at 1 atm) is 1735°F. The corresponding decomposition products are 53.1% H_2O and 46.9% O_2 ; their specific heat ratio $\gamma = c_p/c_v = 1.251$. When 100% H_2O_2 is used as a monopropellant (at $P_c = 300 \rightarrow P_e = 14.7$) the gas temperature $T_c = 1800^\circ\text{F}$ and the theoretical specific impulse is 146 sec.

The kinetics of the catalytic decomposition of H_2O_2 solutions has been investigated extensively in this and other countries. Concentrated calcium and sodium permanganate solutions are effective materials (catalysts) for decomposing hydrogen peroxide. Calcium permanganate, $\text{Ca}(\text{MnO}_4)_2$, is preferred because of its greater solubility in water. The decomposition equation, using $\text{Ca}(\text{MnO}_4)_2$, is



Alundum pellets soaked in a strong solution of calcium permanganate for several hours, dried, and packed into a *decomposition chamber* present a large catalytic surface of $\text{Ca}(\text{MnO}_4)_2$ to the H_2O_2 flowing through the decomposition chamber. Once the decomposition of the hydrogen peroxide has been initiated, it proceeds smoothly.

In the United States the most widely used catalyst is the solid samarium oxide coated silver screen. The coated silver screens are usually arranged as a tightly compressed pack in the decomposition chamber, thereby exposing a large surface to the hydrogen peroxide passing

over and around the screens. Silver ions pass into the solution of H_2O_2 and react with the H_2O_2 decomposing it into H_2O and O_2 with the liberation of heat, which increases the rate of decomposition and raises the temperature of the screens and the H_2O_2 . The adiabatic decomposition temperature for the H_2O_2 is attained in a few milliseconds, and, in theory, the reaction rate would remain constant indefinitely, if required, unless the catalyst is poisoned by foreign matter. In practice, however, there are several factors which limit the useful life of the catalyst pack^{1 6}.

As a rocket propellant, hydrogen peroxide suffers from the following disadvantages: it is thermally sensitive, chemically unstable at high temperature, and has a relatively high freezing point. The problems of handling and storing solutions of H_2O_2 , however, have been thoroughly investigated. Experience has demonstrated that the pure material can be stored for reasonable periods in vented containers made from specially treated aluminum. The aluminum content of the container should be 99.7% and its copper content should not exceed 0.06%. Great care must be exercised to prevent impurities—such as iron oxide (rust), organic matter, dust, copper, etc.—from entering the container.

It is found that oxygen gas is continuously evolved from concentrated hydrogen peroxide solutions, even at ambient temperatures, but at low temperatures the rate of gas evolution is low enough to be considered negligible.

The relatively high freezing points of concentrated hydrogen peroxide solutions (see Table 9-2) are disadvantageous for many applications. Considerable research has been expended on investigating materials for depressing the freezing points of concentrated hydrogen peroxide solutions. The three which have been investigated most thoroughly are water, ammonium nitrate, and glycols.

Much effort has also been expended on investigating the ternary system hydrogen peroxide-ethylene glycol-water. To obtain a low freezing point with the latter mixture, the water content must be relatively large (more than 20 percent by weight). This reduces the oxygen content of the mixture and makes the latter unsuitable for application as the oxidizer in a bipropellant system. It does, however, have application as a monopropellant; the ethylene glycol increases its energy content.

9-3.3 ETHYLENE OXIDE (C_2H_4O)

Because of the safety with which it can be handled, ethylene oxide (C_2H_4O) has received extensive study during the past decade. This material decomposes into carbon monoxide (CO) and methane (CH_4).

Because it has a low flash point it must be handled as carefully as gasoline. Although it is insensitive to shock it will ignite if in contact with catalytic surfaces. It can be stored in steel or stainless steel drums and is readily available commercially^{18,19}

9-3.4 MIXTURES OF NITROPARAFFINS

Nitromethane, a somewhat oily colorless liquid, has been investigated quite thoroughly as a monopropellant. It gives a reasonable specific impulse 220 sec at $P_c = 300$ psia and $T_c \approx 4000^\circ F$). It is neither toxic nor corrosive. Because of its shock sensitivity and the problem of obtaining efficient combustion in a motor having a reasonable characteristic length, it has found no application.

Studies of mixtures of nitromethane with nitropropane to reduce shock sensitivity demonstrated that as the shock sensitivity of the mixture was reduced—by increasing the percentage of nitropropane—the specific impulse obtained became unacceptably low.

9-3.5 MIXTURES OF NITRIC ACID, NITRO-BENZENE AND WATER (DITHEKITES)

These monopropellants were investigated during World War II. It was found that unless the mixture contained at least 20 percent water by weight it was too sensitive for use as a monopropellant. The specific impulses obtainable with dithekites ranged from 190 to 208 sec.

9-3.6 MIXTURES OF METHYL NITRATE AND METHANOL (MYROLS)

The Germans investigated such mixtures during World War II, and concluded that they gave unacceptably low specific impulses (approximately 180 sec). Furthermore, they were too sensitive to shock. It is worth noting that methyl nitrate is almost as shock sensitive as nitroglycerin.

9-4 OXIDIZERS FOR LIQUID PROPELLANT SYSTEMS

The performance of a liquid bipropellant system depends upon the thermodynamic properties of the oxidizer and of the fuel. Reference to Table 9-1 shows that the characteristics of the oxidizer have a greater effect upon the specific impulse than do those of the fuel. Only a few liquid chemicals are suitable as practical oxidizers. Consequently, when selecting a bipropellant system for a given application, the usual procedure is first to select the oxidizer and then that fuel which when used with the oxidizer gives the most favorable bipropellant system from all points of view (see par. 9-2).

The atoms that are useful as oxidizers in rocket propellant systems are oxygen and fluorine since they give highly exothermic combustion reactions. Consequently, the suitable liquid oxidizers are either the elements oxygen and fluorine or compounds containing a large proportion of those elements¹. For a material to be a suitable oxidizer it should not have a large

enthalpy of formation, otherwise, its enthalpy of combustion will be relatively small²⁰. A low enthalpy of formation indicates low bond energies between the atoms in the molecule. The requirement of low bond energies suggests that the most suitable compounds are those containing the nonmetallic elements (Groups V, VI, and VII of the periodic table). The single exception is hydrogen which occurs in many oxygenated compounds. The large bond energy of hydrogen (103.4 kcal/mole) causes a loss in combustion energy, but the low atomic weight of hydrogen partially compensates for that loss. For those reasons the liquid oxidizers which are useful in rocketry are primarily compounds containing the elements fluorine, hydrogen, nitrogen, and oxygen. The prime oxidizers are, of course, fluorine and oxygen. Table 9-3 presents the physical properties of the more important oxidizers in the following groups:

- A. Oxidizers containing fluorine and no oxygen.
- B. Oxidizers containing oxygen and no fluorine.

Only the more important oxidizers in the above two groups will be discussed.

9-4.1 LIQUID FLUORINE (F_2)

A given fuel yields a larger enthalpy of reaction with liquid fluorine than with liquid oxygen because the hydrogen in the fuel forms HF which does not dissociate as much as the H_2O formed with oxygen (see Fig. 6-1). Because fluorine is monovalent while oxygen is divalent, more fluorine than oxygen is required for burning a given fuel. Since the specific gravities of oxidizers are, in general, larger than those of fuels, the larger mixture ratios required with fluorine oxidizers result in the propellant system (fuel plus oxidizer) having a higher average density. To illustrate, consider the combustion

of anhydrous liquid ammonia (NH_3) in stoichiometric proportions with fluorine and with oxygen. The specific impulse obtained from the F_2-NH_3 system is 313 sec and its average density is 1.20 g/cc. For the O_2-NH_3 system the corresponding values are 255 sec and 0.89 g/cc. Fig. 9-1 is a bar-graph chart which compares the performances of several fuels when burned with either liquid fluorine or liquid oxygen, at 500 psia combustion pressure^{22,23,24}. It is seen that the largest value of specific impulse is obtained with the fluorine-hydrogen system (373 sec at 500 psia). The corresponding flame temperature is 7940°F and the molecular weight of the propulsive gas is 8.9.

Although liquid fluorine is the best oxidizer for obtaining high specific impulse and a large average density, it has several disadvantages, the three principal ones being (1) its low boiling point ($-188^\circ C$), (2) its extreme chemical activity, and (3) its high toxicity. Compared to liquid oxygen it is much more expensive, less available, and more hazardous to handle. The logical application for liquid fluorine is in the upper stages of long-range missiles where the superior performance obtainable with fluorine can be utilized advantageously.

Fluorine reacts readily with most metals, organic matter, concrete, glass, and water. Consequently, water cannot be used to quench the reaction of fluorine with metals, organic matter, etc., once the reaction has started. Fluorine can be stored, however, at temperatures below $100^\circ C$, in clean dry containers made from copper, nickel, monel metal, and aluminum; a protective film of metal fluoride is formed that adheres tenaciously to the metal surface.

Because of the difficulties in handling liquid fluorine and its low availability, it appears that for the next few years at least, liquid fluorine will be considered only for special applications.

TABLE 9-3
PHYSICAL PROPERTIES OF SEVERAL LIQUID OXIDIZERS

Oxidizer	Formula	\bar{m}^1	ρ^2	$\Delta H_f^O^3$	F.P.T. ⁴	B.P.T. ⁵	T _{cr} ⁶	P _{cr} ⁷
A. OXIDIZERS CONTAINING FLUORINE								
Fluorine	F ₂	37.95	1.50 ⁸	-3.03 ⁸	-217.96	-187.97	-129.2	55.0
Nitrogen Trifluoride	NF ₃	71.00	1.54 ⁸	-34.8 ⁸	-206.79	-129.01	-39.1	44.7
Chlorine Trifluoride	ClF ₃	92.45	1.81 ¹⁰	-44.3 ¹⁰	-76.3	11.75	174.	57.
Tetrafluoro Hydrazine	N ₂ F ₄	104.01	1.5 ⁸	-5.2 ⁸	-163.	-73.	36.	77.
Chlorine Pentafluoride	ClF ₅	130.45	1.74 ¹⁰	-60. ¹⁰	-103.	-13.6	119.	41.2
Bromine Pentafluoride	BrF ₅	174.90	2.47	-109.6	-62.5	40.3	196.8	53.6
B. OXIDIZERS CONTAINING OXYGEN								
Oxygen	O ₂	32.0	1.14 ⁸	-3.08 ⁸	-218.8	-183.0	-118.9	49.7
Ozone	O ₃	48.0	1.46 ⁸	+30.2 ⁸	-142.5	-111.9	-12.1	54.6
Hydrogen Peroxide (90%)	H ₂ O _{1.96}	33.38	1.39	-49.1 ⁹	-11.5	141.	395.	214.7
Hydrogen Peroxide (100%)	H ₂ O ₂	34.02	1.44	-44.8	-0.89	151.4	457.	214.
Nitrogen Tetroxide	N ₂ O ₄	92.01	1.43 ¹⁰	-4.66 ¹⁰	-11.23	21.15	157.8	99.0
MON-25 N ₂ O ₄ 75% NO 25%	N ₂ O _{3.32}	81.13	1.37 ⁸	+6.68 ^{9,10}	-54.	-15.	—	—
Tetranitromethane	CN ₄ O ₈	196.0	1.63	+10.3	14.1	126.	Ex- plodes	
TNM eutectic CN ₄ O ₈ 64% N ₂ O ₄ 36%	CN ₆₄ O _{12.8}	306.4	1.55	+4.7	-30.5	32.2	Ex- plodes	

TABLE 9-3 (Continued)

Oxidizer	Formula	\bar{m}^1	ρ^2	$\Delta H_f^O^3$	F.P.T. ⁴	B.P.T. ⁵	T _{cr} ⁶	P _{cr} ⁷
Nitric Acid	HNO ₃	63.01	1.50	-41.6	-42.0	86.0	255.	84.4
RFNA-III								
HNO ₃	85.7%							
N ₂ O ₄	14.7							
H ₂ O	2.6	HN _{1.02} O _{2.95}	62.49	1.55	-41.6 ⁹	-54.	60.	—

* Molecular weights, freezing points, and meeting points (where available) were taken from the *Handbook of Chemistry and Physics*, College Edition, 46th Edition, 1965-1966. All other data were taken from *Liquid Propellant Handbook*, CPIA.

¹ \bar{m} - molecular weight

² ρ - density at 25°C, g/cc

³ ΔH_f^O - enthalpy of formation at 25°C, unless otherwise noted, kcal/mole

⁴ F.P.T. - freezing or melting point, °C

⁵ B.P.T. - boiling point, °C

⁶ T_{cr} - critical temperature, °C

⁷ P_{cr} - critical pressure, atm

⁸ liquid at normal boiling point

⁹ heat of mixing included

¹⁰ liquid at 25°C under own vapor pressure

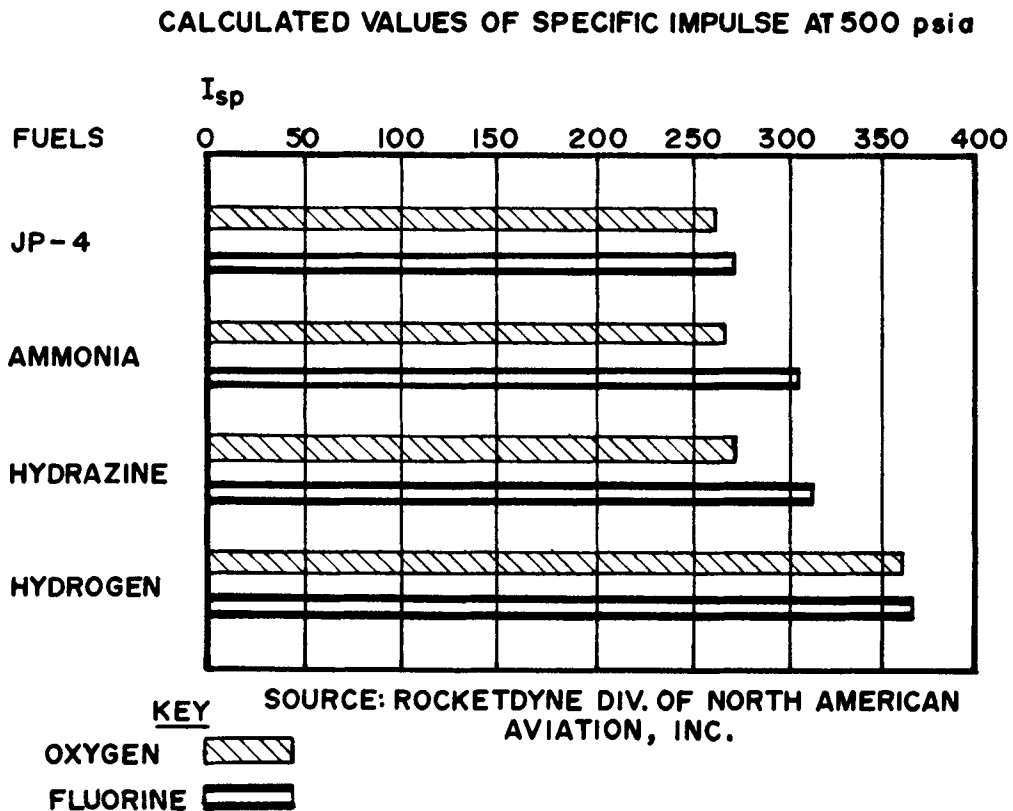


Figure 9-1. Comparison of Specific Impulses Obtained With Several Liquid Fuels Reacted With Liquid Fluorine and With Liquid Oxygen

In general, the gases ejected from rocket motors burning oxidizers containing fluorine contain large quantities of HF. Experiments have demonstrated that there is insignificant contamination and corrosion of the firing site associated with burning fluorine in rocket engines of moderate size. Because HF has a low molecular weight it tends to dissipate rapidly in the air.

9-4.2 LIQUID OXYGEN (LOX)

Historically, LOX was one of the first oxidizers used in liquid propellant rocket systems. LOX is the oxidizer which was used in the REDSTONE and JUPITER missiles, and is currently used in such ballistic missiles as the

ATLAS, TITAN, and THOR. With the exception of ozone and the fluorine group of oxidizers, LOX gives the best performance, on a weight basis, of any oxidizer. Since LOX is prepared from liquid air by fractional distillation, it can be produced cheaply (about 3 cents per lb) at any desired site. Furthermore, because of its widespread industrial use, its manufacturing and handling technology is well developed. Recent years have brought the development of air transportable LOX generators.

The principal disadvantages of LOX arise from its being liquefied gas, and the fire risk attendant to its use. Because of its volatility, its transport and storage introduce severe problems. If stored in bulk in insulated tanks, the loss due

to evaporation is of the order of 2 percent per day but, stored in vacuum jacketed tanks, the evaporation loss can be reduced to a fraction of a percent per day. It does not appear feasible at this time either to transport or store LOX in the oxidizer tanks of either launch vehicles for spacecraft or ballistic missiles, hence these tanks must be filled with LOX in the field or at the launching site. Consequently, LOX generators must be provided to replace the losses of LOX due to evaporation.

Even though a relatively small quantity of LOX is actually consumed in firing a missile, its real cost is much greater than might be assumed from the factor that LOX is plentiful and can be produced cheaply. The cost of storage tanks, LOX generators, evaporation losses, and the maintenance of an extensive crew to service launch vehicles or missiles using LOX must be included in the actual cost of LOX consumed. Thus, despite its plentiful supply, low cost of production, and broad background of industrial and military use, LOX is really unsuitable as the oxidizer for tactical missiles. In fact, when all the problems and costs concerned with handling, storing, servicing, complexity, and cost of LOX missiles are considered, it appears probable that LOX may not even be the best choice of oxidizer for some of the missiles in which it is currently being used.

9-4.3 OXIDIZERS CONTAINING FLUORINE

9-4.3.1 GENERAL CONSIDERATIONS

The compounds of fluorine with the non-metallic elements nitrogen, chlorine, bromine, and iodine are of interest because the fluorine atoms are relatively loosely held in those compounds. The properties of several fluorine compounds are presented in Table 9-3 (see A. Oxidizers Containing Fluorine).

Of the compounds listed in Table 9-3, only ClF_3 and NF_3 contain a large enough percentage by weight of fluorine to give good performance. Bromine pentafluoride (BrF_5) may be of interest because of its high density, 2.47 g/cc at 25°C.

9-4.3.2 CHLORINE TRIFLUORIDE (ClF_3)

Although nitrogen trifluoride (NF_3) gives higher performance than chlorine trifluoride (ClF_3) it has not received as much attention as ClF_3 because NF_3 is a liquefied gas at ambient temperatures (see Table 9-3). Chlorine trifluoride has a large density (1.81 g/cc), a low freezing point (-76.3°C), and can be handled as a liquid at ambient conditions; its vapor pressure is less than 100 psia at 71°C . Reference to Table 9-1 shows that if ClF_3 is reacted with hydrazine (N_2H_4) at 1000 psia, the specific impulse obtained – based on shifting equilibrium – is 293.1 sec.

Since ClF_3 is produced by the direct reaction between gaseous chlorine and gaseous fluorine its availability depends upon the potential supply of fluorine.

The exhaust products of a rocket motor burning ClF_3 contain both hydrogen fluoride (HF) and hydrogen chloride (HCl). The higher molecular weight of the latter can cause it to persist in the launching area especially on a humid day.

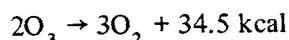
9-4.4 OXIDIZERS CONTAINING OXYGEN

The principal oxidizers containing oxygen atoms and no fluorine atoms are liquid ozone (O_3), hydrogen peroxide (H_2O_2), nitric acid (HNO_3), and a mixture of nitric oxide (NO)

with nitrogen tetroxide (N_2O_4) for brevity termed mixed oxides of nitrogen (MON). Table 9-3 presents the physical properties of the principal oxidizers containing oxygen.

9-4.4.1 LIQUID OZONE (LOZ)

Liquid ozone, for brevity designated as LOZ, is a deep blue liquid. It boils at -112°C , its density is 1.46 g/cc at -183°C and it has a negative heat of formation (-30.2 kcal/mole at -112°C). Propellant systems based on LOZ give specific impulse values comparable to those based on liquid fluorine (see Table 9-1). LOZ is made by the silent discharge of electricity through oxygen gas^{25,26}. The O_3 molecule is thermally unstable and sensitive to shock. These factors combined with its large oxidizing potential make LOZ hazardous to handle. It decomposes with explosive violence according to the equation



It is important to keep LOZ chemically pure. Hence, the oxygen used in making LOZ must be free of even traces of impurities. The sensitivity of LOZ can be reduced by making mixtures of LOZ in LOX. Thus a solution of LOX containing approximately 25 percent LOZ is quite stable to shock, and the mixture boils as a single phase at -112°C . Calculations show, however, that burning the 75LOX-25LOZ mixture with gasoline increases the specific impulse above that when LOX alone is used by approximately 6 sec. Since LOX is more volatile than LOZ (see Table 9-3), the 75-25 mixture tends on storage to increase the LOZ content due to the evaporation of LOX. When the LOZ concentration exceeds approximately 30 percent, explosions of extreme violence can result from contamination with minute traces of organic matter²⁶.

Since LOZ has not as yet been effectively stabilized, and because of the small increase in performance with the 75LOX-25LOZ mixture, LOZ cannot be considered to be a promising oxidizer at this time.

9-4.4.2 HYDROGEN PEROXIDE (H_2O_2)

For completeness, hydrogen peroxide is listed here as an oxidizer. The principal characteristics of concentrated solutions of H_2O_2 were presented in par. 9-3.2 where its use as a monopropellant was discussed. Despite their relatively high freezing points, water solutions of H_2O_2 containing 90 percent or more H_2O_2 have been considered for certain applications. The high density, high boiling point, and good performance (see Table 9-1) obtainable with such solutions make them attractive as a replacement for liquid oxygen. In applications where a large value of density impulse is of importance, certain hydrogen peroxide propellant systems may be suitable. Furthermore, in a missile using hydrogen peroxide as the oxidizer, "monopropellant runout" can be employed if the fuel is consumed but not all of the hydrogen peroxide.

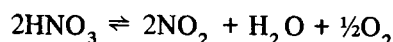
9-4.4.3 NITRIC ACID (HNO_3)

The following fuming nitric acids have been considered as oxidizers: white fuming nitric acid (WFNA), red fuming nitric acid (RFNA), and mixed acid (MA). The principal disadvantages of nitric acids are the tendency to decompose thermally, and their high corrosivity. These disadvantages introduce storage problems.

WFNA has been used in this country in several liquid propellant engines for rocket-

assisted take-off (RATO) and in-flight-thrust-augmentation (IFTA). Its composition is 98 percent HNO_3 , 2 percent H_2O with traces of N_2O_4 .

Considerable effort has been expended on improving the stability of fuming nitric acid and decreasing its corrosivity. The thermal decomposition of HNO_3 may be expressed by the equilibrium equation^{27,28,29}



Studies of the above reaction indicate that its rate is slow at temperatures below 71°C but increases rapidly above that temperature. Because the oxygen gas formed is relatively insoluble in the acid, very high storage pressures can be encountered in containers having small ullages. Moreover, since the NO_2 and H_2O are more soluble in the acid than the oxygen, the composition of the acid changes with the storage time within the range of the initial and equilibrium concentrations of NO_2 and H_2O . If the thermal decomposition is accompanied by corrosion of the container material, then the composition of the acid changes continuously in storage, which is undesirable³².

Although a great deal of effort has been expended, no inhibitor has been discovered for reducing the rate of thermal decomposition to a negligible value. Consequently, attention has been given to the use of additives for lowering the equilibrium decomposition pressure^{30,33}.

It is apparent from the decomposition equation for nitric acid that the addition of NO_2 and H_2O to the acid should decrease the amount of O_2 formed, since they appear in the equation and, consequently, reduce the equilibrium storage pressure. A satisfactory red fuming nitric acid (RFNA) — containing on a weight basis approximately 83-84% HNO_3 , 14% NO_2 , and 2

to 3% water—will reduce the oxygen pressure to less than 100 psia where filling voids are of the order of 10%. The latter storage pressure is satisfactory for many purposes.

It has been found that the addition of small amounts of hydrofluoric acid (HF) to fuming nitric acid will reduce its corrosion attack on certain stainless steels and aluminum alloys³³.

A fuming nitric acid containing 84.4% HNO_3 , 14% N_2O_4 , 1% H_2O , and 0.6% HF is known as IRFNA, *inhibited red fuming nitric acid*. It freezes at -65°F , has a density of 1.56 g/cc at 65°F , and can be stored for practically indefinite periods, at temperatures up to 160°F , in either aluminum or stainless steel containers with no serious corrosion. Where the ullage volume is of the order of 10 percent of the storage container volume, the equilibrium storage pressure does not exceed 100 psia. IRFNA was the oxidizer used in the CORPORAL missile and is currently used in the LANCE missile.

IRFNA is the only oxidizer in current use that has a low freezing point (-65°F), a high density (1.56 g/cc) a reasonable vapor pressure at ambient temperature (7 psia at 120°F), and a low viscosity. Propellant systems based on IRFNA (see Table 9-1) do not give as high a specific impulse values as those based on either F_2 or LOX. IRFNA appears to be ideally suited, however, to those applications where the propellant system must be *storable* and the lower specific impulse is acceptable; for example, for *prepackaged storable* tactical missiles for short and medium ranges such as BULLPUP, CONDOR, and LANCE⁸.

9-4.4.4 MIXED OXIDES OF NITROGEN (MON)

Table 9-4 presents the physical properties of the seven known oxides of nitrogen: N_2O , NO ,

N_2O_3 , NO_2 , N_2O_4 , N_2O_5 and NO_3 . It is evident from the data listed in Table 9-4 that N_2O_3 , N_2O_5 , and NO_3 are too unstable under ordinary conditions to be satisfactory liquid propellants. Of the remaining oxides only nitric oxide (NO) and nitrogen tetroxide (N_2O_4) have been applied as oxidizers in liquid bipropellant systems. NO and N_2O_4 appear together in a mixture termed *mixed oxides of nitrogen* (MON) (See Table 9-3).

The principal advantage of nitrogen tetroxide is that at low concentrations of water (less than 0.1 percent by weight) it can be stored practically indefinitely in either mild steel or aluminum containers. Its two principal disadvantages are its high melting point (11.2°C) and its extreme toxicity.

A number of freezing point depressants have been investigated and the most promising one is nitric oxide (NO). Because of the high volatility of the NO, the vapor pressure of solutions of NO in N_2O_4 becomes quite high at a storage temperature of 160°F. Thus a solution containing 16.85 percent NO by weight has a freezing point of approximately -29°F, and a vapor pressure of approximately 240 psia. Reference 35 presents data on the freezing point and vapor pressure of solutions of NO in N_2O_4 —i.e., MON solutions—as a function of the NO concentration.

As noted above, MON is extremely toxic. The maximum tolerable concentrations are quite small, 500 parts per million being rapidly fatal and exposure for 30 to 60 minutes to a concentration of 100 parts per million being dangerous. Since missiles using MON or N_2O_4 as the oxidizer could be filled at the factory, thereby eliminating the need for handling it in the field, its toxicity should not rule it out as a possible oxidizer. Where space is limited, however, as on board a ship or submarine the dangers from accidental damage to a storage tank may be sufficiently great to prohibit its

use. Recent experience with N_2O_4 has been favorable from the standpoints of handling and hazard to personnel⁸. It is the oxidizer used in the TITAN II missile.

9-4.5 OXIDIZERS CONTAINING FLUORINE AND OXYGEN

Fuels containing hydrogen, carbon, and certain metals, such as boron, yield the maximum values of specific impulse when they are burned with an oxidizer containing both fluorine and oxygen. The combustion products obtained by burning such fuels with either oxygen or fluorine are tabulated below.

Element	Combustion Products	
	With Oxygen	With Fluorine
Hydrogen (H)	H_2O	HF
Carbon (C)	CO, CO_2	CF_4 , CF_3 , CF_2 , CF
Boron (B)	B_2O_3	BF_3

The molecular weights of H_2O and HF are comparable, 18.016 and 20.008, respectively, but HF is much more stable thermally than H_2O . Hence, if the predominant constituent of a fuel is hydrogen, then it will give a larger specific impulse with fluorine than with oxygen.

The molecular weights of CO and CO_2 , on the other hand, are smaller than those of the fluorocarbon species. Hence, if a fuel has a large carbon content, it gives its largest specific impulse with oxygen as the oxidizer.

TABLE 9-4
PHYSICAL PROPERTIES OF OXIDES OF NITROGEN

Oxide	Formula	\bar{m}^1	ρ^2	F. PT. ³	B.P.T. ⁴	ΔH_f° ⁵	Stability at Room Temp.
Nitrous Oxide	N ₂ O	44.01	1.226 ⁻⁸⁹	-90.8	-88.5	19.49 ⁶	Stable
Nitric Oxide	NO	30.01	1.269 ⁻¹⁵²	-163.6	-151.8	21.6 ⁶	Stable
Nitrogen Trioxide	N ₂ O ₃	76.01	1.447 ²	-102	3.5	20.0 ⁶	Unstable
Nitrogen Dioxide	NO ₂	46.01	1.45 ²⁰	-11.2	21.2	8.09 ⁶	Stable
Nitrogen Tetroxide	N ₂ O ₄	92.01	1.45 ²⁰	-11.2	21.2	2.31 ⁶	Stable in equilibrium with NO ₂
Nitrogen Pentoxide	N ₂ O ₅	108.01	1.63 ¹⁸	-32.4*	47	0.70 ⁶	Low stability
Nitrogen Peroxide	NO ₃	62.00	—	-142**	—	13.0 ⁶	Very unstable

¹ \bar{m} - molecular weight

² ρ - density at °C temperature indicated, g/cc

³ F.P.T. - freezing or melting point, °C

⁴ B.P.T. - boiling point, °C

⁵ ΔH_f° - enthalpy of formation at 25°C, kcal/mole (Values of ΔH_f° are taken from Reference 38)

⁶ - gas

* - N₂O₅ sublimates and decomposes rapidly.

** - Solid NO₃ trapped at -185°C began decomposing rapidly at -143°C

The carbon fluorides— CF_4 , CF_3 , CF_2 , CF —are seldom found in the propulsive gas ejected from the exhaust nozzle of a rocket motor burning fluorine and a carbonaceous fuel. Instead, one finds that the gas contains free carbon.

It appears, therefore, that in the case of fuels containing the elements H and C, the maximum values of I_{sp} are obtained with oxidizers containing both fluorine and oxygen; the hydrogen reacting with the fluorine and the carbon with the oxygen. A similar situation occurs in the case of fuels containing boron. Calculations show that the maximum specific impulse is obtained with an oxidizer containing oxygen and fluorine.

Table 9-5 presents the physical properties of some oxidizers which are compounds containing fluorine and oxygen. A few of these oxidizers are discussed below.

9-4.5.1 OXYGEN BIFLUORIDE (OF_2)

Oxygen bifluoride (OF_2), also called fluorine monoxide, and the 70% F_2 + 30% O_2 mixture give reasonably high values of specific impulse with noncarbonaceous fuels, and also with fuels containing boron. OF_2 has a higher boiling point than the aforementioned mixture and is easier to handle. Moreover, there is the advantage that the proportions of a fluorine-oxygen mixture can be adjusted to the carbon-hydrogen ratio of a carbonaceous fuel. Since OF_2 is made from fluorine and the process gives a low yield of OF_2 , it is more expensive than either fluorine or fluorine-oxygen mixtures.

9.4.5.2 PERCHLORYLFLUORIDE (ClO_3F)

This oxidizer is a relatively recent development. Its basic advantages are that it is compatible with most materials of construction, and its density is relatively high (1.41 g/cc at 25°C). Its principal disadvantages are the HCl and HF in the exhaust products, its low availability, and high cost.

From an overall standpoint ClO_3F does not appear to offer any substantial advantages over oxidizers such as H_2O_2 , IRFNA, and MON. Moreover, its high vapor pressure is a disadvantage in using it in prepackaged missiles, and also in turbopump pressurizing systems without refrigerating the ClO_3F .

9-5 FUELS FOR LIQUID BIPROPELLANT SYSTEMS

The factors to be considered in selecting a liquid chemical compound which will be a satisfactory rocket fuel have been discussed in par. 9-1. From a performance viewpoint they must have high enthalpies of combustion and yield gas products having a low value of molecular weight \bar{m} . As pointed out earlier, while the number of practical oxidizers is limited, there are many fuels suitable for rocket propellant systems and the physical properties of several of them are presented in Table 9-6. For convenience the fuels are grouped into the following classes:

1. Cryogenic fuels rich in hydrogen
2. Borohydride fuels
3. Organic fuels containing C, H, and O
4. Organic fuels containing C, H, and N
5. Hydrocarbon fuels
6. Nitrogen hydrides and their derivatives

Some of the more important fuels will be discussed below.

9-5.1 CRYOGENIC FUELS RICH IN HYDROGEN

Liquid hydrogen gives the largest values of I_{sp} of all fuels, and with all liquid oxidizers (see Table 9-1). Because of its low boiling point (−259°C), its handling and storage is a difficult

TABLE 9-5
PHYSICAL PROPERTIES OF SEVERAL OXIDIZERS CONTAINING
FLUORINE AND OXYGEN*

Name	Formula	\bar{m}^1	ρ^2	$\Delta H_f^O^3$	F.P.T. ⁴	B.P.T. ⁵	T _{cr} ⁶	P _{cr} ⁷
Oxygen Bifluoride	OF ₂	54.0	1.53 ⁸	-8.4 ⁸	-224.0	-144.8	-57.96	48.9
Nitrosyl Trifluoride	ONF ₃	87.0	1.55 ⁸	-41. ⁸	-160.	-87.5	29.5	63.5
Nitryl Fluoride	O ₂ NF	65.0	1.50 ⁸	-22.5 ⁸	-166.	-72.4	76.3	96.
Perchloryl Fluoride	ClO ₃ F	102.5	1.41 ⁹	-9.2 ⁹	-146.	-46.8	95.2	53.

* Based on *Liquid Propellant Handbook*, CPIA.

¹ \bar{m} - molecular weight

² ρ - density at 25°C, g/cc

³ ΔH_f^O - enthalpy of formation at 25°C, unless otherwise noted, kcal/mole

⁴ F. PT. - freezing or melting point, °C

⁵ B. PT. - boiling point, °C

⁶ T_{cr} - critical temperature, °C

⁷ P_{cr} - critical pressure, atm

⁸ liquid at normal boiling point

⁹ liquid at 25°C under its own vapor pressure

problem; and its small specific gravity (0.07 g/cc at -259°C) is a disadvantage. It must be handled with care because hydrogen gas forms explosive mixtures with air. The experience with liquid hydrogen indicates that it can be handled in much the same manner as liquid oxygen. It appears that liquid hydrogen will be used in those special applications as for example, the upper stage engines for space propulsion, for which a high specific impulse is of prime importance.

Light metals appear to be attractive as fuels for rocket motors because, when they combine with oxygen to form oxides, they have large enthalpies of combustion. Since the gaseous combustion products must have a low molecular weight, only such light metal elements as lithium, beryllium, boron, and aluminum are of interest. In all cases the combustion temperatures are very high and when allowance is made for the evaporation and dissociation of the oxides, it is found that they give major gains in specific impulse. Figs. 9-1 and 9-2 are bar graphs comparing the enthalpies of combustion of several fuels.

A disadvantage accompanying the use of light metals as rocket fuels is that their oxides appear in the exhaust and make it smoky. Moreover, beryllium is extremely toxic, and lithium is quite scarce.

9-5.2 THE BOROHYDRIDES

Table 9-6 presents some of the physical properties of the borohydrides. Calculations show that after hydrogen the next highest performance fuels are the boron compounds containing hydrogen. In this country much research has been devoted to diborane (B_2H_6) and pentaborane (B_5H_9).

The borohydride fuels when reacted with F_2O , F_2 , O_2 , and H_2O_2 offer theoretical maximum specific impulses, based on mobile

equilibrium, of approximately $300 \text{ sec}^{1/2}$. The borohydride fuels, however, have certain undesirable properties. Thus, diborane (B_2H_6) boils at -92.5°C and is unstable. It decomposes slowly to form large quantities of hydrogen. Pentaborane (B_5H_9) has more favorable properties than diborane. It melts at -46.8°C and its rate of decomposition at room temperature is comparatively slow. Decaborane is a solid at room temperature.

Neither pure diborane nor pure pentaborane appear to ignite spontaneously when in contact with air. Apparently they decompose to form self-igniting boron hydrides, and the mixture increases in inflammability. None of the borohydrides decompose explosively, and they decompose slowly even when heated. Violent decomposition can occur when they are in contact with other metals.

Considerable effort was expended, until approximately a decade ago, on the development of boron compounds for use as additives to conventional hydrocarbon fuels (JP fuels) for use in rocket engines and air-breathing engines. When reacted with oxygen these fuels yield 60 percent more heat of combustion than does a conventional jet engine fuel. Unfortunately, the solid boron oxides which deposit in the flow passages of the engines—such as nozzles and turbine blade passages—preclude the use of such fuels in rocket and gas-turbine type air-breathing engines (see Chapter 12). Moreover, the solid particles in the propulsive gas decrease the efficiency of the nozzle expansion process, due primarily to their effect upon the average properties of the propulsive gas, and the *velocity lag* of the solid particles with reference to the gas (see Chapter 4, Reference 39).

9-5.3 ORGANIC FUELS

All liquid fuels containing carbon and hydrogen are termed organic fuels, and several have been investigated for use in liquid rocket

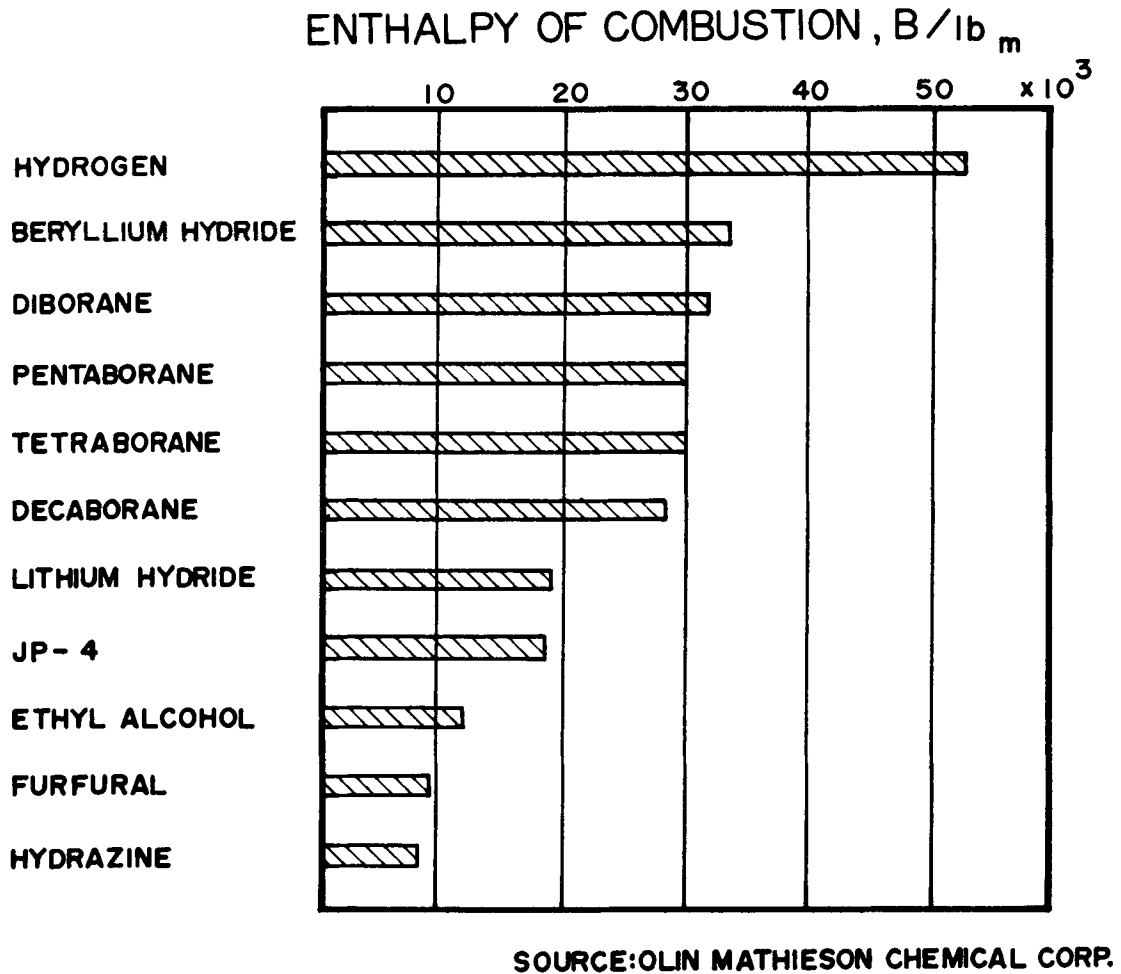


Figure 9-2. Enthalpy of Combustion of Several Fuels With Liquid Oxygen

TABLE 9-6
PHYSICAL PROPERTIES OF LIQUID FUELS*

Name	Formula	\bar{m}^1	ρ^2	$\Delta H_f^O^3$	F.P.T. ⁴	B.P.T. ⁵	T _{cr} ⁶	P _{cr} ⁷
1. CRYOGENIC FUELS RICH IN HYDROGEN								
Liquid Hydrogen (LH)	H ₂	2.016	0.070 ⁸	-2.50 ⁸	-259.2	-252.8	-240.2	12.8
Liquid Methane (LM)	CH ₄	16.043	0.424 ⁸	-21.6 ⁸	-182.5	-161.5	-82.1	45.8
2. BOROHYDRIDE FUELS								
Diborane	B ₂ H ₆	27.67	0.433 ⁸	+2.71 ⁸	-165.5	-92.5	16.7	39.5
Pentaborane	B ₅ H ₉	63.13	0.618	+7.8	-46.8	58.4	Pyrolizes	
Decaborane	B ₁₀ H ₁₄	122.3	0.94		99.5	213		
3. ORGANIC FUELS CONTAINING (C, H, and O)								
Furfuryl Alcohol	C ₅ H ₆ O ₂	98.10	1.129	-68.0	-31.0	169.3	—	—
Methanol	CH ₄ O	32.04	0.787	-57.0	-97.8	64.9	240.	78.5
Ethanol	C ₂ H ₆ O	46.07	0.785	-66.4	-117.3	78.5	243.	63.0
Denatured Alcohol (3A):	C _{1.62} OH _{5.24}	40.74	0.814	-66.14 ¹⁰				
(Other properties close to these of ethanol)								
Ethanol		88.2						
Methanol		4.7						
Water		7.1						
Isopropanol	C ₃ H ₈ O	60.1	0.780	-74.3	-89.5	82.4	235.6	53
4. ORGANIC FUELS CONTAINING (C, H, and N)								
TEA ¹¹	C ₆ H ₁₅ N	101.2	0.729	-39.9	-114.7	89.4	259.	30.
DETA ¹²	C ₄ H ₁₃ N ₃	103.2	0.953	-15.4	-35.	207.1	—	—
Commercial DETA contains approximately 9% N. amino ethyl piperazine								
Acetonitrile	C ₂ H ₃ N	41.05	0.783	+13.9	-45.7	80.0	474.7	47.7

TABLE 9-6 (Continued)

Name	Formula	\bar{m}^1	ρ^2	$\Delta H_f^O^3$	F.P.T. ⁴	B.P.T. ⁵	T _{cr} ⁶	P _{cr} ⁷
Aniline	C ₆ H ₇ N	93.13	1.021	+7.34	-6.2	184.3	425.6	52.3
NEA ¹³	C ₈ H ₁₁ N	121.18	0.962	-1.28	-63.5	204.7		
Commercial NEA contains approximately 10% N, N, diethylaniline 26% aniline								
5. HYDROCARBON FUELS								
N-octane	C ₈ H ₁₈	114.2	0.703	-59.7	-56.5	125.7	296.7	24.61
RP-1	(CH _{1.95}) _n	13.98	0.807	-5.76	-48.	219.	406.	23.1
RP-1 is a mixture of naphthenes, paraffins and olefins in the C ₁₂ region. All values in table are approximate.								
Diethyl Cyclohexane	C ₁₀ H ₂₀	140.3	0.805	-73.5 ⁸	<-79.	207.1	366.	25.
6. NITROGEN HYDRIDES AND THEIR DERIVATIVES								
Ammonia	NH ₃	17.03	0.682 ⁸	-17.14 ⁸ 0.603 ⁹	-77.7	-33.4	132.3	111.3
Hydrazine	N ₂ H ₄	32.05	1.004	+12.0	1.4	113.5	380.	145.
MMH ¹⁴	CH ₆ N ₂	46.07	0.874	+12.7	-52.4	87.	312.	81.3
UDMH ¹⁵	C ₂ H ₈ N ₂	60.1	0.786	+12.74	-57.2	63.	250.	53.5
* Based on <i>Liquid Propellant Handbook</i> , CPIA.								
¹ \bar{m}	- molecular weight							
² ρ	- density at 25°C, unless otherwise noted, g/cc							
³ ΔH_f^O	- enthalpy of formation at 25°C, unless otherwise noted, kcal/mole							
⁴ F. PT.	- freezing or melting point, °C							

TABLE 9-6 (Continued)

	Name	Formula	\bar{m}^1	ρ^2	$\Delta H_f^{O^3}$	F.P.T. ⁴	B.P.T. ⁵	T_{cr}^6	P_{cr}^7
⁵	B. PT.	- boiling point, °C							
⁶	T_{cr}	- critical temperature, °C							
⁷	P_{cr}	- critical pressure, atm							
⁸		- liquid at normal boiling point							
⁹		- liquid at 25°C under its own vapor pressure							
¹⁰		- heat of mixing included							
¹¹	TEA	- Triethylamine, $C_6H_4(NH)$							
¹²	DETA	- Diethylene triamine, $C_2H_{13}N_3$							
¹³	NEA	- Normal Ethylaniline, $C_8H_{11}N$							
¹⁴	MMH	- Monomethyl Hydrazine, $N_2H_3CH_3$							
¹⁵	UDMH	- Unsymmetrical Dimethyl Hydrazine, $(CH_3)_2N_2H_2$							

bipropellant systems. The discussions here will be limited to those organic fuels that are of either current or recent interest:

1. Ethyl alcohol
2. Light hydrocarbons (JP fuels)
3. Unsymmetrical dimethylhydrazine (UDMH)
4. Diethylenetriamine (DETA)

9-5.3.1 ETHYL ALCOHOL (C_2H_5OH)

Ethyl and methyl alcohols are the only lower alcohols which have been investigated and used as fuels in rocket engines. They are slightly inferior to the hydrocarbons in performance. Ethyl alcohol was used in the German V-2 missile and has been used in the REDSTONE missile.

Ethyl alcohol (C_2H_5OH), also called ethanol, melts at $-117^\circ C$ and boils at $78.5^\circ C$. It is plentiful and inexpensive and is a good regenerative coolant. Its main disadvantage is its low specific gravity (0.79 at $20^\circ C$). It is compatible with most normal construction materials, is nontoxic, and noncorrosive. Hot ethanol is said to etch aluminum. With LOX the maximum obtainable specific impulse is approximately 240 sec (based on frozen composition) and its combustion is smooth. Ethanol is nonhypergolic with most oxidizers.

9-5.3.2 LIGHT HYDROCARBON FUELS

Table 9-6 presents the physical properties of some hydrocarbon fuels. The common light hydrocarbon fuels are mixtures of aromatics, olefins, paraffins, and naphthenes that are termed jet engine fuels, and are designated by "JP" with a numerical suffix. In general, they have a carbon-hydrogen ratio of approximately

6 and a lower heating value of approximately 18,500 B/lb. Table 9-7 presents some of the characteristics of several such fuels. JP fuels are used in air-breathing engines.

The JP fuels are plentiful and inexpensive, have good handling characteristics, are compatible with most of the common materials of construction, are nontoxic, have good storage properties, and give reasonable high values of specific impulse either with oxygen or mixtures of oxygen and fluorine.

The disadvantages of JP fuels as rocket fuels are their low density and their tendency to pyrolyze or crack and deposit solids when used as regenerative coolants. They also tend to deposit solids in the nozzles of the gas turbine for driving propellant pumps when burned with LOX in fuel-rich reactions to produce gases for driving the gas turbine.

With nitric acid and MON, the JP fuels give rather low values of I_{sp} and the combustion is apt to be rough. It is found advantageous to employ additives to the JP fuel when it is used with either IRFNA or MON to improve the combustion characteristics.

In applying JP fuels to long-range rocket-propelled missiles, problems arise due to the variations in the density and composition of the fuel. These changes materially affect the performance of the engine and also complicate the accurate fueling of the missiles.

The JP fuels are nonhypergolic with most liquid oxidizers.

9-5.3.3 UNSYMMETRICAL DIMETHYL-HYDRAZINE (UDMH)

This fuel is currently being produced in relatively large quantities under the trade name "Dimazine." UDMH possesses excellent physical properties and is compatible with common

TABLE 9-7
PHYSICAL PROPERTIES OF LIGHT HYDROCARBON FUELS

Hydrocarbon Fuel	Distillate Range, °F	Gravity deg, API	Freeze Point °F, max	Flash Point, °F, min	General Description
JP-1	400-570	50-60	-76	110	Low freeze kerosene
JP-3	150-500	50-60	-76	NR ¹	High vapor pressure JP-4
JP-4	200-550	45-57	-76	NR ¹	Wide-cut gasoline
JP-5	350-550	36-48	-40	140	High flash kerosene
JP-6	250-550	37-50	-65	NR ¹	Thermally stable kerosene
RJ-1	400-600	32.5-36.5	-40	190	Thermally stable, heavy kerosene
RP-1	380-525	42-45	-40	110	Pure, light cut kerosene

¹ NR: No requirement.

construction materials. It burns smoothly with most oxidizers and gives relatively high performance (see Table 9-1). Its density is rather low being 0.786 g/cc at 25°C.

UDMH is thermochemically unstable and has the potentialities of being used as a monopropellant, but this requires more investigation. It is hypergolic with fuming nitric acids at very low temperatures and gives extremely short ignition delays, approximately 2 milliseconds at -75°F. It appears to be the most suitable fuel for use with IRFNA because of its excellent combustion characteristics with that oxidizer.

9-5.3.4 AEROZINE - 50 (N₂H₄ + UDMH-50/50)

Aerozine-50 is a 50/50 mixture of hydrazine and UDMH. It has the following physical properties:

$\bar{m} = 41.797$, F.Pt. = 18°F, B.Pt. = 170°F,

$\Delta H_f^0 = 11.789$ kcal/mole, $\rho = 0.9$ g/cc at 70°F,

$\Delta H_v = 425.8$ B/lb_m, $c_p = 0.69$ B/lb_m °F

Aerozine-50 is hypergolic with nitrogen tetroxide, and is used in the TITAN II ICBM.

9-5.3.5 DIETHYLENETRIAMINE (DETA)

There are several organic amines which may be useful as rocket fuels. Some of them give reasonably high values of specific impulse and have good physical properties. All of them are toxic to some degree. Since they are reasonably stable at high temperatures, they may be good regenerative coolants.

DETA, [NH₂(CH₂)₂]₂NH, has a relatively high density, 0.95 g/cc at 25°C, (see Table 9-6), is available in large quantities at fairly low cost,

has a moderately low freezing point (-38°F), and gives a larger I_{sp} with LOX than the JP fuels give. It also gives better general performance with fuming nitric acid (FNA), being hypergolic with very short ignition delays. It can be substituted for the JP fuels in missiles designed originally for JP fuels, without introducing any major problems. Because of the greater density of DETA the performance of the missile is improved. DETA is compatible with common construction materials and has good storage, handling, and heat transfer characteristics.

9-5.4 NITROGEN HYDRIDES

Two stable nitrogen hydrides are of interest as rocket fuels: ammonia (NH_3) and hydrazine (N_2H_4).

9-5.4.1 ANHYDROUS AMMONIA (NH_3)

Ammonia (NH_3) is available commercially in large quantities, is cheap, and can be stored in steel containers. It is moderately toxic but its presence is easily detected. NH_3 gives reasonably high values of specific impulse with most oxidizers and is nonhypergolic with most of them.

Ammonia has a low specific gravity (0.61 at 70°F) and a high vapor pressure (493 psia at 160°F). When used as a liquefied gas, the vapor pressure problem is eliminated by applying refrigeration. Its low density detracts from its usefulness as a rocket fuel, but it appears to be of interest when used with fluorine as the oxidizer. Information is lacking, however, on the capabilities of ammonia as a regenerative coolant under the high heat flux conditions occurring when it is burned with fluorine.

Ammonia gives smooth combustion with IRFNA and RFNA. The starting and stopping of the rocket engine is also smooth. Although it is nonhypergolic with FNA, ignition can be made hypergolic by causing liquid NH_3 to flow over a

small amount of lithium before entering the combustion chamber.

9-5.4.2 HYDRAZINE (N_2H_4)

The physical characteristics of hydrazine (N_2H_4) as well as its storage and handling characteristics are discussed in paragraph 9-3.1, where its use as a monopropellant was described. Reference to Table 9-1 shows that when used as a fuel in a bipropellant system, it gives high values of specific impulse with every oxidizer. Its main disadvantage is its high freezing point (35°F), and the lack of adequate information as to its characteristics as a regenerative coolant. In a missile application it offers the advantage of monopropellant runout, i.e., complete utilization of propellant.

Hydrazine is hypergolic and gives small ignition delays with all of the common oxidizers except LOX. It appears to be the best fuel for use with liquid fluorine, ClF_3 , H_2O_2 , and MON. It is worth noting that the high freezing point of N_2H_4 (35°F) is of the same order of magnitude as the freezing points of N_2O_4 (12°F) and H_2O_2 (30°F).

9-5.4.3 MIXTURES OF HYDRAZINE AND AMMONIA

There is interest in N_2H_4 - NH_3 mixtures because they have certain properties which are superior to those of the individual constituents¹². It has been pointed out that NH_3 is cheap, plentiful, stable under storage conditions, has a low freezing point (-78°C), gives reasonable values of specific impulse, but has a low density and a high vapor pressure. Hydrazine, on the other hand, is relatively expensive and has a high freezing point (35°F), but its density is high and it gives larger values of specific impulse than does NH_3 . By adding NH_3 to N_2H_4 a mixture can be made that has a reasonably low freezing point, good performance, and a reasonable density. For example, a mixture of 38

percent by weight NH_3 in N_2H_4 freezes at -30°F , while the 50 percent NH_3 -50 percent N_2H_4 mixture freezes at -40°F . As the NH_3 content is increased the vapor pressure increases, especially at high temperatures. For 36 percent NH_3 in N_2H_4 , the vapor pressure at 158°F is 18.5 atm. The mixture 37 percent NH_3 , 59 percent N_2H_4 , and 4 percent water gives an experimental value of specific impulse of approximately 280 sec when burned with liquid fluorine at 300 psia combustion pressure.

9-6 GELS, SLURRIES, AND EMULSIONS (HETEROGENEOUS PROPELLANTS)*

Early in the history of rocketry (1909) consideration was given to the idea of increasing the performance of a liquid bipropellant system by adding a finely divided active light metal to the liquid fuel³⁹. The object was to take advantage of the large enthalpy of combustion of the metal to increase the specific impulse of the resulting fuel,—hereafter termed a *heterogeneous propellant*—and simultaneously increase density impulse (see par. 6-3.7.2). It was soon found that the problem of developing a stable uniform dispersion of a high energy solid material in a liquid fuel was a difficult one. Consequently, for many years the concept of a heterogeneous propellant remained in the conceptual stage.

Approximately a decade ago, the idea of gelling liquid propellants received earnest consideration, due primarily to the interest in *prepackaged* missiles equipped with liquid propellant rocket engines. It was argued that a *gelled propellant* having the consistency of a stiff jelly would greatly reduce, and might even eliminate, the fire hazard presented by a leak in a propellant tank of a prepackaged missile.

9-6.1 THIXOTROPIC GELS

Because a gelled propellant must—in addition to behaving as a solid under storage and handling conditions—be capable of flowing like a liquid when its tank is pressurized for feeding it into a rocket motor, the development of *thixotropic gels* was undertaken. A thixotropic gel is a material which behaves like a solid when it is subjected to a shear stress smaller than a specified value, hereafter termed the *yielding stress* but flows like a liquid when it is subjected to a shearing stress exceeding the yielding stress. Furthermore, the gel reverts to the semi-solid state when the shear stress falls below the yielding stress. For most gelled propellants the yielding stress is in the range of 300 to 2,000 dynes/cm² (1 dyne/cm² = 14.5×10^{-6} psia $\approx 10^{-6}$ atm). Its proper value, however, depends upon the application.

Thixotropic gels have been prepared for several liquid fuels and liquid oxidizers. As to be expected, the formation of gels from liquid oxidizers entails problems not encountered with liquid fuels because organic gelling agents cannot be used with oxidizers. In any case, however, the gelling agent must be compatible with the liquid propellant. For a gel to be satisfactory for military use it must be stable—i.e., the solids do not separate out—under high g-loadings, mechanical shock, and mechanical vibration. In addition, it must be thermally stable under temperature cycling conditions over the required operating and storage range (usually -60°F to $+160^\circ\text{F}$).

Thixotropic gels, as such, are considered primarily as a means for improving safety and handling, and for preventing or reducing sloshing in propellant tanks. The research and development effort in that connection has been and is considerably smaller than that devoted to the development of gelled heterogeneous fuels. A typical gelled heterogeneous fuel consists of the liquid fuel, approximately 50%, by weight, of a

*Paragraph 9-6 is based on private communications from Dr. John D. Clark, LRPL, MUCOM, Picatinny Arsenal, and Dr. Paul Winternitz, New York University.

powdered solid—such as aluminum, boron, etc.—plus less than 5% of a gelling agent.

9-6.2 THIXOTROPIC SLURRIES

If the solid material is sufficiently finely divided, a gelling agent may not be needed to keep it in suspension. The resulting mixture is called a *slurry* and has the appearance of a jelly-like mud. Heterogeneous fuels in the form of *thixotropic slurries* are desirable because they contain no gelling agents. Thixotropic slurries must, of course, satisfy all of the requirements discussed under thixotropic gels.

Several thixotropic slurries have been made of aluminum, boron, and other high energy solids in both amine-type and hydrocarbon fuels. Such slurries are expected to raise the specific impulse of current storable liquid bipropellant systems and simultaneously increase their density impulse. For *volume-limited* propulsion systems, the larger density impulse yields a larger burnout velocity for the missile (see par. 5-9.2).

The compatibility of the solid constituent of a thixotropic slurry with its liquid carrier appears to be a more serious problem than it is for a gel. For example, it is only recently that the continuous gassing of *Alumizine*, a slurry of 30-45 percent of aluminum in hydrazine, has been eliminated. Alumizine is the best known and furthest developed heterogeneous propellant. Its application is limited, however, because it freezes at 1.5°C. Moreover, many promising heterogeneous fuels, such as a slurry of boron in amine-type fuels, show slow chemical reactions at ambient or somewhat higher temperatures.

Several slurry-type fuels are being studied, but none has progressed as far as Alumizine. At this time the only heterogeneous fuel which appears ready for engineering applications is a slurry of boron in a hydrocarbon; it can be used in ramjet engines.

9-6.3 EMULSIONS

Emulsions are being studied because they offer the possibility of allowing higher loadings of solids in the liquid fuel than do gels or slurries. It has been difficult, however, to develop emulsions having the desired thixotropic properties.

9-6.4 SUMMARY

Heterogeneous propellants offer performance advantages, in certain applications, over neat liquid propellant. The difficulties encountered in developing a satisfactory heterogeneous propellant have been, and are, formidable. Many common fuels, such as the hydrazines, are sensitive to catalytic decomposition and a finely divided metal dispersed in the hydrazine aggravates its catalysis. Moreover, it is difficult to attain complete combustion of the powdered metal, and solid or liquid particles may be formed in the propulsive gas with the result that the anticipated increase in specific impulse is not realized. Nevertheless, thixotropic slurry-type propellants offer the only tangible approach at this time toward substantially advancing the technology of chemical propellants for both rocket and air-breathing engines.

REFERENCES

1. M.J. Zucrow, *Aircraft and Missile Propulsion*, John Wiley and Sons, Inc., Vol 2. Second Printing, 1964, Ch. 10.
2. C.W. Besserer, *Missile Engineering Handbook, Principles of Guided Missile Design*, Edited by G. Merrill, D. Van Nostrand Company, 1958.
3. G.P. Sutton, *Rocket Propulsion Elements*, John Wiley and Sons, Inc., Third Ed., 1963, Ch. 8.
4. J.F. Tormey, "Liquid Rocket Propellants", *Aero. Eng. Rev.*, Vol. 16, October 1957, p. 55.
5. M.J. Zucrow and J.R. Osborn, "An Experimental Study of High Frequency Combustion Pressure Oscillations", *Jet Propulsion*, Vol. 28, No. 10, October 1958, p. 654.
6. A.J. Stepanoff, *Centrifugal and Axial Flow Pumps*, John Wiley and Sons, Inc., 1958.
7. D.R. Bartz, *Factors Which Influence the Suitability of Liquid Propellants as Rocket Motor Regenerative Coolants*, Jet Propulsion Laboratory, Calif., Institute of Technology, Technical Memorandum No. 20-139, Dec. 1956.
8. C.J. Grelecki and S. Tannenbaum, "Survey of Current Storable Propellants", *ARS Jour.*, August 1962, p. 1189.
9. *Performance and Properties of Liquid Propellants* (Revision A), Aerojet-General Corporation, Liquid Rocket Plant, Sacramento, Cal., 8160-6S, June 1961.
10. H.A. Liebhafsky, "Use of Hydrazine Hydrate as a Fuel", *Chemie et Industrie*, Vol. 56, 1946, p. 19.
11. T.C. Hill and J.F. Sumner, "The Freezing-Point Diagram of the Hydrazine-Water System," *J. Chem Soc.*, March 1951, p. 838.
12. L.F. Audrieth and P.H. Mohr, "Autoxidation of Hydrazine", *Ind. Eng. Chem.*, Vol. 43, August 1951, p. 1774.
13. G.S. Sutherland and M.E. Maes, "A Review of Microrocket Technology 10^{-6} to 1 lb_f Thrust", *Journal of Spacecraft and Rockets*, Vol. 3, No. 8, August 1966, p. 1153.
14. *High Strength Hydrogen Peroxide Monopropellant and Bipropellant Performance Data*, Becco Chemical Division, Food Machinery and Chemical Corporation, Bulletin No. 107.
15. J.G. Tschinkel, "Calculation of a Mollier Diagram for the Decomposition Products of Aqueous Hydrogen Peroxide Solutions of 90 Percent H₂O₂ Content", *Jet Propulsion*, Vol. 26, No. 7, Pt. 1, July 1956, p. 569.
16. N.S. Davis, Jr., and J.C. McCormick, *Design of Catalyst Packs for the Decomposition of Hydrogen Peroxide*, ARS Preprint 1246-60, ARS Propellants, Combustion and Liquid Rockets Conference, The Ohio State University, July 18-19, 1960.
17. R.J. Matt, "The Problems of Sealing Hydrogen Peroxide in a 3000°F Environment", *Trans. Am. Sec. Mech. Engrs.*, Paper No. 61-WA-76, July 19, 1961.
18. L.G. Hess and V.V. Tilton, "Ethylene Oxide Hazards and Methods of Handling", *Ind. Eng. Chem.*, Vol. 42, 1950, p. 1251.

REFERENCES (Continued)

19. E.M. Wilson, "The Stability of Ethylene Oxide", *ARS Jour.*, Vol. 23, No. 6, Nov.-Dec. 1953, p. 368.
20. P.F. Winternitz and D. Horvitz, "Rocket Propellant Performance and Energy of the Chemical Bond", *ARS Jour.*, Vol. 21, No. 85, June 1951, p. 51.
21. D. Altman and S.S. Penner, "Combustion of Liquid Propellants", Princeton Aeronautical Paperbacks, C. Du P. Donaldson, General Editor, *Liquid Propellant Rockets*, Princeton University Press, 1960, Section L, p. 84.
22. "Fluorine Figures Big", *Jet Propulsion*, Vol. 27, No. 6, June 1957, p. 678.
23. *Physical Properties and Thermodynamic Functions of Fuels, Oxidizers and Products of Combustion, II - Oxidizers*, R-129, Rand Corporation February 1949.
24. D. Altman, "A Review of Liquid Propellant Oxidizers", Office of the Ass't Sec. of Defense (R&D), *Symposium on Liquid Propellants*, Washington, D.C., Vol. 1, 13 May 1955.
25. A.H. Taylor, *Ozone Preparation and Stability in High Concentrations*, Air Reduction Sales Company, Final Report, Vol. 1, 27 December 1949.
26. *Research on the Properties of Ozone*, Linde Air Products Company Progress Report No. 13, 1 January 1955 (Confidential).
27. W.B. Kay and S.A. Stern, "Phase Relation of Nitric Acid at Physicochemical Equilibrium", *Ind. Eng. Chem.*, Vol. 47, July 1955, p. 1463.
28. G.D. Robertson, D.M. Mason and W.H. Corcoran, *The Kinetics of the Thermal Decomposition of Nitric Acid in the Liquid Phase*, JPL, CIT, Prog. Report No. 20-223, 29 January 1954.
29. H.S. Johnston, L. Foering and T. Yu-Sheng, *The Kinetics of the Thermal Decomposition of Nitric Acid Vapor*, Stanford University (Final Report to M-W. Kellogg Co.).
30. D.M. Mason, "Properties of Fuming Nitric Acid Affecting its Storage and Use as a Rocket Propellant", *Jet Propulsion*, Vol. 26, No. 9, Sept. 1956, p. 741.
31. C.E. Levee and D.M. Mason, *Inhibiting Effect of Hydrofluoric Acid in Fuming Nitric Acid on Corrosion of Austenitic Chromium-Nickel Steels*, JPL, CIT, Prog. Report 20-253, 14 January 1955.
32. D.M. Mason and L.L. Taylor, *Inhibiting Effect of Hydrofluoric Acid in Fuming Nitric Acid on Liquid and Gas-Phase Corrosion of Several Metals*, JPL, CIT, Prog. Report 20-255, 24 January 1955.
33. E.C. Fetter, "Nitric Acid Versus Construction Materials", *Chemical Engineering Corrosion Forum*, Vol. 55, Feb., March, April 1948, pp. 233-225-219.
34. *Nitrogen Tetroxide*, Allied Chemical and Dye Corp., Solvay Process Division, New York, Product Development Booklet NT-1.
35. A.G. Whitaker et al., "Vapor Pressures and Freezing Points of the System Nitrogen Tetroxide-Nitric Oxide", *J. Am. Chem. Soc.*, Vol. 74, 1952, p. 4794.

REFERENCES (Continued)

36. L.G. Cole, "The Nitrogen Oxides as Rocket Fuel Oxidants Including the Theoretical Performances of Propellant Systems Employing Nitrogen Tetroxide", JPL CIT, Prog. Report 9-23, 18 Oct. 1948.
37. "Gasoline to Kerosene to 'Zip' - With Energy Calling the Signals", *Jet Propulsion*, Vol. 27, No. 6, June 1957, p. 682.
38. S.S. Penner, *Chemistry Problems in Jet Propulsion*, Pergamon Press, 1957, p. 57.
39. F.A. Tsander, *Problems of Flight by Jet Propulsion*, (Russian translation by Israel Program for *Scientific Translations*), Published by National Aeronautics and Space Administration and National Science Foundation, Washington, D.C., 1964, p. 185.
40. M.C. Hardin and A.I. Masters, "Lithium Propellant Shows Low Combustion Loss," *Space/Aeronautics*, September 1961, p. 63.
41. A.H. Mitchell and H.A. Kirschner, "Compression-Ignition Studies of a Liquid Monopropellant," *AIAA Jour.*, Vol. 1, No. 9, September 1963, p. 2083.

CHAPTER 10

LIQUID PROPELLANT ROCKET ENGINES

10-0 PRINCIPAL NOTATION FOR CHAPTER 10*

a_o	stagnation acoustic speed $= \sqrt{\gamma RT_o}$	\dot{m}_f	mass rate of fuel flow
A	cross-sectional area	\dot{m}_o	mass rate of oxidizer flow
A_c	area of entrance cross-section of exhaust nozzle	\dot{m}_p	mass rate of propellant flow $= \dot{m}_f + \dot{m}_o$
A_e	area of exit cross-section of exhaust nozzle	M	Mach number
A_t	area of throat cross-section of exhaust nozzle	p	static pressure, psia
A^*	critical area where $M = 1$ for an isentropic flow	P	static pressure, psf
c	effective jet velocity	P_o	stagnation or total pressure
C_d	discharge coefficient	Δp	static pressure drop
g_c	gravitational conversion factor $= 32.174 \text{ slug-ft/lb-sec}^2$	q	heat flux, B/sq in.-sec
h_g	gas film conductance coefficient	\dot{Q}	volumetric rate of flow
h_L	liquid film conductance coefficient	\dot{Q}_{ch}	volumetric rate of flow of gas in the combustion chamber
I_{sp}	specific impulse $= F g_c / \dot{m}$	r	mixture ratio $= \dot{m}_o / \dot{m}_f$
L^*	characteristic length $= V_{ch} / A_t$	t	time
m	mass	t_s	stay or residence time
\dot{m}	mass rate of flow, slug/sec	T	static temperature, °R
		T_c	static temperature at entrance section of exhaust nozzle, °R
		T_o	stagnation temperature, °R
		V	volume
		V_{ch}	volume of combustion chamber

*Any consistent set of units may be employed; the units presented here are for the American Engineers System (see par. 1-7).

SUBSCRIPTS

amb	ambient
c	entrance section of exhaust nozzle
ch	combustion chamber
e	exit section of exhaust nozzle
g	gas
i	injection
p	propellant

GREEK LETTERS

γ	specific heat ratio = c_p/c_v
Γ	$\sqrt{\gamma} \left(\frac{2}{\gamma+1} \right)^{(\gamma+1)/[2(\gamma-1)]}$
Δ	increment or finite change
ϵ	area ratio = A/A_t
ρ	density
ρ_{ch}	density of the gas flowing in the combustion chamber
ϕ	velocity coefficient

10-1 INTRODUCTION

As indicated in par. 1-6.1, liquid propellant rocket engines may be classified into two broad groups: (1) liquid bipropellant rocket engines, and (2) liquid monopropellant rocket engines. Although the latter type of engine has a simplicity advantage over the former, because a single propellant is involved, it appears doubtful, at least, that a liquid monopropellant will either be developed or discovered that will give a specific impulse equal to that obtainable from

current liquid bipropellant systems. Consequently, the use of liquid monopropellants will be restricted to such applications as reaction control devices, the generation of gas for pressurizing liquid propellants, and for driving the turbines for auxiliary power units (APU's) and turbopumps. In view of the foregoing the discussions which follow will be concerned, in the main, with liquid bipropellant rocket engines.

10-2 ESSENTIAL COMPONENTS OF A LIQUID BIPROPELLANT ROCKET ENGINE

A liquid bipropellant rocket engine (see Fig. 1-5) comprises four principal subassemblies:

1. One or more *thrust chambers* or rocket motors, into which the liquid propellants are injected, atomized, mixed, and burned to produce large quantities of propulsive gas; the latter is then expanded in a suitable exhaust nozzle thereby developing a propulsive force (*thrust*).
2. Tanks for storing the liquid fuel and liquid oxidizer, hereafter termed the *propellant tanks*.
3. A *pressurizing system* for removing the liquid propellants from their storage tanks, and raising their pressure so they can flow through an *injector*, into the thrust chamber, against the combustion pressure; the injector meters the liquid flow rates.
4. A *control system* for controlling the operation of the engine so that it performs in the desired manner and also incorporates means for protecting the engine against damage in the event of a malfunction.

In general, the requirements imposed upon a liquid rocket engine stem from its application. In several military applications the performance of the engine should be independent of the engine and its liquid propellant temperatures over the range -60° to $+160^{\circ}\text{F}$. Because the physical properties of practically all chemicals vary with their temperature, the number of liquid chemicals that can satisfy the above temperature requirements is quite limited. As a consequence, one finds that a large portion of the engineering effort in developing a new liquid rocket engine is devoted to making the engine operate satisfactorily and reliably over a wide range of temperatures. One of the costly and time-consuming phases of liquid rocket engine development is that concerned with obtaining reliable operation at very low temperatures (below -20°F). In view of the foregoing, the specifications for the required range of operating temperatures should not be made any wider than is warranted from a realistic appraisal of the conditions under which the rocket-propelled vehicle is to be used. Furthermore, wherever it is practicable, means should be provided for protecting the engine and its propellants against cold weather (for example, by employing heating blankets).

10-3 THE THRUST CHAMBER

Figs. 10-1(A) and 10-1(B) illustrate schematically the essential elements of an uncooled and a *regeneratively cooled* thrust chamber, respectively, for a liquid bipropellant rocket engine. In Fig. 10-1(B), the fuel is circulated around the walls of the combustion chamber and nozzle that are wetted by the hot flowing propulsive gas; this method of cooling the walls is known as *regenerative cooling*. The following principal elements are involved^{1,2}:

- (1) The injector for introducing the propellants into the combustion chamber, and for metering their rates of flow (see par. 10-3.1).
- (2) The combustion chamber, wherein occurs the chemical reaction between the propellants. Its dimensions must provide adequate *stay time* for the combustion reaction to produce a propulsive gas having a substantially equilibrium composition when it reaches the entrance cross-section A_c of the exhaust nozzle (see Fig. 10-1).
- (3) The converging-diverging (De Laval) exhaust nozzle for expanding and ejecting the propulsive gas as a supersonic gaseous jet.

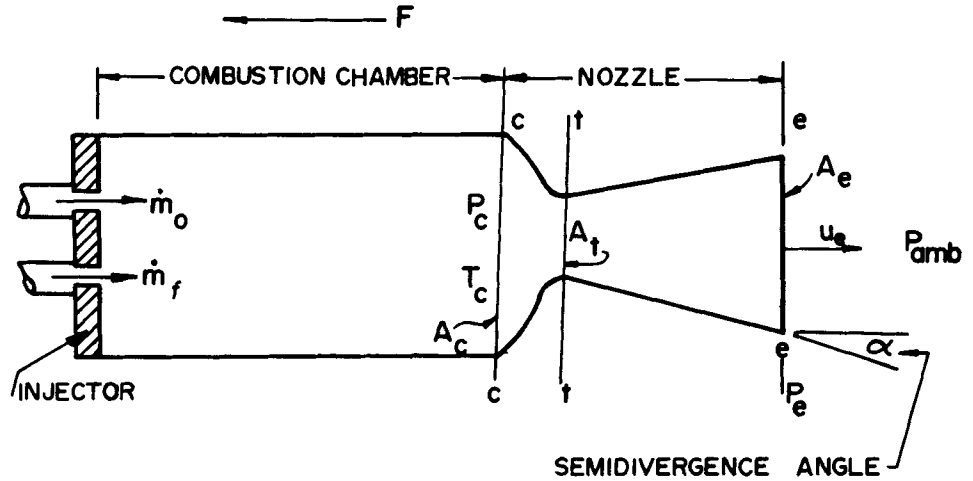
In addition to the three principal elements listed above, there are such pertinent auxiliary devices as various valves and pressure regulators. If the propellants are *diergic*, they do not react on contact with each other; hence, some form of ignition system must be provided. This may be an electrically heated glow plug, a spark plug, a small quantity of liquid fuel which is *hypergolic* with the oxidizer leading the main fuel, or a pyrotechnic igniter which will burn for one or two seconds.

10-3.1 THE INJECTOR

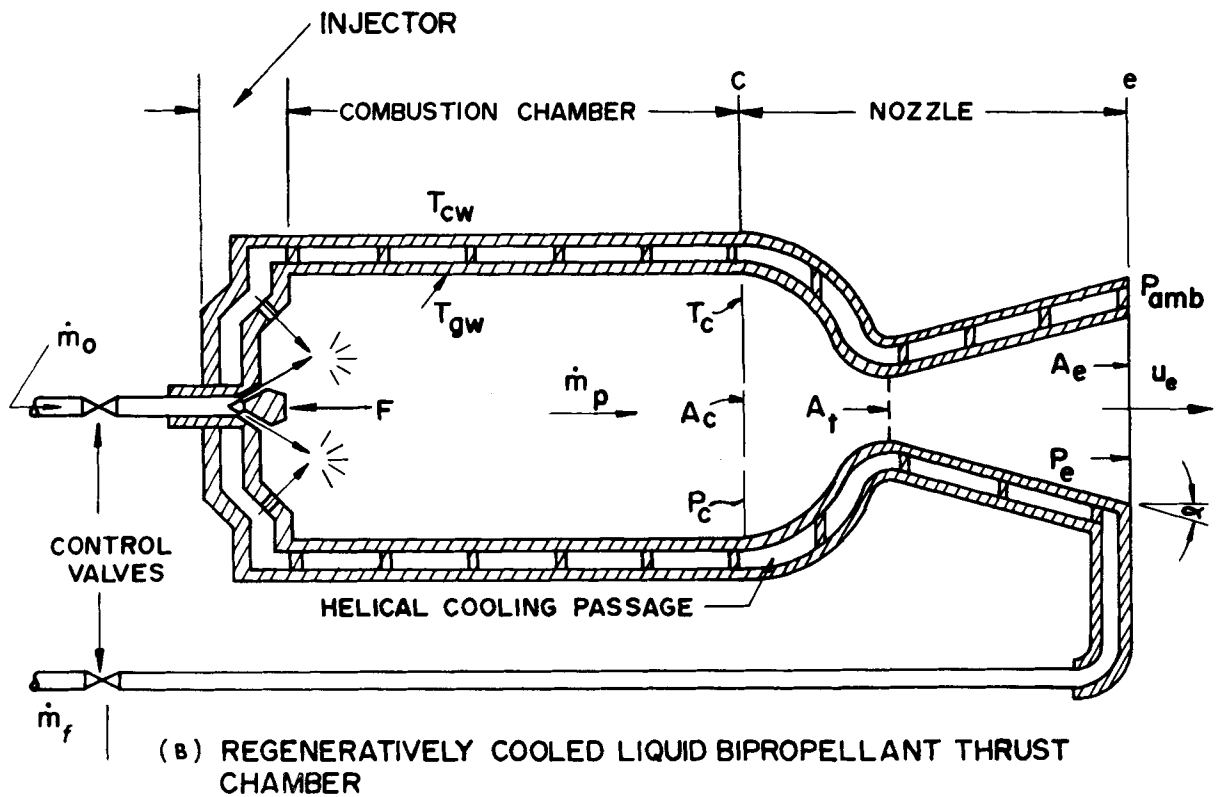
The injector is ordinarily located in the fore-end of the thrust chamber, as illustrated in Fig. 10-1. Its function is to introduce the liquid propellants into the combustion chamber through several injection orifices or nozzles, atomize them to promote their vaporization, and meter and mix the propellants so that they will burn smoothly and efficiently.

If \dot{m}_o and \dot{m}_f denote the mass flow rates of oxidizer and fuel, respectively, the mixture ratio r is accordingly

$$r = \dot{m}_o / \dot{m}_f \quad (10-1)$$



(A) UNCOOLED LIQUID BIROPELLANT THRUST CHAMBER



(B) REGENERATIVELY COOLED LIQUID BIROPELLANT THRUST CHAMBER

Figure 10-1. Essential Elements of a Liquid Bipropellant Thrust Chamber

In general, the mass flow rate of a liquid propellant through an injector nozzle, is given by

$$\dot{m} = A_i V_i \rho = C_d A_i \rho \sqrt{2\Delta P_i / \rho} \quad (10-2)$$

The injection velocity V_i is given by

$$V_i = \phi \sqrt{2\Delta P_i / \rho} \quad (10-3)$$

where

ρ = density of the injected liquid

A_i = exit cross-sectional area of an injector nozzle or orifice

ΔP_i = pressure drop across an injector nozzle or orifice

ϕ = velocity coefficient

Let

A_o = the total exit area of the oxidizer nozzles

A_f = the total exit area of the fuel nozzles

ΔP_o = the pressure drop across A_o

ΔP_f = the pressure drop across A_f

$(C_d)_o$ = the discharge coefficient for A_o

$(C_d)_f$ = the discharge coefficient for A_f

Hence, the mixture ratio r is given by

$$r = \frac{(C_d)_o A_o}{(C_d)_f A_f} \sqrt{\frac{\rho_o \Delta P_o}{\rho_f \Delta P_f}} \quad (10-4)$$

The injection nozzles are essentially short tubes with either well-rounded or chamfered

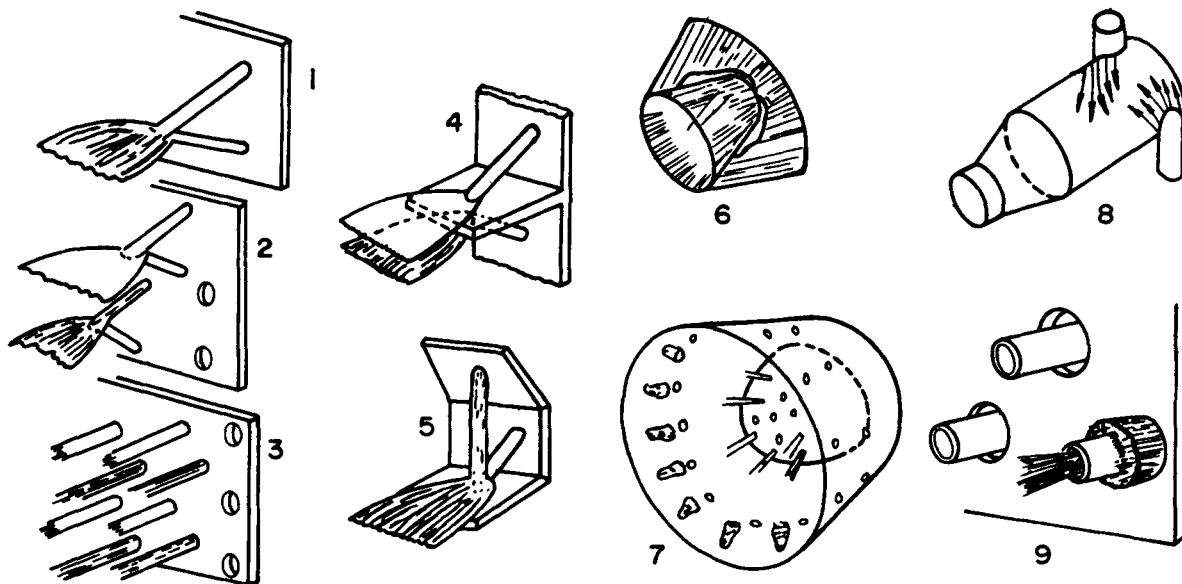
inlets, and their discharge coefficients are functions of their Reynolds numbers. Consequently, the injector should be designed so that the injector nozzles operate in a range where their discharge coefficients are not affected appreciably over the anticipated range of variations in Reynolds number. For well-rounded inlets to the nozzles the discharge coefficient C_d , assuming turbulent flow, will have a value between 0.95 and 0.99. For chamfered inlets a value of $C_d = 0.80$ to 0.84 may be assumed. Sharp-cornered inlets to short tubular passages should be avoided because they are apt to introduce jet contraction phenomena and flow instabilities; for sharp-edged inlets, with steady flow, C_d will range from 0.6 to 0.75.

Fig. 10-2 illustrates schematically nine different types of injectors⁹. In some injector designs an effort is made to assist the processes of atomizing and mixing the liquid oxidizer and liquid fuel streams by causing them to impinge upon each other.

No rational principles have as yet been formulated for relating injector design parameters to the combustion performance. Consequently, there are no rational principle for "scaling" injectors from one size to another, and the development of an injector for a new and larger thrust chamber is a costly, time-consuming empirical process. The success of the development depends upon experience combined with trial and error model experiments. It is not unreasonable to state that the main problems concerned with scaling liquid bipropellant rocket engines are primarily injector development problems.

10-3.2 THE COMBUSTION CHAMBER

Refer to Fig. 10-1. The *combustion chamber* of a liquid bipropellant thrust chamber is defined as the volume located between the downstream face of the injector and the entrance cross-section A_c of the exhaust nozzle. It is in the combustion chamber that the liquid propellants are burned at a substantially high pressure; ordinarily *chamber pressure* P_c has a



(1) UNLIKE IMPINGING. (2) LIKE-ON-LIKE IMPINGING. (3) NONIMPINGING (SHOWERHEAD). (4) SPLASH PLATE. (5) MIX PLATE (ENZIAN). (6) CONVERGING-DIVERGING CONES. (7) INTERSECTING CONES AND JETS (V-2 ROSETTE) WITH O_2 IN CENTER. (8) PREMIX. (9) COAXIAL.

Figure 10-2. Nine Different Injector Patterns for Liquid Bipropellant Thrust Chambers

value of 300 to 1200 psia. In more advanced designs P_c may exceed 3000 psia.

The combustion chamber is utilized for completing such processes as the injection of the liquid bipropellants in the form of several liquid streams, the pulverization and atomization of those liquid streams, the mixing of the atomized liquids, the vaporization of the liquid droplets, the mixing of the vaporized fuel and oxidizer, the thermal decomposition of the oxidizer to release its oxygen when required, the ignition of the fuel-oxidizer mixture, and combustion of that mixture. To obtain the maximum specific impulse obtainable from a given propellant system, its chemical reaction should be completed when the gaseous products of combustion

reach the entrance section of the exhaust nozzle. In the interest of keeping the weight of the thrust chamber as low as possible, the combustion volume should be the minimum that is consistent with no appreciable decrease in the characteristic velocity c^* (see par. 6-3.6) obtainable from the equilibrium combustion of the propellants at the prevailing chamber pressure P_c and mixture ratio r .

10-3.2.1 CHARACTERISTIC LENGTH FOR A LIQUID PROPELLANT THRUST CHAMBER (L^*)

Let V_{ch} denote the combustion chamber volume for providing the required *residence* or *stay time* t_s for completing the physical and

combustion processes discussed above. It is difficult, if not impossible, to measure t_s directly. In general, the more reactive either the propellant system or the conditions prevailing during combustion, the smaller the magnitude of t_s .

A measurable criterion which is closely related to t_s can be derived by assuming the following: (1) the propellants are completely mixed as they enter the combustor, (2) the entire combustor is filled with flowing gaseous products at a constant static temperature T_c and density ρ_{ch} , and (3) the gas flow is isentropic. In view of the aforementioned assumptions, the stay time t_s is given by

$$t_s = \frac{V_{ch}}{\dot{Q}_{ch}} = \frac{\rho_{ch} V_{ch}}{\dot{m}_p} \quad (10-5)$$

where \dot{m}_p is the mass rate of propellant consumption and \dot{Q}_{ch} is the volumetric rate of gas flow for the combustion chamber.

It is customary to express the size of the combustion chamber in terms of a *characteristic length*, denoted by L^* , which is defined by

$$L^* = \frac{V_{ch}}{A_t} = \frac{V_{ch}}{A^*} \quad (10-6)$$

since for the assumed isentropic flow $A_t = A^*$ (see Chapter 3).

From Eq. A-134 it follows, since $M=1$ in A^* , that

$$\frac{\dot{m}_p}{A^*} = \frac{P_o}{\sqrt{RT_o}} \sqrt{\gamma} \left(\frac{2}{\gamma+1} \right)^{(\gamma+1)/[2(\gamma-1)]} \quad (10-7)$$

It can be shown that

$$a_o = \sqrt{\gamma RT_o} = C_d c^* \Gamma \quad (10-8)$$

where c^* is the characteristic velocity (see par. 6-3.6), and

$$\Gamma = \sqrt{\gamma} \left(\frac{2}{\gamma+1} \right)^{\frac{\gamma+1}{2(\gamma-1)}} \quad (10-9)$$

Hence

$$t_s = \frac{L^*}{C_d c^* \Gamma} \quad (10-10)$$

In Eq. 10-10, the parameter r is a function only of γ , i.e., the propellants and their mixture ratio $r = \dot{m}_o / \dot{m}_f$. Similarly, c^* depends upon the propellant system and its mixture ratio r . It follows, therefore, that the stay time is primarily a function of the specific propellant system, its mixture ratio, and the characteristic length $L^* = V_{ch}/A_t$.

From Eq. 10-10, it follows directly that

$$L^* = t_s C_d c^* \Gamma \quad (10-11)$$

If V_{ch} is expressed in cu in. and A_t is in sq in., then L^* is expressed in inches.

It is desirable, in a thrust chamber design, that L^* be as small as possible consistent with the maximum c^* obtainable from the propellant system under the design operating conditions. The minimum usable value of L^* is determined experimentally; hereafter the symbol L^* will refer to the *minimum usable value*.

Experiments indicate that although the mixture ratio $r = \dot{m}_o / \dot{m}_f$ has a measurable effect on c^* , its influence upon L^* is much smaller. Furthermore, the L^* for a specific propellant system burned at a given combustion pressure and mixture ratio r is substantially independent of the size of the thrust chamber. Consequently, the L^* data for a given propellant system are obtained from experiments with small scale thrust chambers.

As indicated earlier, the L^* for a specific propellant system will, of course, be related to its chemical reactivity faster-reacting liquid propellants have the smallest values for L^* . Some typical values are listed below:

<u>Propellant System</u>	<u>L^*, in.</u>
Diesel fuel and gaseous oxygen	80
Alcohol-water mixtures with LOX	80-120
WFNA - hydrocarbon fuels	60
RFNA - hydrocarbon fuels	40-60

For a cylindrical combustion chamber it is customary to include the volume of the converging portion of the exhaust nozzle in calculating V_{ch} , in $L^* = V_{ch}/A_t$.

The minimum value for L^* is desirable not only from the viewpoint of small weight, but from *heat transfer* considerations (see par. 10-4). The total amount of heat transferred from the hot propulsive gas to the walls of the combustion chamber decreases with a decrease in the surface area exposed to the hot gas. On the other hand, decreasing the volume of the combustion chamber increases the gas velocity past its walls, which tends to increase the heat flux B/L^2T to those walls. For a given thrust chamber configuration, size, and propellant system there will be a volume for which the *product* of the *exposed surface area* and *heat flux* is a *minimum*.

10-3.2.2 GAS-SIDE PRESSURE DROP IN A LIQUID PROPELLANT THRUST CHAMBER

It is desirable that the pressure drop for the gas flowing through the combustion chamber be small because any reduction in the static pressure of the gas at the entrance cross-section A_c of the exhaust nozzle (see Fig. 10-1) reduces the exhaust velocity of the propulsive gas and, hence, the thrust.

The pressure drop in a combustor is due primarily to the addition of heat to the gaseous products of the chemical reaction (combustion) and increases with the Mach number of the flowing gas. Because of the complicated fluid dynamic and combustion phenomena occurring in the combustion chamber of a liquid rocket thrust chamber, it is well-nigh impossible to make an accurate analysis of the pressure drop caused by the aforementioned heat addition process. An approximate estimate, can be made, however, by assuming the process is a steady frictionless one-dimensional flow of an ideal gas with heat addition (see par. A-9). From Eq. A-220

$$\frac{P_2^O}{P_1^O} = \frac{1 + \gamma M_1^2}{1 + \gamma M_2^2} \left[\frac{1 + \left(\frac{\gamma-1}{2}\right) M_2^2}{1 + \left(\frac{\gamma-1}{2}\right) M_1^2} \right]^{\frac{\gamma}{\gamma-1}} \quad (10-12)$$

From Eq. A-216, the static pressure ratio P_2/P_1 , is given by

$$\frac{P_2}{P_1} = \frac{1 + \gamma M_1^2}{1 + \gamma M_2^2} \quad (10-13)$$

At the downstream face of the injector, it may be assumed that $M_1 \approx 0$. Hence, one obtains the following equations for the stagnation pressure ratio P_2^O/P_1^O and the static pressure ratio P_2/P_1 :

$$\frac{P_2^O}{P_1^O} = \frac{1}{1 + \gamma M_2^2} \left[1 + \left(\frac{\gamma-1}{2}\right) M_2^2 \right]^{\frac{\gamma}{\gamma-1}} \quad (10-14)$$

and

$$\frac{P_2}{P_1} = \frac{1}{1 + \gamma M_2^2} \quad (10-15)$$

Assume now that the flow through the exhaust nozzle is an ideal nozzle flow (see par.

4-3), then from Eq. 4-23, letting $A_x = A_c =$ entrance cross-section of exhaust nozzle, and $M_2 = M_x =$ Mach number in A_c , one obtains

$$\frac{A_c}{A^*} = \frac{1}{M_2} \left\{ \frac{2}{\gamma+1} \left[1 + \left(\frac{\gamma-1}{2} \right) M_2^2 \right] \right\}^{\frac{\gamma+1}{2(\gamma-1)}} \quad (10-16)$$

Eq. 10-16 can be employed for estimating the Mach number M_2 from the *contraction ratio* for the exhaust nozzle $A_c/A^* = A_c/A_t$, and the specific heat ratio γ for the propulsive gas.

If M_2 is known, the static pressure drop ($P_1 - P_2$) can be estimated from Eq. 10-15 and the stagnation pressure drop ($P_1^0 - P_2^0$) from Eq. 10-14. Typical values for the contraction ratio for liquid bipropellant rocket nozzles are between 1.5 and 2.0; the corresponding values of M_2 range from approximately 0.4 to 0.3.

10-3.3 THE EXHAUST NOZZLE

As in all jet propulsion engines (see par. 1-4) the exhaust nozzle is the propulsive element of the liquid propellant rocket thrust chamber. The nozzle throat area A_t and its configuration determine the combustion chamber pressure P_c , the propellant flow rate \dot{m}_p , the effective jet velocity c , and the thrust F . The gas dynamics of exhaust nozzles, their general design considerations, and the different nozzle configurations are discussed in Chapter 4 and will not be considered here.

It is essential that the nozzle be cooled adequately. Experiments indicate that *overall* heat flux for the nozzle is approximately 3 to 4 times the overall heat flux for the combustion chamber^{5,6}. The most critical region from the viewpoint of heat transfer is the region immediately upstream of the throat. The local heat transfer for that region can be 3 to 6 times the overall heat flux for the nozzle, and increases with the chamber pressure.

10-4 HEAT TRANSFER IN LIQUID PROPELLANT THRUST CHAMBERS

Reference to Table 9-1 indicates that the temperatures attained by the propulsive gas flowing in a liquid propellant thrust chamber are too high for measurement with conventional measuring instruments. For most propellant systems the gas temperature exceeds the melting temperatures of the stainless steels, Inconel, the titanium alloys, and some refractories. It should be noted that such high melting point materials as tantalum, tungsten, and carbon cannot be used at high temperatures in the presence of oxidizing substances. The propulsive gas temperature T_c depends primarily upon the specific propellant system and the mixture ratio $r = \dot{m}_o/\dot{m}_f$, as indicated in Table 9-1. To a minor degree, however, T_c is also influenced by the chamber pressure P_c .

In general, heat is transferred from the hot flowing propulsive gas to the walls of the thrust chamber that it wets, by forced convection, radiation, and conduction. It is estimated that the total amount of heat transferred to the thrust chamber wall amounts to 0.5% to possibly 5% of the heat released by the heat of reaction of the propellants; for example, the overall heat transfer for the V2 thrust chamber amounted to 0.7% of the heat of combustion for its propellants^{2,3}. It is difficult to determine by measurement the exact contributions of each of the aforementioned three modes of heat transfer to the total amount of transferred heat. Studies indicate, however, that the amount of heat transferred by conduction is so small that it may be assumed that all of the heat is transferred by the other two modes; forced convection and radiation^{7,8,9}. Furthermore, the transfer of heat by radiation is of significance only in the combustion chamber (see Fig. 10-1), and is responsible for approximately 5 to 30 percent of the total amount of transferred heat for temperatures ranging from approximately 4000° to 7500° R (Ref. 2).

Fig. 10-4 illustrates schematically the average heat flux distribution along the wall of a thrust chamber of cylindrical cross-section. There is a slow increase in the heat flux to the combustion chamber wall, due to the progress of the combustion process, as one proceeds from the injector face to the nozzle. The maximum heat flux occurs in the vicinity of the nozzle throat, due primarily to intense heat transfer by forced convection, where the local heat flux can exceed 25 B/sq in.-sec depending upon the combustion pressure and the mixture ratio. Beyond the throat the heat flux decreases rapidly due to the expansion of the propulsive gas and the boundary layer build-up. The heat flux attains its minimum value in the vicinity of the exit section of the nozzle^{2,3}. The mixture ratio r for a propellant system that produces the largest values of heat flux is that value of r which gives the highest flame temperature. Increasing the combustion pressure increases the heat flux due to increasing the density of the propulsive gas and the conductance of the boundary layer⁵.

The design of the cooling system for a liquid propellant thrust chamber involves two distinct steps: (1) the determination of the heat flux transferred to the walls by the hot propulsive gas, and (2) the analysis of the several pertinent cooling systems³.

The heat flux to the walls depends upon the velocity of the propulsive gas, its velocity distribution, the gas composition and its distribution, and the temperature distribution in the flowing gas. Because the flow process in the thrust chamber is quite complicated, it is not possible to predict the heat fluxes to the wall with precision. At best it may be possible to calculate what may be assumed to be the probable maximum heat flux for a given P_c and mixture ratio. The effect of changes in combustion pressure, mixture ratio, chamber and nozzle configurations may then be estimated. In any case, the calculated results must be checked

experimentally; they should be regarded only as a first approximation to the actual heat fluxes.

Ordinarily, it is desirable that the weight of the thrust chamber be as small as possible, which calls for thin, highly stressed walls. For the walls to be capable of maintaining an adequate stress level, they must be cooled to a low enough temperature for maintaining the structural integrity of the thrust chamber while it is exposed to the hot flowing propulsive gas. To accomplish that objective some form of *cooling system* must be provided that will maintain the local wall temperature at any point in the thrust chamber below the *critical structural temperature*, i.e., the temperature above which the structural integrity of the wall starts to deteriorate. The phrase *cooling system*, as employed here, includes those systems where there is no real cooling of the wall, but the thermal capacity of the thrust chamber materials are employed for maintaining the walls below the critical structural temperature.

10-4.1 CLASSIFICATION OF THRUST CHAMBER COOLING SYSTEMS

Thrust chamber cooling systems that have either been applied or conceived can be classified into three broad groups:

1. *Nonregenerative systems* which are based on either employing the thermal capacity of the material as a *heat sink* or the thermal resistance of materials as *heat barriers*.
2. *Regenerative systems* which circulate either the liquid fuel or the liquid oxidizer, or both, around the combustion chamber and nozzle; these are basically *external cooling systems*.
3. *Internal cooling systems* which are based upon interposing some form of coolant between the hot propulsive gas and the internal surface of the wall to be protected.

Fig. 10-3 summarizes diagrammatically the different systems either employed or conceived for cooling rocket thrust chambers which burn either liquid or solid propellants.

10-4.2 NONREGENERATIVE COOLING SYSTEMS

The earliest cooling systems were of the nonregenerative type and were based on employing structures which were capable of either absorbing or resisting the heat flux.

10-4.2.1 HEAT-SINK COOLING OF THRUST CHAMBERS

The heat flux q to the walls of a liquid propellant thrust chamber is ordinarily expressed in B/sq in.-sec, and its magnitude depends upon the propellant system, its mixture ratio, the characteristics of the injector, and the part of the thrust chamber being considered. Because of the uncertainty of the values of q obtained by calculations based on theory alone (convection and radiation), it has become the practice to base the heat sink design on measured values of the average flux for the combustion chamber, the overall heat flux for the nozzle, and the average heat flux for the entire thrust chamber (see Fig. 10-4). The aforementioned values of heat flux are based on thermocouple measurements in an experimental thrust chamber made of the materials to be employed in the design. It is necessary to know the thermal conductivity k , density ρ , and specific heat c_p of the materials involved.

A *heat-sink cooled* liquid propellant thrust chamber, and also a solid propellant rocket motor, does not, of course, attain a state of thermal equilibrium; its local temperatures increase with the operating duration. Consequently, the safe operating duration for such a thrust chamber is limited. The allowable duration is governed by such factors as the construction materials, the propellant system and its

mixture ratio, and the chamber pressure. The general problem is to design the thrust chamber so that its walls stay below the critical structural temperature, defined above, and to maintain the surface temperature of the nozzle throat sufficiently low so that it does not soften and erode.

Uncooled liquid propellant thrust chambers can be used in applications where the smaller specific impulse obtained with low mixture ratios, for reducing the combustion temperature, can be tolerated. Experiments conducted with the RFNA-aniline propellant system, at a mixture ratio $r = 1.5$, indicated that the average heat flux for a heat-sink cooled thrust chamber was $q=0.8$ B/sq in.-sec. For the nozzle the average heat flux was approximately 1.6 B/sq in.-sec. From a heat transfer standpoint the nozzle of a thrust chamber which is to operate heat-sink cooled should be made of a material having a high thermal conductivity so that the heat will be transmitted rapidly through the nozzle material.

For short-duration, one-shot applications, having burning times of less than approximately 2 sec, heat-sink cooled thrust chambers have the advantages of simplicity and low cost.

10-4.2.2 HEAT-BARRIER COOLING OF THRUST CHAMBERS

Heat-barrier cooling (see Fig. 10-3) can be effected by applying refractory liners, special refractory deposits from one (or both) of the liquid propellants, or a compound design comprising several liners of different materials to the internal surfaces of the thrust chamber^{11,12}. Recent experience with large solid propellant rocket motors, such as POLARIS and MINUTEMAN, has demonstrated that ceramic materials are satisfactory heat barriers. They must, however, be carefully selected so that they are

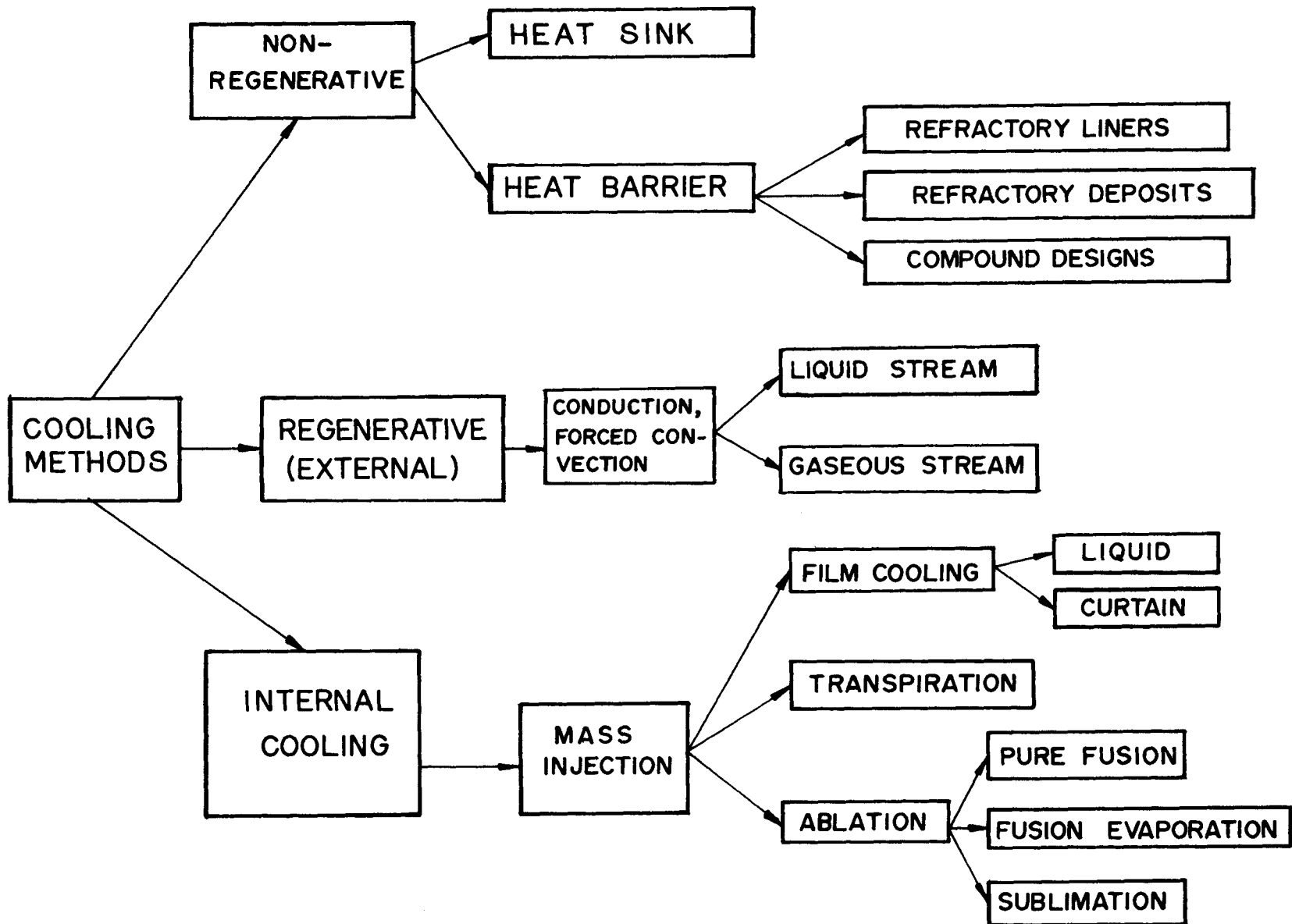


Figure 10-3. Cooling Systems for Rocket Thrust Chambers

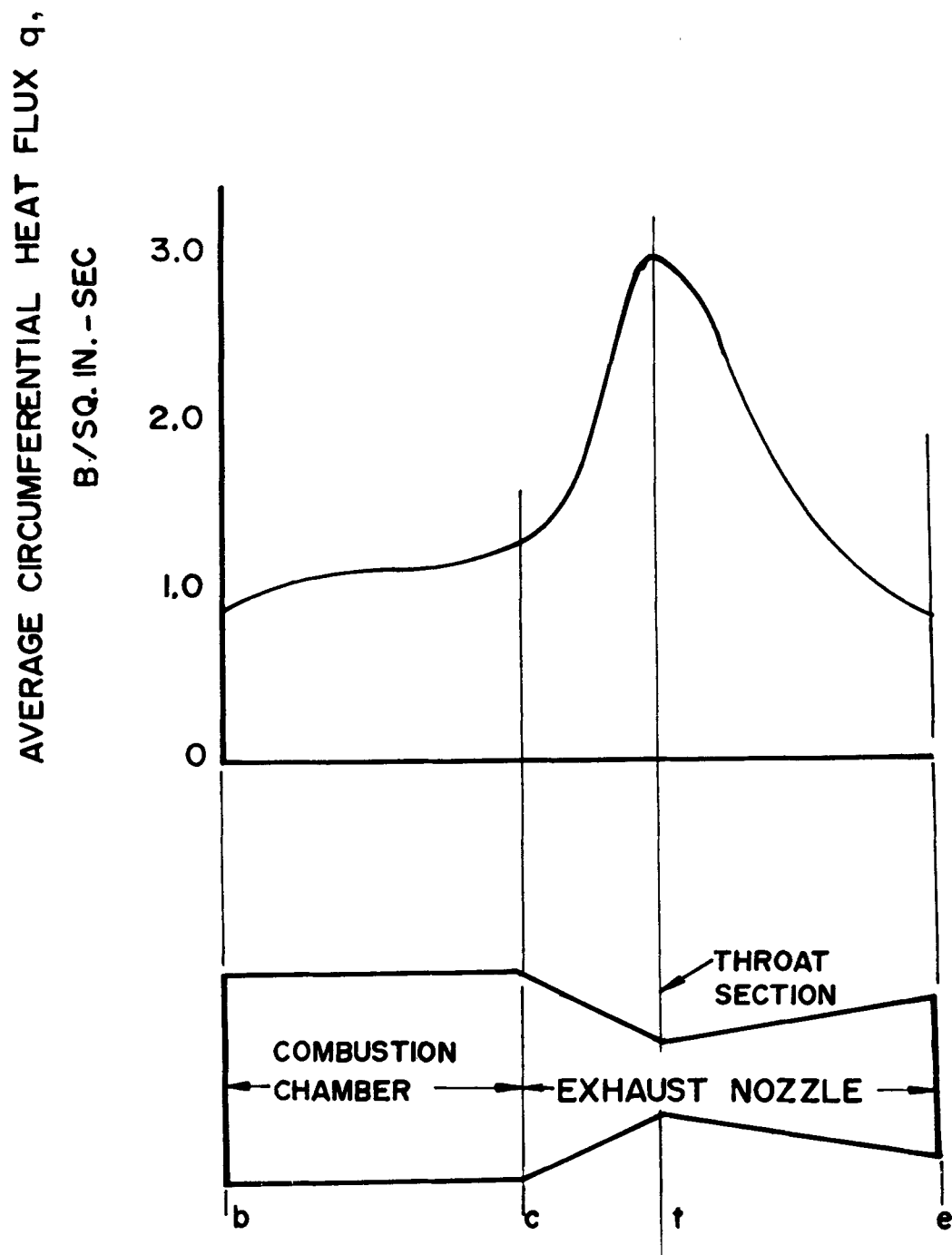


Figure 10-4. Typical Mean Circumferential Heat Flux Distribution
Along a Thrust Chamber Wall

compatible with the constituents of the propulsive gas. The selection of the ceramic material should consider the following^{1 2}:

- (1) It should have good thermal insulating properties.
- (2) It should have a high melting or sublimation temperature.
- (3) It should be resistant to oxidation at high temperatures.
- (4) It should be resistant to thermal shock.
- (5) It should not undergo changes in phase in the thermal range of operation.

Experiments have demonstrated that internal coatings, applied either as a paint before firing or deposits formed from materials added to one of the propellants, can be used as heat-barriers. They suffer from the serious disadvantage that their thicknesses vary during operation, and hence their effectiveness is unpredictable. Experiments with liquid propellant thrust chambers burning fuels such as JP-4 or RP-1 indicated that the deposition of carbon may be effective as a heat-barrier deposit^{5, 16}.

10-4.2.3 COMPOUND HEAT-SINK AND HEAT-BARRIER COOLING OF THRUST CHAMBERS

Compound designs have in the main been utilized for constructing the exhaust nozzles for solid propellant rocket motors (see par. 8-6.5 and Fig. 8-9). The compound designs are based on utilizing the favorable properties of metallic and nonmetallic materials to provide both heat-sink and heat-barrier functions for maintaining the structural integrity of the nozzle.

A typical compound design of an exhaust nozzle would comprise a relatively thin outer metallic shell of molybdenum faced on a thick wall of a refractory material—for example, refrasil, asbestos fiber, zirconium oxide, a silicate, glass fiber, etc.—followed by a layer of graphite, and finally, exposed to the hot propulsive gas, a layer of a ceramic material having a fusion temperature exceeding 4700°F.

10-4.3 REGENERATIVE COOLING SYSTEMS

Figure 10-1(B) illustrates schematically how regenerative cooling is employed for liquid propellant thrust chambers. In the figure the fuel is circulated in a helical fashion around the inner walls before it is injected into the combustion chamber. For large thrust chambers and for those to be operated at combustion pressures above approximately 1800 psia the thrust chamber configuration may comprise an array of truncated or pie-shaped, thin-walled tubes which are formed so that when they are either brazed or welded together their inner surfaces form the passage for the propulsive gas. The propellant used for cooling the heated surfaces flows through the tubes. As pointed out earlier, heat is transferred to the coolant through the tube wall by forced convection and radiation.

It is not possible to predict the heat fluxes from the hot propulsive gas to the heated surfaces with good accuracy because the detailed phenomena are incompletely understood, as explained earlier. Consequently, to calculate predicted values of heat flux one must extrapolate experimental data which are representative for the thrust chamber under consideration. It should be noted that even if the overall heat fluxes could be calculated accurately, their values cannot be regarded as sound criteria of the ability of the thrust chamber to operate with no "burnout". There is experimental evidence indicating that, for a given thrust chamber configuration, the design of the injector can exercise a major influence in producing local "hot spots".

Despite the inadequacies of the current methods for estimating heat transfer rates, the predicted and the experimental values of the heat flux distribution along the wall of the thrust chamber are instructive. They may be considered as preliminary qualitative information regarding the severity of the cooling problem.

For the metals employed for constructing liquid propellant chambers — such as stainless steel, Inconel, nickel, etc. — it is desirable to maintain the surface temperature of the hot gas side of the wall in the range 1500° to 2000°F depending upon the construction material. The choice of the propellant to be the regenerative coolant is based upon its ability to absorb the heat transferred with only local or nucleate boiling; the bulk of the liquid must not reach either its boiling or decomposition temperature^{19,20}.

If the temperature rise of the liquid (propellant) coolant is measured between any two sections of the thrust chamber, the heat flux q is given by

$$q = \frac{1}{A_q} \int_{T_{L1}}^{T_{L2}} \dot{m}_L c_{pL} \Delta T_L$$

$$= \left(\frac{\dot{m}}{A_q} \right)_{av} \bar{c}_{pL} (T_{L2} - T_{L1}) \quad (10-17)$$

where

A_q = area perpendicular to the heat flux q

\dot{m}_L = mass flow rate of coolant

\bar{c}_{pL} = average value of specific heat of the liquid coolant over the temperature range T_{L1} to T_{L2}

T_{L1} = temperature of liquid coolant at Station 1

T_{L2} = temperature of liquid coolant at Station 2

Ordinarily the heat flux for a complete thrust chamber is subdivided into measurement of the flux to the combustion chamber portion A_{qc} , to the nozzle converging portion including the throat A_{qt} , and to the nozzle diverging (or exit) portion A_{qe} .

The heat to the walls of the thrust chamber is conducted not only through the wall but also through the gas film on the hot side of the wall and the liquid film on the cooled side. The rate at which heat flows through a wall of thickness L is given by

$$\dot{Q}_w = \frac{k_w}{L} A_L \Delta T = \frac{k_w}{L} A_L (T_{wL} - T_L) \quad (10-18)$$

where k_w is the thermal conductivity of the wall material at its average operating temperature, T_{wL} is the wall temperature on the liquid coolant side, and T_L is the mean temperature of the main body of liquid coolant.

The ratio k_w/L is termed the *liquid film conductance coefficient* and is denoted by h_L . Thus

$$h_L = k_w/L \quad (10-19)$$

If the measurement of the heat flow through the wall is based on the area of the heated wall area A_q , then the wall temperature on the coolant side T_L is given by

$$T_{wL} = T_L + \frac{\dot{Q}_w}{h_L A_F} \quad (10-20)$$

where

$$T_L = \frac{T_{L1} + T_{L2}}{2} \quad (10-21)$$

and

$$A_F = A_L/A_G \quad (10-22)$$

The temperature of the inner wall wetted by the hot propulsive gas, denoted by T_{wg} , is given by

$$T_{wg} = \frac{q}{h_w} + T_{wL} \quad (10-23)$$

where

h_w = is the conductance of the wall material

q = the heat flux, B/sq in.-sec

If R_1 and R_2 denote the radii to the gas and liquid sides of the wall, respectively, then

$$h_w = \frac{k_w}{R_1 \ln(R_2/R_1)} \quad (10-24)$$

The denominator in Eq. 10-24 is termed the *effective wall thickness*; it is a convenient parameter for accounting for the increase in the heat flow area from the hot gas side to the liquid coolant side.

After T_{wL} and T_{wg} have been calculated from Eqs. 10-20 and 10-23, respectively, the average wall temperature T_w is calculated to determine the allowable stress for the wall material. It is assumed that T_w is given by

$$T_w = (T_{wL} + T_{wg})/2 \quad (10-25)$$

Because the thermal conductivity of the wall material k_w varies with the wall temperature T_w , and the latter is an unknown, the final solution for Eqs. 10-20, 10-23, and 10-25 can be obtained only by trial and error.

In designing the regenerative cooling system it is important that the pressure drop required for forcing the liquid coolant through the cooling passages is not excessive.

The effectiveness of regenerative cooling depends upon the ability of the liquid coolant, usually the fuel, to absorb all of the heat transferred to it without vaporizing. In many current thrust chambers the regenerative cooling is supplemented with a form of *internal cooling*, termed *curtain cooling*, which is a fuel-rich boundary layer of gas adjacent to the walls of the thrust chamber formed by injecting fuel through the outermost ring of injector nozzles^{2,4}.

10-4.4 INTERNAL COOLING SYSTEMS

Fig. 10-3 indicates that all internal cooling systems are based on injecting mass into the thrust chamber so that the injected mass protects the thrust chamber walls from the hot propulsive gas. Internal cooling systems are of three main types:

- (1) Film cooling
- (2) Transpiration cooling
- (3) Ablation cooling

10-4.4.1 FILM COOLING

Film cooling is based on interposing a thin film of fluid, usually the liquid fuel, between the hot propulsive gas and the wall of the thrust chamber to be protected from it. The liquid for forming the film is injected into the thrust chamber at a low velocity and in a manner that will produce a stable liquid film on the wall to be protected^{2,22}. As the film moves downstream it becomes thinner due to evaporation, and a new injection station is located close to the region where all of the liquid in the film is evaporated. For the application of film cooling,

the parameter of interest is the mass flow rate of film coolant \dot{m}_{fc} per unit area of the surface which is film-cooled. Thus

$$\frac{\dot{m}_{fc}}{A_s} \approx h \frac{(T_g - T_v)}{c_{pL}(T_v - T_{oL}) + \Delta H_v} \quad (10-26)$$

where

T_{oL} = inlet temperature of the liquid coolant

T_g = temperature of the flowing gas

T_v = temperature of the surface of the liquid film, assumed to be saturation temperature of the liquid coolant

ΔH_v = enthalpy of evaporation of the liquid coolant

A_s = area of film-cooled surface

c_{pL} = specific heat of the liquid coolant

In Eq. 10-26 the parameter h is the heat transfer coefficient for the two-phase flow. Methods for evaluating h theoretically are given in References 25, 26, 27, and 28.

10-4.4.2 TRANSPIRATION COOLING

This type of cooling refers to methods for establishing a protective fluid film by forcing a fluid, usually a liquid, through a porous material. For the practical realization of transpiration cooling porous walls having the required permeability, flow resistance and light weight are needed. If the porosity is too fine, the porous wall may filter out any solid impurities in the liquid coolant and become "plugged", thereby causing a local hot spot which causes a "burn-out".

In relatively recent years a porous metal made from sintered woven-wire cloth, known as

"Rigimesh", has been developed for transpiration cooling applications. It is reported that most of the U.S. liquid hydrogen-liquid oxygen rocket thrust chambers have injectors employing Rigimesh plate²⁹.

10-4.4.3 ABLATION COOLING

The problem of providing thermal protection to surfaces wetted by hot flowing gases has received considerable study in recent years, particularly for protecting re-entry bodies from aerodynamic heating. A similar problem is encountered in developing means for reducing the thermal flux to the metal portion of the exhaust nozzle of a solid propellant rocket motor. The solution of the aforementioned problems has resulted in the development of ablating materials as means for protecting surfaces from high temperature gases. The ablating material is applied to the metal walls of the thrust chamber, as illustrated in Fig. 10-5.

Due to the flow of hot propulsive gas past the ablating material, heat is transferred to the latter and a phase change occurs in the ablating material which results in what is essentially a *mass transfer*, i.e., the injection of gaseous ablated material into the hot gas boundary layer. The injection of the gas into the boundary layer produces a *thermal blocking effect* to the transfer of heat to the ablating material that is commonly termed either the *mass-transfer effect* or the *transpiration factor*^{29,30}. As stated in Reference 31, "The outstanding assets of successful ablative materials are their high sensible and latent heat capabilities and their suitability for the creation *in situ* of high surface temperature, low-density insulative *char layers*".

Two different ablative processes are possible:

- (1) Ablation with fusion of the ablative material and evaporation of the melted layer (liquid film) as illustrated in Fig. 10-6(A).

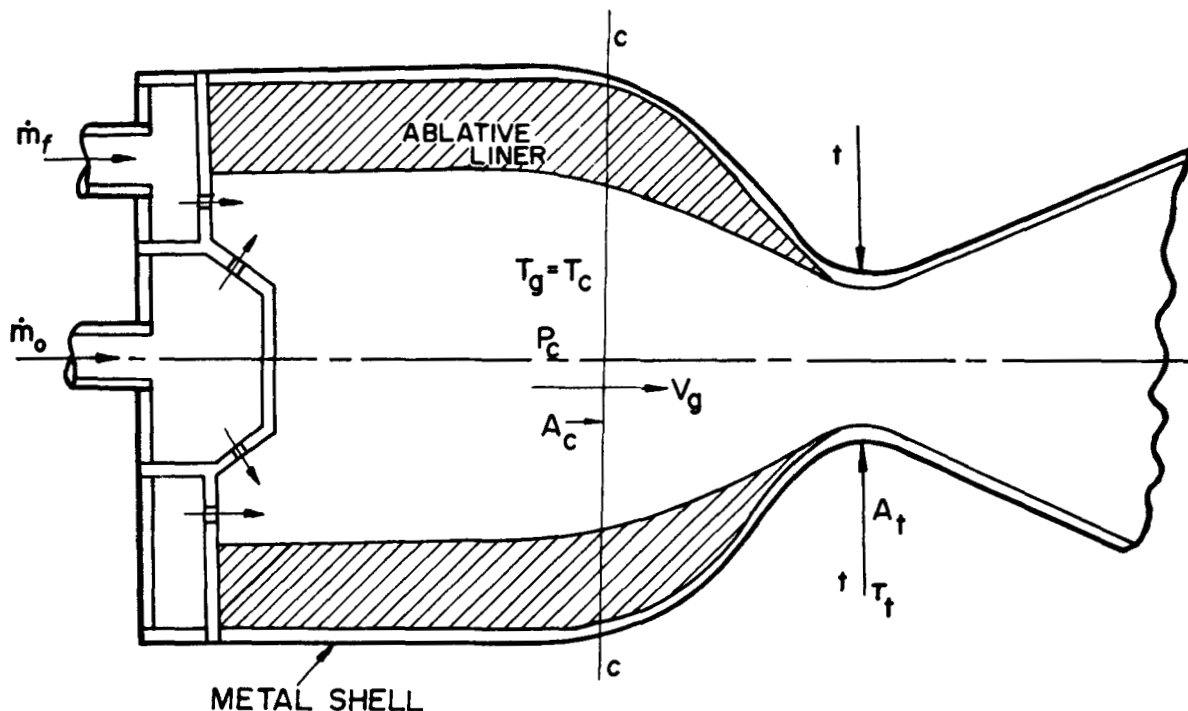


Figure 10-5. Application of an Ablating Material to a Liquid Propellant Thrust Chamber

- (2) Ablation by *sublimation* of the solid ablating material, as illustrated in Fig. 10-6(B).

Figs. 10-6(A) and 10-6(B) illustrate schematically the heat balances for the two ablation processes.

Let

q_c = the incident heat flux, transferred by convection, from the hot propulsive gas to the ablating material

q_{ch} = the heat flux due to chemical reactions of the ablative materials because of its exposure to the high temperature gas stream (e.g., combustion, decomposition, etc.)

q_L = the heat flux absorbed by the liquid (melted) layer of ablative material; the melted material flows downstream and

absorbs more heat than if it remained stationary

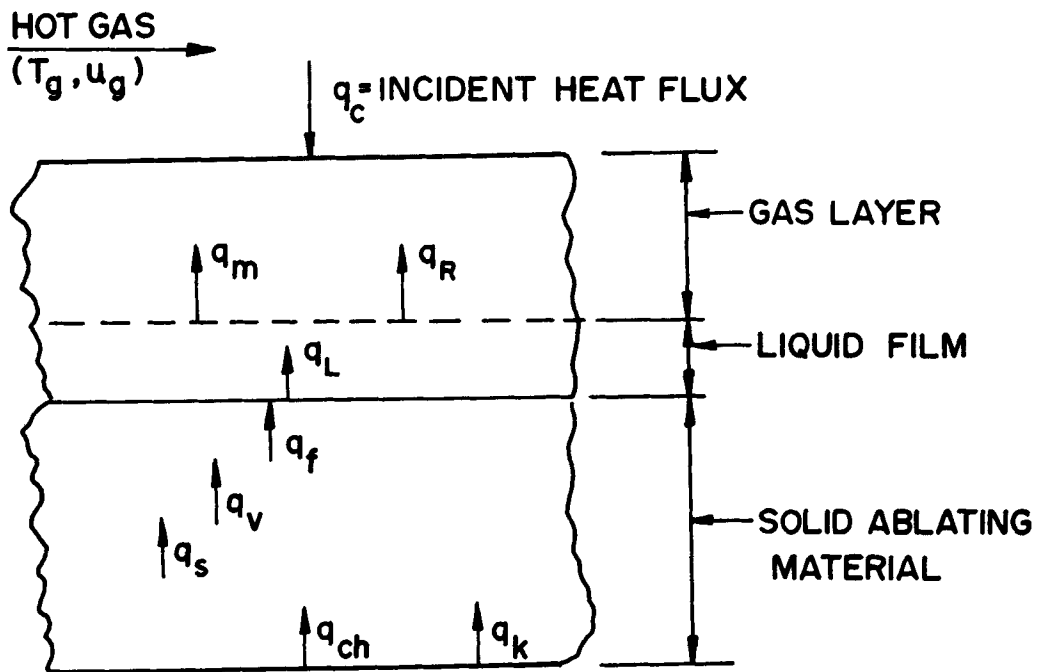
q_f = the heat flux absorbed in melting the ablative material

q_v = the heat flux absorbed in vaporizing the melted ablative material

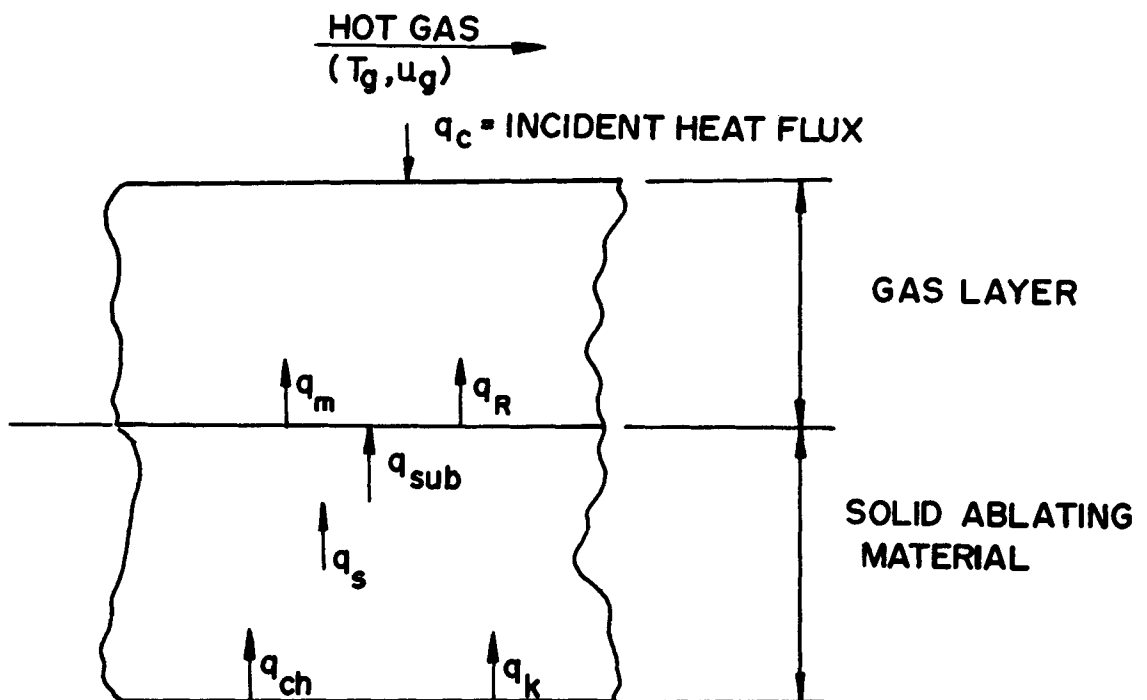
q_s = the heat flux absorbed in raising the temperature of the ablative material from its initial temperature to the fusion temperature

q_R = the heat flux emitted by radiation to the gas layer

q_k = the heat flux absorbed by conduction to the solid ablating material



(A) ABLATION BY FUSION AND VAPORIZATION



(B) ABLATION BY SUBLIMATION

Figure 10-6. Heat Balances for Ablation Cooling

If steady state conditions are assumed, the heat balance equations for the two cases of ablation illustrated in Fig. 10-6, are as follows:

1. *Ablation with fusion and evaporation*

$$q_c \pm q_{ch} - (q_m + q_L + q_f + q_v + q_s + q_R + q_k) = 0 \quad (10-27)$$

2. *Ablation with sublimation*

$$q_c \pm q_{ch} - (q_m + q_{sub} + q_s + q_R + q_k) = 0 \quad (10-28)$$

In Eq. 10-28, q_s denotes the heat flux absorbed in raising the temperature of the ablating material from its initial temperature to the ablation temperature, i.e., the sensible and latent heats of ablation. The term q_{sub} denotes the thermal flux absorbed in causing the sublimation of the ablating material.

Regardless of the type of ablation process, the most significant term is the mass-transfer effect q_m . Introducing gas into the boundary layer causes it to thicken with a simultaneous reduction in skin friction and heat transfer^{2,9}.

Ablative materials have been applied to give thermal protection to the metal walls of liquid propellant thrust chambers employed in the LANCE missile. As is to be expected they can only be applied where the limited operational life for the thrust chamber satisfies the operational requirements.

10-5 FEED SYSTEMS FOR LIQUID PROPELLANT ROCKET ENGINES

There are three principal systems for forcing liquid propellants from the propellant tanks into the thrust cylinder: stored inert gas pressurization, chemical gas pressurization, and turbo-pump pressurization.

10-5.1 STORED (INERT) GAS PRESSURIZATION

Fig. 10-7 illustrates schematically the essential elements of a stored gas pressurization system. A gas such as nitrogen or helium is stored under pressure (1800 to 4000 psia, depending upon the desired chamber pressure) and used for pressurizing the propellant tanks. The system is simple and reliable. Gas is supplied to the propellant tanks at a regulated pressure which maintains the propellant flow rates at the desired values. The gas pressure in each propellant tank exceeds the combustion pressure by the sum of the pressure drops in the propellant feed line and the injector. Consequently, the propellant tanks must be designed to withstand relatively high pressures.

It is usually desirable that the pressurizing gas should not react chemically with, or dissolve in, either the fuel or the oxidizer. Where one or both of the propellants is a liquefied gas, such as liquid oxygen, the pressurizing gas must not condense when it comes in contact with the liquefied gas.

The stored gas pressurization system is most applicable to either short-duration or small thrust rocket engines because of the large weights of the high pressure tanks for the stored gas and for the propellants. It may find application to missiles having a relatively short range (up to approximately 75 miles) where simplicity and reliability are more important than the weight of the missile.

The weight of pressurizing gas required for a given set of operating conditions depends upon the molecular weight and specific heat ratio for the stored gas. Thus, the weight of helium required in a given case, compared to air or nitrogen, is approximately 65 percent. The decrease in the weight of stored gas achieved by using helium has only an insignificant influence upon the overall weight of the pressurization system because the weights of the stored gas and the propellant tanks are practically unchanged.

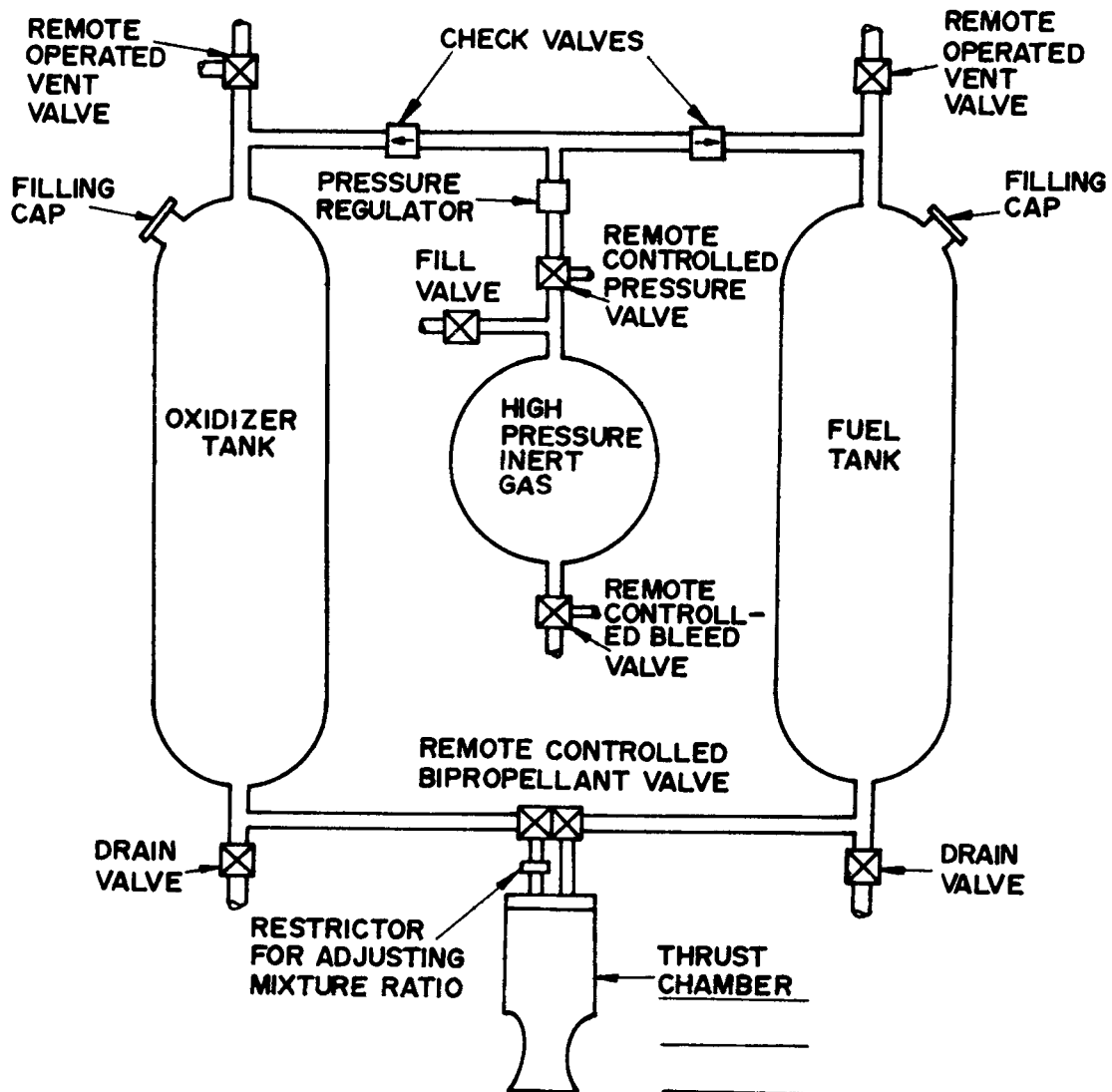


Figure 10-7. Diagrammatic Arrangement of a Stored Gas Pressurization System

10-5.2 CHEMICAL GAS PRESSURIZATION

In a chemical gas pressurization the pressurizing gas is produced by a chemical reaction as it is used, thereby essentially eliminating a large part of the weight of the high pressure tank required in a stored gas pressurization system. The pressurizing gas is produced in a special gas generator either by reacting liquid bipropellants, decomposing a monopropellant such as hydrazine, or by burning a solid propellant.

Irrespective of the method employed, it is important that there be no chemical reaction between the pressurizing gas and the liquid propellant. Neither should they react physically. Moreover, the temperature should be low enough to preclude structural problems due to heating.

Low temperature gases which will not react chemically with the propellants can be obtained by employing two gas generators; one for

pressurizing the oxidizer, and the other the fuel. The former is operated rich in oxidizer and the latter rich in fuel.

10-5.3 TURBOPUMP PRESSURIZATION

The large tank weights required with either the inert gas or the stored gas pressurization systems are greatly reduced by employing a turbopump pressurization system. The latter consists of a set of propellant pumps driven by a turbine which is powered by gases generated in some form of gas generator, as illustrated schematically in Fig. 10-8.

As the thrust of the rocket engine is increased, there is a reduction in the operating duration for which the turbopump pressurizing system becomes lighter than the inert gas pressurizing system; e.g., for a 5000 lb thrust engine the operating duration is approximately 25 sec and for a 50,000 lb thrust engine it is approximately 7 sec. Turbopump pressurization is particularly suitable in the case of liquid rocket engines which must develop either large thrusts, or operate for long durations, or both. This type of engine is particularly adaptable to the propulsion of intermediate and long-range surface-to-surface missiles.

Because of the importance of low weight in the liquid propellant engines for such missiles, the turbines and pumps must be light in weight. Such turbines and pumps are generally operated at high speeds in order to hold weight to a minimum. The pumps are usually centrifugal pumps with radial bladed impellers of high specific speed design and operate with high fluid velocities at their entrance sections^{33,34,35}. To avoid cavitation, which occurs when the static pressure in the flowing fluid is smaller than its vapor pressure, the propellants must be pressurized^{36,37}. Hence, the selection of the pump

speed requires optimization of two influences: (1) the decreasing weight of higher speed pumps, and (2) the increasing weight of the gas pressurizing apparatus required for minimizing cavitation effects.

In most turbopump systems the gases for operating the turbine are produced in a separate gas generator either by reacting suitable propellants or by decomposing a monopropellant. The gases must be supplied at a temperature which the turbine blades can safely withstand.

In cases where the propellants burned in the gas generator are the same as those burned in the thrust cylinder, the mixture ratios must be either fuel-rich or oxidizer-rich in order to limit the gas temperature to approximately 1800°F. If the fuel is a hydrocarbon and the gases are fuel-rich, problems due to carbon depositing in critical passages of the gas generator and turbine are apt to be encountered. If the gases are oxidizer-rich severe corrosion problems may be met.

Gases produced by decomposition of high strength peroxide (HTP) for operation of the turbine consist of steam and oxygen at less than 1000°F. Gases produced by the decomposition of hydrazine (see par. 9-3.1) are at approximately 1800°F.

10-6 THRUST VECTOR CONTROL

Thrust vector control has been discussed in detail in par. 8-7.7.1 and much of the discussion in that paragraph also applies to liquid propellant rocket engines. In many current liquid propellant engines, thrust vector control is achieved by gimbaling the complete thrust chamber and its turbopump so that the thrust chamber can be pivoted with respect to the thrust axis. The hydraulic actuators for moving the assembly are usually operated by liquid fuel tapped from the fuel pump discharge.

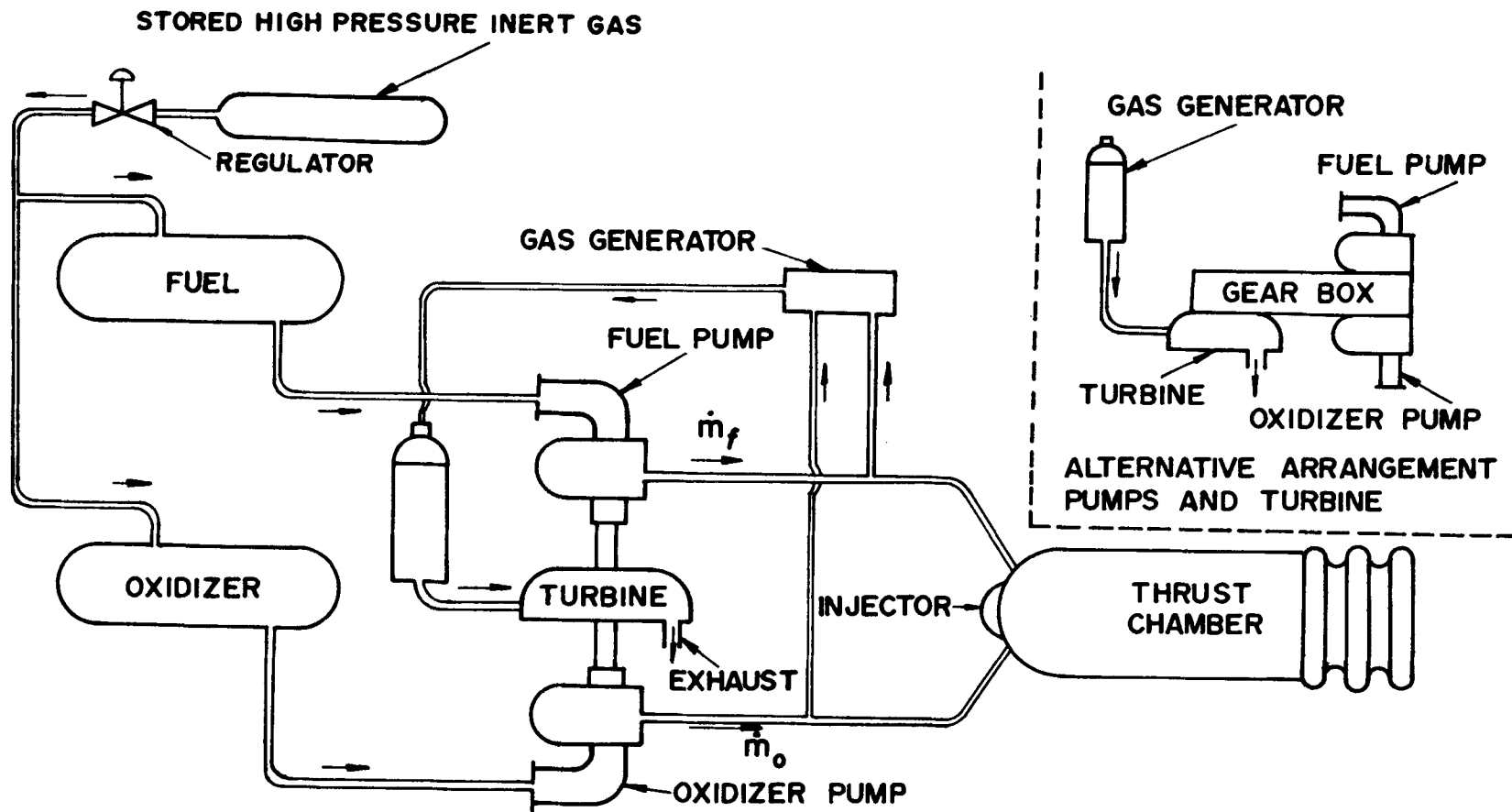


Figure 10-8. Schematic Arrangement of the Components of a Turbopump Pressurization System

10-7 VARIABLE THRUST LIQUID ROCKET ENGINES

The thrust of a rocket thrust chamber is given by Eq. 5-10 which is repeated here for convenience

$$F = C_F A_t P_c = \dot{w} I_{sp} \propto \dot{w} \sqrt{T_c / \bar{m}} \quad (10-29)$$

where, as before, \bar{m} is the molecular weight of the propulsive gas.

Eq. 10-29 indicates that the thrust of a liquid propellant thrust chamber can be varied by varying the mass rate of propellant flow, while the mixture ratio $r = \dot{m}_O / \dot{m}_f$ and the nozzle throat area are maintained constant. The combustion pressure P_c will then vary almost

linearly with the propellant flow rate. Decreasing the flow rate, in addition to reducing P_c also reduces the specific impulse I_{sp} . If $r = \dot{m}_O / \dot{m}_f$ is held constant, the thrust can be varied by varying simultaneously the throat area A_t — by means of a form of plug inserted in the throat — and the propellant flow rate. This method of variable thrust operation keeps P_c , T_c , and \bar{m} essentially constant so that the specific impulse I_{sp} remains substantially constant over the thrust range.

A method for varying thrust by varying the propellant flow rate without causing too small a pressure drop across the injector is to design the latter so that the number of injector orifices through which the liquid fuel and liquid oxidizer can flow can be varied. A mechanical system employing the latter principle is employed in the sustainer motor of the LANCE missile.

REFERENCES

1. M. J. Zucrow, *Aircraft and Missile Propulsion*, John Wiley and Sons, Inc., Vol. 2, Second Printing, 1964, Ch. 10.
2. G. P. Sutton, *Rocket Propulsion Elements*, John Wiley and Sons, Inc., 3rd Edition, 1963, Ch. 4 and 9.
3. M. Summerfield, "Liquid Propellant Rocket Engine", *Liquid Propellant Rockets*, Princeton Aeronautical Paper Backs, Princeton University Press, Section G, 1960, p. 159.
4. H. S. Seifert, "Twenty-Five Years of Rocket Development", *Jet Propulsion*, Vol. 25, Nov. 1955, p. 594.
5. M. J. Zucrow and C. M. Beighley, "Experimental Performance of WFNA-JP-3 Rocket Motors at Different Combustion Pressures", *ARS Jour.*, Vol. 22, Nov.-Dec., 1952, p. 323.
6. D. R. Bartz, "A Simple Equation for Rapid Estimation of Rocket Nozzle Convective Heat Transfer Coefficients", *Jet Propulsion*, Vol. 27, Jan. 1957, p. 49.
7. M. Jacob, *Heat Transfer*, John Wiley and Sons, Inc., Vol I, 1949, Vol. II, 1957.
8. H. Grober, S. Erk and U. Grigull, *Fundamentals of Heat Transfer*, McGraw-Hill Book Company, Inc., 1961.
9. E. R. G. Eckert and R. M. Drake, *Heat and Mass Transfer*, McGraw-Hill Book Company, Inc., 1959.
10. R. D. Turnacliffe, "Rocket Cooling Techniques", *Trans. Am. Soc. Mech. Engrs., Series C, Journal of Heat Transfer*, August 1960, p. 158.
11. J. H. Robinson and K. G. Englar, "Nozzle Wall Materials", *Trans. Am. Soc. Mech. Engrs., Series C, Journal of Heat Transfer*, August 1960, p. 159.
12. C. C. Mu, "Advanced Uncooled Nozzle for Solid Propellant Rockets", *ARS Jour.*, Vol. 31, No. 3, March 1961.
13. R. I. Jaffee and D. K. Maykuth, "Refractory Materials — High Temperature Behavior", *Aerospace Engineering*, July 1960, p. 39.
14. L. E. Dean and L. A. Shurley, "Analysis of Regenerative Cooling in Rocket Thrust Chambers", *Jet Propulsion*, February 1958, p. 104.
15. D. R. Bartz, "Factors Which Influence the Suitability of Liquid Propellants as Rocket Motor Regenerative Coolants", *Jet Propulsion*, Jan. 1958, p. 46.
16. J. P. Sellers, "Effect of Carbon Deposits on Heat Transfer in a LOX/RPP-1 Thrust Chamber", *ARS Jour.*, Vol. 31, No. 5, May 1961, p. 662.
17. E. Mayer, "Analysis of Convective Heat Transfer in Rocket Nozzles", *ARS Jour.*, Vol. 31, No. 7, July 1961, p. 911.
18. A. B. White and E. Y. Harper, "Experimental Investigation of Heat Transfer Rates in Rocket Thrust Chambers", *AIAA Jour.*, Vol. 1, No. 2, Feb. 1963, p. 443.
19. C. M. Beighley and L. E. Dean, "Study of Heat Transfer to JP-4 Jet Fuel", *Jet Propulsion*, May-June 1954, p. 180.

REFERENCES (Continued)

20. R. H. Sabersky and H. E. Mulligan, "On the Relationship Between Fluid Friction and Heat Transfer in Nucleate Boiling", *Jet Propulsion*, Vol. 25, No. 1, Jan. 1955.
21. M. J. Zucrow, C. M. Beighley and E. L. Knuth, *Progress Report on the Stability of Liquid Films for Cooling Rocket Motors*, Tech. Report No. 23, Purdue University, Nov. 1950.
22. M. J. Zucrow and H. R. Graham, "Some Considerations of Film Cooling for Rocket Motors", *Jet Propulsion*, June 1957, p. 650.
23. C. F. Warner and D. L. Emmons, "Effects of Selected Gas Stream Parameters and Coolant Properties on Liquid Film Cooling", *Trans. Am. Soc. Mech. Engrs. Journal of Heat Transfer*, Paper No. 63-HT-38.
24. M. J. Zucrow and J. P. Sellers, "Experimental Investigation of Rocket Motor Film Cooling", *ARS Jour.*, Vol. 31, No. 5, May 1961, p. 668.
25. J. P. Sellers, *Experimental and Theoretical Study of the Application of Film-Cooling to a Cylindrical Rocket Thrust Chamber*, Ph. D. Thesis, Purdue University, 1958.
26. E. L. Knuth, "The Mechanics of Film Cooling", Part 1, *Jet Propulsion*, Nov.-Dec. 1954, p. 359; Part 2, *Jet Propulsion*, Jan. 1955, p. 16.
27. J. P. Hartnett and E. R. F. Eckert, "Mass-Transfer Cooling in a Laminar Boundary Layer with Constant Fluid Properties", *Trans. Am. Soc. Mech. Engrs.*, Vol. 79, February 1957.
28. D. B. Spalding, "Prediction of Adiabatic Wall Temperatures in Film-Cooling Systems", *AIAA Jour.*, Vol. 3, No. 5, May 1965, p. 965.
29. R. Barnhart, "'Rigimesh' Now Heavily Used in Cooling", *Technology Week*, December 19, 1966, p. 36.
30. W. H. Dorrance, *Viscous Hypersonic Flow*, McGraw-Hill Book Company, Inc., 1962.
31. M. C. Adams, "Recent Advances in Ablation", *ARS Jour.*, Vol. 29, No. 9, Sept. 1959, p. 625.
32. S. J. Tick, G. R. Huson and R. Griesse, "Design of Ablative Thrust Chambers and Their Materials", *Journal of Spacecraft*, Vol. 2, No. 3, May-June 1965, p. 325.
33. J. R. Wilhelm, "Ablation of Refrasil-Phenolic Nozzle Inserts in Solid Propellant Exhausts", *Journal of Spacecraft*, Vol. 2, No. 3, May-June 1965, p. 337.
34. M. J. Zucrow, *Jet Propulsion and Gas Turbines*, John Wiley and Sons, Inc., 3rd Printing, 1951, Ch. 2, 9, and 10.
35. A. J. Stepanoff, *Centrifugal and Axial Flow Pumps*, John Wiley and Sons, Inc., 2nd Ed., 1957.
36. A. G. Thatcher, "The Turborocket Propellant Feed System", *ARS Jour.*, Sept. 1950, p. 126.
37. C. C. Ross, "Principles of Turbopump Design", *ARS Jour.*, March 1951, p. 21.
38. C. C. Ross and G. Barnerian, "Some Aspects of High-Suction Specific-Speed Pump Inducers", *Trans. Am. Soc. Mech. Engrs.*, November 1956, p. 1715.

CHAPTER 11

COMPOSITE CHEMICAL JET PROPULSION ENGINES

11-1 INTRODUCTION

For several years theoretical and experimental studies have been conducted for determining the characteristics of composite jet propulsion engines. In such engines the propulsive gas which is to be expanded in an exhaust nozzle, the propulsive element, is produced by reacting chemicals which are in different phases. From a general point of view composite engines may be grouped as follows:

- (1) *Air-augmented* rocket engines. In these engines air is inducted as the oxidant for burning either a *fuel-rich* liquid or solid propellant.
- (2) *Air-turborocket* engines. These are essentially turbojet engines (see Chapter 1) in which the turbine which drives the air compressor is powered by gas produced by reacting chemicals, usually liquid propellants, in a special gas generator. These gases are *fuel-rich* and, after flowing through the turbine, are burned in a combustor with compressed air supplied by the air compressor. The products of combustion, the propulsive gas, then expand in a suitable exhaust nozzle.
- (3) *Hybrid rocket engines*. These are bipropellant rocket engines in which the oxidizer is a liquid and the fuel is a solid. If the phases of the oxidizer and fuel are reversed the engine is termed a *reversed hybrid rocket engine*.

To date the above composite engines have not emerged from the research and development stage.

It is frequently stated that an engine which is an outgrowth of two different engines cannot be superior to its parent engines over the entire range of operation. Nevertheless, the composite engine may have improved characteristics over certain ranges of altitude and flight speeds, and its greater design flexibility may be advantageous for some applications.

In general, the stimuli for developing the composite engines in Groups (1) and (2) are their potential for achieving improved performance at altitude, and faster rate-of-climb for vehicles propelled by conventional air-consuming engines.

The discussions in this chapter will be confined to hybrid-type rocket engines.

11-2 HYBRID-TYPE ROCKET ENGINES

The name hybrid rocket engine applies currently to a bipropellant rocket engine which uses a liquid oxidizer and a solid fuel. The two propellants are stored in separate tanks or chambers within the propelled vehicle. In general, the solid fuel will not burn in the absence of the liquid oxidizer. The solid fuel is normally in the form of a simple internal-burning cylindrical grain, and may or may not be case-bonded. If the solid fuel contains no solid oxidizer, the propellant system is termed a *true hybrid propellant system*.

To achieve ease of ignition, the solid fuel grain may in some hybrid propulsion systems contain varying amounts of a solid oxidizer, ranging from a few percent to an amount which will sustain combustion of the fuel independently of the injection of liquid oxidizer. Compositions not materially different from those for conventional solid propellants have been investigated, as well as fuel-rich solid propellant grains. Such systems are termed *conventional hybrid rocket engines*.

Because the solid fuel in a *true hybrid rocket engine*, hereafter referred to as a *hybrid rocket engine*, contains no solid oxidizer the hybrid rocket engine is capable of *thrust termination* and *restart* by proper regulation of the flow of *liquid oxidizer*; it is assumed that the liquid oxidizer and solid fuel are *hypergolic*.

11-2.1 CLASSIFICATION OF HYBRID-TYPE ROCKET ENGINES

Hybrid rocket engines can be segregated into two groups based on the methods employed for injecting the liquid oxidizer, mixing the oxidizer and fuel gases, and achieving combustion. The two principal methods are:

(1) Head-end Injection

(2) Afterburning Combustion

11-2.1.1 HEAD-END INJECTION HYBRID ROCKET ENGINE

Fig. 11-1 illustrates schematically the essential elements and their arrangement in a

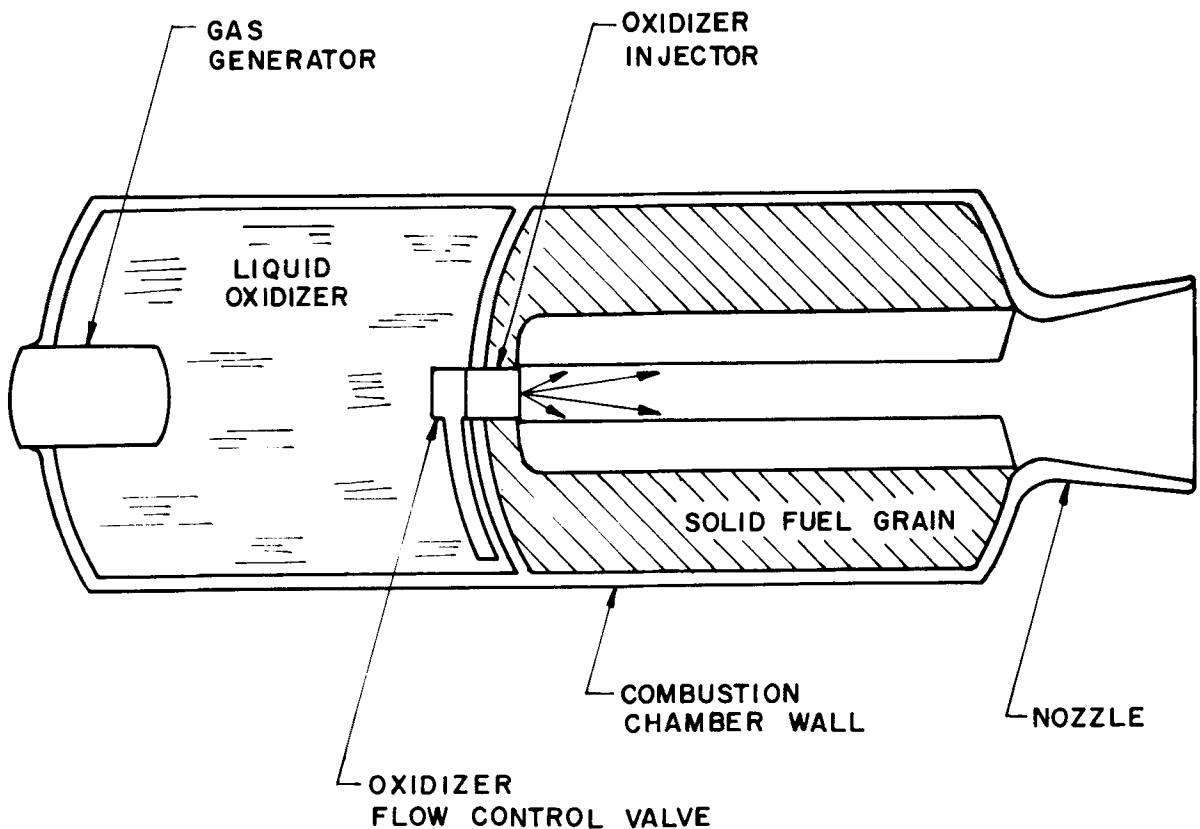


Figure 11-1. Essential Features of a Hybrid Rocket Engine With Head-End Injection of the Liquid Oxidizer

head-end (or *fore-end*) injection hybrid rocket engine. The injector through which the liquid oxidizer is sprayed into the perforation in the solid fuel grain is located at the head-end of the single combustion chamber.

11-2.1.2 AFTERBURNING (CONVENTIONAL) HYBRID ROCKET ENGINE

Fig. 11-2 illustrates diagrammatically the essential features of an *afterburning* (conventional) hybrid rocket engine. In this type of engine the solid propellant grain contains sufficient solid oxidizer to sustain combustion. The fuel-rich gases formed by the combustion of the solid propellant flow toward the afterburner wherein the liquid oxidizer is injected. The fuel-rich gases are mixed with vaporized oxidizer and burned in the afterburner.

A hybrid propellant system cannot be employed in an afterburner engine because the solid fuel has no oxidizer for sustaining its combustion.

Thrust termination in an afterburning conventional hybrid engine cannot be achieved by merely stopping the flow of liquid oxidizer.

11-2.1.3 TRIBRID ROCKET ENGINES

The tribrid rocket engine is an engine employing the hybrid concept, but is uses a *tripropellant* system. A typical tribrid system is one using a solid fuel (such as aluminum hydride), a liquid oxidizer (such as chlorine trifluoride), and a gaseous fuel (such as hydrogen). The liquid oxidizer reacts with the solid fuel to produce high temperature gases,

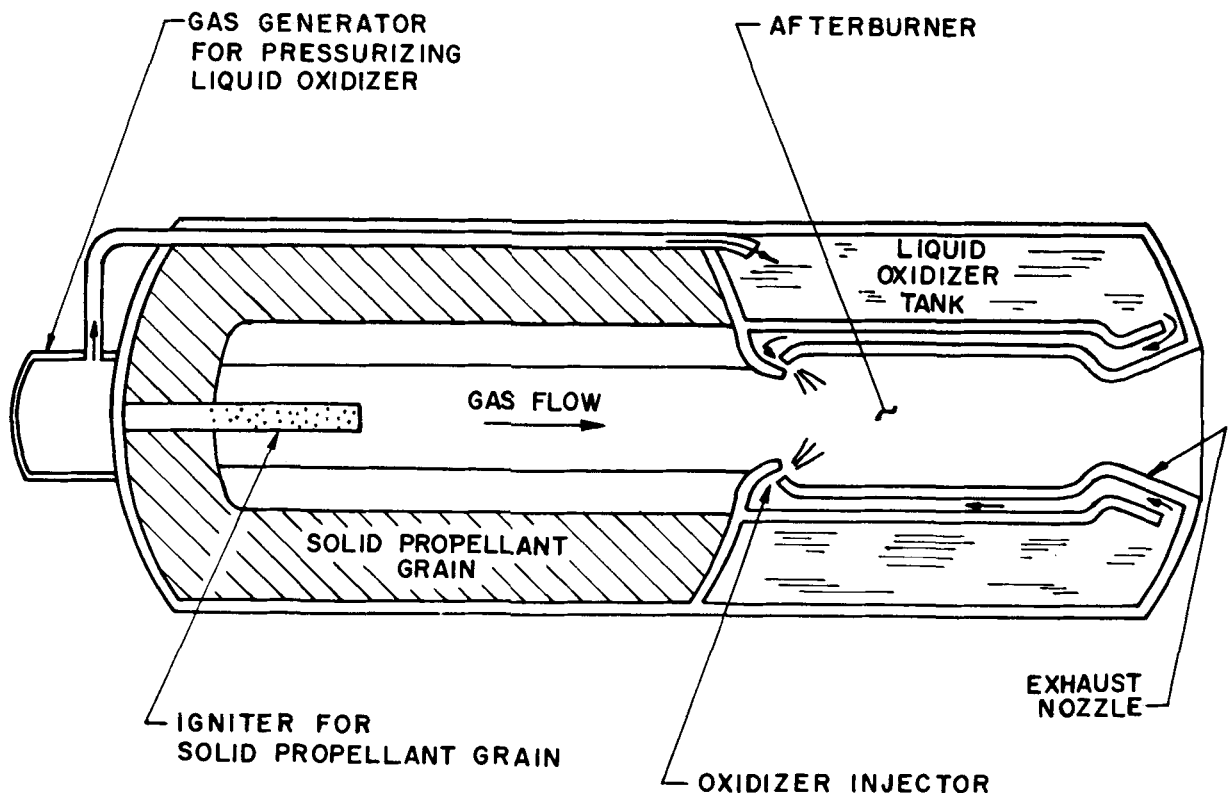


Figure 11-2. Essential Features of an Afterburning Hybrid Rocket Engine

and the hydrogen gas is heated by them so that a low molecular weight propulsive gas is produced. In essence, the tribrid rocket engine is a chemical analogy to a nuclear rocket engine using hydrogen as the working fluid. The hybrid gives higher theoretical values of specific impulse than any of the known chemical bipropellant systems. Only limited experiments have been conducted with tribrid propellant systems.

11-3 POTENTIAL ADVANTAGES OF THE HYBRID ROCKET ENGINE

It is frequently stated, as may be inferred from par. 11-1, that the hybrid rocket engine combines the disadvantageous features of the liquid and solid propellant rocket engines. The proponents of the hybrid rocket engine, however, claim the opposite; i.e., that type of engine combines the most desirable features of its parent engines ^{4,5}. The truth probably lies somewhere between the aforementioned extremes.

The principal advantages of the hybrid rocket engine, real and potential, are related to the following:

- (1) Safety in Handling
- (2) Thrust Termination and Restart
- (3) Volume-limited Propulsion Systems
- (4) Variable Thrust Operation
- (5) Mechanical Properties of the Solid Fuel Grain
- (6) Storability
- (7) Flexibility in Selection of Propellant Systems
- (8) Simplicity

11-3.1 SAFETY IN HANDLING HYBRID PROPELLANTS

Separate storing of the fuel and oxidizer is utilized in liquid bipropellant rocket engines. In a solid propellant rocket motor no such separation is possible. As the performance of solid propellants has been increased, they have become more *shock sensitive*; some formulations are not far different from explosives. The hybrid rocket propellant system eliminates the shock sensitivity associated with high performance solid propellants by separating the fuel and oxidizer until the firing of the engine is desired.

11-3.2 THRUST TERMINATION AND RE-START

The thrust of a true hybrid rocket engine is terminated by terminating the flow of liquid oxidizer. If the liquid oxidizer is hypergolic with the solid fuel, the hybrid rocket engine is restarted by merely restarting the flow of liquid oxidizer.

11-3.3 VOLUME-LIMITED PROPULSION SYSTEMS

The density impulse (see par. 6-3.7.2) is a criterion which gives an approximate indication of the adequacy of a propellant for application to a volume-limited propulsion system. In such a system the amount of energy per unit volume of propellant is important. Since the density impulse I_p is an important parameter — where I_p is the product of the specific impulse and the density of the propellants in cc — the higher the density impulse, the larger is the amount of propellant that can be loaded into a given volume.

The density impulse of some hybrid propellant systems is between 400 and 500 gsec/cc, and some have values exceeding 600 gsec/cc. In comparison, for liquid bipropellant systems, density impulse values are less than 400 gsec/cc,

and for solid propellants they range from 400 to 500 gsec/cc. Consequently, hybrid rocket engines have the potential for storing large amounts of energy per unit volume.

11-3.4 VARIABLE THRUST OPERATION

Hybrid rocket engines offer a relatively simple means for varying the thrust level over a wide range, by merely varying the liquid oxidizer flow rate. Unfortunately, for many hybrid propellant systems the transformation of the solid fuel into the gaseous fuel which reacts with the vaporized (liquid) oxidizer does not vary directly with the oxidizer flow rate. Consequently, the ratio — oxidizer flow rate to fuel flow rate — does not remain constant over the range of thrust variation, and there is a decrease in the specific impulse ⁶.

11-3.5 MECHANICAL PROPERTIES OF THE SOLID FUEL GRAIN

The increase in the specific impulses of modern conventional solid propellants has been achieved in large measure by (1) increasing the percentage of solids (*metal additives and powdered crystalline oxidizers*) in the propellant formulation and (2) simultaneously reducing the percentage of the binder (see par. 7-3). As a result, the mechanical properties of such solid propellant grains have been reduced (see par. 7-5). Since no solid oxidizer or additives are in the formulation for the solid fuel of a hybrid rocket engine, the fuel grain has superior mechanical properties. Furthermore, the solid fuel grain in a *conventional* hybrid rocket engine has improved mechanical properties compared to a solid propellant because of its lower content of solid oxidizer.

11-3.6 STORABILITY OF HIGH ENERGY PROPULSION SYSTEMS

It is possible to use optimum combinations of solid fuel and liquid oxidizer, and there is a great flexibility in the choice of the individual

propellants. In fact, almost any known material which can be handled is a possible candidate as a propellant. Currently, the maximum theoretical specific impulse for hybrid propellant systems is approximately 360 sec, which is comparable with liquid cryogenic bipropellant systems, but with the added feature of storability.

11-3.7 FLEXIBILITY IN PROPELLANT SELECTION

The hybrid concept offers the capability of using optimum propellant systems regardless of the mutual incompatibility of the liquid oxidizer and solid fuel. This gives the engine designer greater flexibility in overcoming the limitations of both solid and liquid propellant rocket propulsion systems ⁶.

11-3.8 SIMPLICITY

The hybrid rocket engine is simpler than a liquid bipropellant rocket engine, but not as simple as a conventional solid propellant rocket motor. If variable thrust, thrust termination, and restart are necessary; then the hybrid rocket engine becomes the simplest rocket engine.

11-4 THEORETICAL SPECIFIC IMPULSES FOR HYBRID ROCKET PROPELLANT SYSTEMS¹⁰

Table 11-1 presents the theoretical specific impulse and the corresponding combustion temperature for hybrid rocket propellant systems using solid fuels and either liquid fluorine or oxygen as the oxidizers. The combustion pressure is $P_c = 1000$ psia in all cases, and the propulsive gas is assumed to expand to standard sea level ($P_{amb} = 14.7$ psia). The calculations are based on shifting equilibrium and a mixture ratio (\dot{w}_o/\dot{w}_f) corresponding to the maximum specific impulse; where \dot{w}_o and \dot{w}_f are the weights of the oxidizer and fuel consumed, respectively.

TABLE 11-1[†]
PERFORMANCE OF HYBRID FUELS WITH FLUORINE
AND OXYGEN OXIDIZERS[‡]

HYBRID PROPELLANT SYSTEM	MIXTURE RATIO, \dot{w}_O/\dot{w}_f	SPECIFIC IMPULSE $P_c = 1000$ psia SEA LEVEL	COMBUSTION TEMP., °K	CHARACTERISTIC VELOCITY c^* , ft/sec
O ₂ /Mg	2.00	222.5	4014	4296
O ₂ /Li	1.50	238.4	3769	4537
O ₂ /B	2.20	260.8	4591	5059
O ₂ /AlH ₃	0.64	308.2	3758	5902
O ₂ /LiBH ₄	2.40	307.6	3773	6035
O ₂ /LiAlH ₄	0.85	307.3	3534	5864
O ₂ /BeH ₂	1.40	379.6	4712	7339
O ₂ /Si	2.00	218.9	3979	4237
O ₂ /SiH ₂	0.80	305.4	4111	6048
O ₂ /Be(BH ₄) ₂	1.77	330.8	3624	6431
F ₂ /Al	2.81	299.7	5480	5903
F ₂ /AlH ₃	3.20	349.0	5247	6872
F ₂ /Be	5.00	355.0	6491	6957
F ₂ /BeH ₂	4.00	391.4	5349	7744
F ₂ /B	5.18	317.5	5278	6241
F ₂ /LiBH ₄	6.00	360.8	4950	7112
F ₂ /LiAlH ₄	3.50	353.2	5144	6962
F ₂ /Li	2.50	378.0	5584	7527
F ₂ /LiH	5.00	362.6	4939	7219
F ₂ /Mg	2.00	302.1	5594	5955
F ₂ /MgH ₂	1.50	367.2	5181	7303
F ₂ /Si	5.00	287.9	4641	5615
F ₂ /SiH ₂	3.00	326.8	5358	6439

[†]Data given at a mixture ratio approximately corresponding to maximum specific impulse.
Shifting equilibrium.

[‡]Unpublished information furnished by Rocketdyne.

It is seen that the F_2 - BeH_2 system gives a theoretical specific impulse of 391.4 sec, which is comparable to the liquid bipropellant system H_2 - F_2 , which for the same conditions gives a theoretical specific impulse of 410 sec.

Table 11-2 presents the same type of information as in Table 11-1 for hybrid solid fuels reacted with hydrogen peroxide and chlorine trifluoride as the liquid oxidizers (see pars. 9-3.2 and 9-4.3.2).

11-4.1 CHARACTERISTICS OF THE PROPULSIVE GAS OF A HYBRID ROCKET ENGINE

It is evident from the propellant systems listed in Tables 11-1 and 11-2 that the chemical reaction of a hybrid propellant system usually produces a propulsive gas having relatively large molecular weight, compared to that of a conventional liquid or solid propellant rocket engine. The higher specific impulse values for

TABLE 11-2[†]

PERFORMANCE OF HYBRID FUELS WITH HYDROGEN PEROXIDE CHLORINE TRIFLUORIDE OXIDIZERS[‡]

HYBRID PROPELLANT SYSTEM	MIXTURE RATIO, \dot{w}_o/\dot{w}_f	SPECIFIC IMPULSE $P_c = 1000$ psia, SEA LEVEL	COMBUSTION TEMP., °K	CHARACTERISTIC VELOCITY c^* , ft/sec
$H_2O_2/.33 Al-67(CH_2)_n$	1.30	290.0	3520	5632
$H_2O_2/(CH_2)_n$	7.30	277.5	2993	5467
H_2O_2/LiH	1.28	266.3	2245	5143
H_2O_2/Al	2.50	266.1	3948	5129
H_2O_2/AlH_3	0.90	321.7	3579	6160
$H_2O_2/LiAlH_4$	1.07	310.7	3211	6052
H_2O_2/SiH_2	1.00	303.1	3256	5880
ClF_3/LiH	5.50	290.0	4086	5893
$ClF_3/19 LiH-1(CH_2)_n$	5.50	288.9	4060	5837
$ClF_3/(CH_2)_n$	3.32	257.8	3543	5165
ClF_3/AlH_3	4.00	289.0	4637	5725
ClF_3/BeH_2	5.00	323.8	4717	6398
$ClF_3/LiAlH_4$	4.00	290.2	4437	5759
ClF_3/SiH_2	5.00	274.0	4461	5339
ClF_3/MgH_2	3.00	278.0	4444	5507

[†]Data given at a mixture ratio approximately corresponding to maximum specific impulse.
Shifting equilibrium
All H_2O_2 calculations for 100% H_2O_2 .

[‡]Unpublished information furnished by Rocketdyne.

hybrid propellant systems are due to their high combustion temperatures. The maximum specific impulse is obtained with several hybrid propellant systems when they are reacted with an excess of oxidizer. Consequently, the hot propulsive gas is *oxidizer rich* so that there occurs a vigorous chemical reaction with the walls of the exhaust nozzle and structural members.

11-4.2 COMBUSTION OF HYBRID PROPELLANTS

The basic problems in developing a hybrid rocket engine are related to the combustion process. Currently, the combustion efficiency of hybrid propellant systems is low, so that the actual specific impulse is, at best, approximately 85 percent of the theoretical specific impulse. Furthermore, the solid fuel burns unevenly along its length and a "burnout" may occur before all of the fuel is consumed. Consequently, the major objectives of the research and development effort for the past several years have been concerned with obtaining a better understanding of the combustion process, and with investigating methods for controlling it⁶.

It is well-recognized that the combustion process in a hybrid rocket engine is quite different from that occurring in either a liquid propellant or solid propellant rocket engine. From the investigations conducted to date it has been determined that the combustion processes in a hybrid engine are amenable to scientific analysis, and that the basic phenomena are now well understood. Also several of the processes can be described by mathematical equations^{6,7}.

It has been established that the actual combustion occurs in a relatively narrow zone which is fed by gaseous decomposition products of the solid fuel and gases from the liquid oxidizer. The heat for producing and heating those gases comes from the combustion zone by

either conduction or radiation, or both. Where the gasified fuel and oxidizer meet, combustion occurs; the products of combustion, the propulsive gases, diffuse away from the combustion chamber.

The surface of the solid fuel in a hybrid rocket engine is much colder than the combustion temperature because it is controlled by the temperature required for either vaporizing or decomposing the solid fuel; for conventional hybrid fuels the surface temperature is between 400° and 750°F. Furthermore, the temperature at the center line of the perforation in the solid fuel grain, termed *the port*, is also relatively low⁶.

The liquid or gaseous oxidizer sprayed into the port (see Fig. 11-1) should not impinge upon the surface of the solid fuel grain after chemical reaction has been initiated. Instead, it should diffuse and vaporize so that it will mix readily with the material in the active combustion zone⁶.

The major factor in improving the performance of a hybrid rocket engine is the control of the processes so that there is a thorough mixing of the vaporized fuel and oxidizer, and combustion is complete, so that no unreacted materials are exhausted through the exhaust nozzle.

Another major combustion problem relates to the low rates of combustion obtained with hybrid propellant systems. Because the solid fuel grain contains no oxidizer, the rate of transformation of the fuel from the solid to the gas phase is governed primarily by the heat transferred to the grain and the energy required for the phase transformation. The ideal hybrid fuel would be one having the lowest possible enthalpy of vaporization or decomposition.

11-5 PERFORMANCE PARAMETERS FOR HYBRID ROCKET ENGINES

The performance parameters for chemical rocket propulsion systems, discussed in Chapter 5, are applicable to hybrid rocket engines. For example, the specific impulse I_{sp} , the characteristic velocity c^* , and the effective jet velocity c have the same meanings for all rocket propulsion systems. Some modifications to some of the performance criteria are needed in applying them to hybrid rocket engines. Two such modifications will be discussed.

11-5.1 SPECIFIC IMPULSE OF A HYBRID ROCKET ENGINE

Two interpretations of the specific impulse are employed quite generally; namely, the *instantaneous specific impulse*, and the *system specific impulse*.

The instantaneous specific impulse is defined by Eq. 5-4, which is repeated here for convenience. Thus

$$I_{sp} = Fg_c / \dot{m}_p = F / \dot{w}_p \quad (11-1)$$

where

F = instantaneous thrust, lb

\dot{m}_p = instantaneous mass rate of consumption of propellants, slug/sec

\dot{w}_p = instantaneous weight rate of consumption of propellants, lb/sec

g_c = gravitational conversion factor = 32.174 slug-ft/lb-sec²

The system specific impulse is defined by

$$I_{sp} = \int_{t=0}^{t=t_B} (Fdt/W_p) \quad (11-2)$$

where

t = time

t_B = time to consume the propellant weight W_p

Eq. 11-1 defines the specific impulse at any instant of time. Its value may vary throughout a firing because it is a function of the combustion conditions. In general, the instantaneous specific impulse corresponds to the maximum value obtainable from the engine. Fig. 11-3 illustrates the manner in which the instantaneous specific impulse could vary during a typical firing of a hybrid rocket engine. The system specific impulse defined by Eq. 11-2 gives the average value for the engine for a complete firing; it, therefore, includes the inefficiencies due to ignition, flow rate variation, sliver loss, etc. In many liquid and solid propellant rocket engines the difference between the two values of specific impulse may not be great. In the case of a hybrid rocket engine, however, values of the instantaneous and system specific impulses may be quite different because of such difficulties as the proper sequencing of the oxidizer liquid flow, fluctuations in its mass flow rate, pressure variations, etc. Fig. 11-4 illustrates a typical pressure-time curve for a hybrid rocket engine.

The system specific impulse more nearly presents the actual capability of a hybrid rocket engine. Moreover, there is no method for accurately determining the fuel consumption rate, hence any stated values of instantaneous specific impulse for a hybrid rocket engine are open to question.

11-5.2 CHARACTERISTIC VELOCITY FOR A HYBRID ROCKET ENGINE

The comments in par. 11-5.1 with regard to the specific impulse are also applicable to the characteristic velocity c^* . The characteristic velocity is defined by Eq. 5-13, which is repeated here for convenience. Thus, the

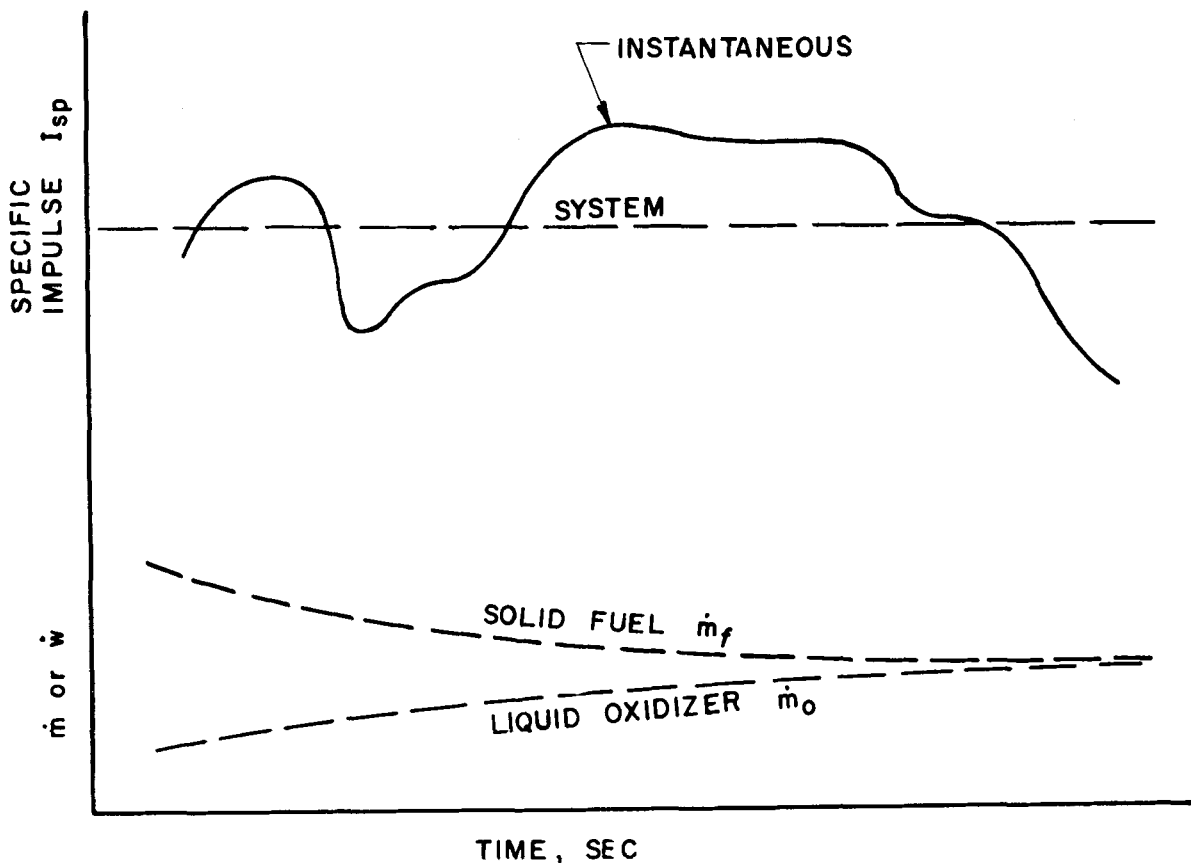


Figure 11-3. Variations in Instantaneous and System Specific Impulse During the Firing of a Hybrid Rocket Engine

instantaneous characteristic velocity is defined by

$$c^* = P_c A_t g_c / \dot{w}_p \quad (11-3)$$

where

P_c = the chamber pressure

A_t = the area of the nozzle throat

Accordingly, the system c^* is given by

$$c^* = \int_{t=0}^{t=t_B} (P_c A_t g_c / \dot{w}_p) dt \quad (11-4)$$

A problem is encountered in determining the system characteristic velocity because the throat of a hybrid rocket engine erodes during the firing. To obtain an average value for the throat area A_t during the complete firing, two methods have been used. One assumes that the throat diameter increases linearly with time, and the other assumes that the value of the throat area is the arithmetic average of the nozzle throat areas before and after the firing.

11-6 INTERNAL BALLISTICS OF THE HYBRID ROCKET ENGINE

In general, the internal ballistic data for designing solid propellant rocket motors may

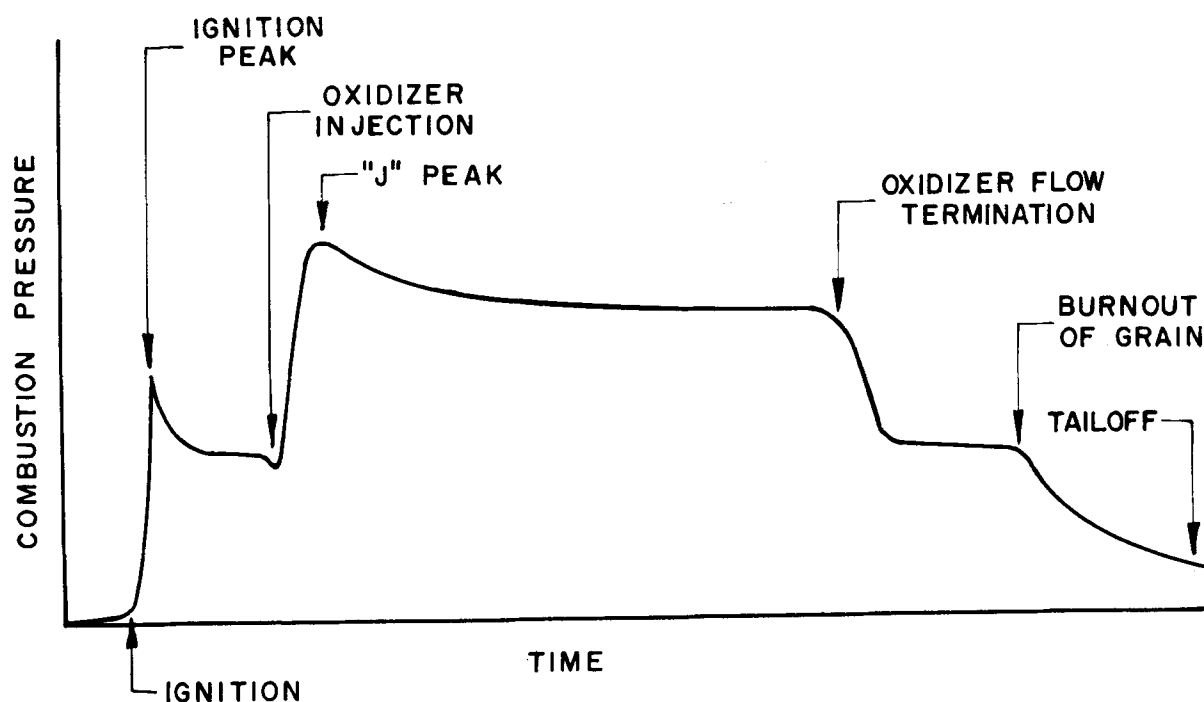


Figure 11-4. Typical Pressure-Time Curve for a Hybrid Rocket Engine

not be applied directly to a hybrid rocket engine. Nevertheless, there are some similarities between the behaviors of these two types of rocket propulsion systems. For example, the thrust equation, given by Eq. 5-10, is also applicable to the hybrid rocket engine.

11-6.1 THRUST EQUATION

From Eq. 5-10, one obtains the following thrust equation for a hybrid rocket engine:

$$F = C_F P_c A_t \quad (11-5)$$

where

C_F = the thrust coefficient (see Chapter 5).

It is not possible to predict either theoretically or empirically the chamber pressure P_c for a hybrid rocket engine. To predict the behavior of a specific hybrid propellant system, data must be available regarding the burning rate laws for that system.

11-6.2 BURNING RATE OF HYBRID PROPELLANTS

In general, Saint-Robert's law for the burning rate of a solid propellant does not apply to the solid fuel grain of a hybrid rocket engine. Experiments indicate that the burning rate, also called the *regression rate* for a hybrid fuel depends upon the flow rate of the liquid oxidizer, in a manner analogous to the dependence of the burning rate of a solid

propellant upon the combustion pressure. The mass flux of the oxidizer has such a predominant influence that, for many hybrid propellant systems, the burning rate depends only slightly on temperature. In general, the regression rate of several nonmetallized solid fuels appears to be independent of the chamber pressure⁸.

Conventional hybrid propellant systems, because they contain oxidizer in the solid fuel grain, are capable of sustaining combustion, and the burning rate follows Saint-Robert's law (see Eq. 8-3). The addition of a liquid oxidizer in the combustion zone alters the behavior of the propellant system, but in a rather predictable manner. For example, the burning rates of several solid propellants are increased approximately 10 percent when they are used in a hybrid application. The increase in burning rate is attributed to the increase in the flame temperature of the hybrid combustion process.

Although several (true) hybrid propellant systems have burning rates which are independent of the chamber pressure, this characteristic does not apply to all hybrid propellant systems¹⁰.

The solid fuel grain of a hybrid rocket engine does burn in accordance with Piobert's law, i.e., the burning surface recedes normal to itself. There are, however, several reservations to that statement. For example, in regions of high concentrations of the oxidizer fluid, the burning surface recedes faster than in those of low oxidizer concentration. This gives rise to what are termed "worm holes" in the solid fuel grain.

The dependence of the burning rate of the hybrid fuel (solid) upon the mass flux of liquid oxidizer has a predominating influence upon the design of the grain configuration for the solid fuel. If the flow of liquid oxidizer is held constant, then the thrust of a hybrid rocket

engine is a function of the solid fuel consumption rate; the latter depends on the rate of production of gaseous fuel per unit area of the grain surface (see par. 8-1.1). Consequently, as the solid fuel surface regresses the port area increases. If the burning surface has a configuration which maintains a constant burning surface, such as an internal burning star, then the thrust will decrease. For the thrust to remain constant, however, the area of the burning surface must be increased. For this reason a tubular internal-burning grain is used in most cases, and is found to give the required increase in burning surface as the burning surface regresses.

11-7 GENERAL DESIGN CONSIDERATIONS PERTINENT TO HYBRID-TYPE ROCKET ENGINES

The unique features of hybrid type rocket engines introduce new design problems in addition to those pertinent to liquid and solid propellant rocket engines. Furthermore, some of the latter design problems are intensified. Some of the new problems still await solutions.

The (true) hybrid rocket engine has been investigated more extensively than the conventional hybrid rocket engine, and as pointed out earlier the hybrid propellants are burned in engines having head-end injection of the liquid oxidizer (see Fig. 11-1). More recently, to improve the combustion efficiency of the hybrid rocket engine, the *post-combustion chamber*—which is inserted between the aft-end of the hybrid combustion chamber and the exhaust nozzle—has been investigated. The arrangement allows a longer "stay time" for mixing of the fuel and oxidizer gases, and improves the combustion process. It must be designed so that it introduces a negligible loss in the stagnation pressure (see par. 10-3.2.2).

In general, the oxidizers used in hybrid type rocket engines are highly reactive chemically. For example, chlorine trifluoride (CTF) reacts

violently with many metals and organic materials (see par. 9-4.3.2). To make use of such an oxidizer, all metal parts exposed to it must be chemically clean and *passivated*. Passivation of a metal surface can be achieved by producing a tenuous and impervious fluoride coating on the metal surface so that the metal is never wetted by the liquid oxidizer. It is important that there be no cracks or "pin-holes" in the passivation coating.

It is important that a thorough study be made for determining those metals, organic and inorganic material, and lubricants that will be compatible with the oxidizer over the required storage life for the hybrid type engine.

11-7.1 PRESSURIZATION OF THE LIQUID OXIDIZER

For all types of hybrid rocket engines the liquid oxidizer which is stored in its own supply tank, must be forced into the combustion region against the combustion pressure. The following pressurizing methods may be employed for injecting the liquid oxidizer into the combustion region: inert gas pressurization, chemical gas pressurizing, or turbopump pressurization (see par. 10-5). Most of the hybrid propulsion systems built to date use inert gas pressurization, but the weight of that pressurizing system is quite high.

11-7.1.1 CHEMICAL GAS PRESSURIZATION

Although chemical gas pressurization systems for hybrid type rocket engines have received considerable attention, some problems are still unresolved. Problems arise because it is essential that the pressurizing gas be clean and that it not react chemically with either the liquid oxidizer or the metal parts of the engine, including the oxidizer storage tank material. Most chemical gas generators use solid propellant grains having formulations which produce *fuel-rich* gases which are cool enough to prevent

chemical reaction with the metal parts of the engine.

Solid propellant chemical gas generators for producing cool oxidizer-rich gases have received scant investigation. Also, chemical gas generators using liquid propellant have not been investigated extensively. In the latter connection, no experiments have been reported on the concept of pressurizing the liquid oxidizer by injecting small amounts of a liquid fuel directly into the oxidizer storage tank.

11-7.1.2 BLADDERS

The possibility of using stainless steel roll-up bladders or separating the liquid oxidizer from the chemical pressurizing gas has been given consideration. The problem of achieving effective separation still remains unsolved.

11-7.1.3 OXIDIZER TANK PRESSURE REQUIREMENTS

The pressure inside the oxidizer tank must be raised sufficiently, by gas pressurization, to insure a steady flow of liquid oxidizer across the injector orifices. For design purposes it can be assumed that a pressure differential of approximately 250 psi will be required across the injector orifices with either head-end injection (true hybrid) or afterburner injection (conventional hybrid).

11-8 DESIGN CONSIDERATIONS PERTINENT TO THE HEAD-END INJECTION HYBRID ROCKET ENGINE

As pointed out earlier, head-end injection can be employed only with a true hybrid rocket engine, i.e., one using a solid fuel grain containing no solid oxidizer (see Fig. 11-1).

11-8.1 THE COMBUSTION CHAMBER

The design of the combustion chamber for housing the solid fuel grain is similar to that for a solid propellant rocket motor (see par. 8-7.4). It should be noted that the propulsive gas temperature T_c (see Tables 11-1 and 11-2) in a hybrid rocket engine is usually higher than in a solid propellant rocket motor, and must be taken into consideration in designing the metal parts.

Certain problems arise with regard to installing the solid fuel grain. Many of them cannot be cast directly into the combustion chamber but must be pressed, sintered or extruded to the required configuration. Additional design problems may be encountered because of the toxicity, vapor pressure, and hygroscopicity of the solid fuel. It may be required, in some cases, that the combustion chamber be sealed and contain an inert dry gas under pressure to satisfy storage requirements.

11-8.2 EXHAUST NOZZLE DESIGN

The propulsive gas produced in a hybrid rocket engine is apt to be *oxidizer-rich*, and at a temperature of 5400° to 7200°R. Consequently, the materials for the exhaust nozzle must be selected carefully if excessive erosion of the throat and walls of the exhaust nozzle is to be avoided. Experiments indicate that it is more difficult to find suitable materials for hybrid rocket engines burning *oxygen-based* oxidizers than those burning *fluorine-based* oxidizers. Graphite has been found to be a suitable nozzle material when burning fluorine-based oxidizers¹⁰. Experimental studies concerned with materials for use in hybrid engines and transpiration cooling (see par. 10-4.4.2) of the nozzles are presented in Reference 6.

11-8.3 INJECTORS FOR THE LIQUID OXIDIZER

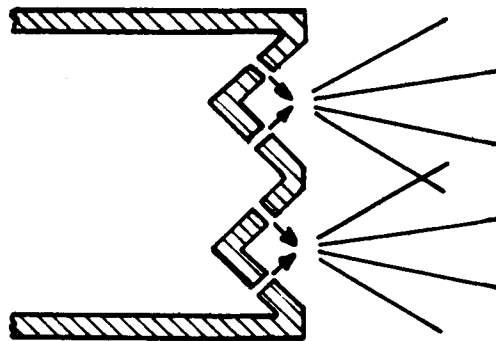
There are little data available for guiding the designer of the injector for a hybrid rocket engine. Fig. 11-5 illustrates schematically three types of injectors that have been investigated with some degree of thoroughness: (A) the impinging jet, (B) the shower head, and (C) the vortex. The combustion efficiencies obtained with all of these injectors have been unsatisfactory.

The low values of specific impulse obtained with the aforementioned injectors are attributed to the poor mixing of the fuel gases and the oxidizer. For the hybrid concept to be successful, the oxidizer vapors and the gases from the solid fuel must be thoroughly mixed. All of the injection schemes illustrated in Fig. 11-5 produce a central core of cool gas in the perforation in the solid fuel grain. Consequently, chemical reaction, if it occurs, is confined to a region exterior to the central cool gas core and is between the fuel vapors evolved from the solid fuel grain and the oxidizer vapor surrounding the core of axially flowing oxidizer stream. It appears that there is no large scale turbulence in the perforation to promote adequate mixing of the fuel and oxidizer vapors. As a consequence, the combustion process is incomplete. That achieving complete combustion is a problem, is demonstrated by the increased combustion efficiency obtained with post-combustion chambers (see par. 11-7).

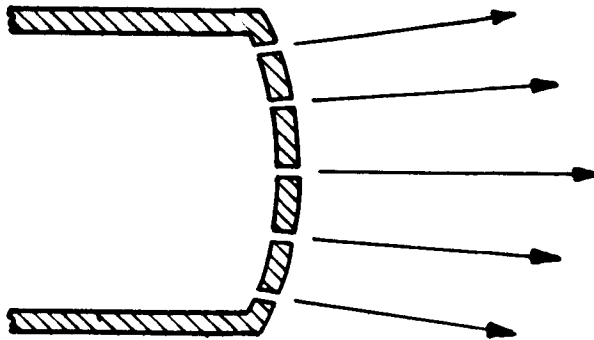
The problem of achieving efficient combustion with a relatively simple and reliable oxidizer injection system is still a major obstacle to the development of an efficient hybrid rocket engine.

11-8.4 IGNITION OF HYBRID ROCKET ENGINES

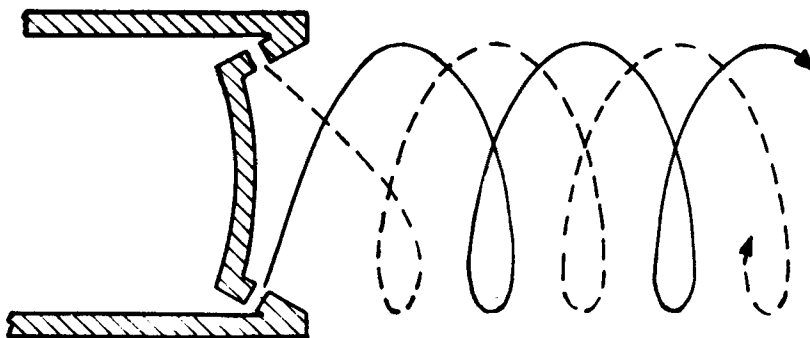
To ignite the solid fuel component a certain amount of oxidizer must be close to its surface.



(A) IMPINGING JET



(B) SHOWER HEAD



(C) VORTEX

HEAD-END INJECTORS

Figure 11-5. Three Types of Injectors That Have Been Utilized in Hybrid Rocket Engines

If the fuel and oxidizer are *hypergolic* no auxiliary ignition system is required. For *non-hypergolic* (also termed *ergolic*) hybrid propellant systems, auxiliary ignition schemes are, of course, necessary. One such scheme is based on coating the solid fuel with a material which is hypergolic with the oxidizer, another utilizes an igniter for vaporizing some of the solid fuel before the oxidizer is introduced into the grain perforation (see Fig. 11-1).

The use of hypergolic hybrid propellant systems appears to not only be the most reliable, but also gives "soft" ignition, i.e., no large ignition pressure peaks. Moreover, hypergolic propellant systems make it possible to terminate and restart the operation of the hybrid rocket engine.

11-9 DESIGN CONSIDERATIONS PERTINENT TO THE AFTERBURNING (CONVENTIONAL) HYBRID ROCKET ENGINE

11-9.1 GENERAL DISCUSSION

Fig. 11-2 illustrates the essential features of the afterburning hybrid rocket engine. As pointed out earlier, this engine is not a true hybrid engine but is essentially a solid propellant rocket motor with an afterburner chamber attached to the outlet of the chamber housing the solid propellant grain. A liquid oxidizer is injected into the afterburner and reacts with the hot combustion gases produced by burning the solid propellant grain.

The design of the solid propellant grain and its combustion chamber is based on the principles, discussed in par. 8-6, applicable to conventional solid propellant rocket motors.

The main reason for the interest in the afterburning (conventional) hybrid engine stemmed from the unsatisfactory combustion efficiencies obtained with (true) hybrid rocket

engines. The after burning hybrid engine does give improved combustion efficiency but at the expense of a larger engine weight, due to adding the afterburner. Experiments indicate, however, that conventional hybrid propellants can be burned with head-end injection with practically the same combustion efficiency as in an afterburning engine. A true hybrid propellant system cannot be burned in an afterburning hybrid engine because a solid fuel containing no solid oxidizer cannot sustain combustion in the absence of a supply of liquid oxidizer.

11-9.2 AFTERBURNER CHAMBER

Refer to Fig. 11-2. The afterburner chamber is similar to the combustion chamber of a liquid propellant rocket motor, in which the fuel is a gas and the oxidizer is a liquid. Insufficient data are available for predicting the required afterburner dimensions for a given (conventional) hybrid propellant system. The available data indicate that, for the propellant systems which have been investigated, a *characteristic length* (see par. 10-3.2.1) of approximately $L^* = 100$ is satisfactory.

The afterburner chamber may or may not be cooled depending on the application of the rocket engine. It is difficult, however, to cool both the chamber and nozzle of small rocket engines because only the oxidizer is available for cooling purposes, and only relatively small amounts of liquid oxidizer are used to obtain the maximum performance of an afterburner hybrid rocket engine. Consequently, the cooling problem is quite difficult, especially in view of the high pressures and temperatures of the propulsive gases used in afterburning hybrid rocket engines.

It is important to design the afterburner so that its stagnation pressure loss is small.

REFERENCES

1. O. Lutz, *Some Special Problems of Power Plants, History of German Guided Missiles Development*, Agardograph 20, Appelhaus, Brunswick, Germany, 1957.
2. E. Ring, *Hybrid Rocket Motor*, General Electric Report R 53A0520, DDC AD 38444, December 1953.
3. F. J. Hendel, *Storable Hybrid Propulsion Systems*, ARS Preprint 1268-60, July 1960.
4. D. D. Ordahl, "Hybrid Propulsion Systems," *Astronautics*, Vol. 4, October 1959, p. 42.
5. J. Gustavson, *The Hybrid Rocket Motor and Its Unique Capabilities*, ARS Preprint 1167-60.
6. D. D. Ordahl and W. A. Rains, "Recent Developments and Current Status of Hybrid Rocket Propulsion," *Journal of Spacecraft*, Vol. 2, No. 6, Nov.-Dec., 1965, p. 923.
7. D. D. Ordahl, "Hybrid Propulsion," *Space/Aeronautics*, April 1964, p. 108.
8. L. D. Smoot and C. F. Price, "Pressure Dependence of Hybrid Fuel Regression Rates," *AIAA Jour.*, Vol. 5, No. 1, Jan. 1967, p. 102.
9. L. D. Smoot and C. F. Price, "Regression Rates of Nometalized Hybrid Fuel Systems," *AIAA Jour.*, Vol. 3, No. 8, Aug. 1965, p. 1408.
10. R. J. Zabelka, *Studies in Hybrid Combustion*, First Annual Report, Jet Propulsion Center, Purdue University, JPC-I-63-2, March 1963.
11. A. T. Robinson, R. L. Alexander, J. D. Ramsdell, and M. R. Wolfson, "Transpiration Cooling with Liquid Metals," *AIAA Jour.*, January 1963, p. 89.

PART TWO

AIR-BREATHING JET PROPULSION ENGINES

CHAPTER 12

CLASSIFICATION AND ESSENTIAL FEATURES OF AIR-BREATHING JET PROPULSION ENGINES

12-0	PRINCIPAL NOTATION FOR PART TWO*	<u>bhp</u>	brake horsepower
a	acoustic speed = $\sqrt{\gamma P/\rho}$, ft/sec	<u>bhp-hr</u>	brake horsepower-hour
a^0	stagnation or total acoustic speed = $\sqrt{\gamma^0 R T^0}$, ft/sec	B	British thermal unit
a^*	critical acoustic speed = $\sqrt{\gamma^* P^*/\rho^*}$, ft/sec	c_p	specific heat at constant pressure, B/slug-°R
a_0	acoustic speed in free-stream = $\sqrt{\gamma_0 P_0/\rho_0}$, ft/sec	c_v	specific heat at constant volume, B/slug-°R
A	cross-sectional area, sq in. or sq ft	\bar{c}_{pc}	mean value of c_p for a compression process
A	air-rate for a turboshaft engine, slug air/ <u>shp-hr</u>	\bar{c}_{pt}	mean value of c_p for turbine expansion process
A_c	cross-sectional area of entrance cross-section of the exhaust nozzle	\bar{c}_{pn}	mean value of c_p for a nozzle expansion process
A_e	cross-sectional area of the exit cross-section of the exhaust nozzle	C	coefficient
A_F	frontal area of engine	C_d	discharge coefficient of a nozzle or orifice
A_m	maximum cross-sectional area of an engine body	C_D	drag coefficient = D/q
A_t	cross-sectional area of the throat of a nozzle	C_F	thrust coefficient for a rocket motor = $F/P_c A_t$
A^*	cross-sectional area, for an isentropic flow, where $M = 1$	C_{Fg}	gross thrust coefficient for a ramjet engine = $F_g/q_0 A_m$
		C_{Fn}	net thrust coefficient for a ramjet engine = $F_n/q_0 A_m$

*Any consistent set of units may be employed; the units presented here are for the American Engineers System (see par. 1-7).

D	drag, lb	<u>F_nSFC</u>	net thrust specific fuel consumption, lb fuel per hr per lb net thrust
D	hydraulic diameter = $4R$	g	acceleration due to gravity, ft/sec ²
D_a	additive drag for an inlet-diffuser	g_c	gravitational correction factor = 32.174 slug-ft/lb-sec ²
D_e	external drag = $D_a + D_f$	G	flow density or mass velocity = \dot{m}/A
D_f	skin friction drag	G*	critical flow density, value of G where $M = 1$
D_i	ram drag = $\dot{m}_a V_0$	h	static specific enthalpy, B/slug
e_R	regenerator effectiveness = $(T_{3R} - T_3)/(T_5 - T_3)$	h^o	stagnation or total specific enthalpy, B/slug
E_f	calorific value of fuel, ft-lb/slug	Δh	a finite change in specific enthalpy, B/slug
E_{in}	rate at which energy is supplied to an engine, ft-lb/sec	Δh_B	increase in specific enthalpy due to combustion process
f	fuel-air ratio = \dot{m}_f/\dot{m}_a	Δh_c	increase in specific enthalpy due to a compression process
f'	ideal fuel-air ratio = f/η_B	Δh_n	decrease in specific enthalpy due to expansion in a nozzle, B/lb
f	friction coefficient in the Fanning equation for pressure drop	Δh_R	heat transferred in regenerator = $h_5 - h_3$, B/slug
F	thrust, lb	Δh_t	decrease in specific enthalpy due to expansion in a turbine, B/lb
F_A	thrust of an afterburning engine, lb	ΔH_c	lower heating value of a liquid fuel, B/slug
F_g	gross thrust for a ramjet engine = $F_i = \dot{m}_7 V_j - \dot{m}_0 V_0$	I_{sp}	specific impulse = F_g/\dot{m} , sec
F_i	thrust due to the internal flow = $\dot{m}_e u_e - \dot{m}_i V_0 + (P_e - P_{amb})A_e$	I_a	air specific impulse or specific thrust = F_g/\dot{m}_a , sec
F_j	jet thrust = $\dot{m}_e V_j$	I_{Fg}	gross thrust specific impulse
F_n	net thrust = $F_g - D_e$		
F_p	pressure thrust = $(P_e - P_{amb})A_e$		
<u>F_gSFC</u>	gross thrust specific fuel consumption, lb fuel per hr per lb gross thrust		

J	mechanical equivalent of heat ≈ 778 B/ft-lb	\tilde{M}_e	momentum of gases crossing A_e , slug-ft/sec
L	length	\tilde{M}_i	momentum of gases inducted by engine, slug-ft/sec
L	specific output of a gas-turbine powerplant or turboshaft engine, <u>shp</u> /lb-air per sec	p	static pressure, psia
L_c	specific output required for driving air compressor	p_a	ambient static pressure, psia
L_t	specific output furnished by turbine	p_c	static pressure in A_c , psia
m	mass, slug	p_e	static pressure in A_e , psia
\dot{m}	mass rate of flow, slug/sec	p^O	stagnation (or total) pressure, psia
\dot{m}_a	mass rate of air induction by the engine, slug/sec	P_{std}	standard static pressure = 14.7 psia
\dot{m}_{aF}	fan air flow rate for a turbofan engine	p	static pressure, psf
\dot{m}_e	mass rate of flow of gas crossing exit cross-section of exhaust nozzle	P_{std}	standard static pressure = 2116 psfa
\dot{m}_f	mass rate of fuel flow, slug/sec	p^O	stagnation (or total) pressure, psfa
\dot{m}_{fa}	mass rate of fuel flow to the afterburner, slug/sec	P_c^O	stagnation pressure in cross-section A_c , psfa
\dot{m}_{fab}	total fuel flow to an afterburning engine = $\dot{m}_f + \dot{m}_a$, slug/sec	P_e^O	stagnation pressure in cross-section A_e , psfa
\dot{m}_i	mass rate of gas flow into an engine, slug/sec	P	propulsive power, energy per unit time
\bar{m}	molecular weight of a gas = R_u/R	P_F	fan power for turbofan engine
M	local Mach number = M/a	P_j	jet power = $FI_{sp}/45.8$, kw
M_0	Mach number of free-stream air (flight Mach number) = V_0/a_0	P_L	leaving (or exit) loss
M_j	effective Mach number of exhaust jet	P_T	thrust power = $FV_0/550$, <u>thp</u>
		P_{Tj}	jet thrust power = $F_j V_0/550$, <u>thp</u>
		P_{cTF}	compressor power for turbofan engine

P_{jTF}	jet thrust power for turbofan engine	R_u	universal gas constant = 49,717 ft-lb/slug-mole $^{\circ}$ R=63.936 B/slug-mole $^{\circ}$ R
P_{tTF}	turbine power for turbofan engine	R	hydraulic radius = (flow area)/(wetted perimeter), ft
P_{aux}	power for driving engine auxiliaries	R_e	Reynolds number = $uL\rho/\mu$
P_{λ}	power for overcoming parasite-loss in engine	s	static specific entropy, B/slug- $^{\circ}$ R
P_{sh}	shaft power	s^O	stagnation specific entropy
$\underline{P_T SFC}$	thrust power specific fuel consumption = $g_c \dot{m}_f / P_T$, lb/thp	S	entropy for a system
q	dynamic pressure = $\rho u^2 / 2$, psf	S	surface area, or control surface, as specified in text
q_0	dynamic pressure of free-stream air = $\rho V_0^2 / 2 = \gamma P_0 M_0^2 / 2$	\underline{shp}	shaft horsepower
Q_i	heat supplied to ideal burner = $g_c \dot{m}_f \Delta H_c$, B/sec	$\underline{shp-hr}$	shaft horsepower-hour
Q'_i	heat supplied to burner = $g_c \dot{m}_a f' \Delta H_c$, B/sec	\underline{SFC}	specific fuel consumption = $\dot{m}_f / P_{sh} = 2545 / \eta_{th} \Delta H_c$, lb fuel/hp-hr
Q_{iR}	heat supplied to regenerative turbo-shaft engine (par. 15-5.3.3)	t	time, sec or hr, as specified in text
Q_R	heat transferred by regenerator to compressed air from the hot gas = $\dot{m}_a (h_{3R}^O - h_3^O)$, B/sec	\underline{thp}	thrust horsepower = $FV_0 / 550$
Q_{avail}	heat available for heat transfer in regenerator = $\dot{m}_g \bar{c}_{pg} (T_5 - T_3)$, B/sec	T	static temperature, $^{\circ}$ R
$\frac{Q_i \eta_B}{c_p T_0}$	dimensionless heat addition parameter (see par. 15-8.1)	T_a	static temperature of ambient air
r_D	stagnation pressure ratio	T_e	static temperature in A_e
R	gas constant = R_u / \bar{m}	T_t	static temperature in A_t
R_a	gas constant for air	T_{std}	standard static temperature = 519 $^{\circ}$ R
R_g	gas constant for hot gas	T^O	stagnation temperature at section indicated by subscript, $^{\circ}$ R
		T_a^O	stagnation temperature of air flow

<u>TSFC</u>	thrust specific fuel consumption = $3600 \text{ g}_c \dot{m}_f / F, \text{ lb}_m$ of fuel per hour per lb thrust
u	velocity parallel to the x-axis, fps
u_e	velocity of gas crossing A_e
U	work-ratio, P_{sh}/P_{turb}
U	overall heat transfer coefficient for regenerator, B/(hr) (sq ft) ($^{\circ}\text{R}$)
V	velocity, fps
V_j	effective jet velocity, fps
V_o	free-stream velocity (flight speed), fps
V_{jF}	effective jet velocity for fan airflow \dot{m}_{aF} of turbofan engine
\bar{V}_{jTF}	mean effective jet velocity for turbofan engine
w	weight, lb
\dot{w}	weight rate of flow, lb/sec
\dot{w}_a	weight rate of flow of air = $g_c \dot{m}_a$, lb/sec
\dot{w}_f	weight rate of flow of fuel = $g_c \dot{m}_f$
W_E	engine weight, lb
z	altitude, ft
Z_c	compression factor for air compressor = $\Theta_c - 1$ (see par. 15-3.2.2)
Z_d	compression factor for diffusion process = $\Theta_d - 1$ (see par. 15-3.1.3)

Z_F	compression factor for fan of turbofan engine = $\Theta_F - 1$ (see par. 15-9.1.4)
Z_n	expansion factor for propulsive nozzle = $1 - \Theta_n$
Z_t	expansion factor for turbine expansion = $1 - \Theta_t$

GREEK LETTERS

α	cycle temperature ratio = $a_d a_1 = T_4^O/T_o^O$ for a gas-turbine engine = T_6^O/T_o^O for a ramjet engine
a_d	diffuser temperature ratio = T_2^O/T_o^O
a_1	T_4^O/T_2^O
a_2	compressor temperature ratio = T_3^O/T_o^O
β	bypass ratio for turbofan engine = \dot{m}_{aF}/\dot{m}_a (see par. 15-9.1.1)
γ	specific heat ratio = c_p/c_v
$\bar{\gamma}$	mean value of γ for process indicated by subscript
δ	corrected pressure = P^O/P_{std}
η	efficiency
η_a	air cycle efficiency = $1 - 1/\Theta_c$
η_B	burner efficiency = $f'/f = Q'_i/Q_i$
η_c	isentropic compressor efficiency = $(T_3^{O'} - T_2^O)/(T_3^O - T_2^O)$
η_d	isentropic diffuser efficiency = $(T_2^{O'} - T_o^O)/(T_2^O - T_o^O)$
η_g	mechanical efficiency of gearbox

η_M	mechanical efficiency	Θ_n	nozzle expansion ratio parameter = $(P_7/P_6^O)^{\frac{\gamma-1}{\gamma}}$
η_{Mc}	mechanical efficiency of compressor	Θ_t	turbine expansion ratio parameter = $(P_5^O/P_4^O)^{\frac{\gamma-1}{\gamma}}$
η_{Mt}	mechanical efficiency of turbine	Θ_{co}	compressor pressure ratio parameter under static conditions ($V_0=0$)
η_n	isentropic efficiency of exhaust nozzle	λ	dimensionless specific thrust = $V_j (1 - \nu)/c_0$
η_o	overall efficiency - $\eta_p \eta_{th} = P_T/Q_i$	ν	effective speed ratio = V_0/V_j
η_p	propulsive efficiency P_T/P	ρ	density, slug/ft ³
η_p	ideal propulsive efficiency = $P_T/(P_T + P_L) = 2\nu/(1 + \nu)$ for a turbojet engine	ρ_0	density of ambient air, slug/ft ³
η_{prop}	efficiency of propeller	σ	density ratio = ρ/ρ_0
η_t	isentropic efficiency of turbine	ϕ	velocity coefficient for a nozzle = $\sqrt{\eta_n}$
η_{tc}	machine efficiency = $\eta_t \eta_c$		
η_{th}	thermal efficiency		

SUBSCRIPTS

Θ	cycle pressure ratio parameter = $(P_3^O/P_0^O)^{\frac{\gamma-1}{\gamma}}$	a	air, or ambient
Θ_c	compressor pressure ratio parameter = $(P_3^O/P_0^O)^{\frac{\gamma-1}{\gamma}}$	A	afterburning
Θ_d	diffuser pressure ratio parameter = $(P_2^O/P_0^O)^{\frac{\gamma-1}{\gamma}}$	B	burner or combustor
Θ_F	fan pressure ratio parameter for turbofan engine = $(P_3^O/P_0^O)^{\frac{\gamma-1}{\gamma}}$	c	compressor, or nozzle inlet section, as specified in text
		d	diffuser
		e	exit cross-section, or external to engine, as specified in text
		f	fuel
		f	friction

F	fan	3	inlet to burner, also exit from air compressor (for a ramjet engine, it denotes exit from burner) (see Fig. 12-1)
g	gas, or gearing, as specified in text	3F	exit from fan of turbofan engine
i	internal, or internal flow	4	inlet to turbine
id	ideal	5	exit from turbine, also inlet to afterburner (see Fig. 12-4)
j	jet	6	inlet to propulsive nozzle
m	maximum value	6F	inlet to propulsive nozzle for cold air-stream in a turbofan engine
n	nozzle	7	exit from propulsive nozzle
o	overall	7F	exit from propulsive nozzle for cold air-stream in a turbofan engine
p	propulsive		
prop	propeller		
P	ideal propulsive		
R	regenerator		
t	turbine		
TF	turbofan engine		

NUMBERS

0	free-stream or ambient, as specified in text
1	inlet to diffuser
2	exit from subsonic diffuser; also inlet to burner for a ramjet engine (see Fig. 12-1), and inlet to air compressor for a gas-turbine jet engine (see Fig. 12-2)
2F	inlet to fan of turbofan engine (see Fig. 15-29)

SUPERSCRIPTS

'	state is reached by an isentropic process
o	stagnation value
-	mean value of variable
*	critical value where $M=1$

12-1 CLASSIFICATION OF AIR-BREATHING PROPULSION ENGINES

This chapter discusses the essential features of those air-breathing engines, other than piston engines, that are employed for propelling winged aircraft, helicopters and target drones. For convenience the engines may be grouped into three main groups, as indicated in Table 12-1.

Engines in Groups A and C are air-breathing jet engines and utilize several common gas

TABLE 12-1

CLASSIFICATION OF AIR-BREATHING
ENGINES

A. PROPULSIVE DUCT ENGINES
1. Ramjet Engine
2. SCRAMJET Engine
B. GAS-TURBINE POWERPLANT ENGINES
1. Turboshaft Engine
2. Turboprop Engine
C. GAS-TURBINE JET ENGINES
1. Turbojet Engine
2. Turbofan Engine
3. Turboramjet Engine

dynamic processes in their functioning (see par. 1-5.1). Engines in Group B are basic gas-turbine powerplants which are employed for driving helicopter rotors, aircraft propellers, and the like. It should be noted, however, that the turboprop engine develops a portion of its thrust by jet propulsion.

The descriptions presented of the different air-breathing engines are primarily for identification purposes; more detailed technical information pertinent to those engines are presented in Chapters 13, 14, and 15. In all of the discussions of Part Two a *relative coordinate system* (see par. 2-2.1) is assumed unless it is specifically stated to be otherwise.

12-1.1 PROPULSIVE DUCT ENGINES

The propulsive duct engines considered here are continuous flow jet engines, and maybe classified into two groups:

- (1) Ramjet engine utilizing subsonic combustion.
- (2) Ramjet engine employing supersonic combustion, hereafter referred to as the SCRAMJET engine.

It is possible, of course, to have combinations of gas-turbine and propulsive duct engines, i.e., the *turboramjet engine*.

Moreover, it is possible to have combinations of air-breathing and rocket engines such as the *air-turbo rocket*, the *air-augmented rocket*, etc.

The discussions in Part Two will be limited to the primary air-breathing engines.

12-1.2 THE RAMJET ENGINE

Fig. 12-1 illustrates diagrammatically the essential features of the ramjet engine for propelling bodies at supersonic flight speeds. The atmospheric air inducted into the ramjet engine forms the so-called *internal flow* and the air flowing past the external housing of the engine is called the *external flow*. The internal flow is decelerated, from the flight Mach number $M_0 > 1$ to a low subsonic Mach number M_2 at the entrance to the *burner*, by a diffusion system comprising a supersonic diffuser followed by a subsonic diffuser (see pars. 3-4.3.2 and 3-5). The highly compressed air flows into the burner with a subsonic Mach number of approximately $M_2 = 0.2$. A liquid fuel is injected into the low velocity compressed air and mixes with it before the fuel-air mixture enters the burner, wherein the *flameholders* are located. The hot combustion gases, at approximately $T_6^0 = 4000^\circ R$, are expanded in an appropriate exhaust nozzle and ejected to the surroundings with a supersonic speed; the nozzle is the propulsive element of the engine, the remaining components comprise the hot gas generator (see par. 1-5).

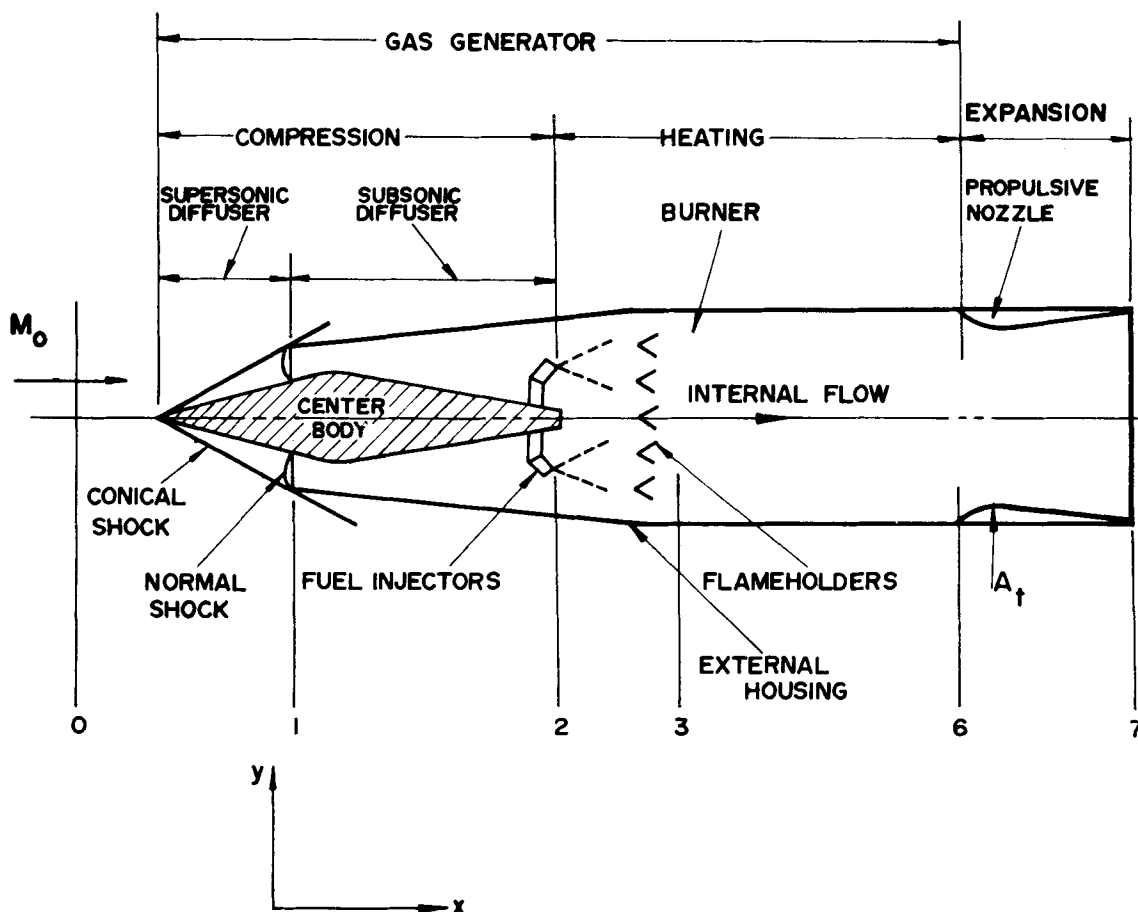


Figure 12-1. Essential Features of the Ramjet Engine

From a purely mechanical viewpoint the ramjet engine is the simplest of all air-breathing jet engines. Although the ramjet engine can be designed to operate at subsonic flight speeds, the nozzle expansion ratio P_7/P_6^0 is too small to give a high thermal efficiency.

The higher the flight Mach number at a given altitude, the larger the cycle pressure ratio P_2^0/P_0 and the more efficient is the ramjet engine. For flight Mach numbers above approximately $M_0=3$, has a lower fuel consumption rate than any gas-turbine jet engine. It should be noted that the isentropic deceleration of a supersonic free air-stream to a subsonic velocity is always accompanied by the formation of shock

waves so that only a fraction of the isentropic stagnation pressure is achieved by the diffusion process, and the loss in the total pressure increases rapidly at values of M_0 exceeding approximately $M_0=2$ (see par. A-10).

If the ramjet engine is to operate over a wide range of flight Mach numbers, a variable area inlet and a variable area exhaust nozzle—which complicates the engine and increases its weight—are required.

The materials employed for constructing the walls of the combustion chamber, also called the burner, and nozzle must be protected from the hot propulsive gas so that their temperatures do

not exceed approximately 2200°R. For engines that are to propel vehicles at flight Mach numbers above $M_0 = 3$ to 4, it becomes necessary to apply *regenerative cooling*, using the liquid fuel as the coolant, to the burner and nozzle walls.

If the fuel is a liquid hydrocarbon, its cooling effectiveness is limited by the temperature at which pyrogenesis, (500°-600°F), with its attendant formation of coke, is initiated. The temperature at which coke formation becomes a serious problem limits the flight Mach number of the ramjet engine to approximately $M = 5$. Higher flight Mach numbers than $M = 5$ are possible if the fuel flow for regenerative cooling exceeds that required for stoichiometric combustion, and the excess fuel may be "*dumped overboard*" which is wasteful. It may be possible, however, to use special coolants having superior heat transfer characteristics, film or transpiration cooling, or a nonhydrocarbon fuel. These solutions to the cooling problem need further study.

If a satisfactory solution to the cooling problem can be developed or a nonhydrocarbon fuel-like liquid hydrogen can be used, the operating flight regime of the ramjet portion of a turboramjet engine could be extended.

When T_6^0 exceeds approximately 4000°R, there may be significant dissociation of the combustion products and the result of injecting more fuel may cause further dissociation instead of an increase in T_6^0 . At flight Mach numbers exceeding approximately $M_0 = 6$, the stagnation pressure recovery of the diffusion system decreases rapidly due to strong shocks, and the static temperature and pressure of the air entering the burner become too high for obtaining a satisfactory ramjet engine. The static temperature can become so high that no heat release can be achieved in the burner.

The basic disadvantage of the ramjet engine, and this also applies to the SCRAMJET engine, is that the nozzle pressure ratio P_6^0/P_7 depends entirely upon the flight Mach number and the performance of the diffusion system. Consequently, a ramjet engine cannot develop static thrust. It must be boosted to a flight Mach number which will make it self-operating by some external means, e.g., a rocket booster engine.

At this time there are no Army missiles employing ramjet engine propulsion, but a supersonic target drone utilizing ramjet engines is under development.

12-1.3 THE SCRAMJET ENGINE

The difficulties which limit the operating flight Mach number of the ramjet engine arise primarily from the necessity of decelerating the inducted air to approximately $M_2 = 0.2$ at the entrance to the burner so that satisfactory combustion of the fuel can be achieved in a subsonic stream of air. The obvious solution is to burn the incoming air without decelerating it to a low subsonic speed. If that can be achieved the static air temperatures and pressures throughout the engine will be considerably below those for a conventional ramjet engine operating at the same flight Mach number. As a result, the cooling problem is less severe. Moreover, since the Mach numbers would be supersonic throughout the engine; its inlet geometry, and possibly that of the exhaust nozzle, may be simplified. It appears, therefore, that by developing the technology of the supersonic combustion ramjet termed the SCRAMJET engine, the high flight Mach number limitations of air-breathing propulsion could be raised markedly, thus enhancing the possibility of achieving hypersonic aircraft flight with air-breathing engines.

The possibilities of the SCRAMJET engine has been investigated for approximately ten

years, and the scope and research programs pertinent to that type of engine have been greatly increased in the past four years. Most of the research has been conducted using liquid hydrogen as the fuel but other possible fuels are being considered. Several difficult problems have to be solved before a practical SCRAMJET engine can be developed⁴.

12-2 GAS-TURBINE JET ENGINES

Brief descriptions of the essential features of the different gas-turbine jet engines will now be presented (see Table 12-1).

12-2.1 THE TURBOJET ENGINE

It was pointed out in par. 12-1.1 that the propulsive duct engines (the ramjet and SCRAMJET engines) suffer from the disadvantage that they cannot develop a static or *takeoff* thrust, at zero flight speed. When $V_0 = 0$, no air flows through the propulsive duct and the thrust F is zero. A gas-turbine engine overcomes the above deficiency by installing a mechanical compressor between the inlet diffuser and the burner system, so that air is inducted into the engine at all flight speeds, including $V = 0$. Fig. 12-2 illustrates diagrammatically the general arrangement of the components of a turbojet engine. It is seen from the figure that the gas generator comprises the following components: an air intake and diffuser, a mechanical air compressor (axial or radial flow), a gas-turbine which drives the air compressor, and a burner or combustion system.

If a subsonic flight Mach number is assumed, the air inducted into the engine is partially compressed in the subsonic intake-diffuser and then further compressed in the air compressor. The high pressure air is then heated by burning a liquid fuel with it in the burner system, the stagnation temperature of the gas entering the turbine T_4^0 is limited by metallurgical considerations. For uncooled blades the *turbine*

inlet temperature for *cruise* of modern commercial aircraft is limited to approximately 1960°R ; the combustion in the burners occurs at sensibly constant pressure. The high temperature gas expands in the turbine which develops just enough power to drive the air compressor and the pertinent auxiliaries. The gas leaves the turbine with a static pressure higher than that of the surrounding atmosphere and at a temperature ranging from 1360° to 1800°R , depending upon the operating condition. The *turbine exhaust gases* are then discharged to the atmosphere through a suitably shaped nozzle; current turbojet engines operate with compressor pressure ratios ranging between 5 and 18 to 1.

Like the ramjet engine, the turbojet engine is a continuous flow engine. Although it does not depend upon the *ram pressure* of the inducted air for functioning, the effectiveness with which the ram pressure is recovered in the diffuser has a significant influence upon its fuel consumption. A 20 percent loss in ram pressure recovery increases the fuel consumption per pound of thrust by approximately 10 percent.

The turbojet engine is eminently suited for propelling aircraft at flight Mach number ranging from $M_0 = 0.65$ to $M_0 = 3$ to 4. As the flight Mach number is increased from $M = 0.9$ the ram pressure increases rapidly and when M_0 is between 3 and 4, the characteristics of the turbojet merge into those for the ramjet, i.e., the optimum compressor pressure ratio P_2^0/P_3 approaches unity.

Turbojet engines which do not have to develop thrusts exceeding approximately 7,000 lb may employ radial (also called centrifugal) air compressors. By far the majority of modern turbojet engines employ axial flow compressors.

12-2.2 THE AFTERBURNING TURBOJET ENGINE

Several methods have been investigated for augmenting the thrust of the turbojet engine.

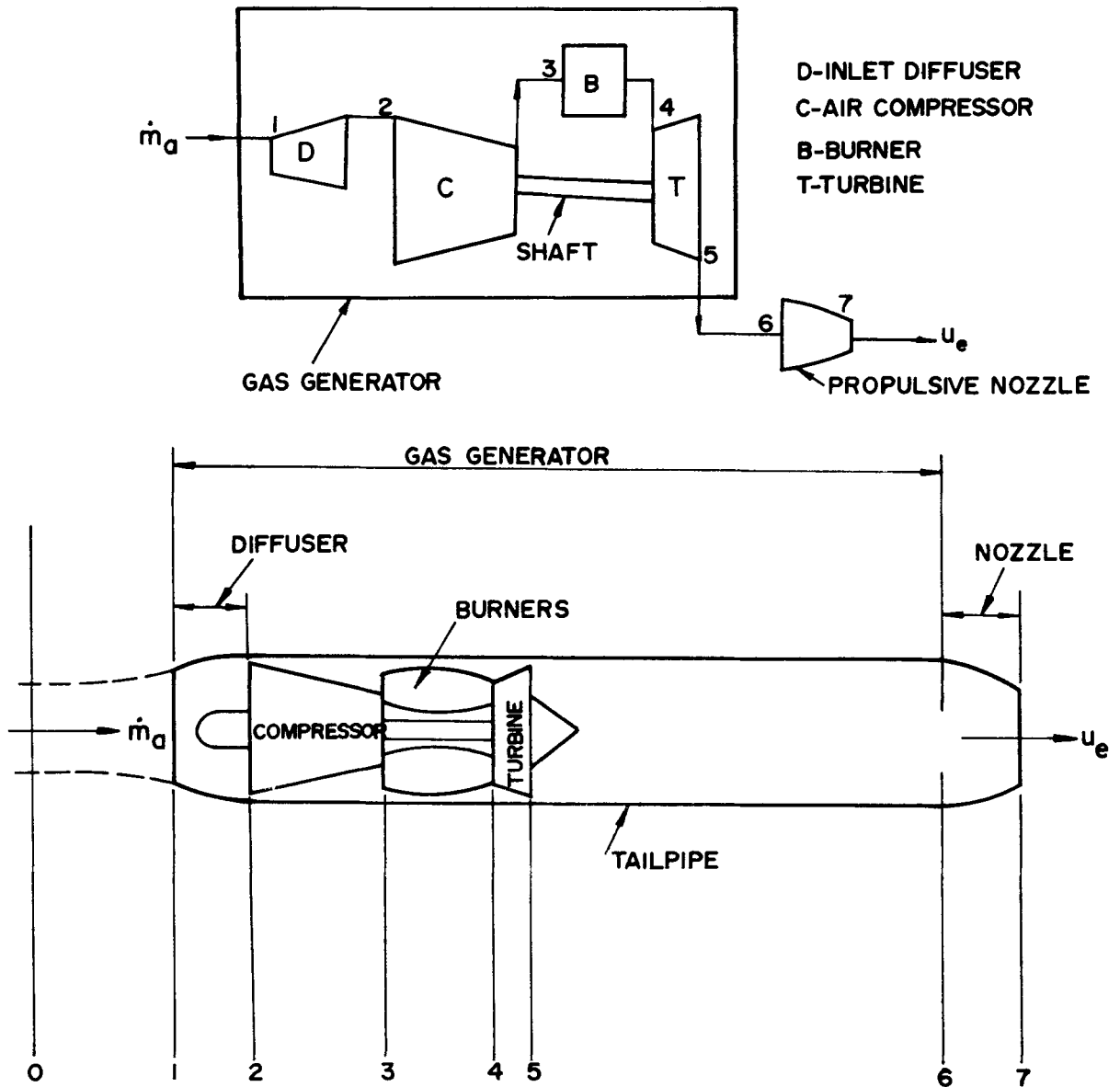


Figure 12-2. Essential Features of the Turbojet Engine

The most common method is termed either "afterburning" or "post-combustion". In an afterburning engine the hot gas generator, as illustrated schematically in Fig. 12-3, comprises the following components: (1) an inlet diffuser, (2) an axial flow compressor, (3) a burner or combustor, (4) an axial flow turbine for driving the air compressor, and (5) a tailpipe equipped with an *afterburner*.

In an afterburning engine the area of the exhaust nozzle must be variable.

Because of the low fuel-to-air ratio (approximately 1/50) utilized in the primary burner of a

turbojet engine, the gas exhausted from the turbine contains a large amount of oxygen, so that additional fuel can be burned in the *tailpipe* section between the turbine and the entrance to the exhaust nozzle. Due to the additional fuel burned in the afterburner, the temperature of the gas entering the exhaust nozzle T_6^0 can be as high as approximately 4000°R. As a result the jet velocity and, consequently, the thrust of engines operated at turbine inlet temperatures of approximately 1800°F can be increased approximately 50 percent above that for the corresponding turbojet engine. Increasing the turbine inlet temperature reduces the percentage increase obtainable by afterburning.

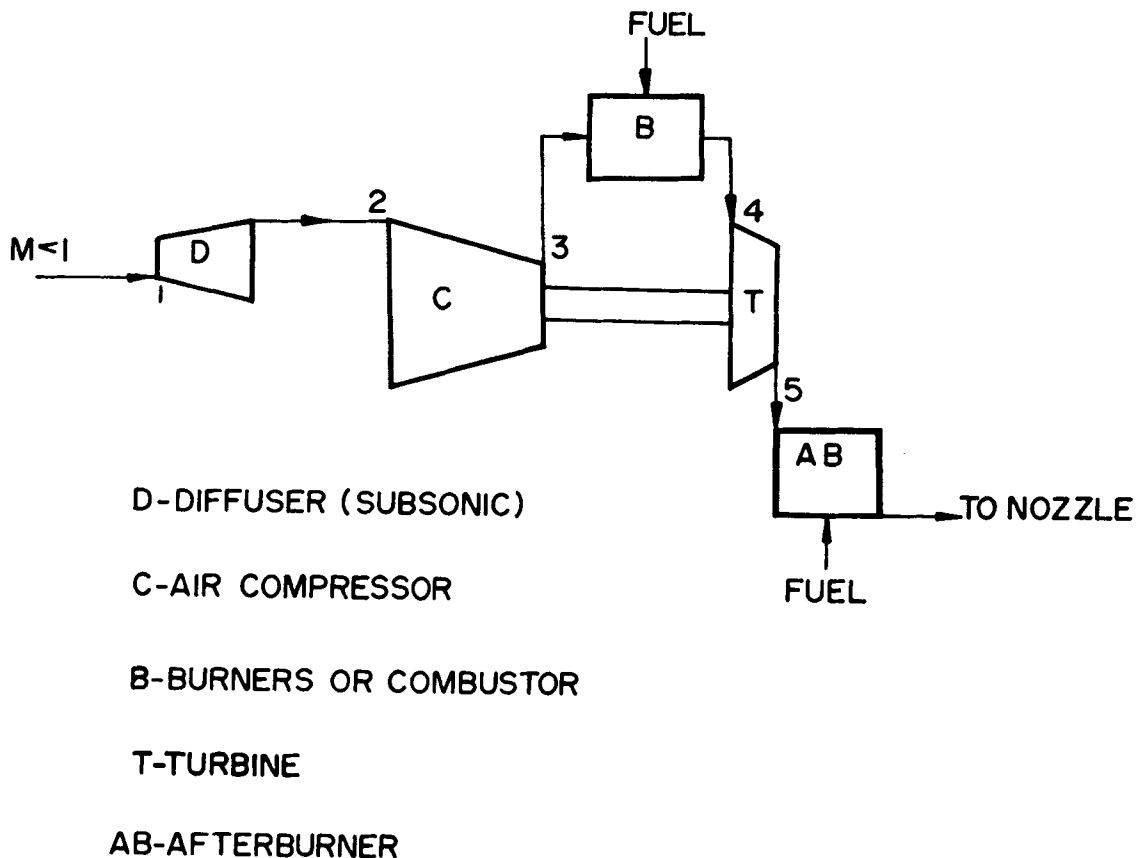


Figure 12-3. Components of Gas Generator for an Afterburning Turbojet Engine

If the afterburning engine is to propel aircraft at supersonic speeds, a diffusion system similar to that for the ramjet engine (see Fig. 12-1) must precede the air compressor.

Fig. 12-4 illustrates schematically the arrangement of the components for an afterburning turbojet engine for propelling an aircraft at supersonic speeds.

12-2.3 THE TURBOFAN ENGINE

Fig. 12-5 illustrates diagrammatically the essential features of an afterburning turbofan engine. It differs from the afterburning turbojet engine by the addition of a fan which compresses a stream of cold air which flows through

a duct surrounding the hot gas generator. Because of the additional power required for driving the fan, a larger turbine is required.

If the afterburner is omitted, then the engine in Fig. 12-5 becomes a *turbofan engine*. Furthermore, if fuel is burned in the duct surrounding the gas generator then the engine is called a *duct-burning turbofan engine*.

To obtain satisfactory performance from a gas-turbine jet engine, it is essential that its components (compressor and turbine) of the hot gas generator have high isentropic efficiencies. In addition the burner must operate with a *high burner efficiency* η_B , a low total pressure loss, have a small frontal area, and be light in weight.

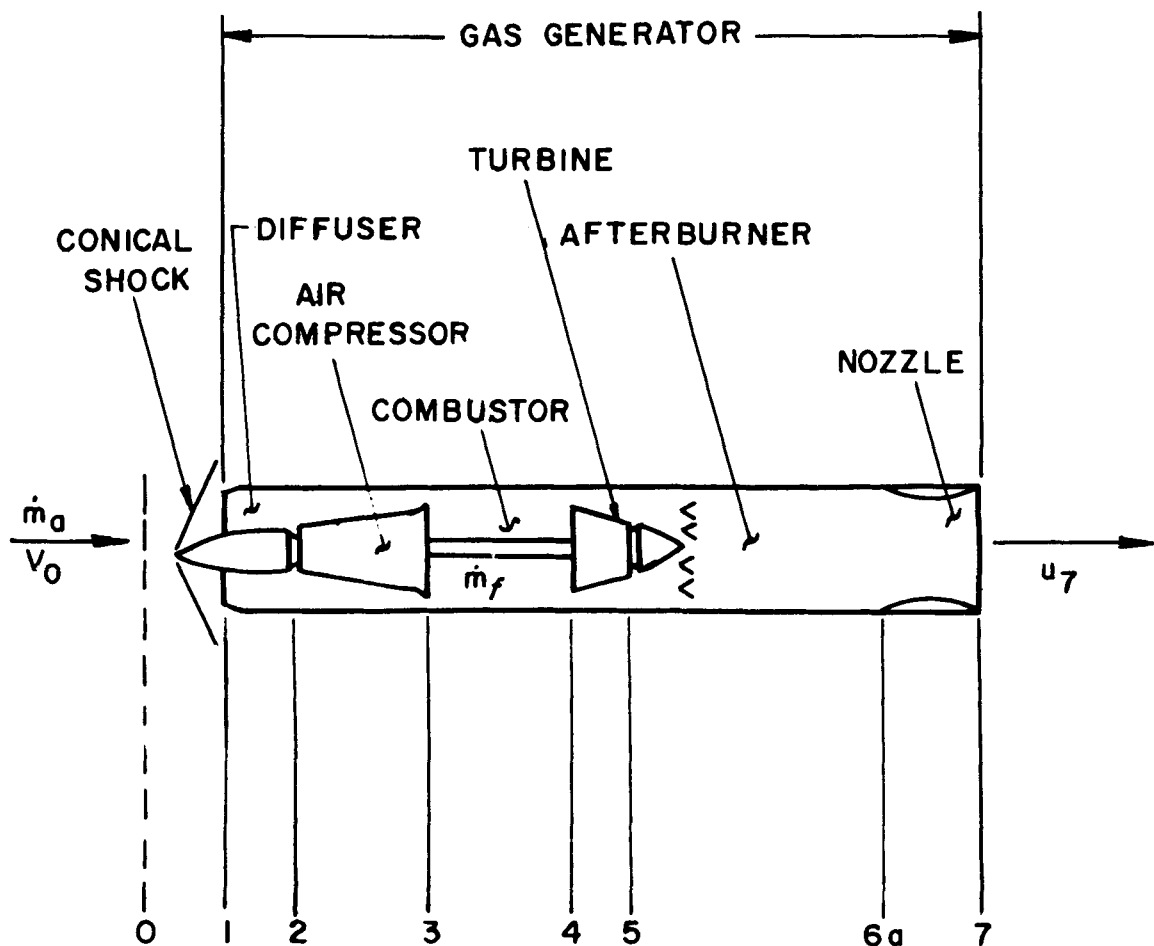
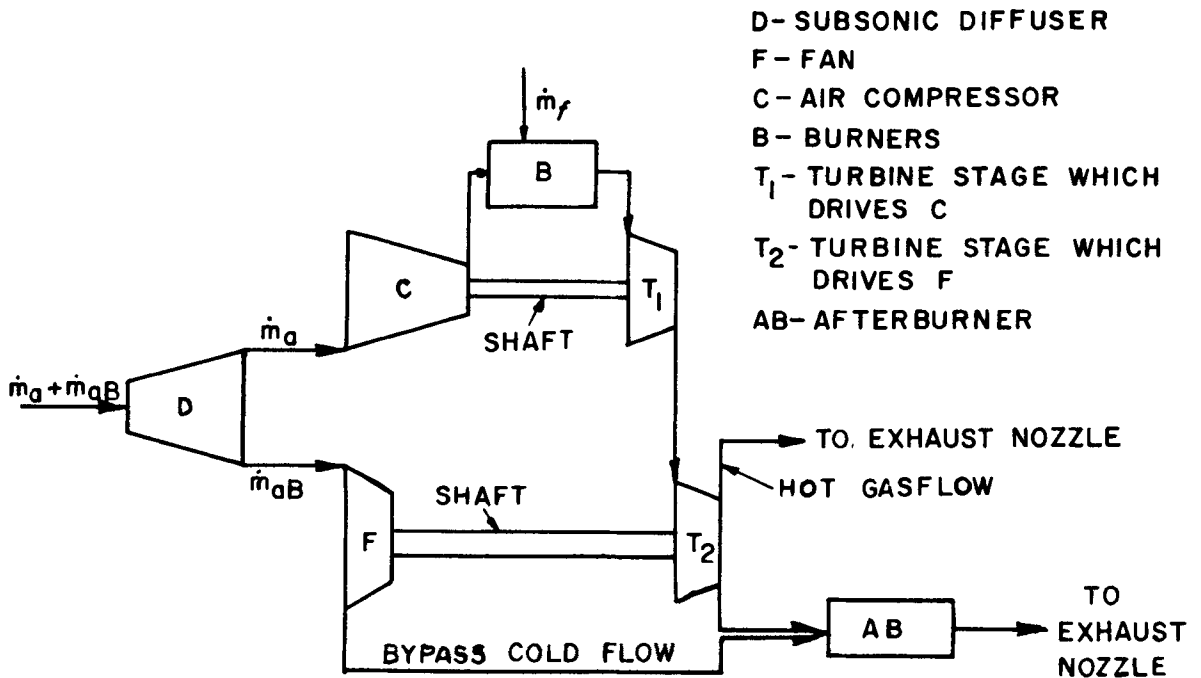
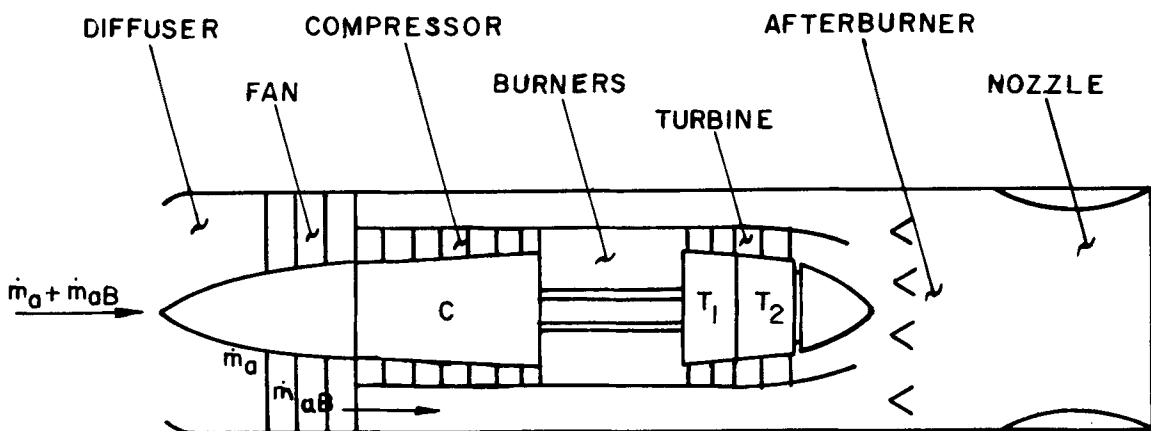


Figure 12-4. Arrangement of the Components of an Afterburning Turbojet Engine



(A) GAS GENERATOR FOR TURBOFAN ENGINE



(B) DUCT - BURNER TURBOFAN ENGINE

Figure 12-5. Essential Features of a Turbofan Engine

The gas leaving the hot gas generator of a turbofan engine—which is operated with the same turbine inlet temperature as its equivalent turbojet engine—has a lower temperature than that leaving the hot gas generator of the equivalent turbojet engine. The reduction in the hot gas temperature is due to the turbine extracting additional energy, required for driving the fan, from the hot gas flowing through it. Most of the aforementioned additional energy is imparted to the cold air which is by-passed around the hot gas generator. The average velocity for the gases ejected from the turbofan engine is smaller than that for the equivalent turbojet engine.

12-2.4 THE TURBORAMJET OR DUAL-CYCLE ENGINE

The turboramjet engine, also called a dual-cycle engine, combines the components of the two engine types in such a fashion that the entire flight regime from take-off ($M_0 = 0$) to cruise, at approximately $M_0 = 4$, is accomplished in a single engine. The turbojet operates from $M_0 = 0$ until at a predetermined value of M_0 the engine is then switched to ramjet operation. The

engine utilizes a common inlet-diffuser system, tailpipe equipped with an afterburner, and exhaust nozzle for both the turbojet and ramjet operations. An air-valve switches the air flowing from the diffuser so that it by-passes the turbo-compressor set and primary burners, and flows directly into the tailpipe. The feasibility of such an engine was demonstrated more than a decade ago, but its flight characteristics have not been determined.

12-2.5 THE TURBOSHAFT ENGINE

Fig. 12-6 illustrates diagrammatically two arrangements of the components of a turboshaft engine which is an open cycle gas-turbine power-plant¹. The simplest configuration is that illustrated in Fig. 12-6(A), where a single air compressor and turbine assembly drives the load—such as a helicopter rotor—through a gearbox G. The arrangement illustrated in Fig. 12-6(A) is termed a *fixed-shaft turboshaft engine*. The arrangement illustrated in Fig. 12-6(B) is a dual turbine configuration termed a *free-turbine turboshaft engine*.

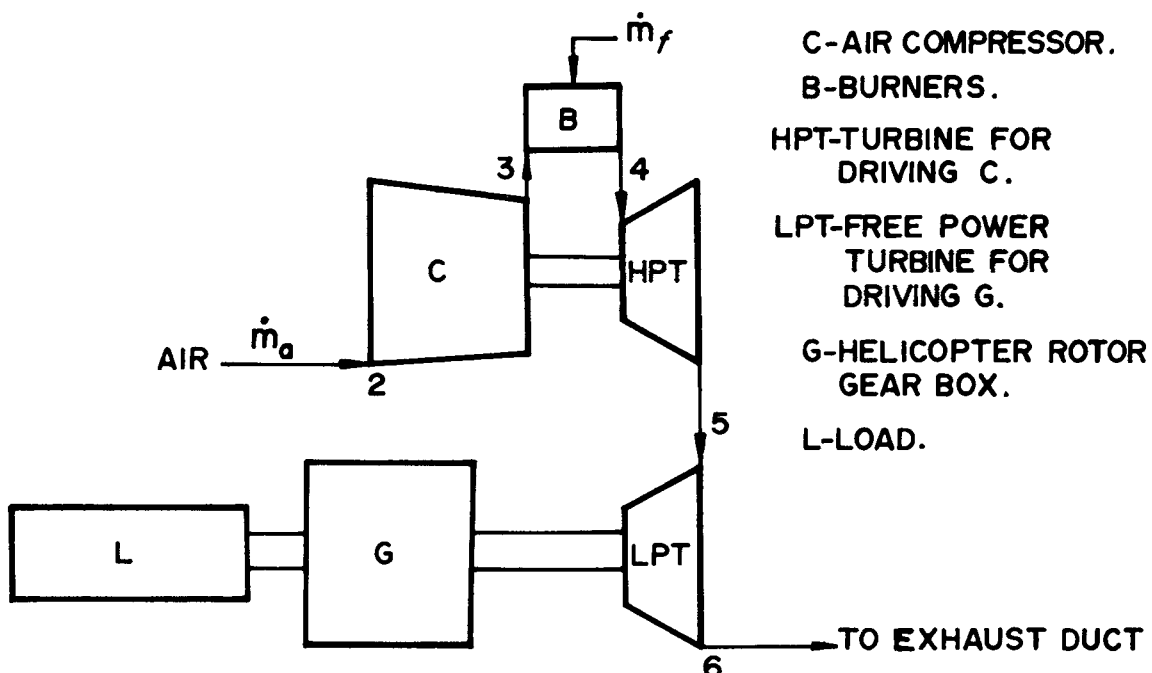


Figure 12-6. Essential Features of a Turboshaft Engine

In Fig. 12-6(B) compressor (C) and a high pressure turbine (HPT) are direct connected with a hollow shaft, and a *free* low pressure turbine (LPT), also called the *power-turbine*, drives the load through the reduction gearbox G. The shaft connecting the power-turbine and the load passes through the hollow shaft connecting the air compressor (C) and the (HPT). The power-turbine has “torque converter” characteristics, so no clutch is required between the load and the turboshaft engine. Because the free-turbine configuration has the flexibility for satisfying a wide range of performance requirements, it is the favored configuration for modern helicopter turboshaft engines.

An arrangement similar to that shown in Fig. 12-6(B) can be employed where the air compression is accomplished by two air compressors in series; a low pressure compressor (LPC) followed by a high pressure compressor (HPC). In such an engine, the power turbine (LPT) drives the (LPC) in addition to the load¹. The air compression is, therefore, accomplished by two air compressors which rotate independently of each other because they are driven by separate turbines. Such an engine is termed a *two-spool* turboshaft engine.

The air compression system for a turboshaft engine usually has a pressure ratio P_3^O/P_2^O in the range 6 to 1 to 13 to 1. It may comprise a single axial flow compressor, an axial flow compressor followed by a radial compressor stage, or a twin-spool axial flow compressor, etc.

In a turboshaft engine the turbines are designed so that the gas leaving the engine (at Station 6) is ejected with the lowest practical velocity. The object is to keep the kinetic energy associated with the ejected gas, termed the *exit loss* as small as possible because it does not contribute any significant thrust.

Modern turboshaft engines in the 3000 to 3500 shp class have ratios shaft horsepower-to-engine weight of approximately 5.0, and operate with a SFC of approximately 0.50 lb fuel/hp-hr.

12-2.6 THE TURBOPROP ENGINE

Fig. 12-7 illustrates diagrammatically the essential elements of a turboprop engine, which is a *turboshaft* engine driving an aircraft propeller. In its essential features these engines are quite similar to the turbojet engine (see Fig. 12-2), the major difference being that the turbines of the turboshaft and turboprop engines are designed to produce shaft power. The turboprop engine differs from the turboshaft engine in that in addition to developing shaft power for driving an aircraft propeller it also delivers some jet thrust (see par. 2-3). In some turboprop engines a separate *power turbine* is employed for driving the propeller, as explained in par. 12-2.5.

The turboprop engine is well adapted to propelling aircraft in the moderate speed range (300-375 knots). To achieve a satisfactory SFC (lb fuel/hp-hr) the engine components must have high efficiencies. The turbine inlet stagnation temperature T_4^O must be as high as possible so that a large value of thrust-to-weight ratio can be realized.

The proportioning of the total thrust of a turbojet engine into *propeller thrust* and *jet thrust* is determined by the application of the engine. It is estimated that the jet thrust practically compensates for the nacelle drag and the propeller losses. Consequently, the shaft horsepower obtained from a turboprop engine installed in an aircraft is substantially equal to the *net* thrust horsepower (thp) *available* for propelling the airplane.

The horsepower rating of a turboprop engine must be based on the power required for

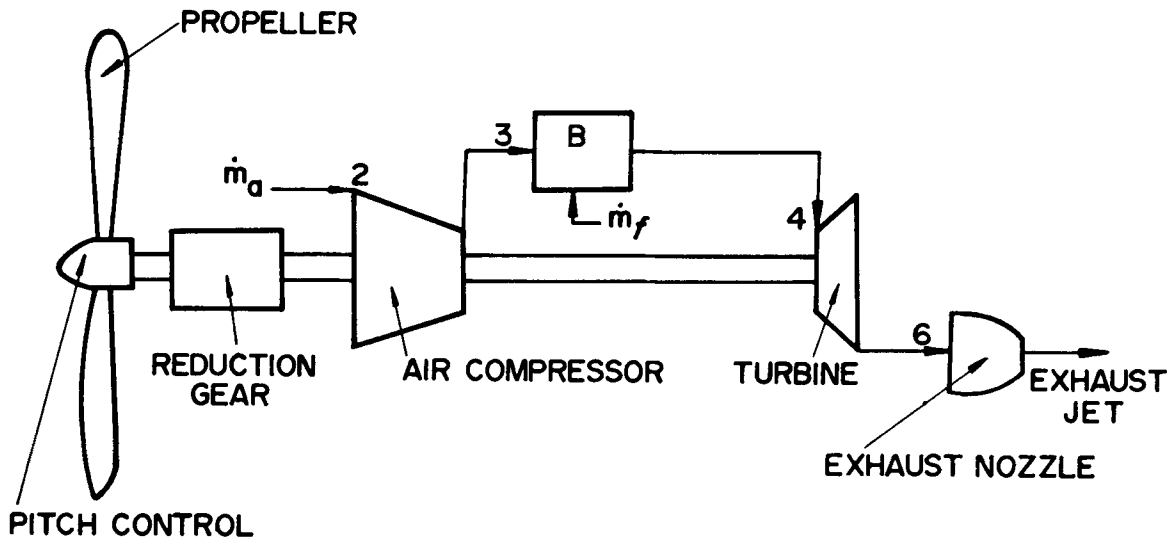


Figure 12-7. Essential Features of a Turboprop Engine

propelling the airplane at a constant flight speed V_0 at the design altitude. Consequently, at lower altitudes the specific power output of the engine increases, and there is considerable excess shp, and hence propeller thrust, available at sea level for accelerating the aircraft. A turboprop engine has, therefore, excellent take-off characteristics.

Regenerative turboshaft engines are discussed in Chapter 15.

12-3 GENERAL THRUST EQUATIONS FOR AIR-BREATHING ENGINES

Equations for the thrust developed by an air-breathing jet engine can be obtained by applying the momentum equation of fluid mechanics to a control surface, fixed in space, enclosing a stationary jet (propulsion) engine. Employing a *relative coordinate system*, a general equation can be derived for the thrust produced by the propellant stream flowing through an engine, i.e., the thrust produced by the *internal flow*. The external flow is assumed to be thermodynamically reversible and, because

of that assumption, the air velocity V_0 and the ambient static pressure P_0 are constant over the entire control surface, except over the exit area of the exhaust nozzle A_e (see par. 2-2.1).

12-3.1 GENERAL THRUST EQUATIONS

For a single propellant stream, the thrust F —which acts in the opposite direction to the relative exit velocity u_e —is given by Eq. 2-28, which is repeated here for convenience. Thus

$$F = \dot{m}_e u_e - \dot{m}_1 V_1 + (P_e - P_0) A_e \quad (12-1)$$

If the exit velocity u_e is *supersonic*, the static pressure P_e can be different from the ambient static pressure P_0 . In Eq. 12-1

$\dot{m}_e u_e$ is called the *jet thrust*

$\dot{m}_1 V_1$ is called the *ram drag*

$(P_e - P_0) A_e$ is called the *pressure thrust*

It is convenient to eliminate the pressure thrust term $(P_e - P_o)A_e$ from Eq. 12-1 by introducing a fictitious velocity V_j termed the *effective jet velocity*. Hence, one may write

$$F = \dot{m}_e V_j - \dot{m}_1 V_1 \quad (12-2)$$

Eqs. 12-1 or 12-2 are applicable to each propellant stream flowing through an air-breathing jet engine.

In the special case where the propulsive gas (assumed to be thermally and calorically perfect) flowing through the exhaust nozzle is expanded completely, so that $P_e = P_o$, then $V_j = u_e$. Thus (see pars. 4-3 and 4-5)

$$V_j = \phi_n \sqrt{2(h_c^o - h_e)} = \phi_n \sqrt{\frac{2\gamma}{\gamma-1} RT_c^o Z_t} \quad (12-3)$$

where

$$Z_t = 1 - \left(\frac{P_e}{P_c^o} \right)^{\frac{\gamma-1}{\gamma}} \quad (12-4)$$

where

h_e = static specific enthalpy of the propulsive gas in the exit cross-section of the exhaust nozzle A_e , B/slug

h_c^o = stagnation specific enthalpy of the propulsive gas in the inlet cross-section of the exhaust nozzle A_c , B/slug

R = gas constant = $1545/\bar{m}$, ft-lb $^\circ$ R

\bar{m} = molecular weight of propulsive gas

T_c^o = stagnation temperature of the propulsive gas at the inlet cross-section of the exhaust nozzle, $^\circ$ R

$\gamma = c_p/c_v$ = specific heat ratio

P_c^o = stagnation pressure in A_c

P_e = static pressure in A_e

Eq. 12-3 shows that the exit velocity of the propulsive jet depends upon the following parameters:

1. The expansion ratio for the exhaust nozzle, P_e/P_c^o
2. The stagnation temperature of the gas entering the exhaust nozzle, T_c^o
3. The molecular weight of the propellant gas, $\bar{m} = R_u/1545$
4. The specific heat ratio of the gas, γ
5. The velocity coefficient for the exhaust nozzle, ϕ_n

For a simple turbojet engine (see Fig. 12-2) the stagnation temperature of the gas entering the exhaust nozzle, T_6^o , will range from 900 $^\circ$ F to 1300 $^\circ$ F depending upon the design of the engine. In the case of an afterburning turbojet engine, (see Fig. 12-3) T_6^o can be as high as approximately 3600 $^\circ$ F.

12-3.2 GENERAL THRUST EQUATIONS IN TERMS OF FUEL-AIR RATIO

Air-breathing engines induct atmospheric air at the mass rate of flow \dot{m}_a and burn a fuel, usually a hydrocarbon liquid, in the air at the rate \dot{m}_f .

Let

$\dot{m}_1 = \dot{m}_a$ = the mass rate of air flow into the engine

and

$\dot{m}_e = \dot{m}_a + \dot{m}_f$ = the mass rate of gas flow leaving engine

By definition

and

$$\nu = V_0/V_j = \text{the effective speed ratio} \quad (12-6)$$

Combining Eqs. 12-2, 12-5, and 12-6 one obtains the following general equation for the thrust produced by an air-breathing engine:

$$F = \dot{m}_a V_0 \left(\frac{1+f}{\nu} - 1 \right) \quad (12-7)$$

Eq. 12-7 is the general equation for the thrust F of an air-breathing jet engine. For chemical engines $f = \dot{m}_f/\dot{m}_a > 0$; for nuclear heat-transfer engines $f = 0$.

For given values of \dot{m}_a , f , and V_0 the thrust increases as the effective jet velocity $V_j = V_0/\nu$ increases, i.e., as more energy is added to the air. Because of structural and thermodynamic considerations, however, the effective jet velocity V_j is limited by the maximum amount of energy that can be added to the inducted air. Consequently, there is a definite limit to the thrust obtainable per unit mass flow of air through an air-breathing jet engine.

12-4 THRUST EQUATIONS FOR SPECIFIC AIR-BREATHING ENGINES

The general thrust equations presented in the preceding paragraphs will now be applied to specific types of air-breathing engines.

12-4.1 THRUST EQUATIONS AND COEFFICIENTS FOR THE RAMJET ENGINE

Refer to Fig. 12-1. The thrust produced by the internal flow of the ramjet engine is termed the *gross thrust* and is denoted by F_g . The fuel flow for such an engine can be large enough for the fuel-air ratio to have a value of approximately $f = 0.08$. Hence, the *gross-thrust* of the ramjet engine is given by Eq. 12-7 which is repeated here for convenience.

Thus

$$F_g = \text{gross thrust} = \dot{m}_a V_0 \left(\frac{1+f}{\nu} - 1 \right)$$

If D denotes the total drag force acting on the ramjet engine, the *net thrust*, denoted by F_n , is defined by

$$F_n \equiv F_g - D \quad (12-8)$$

In discussions of the performance characteristics of a ramjet engine, two *thrust coefficients* are employed:

1. C_{Fg} - the gross thrust coefficient, and
2. C_{Fn} - the net thrust coefficient

If A_m denotes the maximum cross-sectional area of a ramjet engine body, then by definition

$$C_{Fg} \equiv \frac{F_g}{\frac{1}{2} \rho_0 V_0^2 A_m} \quad (12-9)$$

and

$$C_{Fn} \equiv \frac{F_g - D}{\frac{1}{2} \rho_0 V_0^2 A_m} \quad (12-10)$$

where ρ_0 is the density of the atmospheric air in slug/ft³.

12-4.2 THRUST EQUATION FOR SIMPLE TURBOJET ENGINE

Refer to Fig. 12-2. The current and anticipated limitations on the turbine inlet stagnation temperature T_4^0 of turbojet engines to be developed in the next decade are such that the fuel flow rate \dot{m}_f will not exceed approximately 3 percent of the inducted air flow rate \dot{m}_a . It can be assumed that the air bled from the compressor for cooling the bearings and disk will be approximately $0.03 \dot{m}_a$. Hence,

$$\dot{m}_1 = \dot{m}_a$$

and

$$\dot{m}_7 = \dot{m}_a + \dot{m}_f - \dot{m}_{\text{cool}} \approx \dot{m}_a$$

Hence, for a simple turbojet engine, the thrust due to the internal flow is

$$F = \dot{m}_a(V_j - V_0) = \dot{m}_a V_j (1 - \nu) \quad (12-11)$$

The mass rate of air flow \dot{m}_a is determined by the demands of the turbojet engine and not the relative velocity V_0 of the atmospheric air to the turbojet engine. Only for a simple propulsive duct enclosing no flow-controlling devices—such as compressors, burners, etc.—is \dot{m}_a dependent only on V_0 .

Eq. 12-11 shows that—for constant values of the jet velocity V_j and air mass flow rate \dot{m} —the thrust F increases as the flight speed decreases, i.e., as the speed ratio $\nu = V_0/V_j$ is decreased. An important characteristic of a gas-turbine jet engine is that it is capable of providing thrust at zero and low flight speeds. As indicated in earlier paragraphs, a basic disadvantage of propulsive duct jet engines arises from the fact that their cycle pressure ratios are entirely dependent

upon the flight speed and the efficiency of the diffusion processes. They cannot accelerate a vehicle from standstill.

The fuel flow rate \dot{m}_f for a turbojet engine depends upon the required turbine inlet temperature (T_4^0 in Figs. 12-2 and 12-3). Currently, the maximum permissible turbine inlet temperature is limited by metallurgical considerations, assuming uncooled stator vanes and rotating blades, to approximately 1800°F. If higher turbine inlet temperatures are required, the turbine must be cooled. Currently, assuming no cooling of the turbine, the permissible turbine inlet temperature for cruising flight is approximately 1500°F.

Fig. 12-8 illustrates the historical trends in the maximum allowable temperatures for turbine disk, blade, and vane materials⁶. It is evident from the figure that even the most modern materials uncooled are inadequate for operation at the required turbine inlet temperature, approximately 2300°F, for a Mach 3 supersonic transport⁶. The utilization of such a high turbine inlet temperature in the case of the turbojet engine of a Mach 3 SST, combined with the high reliability and the durability so essential to commercial aircraft engines, are the major problems to be solved in developing a satisfactory turbojet engine for such an aircraft. Undoubtedly, the advances in cooled turbine technology will contribute to the development of such an engine.

12-4.3 THRUST EQUATION FOR AFTER-BURNING TURBOJET ENGINE

Refer to Fig. 12-4. For a simple turbojet engine, \dot{m}_f is the fuel consumption rate for the primary burners. For the afterburning engine additional fuel is burned in the afterburner at the rate of \dot{m}_{fa} . The total fuel rate for an afterburning engine is, therefore, the sum $\dot{m}_f + \dot{m}_{fa} = \dot{m}_{fab}$.

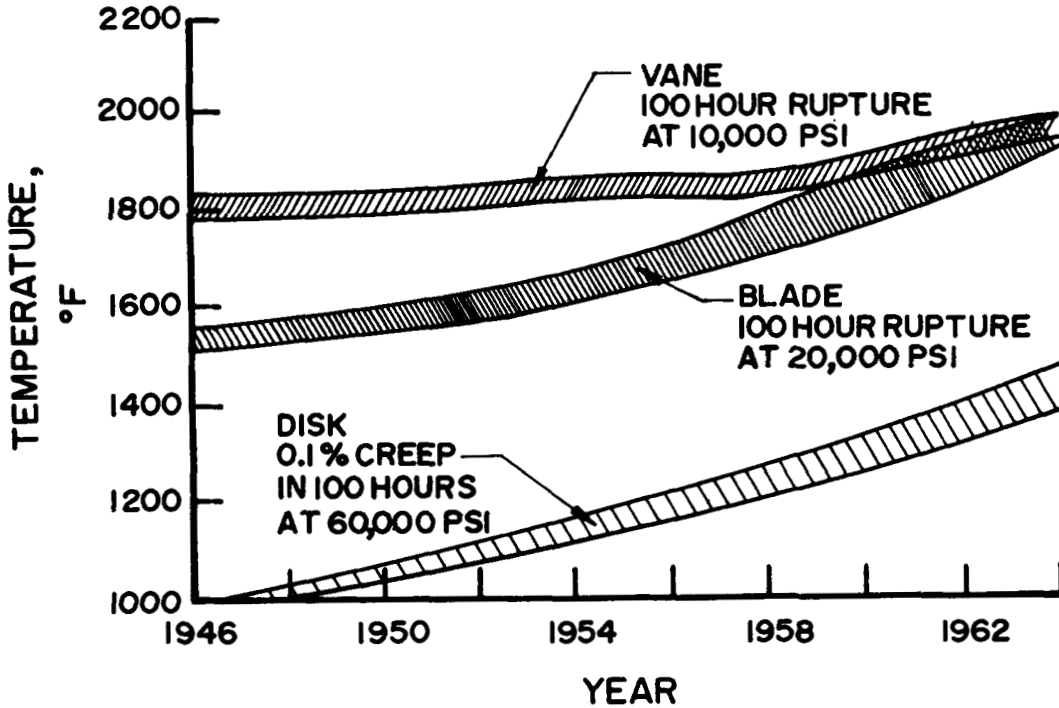


Figure 12-8. Historical Trend in the Maximum Allowable Temperatures for Turbine Disk, Blade, and Vane Materials

For a simple turbojet engine the thrust equation is (see Fig. 12-2) where

$$F = \dot{m}_a (u_7 - V_0) + (P_7 - P_0) A_7$$

$$= F_j - \dot{m}_a V_0 \quad (12-12)$$

For the *afterburning* jet engine the thrust due to the internal flow is denoted by $F_A > F$, and is given by

$$F_A = (\dot{m}_a + \dot{m}_f + \dot{m}_{fa}) V_{jA} - \dot{m}_a V_0$$

$$= F_{jA} - \dot{m}_a V_0 \quad (12-13)$$

The ratio F_A/F is termed the *augmented thrust ratio*. It can be shown that¹

$$\frac{F_A}{F} \approx \frac{\sqrt{T_{6A}^0 / T_6^0} - \nu}{1 - \nu} \quad (12-14)$$

T_6^0 = stagnation temperature of propulsive gas entering the exhaust nozzle with no afterburning

T_{6A}^0 = stagnation temperature of propulsive gas entering the exhaust nozzle with afterburning

12-4.4 THRUST EQUATION FOR TURBOFAN ENGINE

Refer to Fig. 12-5. The internal flow of the turbofan engine comprises two gaseous propellant streams; a hot gas stream leaving the hot gas generator and a cold air stream flowing through the bypass duct. The thrust produced by the engine is the sum of the thrusts produced by the hot and cold gas streams. It can be shown that the thrust developed by a turbofan engine can

be calculated by means of the following equation:

$$F = (\dot{m}_a + \dot{m}_f) V_j - \dot{m}_a V_0 + \dot{m}_{aF} (V_{jF} - V_0) \quad (12-15)$$

where

\dot{m}_a = the mass rate of flow of air through the hot gas generator, slug/sec

\dot{m}_{aF} = the mass rate of flow of cold air through the bypass duct, slug/sec

V_j = the effective jet velocity obtained by expanding the hot gas stream to ambient pressure, fps

V_{jF} = the effective jet velocity obtained by expanding the bypassed cold air to the ambient pressure, fps.

It is readily shown that the *mean effective jet velocity* V_{jTF} for a turbofan engine is given by

$$V_{jTF} = \frac{(1+f) V_j + \beta V_{jF}}{(1+f)} \quad (12-16)$$

where $\beta = \dot{m}_{aF}/\dot{m}_a$ = the *bypass ratio*

Increasing the turbine inlet temperature affects only the temperature of the air flowing through the hot gas generator. Consequently, the thrust increase achieved by raising the turbine inlet temperature is small, and decreases as the bypass ratio β is raised (see par. 15-10.4).

For the same flight speed V_0 and turbine inlet temperature for comparable turbofan and turbojet engines, one may write

$$F_{TFE} < F_{TJE}; \quad \bar{V}_{jTF} < \bar{V}_{jTJE};$$

$$\nu_{TFE} > \nu_{TJE} \quad (12-17)$$

where TFE and TJE refer to turbofan and turbojet engines, respectively.

Increasing the bypass ratio — while holding the hot gas generator conditions constant — reduces the mean jet velocity \bar{V}_{jTF} of the turbofan engine, which increases its *propulsive efficiency* (see par. 12-5).

12-5 EFFICIENCY DEFINITIONS

The performance of an air-breathing jet engine is expressed in terms of the efficiencies presented in par. 2-5.5.

12-5.1 PROPULSIVE EFFICIENCY (η_p)

By definition, in general, the propulsive efficiency is defined by (see par. 2-4)

$$\eta_p = \frac{\text{thrust power } (P_T)}{\text{propulsive power } (P)} \quad (12-18)$$

(a) Propeller efficiency (η_{prop})

If P_{sh} denotes the shaftpower delivered to propeller, and F_{prop} the propeller thrust, then

$$\eta_{prop} = \frac{F_{prop} V_0}{P_{sh}} \quad (12-19)$$

(b) Ideal propulsive efficiency of a jet propulsion engine (η_p)

From par. 2-5.6, for an air-breathing jet engine

$$\eta_p = \frac{2\nu}{1+\nu} \quad (12-20)$$

where $\nu = V_0/V_j$

12-5.2 THERMAL EFFICIENCY (η_{th})

For air-breathing jet engines, the *thermal efficiency* η_{th} is defined by

$$\eta_{th} = \frac{\text{power supplied to propulsive element } (E_p)}{\text{rate of energy consumption in form of fuel } (E_{in})} \quad (12-21)$$

If ΔH_c denotes the lower calorific value of the fuel and \dot{m}_f the rate of fuel consumption, then

$$E_{in} = \dot{m}_f \Delta H_c \quad (12-22)$$

and

$$E_p = \frac{1}{2} [(\dot{m}_a + \dot{m}_f) V_j^2 - \dot{m}_a V_0^2] \quad (12-23)$$

(a) Air-breathing jet engine

$$\eta_{th} = \frac{(1+f)V_j^2 - u^2}{2f\Delta H_c} \quad (12-24)$$

(b) Turboshift engine

Let P_{sh} denote the power output of a turboshift engine; its thermal efficiency is given by

$$\eta_{th} = P_{sh} / (\dot{m}_f \Delta H_c) \quad (12-25)$$

(c) Turboprop engine

The total thrust power developed by a turboprop engine, denoted by P_T , is given by

$$P_T = P_{TP} + P_{Tj} \quad (12-26)$$

where

P_{TP} = the thrust power developed by the propeller

$P_{Tj} = F_j V_j$ = thrust power of the jet

Hence, for a turboprop engine

$$\eta_{th} = \frac{P_{TP} / (\eta_{prop} \eta_g) + P_{Tj}}{\dot{m}_f \Delta H_c} \quad (12-27)$$

where η_{prop} is the propeller efficiency, and η_g is the efficiency of the reduction gearbox.

12-5.3 OVERALL EFFICIENCY (η_o)

Neither the thermal efficiency η_{th} nor the propulsive efficiency η_p when considered alone, is a significant criterion of engine performance. The significant criterion is the overall efficiency η_o because it determines the *thrust specific fuel consumption* (TSFC) of the propulsion system. By definition the overall efficiency η_o is given by

$$\eta_o = \eta_{th} \eta_p = \frac{F V_0}{\dot{m}_f \Delta H_c} = 2 \eta_{th} \frac{v}{1+v} \quad (12-28)$$

12-5.3.1 THRUST SPECIFIC FUEL CONSUMPTION (TSFC)

The thrust specific fuel consumption—in lb fuel per hr per lb thrust—is given by

$$\underline{\text{TSFC}} = 3600 \dot{m}_f g_c / F \quad (12-29)$$

12-5.3.2 SPECIFIC FUEL CONSUMPTION (SFC)

For turboshift engines, P_{sh} denotes the shaft horsepower and the specific fuel consumption—in lb fuel per hp hr—is given by

$$\underline{\text{SFC}} = 3600 \dot{m}_f g_c / P_{sh} \quad (12-30)$$

Typical values of TSFC for turbojet and turbofan engines are as follows:

Engine Type	TSFC (lb/hr-lb)
Turbojet ($V = 0$)	0.75 to 1.0
Turbofan ($V = 0$ and $\beta \approx 2.0$)	0.5 to 0.6

Fig. 12-9 illustrates the increase, since 1945, in the overall efficiency of gas-turbine jet engines for propelling aircraft at subsonic speeds. The following is evident from the figure:

- The gain in overall efficiency (from 16.0% to 21%) during the period 1945 to 1960 was due mainly to increasing the cycle pressure ratio of the turbojet engine.
- The large gain in overall efficiency (from 21% to 25%) since 1960 was due to the introduction of the turbofan engine with its high propulsive efficiency.

The propulsive efficiency of the turbofan engine can be raised by increasing the bypass ratio. When the bypass ratio β is increased above $\beta = 3$ the *rotational speed* required for an efficient lightweight turbine for driving the larger fan becomes incompatible with the required *peripheral speed* for the fan that yields the *optimum fan efficiency*. If the bypass ratio is to be increased to between 4 and 5, it may become necessary to install a *reduction gear* if the optimum combination of overall efficiency η_o and engine weight W_E is to be obtained.

The increase in thrust ΔF , due to adding a fan to a basic turbojet engine, is obtained at the expense of increased nacelle drag ΔD_N because of the larger diameter of the resulting turbofan engine. Hence, the *optimum bypass ratio* is the one which maximizes the *gain in net thrust*, i.e., $(\Delta F - \Delta D_N)$.

Fig. 12-10 compares the TSFC's for rocket engines and air-breathing engines as functions of the flight Mach number M_o .

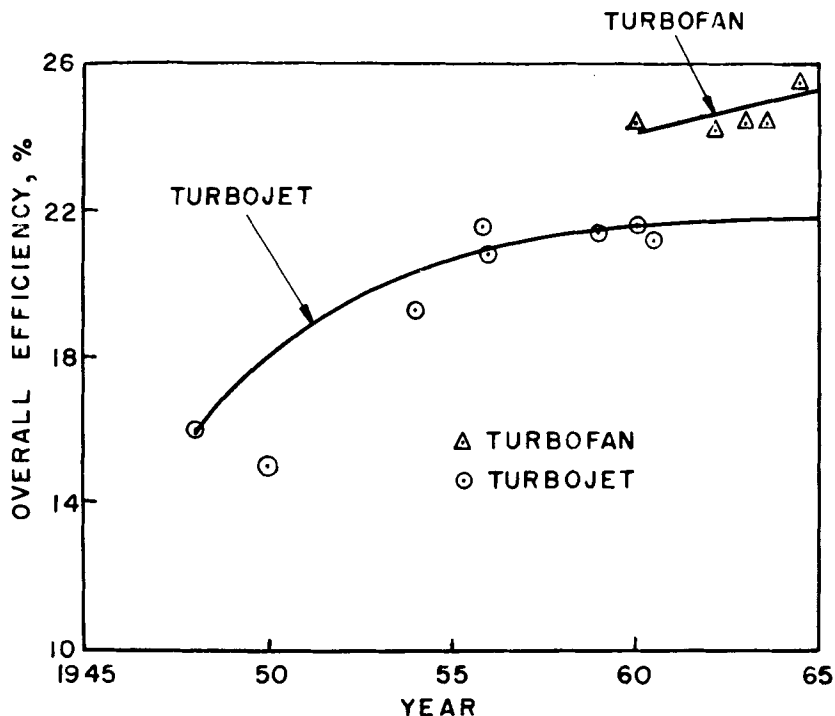


Figure 12-9. Increase in Overall Efficiency of Gas-Turbine Jet Engines Since 1945

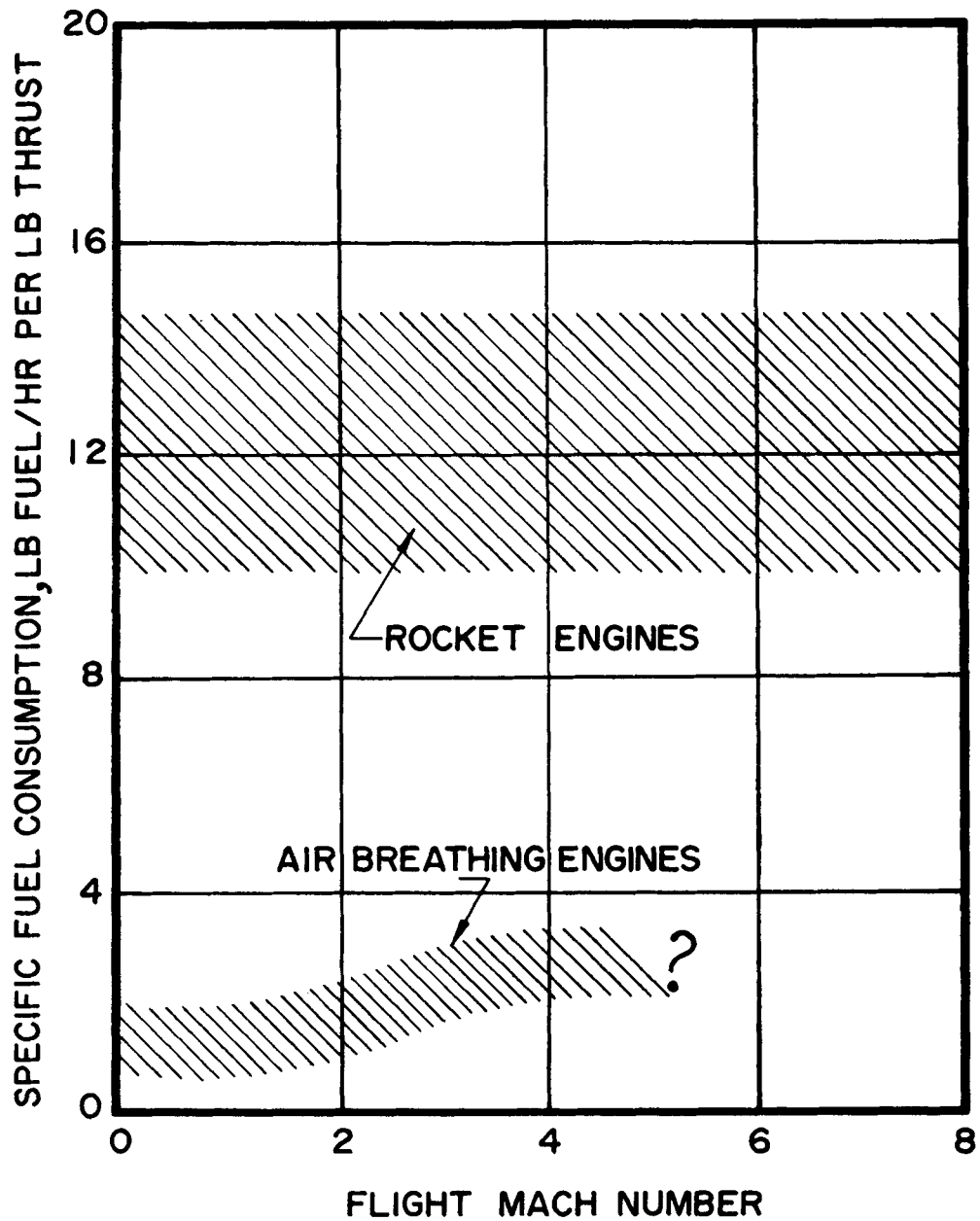


Figure 12-10. Comparison of TSFC's for Air-Breathing and Rocket Engines

12-6 PERFORMANCE PARAMETERS FOR AIR-BREATHING JET ENGINES

The performance parameters for jet propulsion engines are discussed in par. 2-5, in a general manner, but with specific emphasis on rocket engines. In this paragraph the parameters are discussed with reference to air-breathing engines.

There is no single criterion for comparing jet propulsion engines because the *mission* for the propelled vehicle has almost a decisive influence upon the performance characteristics desired for the propulsion engine.

12-6.1 AIR SPECIFIC IMPULSE OR SPECIFIC THRUST (I_a)

This parameter is the net thrust developed per pound of air flowing through an air-breathing engine, and is defined by Eq. 2-42 which is repeated here for convenience. Thus

$$I_a = F_g / \dot{m}_a \quad (12-31)$$

The air specific impulse is a criterion of the physical size of the engine. A large value of specific thrust is desirable. For some aircraft applications a large specific thrust I_a is as important as a high overall efficiency η_o .

In Eq. 12-31, \dot{m}_a is the mass rate of flow of atmospheric air into the engine. For a turbojet engine $\dot{m}_1 = \dot{m}_a$; for a turbofan engine $\dot{m}_1 = \dot{m}_a + \dot{m}_a F$.

The specific thrust depends primarily upon the nozzle inlet stagnation temperature T_6^o and the *nozzle pressure ratio* P_6^o/P_7 . If the nozzle inlet temperature can be increased, then a given thrust can be developed with a smaller mass rate of flow of air, thus making it possible to reduce the *frontal area* of the engine.

The nozzle inlet temperature can, of course, be raised by employing an afterburner. Estimates indicate that the *specific weight* W_E/F_o of an afterburning turbojet engine will be approximately 80% of its nonafterburning counterpart; F_o is the thrust developed when $V_o = 0$. The reduction in specific engine weight is obtained, however, at the expense of a large increase in TSFC. Consequently, the net advantage of employing an afterburning engine for achieving a given mission can be determined only from an analysis which compares the flight performance and ranges for the same aircraft with afterburning and nonafterburning engines.

Another approach to raising nozzle inlet temperature is to cool the turbine vanes and blades, and increase the turbine inlet temperature T_4^o . Considerable research effort is being devoted to developing the technology pertinent to cooled turbines. A cooled turbine offers the additional advantage that its dimensions for a given thrust would be smaller than for its uncooled counterpart.

12-6.2 FUEL SPECIFIC IMPULSE (I_{sp})

By definition

$$I_{sp} = \frac{F_g}{\dot{m}_f} = \frac{3600}{\text{TSFC}} \quad (12-32)$$

where the fuel flow rate \dot{m}_f is in slug/sec.

12-6.3 SPECIFIC ENGINE WEIGHT (W_E/F_o)

The specific engine weight has a direct effect on the *weight of fuel plus payload* that can be carried in an airplane of *gross weight* W_o . A small specific weight is, of course, desirable.

The principal factors which affect the specific engine weight are the following:

- (1) Pressure ratio of the compressor
- (2) Air induction capacity of the inlet
- (3) Frontal area of the engine
- (4) Length of the engine
- (5) Turbine inlet temperature T_4^O because it determines the nozzle inlet temperature T_6
- (6) Allowable stresses for the materials used in constructing the components of the engine

A low specific engine weight W_E/F_0 is probably the most important characteristic for an engine for propelling a supersonic transport. In general, the specific engine weight can be reduced by

- (1) Increasing the turbine inlet temperature.
- (2) Improving the aerodynamic and mechanical design of the engine.
- (3) Developing improved materials for engine components.

12-6.4 TURBINE INLET TEMPERATURE (T_4^O)

Current technology limits the turbine inlet temperature at takeoff to approximately 1800°F, with uncooled blades, and to 2100°F with cooled blades. The corresponding temperature for cruise with uncooled blades is 1500°F. Thermodynamic analyses indicate that for a Mach 3 transport the optimum turbine inlet temperature for cruise is between 2300°F and 2500°F depending upon the cycle pressure⁸. To achieve those high temperatures, the turbine

blades and disk must be cooled with air bled from the air compressor. It is essential that the "bleed" air flowing through the turbine blades does not cause an appreciable degradation of the isentropic efficiency of the turbine.

A thermodynamic study of the application of gas-turbine jet engines to a Mach 3 transport indicates that the required ratios of static thrust F_0 to engine weight W_E range from 9.3 to 11.3 for turbine inlet temperatures ranging from 2300°F to 2500°F. Some idea of the current "state of the art" may be inferred from the GE YJ93 afterburning turbojet engine for the Mach 3 XB70 aircraft (USAF). Its thrust-to-weight ratio is 5.

12-7 GENERAL COMMENTS REGARDING AIR-BREATHING ENGINES

Because of their low TSFC's air-breathing engines are the optimum propulsion engines for vehicles which cruise in the atmosphere.

For accelerating trajectories—such as satellite launchers and sounding rockets—the afterburning jet engine is currently penalized by its poor specific weight characteristics and low top speed limit. If the technology pertinent to the SCRAMJET engine can be developed, the useful operating range of air-breathing jet engines may be increased thereby making them suitable for accelerating trajectories.

In the years immediately ahead, the air-breathing jet engines which are needed for missions requiring high values of overall efficiency will achieve these objectives by increases in, first, the propulsive efficiency, and second, the thermal efficiency. The increases in propulsive efficiency will be accomplished by increasing the bypass ratios of turbofan engines to values between 3 and 8.

The future will see efforts to achieve significant reductions in the specific powerplant

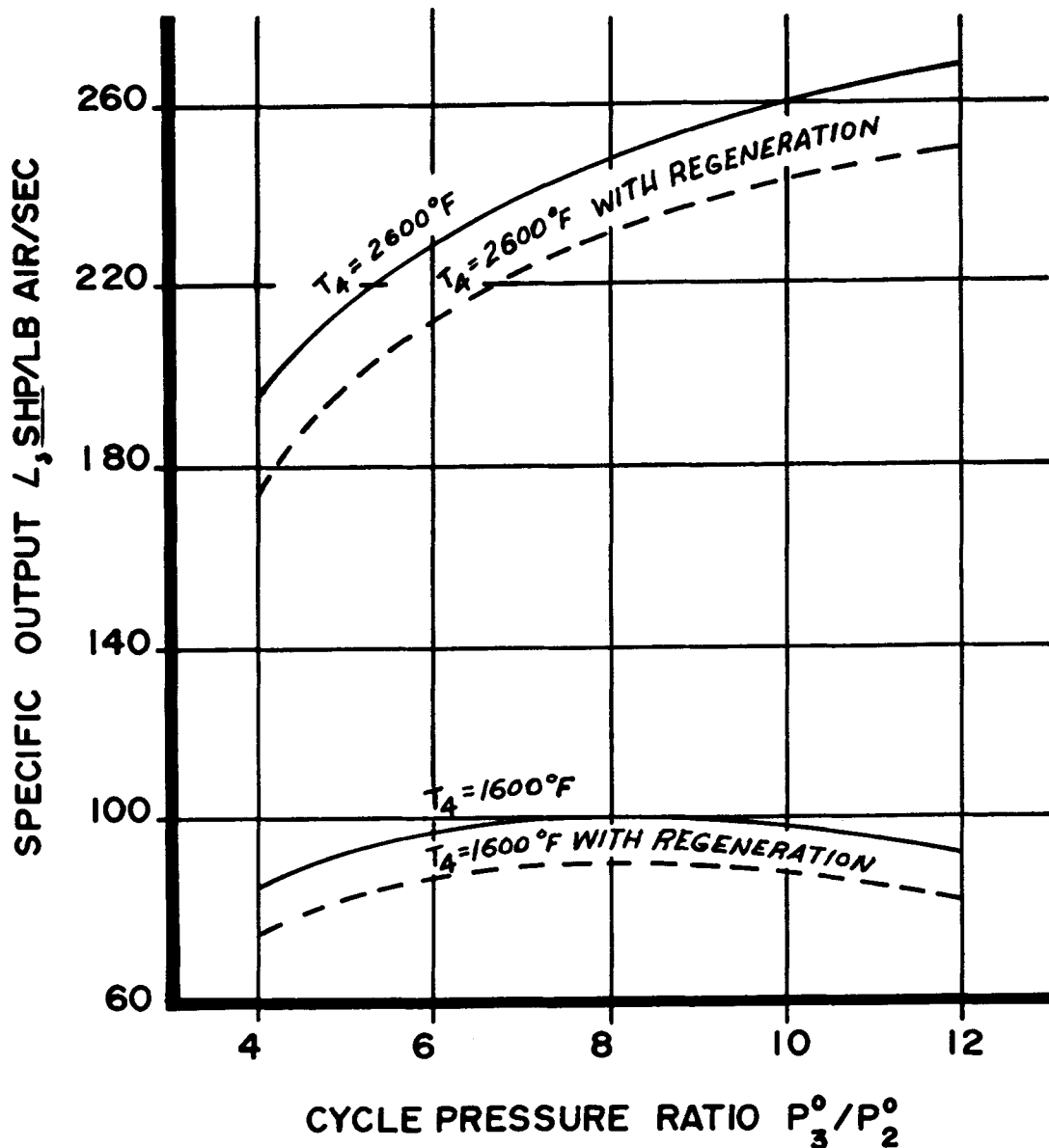


Figure 12-11(A). Specific Output Characteristics As a Function of Cycle Pressures

weight of turbojet and turbofan engines by increasing the turbine inlet temperatures by applying cooling techniques to the turbine, and improvements in aerodynamic design of the rotating machinery.

The air-breathing jet engines for supersonic aircraft must have a good balance between the operating requirements for subsonic and supersonic flight. Consequently, they must have low

specific weight and efficient components so that a high overall efficiency will be realized over the subsonic and supersonic flight regimes. Considerable research and development are required for accomplishing these objectives.

Finally, to extend the flight range of the air-breathing engines into the hypersonic regime, it is necessary that the technology pertinent to

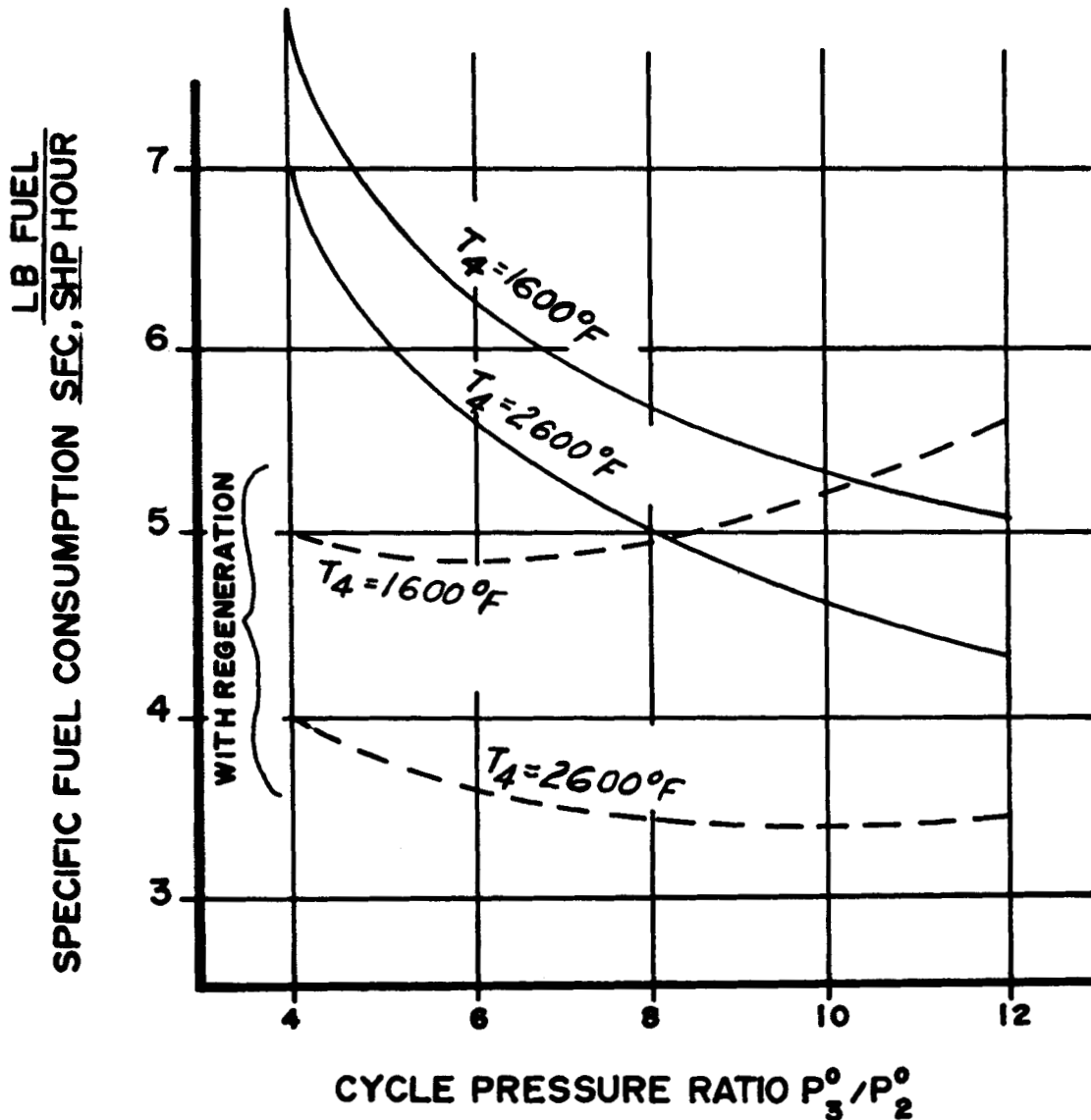


Figure 12-11(B). Specific Fuel Consumption Characteristics As a Function of Cycle Pressures

the SCRAMJET be greatly expanded, so that the hypersonic flight with air-breathing engines can become a reality.

The turbine inlet temperature T_4^0 has a profound influence upon the specific output (see Fig. 12-11(A)) -hp per lb of air per sec - of turboshaft and turboprop engines. Research and development for increasing the turbine inlet temperatures of these engines are highly desirable for increased specific output and for SFC reduction for regenerative engines as shown in

Fig. 12-11(B). An increase in T_4 results in a significant reduction in SFC for a non-regenerative engine (see Fig. 12-11(B)). Furthermore, higher pressure ratio engines are also desirable. Higher turbine inlet temperatures combined with higher pressure ratios for the engine cycle not only reduce the SFC but decrease its sensitivity to decreased loads, a desirable characteristic for an engine which must furnish shaftpower over a wide range of power levels, as in helicopter missions.

REFERENCES

1. M.J. Zucrow, *Aircraft and Missile Propulsion*, John Wiley and Sons, Inc., Vol. II, 2nd Printing, 1964.
2. C.W. Smith, *Aircraft Gas Turbines*, John Wiley and Sons, Inc., 1956.
3. A. Ferri, *Review of SCRAMJET Propulsion Technology*, AIAA Third Annual Meeting, Boston, Mass., Nov. 29-Dec. 2, 1966, AIAA Paper No. 66-826.
4. M.J. Zucrow, "The Problems of the Turbojet Engine as a Propulsion Engine for Supersonic Flight", *Aero Eng. Rev.*, Vol. 15, No. 12, December 1956.
5. B. Pinkel and I.M. Karp, *A Thermodynamic Study of the Turbojet Engine*, NACA Report No. 891, 1947.
6. D.J. Jordan and H.S. Crim, "Evaluation of Modern Air-Transport Power Plants", *Jour. of Aircraft*, Sept.-Oct. 1964, p. 225.
7. J.F. Dugan, R.W. Koenig, J.B. Whitlow, and T.B. McAuliffe, "Power for the Mach 3 SST", *Astro. and Aero.*, September 1964, p. 45.
8. P.W. Pratt, "Aircraft Propulsion Systems—An Evaluation", *Astro and Aero.*, March 1965, p. 60.

CHAPTER 13

COMPRESSIBLE FLOW IN DIFFUSERS

13-1 INTRODUCTION

The efficient diffusion (flow compression) of the air entering an air-breathing engine is essential to the efficient functioning of all air-breathing engines, whether they propel vehicles at either subsonic or supersonic speeds. For a ramjet engine, for example, the combustion process requires that $M_2 \approx 0.2$ (see Fig. 12-1), and for a gas-turbine engine satisfactory performance of the axial flow compressor requires that $M_2 < 0.4$ (see Fig. 12-2). Hence, since the air intake duct for either type of engine acts as a *subsonic diffuser*, it must be designed so that it will decelerate the entering air in an efficient manner, i.e., it should operate with a minimum *stagnation-pressure loss*. Furthermore, the flow over the external surfaces of the air intake should produce the minimum possible *external drag* and the flow leaving the intake-diffuser system should be uniform; a distorted velocity pattern at the inlet of the air compressor can seriously affect its aerodynamic performance.

If the velocity of the free-stream air relative to the intake is *supersonic* (assuming a relative coordinate system), the diffusion problem is complicated by the formation of shock waves at the inlet (Station 1, Figs. 12-1 and 12-2).

Diffusion, also called flow compression, appears at first blush to be merely the reverse of nozzle flow (see Chapter 4). It is considerably more difficult, however, to achieve an efficient diffusion — since the flow moves in the direction of a *positive pressure gradient* — than it is for a flow expansion where the flow has a *negative pressure gradient*. The difference is due to the

difference in the behavior of the *boundary layer* in the two types of flow².

The boundary layer is characterized by being a *thin* layer of fluid adjacent to a solid surface, and in that layer the velocity increases from zero at the surface to practically the main stream velocity in a very short distance perpendicular to the surface, called the *boundary layer thickness*; i.e., the *velocity gradient* in the boundary layer is large. The variation in the velocity of the fluid in the boundary layer is due to *viscous drag*. If the static pressure of the fluid increases in the flow direction, as in a diffusion process, the rate of deceleration of the fluid in the boundary due to the viscous forces exceeds that for the main stream outside of the boundary, where there is no friction. Consequently, the fluid inside the boundary comes to rest while the main stream of fluid has a considerable amount of kinetic energy associated with it. As a result, with further diffusion of the main stream a pressure force is exerted on the stagnant boundary layer — in the direction opposite to that of the main flow — that causes *flow separation* with its attendant large energy dissipation. An expansion process, as in a nozzle, on the other hand adds energy to the boundary layer thereby tending to keep it stable.

A flow passage which converts kinetic energy associated with a *subsonic gas flow* ($M < 1$) into a static pressure rise will be termed a *subsonic diffuser*, and one for decelerating a *supersonic gas flow* ($M > 1$) to approximately the local acoustic speed ($M = 1$), will be called a *supersonic diffuser*. If a vehicle is propelled at a supersonic speed by either a ramjet or turbojet

engine, the complete *diffusion* of the free air stream from $M_0 > 1$ is achieved in two steps: (1) a supersonic diffusion to $M_1 \approx 1$, and (2) followed by a subsonic diffusion from $M_1 \approx 1$ to $M_2 < 1$ (see Figs. 12-1 and 12-2).

Intake-diffusers may be classified into two main groups: (1) subsonic intake-diffusers, and (2) supersonic diffusers. The principal requirements imposed on the intake-diffusers for air-breathing engines are that they convert kinetic energy into static pressure rise with high efficiency; and that the exterior flow over their external surfaces produces the smallest possible drag; and the flow leaving the diffuser should be substantially uniform.

13-2 SUBSONIC INTAKE-DIFFUSERS

All gas-turbine jet engines for propelling aircraft at subsonic flight speeds are equipped with *subsonic intake-diffuser systems*. In such an intake-diffuser the *captured air* is subsonic throughout its flow path. In general, the flow compression of the air inducted by the engine involves two steps: (1) an external compression of the free-stream upstream to the intake (Station 1, Fig. 12-1), and (2) a compression of the air flowing in the duct connecting Stations 1 and 2; see Fig. 12-1. Subsonic diffusers may be grouped into two basic types:

(1) External-Compression Subsonic Diffusers

(2) Internal-Compression Subsonic Diffusers

13-2.1 SUBSONIC EXTERNAL-COMPRESSION DIFFUSERS

Fig. 13-1 illustrates schematically a subsonic external-compression diffuser; for simplicity it is assumed to be of circular cross-section. Its general appearance is a constant area duct with a contoured intake lip. Because the internal flow

passage has a constant area, all of the *diffusion* of the entering air (*the internal flow*) takes place upstream to the inlet (Station 1). The flow streamtube entering the intake has the capture area A_0 far removed from A_1 , where $P_\infty = P_0$, and its cross-section increases to $A_1 > A_0$ at the inlet. All of the transformation of the kinetic energy of the air into pressure rise takes place external to the inlet where there are no solid surface, hence the *external diffusion is isentropic* ($ds = 0$).

Because the capture area $A_0 < A_1$, some of the flowing air is deflected as it approaches the inlet and is accelerated as it flows over the *diffuser lip*; the flow is said to “*spill over*” the inlet. Because of the increased local Mach number due to its acceleration, the “*spilled*” flow causes external drag. It is important that the local Mach number in the vicinity of the lip be less than unity to avoid the formation of shock waves with their attendant large external drag. Consequently, the type of diffuser illustrated in Fig. 13-1 is not satisfactory in the high subsonic speed range.

There is no satisfactory way for designing a subsonic external-compression diffuser; the current theory is quite similar to the airfoil theory employed in analyzing incompressible flow.

13-2.1.1 STATIC TEMPERATURE RATIO FOR AN EXTERNAL-COMPRESSION DIFFUSER

If the subscript 0 denotes the free stream and the subscript 1 the inlet cross-section (Fig. 12-1) then, because the flow is isoenergetic, it follows from Eq. A-109 that

$$\frac{T_1}{T_0} = \frac{1 + \left(\frac{\gamma-1}{2}\right) M_0^2}{1 + \left(\frac{\gamma-1}{2}\right) M_1^2} \quad (13-1)$$

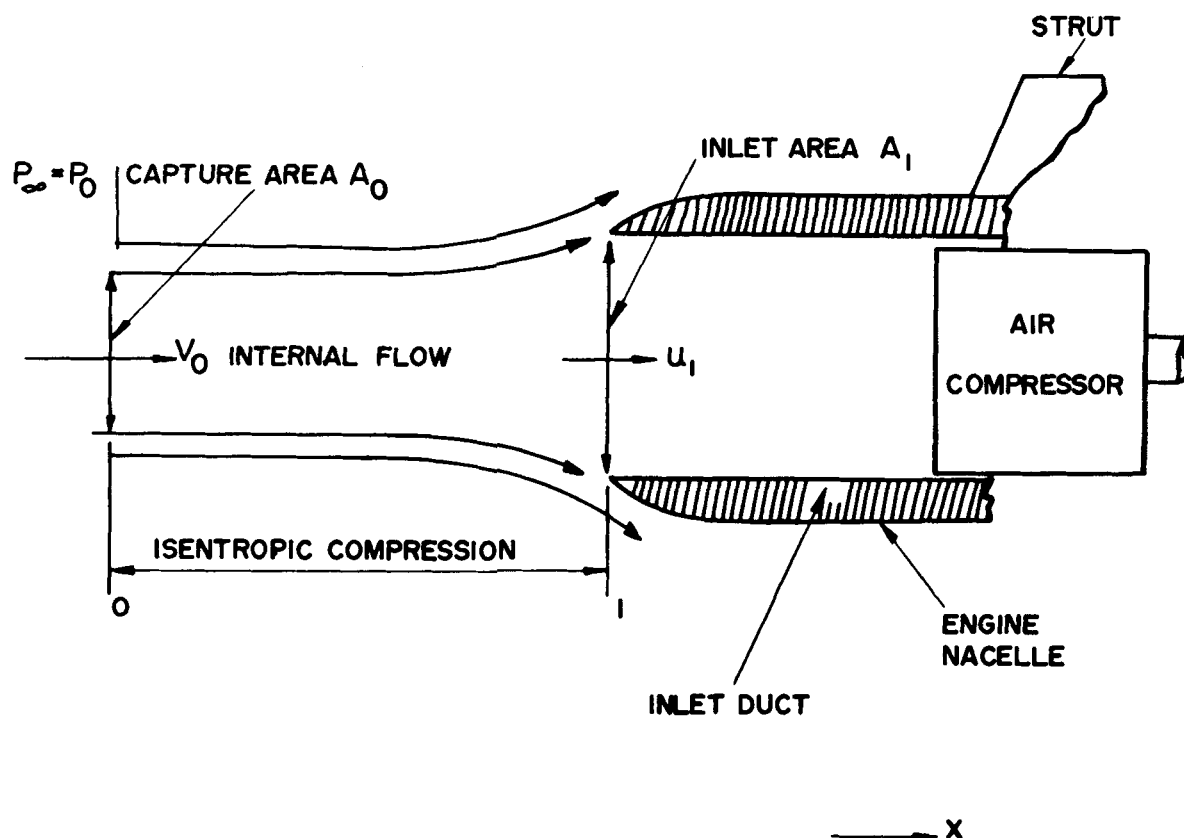


Figure 13-1. Subsonic Inlet With Solely External Compression

13-2.1.2 STATIC PRESSURE RATIO FOR AN EXTERNAL-COMPRESSION DIFFUSER

Because the free-stream flow in the region 0-1 (see Fig. 13-1) may be assumed to be isentropic, the relationships presented in par. A-6 are applicable to that flow. Hence, the static pressure ratio P_1 / P_0 , is given by

$$\frac{P_1}{P_0} = \left(\frac{T_1}{T_0} \right)^{\frac{\gamma}{\gamma-1}} \quad (13-2)$$

There is, of course, no loss in stagnation pressure between Stations 0 and 1.

Ordinarily the subsonic intake-diffuser of a gas-turbine jet engine accomplishes only a small portion of the total compression of the atmospheric air by external diffusion, the balance of the static pressure rise is achieved by *internal compression* in duct 1-2 (see Fig. 12-2).

13-2.2 SUBSONIC INTERNAL-COMPRESSION DIFFUSERS

Subsonic internal-compression diffusers are used in all air-breathing engines. It is accomplished in the duct 1-2 connecting the intake cross-section A_1 and the burner, in a ramjet engine (see Fig. 12-1), and in the duct 1-2 connecting A_1 and the compressor inlet cross-section, in a gas-turbine engine (see Fig. 12-2).

It was pointed out in Chapter 3, that for a one-dimensional isentropic flow the flow area change dA/A , the static pressure change dP/P , and the flow Mach number M are related by Eq. A-156, which is repeated here for convenience. Thus

$$\frac{dA}{A} = \frac{1}{\gamma} \left(\frac{1}{M^2} - 1 \right) \frac{dP}{P} \quad (13-3)$$

Although Eq. 13-3 applies strictly speaking to an isentropic flow ($ds = 0$), it can be employed for obtaining qualitative information regarding an *adiabatic* flow ($ds \neq 0$). The equation shows that area ratio A_2/A_1 for a duct which is to diffuse an isentropic flow must exceed unity, i.e., the flow streamlines must

diverge. Hence, a subsonic internal-compression diffuser is a diverging duct such as that illustrated schematically in Fig. 13-2.

Internal-compression subsonic diffusers have received extensive study but, due to the lack of an adequate theory, their design is largely empirical.

It is apparent from the discussion of the effect of the boundary layer in par. 13-1 that, to prevent the energy losses in an internal-compression diffuser from becoming excessive, the positive pressure gradient dP/dx should be kept small; i.e., the area increase in the direction of flow should be gradual. If the pressure gradient is to be kept small, then the length of

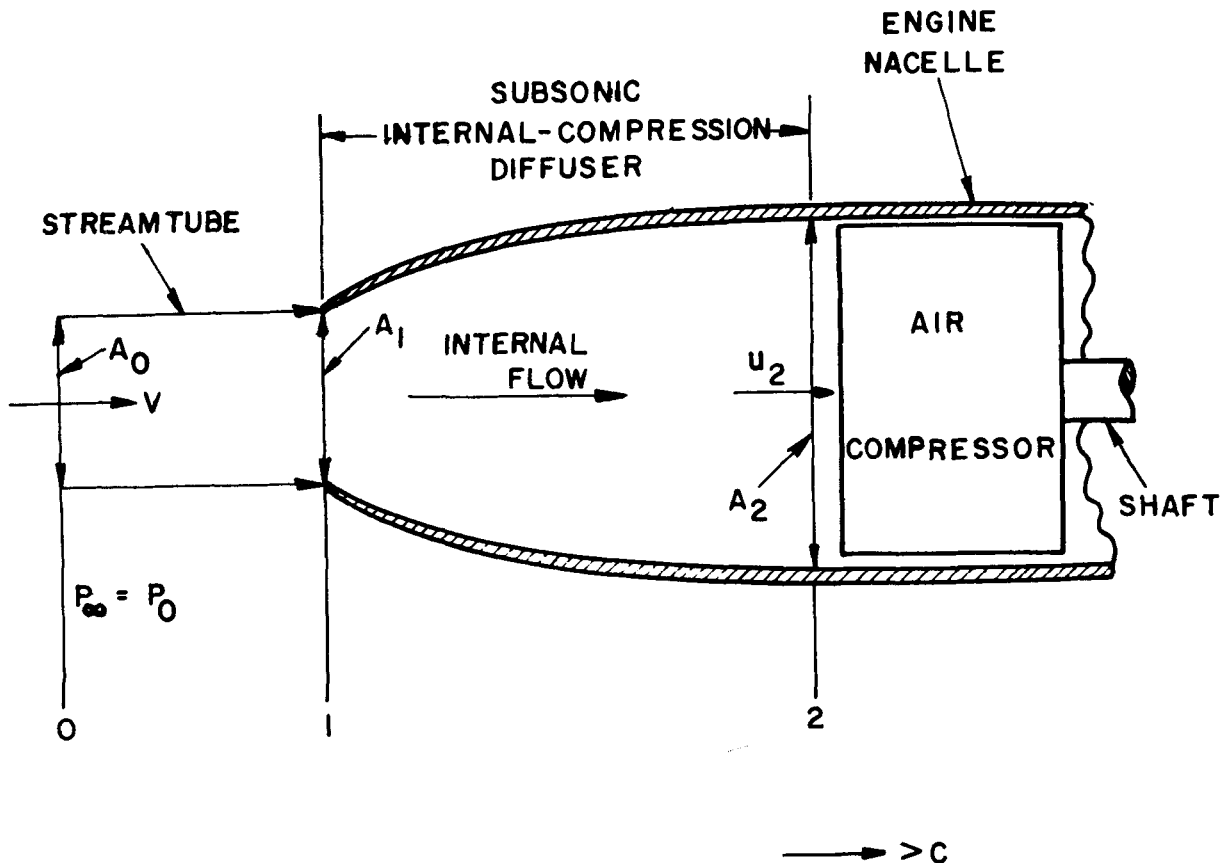


Figure 13-2. Subsonic Internal-Compression Diffuser

the diffuser for accomplishing a specified reduction in the flow Mach number may become so large that the losses in stagnation pressure due to *wall (skin) friction* may be excessive. For a conical internal-compression diffuser, the maximum semiangle of the divergence to avoid flow separation phenomena is between 5° and 7° for a substantially incompressible flow ($M_0 < 0.4$) and decreases approximately as $(1 - M_0^2)$ for higher subsonic Mach numbers⁵. Due to the restrictions on the available space and weight, it is rarely possible to utilize such small divergence angles. Consequently, the design of a subsonic internal-compression diffuser is usually a compromise between stagnation pressure recovery and allowable length.

13-3 PERFORMANCE CRITERIA FOR DIFFUSERS

The performance of a diffuser may be expressed by several different criteria and, if confusion is to be avoided, the bases for defining the different performance criteria should be clearly understood. Three of those criteria will be discussed^{1, 2}.

13-3.1 ISENTROPIC (ADIABATIC) DIFFUSER EFFICIENCY (η_d)

Refer to Fig. 13-3. The isentropic efficiency η_d of a diffusion is given by

$$\eta_d = \frac{h_2^{O'} - h_0}{h_0^O - h_0} \approx \frac{T_2^{O'} - T_0^O}{T_2^O - T_0^O} \quad (13-4)$$

where

$T_2^{O'}$ = the stagnation temperature corresponding to a fictitious isentropic diffusion from P_0 to the actual stagnation pressure P_2^O

T_0^O = the total temperature in the free-stream

$$\text{air} = T_0 \left[1 + \left(\frac{\gamma - 1}{2} \right) M_0^2 \right]$$

In terms of the diffuser pressure ratio P_2^O/P_0 , the isentropic diffuser efficiency is given by

$$\eta_d = \frac{Z_d}{\left(\frac{\gamma - 1}{2} \right) M_0^2} \quad (13-5)$$

where

$$Z_d = \left(\frac{P_2^O}{P_0} \right)^{\frac{\gamma - 1}{\gamma}} - 1 \quad (13-6)$$

From Eq. 13-5 one obtains the following equation for the *diffuser pressure ratio* P_2^O/P_0 . Thus

$$\frac{P_2^O}{P_0} = \left[1 + \eta_d \left(\frac{\gamma - 1}{2} \right) M_0^2 \right]^{\frac{\gamma}{\gamma - 1}} \quad (13-7)$$

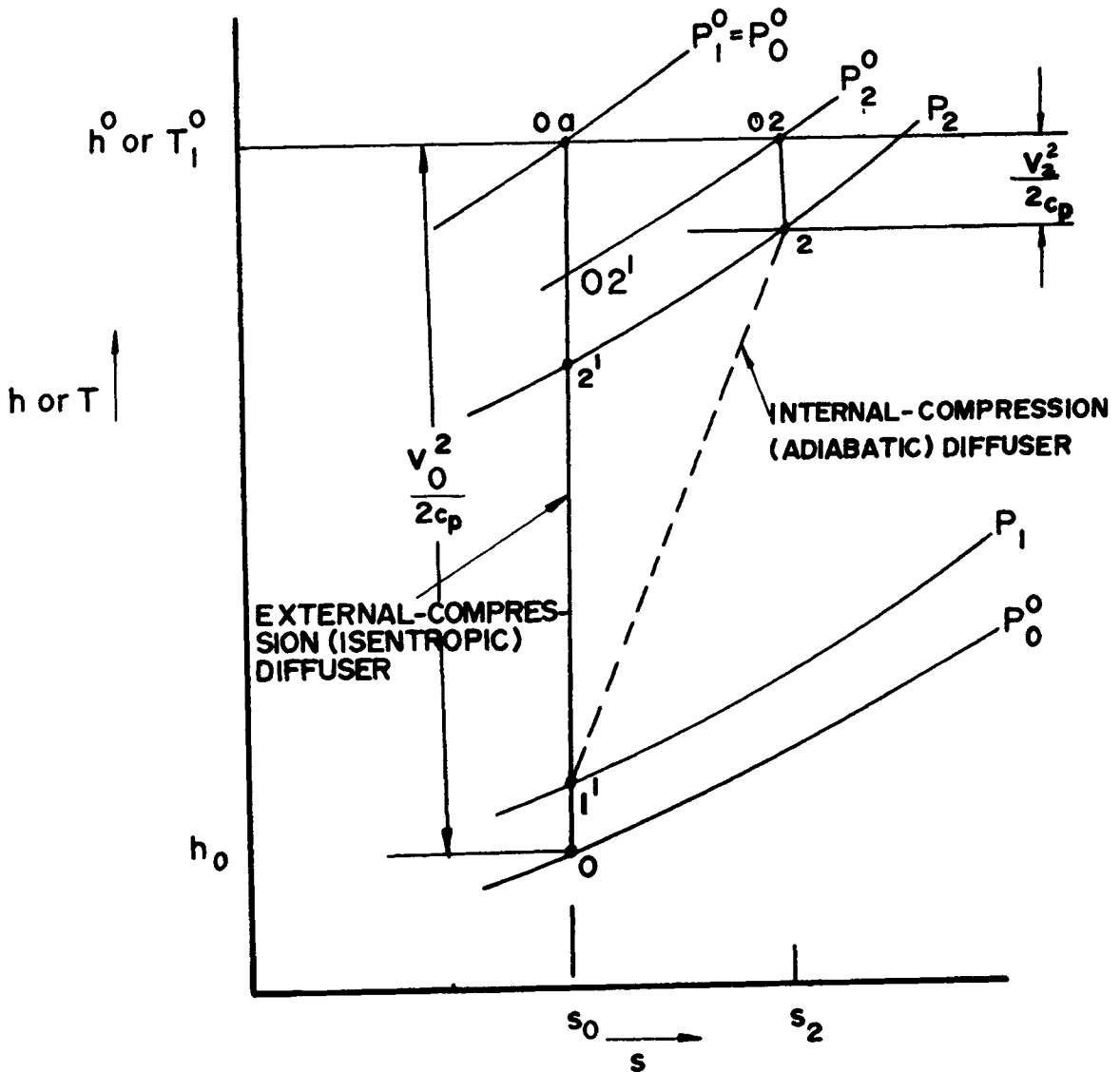
13-3.2 STAGNATION (OR TOTAL) PRESSURE RATIO (r_D)

By definition the stagnation or total pressure ratio is given by

$$r_D = P_2^O/P_0^O \quad (13-8)$$

The stagnation pressure ratio r_D is finding increasing favor as a criterion of diffuser performance for supersonic diffusers and for the overall performance of a supersonic diffuser followed by a subsonic internal-compression diffuser, as in a ramjet engine (see Fig. 12-1). The stagnation pressure ratio r_D and the isentropic diffuser efficiency η_d are related by¹

$$\eta_d = \frac{(T^O/T_0) Z_{rd}}{\left(\frac{\gamma - 1}{2} \right) M_0^2} \quad (13-9)$$

Figure 13-3. Diffusion Processes Plotted on the h - s -plane

where

$$T^0/T_0 = 1 + \left(\frac{\gamma-1}{2} \right) M_0^2 \quad (13-11)$$

$$Z_{rd} = \left(\frac{P_2^0}{P_0^0} \right)^{\frac{\gamma-1}{\gamma}} - 1$$

(13-10)

13-3.3 ENERGY EFFICIENCY OF DIFFUSER (η_{KE})

The energy efficiency η_{KE} is based on comparing the kinetic energy which would be

and

obtained by expanding the diffused air isentropically from state 2 (see Fig. 13-3) to the static pressure P_0 , with that obtainable by expanding the air from the initial stagnation pressure P_0^O to the initial static pressure P_0 . Hence

$$\eta_{KE} = \frac{1 - \left(\frac{P_0}{P_2}\right)^{\frac{\gamma-1}{\gamma}}}{1 - \left(\frac{P_0^O}{P_2}\right)^{\frac{\gamma-1}{\gamma}}} \quad (13-12)$$

By suitable transformations^{1,2}

$$\eta_{KE} = \frac{1 - 2Z_D}{(\gamma-1)M_0^2} \quad (13-13)$$

where

$$Z_D = \left(\frac{P_0^O}{P_2}\right)^{\frac{\gamma-1}{\gamma}} - 1 \quad (13-14)$$

For gases with $\gamma = 1.40$, Eq. 13-14 reduces to

$$\eta_{KE} = 1 - \left(\frac{5}{M_0^2}\right) Z_D \quad (13-15)$$

13-4 SUPERSONIC INLET-DIFFUSERS

All air-breathing engines which propel vehicles at supersonic speeds, except the SCRAM-JET engine (see par. 12-1.1.2), require that the air flow leaving the inlet have subsonic velocity. The design of an efficient supersonic intake is critical because neither the external nor internal compression of a supersonic air stream can be isentropic due to the formation of shock waves (see par. A-10.2.1). The shock waves are accompanied by an increase in the entropy of the flowing air and hence by energy dissipation.

One of the problems in designing a supersonic diffuser is to produce a shock wave pattern which will not cause too large an increase in the entropy of the air. It should be pointed out that in addition to desiring the smallest possible decrease in stagnation pressure (see par. A-5.2.4), the supersonic diffusion should be accomplished with a minimum of external drag. In most cases those two requirements are conflicting, hence a practical design is usually a compromise. Furthermore, the inlet must be capable of operating stably over a range of *angles of attack* and at conditions other than the *design point* with stability, and without serious adverse effects upon either the stagnation pressure recovery or the external drag.

13-4.1.1 NORMAL SHOCK DIFFUSER

From the equations for a normal shock (see par. A-10.3) it is seen that for low supersonic flight Mach numbers a normal shock will give subsonic flow without an excessive loss in stagnation pressure (see par. A-10.3.3). Refer to Fig. 13-4. The maximum static pressure recovery is attained when the normal shock is attached to the inlet; this condition corresponds to the *design point*. When operating at the design point, the *capture area* A_0 for the streamtube of air entering the diffuser has its largest value, and $A_0 = A_1$. Since $V_0 = M_0 a_0$, the mass rate of air induction, at the design point, is

$$\dot{m}_0 = M_0 A_1 \sqrt{\gamma P_0 \rho_0} \quad (13-16)$$

The flow leaving the shock is subsonic and is further compressed in the subsonic internal-compression diffuser downstream from the shock.

If the engine requires a smaller mass rate of air flow than \dot{m}_0 (Eq. 13-16) — due to an increase in back pressure — the excess must be *spilled-over* the lips (leading edges) of the diffuser. To accomplish the spill-over of air, the

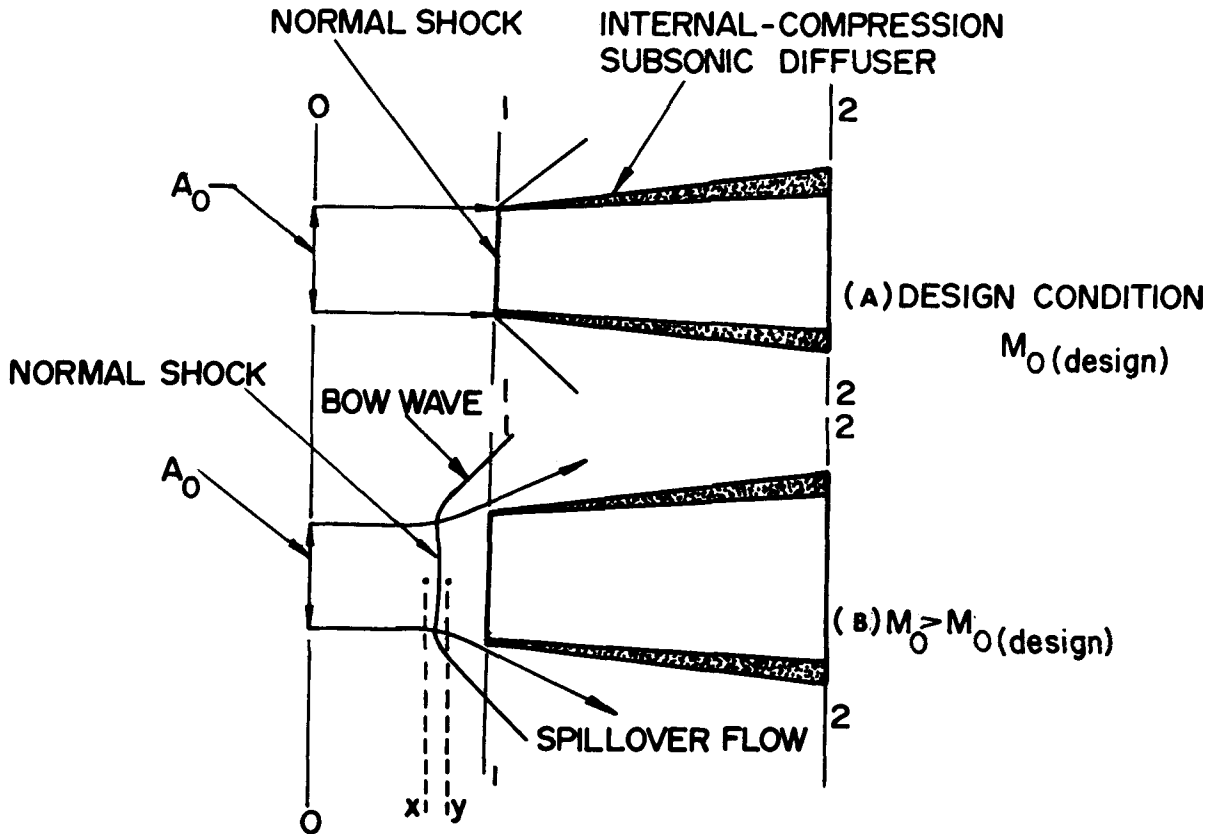


Figure 13-4. Design and Off-Design Operation of the Normal Shock Diffuser

normal shock *detaches* from the diffuser lips, as illustrated in Fig. 13-4(B), and a *bow wave* forms upstream from the intake. One may assume that the portion of the bow wave immediately in front of the inlet is a normal shock, and the conditions in front of and behind the bow wave may be computed by means of the equations for a normal shock (see par. A-10.3.3).

If the back pressure in the outlet section of the diffuser is decreased, the air flow rate into the diffuser increases and the shock wave is *swallowed*, i.e., the shock locates itself inside the diffuser.

13-4.1.2 RAM PRESSURE RATIO FOR A NORMAL SHOCK DIFFUSER

The *ram pressure ratio* for the type of normal shock diffuser illustrated in Fig. 13-3 is defined as the ratio of the stagnation pressure P_0^2 (Station 2) to the static pressure of the free-stream air P_0 . Let η_d be the isentropic efficiency of the subsonic internal-compression diffuser (1-2), then from Eq. 13-7

$$\frac{P_2^O}{P_0} = \left[1 + \eta_d \left(\frac{\gamma-1}{2} \right) M_1^2 \right]^{\frac{\gamma}{\gamma-1}} \quad (13-17)$$

Hence, the ram pressure ratio P_2^O / P_0 is given by

$$\frac{P_2^O}{P_0} = \left(\frac{\gamma-1}{\gamma+1} \right)^{\frac{\gamma}{\gamma-1}} \frac{\left[\left(\frac{2\gamma}{\gamma-1} M_0^2 - 1 \right) + \eta_d \left(1 + \frac{\gamma-1}{2} M_0^2 \right) \right]^{\frac{\gamma}{\gamma-1}}}{\left[\frac{2\gamma}{\gamma-1} M_0^2 - 1 \right]^{\frac{1}{\gamma-1}}} \quad (13-18)$$

The values of P_2^O / P_0 obtained from Eq. 13-18 are larger than those obtainable with an actual normal shock diffuser because of boundary layer effects and wall friction⁸.

The normal shock diffuser is suitable for supersonic Mach numbers less than $M_0 \approx 1.85$. When $M_0 > 1.85$, the ram pressure ratio P_2^O / P_0 decreases rapidly from that for the corresponding isentropic diffusion (see Eq. A-112).

13-4.2 THE REVERSED DE LAVAL NOZZLE SUPERSONIC DIFFUSER

It would be natural to expect that reversing the flow of air through a converging-diverging nozzle, a device for obtaining large supersonic exhaust velocities with high efficiency (see par. 4-5.1), would achieve an efficient supersonic internal compression of the reversed supersonic air flow. Unfortunately, it is practically impossible to achieve shockless diffusion with such a device due to the interactions of the boundary layer and the positive pressure gradient. Furthermore, the presence of shock waves in the converging-diverging passage causes a large increase in the entropy of the air so that the main stream flow is no longer isentropic. Even if it were possible to design a converging-diverging flow passage to achieve a substantially isentropic diffusion at the *design point*, its poor off-design operating characteristics would make it impractical^{1,2}. A fixed-geometry converging-diverging passage having an inlet area A_i and a throat area A_t could give isentropic diffusion

because of its fixed *contraction ratio* A_i / A_t at only one operating point, namely the design point. Furthermore, the *starting* of such a diffuser, as explained in References 1 and 2, presents a critical problem.

13-4.3 EXTERNAL COMPRESSION SUPERSONIC DIFFUSERS

It was pointed out by K. Ostwatitsch that the large decrease in stagnation pressure behind a normal shock could be reduced by decelerating the free-stream air by means of one or more oblique shocks, followed by a *weak* normal shock⁷. By the employment of this principle, an efficient external compression of the air is achievable before the air flows into a subsonic internal-compression diffuser (see par. 13-2.2).

Fig. 13-5 illustrates schematically the essential features of a conical shock supersonic diffuser employing the aforementioned external compression principle. A central body, or *conical spike*, is placed inside an efficient subsonic internal-compression diffuser, so that the system is *axisymmetrical*. The conical nose protrudes through the inlet section of the subsonic diffuser into the free-stream.

When a supersonic flow impinges upon the cone, a conical shock is produced (see par. A-12), as illustrated in Fig. 13-5. The compressed air leaving the conical shock then enters the subsonic internal-compression diffuser through the annular opening formed between the surface of the *central body* and the *housing* of the subsonic diffuser. Theoretically, a *weak normal shock* BB is formed at the lip of the subsonic diffuser, and the air enters that diffuser with a subsonic velocity.

It is evident from Fig. 13-5 that the conical central body deflects the supersonic airstream from its initial flow direction so that the weak normal shock is perpendicular to the direction

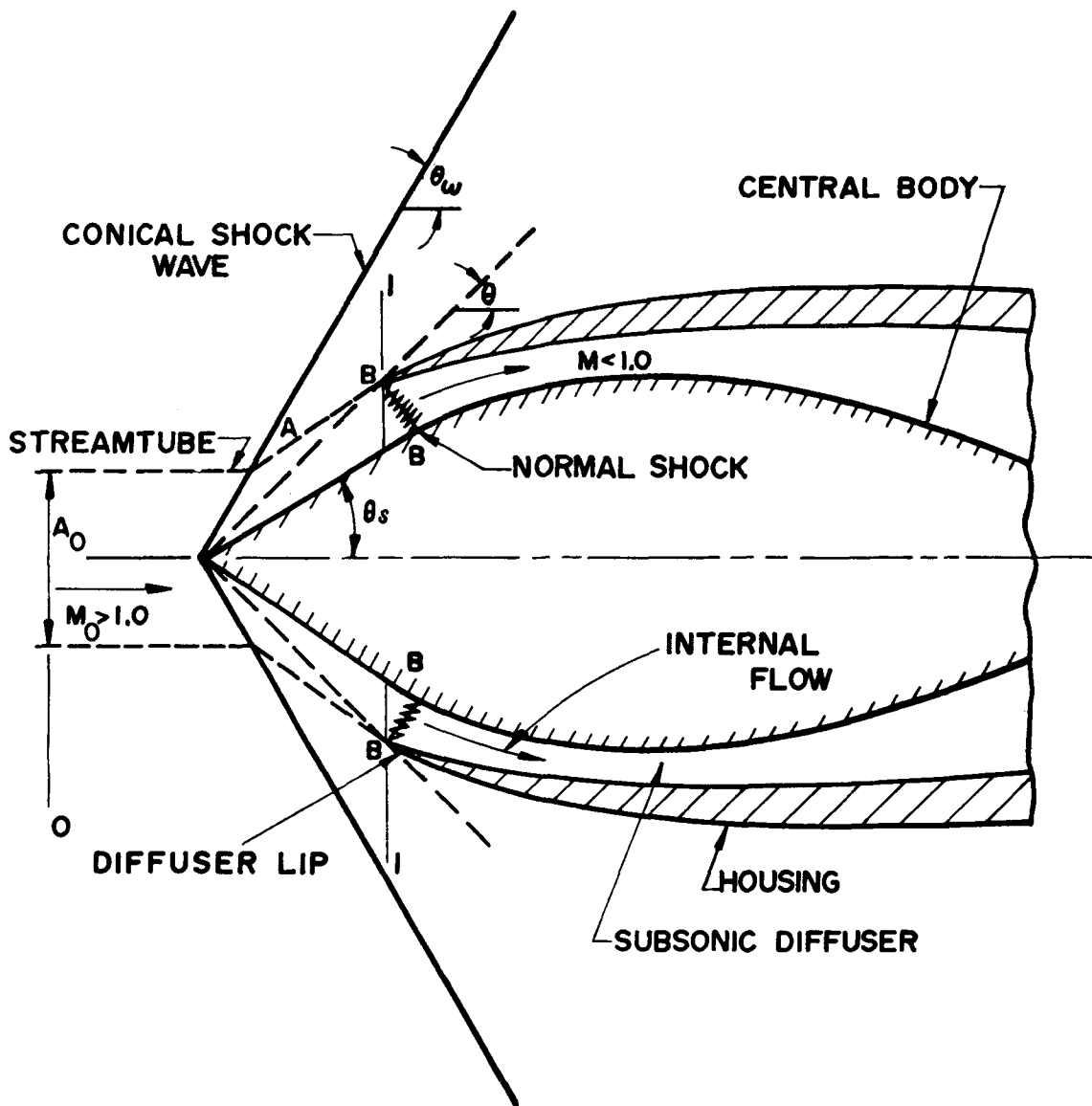


Figure 13-5. Schematic Diagram of a Conical Shock (Oswatitsch type) Supersonic Diffuser

of the stream-lines at the inlet to the subsonic diffuser, and not to the direction of the free-stream air. The supersonic diffusion is accomplished externally before the air enters the subsonic diffuser, and the capture area A_0 for the streamtube entering the diffuser has a radius, assuming circular cross-section throughout, equal to that of the inlet to subsonic diffuser passage. The annular flow area for the *internal*

flow is smaller the A_0 ; the external compression achieved by the conical shock is, therefore, quite strong.

The position of the normal shock with respect to the inlet has a profound influence upon the performance of the diffusion system. If the normal shock occurs near the throat of a converging-diverging section downstream from

the inlet section, the problem of unstable operation encountered with a converging-diverging internal-compression diffuser is also encountered with a spike-type diffuser.

To eliminate the aforementioned instability problem, A. Ferri developed an inlet design employing a conical central body but the housing of the subsonic diffuser is designed so that the annular flow passage beyond the inlet forms an entirely diverging flow channel¹⁰.

If there is a change in the back pressure of the outlet of the diffusion system, due to either increasing fuel flow rate to the engine or decreasing the exit area of the exhaust nozzle, the normal shock may be forced out in front of the diffuser lips with the result that air will "spill" over the diffuser lips. As a result there will be an alteration of the flow pattern entering the subsonic diffuser. There is also a distortion of the conical shock wave pattern.

13-4.4 OPERATING MODES FOR EXTERNAL SHOCK DIFFUSERS

There are three distinct operating conditions under which the supersonic diffusion system for an air-breathing engine can operate. Refer to Fig. 13-6.

13-4.4.1 CRITICAL OPERATION

When the normal shock is positioned at the diffuser lip, as illustrated in Fig. 13-6(A), the operation is said to be *critical*, and that condition usually corresponds to the design point operation.

13-4.4.2 SUPERCRITICAL OPERATION

This type of operation is illustrated in Fig. 13-6(B). It occurs when the exit pressure P_2 , in the subsonic internal-compression diffuser, is too low for keeping the normal shock at the lip of the inlet. Consequently, the air flows into the

subsonic diffuser when a supersonic speed, and the excess energy is dissipated by the formation of a strong shock wave in the diverging portion of the subsonic diffuser.

13-4.4.3 SUBCRITICAL OPERATION

If the exit pressure from the subsonic diffuser P_2 exceeds the static pressure which can be accomplished by the diffusion system, the normal shock is expelled from the diffuser and moves upstream toward the vertex of the conical center body, as illustrated in Fig. 13-6(C). Behind the normal shock the flow is subsonic and, because the normal shock is detached from the intake lips, there is *spillover* of the incoming air over the diffuser cowling, thus the external drag is increased.

In general, the position of the normal shock with reference to the inlet and the amount of *spillover* air for the diffusion system of an air-breathing engine depends upon the flight Mach number, the fuel-air ratio, the combustion efficiency, and the area of the nozzle exit cross-section A_e .

13-5 DIFFUSER PERFORMANCE CHARACTERISTICS AND DESIGN CONSIDERATIONS

Up to this point the maximum recovery of stagnation pressure, at zero angle of attack, has been emphasized as a performance criterion. Inlet diffusers for air-breathing jet engines must, however, give satisfactory performance over the anticipated range of angles of attack. Experience has demonstrated that the *conical spike* type of diffuser (see par. 13-4.3) has satisfactory characteristics with regard to variations in the angle of attack. Ordinarily, a decrease of 20 percent in stagnation pressure recovery results at an angle of attack of 5° .

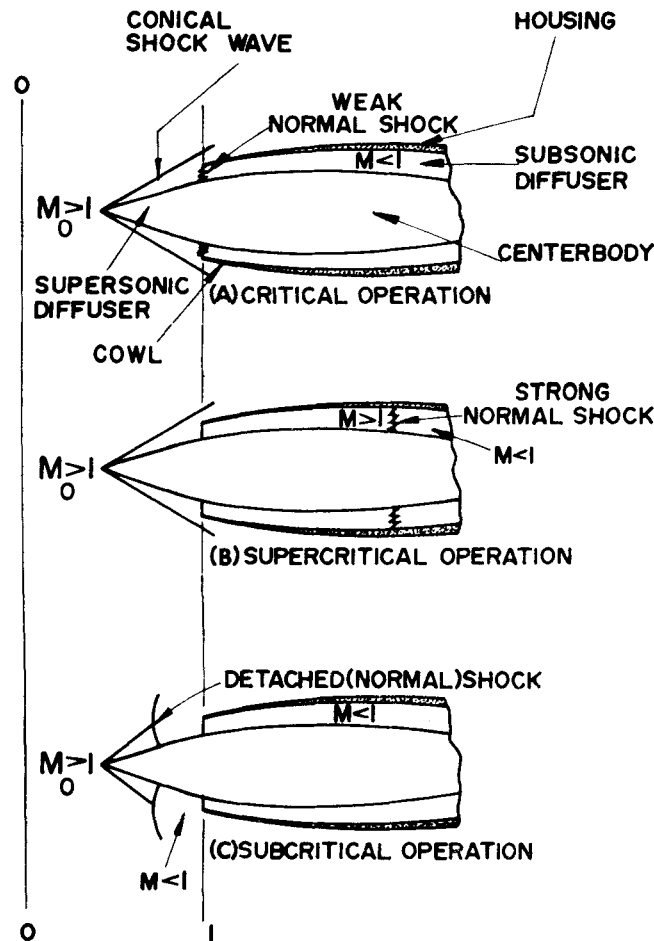


Figure 13-6. Three Principal Operating Modes for Supersonic External Compression Diffusers

Another factor to be considered is the *external drag* of the diffusion system. A conical-spike diffuser introduces a *drag component* known as *additive drag* which arises from the pressure forces acting on the streamtube AAB \bar{B} ; these give rise to a *net force* acting in the flight direction in the relative coordinate system. By positioning the conical shock at the lip of the inlet the additive drag may be eliminated with only a small decrease in the stagnation pressure recovery. The longer the distance between the conical shock wave and the inlet lip, the larger the additive drag.

It is not possible, if the diffuser has a fixed geometry, for the conical shock to be at the

diffuser lip under all operating conditions. For this reason, some diffusers have a movable central body for varying the area of the inlet so that the conical shock is always positioned at the diffuser lip.

In general, high pressure recoveries with a conical-spike diffuser are accompanied by large external drag, and vice versa. In addition to the additive drag, the external drag is high because the large cowl angles employed may induce flow separation on the exterior housing. By careful aerodynamic design, however, the external drag may be kept at tolerable values.

Larger stagnation pressure recoveries are obtainable if several successive weak shocks are utilized for decelerating the air instead of one or two relatively strong conical shocks. To increase the number of shocks, several “breaks” are made on the projecting cone, as illustrated schematically in Fig. 13-7. In the extreme case the spike configuration should be a curved surface giving an infinite number of infinitely weak shocks, i.e., Mach waves (see par. A-10.1). In theory, such a surface would achieve *shockless* deceleration of a supersonic flow to a *sonic* velocity, i.e., the compression would be *isentropic*. A spike of this configuration is termed an *isentropic spike*. Unfortunately, an isentropic spike is satisfactory for only one flight Mach number and is sensitive to changes in the angle of attack. Furthermore, at high flight Mach numbers the flow has to be turned through large angles to enter the subsonic internal-compression diffuser, which can increase the additive drag to prohibitive values and may also affect the pattern of the flow into the subsonic diffuser.

In general, the losses encountered with a conical-spike diffuser system may be grouped

into two classes: (1) those pertinent to the external shock compression in the supersonic inlet, and (2) losses due to wall friction and separation phenomena in the subsonic internal-compression diffuser. It is desirable for the normal shock in front of the inlet to be weak, in order to reduce the tendency for the flow to separate as it flows in the direction of a positive pressure gradient, in the subsonic diffuser.

It appears that a conical-spike diffuser for air-breathing engines for propelling vehicles at Mach numbers up to $M_0 = 2.0$ need have only a single conical shock. For flight Mach numbers above $M_0 = 2.0$, two or more conical shocks may be needed for achieving the desired stagnation pressure recovery. Increasing the number of conical shocks makes the diffusion system more sensitive to changes in the flight Mach number and in the angle of attack. It appears that two conical shocks are sufficient for a design flight Mach number of approximately $M_0 = 2.75$.

Fig. 13-8 presents the total pressure recovery ratio P_2^0/P_0^0 as a function of the free-stream Mach number M_0 for several types of supersonic diffusers¹.

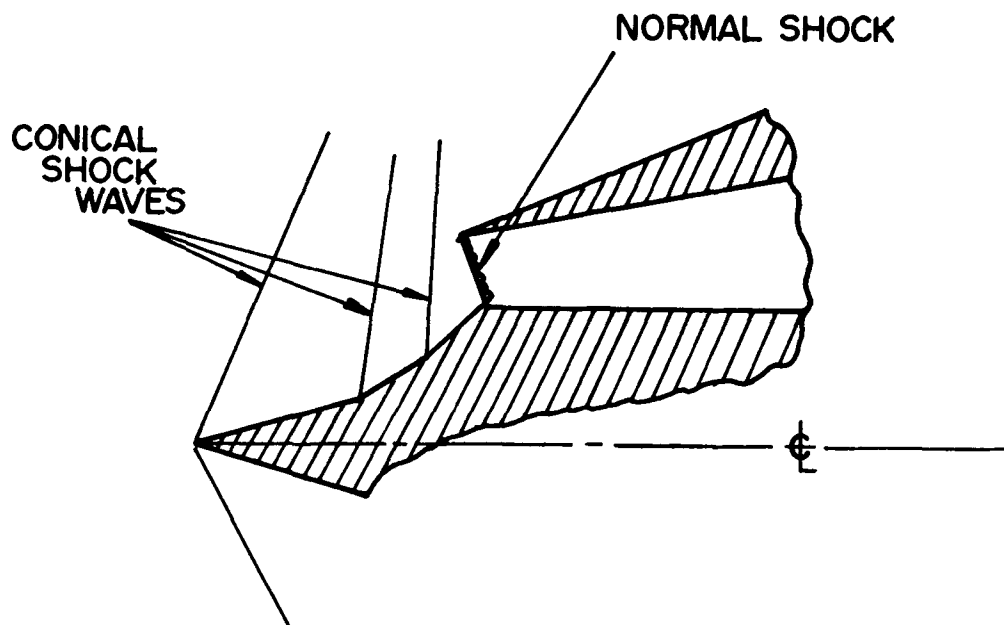


Figure 13-7. Multiple Conical Shock Supersonic Diffusion System

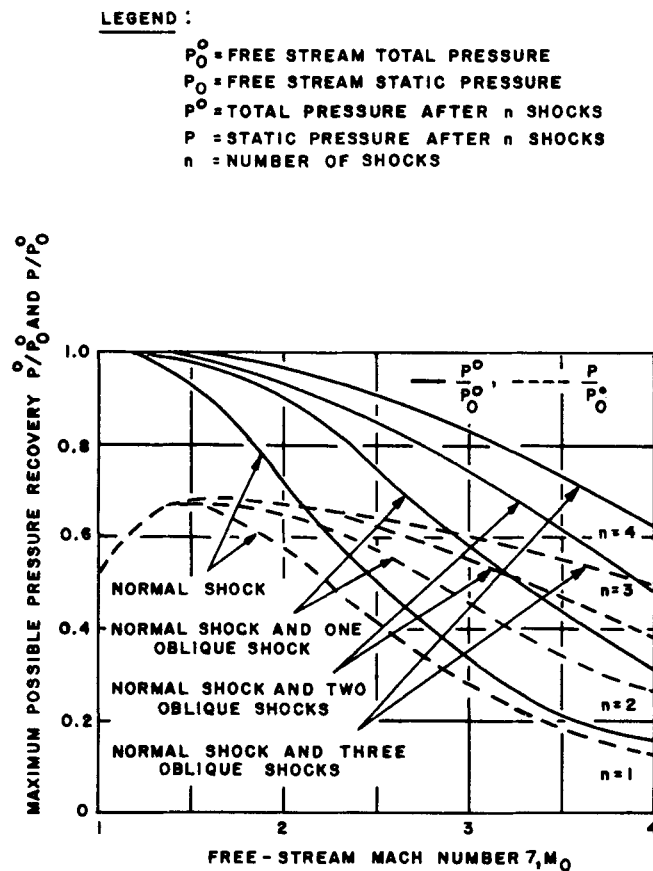


Figure 13-8. Total and Static Pressure Ratios As a Function of the Free-Stream Mach Number for Supersonic Diffusers With Different Numbers of Shocks

REFERENCES

1. M. J. Zucrow, *Aircraft and Missile Propulsion*, John Wiley and Sons, Inc., Vol. 1, 1958, Chapter 5.
2. E. A. Bonney, M. J. Zucrow and C. W. Besserer, "Aerodynamics, Propulsion, and Structures," *Principles of Guided Missile Design*, Editor, G. Merrill, D. Van Nostrand Company, Inc., 1956, Chapter 5.
3. H. Schlichting, *Boundary Layer Theory*, (Translated by J. Kestin), McGraw-Hill Book Company, Inc., 1955.
4. D. Kuchermann and J. Weber, *Aerodynamics of Propulsion*, McGraw-Hill Book Company, Inc., 1953, Chapters 4 and 9.
5. J. V. Foa, *Elements of Flight Propulsion*, John Wiley and Sons, Inc., 1960, Chapter 8.
6. R. Hermann, *Supersonic Diffusers and Introduction to Internal Aerodynamics*, Minneapolis-Honeywell Regulator Co., Aeronautic Division, Minneapolis, Minn.
7. K. Ostwatitsch, *The Efficiency of Shock Diffusers*, FEH Report No. 1005, Trans., NACA TM 1140, 1947.
8. J. D. Stanitz, "Note on the Simple Ram-Intake Preceded by Normal Shock in Supersonic Flight," *Jour. IAS*, Vol. 15, No. 3, March 1948.
9. A. Ferri and L. Nucci, *Preliminary Investigation of a New Type of Supersonic Inlet*, NACA TN 2286, April 1951.
10. A. Ferri, *Elements of Aerodynamics of Supersonic Flows*, The McMillan Company, 1949.
11. De M. Wyatt, "Aerodynamic Forces Associated with Inlets of Turbojet Installations," *Aero. Eng. Rev.*, Vol. 10, No. 10, October 1951, p. 20.

CHAPTER 14

PROPULSIVE DUCT ENGINES

14-1 INTRODUCTION

The essential features of the propulsive duct engines, the ramjet and SCRAMJET engines, are presented in par. 12-1, and the thrust equations for the ramjet engine together with the pertinent thrust coefficients are presented in par. 12-4. The purpose of this chapter is to discuss some of the performance parameters of propulsive duct engines and their performance characteristics.

Fig. 14-1 illustrates the essential features of a ramjet engine for propelling a vehicle at supersonic flight speeds.

14-2 THRUST DEVELOPED BY A PROPULSIVE DUCT ENGINE

Fig. 14-2 illustrates schematically a rotationally symmetrical duct which is stationary in a supersonic flow of air. Assume that no heat is added to the *internal flow*, that a relative coordinate system is employed, and that the flow is one-dimensional and steady (see Chapter 3).

14-2.1 COLD FLOW THROUGH SHAPED DUCT

Because of external and internal compression of the air between Stations 0 and 2, the static pressure $P_2 > P_0$. If no provision is made in designing the duct for supporting the increased static pressure achieved by diffusion, the static pressure P_2 of the internal flow will rapidly decrease to P_0 as the air flows through the duct and no gross thrust will be developed. However, if provisions are incorporated inside the duct that enable maintaining a higher pressure inside the duct than the external pressure acting on the external surfaces of the duct, and

if an area is provided upon which the internal pressure can act in the direction of u_x , then a net axial forward force will be produced, i.e., a thrust F will be produced.

Thus

$$F = \int_1^7 (P_i - P_o) dS \quad (14-1)$$

where

P_i = internal static pressure

P_o = external (atmospheric) static pressure

S = surface wetted by the air flow

14-2.2 METHODS FOR SUPPORTING A STATIC PRESSURE HIGHER THAN THE EXTERNAL STATIC PRESSURE INSIDE A DUCT

There are basically two methods for supporting a static pressure $P_2 > P_0$ inside a duct through which there is a flow of atmospheric air.

1. Restricting the exit area so that $A_7 > A_1$.
2. Heat addition to the flowing air.

14-2.2.1 RESTRICTION OF THE EXIT AREA

Fig. 14-3 illustrates schematically the effect of reducing the exit area A_7 for a duct passing a cold flow of air.

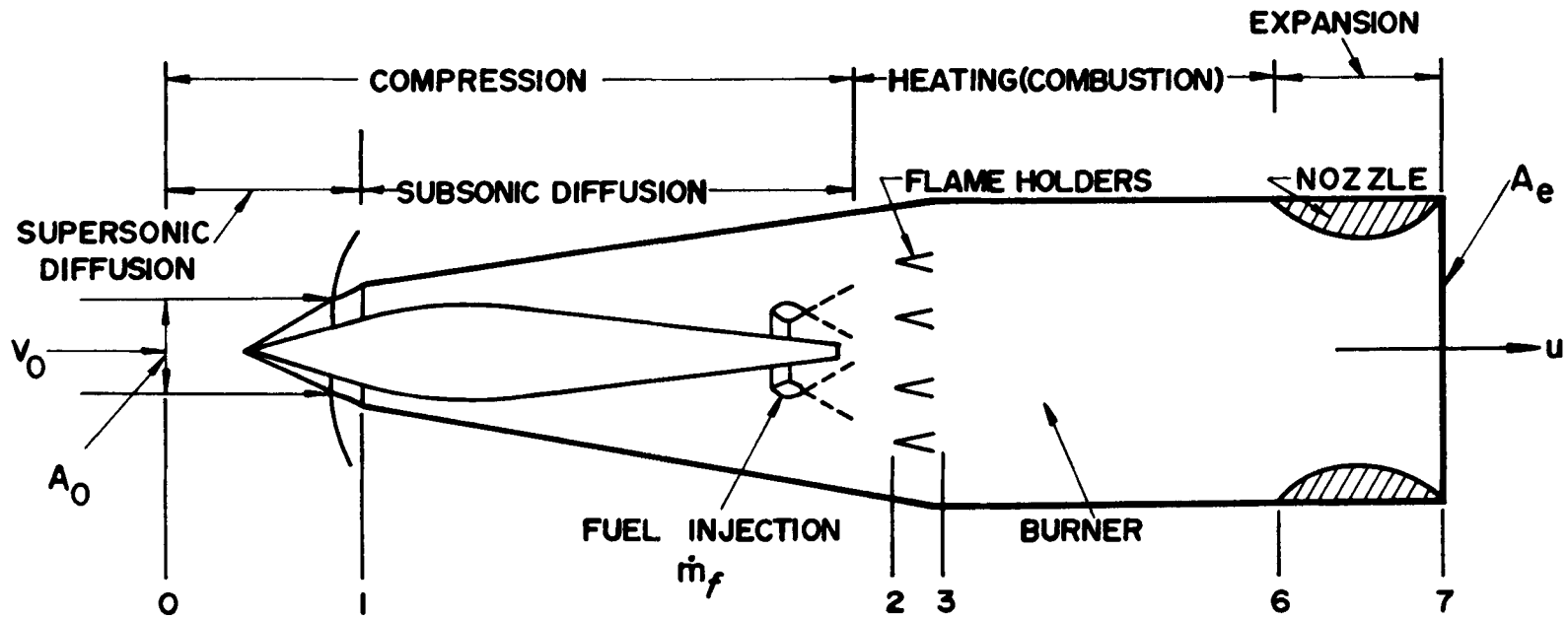


Figure 14-1. Schematic Arrangement of an Axially Symmetric Ramjet Engine for Supersonic Flight

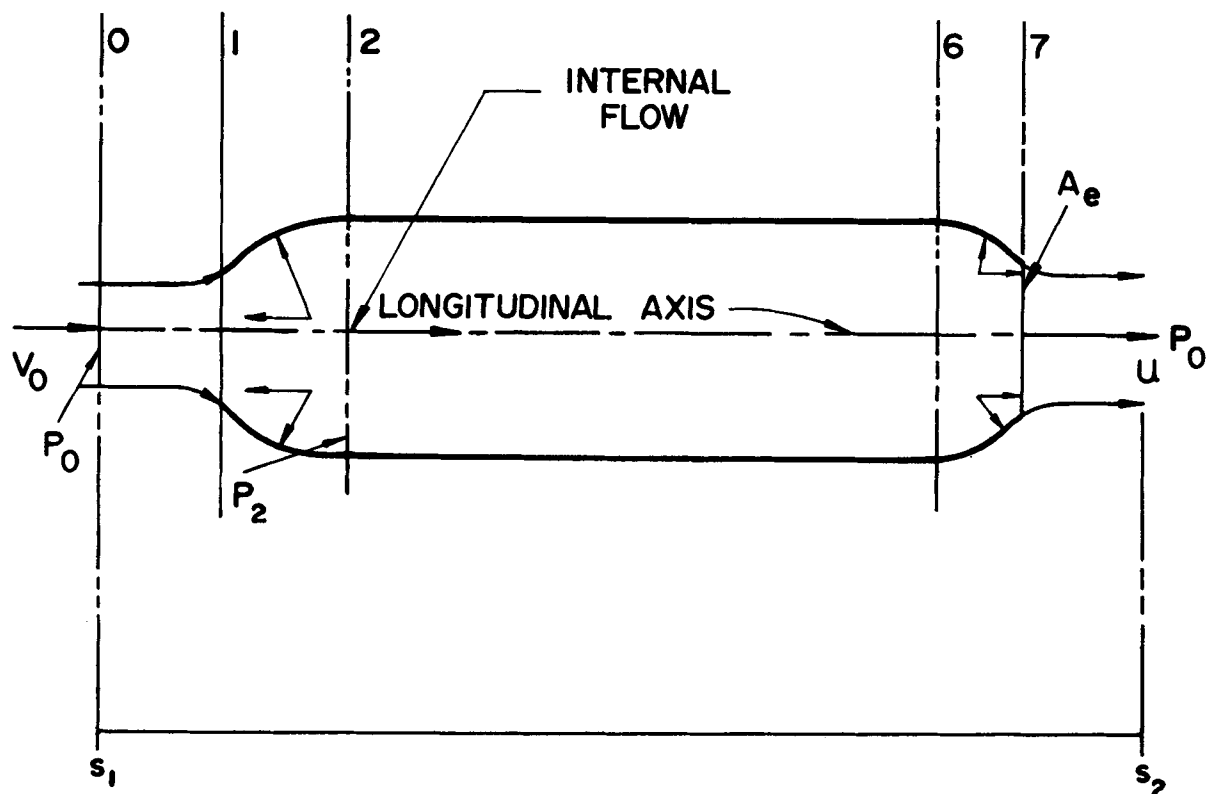


Figure 14-2. Flow of Cold Air Through a Shaped Duct

Fig. 14-3(A) illustrates the condition where the exit area of the duct has no restriction, and a static pressure in the duct higher than the external static pressure cannot be supported.

Let some form of nozzle be installed between Stations 6 and 7, so that $A_7 < A_1$, as illustrated in Fig. 14-3(B). Assume that the air approaches the duct with a free-stream Mach number $M_0 > 1.0$, and that a normal shock is formed in the entrance section A_1 . Suppose now that the exit area A_7 is reduced gradually, all other conditions remaining unaltered, and that the flow downstream from the normal shock is *isentropic*.

Decreasing A_7 causes the static pressure inside the duct to increase until the area $A_7 = A^* = \text{the critical area}$ (see par. A-6.3). When that condition is attained $M_7 = 1$, and

$u_7 = a^* = \text{critical acoustic speed}$ (see par. A-6.1.1). The stagnation pressure at Station 6, P_6^0 , is such that

$$\frac{P_7}{P_6^0} = \frac{P_0}{P_6^0} = \frac{P^*}{P_6^0} = \text{critical expansion ratio}$$

From Eq. A-141

$$\frac{P^*}{P_6^0} = \left(\frac{2}{\gamma+1} \right)^{\frac{\gamma}{\gamma-1}} \quad (14-2)$$

For air, $\gamma = 1.4$, and $P_6^0/P_7 \approx 1.8$.

If A_7 is decreased further so that $A_7 < A^*$ – illustrated in Fig. 14-3(C) – the pressures P_6^0 and P_7 increase, M_7 remains constant at the value $M_7 = 1.0$ (see par. 4-3.3),

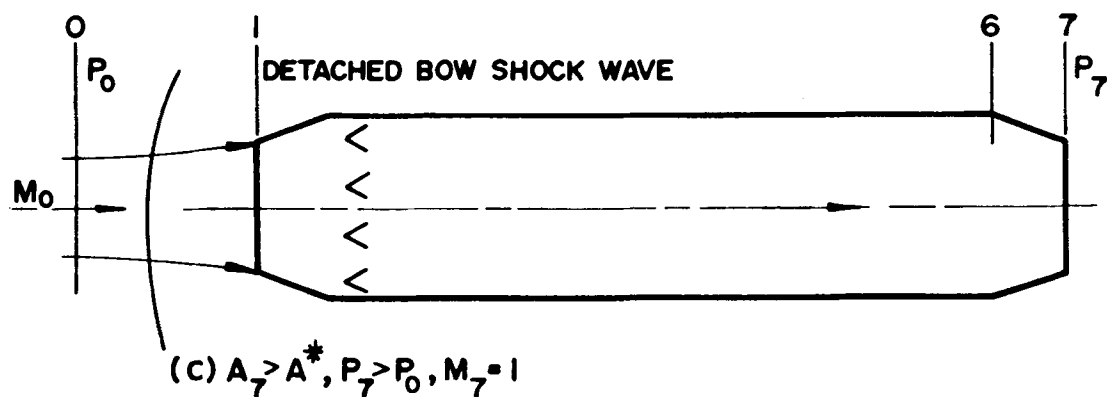
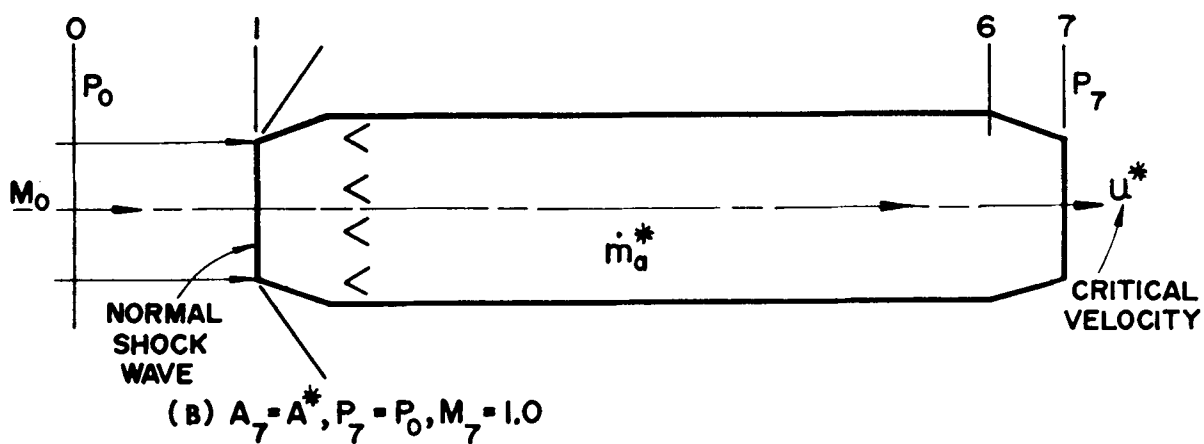
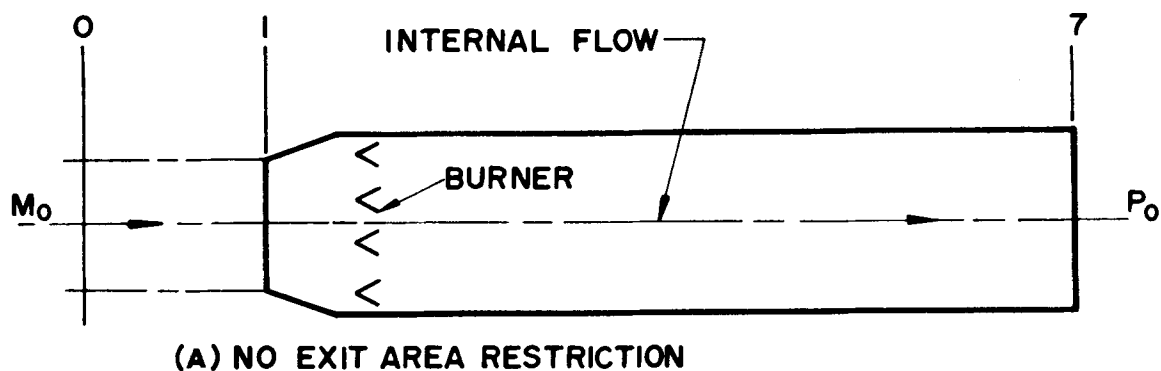


Figure 14-3. Effect of Varying the Exit Area of a Shaped Duct Passing an Internal Flow of Cold Air

the duct operates with *choked flow*, and the expansion of the air from $P_7 > P_0$ to P_0 takes place in the surroundings beyond A_7 .

When choking occurs, a *detached bow shock wave* is formed upstream from the inlet section A_1 and air is "*spilled over*" the lips of the inlet. Further reductions in A_7 cause the detached shock to move further and further upstream and the amount of air "*spilled over*" the inlet lips is increased, accordingly. A point is finally reached where the flow is completely *blocked*, i.e., the static pressure inside the duct becomes equal to that downstream from a normal shock having an inlet Mach number equal to the free-stream Mach number M_0 . Under the blocked condition no gross thrust can be developed because the interior projected area of the diffuser, which produces the forward force, is exactly equal to that of the exhaust nozzle which produces an equal backward force.

14-2.2.2 HEAT ADDITION TO THE INTERNAL FLOW

A high static pressure can be supported in a shaped duct by adding heat to the compressed internal flow by burning a fuel with the compressed (diffused) air. Heating the air causes a large increase in its specific volume and, because the dimensions of the duct (ramjet engine) are fixed, the volumetric rate of flow increases so that the internal flow must be accelerated away from the heat addition region. The geometrical configuration of the duct combined with the high static pressure of the diffused air entering the burner (see Figs. 14-1 and 14-3) causes the air to be accelerated toward the exit section A_7 . The corresponding reaction force supports the high static pressure (due to diffusion) acting on the forward portion of the duct. Increasing the heat addition, by increasing the fuel consumption, raises the acceleration of the internal flow and consequently the gross thrust. The maximum amount of heat that can be added to the internal flow is limited by the calorific value of

the fuel and the efficiency of the burner. Ordinarily, the maximum heat release is obtained when the fuel-air ratio f (where $f = \dot{m}_f/\dot{m}_a$) is slightly richer in fuel than the stoichiometric ratio; for the conventional liquid hydrocarbon fuels, such as jet engine fuels, the stoichiometric fuel-air ratio is close to $f = 0.067$. The maximum value of the static pressure which can be attained by the air entering the burner section of a ramjet engine depends, of course, upon the free-stream Mach number M_0 and the overall effectiveness of the diffusion process (supersonic and subsonic).

Fig. 14-4 illustrates diagrammatically the variation in the static pressure and velocity inside a ramjet engine equipped with a spike-type supersonic diffuser; the curves apply to a flight Mach number of $M_0 = 2.0$.

14-3 DEFINITIONS OF TERMS EMPLOYED IN RAMJET ENGINE TECHNOLOGY

Fig. 14-1 illustrates schematically a static rotationally symmetrical ramjet engine immersed in a uniform supersonic flow of atmospheric air. As before, a relative coordinate system is employed, and in that coordinate system an axial force acting in the *forward direction* (i.e., opposite to V_0) is called a *thrust*, and a force acting in the *backward direction* (i.e., in the same direction as V_0) is termed a *drag*.

14-3.1 GROSS THRUST (F_g)

For a one-dimensional flow the *impulse function* F is given by Eq. A-56. Thus

$$F = \dot{m}u + PA \quad (14-3)$$

where u denotes the velocity of the gas parallel to the x-axis.

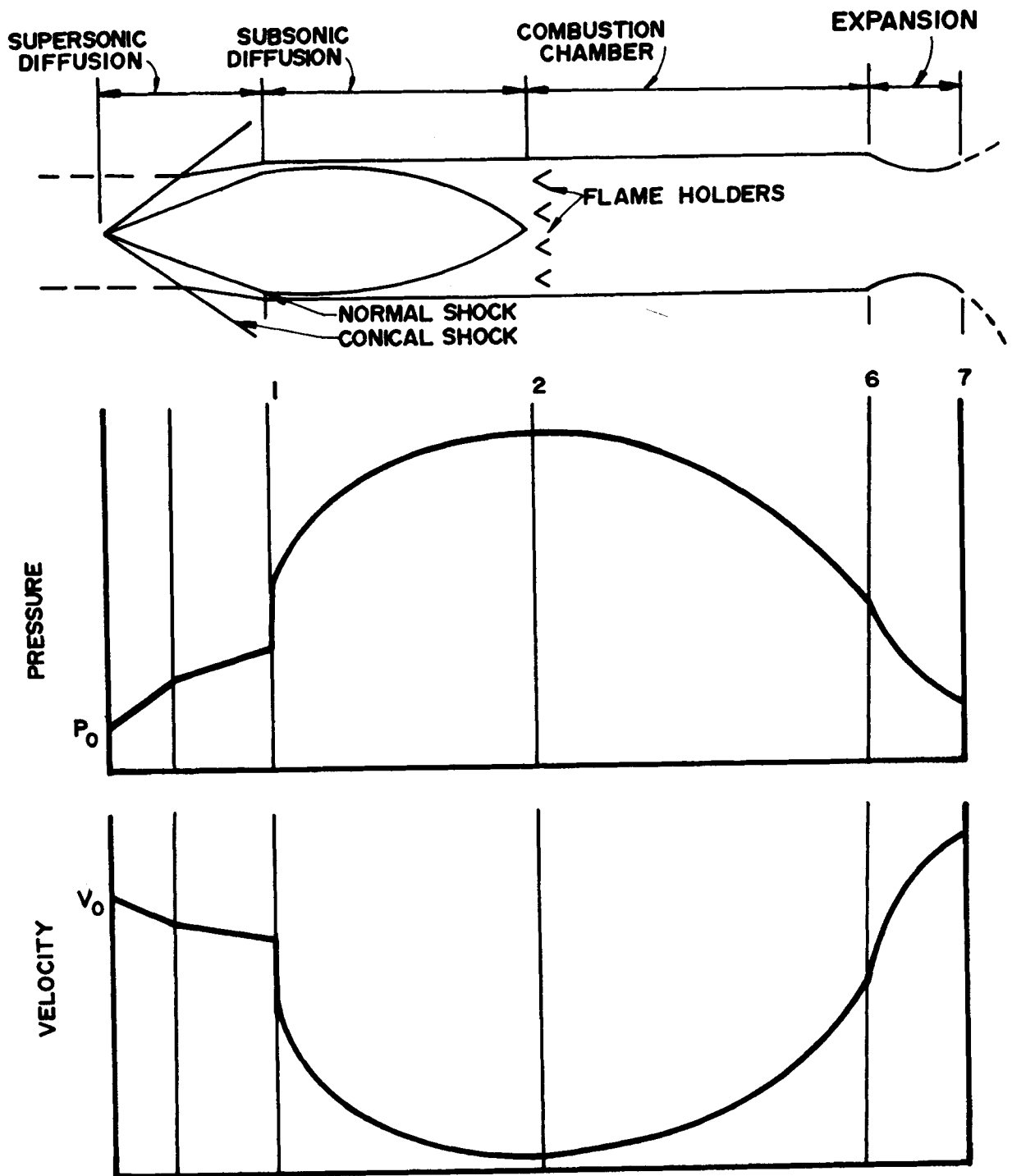


Figure 14-4. Variation in the Static Pressure and Gas Velocity Inside a Ramjet Engine ($M_0 = 2.0$)

By convention, the gross thrust of a ramjet engine, denoted by F_g , is defined by

$$F_g = F_7 - F_0 - P_0 (A_7 - A_0) \quad (14-4)$$

Eq. 14-2 can be transformed to yield^{1,2}

$$F_g = m_7 u_7 - m_0 V_0 + A_7 (P_7 - P_0) \quad (14-5)$$

For the one-dimensional flow of a perfect gas the impulse function in terms of the local Mach number M_1 is given by Eq. A-157. Thus

$$F = PA(1 + \gamma M^2) \quad (14-6)$$

Hence, the gross thrust equation can be written in the form

$$F_g = P_7 A_7 (1 + \gamma_7 M_7^2) - (P_0 A_0 \gamma_0 M_0^2 + P_0 A_7) \quad (14-7)$$

Eq. 14-5 shows that for a given engine configuration operating at a fixed altitude ($P_0 = \text{constant}$) the gross thrust F_g depends upon M_0^2 .

14-3.2 EXTERNAL DRAG (D_e)

The external drag D_e comprises the *skin friction drag* D_f , the *pressure drag* D_p , and the *additive drag* D_a ; as mentioned in par. 13-5, the drag D_a arises from the change in the momentum of the fluid in the diverging streamtube external to the engine (see Fig. 13-1). The external drag D_e is given by

$$D_e = \int_{A_0}^{A_7} \left[(P_e - P_0) + \tau_e \right] dA \quad (14-8)$$

Eq. 14-8 represents the summation of the axial components of the external pressure P_e

and shear forces τ_e acting on the outer surface of the ramjet engine and the streamtube *bounding* the airflow into the engine.

In general, operating a supersonic ramjet engine at *off-design* flight speeds produces similar effects irrespective of the type of inlet. If $M_0 < M_{0d}$, where M_{0d} is the *design flight Mach number*, the drag coefficient C_D and the pressure recovery P_2^0/P_0^0 both increase. On the other hand if $M_0 > M_{0d}$ the reverse effects occur. The variation in C_D is due primarily to changes in the pressure and additive drag coefficients. The additive drag increases with the amount of air "*spilled over*" the intake lips.

14-3.3 NET THRUST (F_n)

By definition

$$F_n = F_g - D_e \quad (14-9)$$

14-3.4 EFFECTIVE JET (OR EXHAUST) VELOCITY (V_j)

Let V_j denote the *effective jet velocity*, also called the *effective exhaust velocity* (see par. 2-2.1), then

$$F_g = \dot{m}_7 V_j - \dot{m}_0 V_0 \quad (14-10)$$

where

$$V_j = u_7 + \frac{A_7}{\dot{m}_7} (P_7 - P_0) \quad (14-11)$$

If the exhaust nozzle operates with complete expansion, then $P_7 = P_0$ and $V_j = u_7$.

It can be shown that if $f = \dot{m}_f/\dot{m}_a =$ the *fuel-air ratio* and $M_j = V_j/A_7 =$ the *effective jet Mach number*, then¹

$$M_j = \frac{V_j}{A_7} = M_7 \left[1 + \frac{1}{\gamma_7 M_7^2} \left(1 - \frac{P_0}{P_7} \right) \right] \quad (14-12)$$

and the gross thrust F_g is given by

$$F_g = A_0 \gamma_0 M_0^2 \left[(1+f) \frac{M_j}{M_0} \sqrt{\frac{\gamma_7 T_7}{\gamma_0 T_0}} - 1 \right] \quad (14-13)$$

14-3.5 NET THRUST COEFFICIENT (C_{Fn})

By definition, the *net thrust coefficient* C_{Fn} is given by

$$C_{Fn} = \frac{F_n}{q_0 A_m} = \frac{F_g - D_e}{\frac{1}{2} \rho_0 V_0^2 A_m} \quad (14-14)$$

Since $a_0^2 = \gamma_0 P_0 / \rho_0$ = the acoustic speed for the free stream, Eq. 14-14 can be expressed in terms of the free-stream Mach number $M_0 = V_0 / a_0$. Thus

$$C_{Fn} = \frac{2(F_g - D_e)}{P_0 A_m \gamma_0 M_0^2} \quad (14-15)$$

where $\gamma_0 = c_p / c_v$ = specific heat ratio for the free-stream air.

Fig. 14-2 presents C_{Fn} as a function of the flight Mach number for three fixed-geometry ramjet engines and one variable-geometry engine. The design Mach numbers for the three fixed-geometry engines are 1.5, 2.3, and 3.5, respectively³. The calculations apply to nacelle-type engines, and the net thrust is the net force transmitted to the strut supporting the engine. The calculations assumed a combustion efficiency $\eta_B = 0.9$, and that the diffuser pressure recovery characteristics were those indicated on the upper left-hand corner of Fig. 14-5.

14-3.6 GROSS THRUST COEFFICIENT (C_{Fg})

The gross thrust coefficient C_{Fg} for a ramjet engine is defined by Eq. 12-9, which can be transformed to read¹

$$C_{Fg} = \frac{F_g}{\frac{1}{2} \rho_0 V_0^2 A_m} = \frac{2F_g}{P_0 A_m \gamma_0 M_0^2} \quad (14-16)$$

In terms of the effective jet Mach number M_j , the gross thrust coefficient is given by¹

$$C_{Fg} = \frac{2A_0}{A_m} \left[(1+f) \frac{M_j}{M_0} \sqrt{\frac{\gamma_7 T_7}{\gamma_0 T_0}} - 1 \right] \quad (14-17)$$

By eliminating M_j from Eq. 14-17, by means of Eq. 14-12, one obtains

$$C_{Fg} = \frac{2A_7/A_m}{\gamma_0 M_0^2} \left[\frac{P_7}{P_0} (1 + \gamma_7 M_7^2) - 1 \right] - 2(A_0/A_m) \quad (14-18)$$

In practically all ramjet engine designs the maximum cross-sectional area A_m is identical with A_3 the cross-section area of the burner (see Fig. 14-1).

The gross thrust coefficient determines the speed range wherein the ramjet engine can propel itself and, consequently, the maximum flight speed. Eq. 14-17 indicates that for constant values of γ_0 , M_0 , and P_0 (fixed values of altitude and flight speed), C_{Fg} for a fixed-geometry ramjet engine ($A_0/A_m = \text{constant}$) depends primarily upon the effective jet speed V_j , where

$$V_j = u_7 + \frac{A_7}{\dot{m}_7} (P_7 - P_0) = M_j \sqrt{\gamma_7 R T_7} \quad (14-19)$$

For calculation purposes it is convenient to express C_{Fg} in terms of P_7^0/P_0 and P_7^0/P_7 . Thus¹

$$C_{Fg} = \frac{2A_7/A_m}{\gamma_0 M_0^2} \left\{ \frac{P_7^0}{P_0} \left[\frac{1 + \gamma_7 M_7^2}{P_7^0/P_7} \right] - 1 \right\} \frac{2A_0}{A_m} \quad (14-20)$$

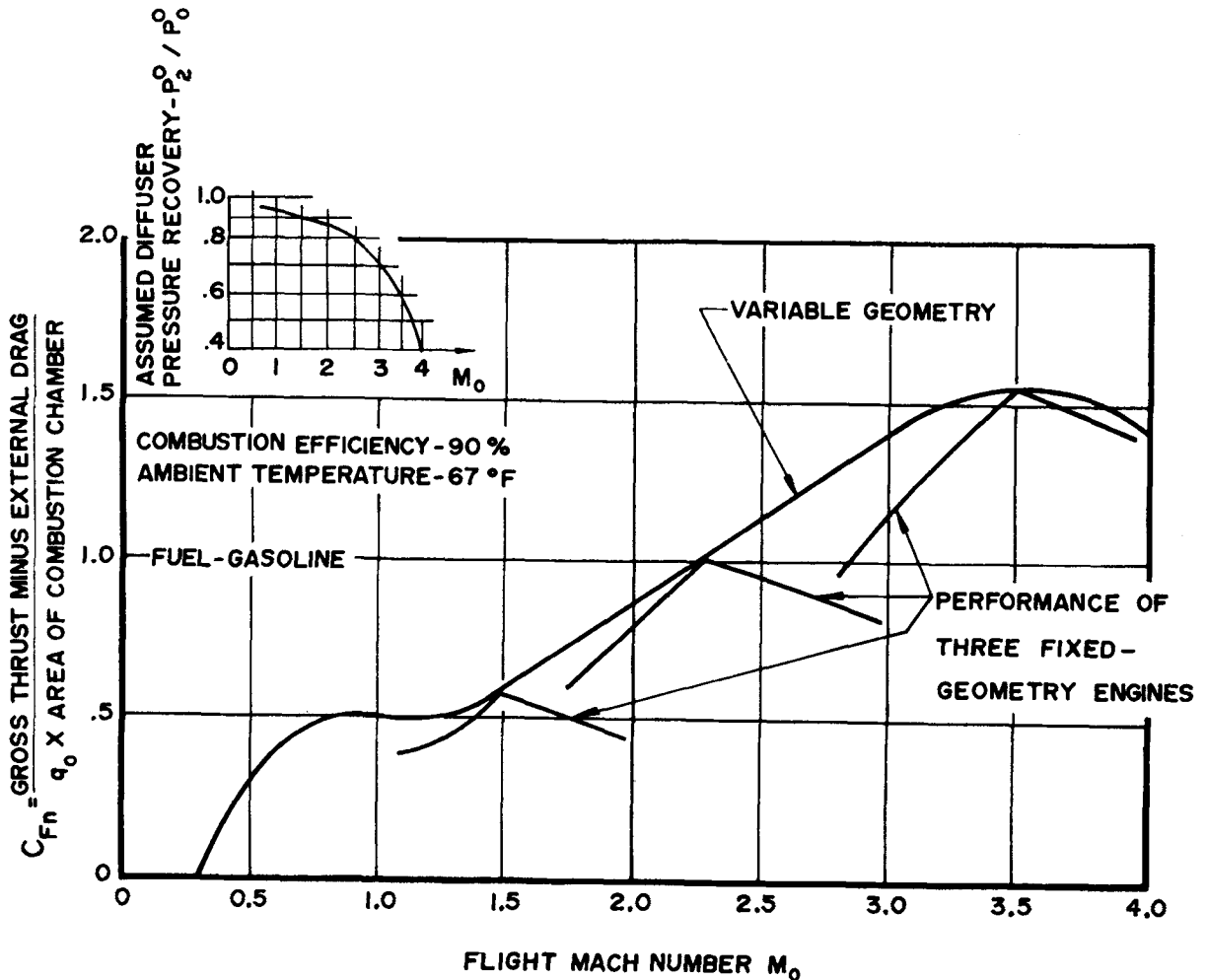


Figure 14-5. Calculated Values of the Net Thrust of Ramjet Engines As a Function of the Flight Mach Number

For a fixed-geometry ramjet engine, M_7 depends upon the combustion temperature T_6 , the fuel-air ratio $f = \dot{m}_f / \dot{m}_a$, the combustion pressure P_6 , and the nozzle efficiency η_n . Hence, for fixed values of M_0 , altitude, and heat addition the thrust coefficient is proportional to the pressure ratio P_7^0 / P_0^0 ; the value of that pressure ratio, and hence the thrust, can be regulated by varying the fuel flow rate \dot{m}_f . As pointed out in par. 14-2.2.2, the heat added in the burner is the means utilized for maintaining the high static pressure inside the ramjet required for developing gross thrust.

For estimating purposes one may assume $\gamma_0 = 1.4$ and $\gamma_7 = 1.28$; the latter value assumes that a liquid hydrocarbon fuel is burned at substantially the stoichiometric fuel-air ratio. The following parameters must be either known or determinable: $T_6^0 = T_3^0$, P_2^0 , M_6 , $P_6^0 = P_2^0 - \Delta P_{\lambda B}$ (where $\Delta P_{\lambda B}$ is the stagnation pressure decrease in the burner), and the area ratio A_0 / A_7 . Ordinarily, the ramjet engine operates with a *choked* exhaust nozzle. Hence, M_t = throat Mach number = 1.0. For the choked operating condition the nozzle area ratio $A_7 / A_t = A_7 / A^*$ is given by (see Chapter 4)

$$\frac{A_7}{A_t} = \left(\frac{\gamma+1}{2} \right)^{\frac{1}{\gamma-1}} \left\{ \left(\frac{P_7}{P_6^O} \right)^{\frac{1}{\gamma}} \sqrt{\frac{\gamma+1}{\gamma-1} \left[1 - \left(\frac{P_7}{P_6^O} \right)^{\frac{\gamma-1}{\gamma}} \right]} \right\} \quad (14-21)$$

The pressure ratio P_7^O/P_0 depends upon M_0 , the stagnation pressure ratio P_2^O/P_0^O , the pressure drop in the burner $\Delta P_{\lambda B}$, and the decrease in stagnation pressure in the exhaust nozzle.

The pressure ratio P_7^O/P_0 is obtained from the relationship

$$\frac{P_7^O}{P_0} = \frac{P_0^O}{P_0} \frac{P_2^O}{P_0^O} \frac{P_6^O}{P_2^O} \frac{P_7^O}{P_6^O} \quad (14-22)$$

Some general conclusions will now be presented regarding the effect of altitude z , flight Mach number M_0 , and fuel-air ratio f upon C_{Fg} for a ramjet engine having a *fixed geometry*.

14-3.6.1 EFFECT OF ALTITUDE (z) ON C_{Fg} ($T_3^O = \text{constant}$)

Assume that a fixed geometry ramjet engine propels a vehicle at a constant altitude ($z = \text{const}$) and the *fuel controls* maintain T_3^O , the *combustion total temperature*, at a fixed value (see Fig. 14-1).

As the engine accelerates the vehicle the net thrust $F_n = (F_g - D_e)$, the flight Mach number, the internal air flow \dot{m}_0 , and stagnation pressure P_2^O , at the diffuser exit section all increase. At a particular value of M_0 one or more shock waves attach themselves to the inlet, and the capture area A_0 (see Fig. 14-1) becomes fixed. Ordinarily, the latter condition is established when M_0 is slightly smaller than M_{0d} , the *design flight Mach number* (see Fig. 14-6). If the engine continues to accelerate the vehicle, a flight Mach number is attained where the flow in the

exhaust nozzle becomes *choked*. Further acceleration causes the normal shock to become detached from the *intake lips*, air is "*spilled over*" the *intake lips*, and the gross thrust decreases as indicated in Fig. 14-6.

Since $C_{Fg} = F_g/q_0 A_m$, the variation of C_{Fg} with M_0 , at $z = \text{constant}$, depends on both F_g and the *dynamic pressure* $q_0 = \gamma_0 P_0 M_0^2/2$. After the exhaust nozzle operates with choked flow, q_0 increases faster than F_g , so that C_{Fg} decreases with M_0 , as illustrated in Fig. 14-7(A), for sea level and altitude z .

It is seen from Fig. 14-7(A) that the thrust coefficient, when T_3^O is constant increases with the altitude z . At altitude, the air temperature T_2^O entering the burner is lower than it is at sea level, so that more heat can be added to the air for achieving the same value of T_3^O .

14-3.6.2 EFFECT OF FUEL-AIR RATIO ON C_{Fg} ($z = \text{const.}$)

Fig. 14-7(B) illustrates schematically the effect of fuel-air ratio f and M_0 on a fixed geometry ramjet operating at a constant altitude.

14-4 CRITICAL, SUPERCRITICAL, AND SUBCRITICAL OPERATION OF THE RAMJET ENGINE

It was pointed out in par. 13-4.4 that a diffuser employing external shocks has three basic modes of operation—critical, supercritical, and subcritical—depending upon the value of the diffused pressure at Station 2 (see Figs. 13-2 and 13-5). The external shock pattern may be produced by either a normal shock diffuser or a conical spike diffuser (see Fig. 13-6). The general conditions in the diffuser are illustrated in Fig. 13-7.

In a ramjet engine the magnitude of the restriction for sustaining a high internal pressure

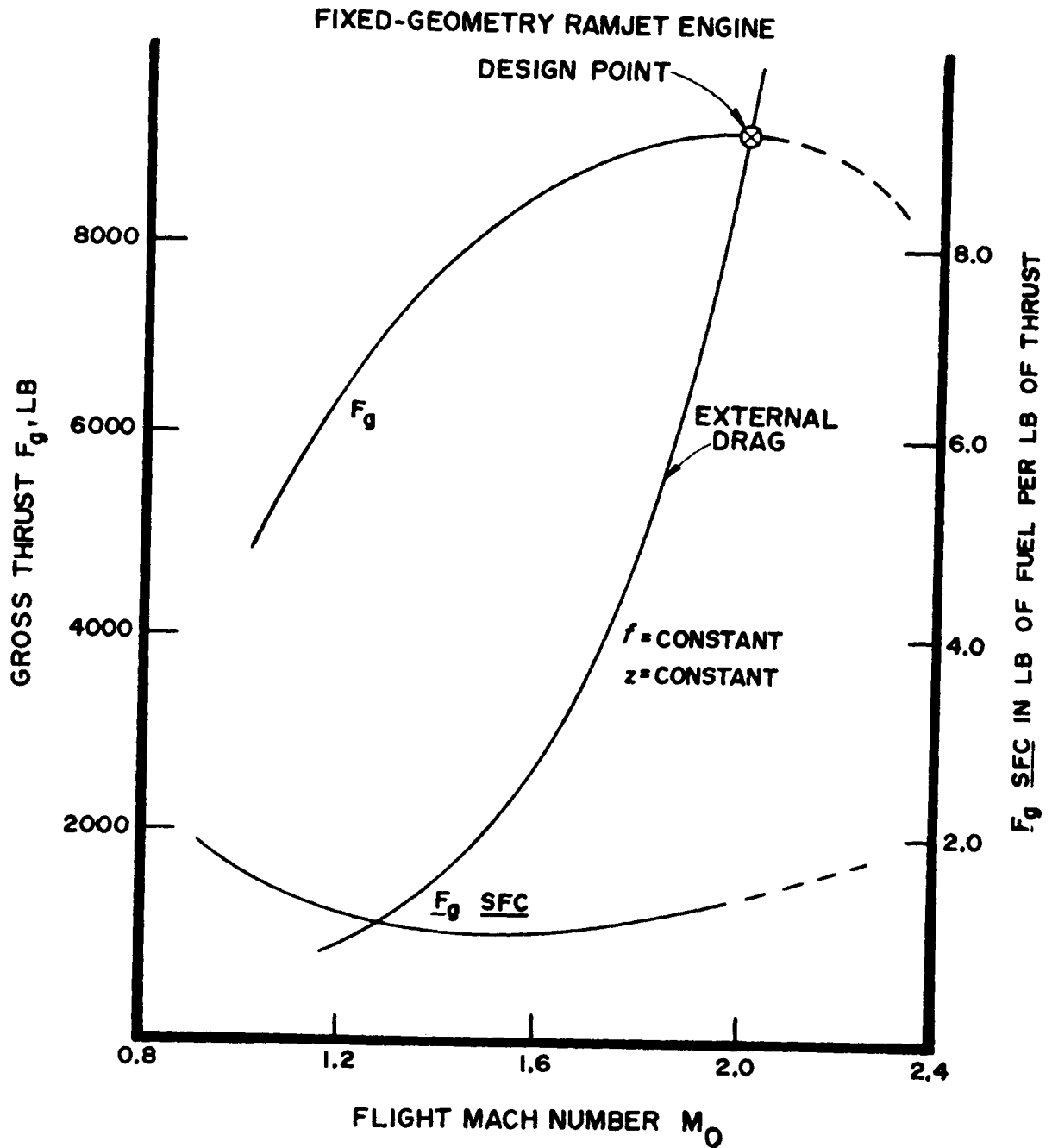
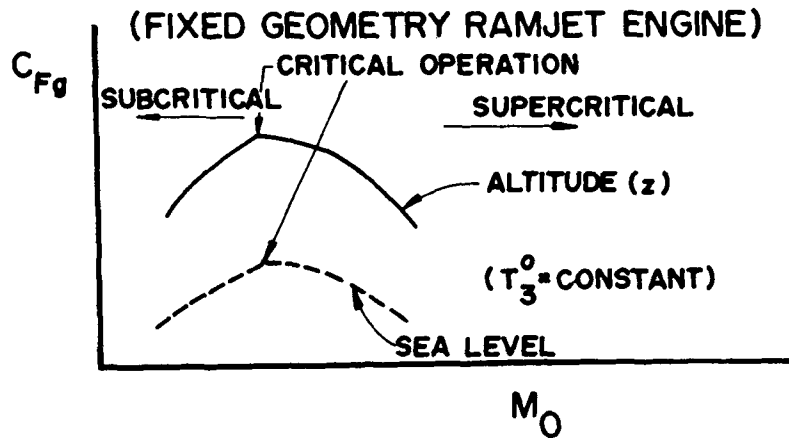
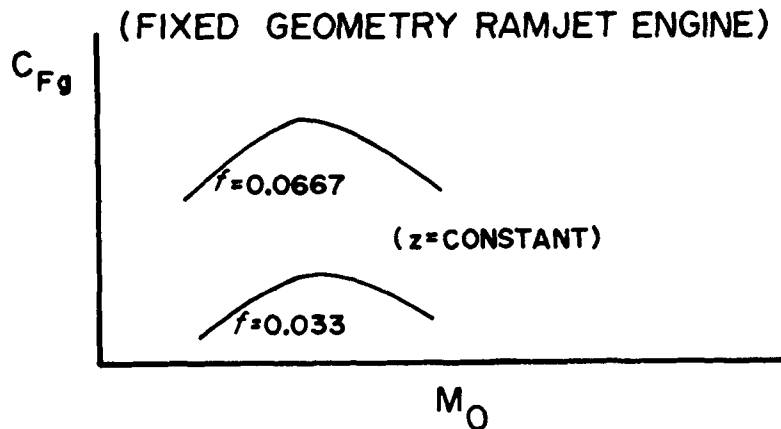


Figure 14-6. Gross Thrust Characteristics of a Fixed-Geometry Ramjet Engine
As a Function of the Flight Mach Number (Constant Fuel-Air
Ratio f and a Fixed Altitude z)



(A) EFFECT OF ALTITUDE FOR A CONSTANT COMBUSTION TEMPERATURE T_3^0



(B) EFFECT OF FUEL-AIR RATIO AT A CONSTANT ALTITUDE

Figure 14-7. Variation of Gross Thrust Coefficient C_{Fg} for a Fixed-Geometry Ramjet Engine With Flight Mach Number M_0 ; (A) With a Constant Combustion Stagnation Temperature T_3^0 at Two Altitudes; and (B) With Two Different Fuel-Air Ratios at a Fixed Altitude

comes from the heat added in the burner. Hence, the basic operating conditions for a ramjet engine are related to the amount of heat added to the air flowing through the burner, i.e., to the *heat released* in the burner.

14-4.1 CRITICAL OPERATION OF THE RAMJET ENGINE

If the heat released in the burner is sufficient for maintaining the normal shock (see Fig. 13-7(A)) at the inlet, the operation of the ramjet is said to be *critical*.

14-4.2 SUPERCRITICAL OPERATION OF THE RAMJET ENGINE

If the heat released in the burner is too small for achieving critical operation, the excess pressure in the air is dissipated within the diffusion system by a discontinuous process, i.e., by a shock wave. Consequently, the air flows into the internal compression (subsonic) diffuser with supersonic velocity. Since dA/A is positive and the flow is supersonic, the flow Mach number increases. Consequently, the excess kinetic energy associated with the air stream is dissipated by a strong shock wave, as illustrated in Fig. 13-7(B).

14-4.3 SUBCRITICAL OPERATION OF THE RAMJET ENGINE

If the heat release in the burner is large enough, the static pressure P_2 may exceed the static pressure achieved by the diffusion system. Consequently, the internal flow becomes *choked* and the normal shock is expelled from the subsonic diffuser and moves upstream toward the vertex of the conical diffuser, as illustrated in Fig. 13-7(C).

The flow behind the detached normal shock is subsonic. Because of the detachment of the normal shock air is “*spilled over*” the diffuser lips. The “*spillover*” reduces the internal flow,

i.e., there is a reduction in the capture area A_0 (see Fig. 14-1). Because of the subsonic flow and high static pressure acting on the diffuser *cowl*, the external drag of the engine is increased. Although the gross thrust of the engine increases due to the decrease in *ram drag* $\dot{m}V_0$ (see par. 12-3.1), the increased external drag may cause the net thrust F_n to decrease.

If M_0 decreases during *subcritical operation* of the ramjet engine, the “*spillover*” increases and the gross thrust F_g decreases. Unless the decrease in M_0 can be halted, the gross thrust will become less than the external drag. There is only one way for increasing F_g when the ramjet operation is subcritical; *the internal area which produces forward thrust must be increased*. To accomplish the latter requires reducing the inlet area A_1 or, in other words, increasing the *area ratio* A_2/A_1 of the internal compression subsonic diffuser. In other words, a *variable-area* subsonic diffuser is required.

In general, flights at low Mach numbers require large values of A_2/A_1 than do flights at high Mach numbers.

The discussions of critical, supercritical, and subcritical operation of the ramjet engine indicate that the position of the normal shock at the inlet to the engine and the amount of “*spillover*” air depend upon the flight Mach number M_0 , the fuel-air ratio f , and the burner efficiency η_B .

14-5 LOSSES IN THE RAMJET ENGINE

An actual ramjet engine encounters losses in the internal flow. The following are the principal sources of loss:

1. Increase in the entropy of the internal flow due to the presence of shock waves in the supersonic diffusion process.

2. Pressure losses due to skin friction and flow separation phenomena in the subsonic diffuser.
3. Pressure loss due to such obstructions in the flow, as injection nozzles, flame-holders, etc.
4. Loss in stagnation pressure due to heat addition in the burner.
5. Loss due to friction in the exhaust nozzle.

For a typical fixed geometry ramjet configuration operating with $M_0 \approx 1.8$, test results indicate that with $M_2 \approx 0.2$ and $T_3^0 \approx 3800^\circ R$ the total pressure ratio across the engine will be of the order of 0.72. Typical values for the stagnation pressure ratios across different parts of the ramjet engine are presented below:

<u>Part of Engine</u>	<u>Pressure Ratio</u>
Supersonic diffuser	$P_1^0/P_0^0 \approx 0.92$
Subsonic diffuser	$P_2^0/P_1^0 \approx 0.90$
Flameholders	$P_3^0/P_2^0 \approx 0.97$
Combustion chamber	$P_6^0/P_3^0 \approx 0.92$
Exhaust nozzle	$P_7^0/P_6^0 \approx 0.97$

14-6 DIFFUSER PERFORMANCE IN A RAM-JET ENGINE

It is important that the supersonic and subsonic diffusers convert a large portion of the kinetic energy associated with the free-stream air into pressure rise at the entrance to the burner.

The selection of the most appropriate configuration for the supersonic diffuser of a ramjet engine depends primarily upon the design flight Mach number M_{0d} , but also upon the configuration of the propelled vehicle. The supersonic

diffusers for some vehicles may be either of the nose-inlet type or the side, scoop, or aft inlet type. The nose-inlet has the advantage that it gives a somewhat larger pressure recovery than the side-inlet. With a side-inlet, however, the ducting of the combustion air through the nose of a missile, for example, is eliminated and the burner can be moved forward in back of the payload; the latter can then be located in the nose. Such an arrangement offers the possibility of reducing the frontal area of the missile and consequently the external drag. Alternatively, it permits "forward looking" radars, etc., to be located in the nose. Few data on the performance of side-inlets have appeared in the unclassified literature. Irrespective of the type of inlet, the development of the supersonic diffuser is concerned with the following problems:

1. The achievement of the largest possible stagnation pressure recovery.
2. The minimizing of the effect of angle of attack upon the pressure recovery and upon the uniformity of the flow pattern entering the burner.
3. Decreasing the external drag during subcritical operation (where the free-stream Mach numbers are less than the design Mach number).
4. Limiting the subcritical operating range to avoid the occurrence of the oscillatory phenomena at the inlet, commonly called diffuser buzz.

The engine designer must make the best possible compromise between the desired high values of pressure recovery and the overall drag of the missile. For that reason and several others, there must be a good coordination between the design and development engineers of the engine and the vehicle manufacturers. Fairly high pressure recoveries can be obtained with the different types of supersonic diffusers

if they are operated within their optimum ranges.

For supersonic flight Mach numbers less than approximately $M_0 = 1.8$, the normal shock supersonic diffuser (see par. 13-4.1) gives satisfactory values of stagnation pressure recovery. For values of M_0 exceeding 1.8, the stagnation pressure recovery of the normal shock diffuser deteriorates quite rapidly. The spike-type diffuser (with a single cone) with one conical shock at the cone vertex and one normal shock at the intake gives good values of stagnation pressure

recovery for Mach numbers ranging from approximately 1.6 to 2.6. For higher pressure recoveries it is necessary to increase the number of conical shocks. It is found, however, that increasing the number of conical shocks also increases the external drag so that there may be little gain in the net thrust. Except at Mach numbers above approximately 2.75, there is no advantage in using more than two conical shocks. Fig. 14-8 illustrates diagrammatically the best operating ranges for the different supersonic diffusers for fixed-geometry ramjet engines.

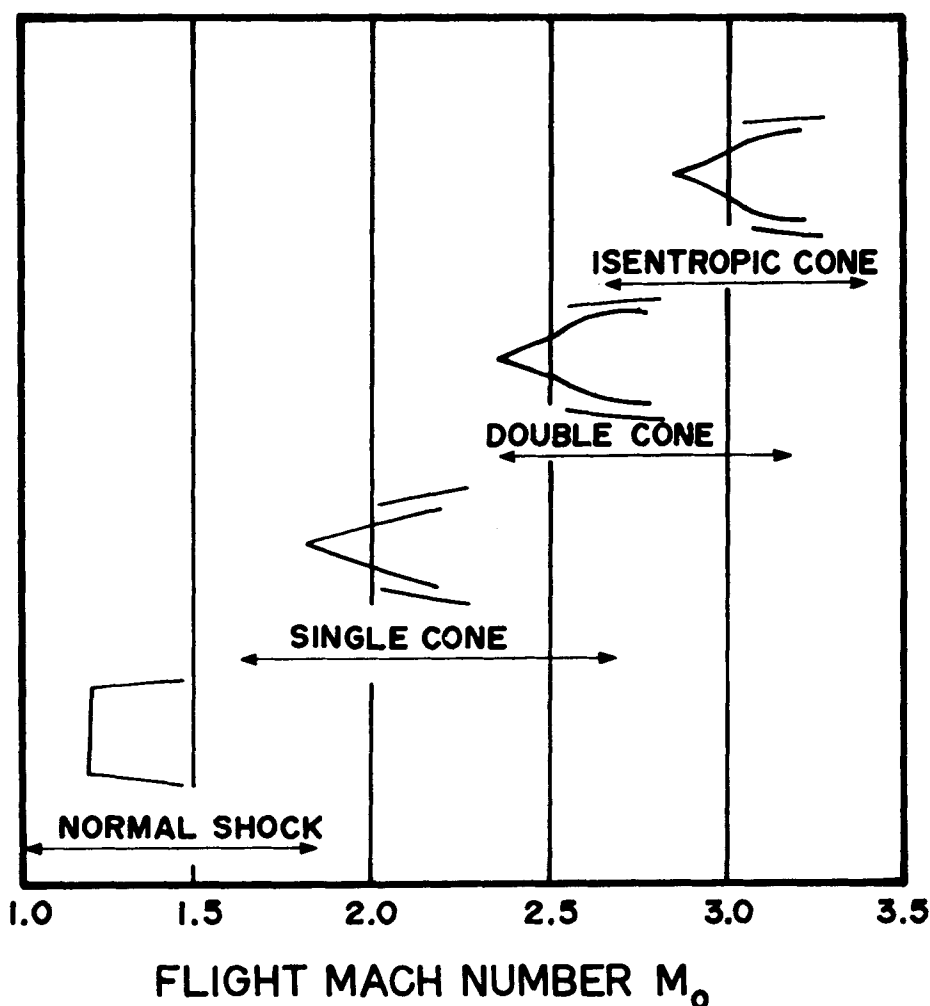


Figure 14-8. Best Operating Ranges for Supersonic Diffusers for Fixed-Geometry Ramjet Engines

14-7 BURNER EFFICIENCY (η_B)

Let \dot{Q}'_i denote the heat actually imparted to the internal flow. Thus

$$\dot{Q}'_i = \dot{m}_a \bar{c}_{pB} (T_3^O - T_2^O) \text{ (B/unit time)} \quad (14-23)$$

where \bar{c}_{pB} is the mean specific heat for the gases raised from T_2^O to T_3^O in the burner.

Let

$$\alpha = T_3^O / T_0 = \text{the cycle temperature ratio} \quad (14-24)$$

and

γ_B = the mean value of γ for the burner.

Then¹

$$\dot{Q}'_i = A_0 P_0 V_0 \left(\frac{\gamma_B}{\gamma_B - 1} \right) \left[\alpha - \left(\frac{1 + \gamma_0}{2} \right) M_0^2 \right] \quad (14-25)$$

Because of inevitable losses, some of the heat supplied to the engine in the form of fuel is not utilized for increasing the enthalpy of the working fluid. Let f' denote the ideal fuel-air ratio corresponding to the ideal heat input \dot{Q}'_i and f the actual fuel-air ratio, then the burner efficiency η_B is defined by

$$\eta_B = \dot{Q}'_i / \dot{Q}_i = f' / f \quad (14-26)$$

14-8 OVERALL EFFICIENCY OF THE RAMJET ENGINE (η_O)

In general, the overall efficiency of a propulsion system, denoted by η_O , is given by

$$\eta_O = P_T / \dot{Q}_i = F_g V_0 / (\dot{Q}_i / \eta_B) \quad (14-27)$$

It can be shown¹ that

$$\eta_O = \frac{P_T}{\dot{Q}_i} = \left[\frac{\gamma_0 (\gamma_B - 1) M_0^2}{\gamma_B} \right] \frac{\left\{ (1 + f) \frac{M_f}{M_0} \left[\frac{\alpha \gamma_f / \gamma_0}{1 + \left(\frac{\gamma_f - 1}{2} \right) M_0^2} \right]^{\frac{1}{2}} - 1 \right\}}{\alpha - \left[1 + \left(\frac{\gamma_0 - 1}{2} \right) M_0^2 \right]^{-1}} \quad (14-28)$$

14-9 GROSS THRUST SPECIFIC FUEL CONSUMPTION OF THE RAMJET ENGINE ($\underline{F_gSFC}$)

The gross thrust specific fuel consumption, denoted by $\underline{F_gSFC}$, is measured in lb of fuel per hr per lb of thrust. It is defined by

$$\underline{F_gSFC} = g_c \dot{m}_f \frac{(3600)}{F_g} = g_c \dot{m}_f \frac{(3600)}{C_{Fg} \left(\frac{1}{2} A_m P_0 \gamma M_0^2 \right)} \quad (14-29)$$

In terms of the fuel-air ratio $f = \dot{m}_f / \dot{m}_a$,

$$\dot{m}_f = f \dot{m}_a = f (\rho_0 V_0 A_0) \quad (14-30)$$

Combining Eqs. 14-29 and 14-30, one obtains

$$\underline{F_gSFC} = 7200 g_c \left(\frac{A_0}{A_m} \right) \left(\frac{f}{C_{Fg}} \right) \left(\frac{1}{a_0 M_0} \right) \quad (14-31)$$

For fixed values of f and M_0 , the $\underline{F_gSFC}$ of a fixed-geometry ramjet engine decreases as C_{Fg} is increased, as indicated in Fig. 14-6.

14-10 VARIABLE-GEOMETRY RAMJET ENGINE

The main advantage of the fixed-geometry engine is its simple construction, but from an aerodynamic and thermodynamic point of view it leaves much to be desired. Its performance decreases rapidly with off-design operation and

if the Mach number at which it becomes self-operating (thrust > drag) is high, the boosters or launching rockets become large and expensive.

A ramjet engine having variable intake and exit areas gives improved performance at low flight speeds and thus reduces the size of the booster rockets. The cruise performance can also be improved because it is not necessary to compromise the design performance.

14-11 SCRAMJET ENGINE PERFORMANCE PARAMETERS

It was pointed out in par. 12-1.2 that the maximum flight Mach number for the ramjet engine, because it utilizes subsonic combustion, is limited to approximately $M_0 = 5$. The limit is due to the high stagnation temperatures and pressures resulting from decelerating the free-stream air to approximately $M_2 = 0.2$, see Fig. 14-1.

The SCRAMJET engine by eliminating the need for decelerating the incoming air to a subsonic Mach number removes the limitations described above. Consequently, such an engine has the potentiality of developing thrust at hypersonic flight speeds and possibly up to orbital speeds. Moreover, it appears that it may be feasible to operate a SCRAMJET engine over

a wide range of Mach numbers with fixed geometry. Moreover, its internal pressure and temperature at the entrance to the burner will not be excessive since the diffused flow is supersonic throughout; u_2 is not too far different from V_0 .

Fig. 14-9 illustrates schematically a longitudinal cross-section through a SCRAMJET engine.

14-11.1 GROSS THRUST (F_g)

The gross thrust F_g is given by

$$F_g = (\dot{m}_7 u_7 + P_7 A_7) - (\dot{m}_0 V_0 + P_0 A_0) - P_0 (A_7 - A_0) \quad (14-32)$$

Rearranging

$$F_g = (\dot{m}_7 u_7 + P_7 A_7) - (\dot{m}_0 V_0 + P_0 A_7) \quad (14-33)$$

14-11.2 GROSS THRUST SPECIFIC IMPULSE (I_{Fg})

By definition

$$I_{Fg} = \frac{F_g g_c}{\dot{m}_f} \quad (14-34)$$

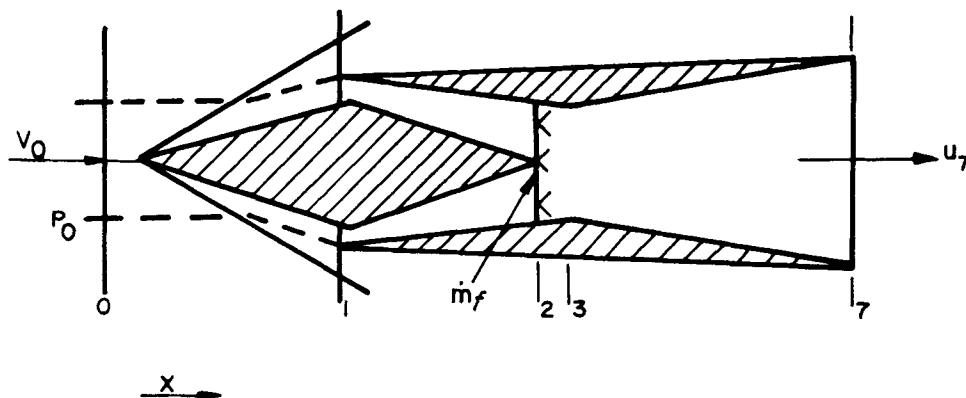


Figure 14-9. Diagrammatic Cross-Section Through a SCRAMJET Engine

where, as before, \dot{m}_f is the fuel consumption rate.

14-11.3 INLET KINETIC ENERGY EFFICIENCY (η_{KE})

Fig. 14-10 illustrates diagrammatically the deceleration of the incoming air from the velocity V_0 to the velocity u_2 . By definition, the kinetic energy efficiency η_{KE} is given by

$$\eta_{KE} = \frac{u^2}{V_0^2} = \frac{h_2^0 - h_0}{h_0^0 - h_0} \quad (14-35)$$

14-11.4 NOZZLE THRUST EFFICIENCY (η_{nF})

By definition

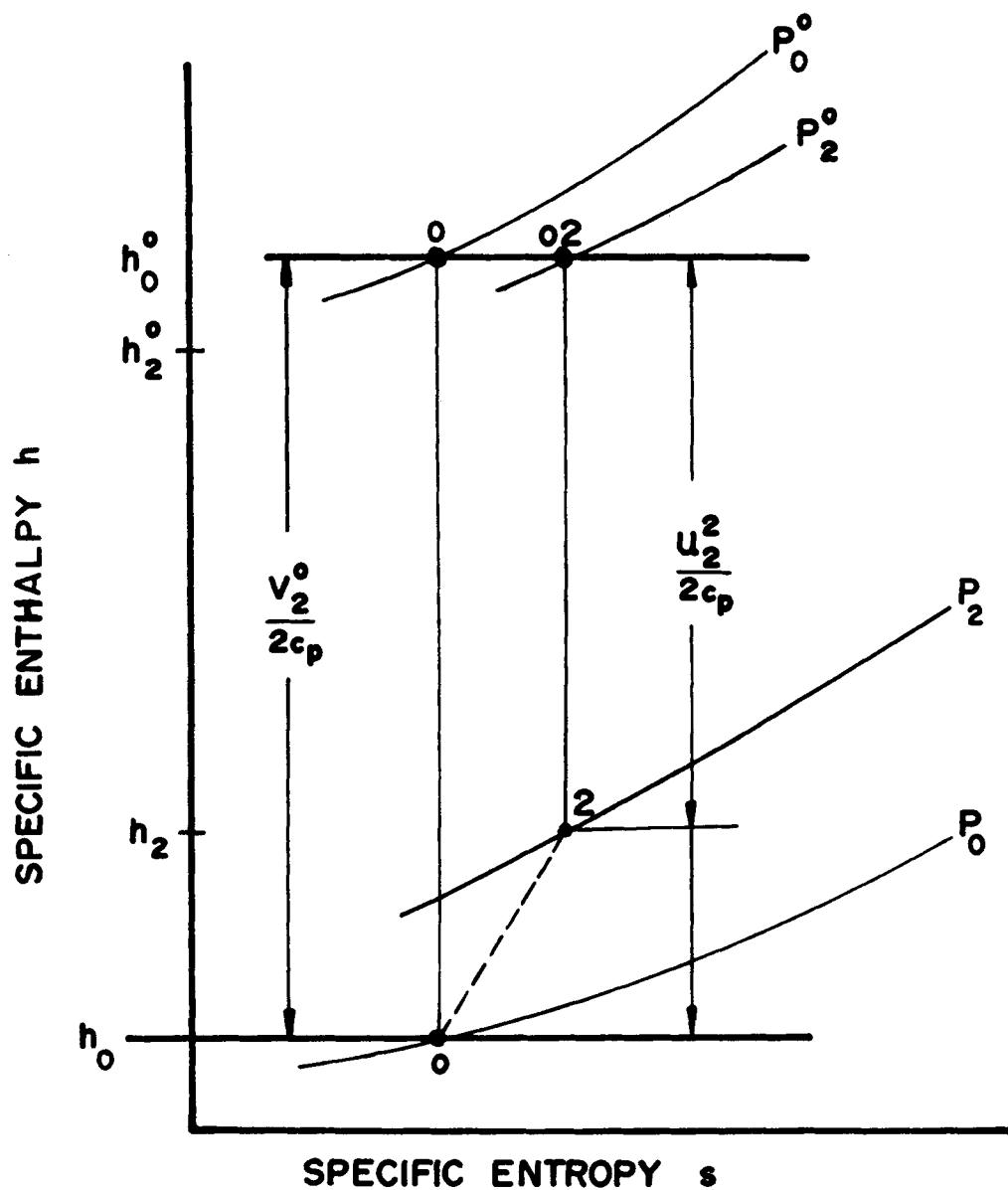
$$\eta_{nF} = \frac{F_7}{F_7'} \quad (14-36)$$

where

$F_7 = \dot{m}_7 u_7 + P_7 A_7$ = stream thrust for the actual nozzle

$F_7' =$ stream thrust for an isentropic nozzle

To date, no operating SCRAMJET engine has been developed, but there is considerable research and development activity pertinent to that engine⁶.

Figure 14.10. SCRAMJET Engine Diffusion Process Plotted in the h - s plane

REFERENCES

1. M.J. Zucrow, *Aircraft and Missile Propulsion*, John Wiley and Sons, Inc. Vol. 2, 2nd Printing, 1964, Ch. 9.
2. M. Harned, "The Ramjet Power Plant", *Aero Digest*, July 1954, p. 38.
3. M. Harned, "The Application of the Ramjet Engine to Aircraft Propulsion", *Aero Digest*, Feb. 1953, p. 44.
4. W.H. Goss and E. Cook, *The Ramjet as a Supersonic Propulsion Plant*, SAE, Annual Meeting, Detroit, Mich., Jan 12 to 16, 1948.
5. J.R. Henry and J.B. Bennett, *Method for Calculating Ram-Jet Performance*, NACA TN 2357, June 1951.
6. A. Ferri, *Review of SCRAMJET Technology*, AIAA, 3rd. Annual Mtg., Boston, Mass., Nov. 29-Dec. 2, 1966, AIAA Paper No. 66-826.

CHAPTER 15

GAS-TURBINE AIR-BREATHING ENGINES

15-1 INTRODUCTION

The essential features of the different types of gas-turbine engines are presented in paragraph 12-2 and illustrated schematically in Figs. 12-2 through 12-7. For convenience of discussion the gas-turbine engines may be classified into the following two groups:

1. Gas-turbine Powerplant Engines
2. Gas-turbine Jet Engines

15-2 GAS-TURBINE POWERPLANT ENGINES

These engines may be grouped into the following types:

- (a) Basic turboshaft engine, for brevity termed the turboshaft engine (see par. 12-2.5)
- (b) Regenerative turboshaft engine
- (c) Turboprop engine (see par. 12-2.6)

Both types of turboshaft engine (a) and (b), are designed for producing *shaft power* only. As pointed out in par. 12-2.6, the turboprop engine develops a small jet thrust in addition to shaft power.

A turboshaft engine — and its modification the regenerative turboshaft engine — is basically an adaptation of the stationary gas-turbine powerplant to aircraft requirements; e.g., low

weight, large thrust per unit weight, etc. Consequently, the thermodynamic methods developed for analyzing stationary gas-turbine power plants are directly applicable to the analytical studies of all of the types of gas-turbine powerplant engines^{1,2}.

The turboshaft engine is employed for driving electric generators, large ground vehicles, ship propellers, helicopter rotors, and airplane propellers. Table 15-1 lists some of the current Army aircraft and their gas-turbine engines.

Because of the large difference in rotative speed of the output shaft of a gas-turbine powerplant engine and its load — helicopter rotor, aircraft propeller, etc. — the load is driven through some form of gearbox, as illustrated in Figs. 12-6 and 15-17. The speed of the output shaft for the larger horsepower engines will range from 10,000 to 14,000 *rpm* and for the smaller horsepower engines the rotative speed may be as large as 40,000 *rpm*. The rotative speeds of helicopter rotors* are ordinarily close to 250 *rpm* while those for aircraft propellers range from 1,000 to 1,500 *rpm*¹. To achieve the required reduction in rotational speed, two stages of speed reduction are generally employed. For a well-designed and well-constructed gearbox one may assume for estimation purposes that the mechanical efficiency of the gearbox, denoted by η_g , will have a value of $\eta_g \approx 0.98$.

*Characteristics of helicopter rotors are presented in Reference 10.

TABLE 15-1

ARMY AIRCRAFT AND THEIR ENGINES

AIRCRAFT DESIGNATION	NAME	ENGINE	hp/ENGINE
UH-1	Iroquois	1-Lycoming T53	1400
CH-47	Chinook	2-Lycoming T55	2850
OH-6A	Cayuse	1-Allison T63	317
OV-1	Mohawk	2-Lycoming T53	1160
CH-54	Flying Crane	2-P&W JFTD-12	4500
U-21A	(Utility Airplane)	2-P&W T74	550
AH-56	Cheyenne	1-GE T64	3400

15-3 EFFICIENCIES OF COMPONENTS OF GAS-TURBINE ENGINES

In this paragraph the definitions of the efficiencies of the components employed in the gas-turbine discussed in Chapter 15 will be presented.

15-3.1 DIFFUSION PROCESS

The flow in an inlet-diffuser may be assumed to be adiabatic, so that $T_0^O = T_2^O = \text{constant}$. Fig. 15-1(A) illustrates schematically the diffusion process on the h - s -plane. The states 0 and 2 correspond to the ambient air and the exit cross-section of the diffuser, respectively, as indicated in Fig. 15-18 (turboprop engine) and Fig. 15-24 (turbojet engine). The diffuser compresses the atmospheric air from P_0^O to P_2^O .

15-3.1.1 DIFFUSER ISENTROPIC EFFICIENCY (η_d)

By definition, the isentropic diffuser efficiency η_d is given by

$$\eta_d = \frac{h_2^{O'} - h_0^O}{h_2^O - h_0^O} \approx \frac{T_2^{O'} - T_0^O}{T_2^O - T_0^O} \quad (15-1)$$

15-3.1.2 DIFFUSER TEMPERATURE RATIO (a_d)

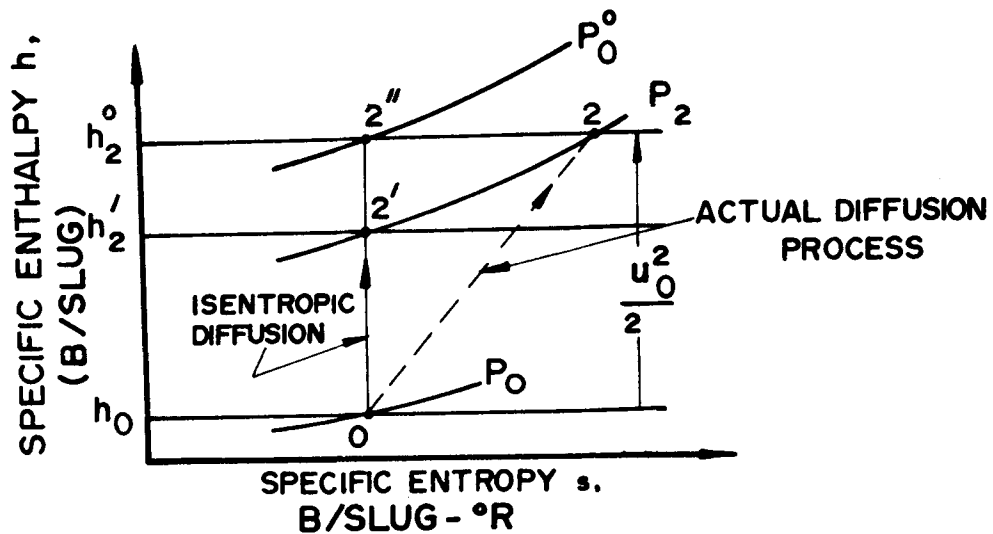
By definition, the diffuser temperature ratio is given by

$$a_d = \frac{T_2^O}{T_0^O} = 1 + \left(\frac{\gamma-1}{2} \right) M_0^2 \quad (15-2)$$

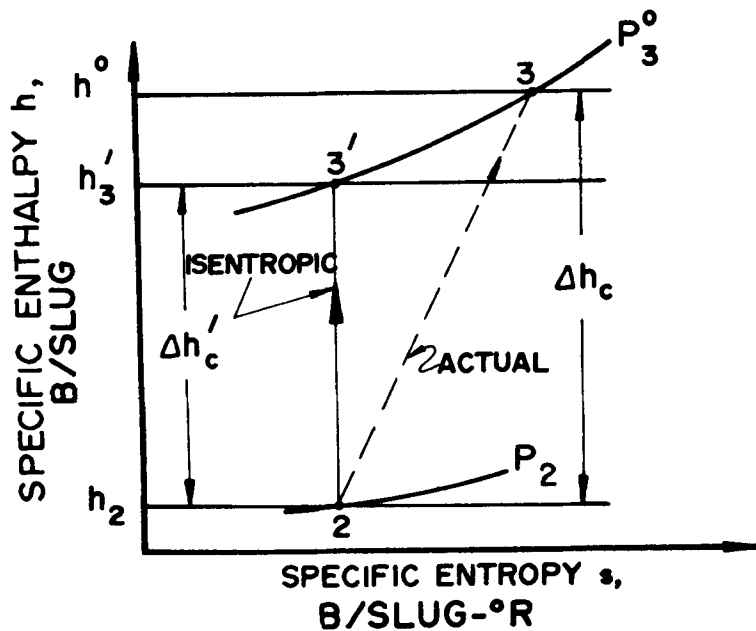
15-3.1.3 DIFFUSER PRESSURE RATIO PARAMETER (Θ_d)

The diffuser pressure ratio P_2^O/P_0^O (see Fig. 15-1(A)) can be related to the flight Mach number M_0 , the diffuser isentropic efficiency η_d , and the diffuser pressure ratio parameter Θ_d , where

$$\Theta_d = \left(\frac{P_2^O}{P_0^O} \right)^{\frac{\gamma-1}{\gamma}} = \text{diffuser pressure ratio parameter} \quad (15-3)$$



(A) SUBSONIC DIFFUSION PROCESS
(TURBOPROP, TURBOJET, AND TURBOFAN ENGINES)



(B) COMPRESSION PROCESS IN AIR COMPRESSOR

Figure 15-1. Isentropic Diffusion and Air Compression Processes
Plotted in the h - s plane

It is readily shown that ^{1,2}

$$\Theta_d = 1 + \eta_d \left(\frac{\gamma-1}{2} \right) M_0^2 \quad (15-4)$$

Fig. 15-2 presents diffuser performance charts obtained by applying Eqs. 15-2 and 15-4. The chart shows that to obtain a large value for Θ_d , for a given M_0 , a large value for η_d is required. For a well-designed inlet-diffuser one may assume for estimation purposes that η_d ranges from 0.7 to 0.9, depending upon M_0 .

15-3.2 COMPRESSION PROCESS

In a turbine-driven air compressor, single- or twin-spool (see par. 12-2.5), the air inducted by a gas-turbine engine is compressed from state 2 to state 3 (see Figs. 15-18 and 15-24).

15-3.2.1 COMPRESSOR ISENTROPIC EFFICIENCY (η_c)

Let Δh_c denote the work actually required to compress the air, in B/slug, from P_2^O to P_3^O , and $\Delta h'_c$ the corresponding work for an isentropic compression; where

$$\Delta h_c = h_3^O - h_2^O = \bar{c}_{pc} (T_3^O - T_2^O) \quad (15-5)$$

and

$$\Delta h'_c = h_3^{O'} - h_2^O = \bar{c}_{pc} (T_3^{O'} - T_2^O) \quad (15-6)$$

where \bar{c}_{pc} is the mean value of c_p for the temperature change accompanying the compression process.

By definition, the compressor isentropic efficiency η_c is given by

$$\eta_c = \frac{\Delta h'_c}{\Delta h_c} = \frac{h_3^{O'} - h_2^O}{h_3^O - h_2^O} \approx \frac{T_3^{O'} - T_2^O}{T_3^O - T_2^O} \quad (15-7)$$

For estimation purposes one may assume that η_c will range from 0.85 to 0.90.

15-3.2.2 COMPRESSOR PRESSURE RATIO PARAMETER (Θ_c)

The air compressor raises the stagnation pressure of the air from P_2^O to P_3^O . The ratio P_3^O/P_2^O is called the *compressor pressure ratio*. By definition ^{1,2}

$$\Theta_c = \left(\frac{P_3^O}{P_2^O} \right)^{\frac{\gamma-1}{\gamma}} = \frac{T_3^{O'}}{T_2^O} = Z_c + 1 \quad (15-8)$$

where

$$Z_c = \Theta_c - 1 = \text{compression factor for air compressor} \quad (15-9)$$

accordingly

$$\Delta h'_c = \bar{c}_{pc} T_2^O Z_c \quad (15-10)$$

and

$$\Delta h_c = \frac{1}{\eta_c} \Delta h'_c = \frac{\bar{c}_{pc} T_2^O}{\eta_c} Z_c \quad (15-11)$$

where, as before, \bar{c}_{pc} is the mean value of the specific heat for the compression process.

15-3.2.3 TEMPERATURE RISE IN AIR COMPRESSOR (ΔT_c)

The compression process increases the specific enthalpy of the air by the amount Δh_c where Δh_c is given by Eqs. 15-5 and 15-11. Hence

$$\Delta T_c = T_3^O - T_2^O = \frac{\Delta h_c}{\bar{c}_{pc}} \quad (15-12)$$

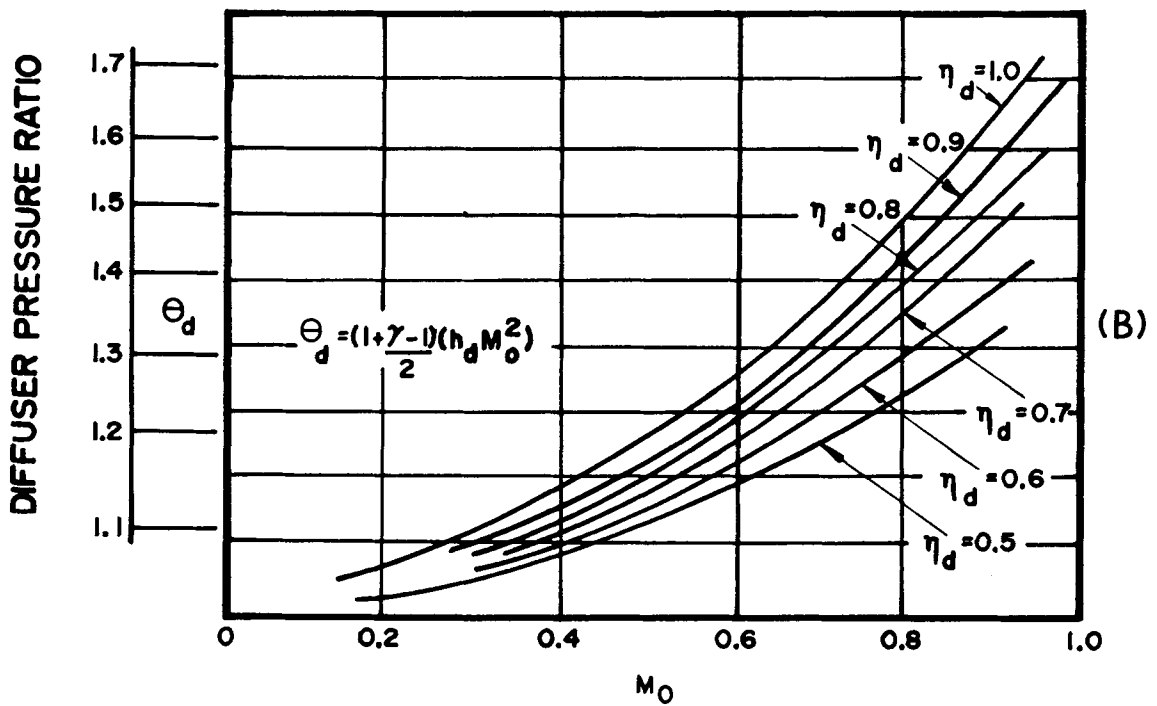
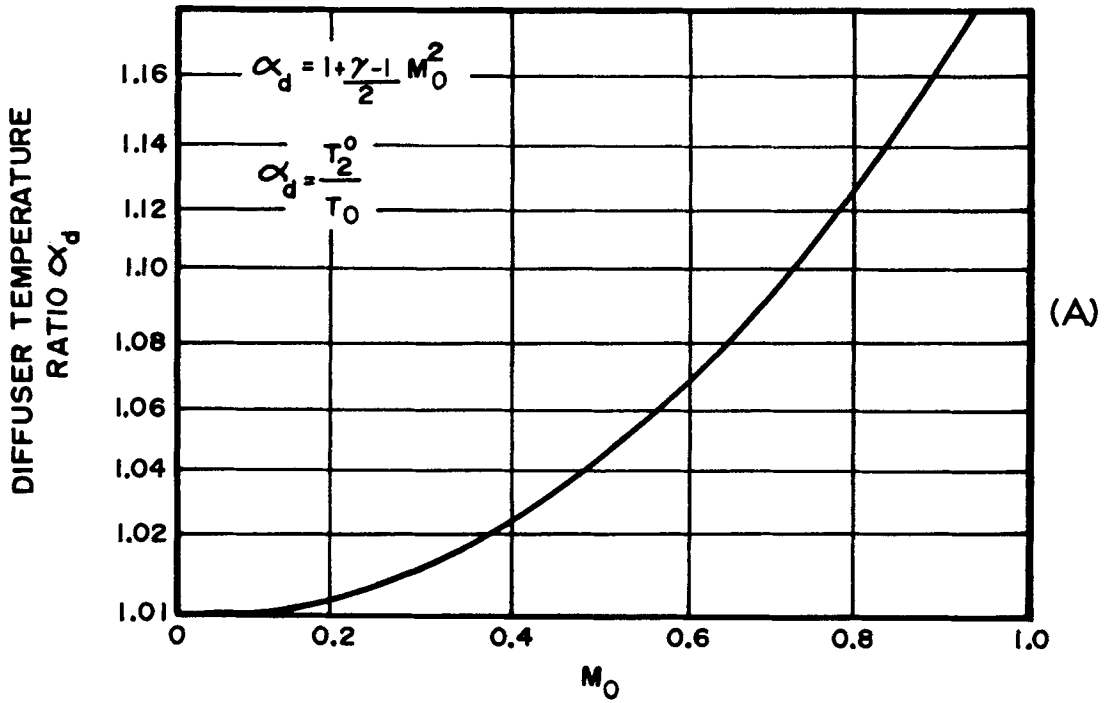


Figure 15-2. Diffuser Performance Charts

It is readily shown that the *compressor discharge temperature* T_3^O is given by ¹

$$T_3^O = T_2^O \left(1 + \frac{Z_c}{\eta_c} \right) = T_2^O \left(1 + \frac{\Theta_c - 1}{\eta_c} \right) \quad (15-13)$$

15-3.3 COMBUSTION PROCESS

The combustion process has the same function in all gas-turbine engines, i.e., to burn a fuel in the compressed air flowing through the *burner* – also called the *combustor* – with a minimum pressure loss and with as complete a utilization of the fuel as possible. Liquid hydrocarbon fuels are the most widely used.

15-3.3.1 BURNER EFFICIENCY (η_B)

Let Q_i denote the heat added in the burner in the form of fuel, having the lower enthalpy of combustion ΔH_c in B/slug, and \dot{m}_f the fuel flow rate in slug/sec, then

$$Q_i = \dot{m}_f \Delta H_c \quad (\text{B/sec}) \quad (15-14)$$

An *ideal burner*, due to the absence of losses due to heat conduction, radiation, and incomplete combustion, would require the *ideal heat input* $Q_i' < Q_i$ to achieve the same temperature in the burner, i.e., T_3^O to T_4^O . Hence, the *ideal fuel flow rate*, denoted by $\dot{m}_f' < \dot{m}_f$, and

$$Q_i' = \dot{m}_f' \Delta H_c \quad (15-15)$$

By definition, if \dot{m}_a denotes the air flow rate for the burner, then

$$f = \dot{m}_f / \dot{m}_a = \text{fuel-air ratio} \quad (15-16)$$

and

$$f' = \dot{m}_f' / \dot{m}_a = \text{ideal fuel-air ratio} \quad (15-17)$$

The effectiveness with which the fuel burned in the burner is converted into enthalpy rise is termed the *burner efficiency* which is denoted by η_B . Hence

$$\eta_B = \frac{Q_i'}{Q_i} = \frac{\dot{m}_f'}{\dot{m}_f} = \frac{f'}{f} \quad (15-18)$$

The burner efficiency η_B is the fraction of the enthalpy $\dot{m}_f \Delta H_c$ that is released in the burner, and is usually between 95 to 99 percent.

15-3.3.2 DIMENSIONLESS HEAT ADDITION PARAMETER ($Q_i \eta_B / \bar{c}_{pB} T_o$)

The heat addition Q_i is also given by

$$Q_i = \frac{\bar{c}_{pB}}{\eta_B} (T_4^O - T_3^O) \quad (\text{B/slug of air}) \quad (15-19)$$

It can be shown that ¹

$$\frac{Q_i \eta_B}{\bar{c}_{pB} T_o} = \alpha - \frac{\Theta_c - 1}{\eta_c} - 1 \quad (15-20)$$

where \bar{c}_{pB} is the mean value of c_p for the burner, and

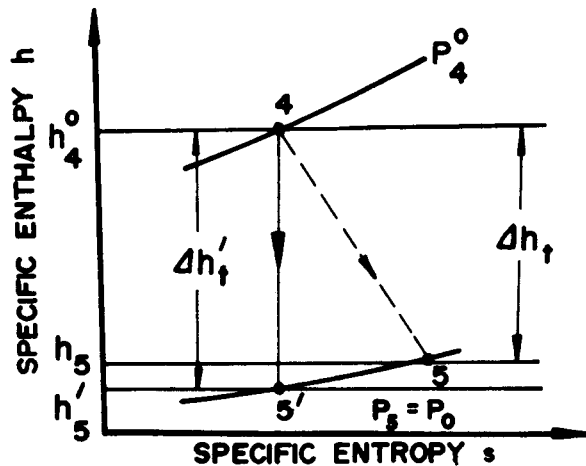
$$\alpha = T_4^O / T_o = \text{cycle temperature ratio} \quad (15-21)$$

The parameter $Q_i \eta_B / \bar{c}_{pB} T_o$ is called the *dimensionless heat addition*.

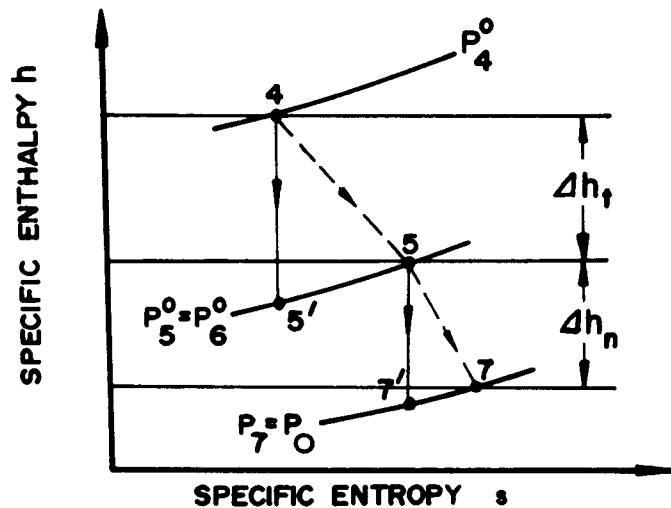
There is always a decrease in the total pressure in a combustor due to the momentum increase resulting from heat addition and the friction losses (see pars. 3-6 and 3-7).

15-3.4 TURBINE EXPANSION PROCESS

The expansion process in the turbine of a gas-turbine engine may be assumed to be adiabatic. Fig. 15-3(A) illustrates the turbine expansion for a turboshaft engine, and Fig. 15-3(B)



(A) EXPANSION PROCESS IN A TURBOSHAFT ENGINE



(B) EXPANSION PROCESS IN TURBOPROP AND TURBOJET ENGINES

Figure 15-3. Expansion Processes for Turboshaft, Turboprop, and Turbojet Engines Plotted in the h - s -plane

illustrates the expansion process for turboprop and turbojet engines. Let T_4^0 denote the *turbine inlet temperature* and h_4^0 the corresponding stagnation enthalpy. The expression for the work performed by a turbine, denoted by Δh_t , will depend upon whether or not useful work is obtained from the kinetic energy of the gas leaving the turbine, i.e., the gas crossing Station 5.

15-3.4.1 TURBINE WORK FOR TURBOSHAFT, TURBOPROP, AND TURBOJET ENGINES

(a) *Turboshaft engines* (see Fig. 15-3(A))

$$\Delta h_t = h_4^0 - h_5 = \bar{c}_{pt} (T_4^0 - T_5) \quad (15-22)$$

and for an ideal turbine

$$\Delta h'_t = h_4^O - h'_5 = \bar{c}_{pt} (T_4^O - T'_5) \quad (15-23)$$

(b) *Turboprop and turbojet engines* (see Fig. 15-3(B))

$$\Delta h_t = h_4^O - h_5^O = \bar{c}_{pt} (T_4^O - T_5^O) \quad (15-24)$$

and

$$\Delta h'_t = h_4^O - h_5^{O'} = \bar{c}_{pt} (T_4^O - T_5^{O'}) \quad (15-25)$$

15-3.4.2 TURBINE ISENTROPIC EFFICIENCY (η_t)

By definition, the turbine isentropic efficiency η_t is given by

$$\eta_t = \frac{\Delta h_t}{\Delta h'_t} \quad (15-26)$$

Hence, for

(a) *Turboshaft engines*

$$\eta_t = \frac{h_4^O - h_5}{h_4^O - h'_5} \approx \frac{T_4^O - T_5}{T_4^O - T'_5} \quad (15-27)$$

(b) *Turboprop and turbojet engines*

$$\eta_t = \frac{h_4^O - h_5^O}{h_4^O - h_5^{O'}} \approx \frac{T_4^O - T_5^O}{T_4^O - T_5^{O'}} \quad (15-28)$$

The values of η_t for turboshaft engines will range from 0.85 to 0.90. For the turboprop and gas-turbine jet engines, η_t will range from 0.88 to 0.95. The larger values for η_t are obtained because there is no *exit loss* charged against the turbines of the latter engines, the kinetic energy associated with the gas leaving Station 5 (see

Fig. 15-3(B)) is used for developing jet thrust, i.e., useful thrust power.

15-3.5 NOZZLE EXPANSION PROCESS AND ISENTROPIC EFFICIENCY (η_n)

Exhaust nozzles for developing thrust are employed in turboprop and gas-turbine jet engines.

The flow in a well-designed nozzle is close to being isentropic. By definition (see Fig. 15-24)

$$\eta_n = \frac{h_6^O - h_7}{h_6^O - h'_7} \approx \frac{T_6^O - T_7}{T_6^O - T'_7} \quad (15-29)$$

The value of η_n for a well-designed exhaust nozzle will range from 0.95 to 0.99 (see Chapter 4).

15-3.6 MACHINE EFFICIENCY (η_{tc})

By definition

$$\eta_{tc} = \eta_t \eta_c \quad (15-30)$$

15-4 THE TURBOSHAFT ENGINE

Fig. 12-6 illustrates schematically two arrangements for the components for a turboshaft engine; (A) a so-called single shaft arrangement, and (B) the free-turbine arrangement where the load is driven by a separate power turbine which is mechanically independent of the hot gas generator. The free-turbine arrangement has greater flexibility for meeting the load demands than does the single shaft configuration. From the viewpoint of thermodynamic analysis the operating cycle is identical for both of the configurations illustrated in Fig. 12-6.

15-4.1 DESIGN CRITERIA FOR TURBO-SHAFT ENGINE

The following criteria are useful for judging the design and performance of a turboshaft engine:

- (a) The thermal efficiency (η_{th})
- (b) The specific output (L)
- (c) The air-rate (A)
- (d) The work-ratio (U)

15-4.1.1 THERMAL EFFICIENCY (η_{th})

The thermal efficiency of a turboshaft engine is defined as the ratio of the *net useful work* delivered by the engine to the heat supplied it in the form of fuel.

Let P_{comp} denote the power expended in driving the air compressors, P_{turb} the power developed by the turbines, and P_λ the parasite power for overcoming losses. The useful or *shaftpower* delivered to the load (helicopter rotor, etc.), denoted by P_{sh} is accordingly

$$P_{sh} = P_{turb} - P_{comp} - P_\lambda \quad (15-31)$$

If \dot{Q}_i denotes the rate at which heat is supplied to the turboshaft engine, then the thermal efficiency η_{th} is given by

$$\eta_{th} = \frac{P_{sh}}{\dot{Q}_i}$$

where $\dot{Q}_i = \dot{m}_f \Delta H_c$, and ΔH_c is in B/slug.

The specific fuel consumption, denoted by SFC measured in lb of fuel per hp-hr, is accordingly

$$\underline{SFC} = \frac{2545}{\eta_{th} \dot{m}_f g_c \Delta H_c} \text{ (lb fuel/hp-hr)} \quad (15-32)$$

where $g_c = 32.174$ slug-ft/lb-sec².

15-4.1.2 SPECIFIC OUTPUT (L)

If \dot{m}_a denotes the rate at which the turboshaft engine inducts air, in slug/sec, and P_{sh} denotes the shaftpower, in hp, then the *specific output* L is given by

$$L = \frac{P_{sh}}{g_c \dot{m}_a} \text{ (hp/lb of air per sec)} \quad (15-33)$$

15-4.1.3 AIR-RATE (A)

The air-rate A is a criterion of the size of the air compressor needed for developing a specified shaftpower P_{sh} . By definition, the air-rate is the quantity of air that must be inducted by the turboshaft air to develop one shaft horsepower (1-shp). The air-rate is generally expressed in lb of air entering the compressor per shp-hr. Hence¹

$$A = \frac{2545}{L} \frac{\text{(B/hp-hr)}}{\text{(B/lb of air)}} \text{ (lb of air/hp-hr)} \quad (15-34)$$

where the specific output L is in B/lb of air.

In the interest of small weight and dimensions for the turboshaft engine, A should be small.

15-4.1.4 WORK-RATIO (U)

The work-ratio U is a criterion of the size of the turbine required for developing a specified shaftpower P_{sh} . By definition¹

$$U = P_{sh}/P_{turb} \quad (15-35)$$

The larger the work-ratio, the smaller is the required turbine. A characteristic of all gas-turbine type engines is that their work ratios are

small compared to other types of powerplants. For a turboshaft engine $U \approx 1/3$ compared to approximately 0.99 for a modern steam powerplant.

The reason for the small work-ratio of a gas turbine engine is that the turbine of such an engine must furnish a large amount of power for driving the air compressor. To obtain values of U exceeding approximately 0.3 the thermodynamic cycle for a gas-turbine type engine must be complicated by incorporating devices such as *intercoolers* (in the air compression circuit) and *reheaters* (in the hot gas expansion circuit) (see Reference 2, Chapters 6 and 7).*

A turboshaft engine (see Fig. 12-6) operating with a turbine inlet total temperature $T_4^0 \approx 2,000^\circ\text{R}$ will have a work-ratio $U \approx 1/3$, i.e., 2 hp of every 3 hp developed by the turbine is used for compressing the air inducted by the engine and only 1 hp is available as shaftpower for driving the load. Moreover, a 5 percent reduction in the isentropic efficiency of the turbine η_t results in a 15 percent reduction in the shaftpower, and a 5 percent reduction in η_c decreases the shaftpower by 10 percent. The foregoing indicates why high values of η_t and η_c are essential if good performance is to be obtained from a gas-turbine engine.

The low work-ratio of the turboshaft engine makes its specific output L sensitive to the values of η_t , η_c , and the turbine inlet temperature T_4^0 . The interdependence of L , T_4^0 , η_t , and η_c is a fundamental characteristic of gas-turbine powerplant engines.

15-4.2 THERMODYNAMIC CYCLE FOR TURBOSHAFT ENGINE AND THERMAL EFFICIENCY OF IDEAL TURBOSHAFT ENGINE (η_a)

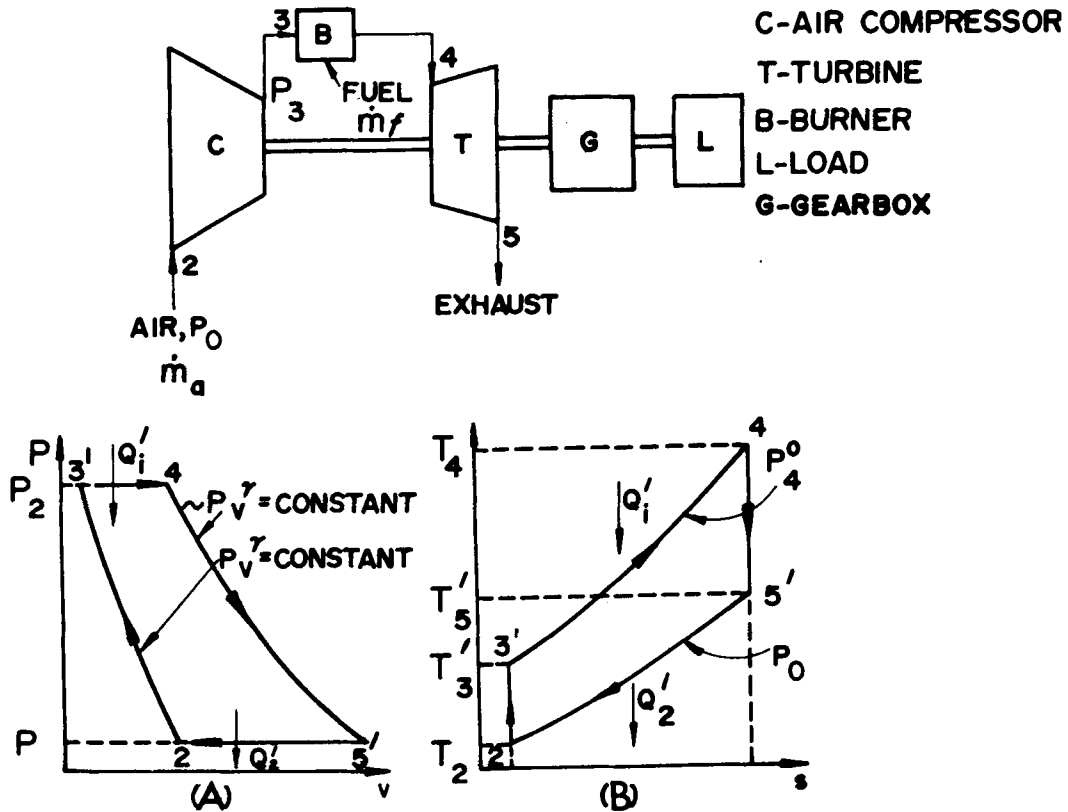
Fig. 15-4 illustrates schematically the thermodynamic cycle for an *ideal turboshaft engine*, plotted in the Pv - and Ts -planes. The

cycle applies to both the fixed-shaft and free-turbine turboshaft engines (see Fig. 15-6). The ideal cycle assumes the following:

- (a) Working fluid is an ideal gas.
- (b) Engine components are perfect, i.e., $\eta_c = \eta_B = \eta_t = 1.0$
- (c) Chemical and physical properties of the working fluid do not change as it flows through the turboshaft engine.
- (d) Mass flow rate of flow of working fluid is the same at all stations in the engine.
- (e) All of the heat added to the working fluid is transferred to it completely and instantaneously.
- (f) Working fluid expands completely in the turbine, i.e., the static pressure of the fluid leaving the turbine is equal to the ambient static pressure P_0 .

It is seen from Fig. 15-4 that the ideal cycle for the turboshaft engine comprises the isentropic compression process 2-3' followed by the isobaric ($dP = 0$) heating process 3-4', and the isentropic expansion process 4-5'. It should be noted that in the turboshaft engine all of the compression of the gas occurs in the compressor and the entire expansion process occurs in the turbine. For the turboprop engine in flight and gas-turbine jet engines a portion of the gas compression is accomplished by *ram compression* in a diffuser located upstream to the compressor. Furthermore, only a portion of the expansion of the gas occurs in the turbine and the remainder is accomplished in an exhaust nozzle.

The numerical results obtained by analyzing the ideal cycle for the turboshaft engines are of theoretical interest only. Nevertheless, the general conclusions regarding the effects of the



$$(\eta_b = \eta_c = \eta_t = 1.0)$$

Figure 15-4. Ideal Thermodynamic Cycle for a Turboshaft Engine

cycle pressure ratio (P_3^0/P_2^0) and cycle temperature ratio ($a = T_4^0/T_0$) upon the performance of the ideal turboshaft engine are indicative of their influences upon actual gas-turbine powerplant engines.

It is readily shown that the thermal efficiency of the ideal turboshaft engine, termed the *air-cycle efficiency* which is denoted by η_a is given by ^{1,2}

$$\eta_a = \eta_{th} = \frac{\Delta h'_t - \Delta h'_c}{Q'_i} = \frac{\Theta - 1}{\Theta} \quad (15-36)$$

where

$$\Theta = \left(\frac{P_3^0}{P_2} \right)^{\frac{\gamma-1}{\gamma}} = \text{cycle pressure ratio parameter}^* \quad (15-37)$$

$$\Delta h'_t = c_p T_2 a \left(\frac{\Theta - 1}{\Theta} \right) \quad (15-38)$$

$$\Delta h'_c = c_p T_2 a (\Theta - 1) \quad (15-39)$$

*If the Mach number for the working fluid is less than $M \approx 0.3$ the stagnation values P^0 and T^0 may be replaced by their static values P and T , respectively.

$$Q'_1 = c_p T_2 (a - \Theta) = \frac{\text{heat added per slug}}{\text{of air}} \quad (15-40)$$

Eq. 15-36 shows that the air cycle efficiency η_a is independent of the cycle temperature, a surprising result which is untrue for an actual engine.

15-4.3 LOSSES IN A TURBOSHAFT ENGINE CYCLE

There are several aspects in which the cycle for a real turboshaft engine differs from the ideal cycle illustrated in Fig. 15-4. The major deviations are summarized below.

- (a) The air inducted by the engine must ordinarily flow through ducting which introduce *pressure drops* at different state points in the cycle and may distort the flow pattern for the air entering the air compressor.
- (b) The air compressor does not compress the air isentropically, so that $\eta_c < 1.0$. Consequently, the compressed air leaves the compressor at a temperature $T_3 < T'_3$.
- (c) Some of the compressed air, approximately 2 percent of the total flow, is utilized for cooling the bearings of the engine and the turbine disk.
- (d) Gas-turbine engines, in general, induct tremendous quantities of atmospheric air and with it foreign material and water vapor. Consequently, the power requirements for the air compressor are affected by the water vapor in the air. It is difficult to predict with accuracy what will be the effect of dust and foreign matter in the air upon the performance of an engine. Experience has demonstrated that operating an axial flow compressor in a dust-laden atmosphere for a short period of time can reduce its isentropic efficiency η_c by at least 2 percentage points.
- (e) Losses occur in the burner due to incomplete combustion, and heat losses by thermal conduction and radiation.
- (f) There is a decrease in stagnation pressure in the burner due to momentum change and friction (see pars. 3-6 and 3-7).
- (g) The turbine exhaust gas is discharged from the engine with a high temperature, above the saturation temperature for water vapor. Consequently, the water vapor formed by burning the fuel leaves the engine as *superheated vapor* and its *enthalpy of vaporization* is lost.
- (h) There are mechanical losses due to friction in the bearings of the compressor and turbine, and in gearboxes.
- (i) The thermodynamic constants for the working fluid may have different values in the different components of the engine.
- (j) In a regenerative turboprop engine, there are pressure drops in the air (*cold*) side and the exhaust gas (*hot*) side of the regenerator.

In view of the deviations listed above an exact thermodynamic analysis of the thermodynamic cycle of a gas-turbine engine is a tedious step-by-step procedure involving engineering judgment based on experimental data ¹.

15-4.4 SIMPLIFIED ANALYSIS OF THE TURBOSHAFT ENGINE CYCLE

The comments presented in par. 15-4.3, while made specifically to the turboshaft engine, are also applicable to gas-turbine engines in

general. Similarly, the simplified thermodynamic analysis presented in this paragraph for the turboshaft engine applies in a general way to other gas-turbine engines. The simplified thermodynamic analysis of the turboshaft engine cycle is based on the following assumptions:

- (a) Working fluid is a perfect gas
- (b) Effect of fuel addition is negligible
- (c) There are no pressure drops
- (d) Compressor and turbine isentropic efficiencies are adjusted to account for bearing and parasite losses
- (e) Specific heat ratio γ is constant

The numerical results obtained by employing the simplified analysis based on the assumptions listed above are quite satisfactory for studies concerned with determining the general characteristics of gas-turbine engines, as in preliminary design studies.

Fig. 15-5 compares the actual and ideal cycles for the turboshaft engine, in the Ts -plane.

15-4.4.1 COMPRESSION WORK (Δh_c)

The enthalpy added to the air flowing through the compressor is given by Eq. 15-11. Thus

$$\Delta h_c = h_3^O - h_2^O = c_p \left(\frac{T_2^O}{\eta_c} \right) Z_c \quad (\text{B/slug of air}) \quad (15-41)$$

where the compression factor Z_c is defined by Eq. 15-9.

15-4.4.2 TURBINE WORK (Δh_t)

From Eq. 15-22, one obtains

$$\Delta h_t = h_4^O - h_5 = c_p \eta_t T_4^O Z_t \quad (15-42)$$

where η_t is defined by Eq. 15-27, and the expansion factor Z_t is given by

$$Z_t = 1 - \Theta_t \quad (15-43)$$

where

$$\Theta_t = \left(\frac{p_5^O}{p_4^O} \right)^{\frac{\gamma-1}{\gamma}} \quad (15-44)$$

15-4.4.3 SPECIFIC OUTPUT (L)

If \dot{m}_a denotes the rate at which air enters the engine, $x\dot{m}_a$ the amount of air bled for cooling purposes, and f is the fuel-air ratio; then the specific output L in B/slug of air, is given by

$$L = (1 - x) (1 + f) \eta_{Mt} \Delta h_t - \frac{\Delta h_c}{\eta_{Mc}} - \Sigma \Delta h_\lambda \quad (\text{B/slug of air}) \quad (15-45)$$

where $\Sigma \Delta h_\lambda$ denotes the sum of the parasite losses.

15-4.4.4 HEAT ADDED (Q_i)

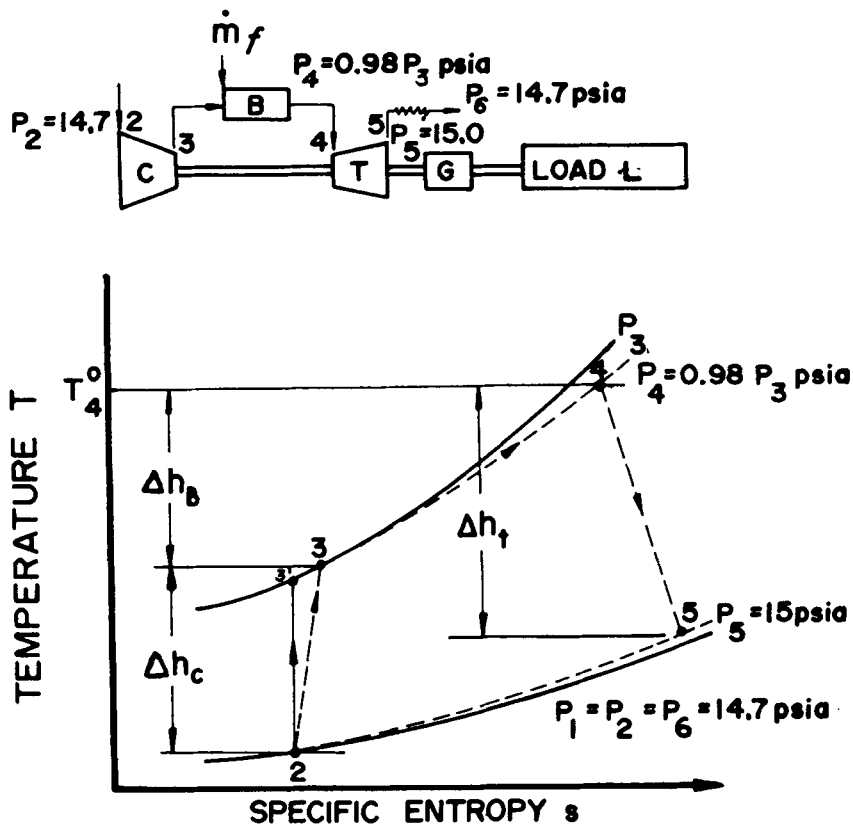
If Δh_c denotes the calorific value of the fuel, in B/slug, and Q_i is the heat added, then

$$Q_i = f \Delta h_c = (1 + f) h_4^O - h_3^O \quad (\text{B/slug of air}) \quad (15-46)$$

15-4.4.5 THERMAL EFFICIENCY (η_{th})

By definition

$$\eta_{th} = \frac{L}{Q_i}$$



$$T_2 = 520^\circ\text{R}, T_4^\circ = 1700^\circ\text{R}, \eta_c = 0.85, \eta_b = 0.98$$

$$\eta_c = 0.87, \eta_{Mc} = \eta_{Mt} = 0.98, \eta_g = 1.00$$

Figure 15-5. Comparison of Actual and Ideal Turbohaft Engine Cycles

If $x = 0$, and $c_p = \text{constant}$, then¹

$$\eta_{th} = \eta_a \frac{a\eta_t - \frac{\Theta}{\eta_c}}{a - \frac{\Theta\eta_a}{\eta_c}} \quad (15-47)$$

where

$$\eta_a = \text{air cycle efficiency} = (\Theta - 1)/\Theta$$

$$a = T_4^\circ/T_2 = \text{cycle temperature ratio}$$

$$\Theta = \left(\frac{P_3^\circ}{P_2} \right)^{\frac{\gamma-1}{\gamma}} = \text{cycle pressure ratio parameter} \quad (\text{Eq. 15-37})$$

15-4.4.6 AIR-RATE (A)

By definition (see Eq. 15-34)

$$A = \frac{2545}{\eta_{Mt}(1-x)(1+f)\Delta h_t - \frac{\Delta h_c}{\eta_{Mc}} - \Sigma \Delta h_\lambda} \quad (15-48)$$

15-4.4.7 WORK-RATIO (U)

By definition (see par. 15-4.1.4)

$$U = \frac{L}{(1-x)(1+f)\Delta h_t \eta_{Mt}} \quad (15-49)$$

where L is given by Eq. 15-45.

15-4.4.8 SPECIFIC FUEL CONSUMPTION (SFC)

The specific fuel consumption in pounds of fuel per horsepower-hour, denoted by SFC, is accordingly

$$\text{SFC} = \frac{2545}{\eta_{th} \Delta H_c}$$

where ΔH_c is in B/lb.

If the analysis takes into account the pressure drops at the pertinent states in the cycle, then the only parasitic loss that needs to be considered is that for supplying the power to drive the auxiliary equipment.

15-4.5 PERFORMANCE CHARACTERISTICS OF THE TURBOSHAFT ENGINE

It is apparent from par. 15-4.4 that the performance parameters for a turboshaft engine – i.e., η_{th} , L , A , and U – depend on a large number of variables. Consequently, the design performance characteristics of such an engine are determined by selecting a *reference engine* and then determining the effect due to varying one parameter at a time. It should be noted that the performance characteristics are sets of curves developed for a series of engines having *constant values* for specified parameters. These parameters cannot be maintained constant when a single engine is operated over a wide range of conditions. Each point of a curve in a performance characteristic chart represents the performance of a different engine.

When a specific engine is operated over a range of conditions – such as altitude, flight speed, turbine inlet temperature, etc. – the corresponding performance curves are termed the *operating characteristics* for the engine.

The equations presented in par. 15-4.4 can be employed for determining the performance characteristics of turboshaft engines.

15-4.5.1 EFFECT OF CYCLE PRESSURE RATIO (Θ)

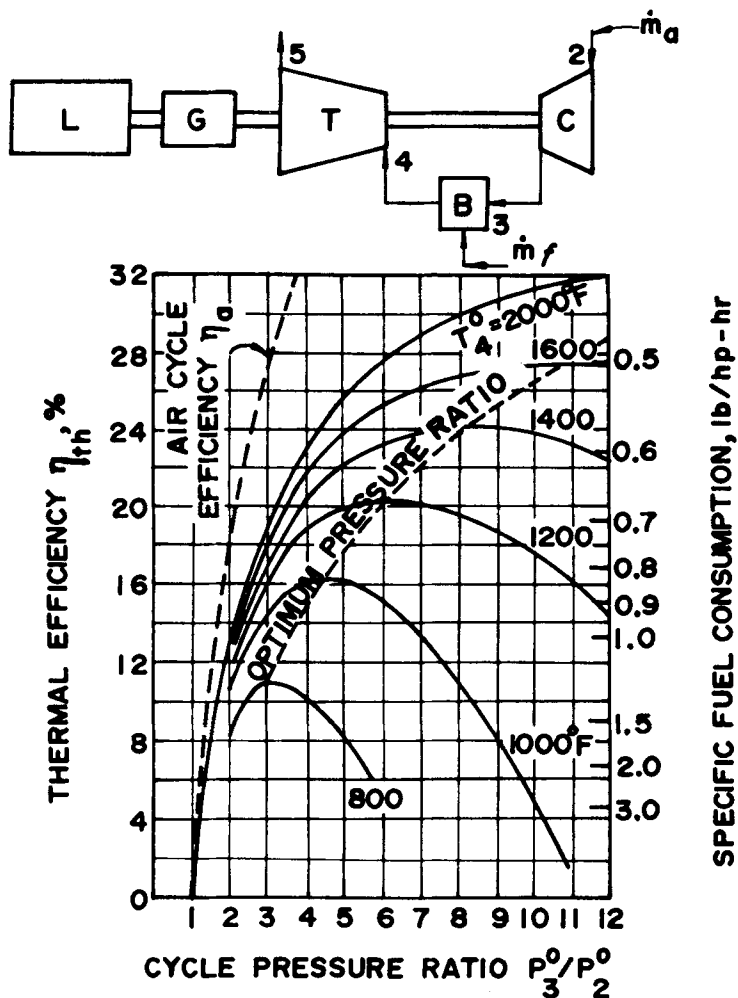
If parameters – such as $T_0 = T_2$, η_t , η_c , and $\alpha = T_4^0$ – are held constant, Eq. 15-47 shows that $\eta_{th} = 0$ for two conditions: (a) $\Theta = 1$ and (b) $\Theta = \alpha \eta_t \eta_c$. This signifies that η_{th} has a maximum value between those two values of Θ . The cycle pressure ratio $P_3^0/P_2^0 = P_3^0/P_0^0$ which yields the maximum value for η_{th} is termed the optimum pressure ratio².

15-4.5.2 EFFECT OF CYCLE PRESSURE RATIO (Θ) AND TURBINE INLET TEMPERATURE (T_4^0)

Fig. 15-6 presents η_{th} as a function of the cycle pressure ratio P_3^0/P_2^0 with the turbine inlet temperature T_4^0 as a parameter. Fig. 15-7 presents the corresponding curves for the specific output L as a function of P_3^0/P_2^0 .

Fig. 15-6 presents the thermal efficiency η_{th} for turboshaft engines as a function of the cycle pressure ratio $P_3^0/P_2^0 = P_3^0/P_0^0$, with turbine inlet temperature T_4^0 as a parameter. For comparison, the air cycle efficiency (see Eq. 15-36) is also plotted. Each point on every curve refers to a different turboshaft engine, and the parameters for the reference engine are presented on the chart.

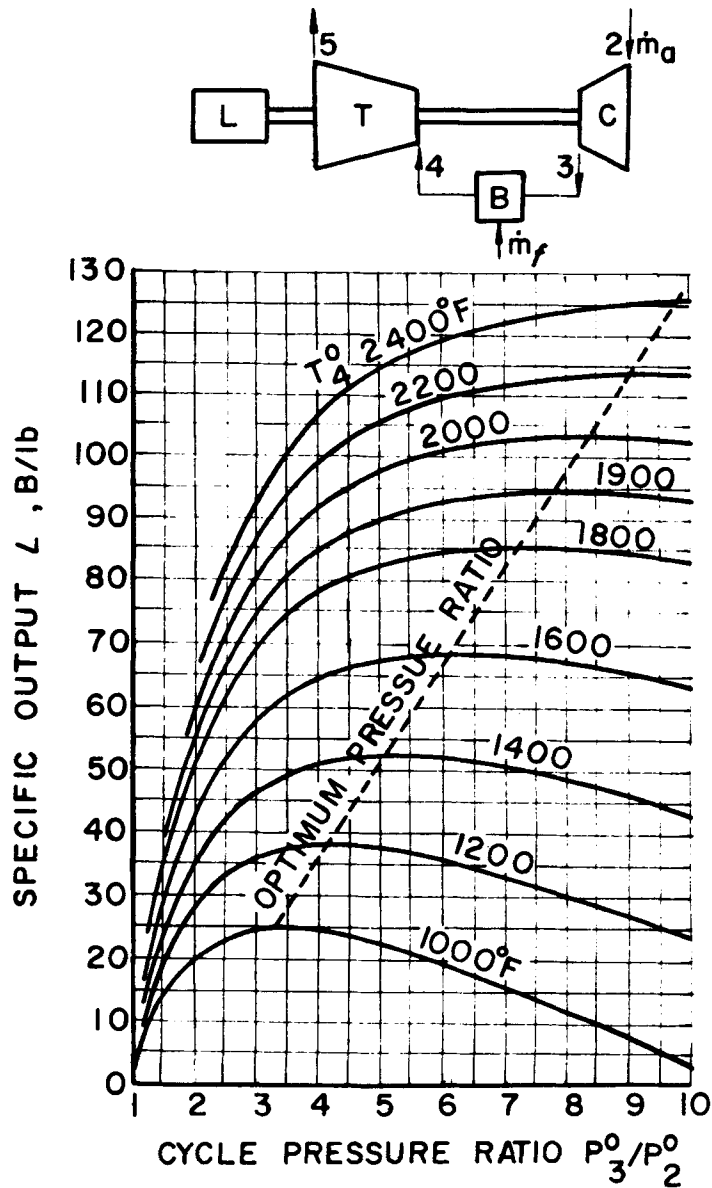
Fig. 15-6 shows that, for a given value of T_4^0 , increasing the cycle pressure ratio P_3^0/P_2^0 increases η_{th} until a maximum value is attained. Further increases in P_3^0/P_2^0 causes the thermal



$$\eta_M = \eta_B = \eta_g = 1.0; \eta_c = 0.84, \eta_t = 0.85, T_2 = T_0 = 530^\circ R$$

$\gamma = 1.395, \Delta H_c = 18,500 \text{ B/lb OF FUEL, PERFECT GAS,}$
NO PRESSURE DROPS

Figure 15-6. Thermal Efficiency of Turboshaft Engine As a Function of the Cycle Pressure Ratio, With the Turbine Inlet Temperature as a Parameter



$$\eta_M = \eta_B = 1.0, \eta_t = 0.85, \eta_c = 0.84, T_2 = 530^\circ \text{R}, \gamma = 1.395,$$

$\Delta H_c = 18,500 \text{ B/lb}$, PERFECT GASES, NO PRESSURE DROPS.

Figure 15-7. Specific Output of Turboshaft Engine as a Function of the Cycle Pressure Ratio, With the Turbine Inlet Temperature as a Parameter

efficiency η_{th} to decrease (see par. 15-4.5.1). The curves show that although the air cycle efficiency η_a – which applies to an ideal turboshaft engine (see par. 15-4.2.1) – depends only upon the cycle pressure ratio P_3^O/P_2^O , the thermal efficiency η_{th} for a real turboshaft engine, however, is sensitive not only to P_3^O/P_2^O but also to the turbine inlet temperature T_4^O .

Fig. 15-7 presents the curves corresponding to those in Fig. 15-6, for the specific output L in B per lb of air. It is evident that for any value of T_4^O , the turbine inlet temperature, the maximum value for η_{th} is obtained at a larger value of P_3^O/P_2^O than that for obtaining the maximum value for the specific output L . For example, for $T_4^O = 1600^\circ\text{F}$, η_{th} is a maximum when $P_3^O/P_2^O = 10.7$, while L attains its maximum value when $P_3^O/P_2^O = 6.1$.

Charts such as those presented in Figs. 15-6 and 15-7 are called *design point charts* and as mentioned earlier each point of each curve applies to a different turboshaft engine. The design point charts do, however, give some indication of the general manner in which η_{th} and L are affected when a specific engine is operated at an *off-design point* (condition) – provided one has a knowledge of the off-design behavior of the components of the engine. When the turboshaft engine is operated at a speed less than its design speed, for example, there is a decrease in the cycle pressure ratio P_3^O/P_2^O , turbine inlet temperature, air flow rate, etc. A reduction in P_3^O/P_2^O , causes both η_{th} and L to decrease. In general, the off-design values for η_{th} and L are smaller than the design values corresponding to the reduced cycle pressure ratio². A detailed discussion of the part-load performance of gas-turbine powerplants is presented in References 1 and 3.

15-4.5.3 AIR-RATE (A)

Fig. 15-8 presents the air-rate A , lb of air per brake horsepower-hour, as a function of the

cycle pressure ratio P_3^O/P_2^O , with T_4^O , the turbine inlet temperature, as a parameter. It is evident that increasing T_4^O decreases the air-rate at all values of cycle pressure ratios, indicating that raising T_4^O increases the work obtained per unit mass of air, an expected result.

15-4.5.4 WORK-RATIO ($U = L/L_t$)

Fig. 15-9 presents the work-ratio U as a function of the cycle pressure ratio P_3^O/P_2^O , with T_4^O as a parameter. Reducing the turbine inlet temperature T_4^O reduces the work ratio at all values of P_3^O/P_2^O . For current turboshaft engines $T_4^O \approx 2260^\circ\text{R}$ and $P_3^O/P_2^O \approx 11$, so that $U \approx 0.3$, e.g., $1/3$ (see par. 15-4.1.4).

The machine efficiency η_{tc} of the turboshaft engine exerts a large influence upon the specific output L (see par. 15-3.6).

15-4.5.5 EFFECT OF MACHINE EFFICIENCY (η_{tc})

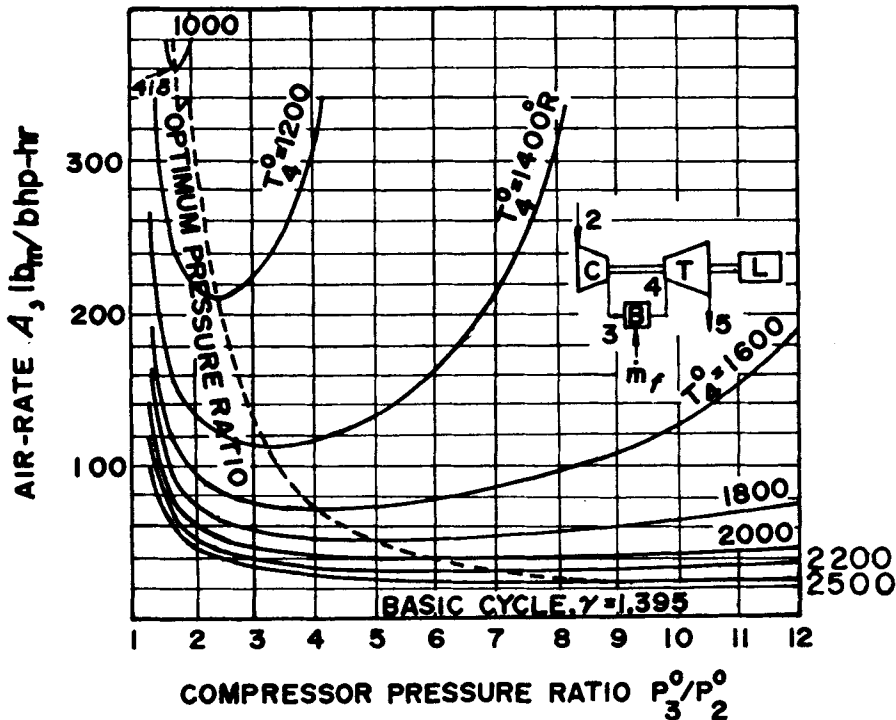
Fig. 15-10 presents η_{th} as a function of the cycle pressure ratio P_3^O/P_2^O for a turboshaft engine having the following characteristics:

$$\eta_M = \eta_B = \eta_g = 1.0; \eta_c = 0.84; T_2 = T_0 = 520^\circ\text{R}; T_4^O = 2000^\circ\text{R}$$

In the same figure curves are plotted for different values of η_c with $\eta_t = 0.85 = \text{constant}$, and for different values of η_t with $\eta_c = 0.84 = \text{constant}$.

The curves in Fig. 15-10 show that reducing either η_c or η_t from the standard values of 0.84 and 0.85, respectively, causes large decreases in η_{th} . Furthermore, the cycle pressure ratio P_3^O/P_2^O for the maximum value of η_{th} decreases if either η_c or η_t is reduced.

Fig. 15-11 presents the specific output L as a function of the cycle pressure ratio P_3^O/P_2^O , with



$$\eta_M = \eta_B = \eta_g = 1.0, \eta_t = 0.85, \eta_c = 0.84, T_2 = T_0 = 530^\circ\text{R}$$

$\Delta H_c = 18,500$ B/lb OF FUEL, PERFECT GAS, NO PRESSURE DROPS

Figure 15-8. Air-rate of the Turboshaft Engine as a Function of the Cycle Pressure Ratio, With the Turbine Inlet Temperature as a Parameter

the machine efficiency η_{tc} as a parameter, and with $T_4^0 = 1500^\circ\text{F} = \text{constant}$.

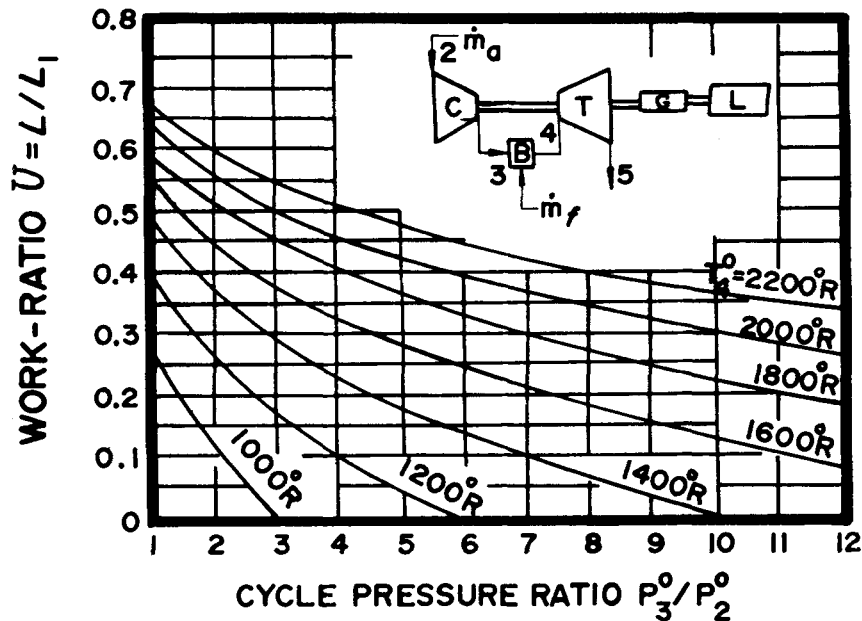
The curves show that to increase L , both η_{tc} and P_3^0/P_2^0 have to be increased, and that for each value of η_{tc} (and also of T_4^0) there is an optimum value for P_3^0/P_2^0 . Furthermore, for a given value of η_{tc} , the value P_3^0/P_2^0 which is optimum for the specific output L , is smaller than that required to give the maximum value for η_{th} (see Fig. 15-11). If $\eta_{tc} > 0.75$ approximately, L is less sensitive to increases in the cycle pressure ratio than η_{th} .

Fig. 15-12 is a chart for determining the optimum cycle pressure ratio P_3^0/P_2^0 for different values of the turbine inlet temperature

T_4^0 and η_{tc} (assuming $\eta_t = \eta_c$). Increasing T_4^0 while holding η_{tc} constant requires raising the cycle pressure ratio if the maximum value is to be obtained for L , the specific output. If T_4^0 is to be maintained constant and L is to be maximized, then if η_{tc} is increased the pressure ratio P_3^0/P_2^0 must also be increased.

15-4.5.6 EFFECT OF AMBIENT AIR TEMPERATURE ($T_0 = T_2$)

The specific output of an air-breathing engine is practically proportional to the mass rate at which it inducts atmospheric air. Furthermore, the work required for compressing the air



$$\eta_M = \eta_B = \eta_g = 1.0; \eta_c = 0.84; \eta_t = 0.85, T_2 = T_0 = 530^\circ\text{R}$$

$$\gamma = 1.395, \Delta h_c = 18,500 \text{ B/lb OF FUEL, PERFECT GAS}$$

NO PRESSURE DROPS

Figure 15-9. Work-ratio of Turboshift Engine as a Function of the Cycle Pressure Ratio, With the Turbine Inlet Temperature as a Parameter

Δh_c , in B/slug, is directly proportional to T_2^0 all other factors remaining unchanged.

Fig. 15-13 presents η_{th} , U , A , and L as functions of the air intake temperature $T_2 = T_0$ for turboshaft engines having fixed values for the parameters presented in the figure. The chart shows that the intake air temperature affects the *design-point performance* of the basic turboshaft engine. A low value for T_2 is beneficial.

15-4.5.7 EFFECT OF PRESSURE DROPS

It is important that a turboshaft engine be designed so that it operates with small pressure

drops. The pressure drops which lower P_2^0 make it necessary to increase the pressure ratio of the compressor if the cycle pressure is to be maintained; consequently, the compression work is increased. Pressure drops either upstream from or downstream from the turbine reduce the turbine expansion ratio P_5^0/P_4^0 and hence, the specific output of the turbine L_t .

Fig. 15-14 presents η_{th} and L as functions of P_3^0/P_2^0 for a turboshaft engine, with pressure drop ΔP_λ as a parameter. If $\Delta P_\lambda = 0.2 P_3^0$, with $P_3^0/P_2^0 = 8$, the thermal efficiency η_{th} decreases from 0.26 to 0.19 and L from 58 B/lb of air to 42 B/lb of air, compared to the engine with $\Delta P_\lambda = 0$.

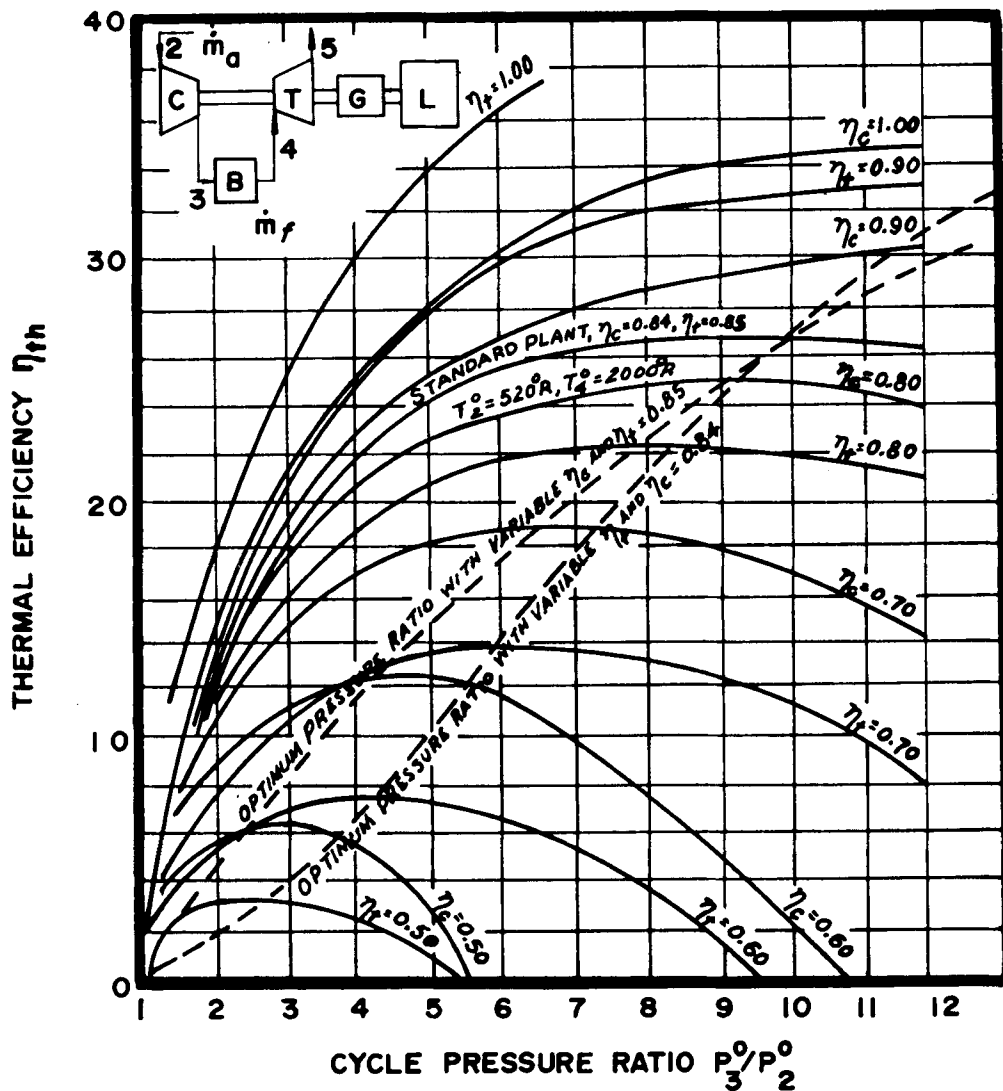


Figure 15-10. Thermal Efficiency of Turboshaft Engine as a Function of the Cycle Pressure Ratio, With η_c and η_t as Parameters

15-4.6 MODIFICATIONS TO BASIC TURBO-SHAFT ENGINE TO IMPROVE ITS PERFORMANCE

The following modifications to the basic gas-turbine powerplant cycle have been applied in several stationary gas-turbine powerplants:

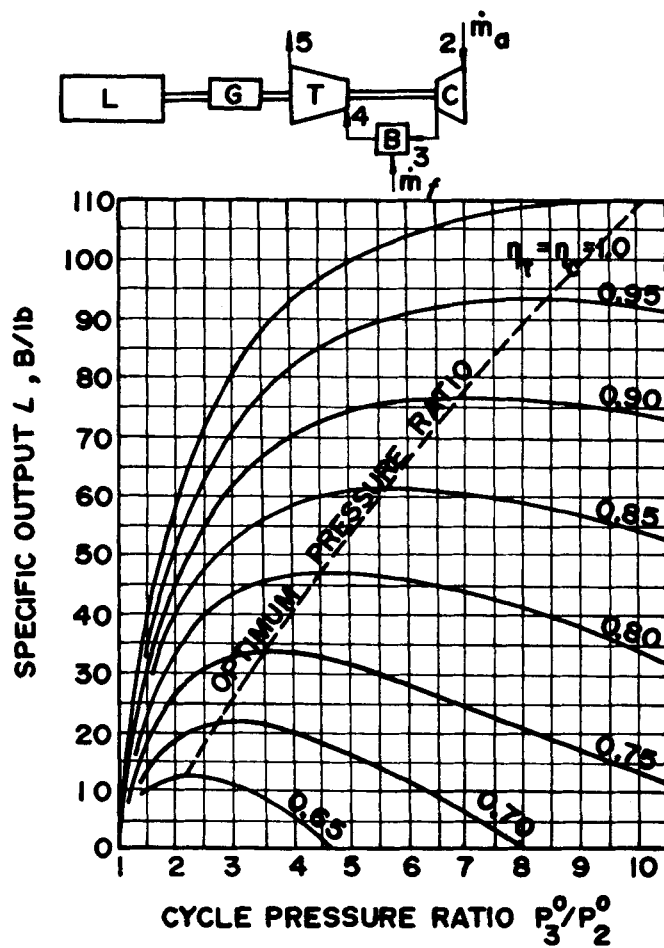
- (a) regeneration – for improving the thermal efficiency of the thermodynamic cycle;

- (b) intercooling – which reduces the work of compression and increases the specific output; and

- (c) reheating – which increases the specific output of the powerplant.

Detailed discussions of these cycle modifications are presented in Reference 2, Chapter 2.

The aforementioned cycle modifications have been applied successfully to stationary and



$\eta_M = \eta_B = \eta_g = 1.0, T_4^0 = 1500^\circ\text{F}, T_0 = T_2 = 70^\circ\text{F}, \gamma = 1.395$
 PERFECT GASES, NO PRESSURE DROPS

Figure 15-11. Specific Output of Turboshaft Engine as a Function of the Cycle Pressure Ratio for Different Values of Machine Efficiency

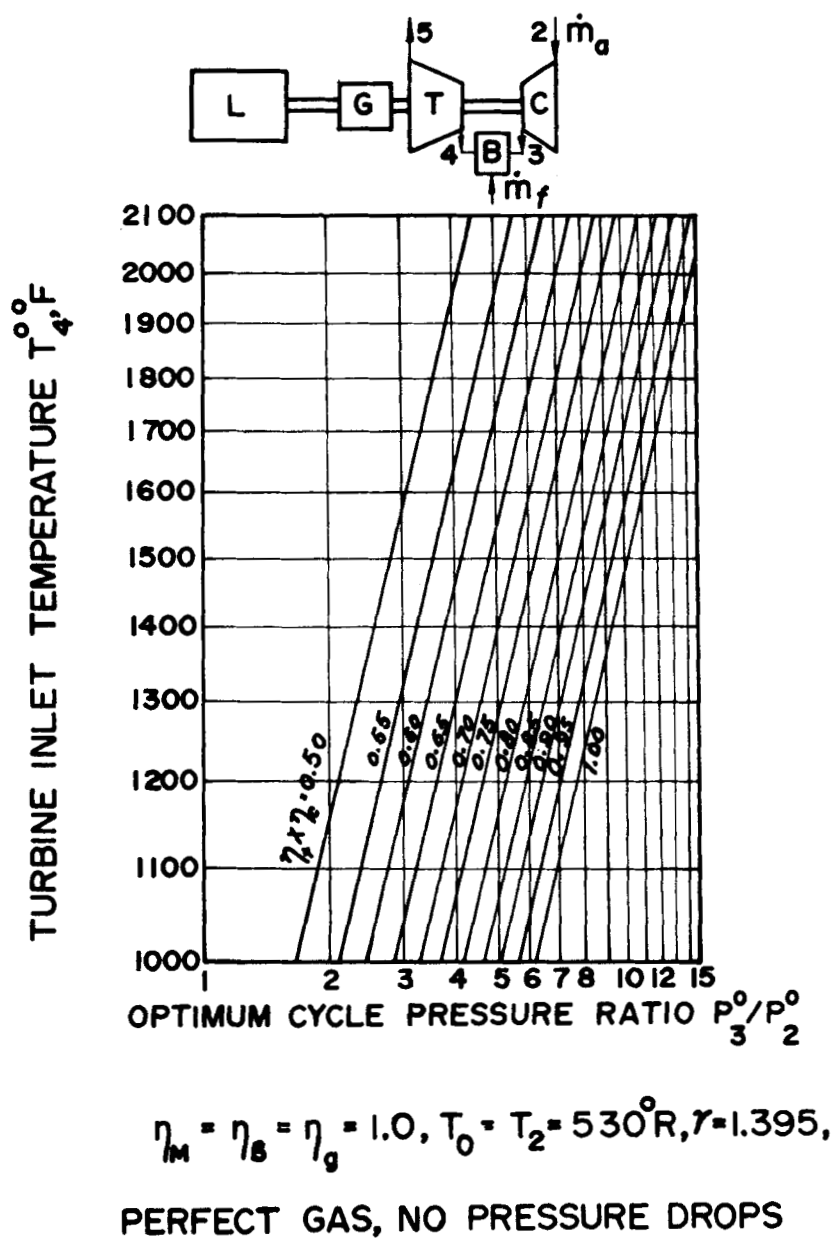
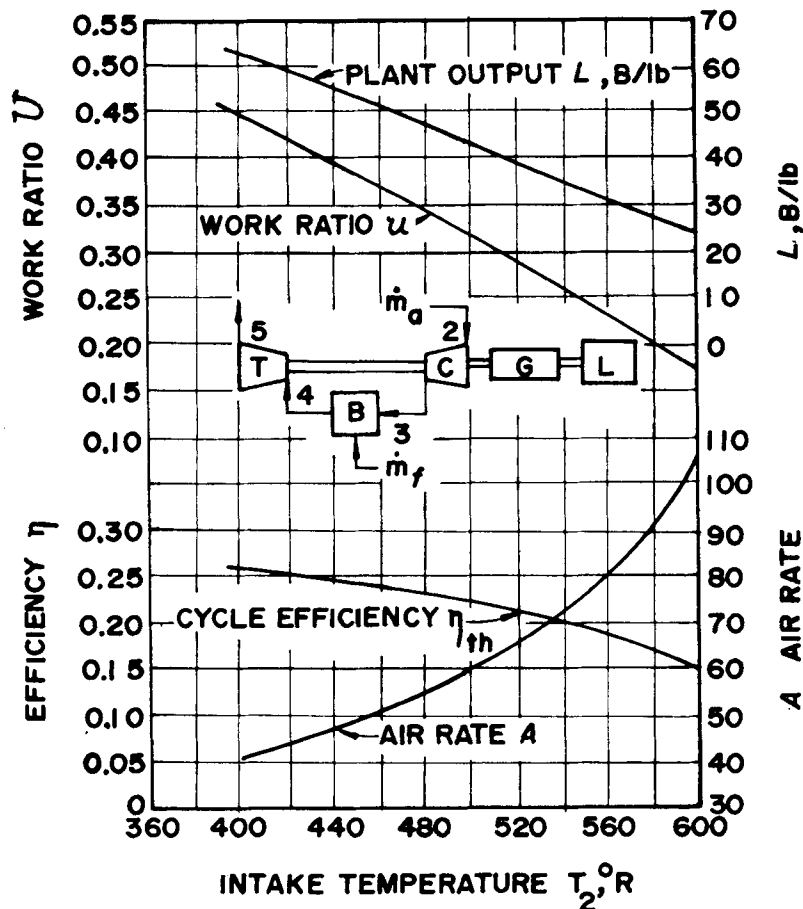


Figure 15-12. Turbine Inlet Temperature T_4° as a Function of the Optimum Cycle Pressure Ratio for Maximum Specific Output (Turboshaft Engine)



$$\eta_M = \eta_B = \eta_g = 1.0, \eta_f = 0.85, \eta_c = 0.84, T_4^0 = 1660^\circ R, P_3^0/P_2^0 = 6.0, \gamma = 1.395$$

PERFECT GAS, NO PRESSURE DROPS

Figure 15-13. Effect of Air Intake Temperature ($T_0 = T_2$) Upon the Designpoint Performance Characteristics of Turbo shaft Engine

marine gas-turbine powerplants, where weight and volume limitations are not as severe as they are for aircraft and ground vehicle turboshaft engines. Currently, the application of regeneration to turboshaft engines for helicopter and/or ground vehicle application is receiving serious development and engineering test.

15-5 REGENERATIVE TURBOSHAFT ENGINE

The thermal efficiency of the turboshaft engine can be raised by incorporating a gas-to-gas heat exchanger, called a *regenerator*, in the manner illustrated schematically in

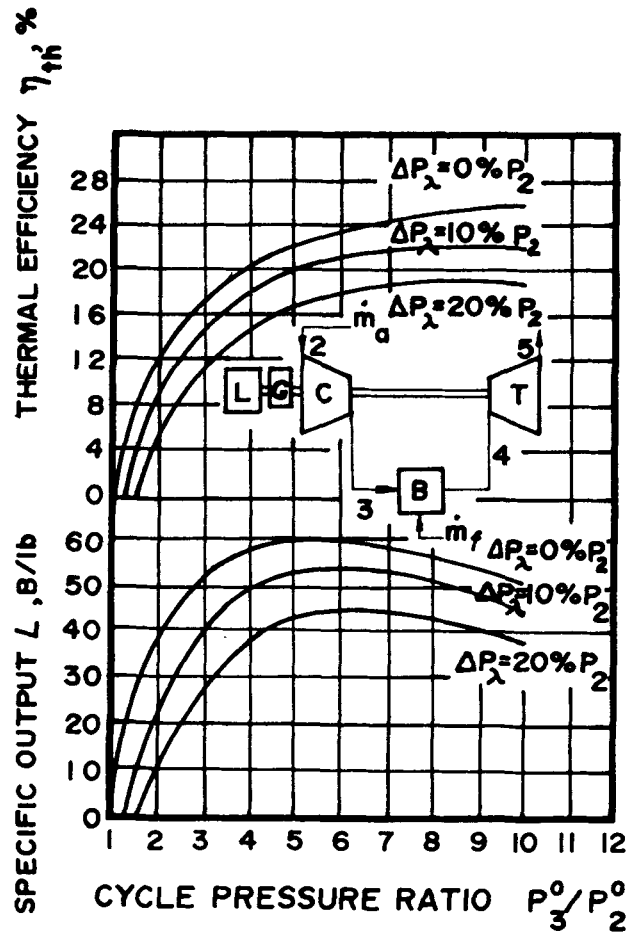


Figure 15-14. Effect of Pressure Drop on the Specific Output and Thermal Efficiency of Turboshaft Engine

Figs. 15-15(A) and 15-15(B). The compressed air discharged by the air compressor C flows through the *cold-side* of the regenerator R and is heated by the hot gas discharged from the turbine T that flows through the *hot-side* of the regenerator. A portion of the enthalpy of the turbine exhaust gas is transferred to the compressed air entering the burner B. Consequently, $h_{3R} > h_3$ and less fuel is required to raise the temperature of the working fluid to the turbine inlet temperature T_4^0 .

15-5.1 THE REGENERATION PROCESS

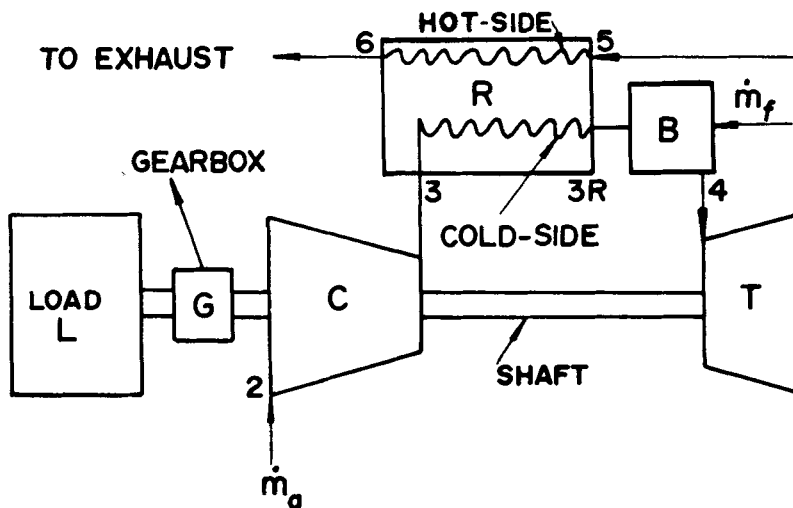
The compressed air and the turbine exhaust gas – hereafter termed the *hot gas* – flowing

through the regenerator may be arranged to form either a *counterflow* heat exchanger, as illustrated in Fig. 15-15, or a *parallel flow* heat exchanger.

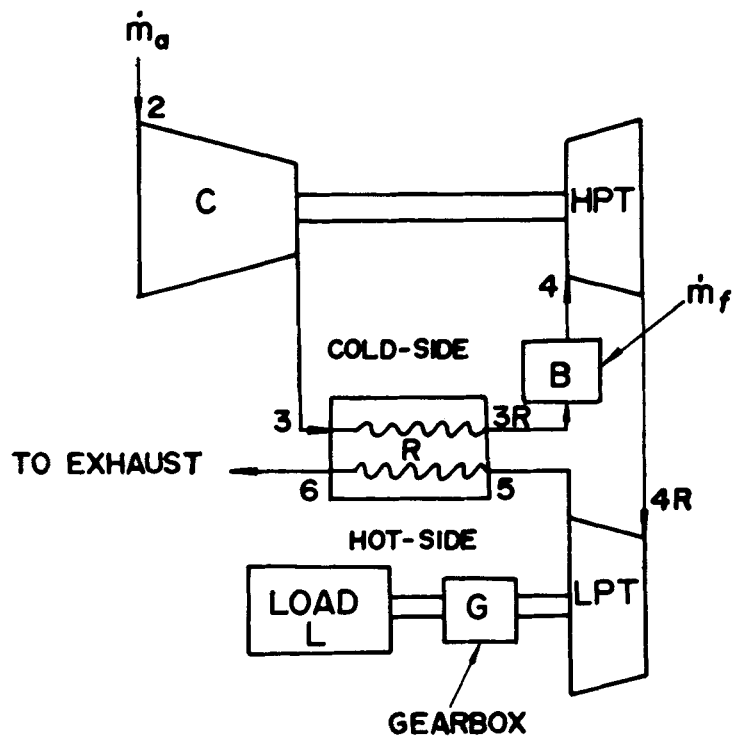
Let h_3^0 denote the specific stagnation enthalpy for the air entering the *cold-side* of the regenerator, h_5^0 the specific stagnation enthalpy for the hot gas entering the *hot-side*, and Δh_R denote the specific enthalpy available for heat transfer in the regenerator. Thus*

$$\Delta h_R = h_5^0 - h_3^0 \approx h_5 - h_3 \text{ (B/slug)} \quad (15-50)$$

*Usually the flow velocities in the regenerator are small enough that the static values may be employed.



(A) SINGLE SHAFT REGENERATIVE TURBOSHAFT ENGINE



(B) FREE TURBINE (LPT) ARRANGEMENT OF A REGENERATIVE TURBOSHAFT ENGINE

Figure 15-15. Component Arrangements for a Regenerative Turboshaft Engine

As a result of the heat transfer, the specific enthalpy of the compressed air is raised from h_3 to h_{3R} . Simultaneously, the specific enthalpy of the hot gas decreases from h_5 to h_6 .

Let Q_R denote the amount of heat transferred from the hot gas to the compressed air. Then

$$Q_R = \dot{m}_g (h_5^0 - h_3^0) = \dot{m}_a (h_{3R}^0 - h_3^0) \quad (15-51)$$

where

\dot{m}_g = mass rate of flow of hot gas, slug/sec

\dot{m}_a = mass rate of flow of compressed air, slug/sec

Let \bar{c}_{pa} and \bar{c}_{pg} denote the mean values of the specific heats of the compressed air and hot gas, respectively, for their respective temperature ranges. Then

$$\dot{m}_a \bar{c}_{pa} (T_{3R} - T_3) = \dot{m}_g \bar{c}_{pg} (T_5 - T_6) \quad (\text{B/sec}) \quad (15-52)$$

15-5.1.1 REGENERATOR EFFECTIVENESS (e_R)

By definition, the *regenerator effectiveness* (also called the *thermal ratio*), denoted by e_R , is given by

$$\begin{aligned} e_R &= \frac{Q_{\text{trans}}}{Q_{\text{avail}}} = \frac{\dot{m}_a (h_{3R} - h_3)}{\dot{m}_g (h_5 - h_3)} \\ &= \frac{\dot{m}_a \bar{c}_{pa} (T_{3R} - T_3)}{\dot{m}_g \bar{c}_{pg} (T_5 - T_3)} \end{aligned} \quad (15-53)$$

For engineering purposes it introduces no significant error if one assumes that $\dot{m}_a \bar{c}_{pa} \approx \dot{m}_g \bar{c}_{pg}$. Hence

$$e_R = \frac{T_{3R} - T_3}{T_5 - T_3} = \frac{T_5 - T_6}{T_5 - T_3} \quad (15-54)$$

In most designs the velocities of the air and hot gas are kept low enough to avoid excessive *pressure drops* in the cold-side and hot-side, respectively. Consequently, the stagnation values are not used in Eqs. 15-53 and 15-54.

The heat not recovered in the regenerator, denoted by λ_R , is given by

$$\lambda_R = 1 - e_R \quad (15-55)$$

15-5.1.2 EFFECT OF PRESSURE DROPS IN THE REGENERATOR

To obtain a high thermal efficiency from a regenerative turboshaft engine, the pressure drops ΔP_a and ΔP_g for the cold-side and hot-side of the regenerator must be kept low. This requirement is inconsistent, however, with the demand that the convective heat transfer rates be as large as possible.

The pressure drop ΔP_a reduces the cycle pressure ratio P_4/P_2 below that for the air compressor P_3/P_2 . Similarly, the pressure drop ΔP_g increases the turbine back pressure.

Let $\Delta h_{\lambda R}$ denote the decrease in the specific output of a regenerative turboshaft engine due to pressure drops in the regenerator. It can be shown that²

$$\Delta h_{\lambda R} \approx 7.73 (1+f) \left(\frac{\gamma-1}{\gamma} \right) T_5' \eta_t \left[\frac{\Delta P_g}{(P_g)_0} + \frac{\Delta P_a}{(P_a)_0} \right] \quad (15-56)$$

where

$f = \dot{m}_f / \dot{m}_a$ = fuel-air ratio for the regenerative turboshaft engine

γ = mean specific heat ratio for the air flowing through the cold-side of the regenerator

T'_5 = the isentropic value of T_5 based on $\Delta P_a = \Delta P_g = 0$

$(P_g)_0$ = pressure of air leaving the compressor based on $\Delta P_g = 0$

$(P_a)_0$ = pressure of hot gas leaving the turbine based on $\Delta P_a = 0$

ΔP_a = pressure drop in cold-side of the regenerator

ΔP_g = pressure drop in hot-side of the regenerator

η_t = isentropic efficiency of the turbine (see par. 15-3.4.2)

Eq. 15-56 is an approximate equation which expresses the loss in specific output, in B/slug of air, in terms of the pressure drops ΔP_a and ΔP_g . If $\Delta P_a = \Delta P_g$, then ΔP_g has a larger deleterious effect upon the thermal efficiency of the regenerative turboshaft engine.

In preliminary design point studies, it is convenient to neglect the influence of ΔP_a and ΔP_g upon the actual pressures in the engine cycle, and to subtract the loss $\Delta h_{\lambda R}$ from the output of the basic turboshaft cycle. The value of $\Delta h_{\lambda R}$, in B/slug of air, in general, increases with the regenerative effectiveness e_R . The values of $\Delta h_{\lambda R}$ listed in Table 15-2 as a function of e_R , are recommended for preliminary studies only. For an accurate performance analysis the actual cycle pressures should be employed together with pertinent experimental data.

For aircraft applications the requirement of lowest possible regenerator weight indicates that to achieve values of $e_R \approx 0.9$ would require rotary regenerators.

TABLE 15-2

VALUES OF LOSS IN SPECIFIC OUTPUT ($\Delta h_{\lambda R}$) AS A FUNCTION OF REGENERATOR EFFECTIVENESS (e_R) (FOR APPROXIMATE PRELIMINARY DESIGN STUDIES)

e_R	$\Delta h_{\lambda R}$ (B/slug of air)
0.50	17.7
0.75	32.2
0.90	70.1

15-5.2 REGENERATOR HEAT TRANSFER SURFACE AREA AND REGENERATOR EFFECTIVENESS

The required regenerator heat transfer surface area denoted by S , the regenerator effectiveness e_R , and the shaft horsepower of the engine P_{sh} are related by

$$S/P_{sh} = \bar{c}_{pa} \frac{A}{U} \frac{e_R}{\lambda_R} \quad (15-57)$$

where

A = the air-rate, slug of air per hp-hr

U = the overall heat transfer coefficient for the regenerator, B/(hr) (sq ft) ($^{\circ}$ R)

S = effective heat-transfer surface, sq ft

P_{sh} = shaft horsepower of the engine

15-5.3 CYCLE ANALYSIS FOR REGENERATIVE TURBOSHAFT ENGINE

The analysis is based on the same assumptions as those for the turboshaft engine (see par. 15-4.4).

15-5.3.1 TEMPERATURE OF AIR LEAVING AIR COMPRESSOR (T_3)

From Eq. 15-13, since $T_2 = T_0$, one obtains

$$T_3 = T_0 \left(1 + \frac{\Theta - 1}{\eta_c} \right) \quad (15-58)$$

where cycle pressure ratio parameter Θ is given by

$$\Theta = \left(\frac{P_3^O}{P_0} \right)^{\frac{\gamma-1}{\gamma}}$$

15-5.3.2 TEMPERATURE OF GAS LEAVING TURBINE (T_5)

From Eq. 15-27, replacing T_4^O by T_4 , one obtains

$$T_5 = T_4 - \eta_t (T_4 - T_5') \quad (15-59)$$

The isentropic turbine exhaust temperature T_5' is given by

$$T_5' = \frac{T_4}{\Theta} \quad (15-60)$$

Introducing the cycle temperature ratio $\alpha = T_4/T_0$ and Eq. 15-60 into Eq. 15-58, yields

$$T_5 = \alpha T_0 (1 - \eta_t \eta_a) \quad (15-61)$$

where η_a is the air cycle efficiency given by Eq. 15-36, and Θ is the cycle pressure ratio parameter given by Eq. 15-37, with P_3^O/P_2 replaced by P_3/P_0 .

15-5.3.3 HEAT SUPPLIED THE REGENERATIVE TURBOSHAFT ENGINE (Q_{iR})

The heat added to the working fluid is the enthalpy change $(h_4 - h_3)$ less the heat Q_R transferred to the compressed air flowing through the regenerator; Q_R depends on the regenerator effectiveness e_R . Hence

$$Q_{iR} = \frac{c_p}{\eta_B} [(T_4 - T_3) - e_R(T_5 - T_3)] \quad (15-62)$$

Substituting for T_3 and T_5 from Eqs. 15-58 and 15-60, respectively, into Eq. 15-62, yields

$$Q_{iR} = \frac{c_p T_0}{\eta_B} (\alpha y - z) \quad (15-63)$$

where

$$y = 1 - (1 - \eta_t \eta_a) e_R \quad (15-64)$$

and

$$z = (1 - e_R) \left(1 + \Theta \frac{\eta_a}{\eta_c} \right) \quad (15-65)$$

where

$$\Theta = \left(\frac{P_3}{P_0} \right)^{\frac{\gamma-1}{\gamma}} \text{ and } \eta_a = \frac{\Theta - 1}{\Theta} \quad (15-66)$$

15-5.3.4 SPECIFIC OUTPUT OF REGENERATIVE TURBOSHAFT ENGINE ($L/c_p T_0$)

Assuming, for convenience, that the mechanical efficiencies $\eta_{Mc} = \eta_{Mt} = \eta_g = 1$, the specific output for a regenerative turboshaft engine is given by

$$L = c_p T_0 \left(\alpha \eta_t - \frac{\Theta}{\eta_c} \right) \eta_a \text{ (B/slug of air)}$$

The dimensionless specific output $L/c_p T_0$ is accordingly

$$\frac{L}{c_p T_0} = \left(\alpha \eta_t - \frac{\Theta}{\eta_c} \right) \eta_a \quad (15-67)$$

Eq. 15-67 applies to both the turboshaft and regenerative turboshaft engines.

15-5.3.5 THERMAL EFFICIENCY OF REGENERATIVE TURBOSHAFT ENGINE (η_{th})

The thermal efficiency is obtained from Eqs. 15-63 and 15-67. Thus

$$\eta_{th} = \frac{L}{Q_{iR}} = \left(\frac{\eta_t a - \frac{\Theta}{\eta_c}}{ay - z} \right) \eta_B \eta_a \quad (15-68)$$

Eq. 15-68 is a general expression for the thermal efficiency of a gas-turbine powerplant engine. It applies to both the regenerative and nonregenerative turboshaft engines. The numerical results obtained from Eqs. 15-67 and 15-68 are sufficiently accurate for obtaining the performance characteristics for turboshaft engines.

To apply Eq. 15-68 to a turboshaft (nonregenerative engine), one sets $e_R = 0$, so that $y = 1$, and $z = 1 + \Theta \eta_a / \eta_c$. Substituting the later values for y and z into Eq. 15-68, one obtains Eq. 15-47, the thermal efficiency equation for the turboshaft (nonregenerative) engine.

15-5.3.6 WORK-RATIO FOR REGENERATIVE TURBOSHAFT ENGINE (U)

The incorporation of a regenerator in the cycle has no effect on the work-ratio U , which is given by

$$U = \frac{L}{L_t} = 1 - \frac{\Theta}{a \eta_t \eta_c} \quad (15-69)$$

Eq. 15-69 applies to turboshaft and regenerative turboshaft engines (see par. 15-4.4). It shows that – for fixed values of η_c , η_t , and Θ – increasing the cycle temperature ratio a increases U .

15-5.4 PERFORMANCE CHARACTERISTICS OF THE REGENERATIVE TURBOSHAFT ENGINE

Fig. 15-16 presents calculated values of thermal efficiency (Eq. 15-68) and dimensionless specific output (Eq. 15-67) as functions of the cycle pressure ratio P_3/P_0 . In the chart, the cycle temperature ratio $a = T_4/T_0$ and the regenerator effectiveness e_R are parameters.

It is seen from Fig. 15-16 that for each value of a there is an *optimum pressure ratio* which maximizes the thermal efficiency. The curve for $e_R = 0$ corresponds to the turboshaft (nonregenerative) engine.

There is also an optimum pressure ratio which maximizes the output. When the specific output is a maximum the air rate A is a minimum.

The pressure ratio for optimizing η_{th} is smaller than that for optimizing L .

In general, increasing e_R always increases the thermal efficiency η_{th} of the engine, but reduces the optimum value of P_3/P_0 that gives the maximum value of η_{th} . The reduction in the optimum cycle pressure ratio results in an increase in the air rate A , so that the turbomachines for a given power output tend to become larger dimensionally.

Fig. 15-17 presents the thermal efficiency η_{th} as a function of the cycle pressure ratio P_3/P_0 , with the regenerator effectiveness e_R as a parameter, for three different turbine inlet temperatures; viz, $T_4^0 = 1200^\circ\text{F}$, 1350°F , and 1500°F .

15-6 TURBOPROP ENGINE

The essential features of the turboprop engine were discussed in par. 12-2.6 and are illustrated schematically in Fig. 15-18. The

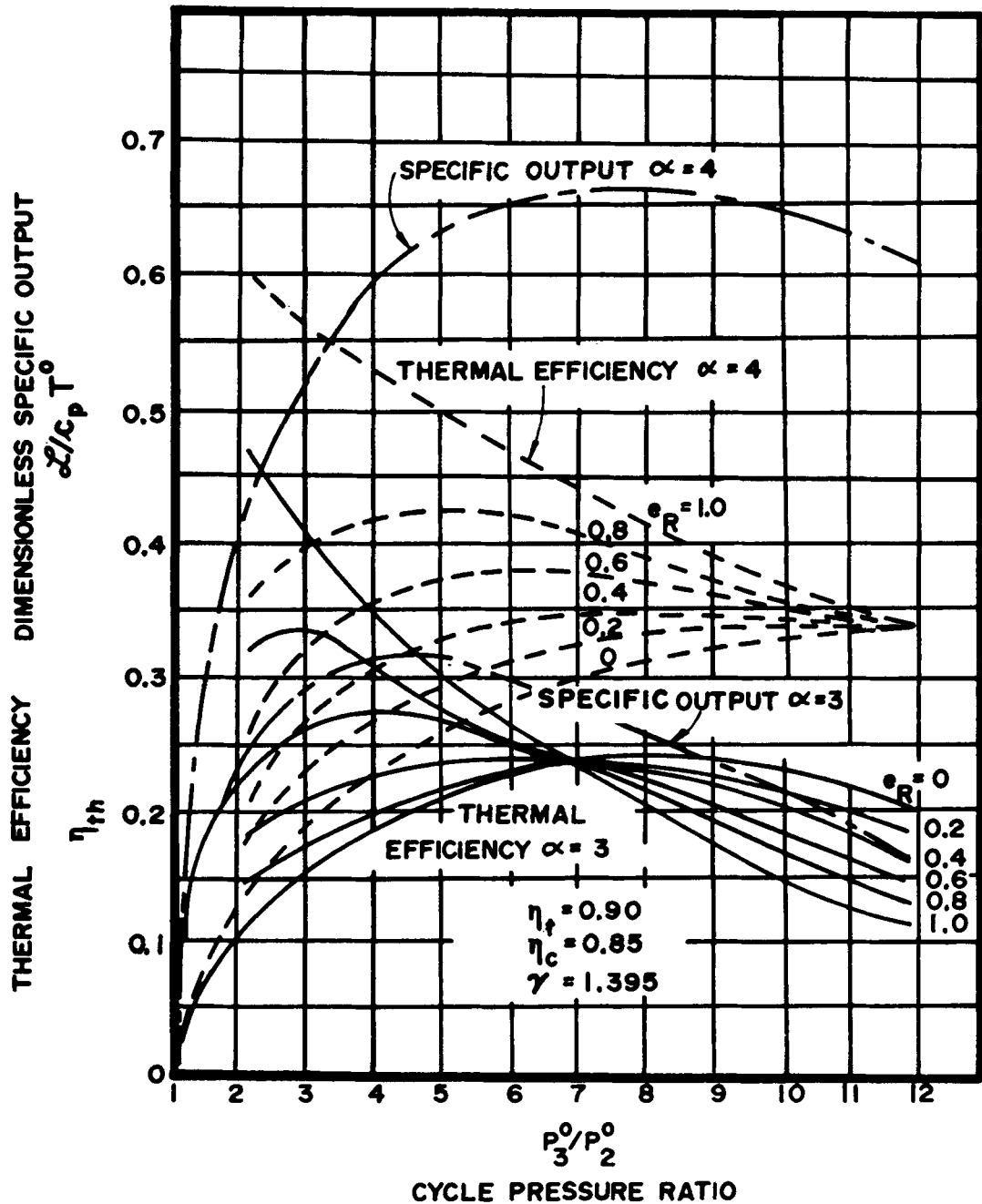
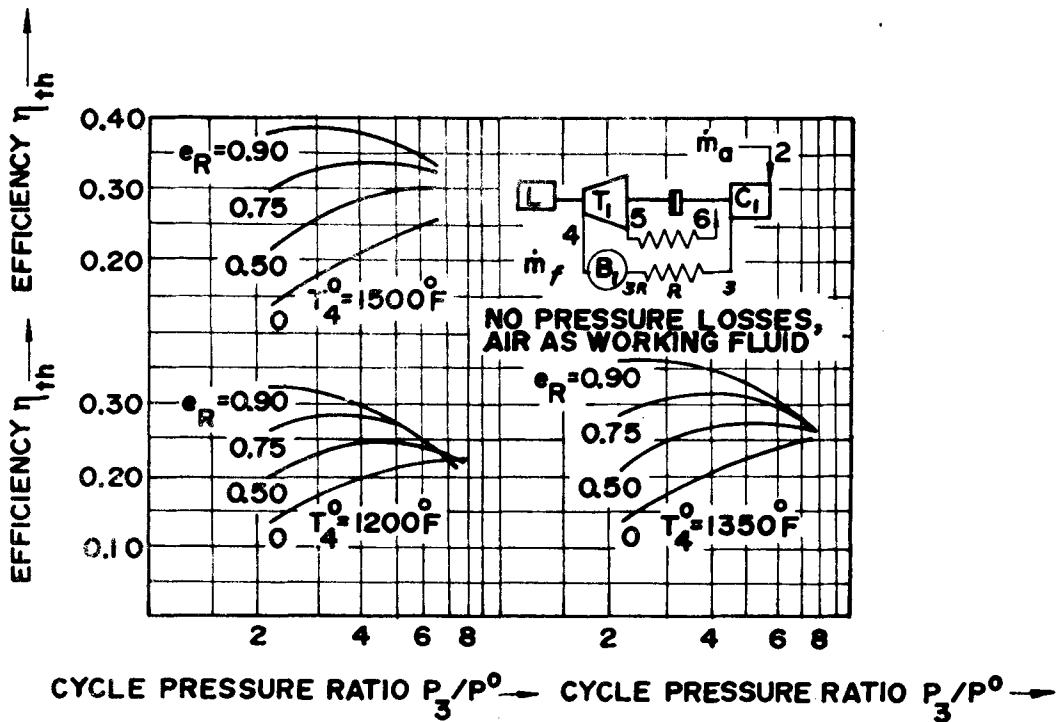


Figure 15-16. Thermal Efficiency and Specific Output as Functions of Cycle Pressure Ratio for Regenerative Turboshaft Engines



$$\eta_{MC} = \eta_{Mt} = 0.98; \eta_c = 0.847; \eta_t = 0.908; \eta_B = 0.98; \eta_g = 1.0; T_2 = T_0 = 530^\circ R$$

$$\Delta h_{\lambda B} = 0.54 \text{ B/lb}; \Delta h_{\lambda P} = 0.60 \text{ B/lb}$$

Figure 15-17. Thermal Efficiency for Regenerative Turboshaft Engines as a Function of Cycle Pressure Ratio, With e_R as a Parameter, for Three Different Turbine Inlet Temperatures

turboprop engine differs from the turboshaft engine in that it develops a small amount of jet thrust as well as shaft power. In other words, of the total amount of enthalpy decrease between stations 4 and 6, the portion $(h_6^0 - h_7)$ occurs in the exhaust nozzle; the latter produces a significant jet velocity. Hence, if Δh_t and Δh_n denote the specific enthalpy drops in the turbine and exhaust nozzle, respectively, then (see Fig. 15-18(D))

$$h_4^0 - h_6 = \Delta h_t + \Delta h_n \text{ (B/slug)} \quad (15-70)$$

The enthalpy drop Δh_t furnishes the energy for driving the air compressor, gearbox, and aircraft propeller, and Δh_n is the specific enthalpy which is converted into the jet kinetic energy $V_j^2/2$. Ordinarily, the engine designer endeavors to achieve a ratio of $\Delta h_t/\Delta h_n$, at the design point, that maximizes the thrust power P_T .

15-6.1 THERMODYNAMIC ANALYSIS OF THE TURBOPROP ENGINE CYCLE

The thermodynamic cycle for the turboprop engine is illustrated schematically in

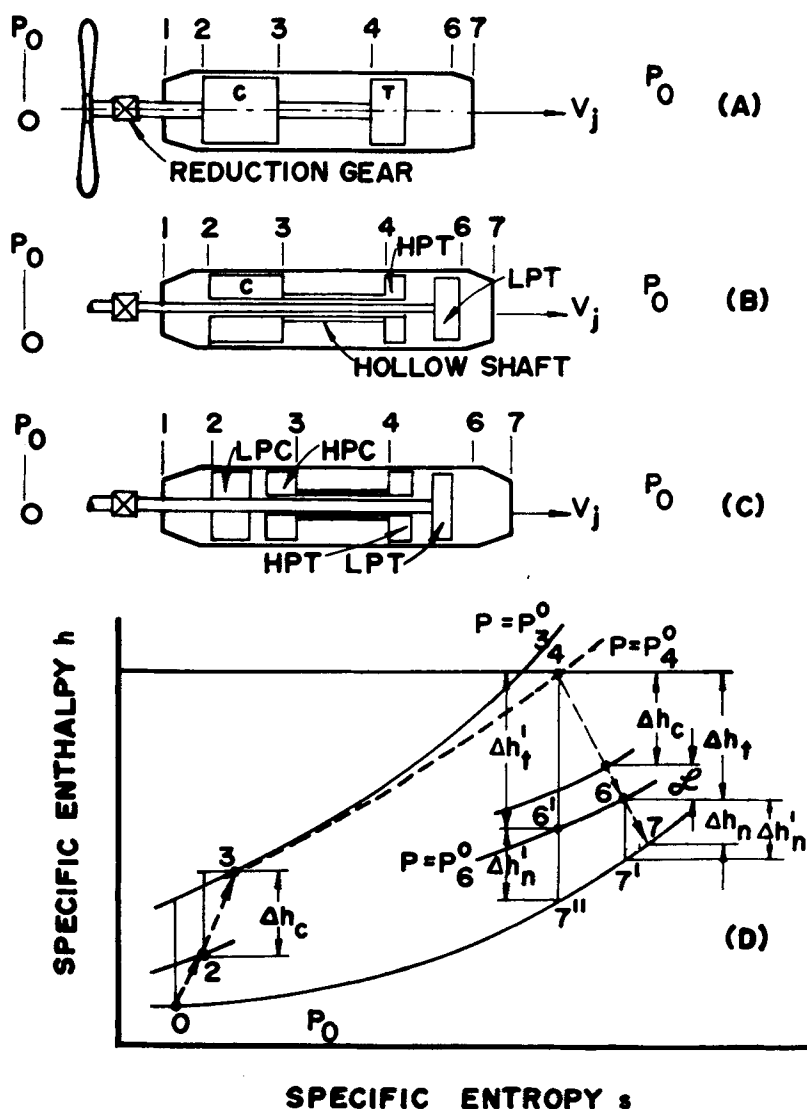


Figure 15-18. Component Arrangement and Thermodynamic Cycle for the Turboprop Engine

Fig. 15-18(D), and it applies to fixed-shaft; free-turbine, and twin-spool configurations.

State point 2 (Fig. 15-18(D)) depends upon the flight speed V_0 of the vehicle propelled by the turboprop engine and the characteristics of the air inlet-diffuser system. The work expended

in diffusing the air entering the engine, is given by*

$$\Delta h_d = h_3^0 - h_2^0 \quad (\text{B/slug})$$

If f denotes the fuel-air ratio for the burner, x the fraction of the inducted air flow \dot{m}_a that is bled from the air compressor for cooling and

*If the Mach number $M_0 < 0.3$, the stagnation values h^0 , p^0 , T^0 , etc., may be replaced by the static values h , P , T , etc.

other purposes, h_4^0 the stagnation specific enthalpy of the hot gas entering the turbine (or the HPT, Fig. 15-18), and h_6^0 the stagnation specific enthalpy of the gas discharged by the turbine (or the LPT), then the work delivered by the turbine per slug of inducted air is given by

$$\Delta h_t = (h_4^0 - h_6^0) (1 + f) (1 - x) \quad (15-71)$$

Of the turbine work Δh_t , an amount equal to $\Delta h_c / \eta_{Mc}$ is required for driving the air compressor; where η_{Mc} is its mechanical efficiency. Hence, the work delivered to the gearbox, denoted by Δh_g , is given by

$$\Delta h_g = \eta_{Mt} \Delta h_t - \Delta h_c / \eta_{Mc} \quad (15-72)$$

where η_{Mt} is the mechanical efficiency of the turbine.

15-6.1.1 PROPELLER THRUST HORSEPOWER (P_{prop})

If η_g denotes the mechanical efficiency of the reduction gearbox, the shaft work delivered to the propeller denoted by W_{prop} , is given by

$$W_{prop} = \eta_g \Delta h_g \text{ (B/slug of air)} \quad (15-73)$$

Let \dot{m}_a denote mass flow rate of inducted air and η_{prop} the propulsive efficiency of the aircraft propeller, then the thrust horsepower (\overline{thp}) delivered by the *propeller* denoted by P_{prop} , is accordingly

$$P_{prop} = g_c \dot{m}_a \eta_g (\eta_t \Delta h_t - \Delta h_c / \eta_{Mc}) \frac{778}{550} (\overline{thp}) \quad (15-74)$$

where $g_c = 32.174$ slug-ft/lb-sec², \dot{m}_a is in slug/sec, and Δh_t and Δh_c are in B/slug.

15-6.1.2 JET THRUST POWER (P_{Tj})

Let P_{Tj} denote the thp developed by the exhaust jet; the effective jet velocity is V_j . Thus

$$V_j = \sqrt{2(h_6^0 - h_7)} \quad (15-75)$$

The jet thrust F_j is given by

$$F_j = \dot{m}_a (1 + f) (1 - x) (V_j - V_0)$$

Hence

$$P_{Tj} = \frac{F_j V_0}{550} = g_c \dot{m}_a (1 + f) (1 - x) (V_j - V_0) \frac{V_0}{550} (\overline{thp}) \quad (15-76)$$

where V_0 is the flight speed in fps, x is the fraction of \dot{m}_a bled for cooling purposes, and f is the fuel-air ratio.

15-6.1.3 TOTAL THRUST HORSEPOWER FOR TURBOPROP ENGINE ($P_{turboprop}$)

The total thp developed by the turboprop engine, denoted by $P_{turboprop}$, is given by

$$P_{turboprop} = P_{prop} + P_{Tj} \quad (15-77)$$

For information on the aircraft propeller the reader is referred to References 1, 6, and 9.

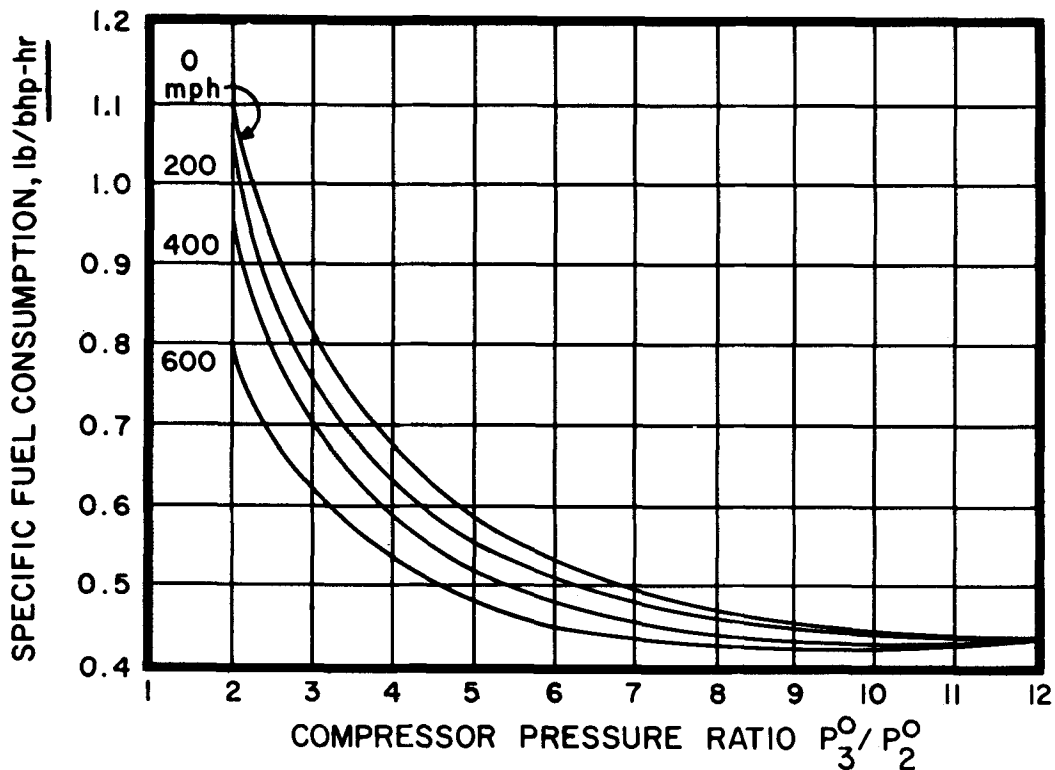
15-6.2 PERFORMANCE CHARACTERISTICS FOR THE TURBOPROP ENGINE

The static performance of the turboprop engine (i.e., $V_0 = 0$) is identical with that for the corresponding turboshaft engine. Hence, the discussions under par. 15-4 are applicable to the turboprop engine under static operating conditions.

Fig. 15-19 presents the SFC of the turbo-prop engine as a function of the compressor pressure ratio P_3^O/P_2^O , with the flight speed V_0 , in mph, as a parameter. The curves are based on the assumption that $(P_6^O/P_7 = P_2^O/P_0^O)$ (see Fig. 15-18). The curves show that increasing the compressor ratio improves the fuel economy of the engine at all flight speeds.

Fig. 15-20 presents the SFC as a function of the percent of the total energy in the propulsive

jet, with the flight speed as a parameter. It is apparent that the optimum division of the energy supplied to the engine – between the exhaust nozzle and the turbine – from the viewpoint of minimum SFC, varies with the flight speed. In general, the optimum division of energy is obtained when $P_6^O/P_7 = P_2^O/P_0^O$. In the region where the energy in the exhaust jet is near the optimum value, both the SFC and the P_T are not affected appreciably by relatively large changes in V_j . Consequently, the ratio



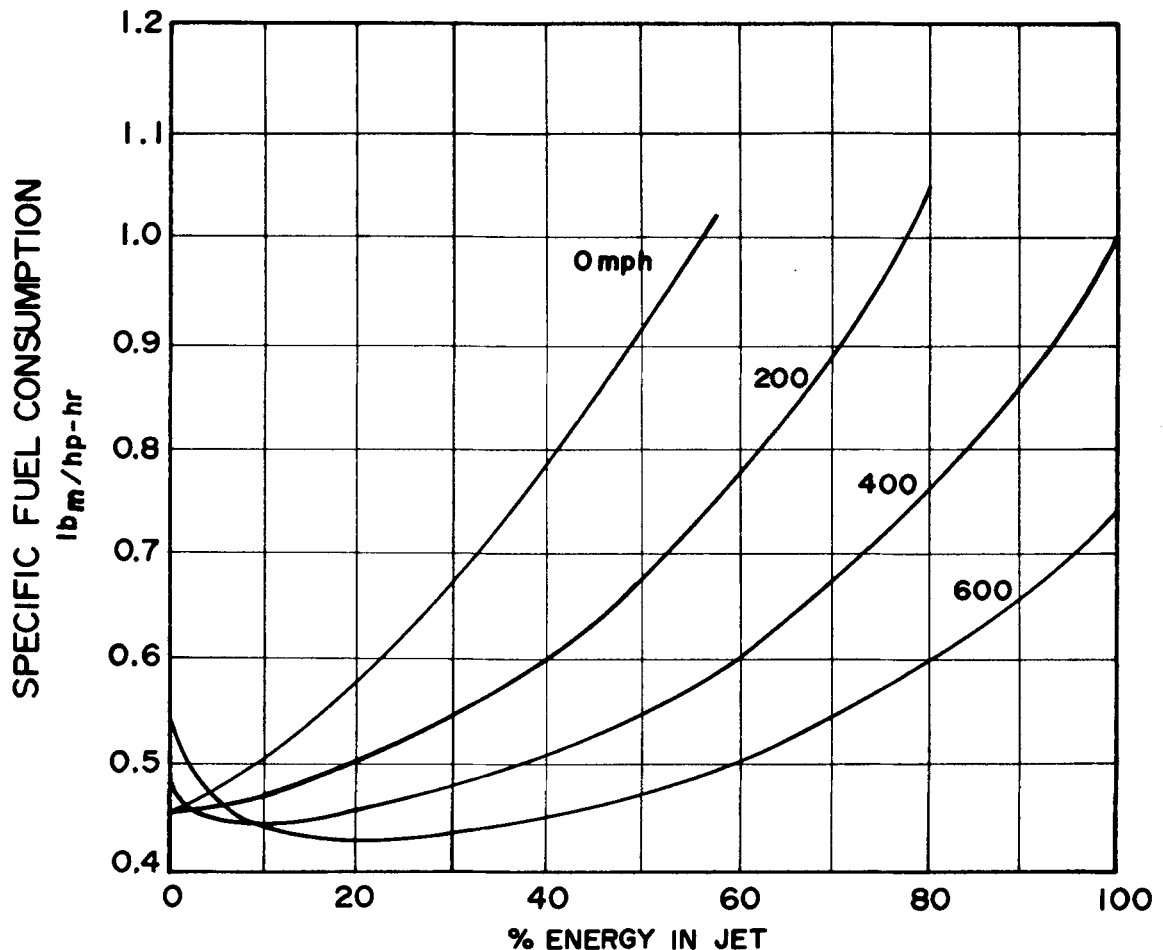
$$\eta_B = 0.98, \eta_c = 0.85, \eta_t = 0.83, \eta_n = 0.98, \gamma_c = 1.395, \Delta P_{3-4} = 0.03 P_2^O,$$

$$\bar{c}_{pB} = 0.26 \text{ B/lb}_m \cdot ^\circ\text{R}, \bar{c}_{pt} = 0.276 \text{ B/lb}_m \cdot ^\circ\text{R}, \gamma_t = 1.33,$$

$$T_0 = 518.4^\circ\text{R}, \Delta H_c = 18,550 \text{ B/lb}_m \text{ OF FUEL}, T_4^O = 1960^\circ\text{R}$$

(BASED ON REFERENCE 8)

Figure 15-19. SFC As a Function of Compressor Pressure Ratio With Flight Speed as a Parameter (Turbo-prop Engine)



(BASED ON ENGINE PARAMETERS IN FIG. 15-19)

Figure 15-20. SFC As a Function of the Percent of Energy in Jet, With Flight Speed as a Parameter (Turboprop Engine)

$\Delta h_n / \Delta h_t$ in a turboprop engine is more apt to be based on the consideration of minimum engine weight — including the weight of the propeller, and reduction gearbox — than on the minimum SFC.

15-6.2.1 EFFECT OF ALTITUDE AND TURBINE INLET TEMPERATURE

Fig. 15-21 illustrates the effect of turbine inlet temperature at static sea level and at 30,000 ft altitude with a flight speed of 400

mph. It is seen that under static sea-level and altitude conditions the minimum SFC is obtained with compressor pressure ratios of 20 to 1 and 60 to 1, approximately, for turbine inlet temperatures of 2000°R and 3000°R, respectively. Fig. 15-22 illustrates the effect of altitude and turbine inlet temperature on the specific power. For each value of T_4^0 the specific power obtained from the engine is larger at the higher altitude (30,000 ft). The beneficial effects of altitude upon both the SFC and specific power indicate that the best performance is obtained if the flight is conducted at a high altitude.

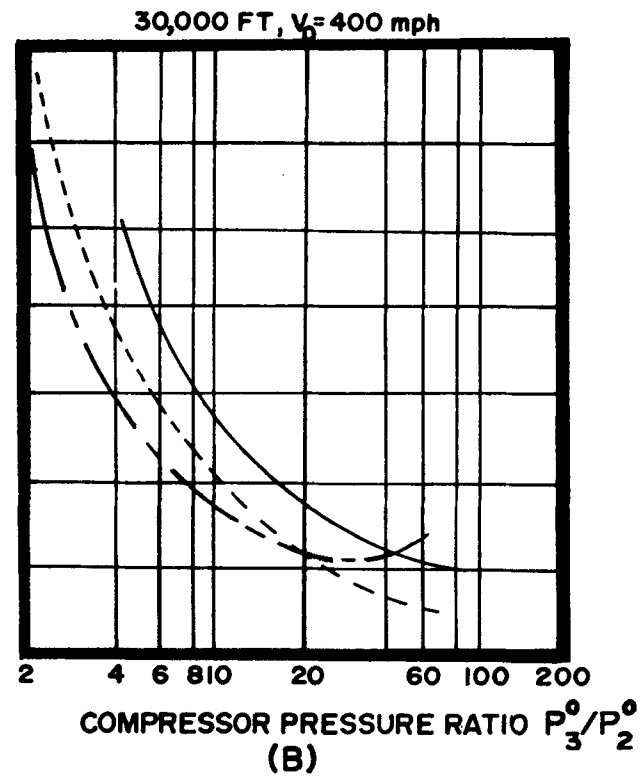
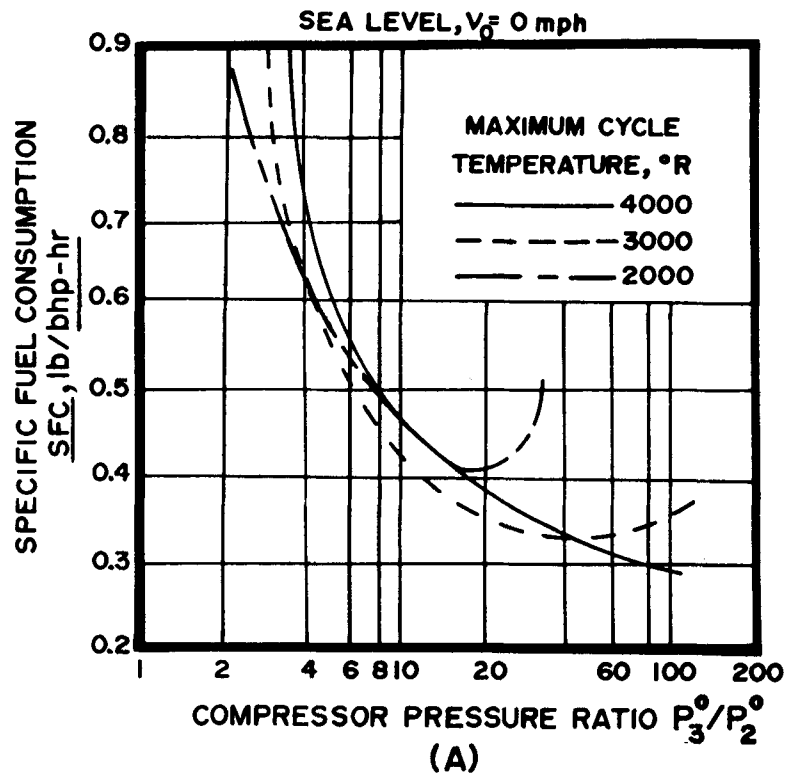


Figure 15-21. Effect of Altitude on the SFC of Turboprop Engines

15-6.2.2 EFFECT OF MACHINE EFFICIENCY (η_c) AND TURBINE INLET TEMPERATURE (T_4^O)

Figs. 15-22(A) and 15-22(B) illustrate the potential gains in the *specific power* of turbo-prop engines resulting from increasing η_c , η_t , and T_4^O . It is apparent that research and development efforts for raising the allowable turbine inlet temperature T_4^O should be encouraged. Successful developments in that field will contribute materially to reducing the size and weight of gas-turbine engines for a given power output.

15-6.3 OPERATING CHARACTERISTICS OF TURBOPROP ENGINE

Fig. 15-23 presents the operating characteristics of a typical turboprop engine.

15-7 GAS-TURBINE JET ENGINES

The gas-turbine jet engines to be discussed here are the turbojet and turbofan engines for propelling aircraft at *subsonic* speeds (see pars. 12-2.1 and 12-2.3). The general thrust equations for gas-turbine jet engines are presented in paragraph 12-3.

For a simple turbojet engine, the thrust equation is Eq. 12-11, which is repeated here for convenience. Thus

$$F = \dot{m}_a (V_j - V_o) = \dot{m}_a V_j (1 - \nu) \quad (\text{lb}) \quad (15-78)$$

For a turbofan engine the thrust equation is given by Eq. 12-15. Thus

$$F = (\dot{m}_a + \dot{m}_f) V_j - \dot{m}_a V_o + \dot{m}_{aF} (V_{jF} - V_o) \quad (15-79)$$

or

$$F = \dot{m}_a V_o \left(\frac{1+f}{\nu} - 1 \right) + \dot{m}_{aF} V_o (\nu_F - 1) \quad (15-79a)$$

where

$$\nu = V_o / \bar{V}_j \quad \text{and} \quad \nu_F = V_o / V_{jF}$$

The mean effective jet velocity V_{jTF} for the turbofan engine is given by Eq. 12-16. In that equation

$$\beta = \dot{m}_{aF} / \dot{m}_a = \text{bypass ratio}$$

15-8 TURBOJET ENGINE

Fig. 15-24 illustrates the arrangement of the components for the turbojet engine and its thermodynamic cycle plotted in the Ts -plane. As pointed out in Chapter 12, the inlet-diffuser, air compressor, combustor, and turbine constitute a gas-generator for supplying the propulsive nozzle – between Stations 6 and 7 in Fig. 15-24 – with a high temperature, high pressure gas.

Fig. 15-24(A) illustrates the flow circuit for the turbojet engine, and Fig. 15-24(B) its thermodynamic cycle.

Because of energy loss in the air intake-diffuser system, the diffusion process (0-2) is not isentropic, and the total pressure of the air leaving the diffuser $P_2^O < P_0^O$. The air compressor (axial or radial flow) raises the total pressure of the air from P_2^O to P_3^O . In the burner (3-4) there is a decrease in the total pressure of the working fluid (see par. 15-3.3). If ΔP_{34} denotes the decrease in stagnation pressure in the burner, then P_4^O is accordingly

$$P_4^O = P_3^O - \Delta P_{34} \quad (15-80)$$

The most significant characteristic of the turbojet engine cycle is that the work done by the gases which expand in flowing through the turbine is exactly equal to that required to drive the air compressor plus the engine auxiliaries.

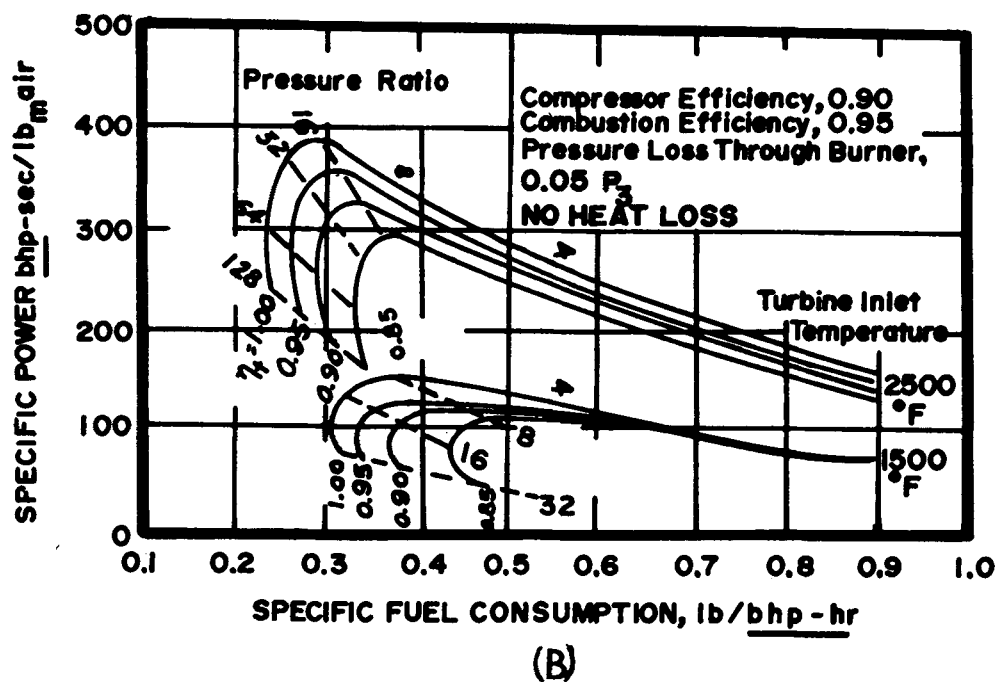
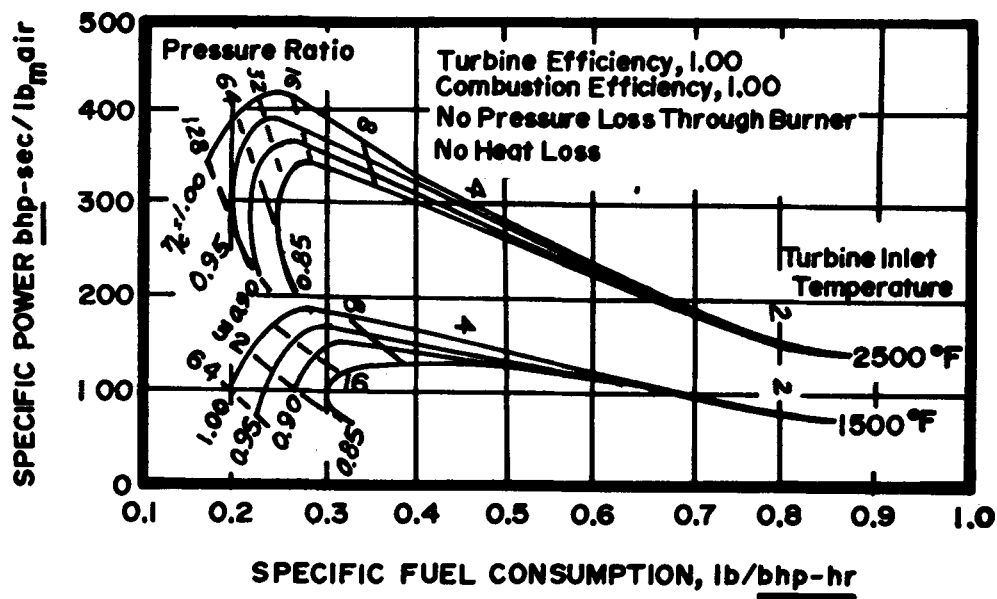
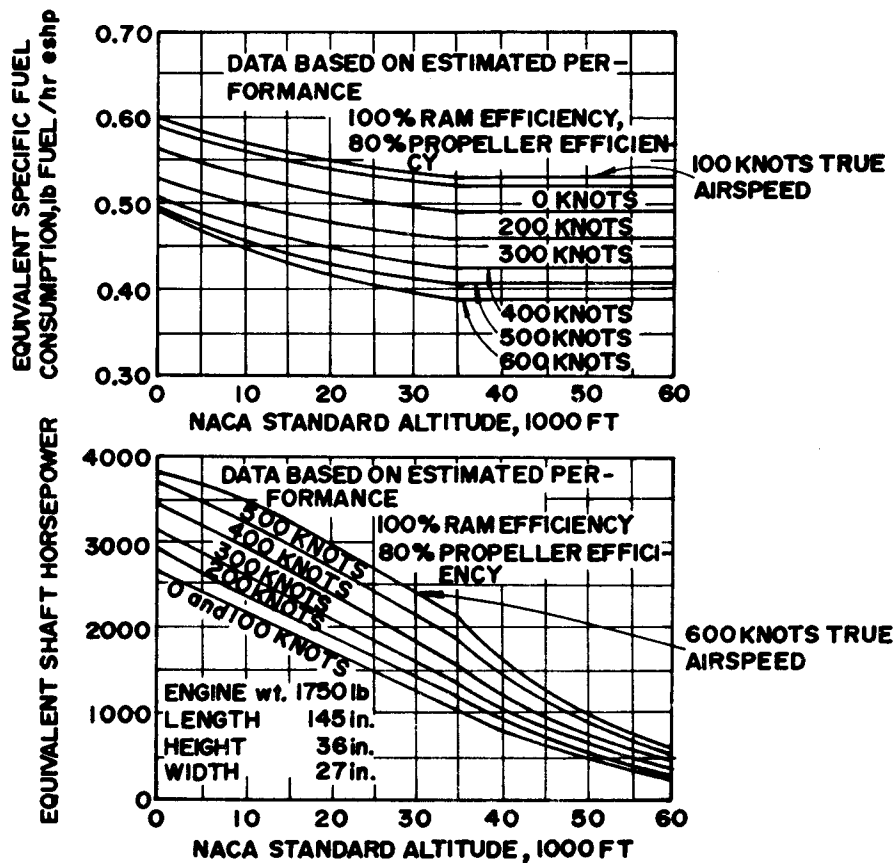


Figure 15-22. Effect of Turbine and Compressor Isentropic Efficiencies and Turbine Inlet Temperature Upon the Performance Characteristics of Turboprop Engines



PERFORMANCE DATA ARE AT STANDARD SEA-LEVEL STATIC CONDITIONS

RATINGS	Rpm	TURBINE INLET TEMPERATURE, °F	EQUIVALENT shp	PROPELLER shp	JET THRUST, lb	FUEL CONSUMPTION, lb/hr eshp
TAKE-OFF	13,820	1780	3750	3460	726	0.540
MAX. CONT.	13,820	1700	3375	3094	702	0.552
CLIMB 92%	13,820	1645	3105	2830	684	0.566
CRUISE 80%	13,820	1557	2700	2437	657	0.589
GD. IDLE	10,000	1015	88	40	120	6.250

Figure 15-23. Operating Characteristics of a Typical Turboprop Engine

An accurate thermodynamic analysis of the turbojet engine cycle is time-consuming and requires a step-by-step calculation of each process, taking into account the changes in the mass flow rates of the working fluid, the change in its chemical composition, the fact that its specific heat varies with the temperature, the different energy losses that are encountered, etc. For a preliminary design analysis for obtaining general performance characteristics (see Ref. 2, Chap. 7), such an analysis is unwarranted.

The component efficiencies for the gas-turbine jet engines are discussed in par. 15-3 and will not be repeated here.

15-8.1 DIMENSIONLESS HEAT ADDITION FOR TURBOJET ENGINE $\left(\frac{Q_i \eta_B}{c_p T_0}\right)$

The heat supplied to a turbojet engine in flight, denoted by Q_i , is given by

$$Q_i = \frac{c_p}{\eta_B} (T_4^O - T_3^O) \text{ (B/slug of air)} \quad (15-81)$$

From Eqs. 15-7 and 15-13

$$T_3^O = T_2^O + \frac{T_3^{O'} - T_2^O}{\eta_c} = T_2^O \left(1 + \frac{\Theta_c - 1}{\eta_c}\right) \quad (15-82)$$

Combining Eqs. 15-81 and 15-82, and noting that $T_4^O = a_1 T_2^O$, $T_2^O = a_d T_0^O$ and $a = a_d a_1$, one obtains on rearranging terms

$$\frac{Q_i \eta_B}{c_p T_0} = \frac{1}{\eta_c} a_d \left(\frac{a}{a_d} \eta_c - \eta_c - \Theta_c + 1 \right) \quad (15-83)$$

where $\Theta_c = T_3^{O'}/T_2^O = \text{cycle pressure ratio parameter}$ (see Eq. 15-8).

The parameter $Q_i \eta_B / c_p T_0$ is called the *dimensionless heat addition*. Eq. 15-83 can be

employed for determining the influences of M_0 , Θ_c , a , and η_c upon the heat which must be supplied to the turbojet engine.

15-8.2 TURBINE PRESSURE RATIO (P_4^O / P_5^O)

A characteristic of the turbojet engine is that $\Delta h_t = \Delta h_c$ (see Eqs. 15-11, 15-24, and 15-28). From those equations it is readily shown that if it is assumed that $\bar{c}_{pc} \approx \bar{c}_{pt} = c_p$, then²

$$\Theta_t = 1 - \frac{\Theta_c - 1}{\eta_1 \eta_{tc}} = \left(\frac{P_5^O}{P_4^O} \right)^{\frac{\gamma-1}{\gamma}} = \frac{T_5^{O'}}{T_4^O} \quad (15-84)$$

where $\eta_{tc} = \text{machine efficiency}$ (see par. 15-3.5).

15-8.3 DIMENSIONLESS ENTHALPY CHANGE FOR THE PROPULSIVE

NOZZLE $\left(\frac{\Delta h_n}{c_p T_0}\right)$

It is assumed that the propulsive gas expands completely in the exhaust nozzle, i.e., $P_7 = P_0$. Then

$$\frac{1}{\Theta_n} = \Theta_d \Theta_c \Theta_t = \left(\frac{a_1 \eta_{tc} - \Theta_c + 1}{a_1 \eta_{tc}} \right) \Theta_d \Theta_c \quad (15-85)$$

See Eqs. 15-3, 15-4, 15-8, and 15-84.

The enthalpy change for the propulsive nozzle, denoted by Δh_n (see Eq. 15-29), is given by

$$\Delta h_n = c_{pn} T_6^O (1 - \Theta_n) \eta_n \quad (15-86)$$

Since the flow from Station 5 to Station 6 (see Fig. 15-24) is adiabatic $T_5^O = T_6^O$ so that

$$T_6^O = T_5^O = T_4^O - \frac{T_3^{O'} - T_2^O}{\eta_c} \quad (15-87)$$

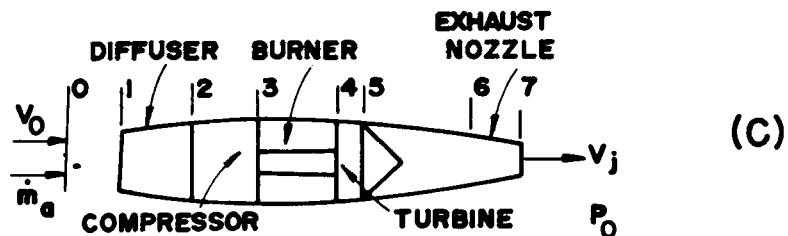
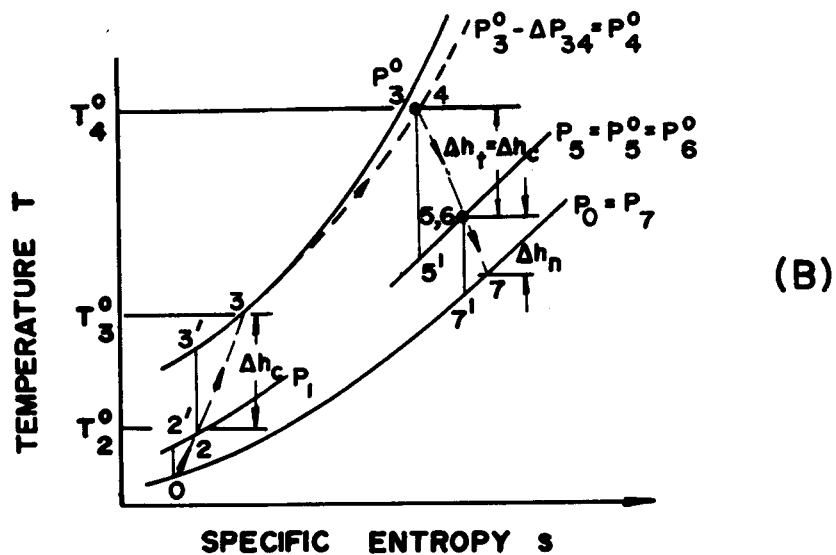
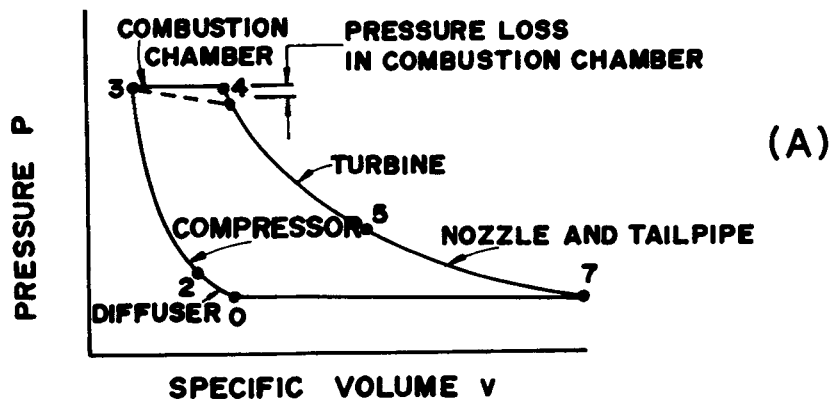


Figure 15-24. Thermodynamic Cycle and Component Arrangement for the Turbojet Engine

Substituting Eq. 5-87 into Eq. 5-86 and rearranging, one obtains

$$\frac{\Delta h_n}{c_p T_0} = [a \eta_c - a_d (\Theta_c - 1)] \frac{\eta_n}{\eta_c} \times \left\{ 1 - \frac{\eta_1 \eta_{tc}}{\Theta_c [1 + \eta_d (a_d - 1)] [a_1 \eta_{tc} - (\Theta_c - 1)]} \right\} \quad (15-88)$$

where $a_1 = T_4^O / T_2^O$, $a_d = T_2^O / T_0$, $a = T_4^O / T_0$, and $\Theta_c = T_3^{O'} / T_2^O$.

The parameter $\Delta h_n / c_p T_0$ is termed the *dimensionless enthalpy change for the propulsive nozzle* (see Fig. 15-25).

Fig. 15-25 presents the dimensionless enthalpy change for the propulsive nozzle ($\Delta h_n / c_p T_0$) as a function of the compressor pressure ratio P_3^O / P_2^O , with the flight Mach number M_0 as a parameter.

15-8.4 DIMENSIONLESS THRUST PARAMETER (λ)

The specific thrust also called the air specific impulse, denoted by I_a , is given by Eq. 2-42 (see also par. 12-6.1). Thus

$$I_a = \frac{F g_c}{\dot{m}_a} \quad (\text{sec}) \quad (15-89)$$

By definition, the dimensionless thrust parameter λ is given by²

$$\lambda = \frac{I_a}{c_0} g_c = \frac{V_j}{c_0} (1 - \nu) \quad (15-90)$$

where $c_0 = \sqrt{2 c_p T_0^O} = \text{maximum isentropic speed}$.

It can be shown that²

$$\lambda = \left(\frac{\Delta h_n}{c_p T_0} \right)^{1/2} - M_0 \left(\frac{\gamma - 1}{2} \right)^{1/2} \quad (15-91)$$

In Eq. 15-91 the first parameter on the right-hand side is calculated by means of Eq. 15-88.

15-8.5 THERMAL EFFICIENCY OF TURBO-JET ENGINE (η_{th})

By definition

$$\eta_{th} = \frac{\Delta h_n}{Q_i} - \frac{V_0^2}{2 Q_i} = \frac{F V_0}{\dot{m}_f \Delta h_c} \quad (15-92)$$

The thermal efficiency η_{th} is primarily of theoretical interest. The important criterion is the overall efficiency η_o which is discussed in the next paragraph.

15-8.6 OVERALL EFFICIENCY OF TURBO-JET ENGINE (η_o)

By definition η_o is given by (see Eq. 12-28)

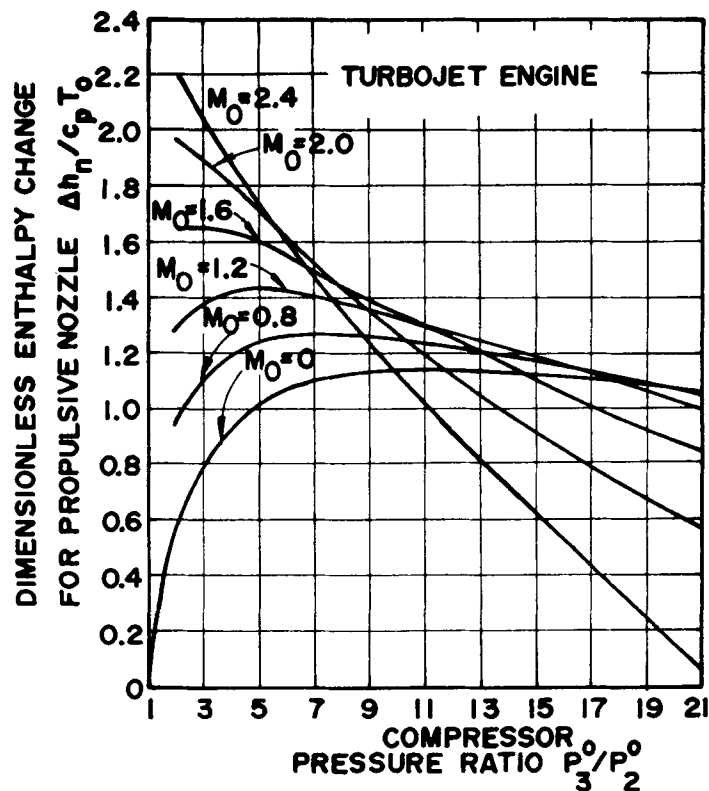
$$\eta_o = \eta_{th} \eta_p = \frac{F V_0}{\dot{m}_f \Delta H_c} \quad (15-93)$$

where from Eq. 12-28, the *ideal propulsive efficiency* η_p is given by

$$\eta_p = \frac{2\nu}{1 + \nu} \quad (15-94)$$

It can be shown that²

$$\eta_o = 2 \eta_B \eta_c \left[\frac{\lambda M_0 \left(\frac{\gamma - 1}{2} \right)^{1/2}}{a \eta_c - \left(1 + \frac{\gamma - 1}{2} M_0^2 \right) (\eta_c + \Theta_c - 1)} \right] \quad (15-95)$$



$\gamma = 1.4$	$\eta_d = 0.91$ FOR $M_0 = 0.8, 1.2$
$\alpha = T_4^0/T_0 = 5.0$	$\eta_d = 0.90$ FOR $M_0 = 1.6$
$\eta_c = 0.85$	$\eta_d = 0.89$ FOR $M_0 = 2.0$
$\eta_f = 0.90$	$\eta_d = 0.88$ FOR $M_0 = 2.4$
$\eta_n = 0.93$	

Figure 15-25. Dimensionless Enthalpy Change for Propulsive Nozzle as a Function of the Compressor Pressure Ratio, With Flight Mach Number as a Parameter (Turbojet Engine)

15-8.7 PERFORMANCE CHARACTERISTICS OF TURBOJET ENGINE

The equations in the preceding paragraphs are useful for determining the performance characteristics of the turbojet engine. Each point on a characteristic curve represents a different engine. Detailed consideration of the characteristics curves for a turbojet engine are presented in References 2 and 7.

15-8.7.1 EFFECT OF CYCLE TEMPERATURE RATIO (α) AND COMPRESSOR PRESSURE RATIO (P_3^0/P_2^0) FOR A CONSTANT FLIGHT SPEED

Fig. 15-26 illustrates the effect of $\alpha = T_4^0/T_0$ and P_3^0/P_2^0 on the subsonic flight performance of the turbojet engine. In the figure η_0 and λ are plotted as functions of Θ_c , P_2^0/P_3^0 , and α .

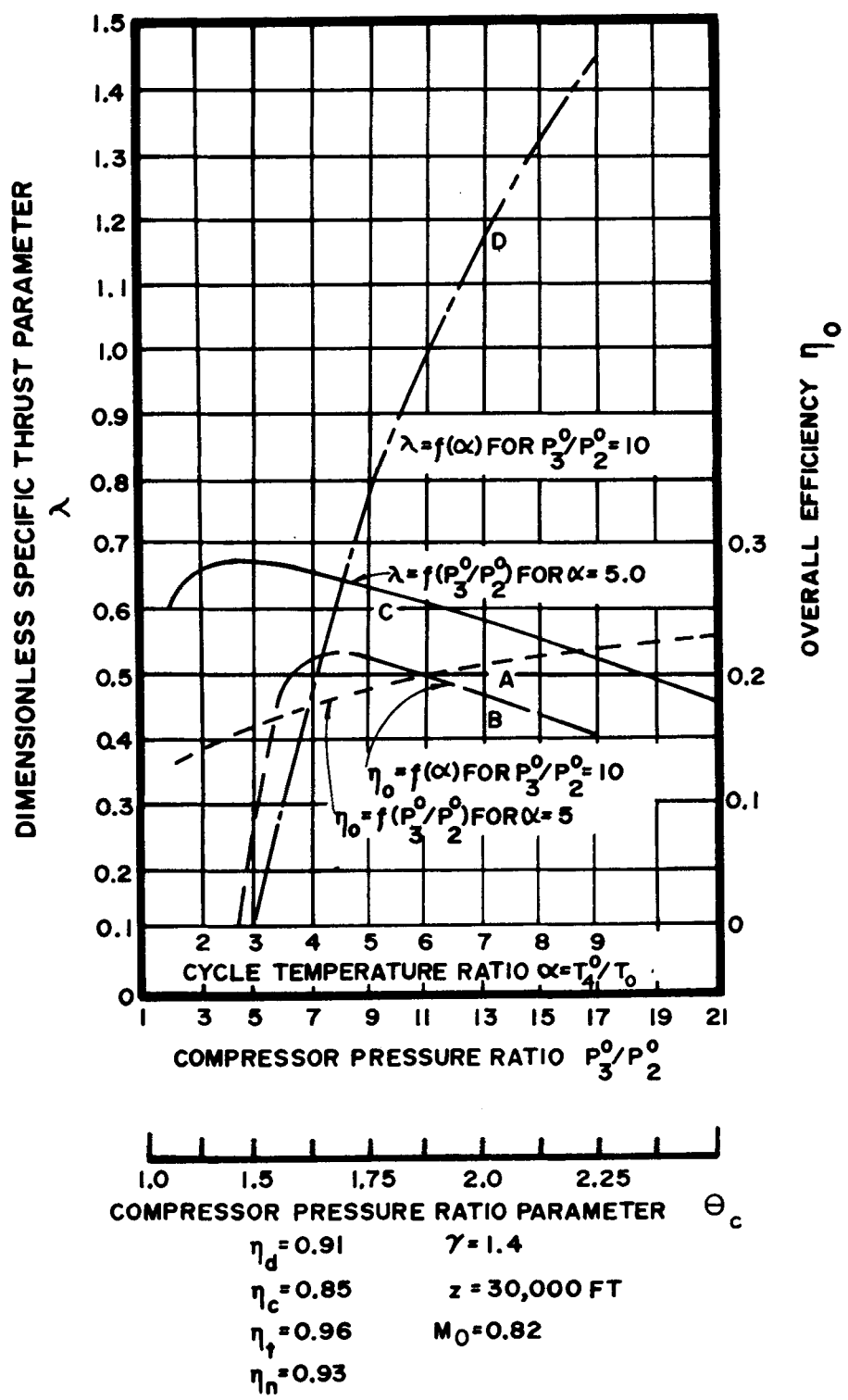


Figure 15-26. Dimensionless Thrust Parameter λ and Overall Efficiency η_0 as Functions of the Compressor Pressure Ratio (Turbojet Engine)

The curves are for $M_0 = 0.82$ at an altitude of 30,000 ft.

Curve A, Fig. 15-26, presents η_O as a function of Θ_c with $a = T_4^O/T_0 = 5.0 = \text{constant}$. As Θ_c is increased, the overall efficiency η_O increases rather slowly and approaches a maximum value at approximately $\Theta_c = 2.3$; i.e., $P_3^O/P_2^O \approx 19$ to 1. The curve for $\eta_c = f(\Theta_c)$ for $a = 5$ is rather flat beyond $\Theta_c \approx 1.75$.

Curve B, Fig. 15-26, presents $\eta_O = f(a)$ for $\Theta_c = 1.932 = \text{constant}$; i.e., $P_3^O/P_2^O = 10$ to 1. The curve shows that if the state of the art pertaining to air compressors limits the compressor pressure ratio, from an isentropic efficiency standpoint, little improvement in TSFC is achieved by increasing the turbine inlet temperature T_4^O above a certain value at the altitude being considered. The curve for $\eta_O = f(a)$, for $\Theta_c = 1.932$, decreases rather slowly for a wide range of values of a . It is essential that a have a sufficiently large value, however, because η_O decreases rapidly when a is less than 3. If Θ_c is limited, the value for a should be that which is consistent with reasonable overall efficiency and long engine life.

Eq. 15-93 shows that η_O is the product of η_{th} and η_p . The thermal efficiency η_{th} increases with Δh_n , and the latter increases with $a = T_4^O/T_2^O$ (see Eq. 15-88). The ideal propulsive efficiency η_p , on the other hand, decreases as V_j increases; i.e., as Δh_n increases. Hence, if the flight speed V_0 is constant, as assumed in this discussion, the value of η_p decreases as the cycle temperature ratio a is increased. Hence, if V_0 is constant, η_{th} increases while η_p decreases as a is raised. These characteristics of η_{th} and η_p cause the curve B for $\eta_O = f(a)$ to be quite flat for a large range of values for a .

Curve C, Fig. 15-26, presents the dimensionless thrust parameter λ (see Eq. 15-90) as a function of Θ_c , for $a = 5.0 = \text{constant}$. The curve shows that the maximum specific thrust is

obtained at a relatively low compressor pressure ratio; i.e., at approximately $\Theta_c = 1.6$ or $P_3^O/P_2^O \approx 5$ to 1.

Curve D, Fig. 15-26, presents λ as a function of a for $P_3^O/P_2^O = 10$. It shows that λ increases as a increases. A comparison of curves B and D shows that although η_O decreases slightly as a is increased, in the range under consideration, large values of specific thrust can be obtained only by increasing the turbine inlet temperature T_4^O . For a fixed value of compressor pressure ratio P_3^O/P_2^O , the higher T_4^O the larger will be thrust per unit area (F/A_F) for the turbojet engine.

15-8.7.2 EFFECT OF FLIGHT MACH NUMBER (M_0) AND CYCLE TEMPERATURE RATIO (a) ON THE DIMENSIONLESS THRUST PARAMETER (λ)

Fig. 15-27 presents the dimensionless thrust parameter λ and η_O as functions of the cycle temperature ratio $a = T_4^O/T_0$, with the flight Mach number as a parameter. Curves are presented for two different compressor pressure ratios $P_3^O/P_2^O = 4$ to 1 and 12 to 1. It is seen that for any value of a , increasing the flight Mach number M_0 causes λ to decrease. For any value of M_0 , however, increasing a increases λ .

15-8.7.3 EFFECT OF FLIGHT SPEED AND COMPRESSOR PRESSURE RATIO (P_3^O/P_2^O) ON PERFORMANCE OF TURBOJET ENGINE

Fig. 15-28 presents the specific thrust I_a and the TSFC as functions of the compressor pressure ratio P_3^O/P_2^O for different values of the flight speed — i.e., 500, 1000, and 1500 mph — at an altitude of 30,000 ft. The curves show that in the range of compressor pressure ratios employed in current turbojet engines (6 to 16 approximately), the flight speed exerts only a small effect on the thrust specific fuel consumption TSFC. The specific thrust I_a in the same

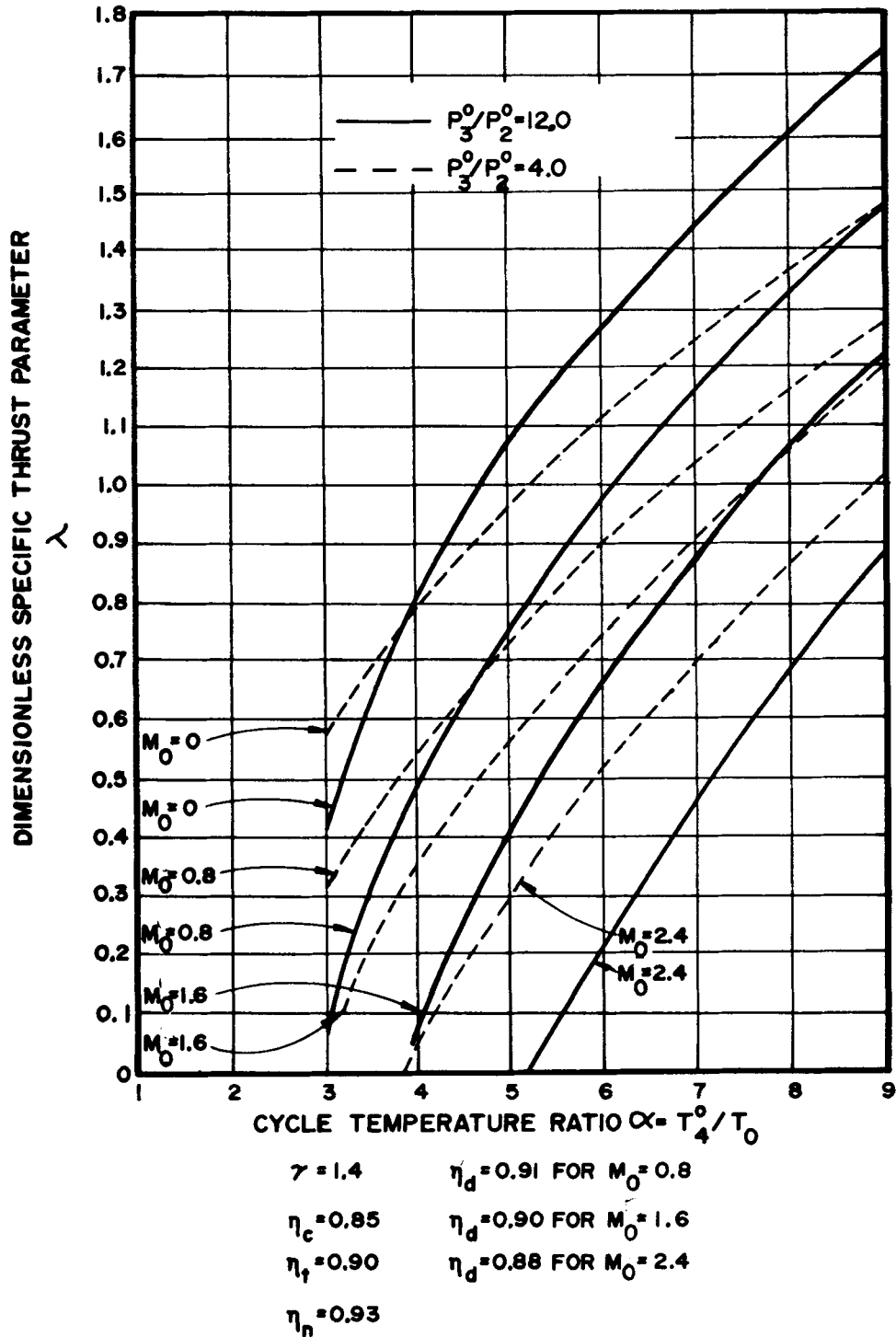
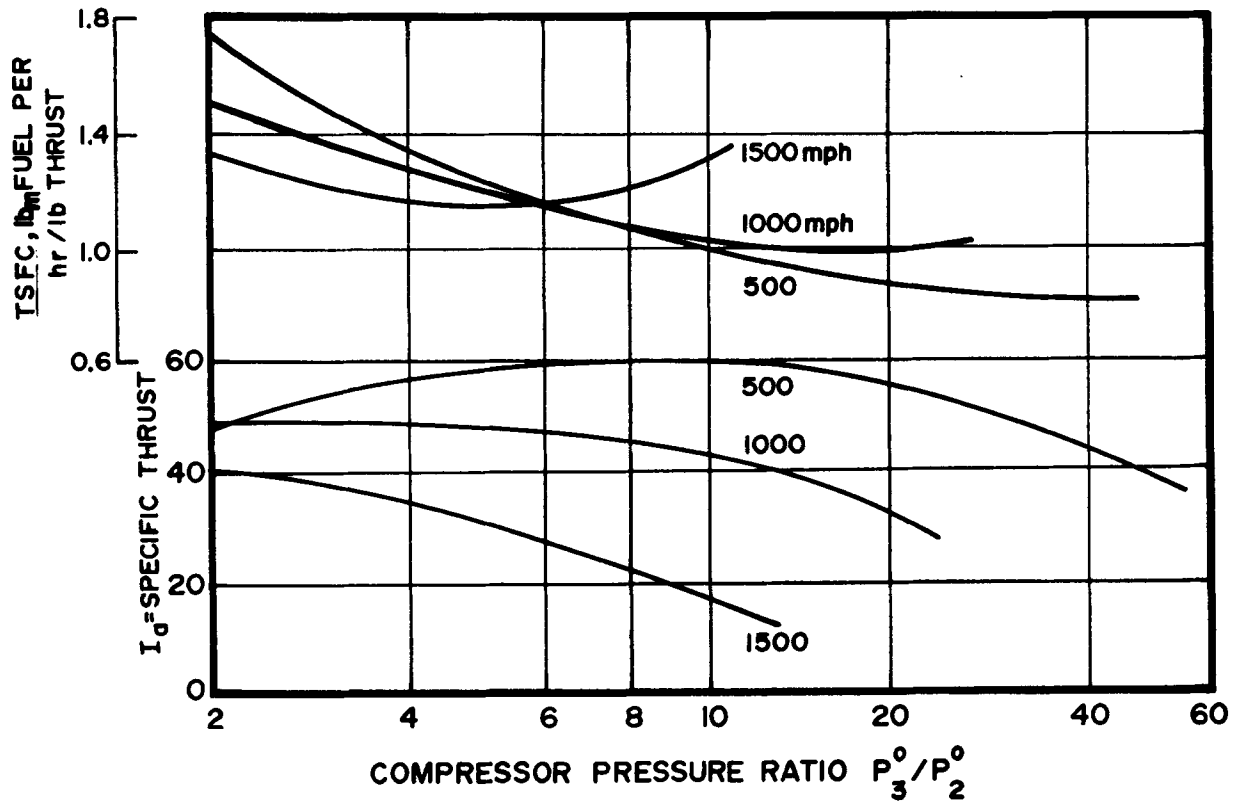


Figure 15-27. Dimensionless Thrust Parameter λ for Turbojet Engine, and Its Overall Efficiency η_o as Functions of the Cycle Temperature Ratio α , With Flight Mach Number as a Parameter



$$\eta_c = 0.85$$

$$\gamma = 1.40 \text{ FOR COMPRESSIONS}$$

$$\eta_t = 0.90$$

$$\gamma = 1.34 \text{ FOR EXPANSIONS}$$

$$\eta_b = 0.95$$

$$z = 30,000 \text{ FT ALTITUDE}$$

$$T_4^0 = 2000^\circ \text{R}$$

$$\Delta H_c = 18,700 \text{ B/lb}$$

Figure 15-28. TSFC and Specific Thrust I_a as Functions of the Compressor Pressure Ratio, With Flight Speed as a Parameter (Turbojet Engine)

range of compressor pressure ratios, decreases markedly when the flight speed exceeds 1000 mph.

The curves show that the optimum values of P_3^0/P_2^0 for I_a and TSFC both decrease as the flight speed is increased. When the flight speed $V_0 \approx 1500$ mph, the compressor pressure ratio for maximizing I_a reduces to 1 to 1, indicating that turbo-machinery is unnecessary. The requirement for maximum I_a would be satisfied by a ramjet engine.

15-9 TURBOFAN ENGINE

The essential features of the turbofan engines are presented in par. 12-4.4, and illustrated schematically in Fig. 12-5. From the point of view of analysis it is convenient to assume that the hot gas and cold air-streams are ejected from the engine through two separate nozzles, as illustrated in Figs. 15-29(A) and 15-29(B); which illustrate schematically the arrangements of the components for an aft-fan and a

ducted-fan turbofan engine, respectively. A turbofan engine, like a turboprop engine (see par. 15-6), accelerates the hot gas from the hot gas generator to the effective jet velocity V_j (see Fig. 15-29) but it also accelerates a large flow of cold air to a smaller effective jet velocity V_{jF} (see par. 12-4.4 and Eqs. 12-16 and 12-17). For convenience it is assumed that the propulsive gas from the hot gas generator and the cold air from the fan are ejected through individual nozzles, as illustrated in Fig. 15-29.

15-9.1 DEFINITIONS PERTINENT TO THE TURBOFAN ENGINE

The parameters discussed below are pertinent to the analysis of the turbofan engine for the purpose of developing the equation for its performance characteristics. The interest here is in turbofan for subsonic aircraft. It is assumed that converging propulsive nozzles are employed for ejecting the individual streams of hot gas and cold air (see Fig. 15-29). The propulsive nozzles have the exit areas A_7 for the hot gas generator, and A_{7F} for the cold air; and in those exit areas $P_7 = P_{7F} = P_0 = \text{static pressure of the ambient air}$.

15-9.1.1 BYPASS RATIO (β)

Let \dot{m}_a and \dot{m}_{aF} denote the mass rates of airflow for the hot gas generator and the fan circuits, respectively. By definition, the *bypass ratio* β is given by

$$\beta = \frac{\dot{m}_{aF}}{\dot{m}_a} = \text{bypass ratio} \quad (15-96)$$

Current turbofan engines operate with bypass ratios of approximately $\beta = 1.5$, or less, and have reduced cruise TSFC by approximately 15 percent compared with their counterpart turbojet engines¹¹. All studies pertinent to turbofan engines for long-range, long-endurance subsonic aircraft conclude that future turbofan engines

for such aircraft will have larger bypass ratios, the optimum value for β will depend upon the allowable turbine inlet temperature T_4^O , i.e., increasing T_4^O increases the optimum value for β ^{11,12,13}.

15-9.1.2 FAN ISENTROPIC EFFICIENCY (η_F)

The fan isentropic efficiency, denoted by η_F , is defined in an analogous manner to the definition for η_c (see par. 15-3.2.1). Hence, (see Fig. 15-29)

$$\begin{aligned} \eta_F &= \frac{\Delta h'_F}{\Delta h_F} = \frac{h_{3F}^{O'} - h_{2F}^O}{h_{3F}^O - h_{2F}^O} \approx \frac{T_{3F}^{O'} - T_{2F}^O}{T_{3F}^O - T_{2F}^O} \\ &= \frac{T_{3F}^O - T_0^O}{T_{3F}^O - T_0} \end{aligned} \quad (15-97)$$

Since the flow from Station 0 to Station 2F is adiabatic, $h_0^O = h_{2F}^O = \text{constant}$. Assuming the specific heat of the air to remain constant between these stations, one obtains (see Eq. 3-52)

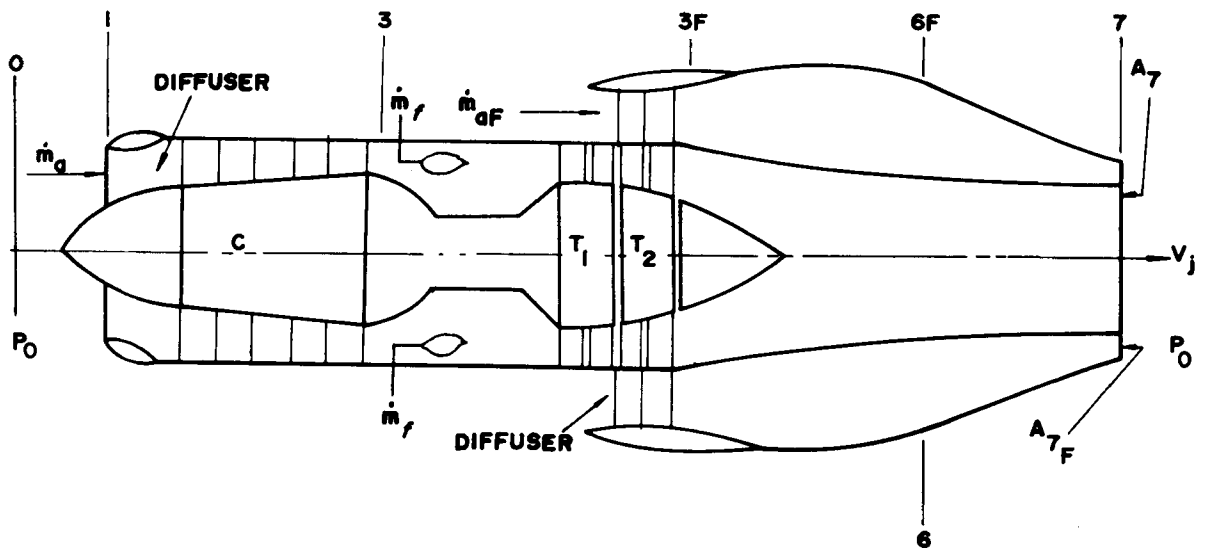
$$T_{2F}^O = T_0^O = 1 + \left(\frac{\gamma - 1}{2} \right) M_0^2 \quad (15-98)$$

15-9.1.3 FAN PRESSURE RATIO PARAMETER (Θ_F)

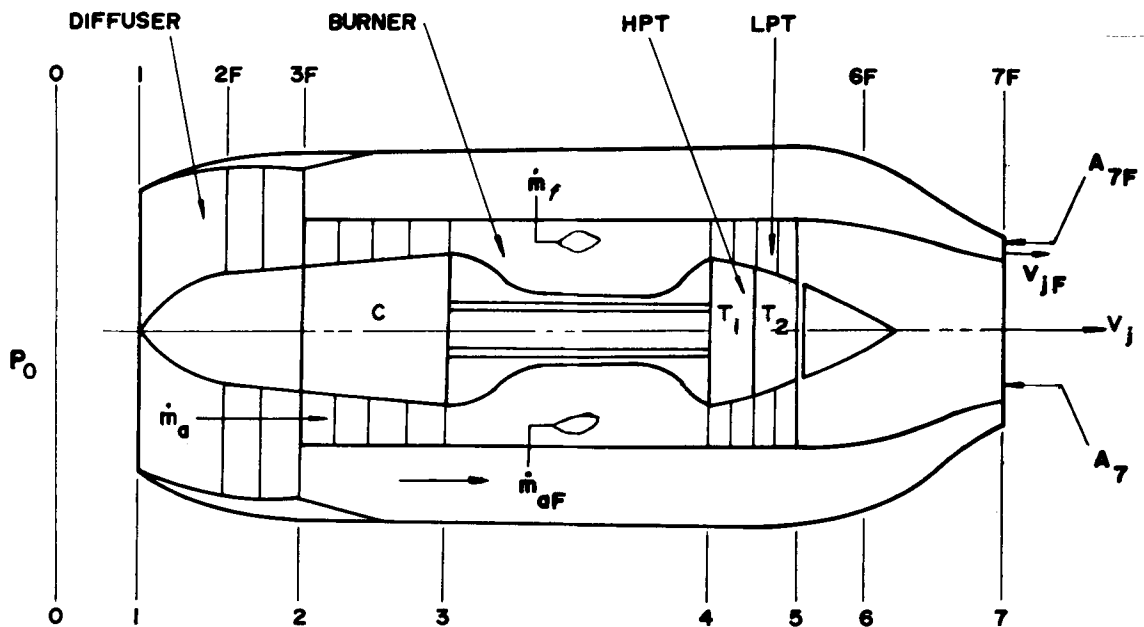
The fan pressure ratio P_{3F}^O/P_{2F}^O influences the mean effective jet velocity \bar{V}_{jTF} for the turbofan engine (see par. 12-4.4). In general, the *optimum fan pressure ratio* is that which makes \bar{V}_{jTF} a maximum¹².

Let Θ_F denote the *fan pressure ratio parameter*. By definition

$$\Theta_F = \left(\frac{P_{3F}^O}{P_0^O} \right)^{\frac{\gamma-1}{\gamma}} = \frac{T_{3F}^{O'}}{T_0^O} \quad (15-99)$$



(A) AFT-FAN TURBINE ENGINE



(B) DUCTED-FAN TURBOFAN ENGINE

Figure 15-29. Arrangement of Components for a Turbofan Engine

The stagnation pressure P_{2F}^O depends upon the isentropic efficiency of the intake-diffuser η_{dF} preceding the fan. From Eqs. 15-3 and 15-4

$$\frac{P_{2F}^O}{P_0^O} = \left[1 + \eta_{dF} \left(\frac{\gamma - 1}{2} \right) M_0^2 \right]^{\frac{\gamma}{\gamma-1}} \quad (15-100)$$

where η_{dF} is the *diffuser isentropic efficiency* for the air-stream entering the fan.

15-9.1.4 FAN POWER (P_F)

Let

$$Z_F = \Theta_F - 1 = \text{compression factor for the fan} \quad (15-101)$$

The work done by the fan upon the air flowing through it, in raising its pressure from P_{2F}^O to P_{3F}^O , is given by

$$\Delta h_{cF} = \bar{c}_{pF} T_0^O \frac{Z_F}{\eta_F} = \bar{c}_{pF} \frac{T_3^{O'} - T_0^O}{\eta_F} \quad (\text{B/lb}) \quad (15-102)$$

Hence, the fan power P_F is given by

$$P_F = \beta \dot{m}_a \bar{c}_{pF} T_0^O \frac{Z_F}{\eta_F} \quad (\text{B/sec}) \quad (15-103)$$

where \dot{m}_a is mass rate of flow of air into the hot gas generator. To obtain P_F in horsepower divide Eq. 15-103 by 0.707 B/hp-sec.

15-9.2 ANALYSIS OF PROCESSES IN TURBOFAN ENGINE

The diffusion and compression processes in the cold air circuit have been discussed in par. 15-9.1. The remaining gas dynamic processes will now be discussed.

15-9.2.1 DIFFUSION FOR HOT GAS GENERATOR CIRCUIT

The equations presented in par. 15-3.1 are directly applicable to the intake-diffuser preceding the hot gas generator (Stations 0 to 2) and need not be repeated here. By means of Eqs. 15-2 and 15-3, the values of T_2^O and P_2^O can be determined. Since the diffusion process is isoenergetic (see par. 3-5.2.2), $T_2^O = T_0^O$ and is defined by Eq. 15-98.

15-9.2.2 COMPRESSOR POWER FOR TURBOFAN ENGINE (P_{cTF})

The total compression work performed on the air inducted by a turbofan engine is the sum of the work performed by the air compressor, denoted by Δh_c , and that performed by the fan Δh_F (see Eq. 15-102). The work Δh_c , in B/slug of air, is given by Eqs. 15-6 and 15-11, and the compressor isentropic efficiency η_c is given by Eq. 15-7. Hence, the total compression work, Δh_{cTF} , noting that $T_{2F}^O = T_2^O = T_0^O$, is given by (see Eq. 15-102)

$$\begin{aligned} \Delta h_{cTF} &= \frac{\dot{m}_a \Delta h_c + \beta \dot{m}_a \Delta h_{cF}}{\dot{m}_a (1 + \beta)} \\ &= \frac{\bar{c}_{pc} T_0^O \left(\frac{Z_c}{\eta_c} + \beta \frac{Z_F}{\eta_F} \right)}{1 + \beta} \quad (\text{B/slug}) \quad (15-104) \end{aligned}$$

In Eq. 15-104, it is assumed that $\bar{c}_{pc} = \bar{c}_{pF}$ which introduces no significant error. The compression factor Z_c is given by Eq. 15-8, Z_F by Eq. 15-101; \dot{m}_a is in slug/sec, and Δh_{cTF} is in B/slug.

Hence, the power required for compressing the air inducted by a turbofan engine, denoted by P_{cTF} , is given by

$$P_{cTF} = 1.413 \dot{m}_a (1 + \beta) \Delta h_{cTF} \quad (\text{hp}) \quad (15-105)$$

In Eq. 15-105, the constant 1.413 transforms B/sec into hp.

15-9.2.3 BURNER FUEL-AIR RATIO FOR TURBOFAN ENGINE (f)

In the case of turbofan engines for propelling aircraft at subsonic speeds fuel is burned only in the hot gas generator circuit, between Stations 3 and 4 (see Fig. 15-29(B)). Turbofan engines for supersonic propulsion utilize *afterburning* in the hot gas stream (see par. 12-4.3) and also *coburning* in the cold air stream. The discussion here is limited to turbofan engines for propelling subsonic aircraft.

The heat added in the combustor Q_i raises the enthalpy of the working fluid from $\dot{m}_a h_3^O$ at the entrance to the burner to $\dot{m}_a(1+f)h_4^O$ at its exit section. If the sensible enthalpy of the inject fuel is neglected², then

$$\dot{m}_f Q_i = \dot{m}_a (1+f) h_4^O - h_3^O$$

In terms of the mean specific heat for the burner \bar{c}_{pB} and the temperature ratio $a = T_4^O/T_0$, $a_2 = T_3^O/T_0$, and the fuel-air ratio $f = \dot{m}_f/\dot{m}_a$, the last equation can be transformed to read

$$\frac{f Q_i}{\bar{c}_{pB} T_0} = (1+f)a - a_2 \quad (15-106)$$

Hence, the fuel-air ratio f is given by

$$f = \frac{a - a_2}{(Q_i/\bar{c}_{pB} T_0) - a} \quad (15-107)$$

15-9.2.4 TURBINE POWER FOR TURBOFAN ENGINE (P_{tTF})

The efficiency η_t of the turbine and the turbine work Δh_t in B/unit mass of working

fluid are given by Eqs. 15-28 and 15-24, respectively, and need not be repeated here.

The turbine expansion ratio parameter, denoted by Θ_t , is given by Eq. 15-84. Hence

$$\Delta h_t = \bar{c}_{pt} \eta_t T_4^O Z_t \quad (15-108)$$

where

$$Z_t = 1 - \Theta_t = 1 - \left(\frac{P_5^O}{P_4^O} \right)^{\frac{\gamma-1}{\gamma}} \quad (15-109)$$

The turbine furnishes the power for compressing the air, overcoming friction in the bearings of the engine, gearing, and auxiliary power.

The turbine delivers the power for compressing the air P_{tTF} plus that required to overcome mechanical inefficiencies in the machinery, auxiliary power, and any other losses. For simplicity the aforementioned parasitic power requirements will be neglected. Hence, the turbine power P_{tTF} is given by

$$\begin{aligned} P_{tTF} &= \dot{m}_a (1+f) \eta_t (1 - \Theta_t) \\ &= \dot{m}_a (1+f) \bar{c}_{pt} (T_4^O - T_5^O) \end{aligned} \quad (15-110)$$

where η_t is given by Eq. 15-28 and

$$\Theta_t = \left(\frac{P_5^O}{P_4^O} \right)^{\frac{\gamma-1}{\gamma}} = \text{turbine expansion ratio parameter} \quad (15-111)$$

In view of the above assumptions, $P_{tTF} = P_{cTF}$. One may write, therefore, that

$$\dot{m}_a (1+f) \bar{c}_{pt} (T_4^O - T_5^O) = \dot{m}_a \bar{c}_{pc} T_2^O \left[\left(\frac{T_3^O}{T_2^O} - 1 \right) + \beta \left(\frac{T_{3F}^O}{T_{2F}^O} - 1 \right) \right]$$

For the adiabatic flow between Stations 0 and 2 and 2F (see Fig. 15-29(B)) $T_0^O = T_2^O = T_{2F}^O$. Hence, the last equation becomes

$$\dot{m}_a (1+f) \bar{c}_{pt} (T_4^O - T_5^O) = \dot{m}_a \bar{c}_{pc} T_0^O \left[\left(\frac{T_3^O}{T_0^O} - 1 \right) + \beta \left(\frac{T_{3F}^O}{T_0^O} - 1 \right) \right] \quad (15-112)$$

The last equation can also be written in terms of the pressure ratios P_3^O/P_2^O , P_{3F}^O/P_{2F}^O , and the turbine expansion ratios P_5^O/P_4^O . Thus

$$\dot{m}_a (1+f) \eta_t T_4^O \left[1 - \left(\frac{P_5^O}{P_4^O} \right)^{\frac{\gamma_t-1}{\gamma_t}} \right] = \dot{m}_a \bar{c}_{pc} T_0^O \left\{ \left[\left(\frac{P_3^O}{P_2^O} \right)^{\frac{\gamma-1}{\gamma}} - 1 \right] \frac{1}{\eta_c} + \beta \left[\left(\frac{P_{3F}^O}{P_{2F}^O} \right)^{\frac{\gamma-1}{\gamma}} - 1 \right] \frac{1}{\eta_F} \right\} \quad (15-113)$$

Solving Eq. 15-113 for the turbine expansion ratio P_5^O/P_4^O one obtains

$$\frac{P_5^O}{P_4^O} = \left[1 - \frac{\frac{1}{\eta_c} (\Theta_c - 1) + \frac{\beta}{\eta_F} (\Theta_F - 1)}{\frac{\bar{c}_{pt}}{\bar{c}_{pc}} \left(\frac{T_4^O}{T_0^O} \right) (1+f) \eta_t} \right]^{\frac{\bar{\gamma}_t}{\bar{\gamma}_t - 1}} \quad (15-114)$$

where $\bar{\gamma}_t$ is the mean value of γ for the turbine expansion process. The variables Θ_c , η_c , Θ_F , η_F , and η_t are given by Eqs. 15-8, 15-7, 15-99, 15-97 and 15-28, respectively.

15-9.2.5 NOZZLE EXPANSIONS FOR TURBOFAN ENGINE

It is assumed that the hot gas generator propulsive nozzle (see Fig. 15-29, section 6-7)

and the cold air propulsive nozzle (section 6F - 7F) both expand the gas flowing through them to the atmospheric back pressure P_0 . Furthermore, it is assumed that there are no pressure drops between Stations 3 and 6, and 3F and 6F. Also each nozzle has the same nozzle isentropic efficiency η_n . Hence

$$P_5^O = P_6^O; P_{3F}^O = P_{6F}^O; P_7 = P_{7F} = P_0$$

also

$$h_5^O = h_6^O = h_7^O; h_{3F}^O = h_{6F}^O = h_{7F}^O$$

15-9.2.5.1 NOZZLE EXPANSION WORK FOR GAS GENERATOR NOZZLE

$$\Delta h_n = h_6^O - h_7 = \bar{c}_{pn} T_6^O (1 - \Theta_n) \eta_n \quad (\text{B/lb}) \quad (15-115)$$

where

$$\Theta_n = \left(\frac{P_0}{P_6^O} \right)^{\frac{\bar{\gamma}_n - 1}{\bar{\gamma}_n}} = \frac{T_7^O}{T_6^O} \quad (15-116)$$

where $\bar{\gamma}_n$ is the mean value of γ for the nozzle expansion.

From Eq. 15-75, the effective jet velocity V_j for the gas flowing through the hot gas generator nozzle is accordingly

$$V_j = \sqrt{2(h_6^O - h_7)} = \phi_n \sqrt{2 \frac{\bar{\gamma}_n}{\bar{\gamma}_n - 1} R_g T_6^O [1 - \Theta_n]} \quad (15-117)$$

where Θ_n is given by Eq. 15-116, R_g is gas constant for hot gas, and

$$\phi_n = \sqrt{\eta_n} = \text{nozzle velocity coefficient} \quad (15-118)$$

15-9.2.5.2 NOZZLE EXPANSION WORK FOR COLD AIR-STREAM

$$\Delta h_{nF} = h_{6F}^O - h_7 = \bar{c}_{pnF} T_{6F}^O (1 - \Theta_{nF}) \eta_n \quad (15-119)$$

where

$$\Theta_{nF} = \left(\frac{P_0}{P_{6F}^O} \right)^{\frac{\bar{\gamma}_{nF} - 1}{\bar{\gamma}_{nF}}} = \frac{T_{7F}^O}{T_{6F}^O} \quad (15-120)$$

where $\bar{\gamma}_{nF}$ is the mean value of γ for the cold air nozzle expansion process, and \bar{c}_{pnF} is the mean specific heat for that process.

By analogy with Eq. 15-118, one obtains for the cold air nozzle

$$V_{jF} = \phi_{nF} \sqrt{2 \frac{\bar{\gamma}_{nF}}{\bar{\gamma}_{nF} - 1} R_a T_{6F}^O (1 - \Theta_{nF})} \quad (15-121)$$

where R_a is the gas constant for air, and Θ_{nF} is given by Eq. 15-120.

15-10 PERFORMANCE PARAMETERS FOR TURBOFAN ENGINE

The equations for the more important performance parameters are presented below.

15-10.1 THRUST EQUATION (F)

The thrust of the turbofan engine is given by Eq. 12-15 which is repeated here for convenience. Thus

$$F = \dot{m}_a (1 + f) V_j + \beta \dot{m}_a V_{jF} - \dot{m}_a V_0 (1 + \beta) \quad (15-122)$$

15-10.2 MEAN JET VELOCITY FOR TURBOFAN ENGINE (\bar{V}_{jTF})

By the introduction of a fictitious mean jet velocity \bar{V}_{jTF} , the thrust equation becomes

$$F = \dot{m}_a (1 + f) \bar{V}_{jTF} - \dot{m}_a V_0 (1 + \beta) \quad (15-122a)$$

Equating Eqs. 15-122 and 15-122a and solving for \bar{V}_{jTF} yields

$$\bar{V}_{jTF} = \frac{(1 + f) V_j + \beta V_{jF}}{1 + f} \quad (15-123)$$

15-10.3 AIR SPECIFIC IMPULSE (OR SPECIFIC THRUST) (I_a)

By definition (see pars. 12-6.1 and 15-8.4)

$$I_a = \frac{F g_c}{\dot{m}_a} = (1 + f) \bar{V}_{jTF} - V_0 (1 + \beta) \quad (15-124)$$

where the mean effective jet velocity is given by Eq. 15-123, which shows that its value depends on f , V_j , V_{jF} , and β . Studies of the effect of varying the bypass ratio are presented in Reference 11. In general, increasing the bypass ratio increases the air specific impulse I_a .

15-10.4 CONCLUSIONS

The following conclusions may be derived from studies of propulsion system requirements for long-range subsonic aircraft.

- (a) For each selected turbine inlet temperature T_4^O there is an optimum value for the bypass ratio β , for a given pressure ratio.
- (b) To achieve the maximum possibilities from the turbofan engine, high turbine inlet temperatures are required; i.e., cooled turbine blading must be developed. There is a limit, however, to the maximum T_4^O , above which the TSFC increases.
- (c) At very high values of T_4^O , increasing T_4^O raises the optimum value for β , because excessive leaving losses must be prevented.
- (d) The TSFC is improved by increasing the cycle pressure ratio, particularly for the higher values T_4^O .
- (e) Design studies show that incorporating a regenerator in the turbofan engine cycle can effect significant reductions in the TSFC¹³.

REFERENCES

1. M. J. Zucrow, *Jet Propulsion and Gas Turbines*, John Wiley and Sons, Inc., 3rd Printing, 1951, Chapter 7.
2. M. J. Zucrow, *Aircraft and Missile Propulsion*, John Wiley and Sons, Inc., 2nd Printing, 1964.
3. W. M. Rosenhow and J. P. Hunsaker, *Part Load Characteristics of Marine Gas-Turbine Plants*, ASME, Annual Mtg., New York December 2-6, 1946.
4. W. J. Hesse and N. V. S. Mumford, Jr., *Jet Propulsion for Aerospace Applications*, Pitman Publishing Corporation, 2nd Ed., 1964.
5. C. R. Soderberg and R. B. Smith, "The Gas Turbine as a Possible Marine Prime Mover", *Trans. Soc. Naval Architects and Marine Eng.*, November 11, 1943.
6. M. J. Zucrow, "Potentialities and Development Problems of the Turboprop Engine", *ARS Jour.*, September 1949, p. 116.
7. B. Pinkel and I. M. Karp, *A Thermodynamic Study of the Turbine-Propeller Engine*, NACA TN 2653, March 1952.
8. F. W. Godsey and C. D. Flagle, "The Place of the Gas Turbine in Aviation", *Westinghouse Engineers*, July 1945.
9. K. S. Coward, "Propeller Static Thrust", *Aerospace Eng.*, March 1959, p. 64.
10. J. Shapiro, *Principles of Helicopter Engineering*, McGraw-Hill Book Co., Inc., 1955.
11. R. E. Neitzel and M. C. Hemsworth, "High-Bypass Turbofan Cycles for Long Range Subsonic Transports", *Jour. of Aircraft*, July-Aug. 1966, p. 354.
12. C. L. Bagby and W. L. Anderson, "Effect of Turbofan Cycle Variables on Aircraft Cruise Performance", *Jour. of Aircraft*, Sept.-Oct. 1966, p.385.
13. J. A. Bogdanoric, A. Feder, and R. J. Wheaton, "A Method of Determining Propulsion System Requirements for Long-Range, Long-Endurance Aircraft", *Jour. of Aircraft*, Nov.-Dec. 1965, p. 499.
14. B. J. Piearcy and F. L. Versnyder, "New Development in Gas Turbine Materials: The Properties and Characteristics of PWA 664", *Jour. of Aircraft*, Sept.-Oct., 1966, p. 390.
15. J. T. Kutney, "Propulsion System Development for V/STOL Transports", *Jour. of Aircraft*, Nov.-Dec. 1966, p. 489.
16. R. J. E. Glenney and J. F. Barnes, "Some Materials and Cooling Techniques Applicable to Air-Breathing Engines at High Flight Speeds", *Jour. of Aircraft*, Nov.-Dec. 1966, p. 507.

APPENDIX A

ELEMENTARY GAS DYNAMICS

A-0 PRINCIPAL NOTATION FOR APPENDIX A*

a	acoustic or sonic speed, fps	C_c	contraction coefficient
a*	critical acoustic speed, where $M = 1$, fps	C_d	discharge coefficient
a⁰	stagnation or total acoustic speed, fps	d	diameter, ft or in., as specified in text
A	flow cross-sectional area, sq ft or sq in., as specified in text	D	drag force, lb
A*	critical cross-sectional area where $u = a^*$	D	hydraulic diameter = $4R$ where R is the hydraulic radius
A_m	maximum cross-sectional area	e	stored energy per unit mass of fluid
B	British thermal unit	E	total amount of stored energy associated with a system
c	effective jet or exhaust velocity; specific heat, B/slug-°R	E_{KE}	kinetic energy
c₀	maximum isentropic speed = $q'_{\max} = \sqrt{2c_p T^0}$	E_{PE}	potential energy
c_p	instantaneous specific heat at constant pressure, B/slug-°R	δE_f	energy expended in overcoming friction
\bar{c}_p	mean value of c_p for a specified temperature range	f	friction coefficient in the Fanning equation for pressure loss
c_v	instantaneous value of the specific heat at constant volume	F	thrust, lb
		F_f	friction force, lb
		F	impulse function, lb
		g	local acceleration due to gravitational attraction of earth, ft/sec ²
		g_c	gravitational conversion factor = 32.174 slug-ft/lb-sec ²

*Any consistent set of units may be employed; the units presented here are for the American Engineers System (see par. 1-7).

G	flow density or mass velocity = \dot{m}/A , slug/sec-ft ²	M*	dimensionless velocity (q/a^* or u/a^*)
G*	critical flow density, value of G where $M = 1$	\vec{M}	momentum vector
h	static specific enthalpy, B/slug	$\dot{\vec{M}}$	rate of change in momentum = $d\vec{M}/dt$, (ML/T)
h^o	stagnation or total specific enthalpy, B/slug	n	number of degrees of freedom of a gas molecule
Δh	finite change in specific enthalpy	N_A	Avogadro's number, $(6.02472 \pm 0.006) (10)^{23}$ molecules/gram-mole; corresponds to $2.70(10)^{19}$ molecules/cc (at 0°C and 760 mmHg) = 2.7237×10^{26} molecules per lb mole
Δh_c	finite specific enthalpy change for a compression process, B/slug	p	absolute static pressure, psia
Δh'_c	finite specific enthalpy change for an isentropic compression process, B/slug	p_a	ambient static pressure, psia
Δh_t	finite specific enthalpy change for an expansion process, B/slug	p*	critical static pressure, where $u=a^*$, psia
Δh'_t	finite specific enthalpy change for an isentropic expansion process, B/slug	P	absolute static pressure, psf
J	mechanical equivalent of heat ≈ 778 ft-lb/B	P*	critical static pressure, where $u = a^*$, psf
k_B	Boltzmann's constant = $1.3804(10)^{-16}$ erg/mole-°K	P	power, dW/dt
K	bulk modulus of fluid	ΔP_λ	pressure loss
L	length, unit as specified in text	\vec{q}	velocity vector
m	mass, slug	q	magnitude of q or the dynamic pressure, as specified in text
\dot{m}	mass flow rate, slug/sec	q_n	velocity of fluid normal to flow area dS , fps
\bar{m}	molecular weight, slug/mole	q'	isentropic velocity, fps
M	Mach number (q/a or u/a), or magnitude of momentum vector, as specified in text	q'_{max}	maximum isentropic speed $= c_o = \sqrt{2c_p T^o}$

\dot{Q}	volumetric rate of flow, cfs	t	time, sec
δQ	heat added, B/slug	T	absolute static temperature ($^{\circ}\text{F} + 460$), $^{\circ}\text{R}$
δQ_R	heat added reversibly, B/slug	T^*	critical static temperature, value of T where $u = a^*$
r	pressure ratio	T°	stagnation or total temperature, $^{\circ}\text{R}$
r_c	pressure ratio for a compression process = P_2/P_1 (or p_2/p_1), where $P_2 > P_1$	u	specific internal energy, B/slug
r_t	expansion ratio for an expansion process = P_2/P_1 (or p_2/p_1), where $P_1 > P_2$	u	velocity parallel to the x-axis, fps
r^*	expansion ratio which makes $u = a^*$	u_e	adiabatic exhaust velocity
\tilde{R}	force due to interaction of flowing fluid with surfaces wetted by fluid, lb	u^*	critical value of u , where $u = a^*$
R	gas constant = R_u/\bar{m}	u'	isentropic exhaust velocity = $a^{\circ} \sqrt{\left(\frac{2}{\gamma - 1}\right) Z_t}$
R	hydraulic radius = $D/4$, ft or in. as specified in text	U	internal energy of a system, B
Re	Reynolds number	v	specific volume = $1/\rho$, ft^3/slug
R_u	universal gas constant = $49.717 \text{ ft-lb/slug-mole-}^{\circ}\text{R} = 63.936 \text{ B/slug-mole-}^{\circ}\text{R}$	v	velocity parallel to the y-axis
s	static specific entropy, B/slug- $^{\circ}\text{R}$	v°	stagnation value of specific volume = $1/\rho^{\circ}$
s^*	critical value of s , where $u = a^*$	V	total volume or velocity, as specified in text
Δs	finite change in static specific entropy	V	control volume in a region of a flowing fluid
S	control surface	w	weight, mg_c , lb
S	entropy for a system, B/ $^{\circ}\text{R}$	w	velocity in direction of z-axis, or dimensionless linear velocity ($w = u/a^{\circ}$)
S_w	area of interior surface of flow, i.e., passage wetted by flowing fluid	(wp)	wetted perimeter

W	work	Θ_c	pressure ratio parameter for a compression process
${}_1W_2$	work done by system in going from state 1 to state 2	Θ_t	pressure ratio parameter for an expansion process
\dot{w}	weight rate of flow = $\dot{m}g_c$ lb/sec	λ	mean free path for gas molecules
\dot{W}	power P , rate of doing work, dW/dt	μ	absolute or dynamic viscosity of a fluid
X	net force acting parallel to x-axis	μ	Mach angle, or compressibility factor for a real gas
Y	net force acting parallel to y-axis	ρ	density, slug/ft ³
z	elevation above datum line	ρ^*	critical density = $1/v^*$, value of ρ where $u = a^*$
Z	net force acting parallel to z-axis	ρ^0	stagnation or total density
Z_c	compression factor = $r_c^{\frac{\gamma-1}{\gamma}} - 1$	τ	shear stress (friction force per unit area)
Z_t	expansion factor = $1 - r_t^{\frac{\gamma-1}{\gamma}}$	ϕ	velocity coefficient = u/u'

GREEK LETTERS

α	angle between velocity vector and normal to flow cross-sectional area
β	angle between the flow leaving an oblique shock and the shock front
γ	specific heat ratio = c_p/c_v
δ	angle for the deflection of a flow after passing through an oblique shock
ϵ	angle between the incident flow and an oblique shock
η	efficiency
θ_c	semi-cone angle, deg
θ_w	semiangle for a symmetrical wedge

SUBSCRIPTSNumerals

0	free stream
1	initial state, or reference Station 1
2	final state, or reference Station 2

Letters

a	ambient or atmospheric
B	burner or combustion chamber
c	compression
d	diffuser

e	exit cross-sectional area normal to flow direction
ext	external
f	friction
h	hydraulic
imp	impact
int	internal
L	limiting value
max	maximum value
min	minimum value
n	nozzle
p	propulsive
P	ideal propulsive; at constant pressure
s	at constant entropy
t	expansion or turbine, as specified in text
T	at constant temperature
th	thermal
V	at constant volume

SUPERSCRIPTS

'	(prime) denotes the value is obtained by means of an isentropic process
*	critical condition, where $u=a^*$ and the Mach number is unity
o	stagnation or total value

A-1 INTRODUCTION

Gas dynamics, which is the theory of the flow of a compressible fluid, is of fundamental importance to the design and analysis of all jet propulsion systems. The thrust developed by a jet propulsion system is governed in large measure by the interactions of the compressible fluid flowing through the system with its internal surfaces.

The object of applying gas dynamic analysis to a jet propulsion system is to determine, thereby, those parameters which characterize the motion of the compressible fluid and its thermodynamic states at pertinent locations in the flow path of the compressible fluid as it flows through the jet propulsion system.

In most jet propulsion engines the gas dynamic processes are such that, except for transients, the flow may be assumed to be *steady* and *one-dimensional*. The results calculated from the relationships derived for one-dimensional flow will be correct in principle but only approximate if the flows are multidimensional. There are certain flow processes that occur in the functioning of the jet propulsion engines, see Chapter 1, and several of them are essentially one-dimensional in character.

For analyzing the flow processes pertinent to jet propulsion engines, the following physical principles are available:

- (a) The principle of the conservation of matter for a flowing fluid, which is discussed in par. A-1.
- (b) The principle of the conservation of momentum which is expressed by the momentum theorem of fluid mechanics discussed in par. 2-1 (see Eqs. 2-11 and 2-21).

- (c) The principle of the conservation of energy which was first demonstrated for an *isolated mechanical system* by Leibnitz (1693). For a flowing fluid the principle leads to the so-called *energy equation*, discussed in par. A-3.3.
- (d) The second law of thermodynamics from which one obtains the entropy equation for a flowing fluid (discussed in par. A-3.4).
- (e) The thermodynamic properties of the flowing compressible medium under consideration; these can be represented by either some form of defining equation relating the static pressure, density, and temperature of the flowing fluid, or by tables.

The pertinent equations derived by applying the principles listed above are then combined to obtain the relationships between the variables of interest. In many cases the desired information can be obtained without applying all of the aforementioned principles.

The motion of a compressible fluid is considered to be determined when the three rectangular components of a *velocity vector* \mathbf{q} , the static pressure P , and the density of the fluid ρ , are known as functions of the Cartesian coordinates x , y , z and of the time t .

In general, any two of the following thermodynamic properties of the fluid must either be known or calculable so that the (macroscopic) *thermodynamic state* of the fluid can be determined; P , the absolute static pressure; T , the absolute static temperature; ρ , the static density; h , the static specific enthalpy; and s , the static specific entropy.

The thermodynamic state of a system is determined by its thermodynamic properties just insofar as they are measured directly or

indirectly by experiment. The properties give no information of the previous history of the state of the system.

The equations of motion for a fluid can be written in either the *Eulerian* or *Lagrangian* form. In the Eulerian form, the one employed in this handbook, unless it is specifically stated to be otherwise, the parameters for characterizing the state of a flowing compressible fluid are referred to a *fixed point in space and time*. From the thermodynamic state of the fluid, assuming that either its *equation of state* is known or that appropriate tables of its thermodynamic properties are available, the thermodynamic state of the fluid at the point under consideration can be determined.

From the rectangular components of the momentum equation (see par. 2-1.2) one obtains three equations of motion, one referred to each of the three Cartesian coordinate axes. The conservation laws for matter (or mass) and energy yield two additional equations. Consequently, one obtains a system of five equations for determining five unknown quantities; the velocity components (u, v , and w), the static pressure P , and the fluid density ρ . In general, the equations are nonlinear, first order, partial differential equations^{4, 28}.

The mathematical methods employed in gas dynamic studies are concerned with solving the aforementioned system of nonlinear first order differential equations. Exact mathematical solutions are obtained for flows which are *steady and one-dimensional*; i.e., flows in which the variables P, ρ , and q , or their equivalents, change appreciably only in a single direction and do not vary with time. It will be assumed in the discussions, unless it is specifically stated to be otherwise, that the flow is steady and one-dimensional.

The thermodynamic properties of a flowing fluid are related to the flow variables by relating

the fluid velocity to its density. If the flowing fluid is an *ideal gas*—one which is both *thermally* or *calorically perfect*—the solution of the gas dynamic equations is greatly simplified. The characteristics of the ideal gas are discussed in par. A-2.

A-2 THE IDEAL GAS

The ideal gas is the simplest working fluid in thermodynamics. Consequently, it is a most valuable concept in the study of gas dynamic processes. Moreover, as will be seen later, the propellant gas which flows through the exhaust nozzle of a jet propulsion system approximates the ideal gas.

A-2.1 THE THERMALLY PERFECT GAS

It was shown empirically by the early experimenters that the so-called permanent gases, air, nitrogen, oxygen, hydrogen, etc., under ordinary conditions of pressure and temperature behaved in accordance with the following equation of state:

$$P = \rho RT = \frac{R_u}{\bar{m}} \quad (\text{psf}) \quad (\text{A-1})$$

where, in the AES system of units (see par. 1-7)

T = absolute temperature of the gas, °R

P = absolute pressure of the gas, psf

ρ = density of gas, slug/ft³

R_u = universal gas constant = 49.717 ft-lb/slug-mole-°R = 63.936 B/slug-mole-°R

\bar{m} = molecular weight of the gas, slug/mole

A medium which behaves in accordance with Eq. A-1 is called a *thermally perfect gas*. Experimental studies of the behavior of *real*

gases indicate that Eq. A-1 is an approximation to the correct equation of state for a real gas. In general, the correct equation of state is a functional relationship of the form

$$P = P(\rho, T) \quad (\text{A-2})$$

or

$$\rho = \rho(P, T) \quad (\text{A-2a})$$

In the case of a *thermally perfect gas*

$$\frac{P}{\rho RT} = 1 \quad (\text{A-3})$$

For a *real* gas, the deviations of the ratio $P/\rho RT$ from unity become significant at very high pressures, such as those occurring in guns, and at very low temperatures. The deviations arise from the fact that *every real gas can be liquefied*.

Logarithmic differentiation of Eq. A-1 gives the following differential equation for the behavior of a *thermally perfect gas*:

$$\frac{dP}{P} = \frac{d\rho}{\rho} + \frac{dT}{T} \quad (\text{A-4})$$

A-2.2 THE CALORICALLY PERFECT GAS

For a unit mass of gas (1-slug) that has undergone a *reversible* change of state, the *first law of thermodynamics* yields

$$\delta Q_R = du + Pdv \quad (\text{B/slug}) \quad (\text{A-5})$$

where

δQ_R = the heat added reversibly, B/slug

du = the change in the specific internal energy of the gas, B/slug

$dv = 1/d\rho$ = the change in the specific volume of the gas, cu ft

P = the absolute pressure of the gas, psf

By definition, the *specific heat* of a medium is given by

$$c = \frac{\delta Q}{dt} \quad (\text{B/slug} \cdot ^\circ \text{R}) \quad (\text{A-6})$$

In Eq. A-6 the magnitude of the specific heat c depends upon the manner by which the heat increment δQ , which is *not* an exact differential because Q is not a thermodynamic property, is added to the medium.

The specific internal energy u see Eq. A-5, is a *property* of the system and depends only upon its state. For a *simple system* one may write: ^{1, 6, 19}

$$u = u(T, v) \quad (\text{B/slug}) \quad (\text{A-7})$$

Eq. A-7 is known as the *caloric equation of state*. The *exact differential* du , is accordingly

$$du = \left(\frac{\partial u}{\partial T} \right)_v dT + \left(\frac{\partial u}{\partial v} \right)_T dv \quad (\text{A-8})$$

If δQ is added to a unit mass of gas under isovolumic conditions ($dv = 0$), then

$$c_v = \left(\frac{\delta Q}{dT} \right) = \left(\frac{\partial u}{\partial T} \right)_v = \text{specific heat at constant volume} \quad (\text{A-9})$$

From Eq. A-9 the specific internal energy of a gas can be calculated from

$$u = \int_{T_0}^T c_v dT + u_0 \quad (\text{B/slug}) \quad (\text{A-10})$$

For a gas which is *calorically perfect* the specific heat c_v is a constant, independent of the gas temperature so that

$$u - u_0 = c_v (T - T_0) \quad (\text{A-11})$$

For a gas which is *thermally perfect but not calorically perfect*

$$P = \rho RT \quad \text{and} \quad c_v = f(T)$$

An *ideal gas* is one which is both thermally and calorically perfect. Such a gas is often called a *polytropic gas*⁴.

A-2.3 SPECIFIC HEAT RELATIONSHIPS FOR THE IDEAL GAS

If the heat is added to a gas under *isobaric conditions* ($dP = 0$), then the specific heat at *constant pressure* c_p is given by

$$c_p = \frac{\delta Q}{dT} = \left(\frac{du}{dT} \right)_v + \left[\left(\frac{\partial u}{\partial v} \right)_T + P \right] \left(\frac{\partial v}{\partial T} \right)_P \quad (\text{B/slug}) \quad (\text{A-12})$$

It is apparent from Eq. A-12 that $c_p > c_v$ as is to be expected. In Eq. A-12

$$P \left(\frac{\partial v}{\partial T} \right)_P dT = \text{work done against external forces}$$

and

$$\left(\frac{\partial u}{\partial v} \right)_T \left(\frac{\partial v}{\partial T} \right)_P dT = \text{work done against internal forces}$$

For an ideal gas, the specific heat c_p is given by

$$c_p = \frac{dh}{dT} \quad (\text{B/slug}) \quad (\text{A-13})$$

By definition, the *specific enthalpy* h which is a property of the gas, is defined by

$$h \equiv u + P/\rho \quad (\text{B/slug}) \quad (\text{A-14})$$

By definition

$$\gamma \equiv \frac{c_p}{c_v} = \text{the specific heat ratio} \quad (\text{A-15})$$

For an ideal gas c_v, c_p , and γ are constants independent of the gas temperature. These constants are related by the equations which follow. Thus

$$c_p - c_v = R \quad (\text{Regnault Relationship}) \quad (\text{A-16})$$

and

$$c_v = R \left(\frac{1}{\gamma-1} \right) \text{ and } c_p = R \left(\frac{\gamma}{\gamma-1} \right) \quad (\text{A-17})$$

The changes of state of usual interest for an ideal gas may be regarded as special cases of the *polytropic change of state* $Pv^n = \text{constant}$. Thus

Value of n	Process
1	Isothermal ($dT = 0$)
0	Isobaric ($dP = 0$)
∞	Isovolumic ($dv = 0$)
γ	Isentropic ($ds = 0$)

A-2.4 SOME RESULTS FROM THE KINETIC THEORY OF GASES

From kinetic theory, the following principal equations are obtained for an ideal gas^{1,15,17,20,25}.

(a) Molecular mean free path (λ)

$$\lambda = \frac{1}{\sqrt{2}n\pi d^2} \quad (\text{cm}) \quad (\text{A-18})$$

where

n = number of molecules per cc

d = effective diameter of molecule, cm

(b) Temperature (T)

If $(E_{KE})_{tr}$ is the kinetic energy of an ideal gas due to its random translatory motion, N is the number of molecules in volume V , and m is the mass of each molecule then

$$(E_{KE})_{tr} = 1/2 Nm\bar{C}^2 \propto T \quad (\text{A-19})$$

where $(E_{KE})_{tr}$ constitutes the internal energy of the gas, and $\sqrt{\bar{C}^2}$ is the *rms*-velocity. If T is fixed then the internal energy of the gas is also fixed.

(c) Pressure (P)

According to the kinetic theory the pressure P acting upon the walls of a container, of volume V , is due to the impacts of the gas molecules on these walls. It can be shown that

$$PV = \frac{2}{3} (1/2 Nm\bar{C}^2) = \frac{2}{3} (E_{KE})_{tr} \quad (\text{A-20})$$

Since, the density of the gas is given by

$$\rho = \frac{NM}{V}$$

Hence

$$P = \frac{2}{3} \left(\frac{1}{2} \rho \bar{C}^2 \right) \quad (\text{A-21})$$

(d) Boltzmann's Constant (k_B)

If N_A is *Avogadro's number*, and R_u the universal gas constant, then, by definition

$$k_B \equiv R_u/N_A \quad (\text{A-22})$$

where

$N_A = (6.02472 \pm 0.006)(10)^{23}$ molecules/gram-mole, which corresponds to $2.70(10)^{19}$ molecules/cc at 0°C and 760 mm Hg

$$k_B = 1.3804(10)^{-16} \text{ erg/mole-}^\circ\text{K}$$

It is readily shown that

$$R_u T = \frac{2}{3} (E_{KE})_{tr} \quad (A-23)$$

(e) *Viscosity* (μ)

For an ideal gas

$$\mu = 0.49 \rho \bar{C} \lambda \propto \bar{C} T \quad (A-24)$$

As ρ decreases, the mean free path λ increases so that the product $\rho \lambda$ tends to remain constant. The equation indicates that for an ideal gas the viscosity depends only on the gas temperature T , and increases with T .

(f) *Maxwell's Equipartition Law*

For one mole of a monatomic gas

$$(E_{KE})_{tr} = \frac{3}{2} R_u T \quad (\text{B/mole}) \quad (A-25)$$

If $\bar{m}c_v$ = the molar heat capacity of the gas at constant volume, then

$$\bar{m}c_v = \frac{3}{2} R_u = \frac{3}{2} (63.94) = 95.91 \text{ B/slug-mole-}^\circ\text{R}$$

According to the above law, the kinetic energy of a gas molecule is equally divided among all of its degrees of freedom. Since a monatomic gas has 3 degrees of freedom, the energy per mole of gas is

$$\bar{m}c_v = \frac{3}{2} R_u \quad (A-26)$$

A rigid diatomic molecule has 5 degrees of freedom, so that

$$\bar{m}c_v = \frac{5}{2} R_u \quad (A-27)$$

In general, if n is the number of atoms in the ideal gas molecule the number of degrees of freedom for translatory, rotational, and vibratory motions is $3n$. Since each molecule has 3 degrees of translatory freedom, the number of degrees of freedom for rotation and vibration is $3n - 3$. Consequently, a monatomic molecule ($n=1$) has no rotational or vibratory degrees of freedom^{17,26}.

(g) *Specific Heat Ratio* (γ)

The kinetic theory indicates that the specific heat ratio γ has the following values depending upon the atoms in the gas molecule:

(1) Monatomic gases $\gamma = 1.66$

(2) Diatomic gases $\gamma = 1.40$

(3) Triatomic gases $\gamma = 1.30$

The above values are accurate for monatomic gases, less accurate for diatomic gases, and least accurate for triatomic gases.

For *air* under ordinary values of P and T , $\gamma_a \approx 1.40$. At high air temperature γ_a decreases from the value 1.40. If one *assumes* that air is an *ideal gas* with $\gamma = 1.40 = \text{constant}$, then

$$\frac{\gamma + 1}{2(\gamma - 1)} = 3; \frac{2}{\gamma - 1} = 5; 2 \left(\frac{\gamma}{\gamma - 1} \right) = 7 \quad (A-28)$$

where $\gamma = \gamma_a$.

Fig. A-1 presents the dimensionless ratios c_v/R and c_o/R for ideal gases as functions of the specific heat ratio $\gamma = c_p/c_v$ (from par. A-2, $R_u = 63.936 \text{ B/slug-mole-}^\circ\text{R}$ and $R = R_u/\bar{m}$).

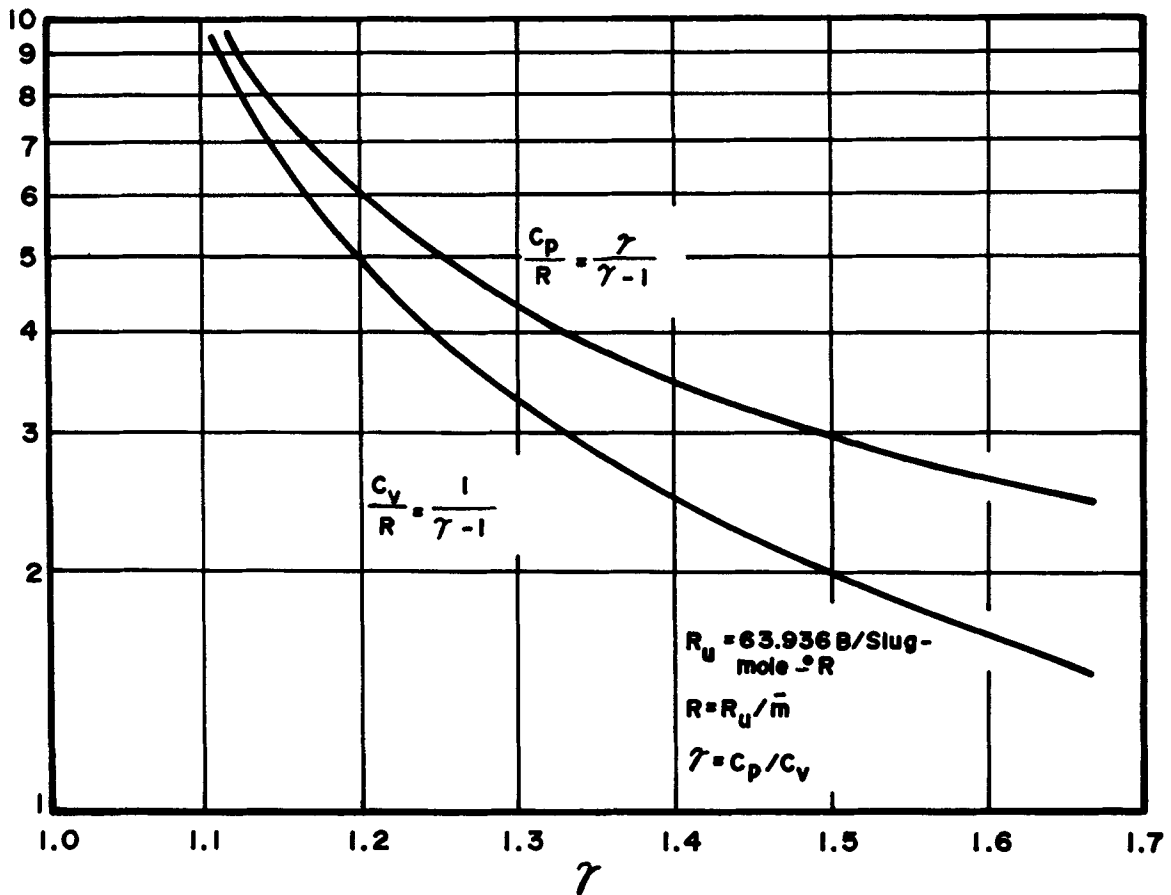


Figure A-1. Specific Heats of Ideal Gases as Functions of the Specific Heat Ratio

A-2.5 SOME CHARACTERISTICS OF REAL GASES

The ideal gas laws do not hold exactly for real gases. Every real gas is characterized by the magnitudes of the parameters which follow:

- The *critical temperature* T_{cr} which is the highest temperature at which a gas can be liquefied.
- The *critical pressure* P_{cr} , the pressure corresponding to T_{cr} .
- The *critical density* ρ_{cr} , the density corresponding to T_{cr} and P_{cr} .

Thus T_{cr} , P_{cr} , and ρ_{cr} are characteristic properties of a real gas; their values are related to the intermolecular forces of the gas. The deviation of a real gas from the ideal gas is expressed in terms of the so-called *compressibility factor*, denoted by μ , defined by

$$\mu = \frac{P}{\rho RT} \quad (\text{A-29})$$

The degree to which μ departs from the value unity is a measure of the *nonideal* character of a gas¹⁸.

For a given gas it is customary to plot the compressibility factor μ as a function of the

reduced pressure P_r and reduced temperature T_r where

$$P_r = \frac{P}{P_{cr}} \text{ and } T_r = \frac{T}{T_{cr}} \quad (\text{A-30})$$

Such plots are presented in several texts on thermodynamics^{1,9,20,21}. They show that if P_r and T_r are close to unity, there can be large deviations from the perfect gas law; μ becoming less than unity due to the cohesive forces between the gas molecules.

If T_r is close to unity but P_r is larger than unity, deviations occur in the opposite direction due to the *covolume* of the molecules.

Many special forms of the equation of state for a real gas have been suggested; e.g., the Noble-Abel equation commonly used in the interior ballistics for guns⁷. Because it is impossible to have a single equation which holds over a wide range of conditions, empirical methods are employed^{2,22,23}.

The temperatures (3500° to 8000°F) encountered in jet propulsion systems are well above the *critical temperatures* of the individual component gases entering the exhaust nozzle, and the combustion pressures (250-3000 psia) are moderate compared to the *critical pressures*. It is reasonable, therefore, to assume for engineering calculations that the propellant gas flowing through the exhaust nozzle of a jet propulsion system, air-breathing or rocket, behaves as a thermally perfect gas^{1,12}. Only in exceptional cases is it necessary to employ an empirical equation of state.

On the other hand, the assumption that the propellant gas is calorically perfect over a wide range of temperatures is unreliable except for monatomic gases^{1,9,10,11}.

The specific heat at constant pressure for propellant gases depends primarily on the

molecular weight of the gas \bar{m} . For estimation purposes it can be assumed that¹⁴

$$c_p \approx \frac{321}{\bar{m}} \text{ (B/slug-°R)} \quad (\text{A-31})$$

When the temperature of a gas is high enough to cause dissociation, caution must be exercised in employing the perfect gas laws because the chemical composition of the gas becomes variable. If it is assumed that thermochemical equilibrium is achieved at every condition, the gas composition can be calculated as a function of P and T ^{23,24}. Even though each component of the gas mixture obeys the law $P = \rho RT$, the latter law is not applicable to the dissociated gas mixture. The temperature at which that law ceases to be applicable increases with the pressure because increasing the pressure decreases the dissociation.

In summary, for most of the problems encountered in jet propulsion systems, excepting dissociation, the equation of state of a flowing gas may be assumed to be $P = \rho RT$, with engineering accuracy. The assumption is of advantage because it greatly simplifies the gas dynamic equations. One should be aware, however, that inaccuracies result if the simplification is employed outside the range of its applicability.

Table A-I lists the values of P_{cr} and T_{cr} for several common gases.

A-2.6 ACOUSTIC OR SONIC SPEED (a)

The speed with which a sound wave (or a very small pressure disturbance) is propagated in a fluid is termed either the *acoustic* or *sonic speed*, and is denoted by a . If the fluid may be assumed to be a continuum—molecular free path λ very small compared to mean diameter of molecules—then the acoustic speed depends only upon the isentropic bulk modulus of the fluid K_s and its density ρ .

TABLE A-I
CRITICAL PRESSURE P_{cr} AND CRITICAL TEMPERATURE T_{cr}
FOR SEVERAL GASES

GAS	CHEMICAL FORMULA	P_{cr} (atm)	T_{cr} (°R)
Carbon Dioxide	CO ₂	73	547
Carbon Monoxide	CO	35	241
Chlorine	Cl ₂	76	751
Hydrogen	H ₂	84	653
Hydrogen Sulfide	H ₂ S	89	673
Nitric Oxide	NO	65	322
Nitrous Oxide	N ₂ O	72	558
Nitrogen	N ₂	34	227
Hydrogen Chloride	HCl	82	585
Oxygen	O ₂	50	277
Sulfur Dioxide	SO ₂	78	764
Water Vapor	H ₂ O	218	1165
To obtain P_{cr} and T_{cr} for a mixture of gases, the molal averages of P_{cr} and T_{cr} for the constituent gases are employed.			

A-2.6.1 ISENTROPIC BULK MODULUS (K_s)

The isentropic bulk modulus is defined by^{1 5}

$$K_s = -\left(\frac{dP}{dv/v}\right)_s = \left(\frac{dP}{d\rho/\rho}\right)_s \quad (A-32)$$

where $v = 1/\rho$ = specific volume of the fluid, and $dv/v = -d\rho/\rho$. Hence, the acoustic speed depends on the derivative $dP/d\rho$. Thus

$$a = \sqrt{\left(\frac{dP}{d\rho}\right)_s} \quad (A-33)$$

where the subscript *s* denotes that the compression process is isentropic, i.e., at constant entropy.

A-2.6.2 ACOUSTIC SPEED IN AN IDEAL GAS

For an ideal gas

$$K_s = \gamma P \quad (A-34)$$

where $\gamma = c_p/c_v$ is the specific heat ratio for the gas.

Hence, for an ideal gas

$$a = \sqrt{\frac{\gamma P}{\rho}} = \sqrt{\gamma R T} = \sqrt{\gamma R_u} \sqrt{\frac{T}{m}} \quad (A-35)$$

Logarithmic differentiation of $a^2 = \gamma P/\rho$ yields

$$\frac{da^2}{a^2} = \frac{d\gamma}{\gamma} + \frac{dP}{P} - \frac{d\rho}{\rho} \quad (A-36)$$

A-2.7 MACH NUMBER

When there is a large relative speed between a body and the compressible fluid in which it is immersed, the *compressibility* of the fluid—which is the variation of its density with speed—affects the drag of the body. The ratio of the local speed of the body *u*, to its acoustic speed *a*, is called the local Mach number which is denoted by *M*. For an ideal gas

$$M = \frac{u}{a} = \frac{u}{\sqrt{\gamma R T}} ; \quad (A-37)$$

or

$$M^2 = \frac{u^2}{a^2} = \frac{u^2}{\gamma R T} \quad (A-37a)$$

The speed *u* measures the directed motion of the gas molecules, and *u*² is a measure of the kinetic energy of the directed flow. According

to the kinetic theory of gases the temperature *T* is a measure of the random kinetic energy of the gas molecules. Hence, $M^2 = u^2/a^2$ is a measure of the ratio of the kinetic energies of the directed and random flows of the gas molecules.

For an ideal gas one obtains the equation below by differentiating Eq. A-37a logarithmically. Thus

$$\frac{dM}{M} = \frac{du}{u} - \frac{1}{2} \frac{dT}{T} \quad (A-38)$$

For an ideal gas, the density ρ can be expressed in the form

$$\rho = \frac{\gamma P}{u^2/M^2} \quad (A-39)$$

The Mach number *M* is a useful dimensionless parameter.

A-3 STEADY ONE-DIMENSIONAL FLOW*

The one-dimensional approximation to the flow of a fluid gives the simplest solutions to the flow equations. It is based upon the *assumptions* presented below:

- (a) The flow passage—diffuser, pipe, nozzle, etc.—has a *small divergence* and the streamlines of the flow have large radii of curvature.
- (b) The flow is steady, the variations of the flow parameters with time are negligible.
- (c) The area of the flow passage is small compared to the radius of curvature of its axial streamline.
- (d) The transverse pressure gradients are negligible, so that the static pressure at

*The equations in this paragraph apply to the steady one-dimensional flow of any compressible fluid.

any cross-section of the flow passage can be assumed constant over that cross-section. Hence, the static pressure of the fluid is a function only of the axial coordinate of the flow passage.

- (e) The velocity components of the flow normal to the axial line of the flow passage are negligible compared to the axial velocity components.
- (f) At every section of the flow passage the acceleration components *normal to the axial line* for the passage are negligible compared to those along the axial line.
- (g) At each point in a given cross-section of the flow passage the static pressure P , the static temperature T , the concentrations of the different chemical species, and all of the parameters related to the chemical conditions of the fluid are *uniformly distributed*.
- (h) No fluid is either *injected into* or *extracted from* the flow passage between the selected reference cross-section.

The assumption that the flow passage has a small divergence (Assumption a) is approximated in a large number of practical flow passages. On the other hand, the uniformity assumption (Assumption g) is rarely realized even in a one-dimensional flow passage. The flow in a *real* flow passage is characterized by the following:

- (i) the velocity at a cross-section is *never* uniform because it must be zero at the bounding wall; and
- (ii) The transfer of heat and mass into the control volume requires that there be gradients of temperature or of concentrations at the walls.

It is assumed quite generally, however, that if one defines proper *mean values* for the static pressure P , the static temperature T , the velocity u , and other physical variables, one can approximate the *actual nonuniform* flow at a cross-section by an *equivalent uniform flow* characterized by the values of pressure, temperature, velocity, and other physical parameters equal to the aforementioned mean values.

The important consequence of the *uniformity assumption* (Assumption g) is that *all changes—physical and chemical—are restricted to the axial direction* of the flow passage. Consequently, each variable becomes a function of a single spatial coordinate defined along the axial line.

If the flow passage has a large divergence, caution must be exercised in applying the one-dimensional approximation. Also there are cases where large transverse velocities may occur in a “well-behaved” duct due to separation of the fluid from the walls.

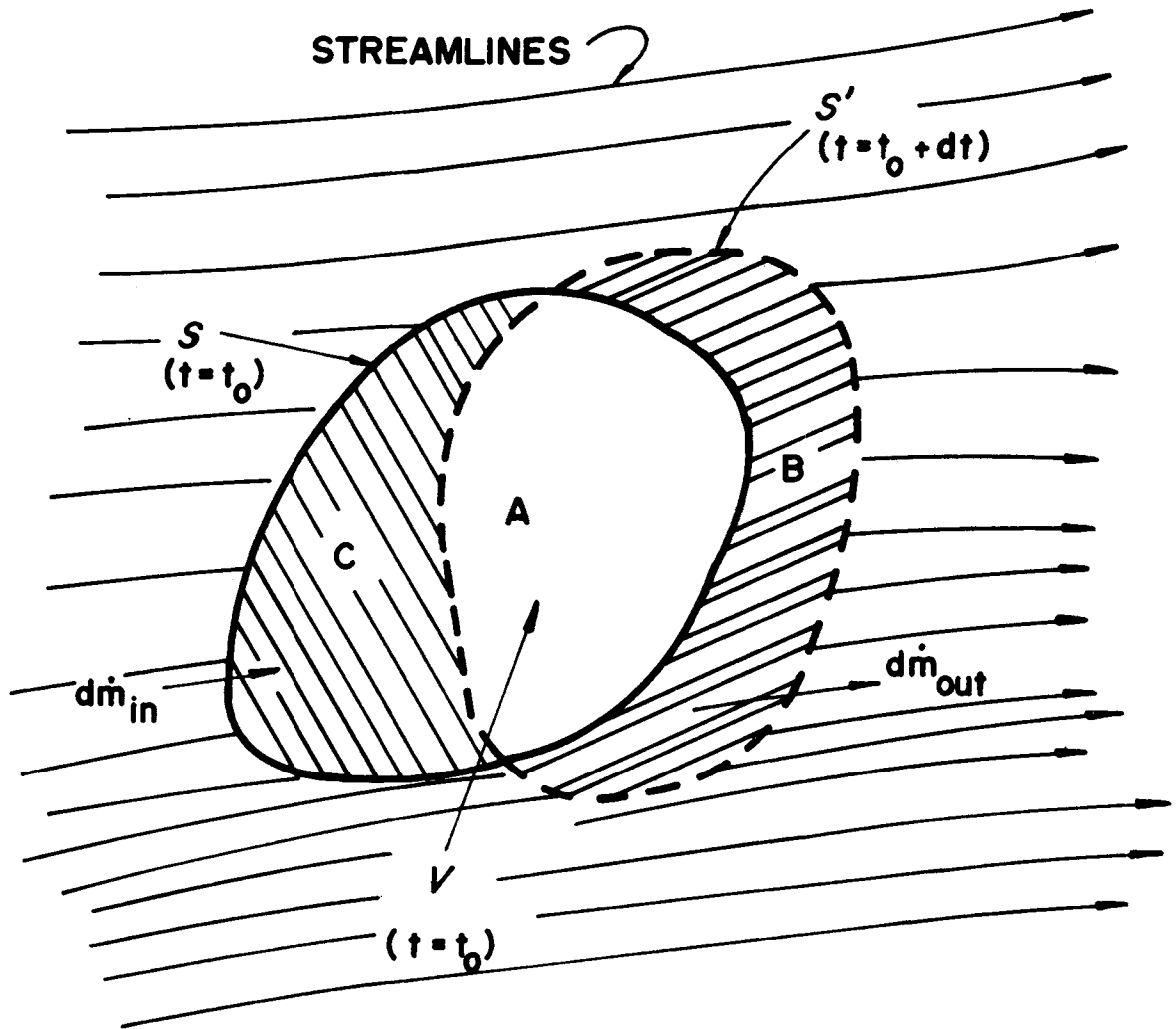
Despite the simplifying assumptions, approximate relations of great engineering usefulness are obtained. Moreover, they are often of good engineering accuracy. In fact the interior ballistics theory of rocket motors is based on the one-dimensional, steady flow assumptions.

A-3.1 CONTINUITY EQUATION

Fig. A-2 illustrates diagrammatically a control surface S enclosing a control volume V in a region of a flowing fluid. In general, the continuity equation in its integral form is

$$\frac{\partial}{\partial t} \int_V \rho dV + \int_S \rho \mathbf{q} \cdot \mathbf{n} dS = 0 \quad (\text{A-40})$$

If the flow is *steady* which is assumed here, it signifies that even though the fluid inside the control volume changes continuously with time,



(V = VOLUME A + VOLUME C) = CONTROL VOLUME

S = CONTROL SURFACE

Figure A-2. Control Surface Enclosing a Control Volume in a Region of Flowing Fluid

the mass of fluid enclosed by the control surface S is *invariant*. Hence

$$\frac{\partial}{\partial t} \int_V \rho dV = 0$$

Hence, for a *steady flow*

$$\int_S \rho \mathbf{q} \cdot \mathbf{n} dS = \int_S \rho q_n dS = 0 \quad (\text{A-41})$$

where $q_n = q \cos \alpha$ = the *normal velocity*, i.e., the velocity normal to the flow area dS .

u_1 and u_2 are normal to A_1 and A_2 , respectively.

For an *unsteady, one-dimensional flow*, it follows from Eq. A-38 that

$$\frac{\partial \rho}{\partial t} + \frac{\partial}{\partial x} (\rho u) = 0$$

or

$$\frac{\partial \rho}{\partial t} + \rho \frac{\partial u}{\partial x} + u \frac{\partial \rho}{\partial x} = 0 \quad (\text{A-44})$$

For a *steady one-dimensional flow* ($d\rho/dt = 0$), and Eq. A-44 reduces to

$$\rho \frac{\partial u}{\partial x} + u \frac{\partial \rho}{\partial x} = 0 \quad (\text{A-45})$$

The corresponding integral equation is

$$\int_A (\rho u) dA = d(\rho u A) = 0 \quad (\text{A-46})$$

or

$$\dot{m} = \frac{dm}{dt} = \rho u A = \text{constant} \quad (\text{A-47})$$

Eq. A-47 states that if the flow is steady, the same mass rate of flow crosses every cross-section of a one-dimensional flow passage.

By definition, the *mass velocity*, also called the *flow density* G , is given by

$$G \equiv \rho u = \dot{m}/A \quad (\text{slug/sec-ft}^2) \quad (\text{A-48})$$

Logarithmic differentiation of Eq. A-47, yields the differential equation for a steady one-dimensional flow. Thus

$$\frac{dA}{A} + \frac{d\rho}{\rho} + \frac{du}{u} = 0 \quad (\text{A-49})$$

As pointed out in the foregoing (see par. A-3), the values of u and ρ in the equations for a steady one-dimensional flow are the *effective mean values* for the cross-sectional area A .

A-3.2 MOMENTUM EQUATION

The general form of the momentum equation is given by Eq. 2-11, which is repeated here for convenience. Thus

$$\begin{aligned} \sum \underline{F}_{\text{ext}} &= \frac{\partial}{\partial t} \int_V (\rho \underline{q}) dV + \int_S (\rho \underline{q}) q_n dS \\ &= \frac{dM}{dt} = \dot{\underline{M}} \end{aligned}$$

where the net external force $\underline{F}_{\text{ext}}$ is given by

$$\sum \underline{F}_{\text{ext}} = \underline{W} + \underline{R} - \int_S \underline{P} n dS$$

(a) *Steady flow.* For a steady flow the volume integral on the right-hand side of Eq. 2-11 vanishes, and

$$\sum \underline{F}_{\text{ext}} - \int_S \rho \underline{q} q_n dS = 0 \quad (\text{A-50})$$

Eq. A-50 is a vector equation and is applicable to

- (1) A steady flow or a mean steady flow, and
- (2) steady viscous and nonviscous flows.

For fluids of *small density*, such as gases, the body force is negligible so that $\underline{W} \approx 0$. In that

case, the momentum equation for a steady flow is

$$\tilde{\mathbf{R}} = \int_S \rho \mathbf{q}_n \tilde{\mathbf{q}} dS + \int_S \tilde{\mathbf{P}} n dS \quad (\rho \text{ small}) \quad (\text{A-51})$$

If there are no solid bodies immersed in the fluid, no body forces, and no friction, then

$$\int_S \tilde{\mathbf{P}} n dS + \int_{S^1} \rho \mathbf{q}_n \tilde{\mathbf{q}} dS = 0 \quad (\tilde{\mathbf{W}} = \tilde{\mathbf{R}} = 0) \quad (\text{A-52})$$

(b) *One-dimensional reversible steady flow.*

It is readily shown that for a one-dimensional steady *frictionless flow*, the momentum equation reduces to ^{1,2,27}

$$\mathbf{u} du + \frac{dP}{\rho} = 0 \quad (\text{A-53})$$

or

$$\mathbf{u} du + \mathbf{v} dP = 0 \quad (\text{A-54})$$

where $\mathbf{v} = 1/\rho$ = the specific volume, ft³/slug

Eq. A-53 is a form of *Euler's equation of motion* and applies only to a *reversible flow*. To integrate Eq. A-53 requires a relationship between \mathbf{P} and ρ . In integral form, Eq. A-53 is

$$\frac{u^2}{2} + \int \frac{dP}{\rho} = \text{constant} \quad (\text{A-55})$$

A-3.2.1 IMPULSE FUNCTION

In certain cases the interest is in the force exerted by a flowing stream of fluid rather than in the characteristics of the flow. In the general case where friction is present, the force will arise both from the reaction of the projected wall

area to the mean hydrostatic pressure and to the shearing force.

The dimensional formula for the rate of change in momentum $\dot{\tilde{\mathbf{M}}}$ is [MLT⁻²] which is the same as that for a force. Consequently, the value of $\dot{\tilde{\mathbf{M}}}$ in the direction of the normal to a flow cross-section is often termed the stream effective force acting on that cross-section. By definition, the *impulse function* is given by

$$F \equiv \mathbf{P} \mathbf{A} + \dot{\tilde{\mathbf{M}}} = \mathbf{P} \mathbf{A} + \dot{m} \mathbf{u} \quad (\text{lb}) \quad (\text{A-56})$$

where

\mathbf{A} = area of cross-section normal to \mathbf{P} , sq ft

\mathbf{u} = velocity of fluid normal to \mathbf{A} , fps

\dot{m} = mass rate of flow, slug/sec

For a steady one-dimensional flow one may write

$$\mathbf{P}_1 \mathbf{A}_1 + \rho_1 \mathbf{A}_1 \mathbf{u}_1^2 = \mathbf{P}_2 \mathbf{A}_2 + \rho_2 \mathbf{A}_2 \mathbf{u}_2^2 \quad (\text{A-57})$$

Eq. A-57 is frequently called the momentum equation for the steady one-dimensional flow of a flowing fluid²⁷. By applying Eq. A-56 one can compute the thrust, or total force acting on the flow passage, as the difference between the values of F_2 and F_1 at \mathbf{A}_2 and \mathbf{A}_1 , respectively. The impulse function F is useful for computing the thrust of an air-breathing jet engine.

A-3.2.2 RAYLEIGH LINE EQUATION

If the cross-sectional area of a one-dimensional flow passage is sensibly constant, so that it may be assumed that $\mathbf{A}_1 = \mathbf{A}_2 = \mathbf{A} = \text{constant}$, then Eq. A-55 becomes

$$\frac{F}{\mathbf{A}} = \mathbf{P} + \mathbf{G} \mathbf{u} = \text{constant} \quad (\text{A-58})$$

where

$$G = \dot{m}/A = \text{mass velocity, slug/sec-ft}^2$$

Eq. A-58 states that the value of F/A does not change in a duct having a constant cross-sectional area, wherein the flow is *steady* and *reversible*. Eq. A-58 is known as the *Rayleigh line equation* (see also par. A-9.1).

A-3.3 ENERGY EQUATION FOR STEADY ONE-DIMENSIONAL FLOW

The concept termed *energy* and the principle regarding its conservation in an isolated (or given) system originated in the science of mechanics. The principle of the conservation of energy for an isolated system states that if E denotes the *total energy* associated with the system, then

$$E = E_{KE} + E_{PE} = \text{constant} \quad (\text{A-59})$$

here

E_{KE} = the kinetic energy associated with the system

E_{PE} = the potential energy associated with the system

Eq. A-59 indicates that if the system interacts with its surroundings, so that external forces act upon it, then E_{KE} and E_{PE} are converted into work done against external forces. Otherwise, there can only be changes of E_{KE} into E_{PE} and vice versa.

Because *heat* and mechanical energy are generically equivalent quantities which are *mutually interconvertible*, the principle of the conservation of energy is embodied in the *first law of thermodynamics*; the mechanical equivalent of heat J is accordingly

$$J = 778.26 \approx 778 \text{ ft-lb/B} \quad (\text{A-60})$$

If E denotes the total energy associated with a closed system, called the *stored energy*, then E is a function of the thermodynamic state of the system. Consequently, E can be changed only by changing the state of the system.

Fig. A-4 illustrates diagrammatically a stationary control surface S enclosing the control volume V in a region of a flowing fluid. According to the first law of thermodynamics, if δQ denotes the amount of heat *added* to the mass of fluid instantaneously enclosed by S , and δW^* denotes the amount of work done by the same mass of fluid on the surrounding in time dt , then

$$dE = \delta Q - \delta W^* \quad (\text{A-61})$$

By convention δQ is positive if heat is transferred to the system, and δW^* is positive if the system does work on its surroundings. The notation signifies that δQ and δW^* are *inexact differentials* because Q and W are *not properties* of the system. The stored energy E is a property and dE is, therefore, an exact differential^{1,6}.

Fig. A-5 illustrates schematically the conditions at an arbitrary element dS of the control surface S . If the flow is *steady*, the stored energy associated with the fluid occupying the control volume V does not change with time. For a *steady flow* the integral form of the energy equation is¹

$$\frac{\delta Q}{dt} - \frac{\delta W}{dt} = \int_S \rho \left(h + \frac{u^2}{2} + gz \right) q_n dS \quad (\text{B/slug-sec}) \quad (\text{A-62})$$

where

δQ = the heat added to the fluid, B/slug

δW = the shaft work done by the fluid, B/slug

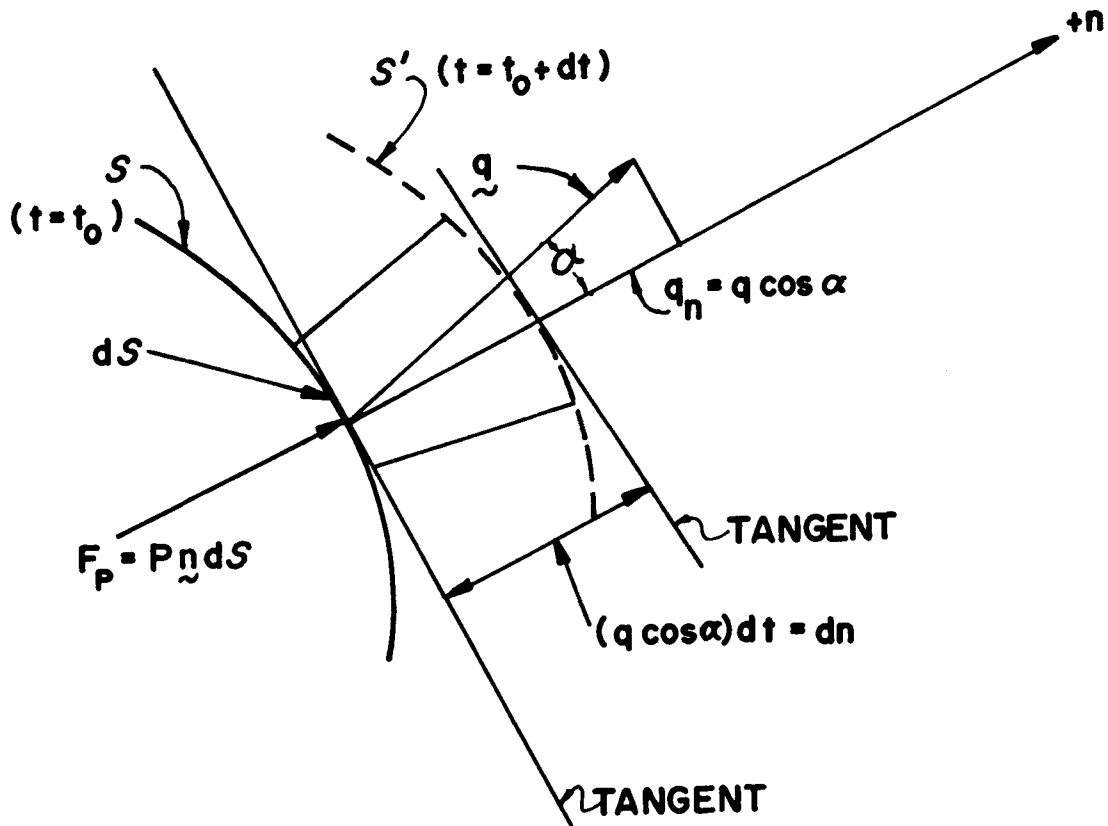


Figure A-5. Element of a Control Surface Which Encloses a Region in a Flowing Fluid

Applying Eq. A-62, yields

$$\frac{\delta Q}{dt} - \frac{\delta W}{dt} = \int_{A_{out}} \rho u \left(h + \frac{u^2}{2} + gz \right) dA - \int_{A_{in}} \rho u \left(h + \frac{u^2}{2} + gz \right) dA \quad (\text{A-63})$$

Eq. A-63 is the integral form of the energy equation for a steady one-dimensional flow. For such a flow

$$\dot{m}_{out} = \dot{m}_{in} = \Sigma(\rho u A)_{out} = \Sigma(\rho u A)_{in}$$

For a single one-dimensional flow passage, integration of Eq. A-62, between reference sections 1 and 2, yields

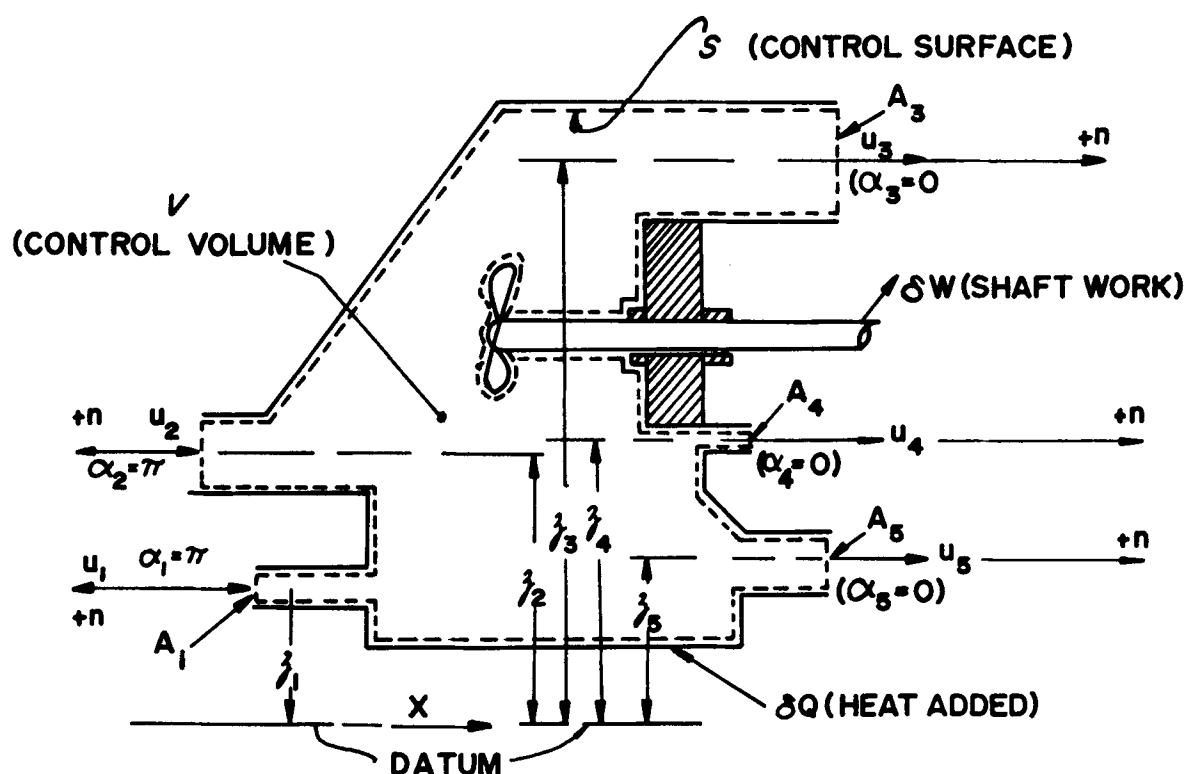
$${}_1Q_2 - {}_1W_2 = h_2 - h_1 + \frac{1}{2}(u_2^2 - u_1^2) + (z_2 - z_1)g \quad (\text{B/slug}) \quad (\text{A-64})$$

where

${}_1Q_2$ = the heat added per unit mass between the reference sections 1 and 2, B/slug

${}_1W_2$ = the work done by the fluid between reference sections 1 and 2, B/slug

h = specific static enthalpy, B/slug



$$\begin{aligned}
 \frac{\delta Q}{dt} - \frac{\delta W}{dt} &= \int_{A_{out}} (h + \frac{u^2}{2} + gz) \rho u \cos \alpha dA - \int_{A_{in}} (h + \frac{u^2}{2} + gz) \rho u \cos \alpha dA \\
 &= (h_3 + \frac{u_3^2}{2} + z_3) \dot{m}_3 + (h_4 + \frac{u_4^2}{2} + z_4) \dot{m}_4 + (h_5 + \frac{u_5^2}{2} + z_5) \dot{m}_5 \\
 &\quad - (h_1 + \frac{u_1^2}{2} + z_1) \dot{m}_1 - (h_2 + \frac{u_2^2}{2} + z_2) \dot{m}_2
 \end{aligned}$$

Figure A-6. Energy Balance for a Steady One-dimensional Flow

u = velocity of fluid, fps

z = elevation of fluid above a datum line, ft

Subscripts 1 and 2 refer to the reference cross-sections A_1 and A_2

Eq. A-63 applies to a unit mass of fluid in steady one-dimensional flow between cross-sections A_1 and A_2 ; it is assumed that no fluid is either injected or *extracted* between the two reference sections. The differential form of Eq. A-63 is

$$\delta Q - \delta W = dh + d\left(\frac{u^2}{2}\right) + g dz \quad (\text{B/slug}) \quad (\text{A-65})$$

For fluids of small density, such as is the case for most of the gases used in jet propulsion systems, $g dz \approx 0$, Eq. A-64 reduces to

$$\delta Q - \delta W = dh + d\left(\frac{u^2}{2}\right) \quad (\text{A-66})$$

If there is no heat transfer ($\delta Q=0$) and the fluid does not do any external work ($\delta W=0$) the flow is said to be *adiabatic*. By definition, an adiabatic flow is an irreversible flow which is characterized by $\delta Q=0$, $\delta W=0$, and $dS>0$. Hence, the *adiabatic energy equation* is

$$dh + d\left(\frac{u^2}{2}\right) = 0 \quad (\text{A-67})$$

Assume now that the fluid is expanded as it flows adiabatically through an exhaust nozzle and let

$$h^0 \equiv h + \frac{u^2}{2} = \text{total or stagnation enthalpy} \quad (\text{A-68})$$

Then integrating Eq. A-67 between the entrance and exit sections of a nozzle yields

$$\frac{u_{\text{ex}}^2}{2} + h_{\text{ex}} = h^0 \quad (\text{A-68a})$$

A-3.4 ENTROPY EQUATION FOR STEADY ONE-DIMENSIONAL FLOW

The *second law of thermodynamics* presents an inequality which cannot be violated in any real process^{1,6,23}. Thus for a closed system the change in *entropy*, denoted by dS is given by

$$dS > \left(\frac{\delta Q}{T}\right)_{\text{rev}} \quad (\text{A-69})$$

The inequality A-69 imposes a limitation which must be observed in obtaining the solution to a gas dynamic problem, if the result is to be a meaningful solution. For a natural process, due to its *irreversibility*, the entropy change dS is always positive. Only for a *reversible process* is $dS = \delta Q/T$.

Consider now the rate of change in the entropy per unit volume for the fluid instantaneously occupying a control volume V in a region of a flowing fluid (see Figs. A-3 and A-4). For a *steady flow*

$$\int_S \frac{\dot{Q}}{T} dS < \int_S (\rho s) q_n dS \quad (\text{A-70})$$

where

\dot{Q} = rate of heat transfer per unit area per unit time to fluid inside control volume

T = temperature at which a reversible heat exchange occurs

s = specific entropy of fluid, B/slug-°R.

Flow processes that are rapid, such as the flow through a rocket exhaust nozzle, are substantially adiabatic due to the short time available for heat transfer. Such processes are never *isentropic* because they are invariably

accompanied by turbulence, eddies, wall friction, etc., — all irreversible processes. Consequently, in gas dynamic problems a *first approximation* is to assume the change of state to be reversible and then modify the resulting equation to account for the effect of the irreversibility of the actual process¹.

For a *reversible change of state*, the first law of thermodynamics yields

$$Tds = dh - \frac{dp}{\rho} \quad (\text{A-71})$$

Eq. A-71 is applicable if the following conditions are fulfilled:

- (a) The medium is homogeneous and has a fixed composition (*frozen chemical equilibrium*), and
- (b) the medium is in *thermal equilibrium*.

Eq. A-71 may be applied to the reactants comprising a combustible mixture provided the mixture is physically and chemically homogeneous throughout. The equation is also applicable to the *products of combustion* provided the chemical transformations are either

- (a) so *slow* that thermodynamic equilibrium is observed, or
- (b) so *rapid* that the chemical composition of the products does not change appreciably, so that the composition may be assumed to be frozen.

Eq. A-71 does not apply to the products formed in the *intermediate* stages of a chemical reaction where chemical reaction kinetics plays a predominant role; i.e., where *time* enters as a significant parameter, a parameter which is essentially independent of the thermodynamic properties that govern the state of a system.

A-4 STEADY ONE-DIMENSIONAL FLOW OF AN IDEAL GAS

The assumption that the flowing medium is an ideal gas greatly simplifies the mathematical analysis of compressible media and reduces the complexity of the resulting equations (see par. A-2).

A-4.1 CONTINUITY EQUATION FOR AN IDEAL GAS

The continuity equation for the steady one-dimensional flow of a compressible medium is given by Eq. A-47 which is repeated here for convenience. Thus

$$\dot{m} = \rho u A = \text{constant}$$

If the flowing compressible medium is an ideal gas, its density ρ can be expressed in terms of the local flow Mach number M by employing Eq. A-39 which is repeated here for convenience. Thus

$$\rho = \gamma P \left(\frac{M}{u} \right)^2$$

where $\gamma = c_p/c_v$ = the specific heat ratio = constant. Combining Eqs. A-47 and A-39 yields the continuity equation for the *steady one-dimensional flow of an ideal gas*. Thus

$$\dot{m} = A P M \sqrt{\frac{\gamma}{RT}} = A P M \sqrt{\frac{\gamma \bar{m}}{R_u T}} \quad (\text{slug/sec}) \quad (\text{A-72})$$

where A is the flow area in sq ft, P is the absolute static pressure in psf, and \bar{m} is the molecular weight of the gas.

Eq. A-72 gives the mass flow rate of an ideal gas crossing the area A with a flow Mach number equal to M .

EXAMPLE A-2.

A duct is designed for the isothermal flow of an ideal gas. At Station 1, where the cross-sectional area is A_1 , the static pressure p_1 is to be 30 psia, and the Mach number $M_1=0.4$. It is desired that at Station 2, where $A_2=0.8A_1$, that the Mach number be $M_2=0.75$. What must be the decrease in the static pressure Δp between A_1 and A_2 ?

SOLUTION.

From data:

$$T_1 = T_2 = T, \quad A_2 = 0.8A_1, \quad p_1 = 30 \text{ psia}$$

$$M_1 = 0.4, \quad M_2 = 0.75, \quad \gamma_1 = \gamma_2 = \gamma,$$

$$R_1 = R_2 = R$$

Eq. A-72

$$A_1 p_1 M_1 \sqrt{\frac{\gamma}{RT}} = 0.8A_1 p_2 (0.75) \sqrt{\frac{\gamma}{RT}}$$

Hence

$$A_1 p_1 (0.4) = 0.8A_1 p_2 (0.75)$$

$$p_2 = 20 \text{ psia}$$

and

$$\Delta p = p_1 - p_2 = 10 \text{ psia}$$

A-4.2 MOMENTUM EQUATION FOR THE STEADY ONE-DIMENSIONAL FLOW OF AN IDEAL GAS

The general momentum equation for the steady *reversible* one-dimensional flow of a compressible fluid, in the absence of body forces, is given by Eq. A-55, which is repeated here for convenience.

Thus

$$\frac{u^2}{2} + \int \frac{dP}{\rho} = \text{constant}$$

A-26

A-4.2.1 REVERSIBLE STEADY ONE-DIMENSIONAL FLOW OF AN INCOMPRESSIBLE FLUID

If the flowing fluid is a liquid or if the Mach number for the flow of a compressible fluid is less than 0.3, the flow may be regarded as one in which ρ is a constant. Hence, for an *incompressible flow* Eq. A-55 integrates to

$$\frac{P_1}{\rho} + \frac{u_1^2}{2} = \frac{P_2}{\rho} + \frac{u_2^2}{2} = \text{constant} \quad (\text{A-73})$$

A-4.2.2 REVERSIBLE STEADY ONE-DIMENSIONAL FLOW OF A COMPRESSIBLE FLUID

For a compressible flow it is desirable to express the flow equation in terms of the Mach number. Rewrite Eq. A-53 in the form

$$u du + \left(\frac{dP}{d\rho} \right)_s \frac{d\rho}{\rho} = 0$$

But

$$\left(\frac{dP}{d\rho} \right)_s = a^2 = (\text{acoustic speed})^2$$

Hence

$$\frac{dP}{\rho} + M^2 \frac{du}{u} = 0 \quad (\text{A-74})$$

A-4.2.3 IRREVERSIBLE STEADY ONE-DIMENSIONAL FLOW

Let δF_f denote the x-component of the wall friction force acting on a fluid element, and δD the x-component of the internal *drag* due to obstructions submerged in the flowing fluid; for example, struts, baffles, screens, etc. The irreversibility of the flow is due to the forces δF_f and δD , which act in the direction opposite

to that for the flow velocity. In this case, the momentum equation takes the following form¹:

$$\frac{dP}{P} + \frac{\rho}{P} u du + \frac{\rho}{P} \left(\frac{u^2}{2} \right) \left(\frac{4f dL}{D} \right) + \frac{1}{2} \left(\frac{\delta D/A}{q} \right) = 0 \quad (A-75)$$

where

$$q = \frac{1}{2} \rho u^2 = \text{dynamic pressure (psf)} \quad (A-76)$$

and

$$f = \tau/q = \text{friction coefficient} \quad (A-77)$$

$$\delta F_f = \tau dS_w = \text{wall friction force}$$

$$dS_w = \text{area of interior surface of the flow passage wetted by the flowing fluid}$$

$$dL = \text{length of the flow passage}$$

$$\tau = \delta F_f / dS_w = \text{shearing stress}$$

$$D = 4A/(wp) = 4A(dL/dS_w) = \text{hydraulic diameter (A-78)}$$

$$(wp) = A(dL/dS_w) = \text{wetted perimeter of the flow passage} \quad (A-79)$$

A-4.2.4 IRREVERSIBLE STEADY ONE-DIMENSIONAL FLOW OF AN IDEAL GAS

For an ideal gas (see par. A-2)

$$a^2 = \gamma P / \rho; \gamma = c_p / c_v; M^2 = u^2 / a^2; \rho = \gamma P (M/u)^2$$

Introducing the preceding relationships into Eq. A-79 yields

$$\frac{dP}{P} + \gamma \left(\frac{M^2}{2} \right) \left(\frac{du^2}{u^2} \right) + \gamma M^2 \left[4f \frac{dL}{D} + \frac{\delta D/A}{\frac{1}{2} (\gamma P M^2)} \right] = 0 \quad (A-80)$$

Eq. A-80 is the differential form for the momentum equation, also called the *dynamic equation* for the irreversible, steady one-dimensional flow of an ideal gas.

A-4.3 ENERGY EQUATION FOR STEADY ONE-DIMENSIONAL FLOW

The differential equation for the steady one-dimensional flow of a fluid of small density is given by Eq. A-66 which is repeated here for convenience. Thus

$$\delta Q - \delta W = dh + d \left(\frac{u^2}{2} \right)$$

In the above equation the enthalpy change dh may be due to one or both of the following causes:

- (a) A physical change in the state of the flowing fluid.
- (b) Chemical reactions inside the flow passage, as in the combustor of a ramjet engine (see Fig. 2-6).

The heat addition term δQ includes all of the heat which is transferred to the fluid across the control surface. In general, δQ includes the following:

- (a) δQ_w the heat transferred through the walls of the flow passage, and
- (b) δQ_b the heat transferred to the fluid by bodies immersed in the fluid.

Hence, in general

$$\delta Q = \delta Q_w + \delta Q_b \quad (\text{A-81})$$

A-4.3.1 ENERGY EQUATION FOR A SIMPLE ADIABATIC FLOW

In the flow passages of a jet propulsion system—such as ducts, diffusers, and nozzles—the flowing medium is a gas (low density) and, due to the speed of the flow, the flow process may be assumed to be adiabatic ($\delta Q = 0$). By definition, the *simple adiabatic flow* of a fluid is characterized by

$$\delta Q = 0; \delta W = 0; dz = 0; ds > 0$$

The energy equation for a simple adiabatic flow is accordingly

$$dh + d\left(\frac{u^2}{2}\right) = 0 \quad (\text{A-82})$$

Eq. A-82 applies to both irreversible ($ds = 0$) and reversible flows ($ds > 0$). Integrating between any two cross-sections of a flow passage, denoted by the subscripts 1 and 2, yields

$$h_1 + \frac{u_1^2}{2} = h_2 + \frac{u_2^2}{2} = \text{constant} \quad (\text{A-83})$$

Eqs. A-55 and A-56 give no indication of the effect of irreversibility (friction) upon a simple adiabatic flow.

A-4.3.2 ENERGY EQUATION FOR THE SIMPLE ADIABATIC FLOW OF AN IDEAL GAS

For an ideal gas, the simple adiabatic flow is characterized by the following:

$$\delta Q = 0; \delta W = 0; gdz = 0; c_p = \gamma R / (\gamma - 1);$$

$$c_v = R / (\gamma - 1); dh = c_p dT; a^2 = \gamma P / \rho = \gamma RT;$$

$$\text{and } \gamma = c_p / c_v.$$

The energy equation for the simple adiabatic flow of ideal gas is accordingly

$$c_p dT + d\left(\frac{u^2}{2}\right) = 0 \quad (\text{A-84})$$

Integrating between Stations 1 and 2 yields

$$c_p T_1 + \frac{u_1^2}{2} = c_p T_2 + \frac{u_2^2}{2} = \text{constant} \quad (\text{A-85})$$

Let $M_1 = u_1 / a_1$ and $M_2 = u_2 / a_2$ and substituting for c_p yields

$$a_1^2 \left[1 + \left(\frac{\gamma - 1}{2} \right) M_1^2 \right] = a_2^2 \left(1 + \frac{\gamma - 1}{2} \right) = \text{constant} \quad (\text{A-86})$$

or

$$\frac{u_1^2}{2} + \frac{a_1^2}{\gamma - 1} = \frac{u_2^2}{2} + \frac{a_2^2}{\gamma - 1} = \text{constant} \quad (\text{A-87})$$

From Eq. A-86 one obtains¹

$$T_2 = T_1 \left\{ 1 + \left(\frac{\gamma - 1}{2} \right) M_1^2 \left[1 - \left(\frac{u_2}{u_1} \right)^2 \right] \right\} \quad (\text{A-88})$$

A flow process for which $u_2 > u_1$ is called a *flow expansion* and the flow passage for achieving the expansion is termed either a *nozzle* or an *effuser*. Conversely, a passage which causes a flow compression, $u_2 < u_1$, is called a *diffuser*.

A-4.4 ENTROPY EQUATION FOR THE STEADY ONE-DIMENSIONAL FLOW OF AN IDEAL GAS

In general (see par. A-3.4) the entropy change for a system is given by

$$dS \geq \left(\frac{\delta Q}{T} \right)_{\text{rev}}$$

Because entropy is a thermodynamic property, the change in the entropy of a system can be calculated by the value of $(\delta Q/T)$ for any arbitrarily selected reversible process connecting the same initial and final states^{1,19,23}. Hence

$$\Delta S = S_2 - S_1 = \int_1^2 \frac{dU + PdV}{T} \quad (\text{A-89})$$

For a unit mass of a thermally perfect gas $Pv = RT$, $du = c_v dT$, and $dh = c_p dT$. Introducing these relationships into Eq. A-89 yields

$$\begin{aligned} ds &= c_v \frac{dT}{T} + R \frac{dv}{v} \\ &= c_v \frac{dT}{T} - \frac{Rd\rho}{\rho} \quad (\text{thermally perfect gas}) \quad (\text{A-90}) \\ &= c_p \frac{dP}{P} - c_p \frac{d\rho}{\rho} \\ &= c_p \frac{dT}{T} - R \frac{d\rho}{\rho} \end{aligned}$$

Integrating Eq. A-90 between states 1 and 2, and assuming an ideal gas yields

$$\begin{aligned} \Delta s = s_2 - s_1 &= c_v \ln \left(\frac{T_2}{T_1} \right) - R \ln \left(\frac{\rho_2}{\rho_1} \right) \\ &= c_p \ln \left(\frac{T_2}{T_1} \right) - R \ln \left(\frac{P_2}{P_1} \right) \quad (\text{ideal gas}) \quad (\text{A-91}) \\ &= c_v \ln \left(\frac{P_2}{P_1} \right) - c_p \ln \left(\frac{\rho_2}{\rho_1} \right) \end{aligned}$$

Eqs. A-91 can also be written in exponential form; for example

$$\begin{aligned} \frac{T_2}{T_1} &= \left(\frac{P_2}{P_1} \right)^{R/c_v} \exp \left[\frac{s_2 - s_1}{c_v} \right] \\ \frac{T_2}{T_1} &= \left(\frac{P_2}{P_1} \right)^{R/c_p} \exp \left[\frac{s_2 - s_1}{c_p} \right] \quad (\text{ideal gas}) \quad (\text{A-92}) \\ \frac{P_2}{P_1} &= \left(\frac{\rho_2}{\rho_1} \right)^{\gamma} \exp \left[\frac{s_2 - s_1}{c_v} \right] \end{aligned}$$

It is convenient for some purposes to express the entropy equation for an ideal gas in the following form¹

$$ds = c_p d \left[\ln \left(\frac{T}{P^{\frac{\gamma-1}{\gamma}}} \right) \right] \quad (\text{A-93})$$

A-5 STEADY ONE-DIMENSIONAL ISENTROPIC FLOW

The assumption that the flow is isentropic infers that the flow is adiabatic and reversible; i.e., that the flowing fluid is *inviscid*. A steady one-dimensional isentropic flow is characterized by the following conditions:

$$\delta Q = \delta W = \dot{m} = ds = 0$$

The assumption of isentropicity is valid in those regions of a flow field where the velocity gradients perpendicular to the direction of flow are negligible; i.e., to the regions of an adiabatic flow field that are external to *boundary layers*. According to boundary layer theory all frictional effects in a flowing fluid are confined to the boundary layers adjacent to the surfaces wetted by the flowing fluid, wherein the velocity gradients are large. Consequently, the fluid in the regions external to the boundary layers may be assumed to be a *perfect fluid*; i.e., a fluid characterized by the following two properties.

- (a) It possesses bulk elasticity so that $K \neq 0$.
- (b) It has no rigidity so that the *shear modulus* N is equal to zero, i.e., it is inviscid.

If the fluid is an *ideal gas*, then¹⁵

- (a) its isothermal bulk modulus is given by

$$K_T = -v \left(\frac{\partial P}{\partial v} \right)_T = P \quad (\text{A-94})$$

- (b) its isentropic bulk modulus is given by

$$K_s = -v \left(\frac{\partial P}{\partial v} \right)_s = \gamma P \quad (\text{A-95})$$

If an ideal gas undergoes an isentropic change of state, then

$$Pv^\gamma = \text{constant} \quad (\text{A-96})$$

To indicate that a state is reached by an isentropic process the *superscript prime* (') will be attached to the pertinent properties of the fluid corresponding to the state reached by the isentropic change of state. For example, if an

ideal gas at a static pressure P_1 and a static temperature T_1 is compressed isentropically to the static pressure P_2 , then the temperature of the gas corresponding to P_2 is denoted by T_2 and computed from the relationship

$$\frac{T_2'}{T_1} = \left(\frac{P_2}{P_1} \right)^{c_p/R} = \left(\frac{P_2}{P_1} \right)^{(\gamma-1)/\gamma} \quad (\text{A-97})$$

The assumption of isentropicity is realistic for subsonic and supersonic flows when the conditions discussed above are closely approximated. It should be noted, however, an adiabatic diffusion of a compressible fluid may be assumed to be isentropic—when $\delta Q \approx 0$ and friction is negligible—only if the flow is *subsonic* throughout.

If a *supersonic* compressible fluid is being diffused the flow may be assumed to be isentropic—when $\delta Q = 0$ and friction is negligible—only if no *shock waves* are produced in the flow field. Shock waves increase the entropy of the flowing fluid. Consequently, even though the flow is adiabatic and frictionless on both sides of a *shock wave* which may be regarded as a discontinuity in the flow, a flow in which one or more shock waves are present cannot be an isentropic flow.

A-5.1 ENERGY EQUATION FOR THE STEADY ISENTROPIC ONE-DIMENSIONAL FLOW OF AN IDEAL GAS

The differential form of the energy equation for either a reversible ($ds=0$) or an irreversible adiabatic flow is given by Eq. A-67 which is repeated here for convenience. Thus

$$dh + d \left(\frac{u^2}{2} \right) = 0 \quad (\text{B/slugg})$$

Eq. A-67 does not indicate explicitly the effect of irreversibility, if present, upon an adiabatic flow process. The effect of irreversibility in the flow is indicated in the integration of Eq. A-67. If a simple adiabatic flow is reversible (isentropic) then it is characterized by

$$\delta Q = 0; \delta W = 0; d\dot{m} = 0; dz = 0; ds = 0.$$

To distinguish an isentropic flow from a simple adiabatic flow, the upper limit of the integration of the adiabatic energy equation is denoted by 2', while for the simple adiabatic it is denoted by 2 (without a prime sign). Thus

(a) *Simple adiabatic flow*

$$(d\dot{m}/\dot{m} = \delta Q = \delta W = dz = 0, ds > 0)$$

$$\int_1^2 dh + \int_1^2 u du = \text{constant}$$

so that

$$h_2 + \frac{u_2^2}{2} = h_1 + \frac{u_1^2}{2} = \text{constant} \quad (\text{A-98})$$

If $h_2 < h_1$, then $u_2 > u_1$ and the process is a flow expansion. Hence, the specific enthalpy change for a *simple adiabatic flow expansion*, denoted by $\Delta h_t = h_1 - h_2$, is given by

$$\Delta h_t = \frac{1}{2} (u_2^2 - u_1^2) \quad (\text{B/slug})$$

For a simple adiabatic *flow compression*, $h_2 > h_1$ and $u_2 < u_1$, the corresponding change in the specific enthalpy of the fluid is denoted by $\Delta h_c = h_2 - h_1$, so that

$$\Delta h_c = \frac{1}{2} (u_1^2 - u_2^2) \quad (\text{B/slug}) \quad (\text{A-99})$$

The corresponding equations for an isentropic flow are presented below.

(b) *Isentropic flow* ($d\dot{m}/\dot{m} = \delta Q = \delta W = dz = ds = 0$)

$$h_2' + \frac{(u_2')^2}{2} = h_1 + \frac{u_1^2}{2} = \text{constant} \quad (\text{A-100})$$

$$\Delta h_t' = h_1 - h_2' = \frac{1}{2} [(u_2')^2 - u_1^2] \quad (\text{A-101})$$

$$\Delta h_c' = h_2' - h_1 = \frac{1}{2} [u_1^2 - (u_2')^2] \quad (\text{A-102})$$

Figs. A-7(A) and A-7(B) compare the simple adiabatic and the isentropic flow expansion and compression processes in the h - s plane. It is seen that for identical values of the initial and final static pressures P_1 and P_2 , respectively

(a) *flow expansions*

$$\Delta h_t' > \Delta h_t, h_2' < h_2, u_2' > u_2$$

(b) *flow compressions*

$$\Delta h_c' < \Delta h_c, h_2' < h_2, u_2' > u_2$$

The difference between the specific enthalpy changes for an isentropic flow and its corresponding simple adiabatic flow is equal to the energy expended in overcoming *irreversible* processes. To illustrate: if δQ_f denotes the energy per unit mass expended in overcoming irreversible phenomena, then for an expanding flow process

$$\Delta h_t = \Delta h_t' - \delta Q_f \quad (\text{A-103})$$

For an isentropic process $\delta Q_f = 0$.

A-5.2 STAGNATION (OR TOTAL) CONDITIONS

Consider the steady, one-dimensional, adiabatic flow of a compressible fluid between sections 1 and 2 of a flow passage. The integrated form of the energy equation, from Eq. A-98, is

$$h_1 + \frac{u_1^2}{2} = h_2 + \frac{u_2^2}{2} = \text{constant}$$

Eq. A-98 applies to both reversible and irreversible adiabatic flows.

A-5.2.1 STAGNATION (OR TOTAL) ENTHALPY (h^0)

Consider the case where the fluid is decelerated isentropically to zero speed ($u_2 = 0$); i.e., the process is an *isentropic diffusion* or flow compression. Then by definition

$$h^0 \equiv h + \frac{u^2}{2} = \text{constant} \quad (\text{A-104})$$

where h^0 is the *stagnation* or *total enthalpy*.

Eq. A-104 applies to either a simple adiabatic or an isentropic one-dimensional steady flow of a compressible fluid.

A-5.2.2 STAGNATION (OR TOTAL) TEMPERATURE (T^0)

If the flowing fluid is a thermally perfect gas, then $dh = c_p dT$, and Eq. A-67 becomes

$$c_p dT + d \left(\frac{u^2}{2} \right) = 0 \quad (\text{A-105})$$

If the fluid is an *ideal gas* ($c_p = \text{constant}$), and if T^0 denotes the *stagnation temperature*, also called the *total temperature*, one may write

$$c_p T^0 \equiv h^0 = c_p T + \frac{u^2}{2} = \text{constant} \quad (\text{A-106})$$

or

$$T^0 = h^0 / c_p = T + \frac{u^2}{2c_p} = \text{constant} \quad (\text{A-107})$$

Eq. A-107 is the energy equation for the steady one-dimensional flow of an ideal gas under either adiabatic or isentropic conditions.

According to Eq. A-107, the total temperature remains constant along the flow path for either a simple adiabatic or an isentropic flow of an ideal gas. Such a flow is said to be *isoenergetic*.

For an ideal gas

$$c_p = R \left(\frac{\gamma}{\gamma - 1} \right), \quad T = \frac{P}{\rho R}, \quad a^2 = \frac{\gamma P}{\rho}$$

Applying Eq. A-107 to reference sections 1 and 2 of a one-dimensional flow path, and solving for T_2 , yields

$$T_2 = T_1 \left\{ 1 + \left(\frac{\gamma - 1}{2} \right) M_1^2 \left[1 - \left(\frac{u_2^2}{u_1^2} \right) \right] \right\} \quad (\text{adiabatic}) \quad (\text{A-108})$$

If the flow process is isentropic, T_2 is replaced by T_2' and u_2 by u_2' .

In Eq. A-108 if $u_2 = 0$, the corresponding value of T_2 is denoted by T^0 and is called either the *stagnation* or the *total temperature*.

Hence

$$\frac{T^0}{T} = 1 + \left(\frac{\gamma - 1}{2} \right) M^2 = \text{constant} \quad (\text{A-109})$$

Logarithmic differentiation of Eq. A-109 yields

$$\frac{dT^0}{T^0} = \frac{dT}{T} + \frac{\left(\frac{\gamma - 1}{2} \right) M^2}{1 + \left(\frac{\gamma - 1}{2} \right) M^2} \frac{dM^2}{M^2} \quad (\text{A-110})$$

A-5.2.3 STAGNATION (OR TOTAL) PRESSURE (P^0)

The total temperature T^0 may be considered to be the temperature of the gas in an *infinite reservoir* from which it flows and accelerates (under the conditions $d\dot{m}/\dot{m} = \delta Q = \delta W = 0$) to the actual gas velocity u . The corresponding value of the static pressure in the infinite reservoir (where $u=0$) is called either the *stagnation* or *the total pressure*, and is denoted by P^0 .

In a corresponding manner the density of the gas in the infinite reservoir is termed the *stagnation* or *total density*, and is denoted by $\rho = \rho^0$. Hence, for a thermally perfect gas, one may write

$$P^0 = \rho^0 R T^0 \quad (\text{A-111})$$

In the case of the *isentropic flow* of an ideal gas

$$\frac{P^0}{P} = \left(\frac{T^0}{T} \right)^{\frac{\gamma}{\gamma-1}} \quad (\text{isentropic}) \quad (\text{A-112})$$

Combining Eqs. A-109 and A-112, yields the following relationship between the *stagnation pressure ratio* and the flow Mach number:

$$\frac{P^0}{P} = \left[1 + \left(\frac{\gamma - 1}{2} \right) M^2 \right]^{\frac{\gamma}{\gamma-1}} \quad (\text{isentropic}) \quad (\text{A-113})$$

It should be noted that the total pressure P^0 for any flow can always be calculated by merely assuming that it originated from an infinite reservoir and accelerated *isentropically* to its actual values of static pressure P and flow Mach number M .

Table A-1 presents T/T^0 , P/P^0 , and ρ/ρ^0 as functions of M for the isentropic flow of several gases.

A-5.2.4 RELATIONSHIP BETWEEN STAGNATION PRESSURE AND ENTROPY

For a unit mass of an ideal gas, the change in entropy ds for a closed system is given by Eq. A-93, which is repeated here for convenience. Thus

$$ds = c_p d \left[\ln \left(\frac{T}{P^{\frac{\gamma-1}{\gamma}}} \right) \right] \geq 0$$

Substituting for T from Eq. A-109 and for P from Eq. A-113, one obtains

$$ds = c_p d \left[\ln \left(\frac{T^0}{P^0^{\frac{\gamma-1}{\gamma}}} \right) \right] \geq 0 \quad (\text{A-114})$$

For an isoennergetic flow (see par. A-5.1.3) the total temperature T^0 remains constant

throughout the flow path. Hence, for a real isoenergetic flow, since $ds \geq 0$, the total pressure P^O decreases in the direction of flow. For an isentropic flow, however, $ds = 0$ and the total pressure remains constant throughout the flow path. In other words, the decrease in the magnitude of the stagnation pressure of the gas may be regarded as a measure of the increase in its specific entropy, i.e., a measure of gas irreversibility of the flow process.

From Eq. A-114 one obtains for an irreversible simple adiabatic flow ($T^O = \text{const.}$) that

$$\Delta s = s_2 - s_1 = R \ln (P_1^O / P_2^O) > 0 \quad (\text{A-115})$$

or

$$\frac{P_2^O}{P_1^O} = e^{-\Delta s/R} \quad (\text{A-116})$$

Eq. A-114 can be transformed to read

$$\frac{ds}{c_p} = \frac{dT^O}{T^O} - \left(\frac{\gamma - 1}{\gamma} \right) \frac{dP^O}{P^O} \quad (\text{A-117})$$

The relative change in total pressure, dP^O/P^O , is obtained by logarithmic differentiation of Eq. A-113. Thus

$$\frac{dP^O}{P^O} = \frac{dP}{P} + \left[\frac{\gamma M^2 / 2}{1 + \left(\frac{\gamma - 1}{2} \right) M^2} \right] \frac{dM^2}{M^2} \quad (\text{A-118})$$

It should be noted that if heat is transferred to a flowing gas or if it performs external work, there *cannot be a conservation of the total pressure*. The heat added to a compressible fluid causes the total pressure to decrease even if the heating process is reversible. If the heating

process is *irreversible*, the decrease in the total pressure is larger than it would be for a corresponding reversible heat-exchange process.

A-5.2.5 STAGNATION (OR TOTAL) DENSITY (ρ^O)

The stagnation density is calculated from Eq. A-111. Thus

$$\rho^O = \frac{1}{v^O} = \frac{P^O}{RT^O} \quad (\text{slug/ft}^3) \quad (\text{A-119})$$

where $v^O = 1/\rho^O$ = the *total specific volume*.

Combining Eqs. A-113 and A-119 yields the following relationship between the stagnation density ratio ρ^O/ρ and the flow Mach number M . Thus

$$\frac{\rho^O}{\rho} = \left[1 + \left(\frac{\gamma - 1}{2} \right) M^2 \right]^{1/(\gamma - 1)} \quad (\text{A-120})$$

A-5.2.6 STAGNATION ACOUSTIC SPEED (a^O)

It was shown in par. A-5.2.1 that the energy equation for the steady one-dimensional isoenergetic flow of an ideal gas can be written in the form of Eq. A-109, which is repeated here for convenience. Thus

$$\frac{T^O}{T} = 1 + \left(\frac{\gamma - 1}{2} \right) M^2$$

It is seen from the above equation that the local gas temperature T in an isoenergetic flow varies with the velocity of the flowing ideal gas. Consequently, the local value of the acoustic speed a (see par. A-2.6.2) is a variable. An isoenergetic flow is characterized by $T^O = \text{constant}$, hence an acoustic speed referred to T^O

is a constant and can be employed as a *reference speed* for the flow. By definition, the *stagnation acoustic speed* a^0 is given by

$$a^0 \equiv \sqrt{\gamma R T^0} \quad (\text{ideal gas}) \quad (\text{A-121})$$

where R is the gas constant = R_u/\bar{m} .

Hence

$$\frac{(a^0)^2}{a^2} = \frac{T^0}{T} = 1 + \left(\frac{\gamma - 1}{2} \right) M^2 \quad (\text{A-122})$$

A-5.2.7 NONDIMENSIONAL LINEAR VELOCITY ($w = u/a^0$)

The *nondimensional linear velocity* w is defined by¹

$$w \equiv \frac{u}{a^0} = \frac{M}{\left[1 + \left(\frac{\gamma - 1}{2} \right) M^2 \right]^{\frac{1}{2}}} \quad (\text{A-123})$$

In terms of the expansion ratio P/P^0

$$w = \frac{u}{\sqrt{\gamma R T^0}} = \sqrt{\frac{2}{\gamma - 1}} \sqrt{1 - \left(\frac{P}{P^0} \right)^{(\gamma - 1)/\gamma}} \quad (\text{A-124})$$

A-5.3 ADIABATIC EXHAUST VELOCITY (u_e)

The gas velocity obtained by expanding a propulsive gas flowing through the exhaust nozzle of a jet propulsion system is obtained directly from Eq. A-98. Thus

$$u_e = \sqrt{2(h^0 - h_e)} \quad (\text{A-125})$$

where h_e denotes the specific enthalpy (B/slug) in the flow cross-section A_e , and h^0 is the stagnation specific enthalpy. The expansion process is assumed to be a simple adiabatic process ($\delta Q = \delta W = 0$).

For an ideal gas, $h^0 = c_p T^0$ and $h = c_p T$, so that

$$u_e = \sqrt{2c_p T^0 \left(1 - \frac{T_e}{T^0} \right)} \quad (\text{A-126})$$

One may write, in general, that if T is the static temperature of an ideal gas moving with the velocity u , then

$$T = T^0 - \frac{u^2}{2c_p} = T^0 - \Delta T_{\text{imp}} \quad (\text{A-127})$$

In Eq. A-127 the ratio $u^2/2c_p$ is often called the *impact temperature rise* and is denoted by ΔT_{imp} .

A-5.4 ISENTROPIC EXHAUST VELOCITY (u')

Let h' denote the final specific static enthalpy of a flowing compressible fluid which undergoes an isentropic flow expansion. The corresponding velocity of the fluid is termed the *isentropic exhaust velocity*, and is denoted here by u' .

Let h^0 denote the stagnation specific enthalpy of the fluid, then

$$u = \sqrt{2(h^0 - h')} = \sqrt{2\Delta h'_t}$$

If the flowing fluid is an ideal gas, then $P/\rho^\gamma = \text{constant}$ and

$$\frac{u^2}{2} + \left(\frac{1}{\gamma-1}\right) \frac{P^0}{\rho^0} \left(\frac{P^0}{P}\right)^{(1-\gamma)/\gamma} = \frac{\gamma}{\gamma-1} \frac{P^0}{\rho^0} \quad (\text{A-128})$$

For an ideal gas

$$\frac{P^0}{\rho^0} = \frac{R_u T^0}{\bar{m}}$$

Combining the last equation with Eq. A-128, yields

$$u' = \sqrt{2 \left(\frac{\gamma}{\gamma-1}\right) R_u} \sqrt{\frac{T^0}{\bar{m}}} \sqrt{1 - \left(\frac{P}{P^0}\right)^{(\gamma-1)/\gamma}} \quad (\text{A-129})$$

or

$$u' = \sqrt{2c_p T^0} \left[1 - \left(\frac{P}{P^0}\right)^{R/c_p} \right] \quad (\text{A-129a})$$

Let

$$Z_t = 1 - \left(\frac{P}{P^0}\right)^{\frac{\gamma-1}{\gamma}} = \text{expansion factor}$$

$$a^0 = \sqrt{\gamma R_u T^0 / \bar{m}} = \text{stagnation acoustic speed}$$

Then, the isentropic exhaust velocity is given by

$$u' = a^0 \sqrt{\left(\frac{2}{\gamma-1}\right) Z_t} \quad (\text{A-130})$$

Eq. A-129 is known as the *St. Venant-Wantzel* equation and applies to the steady, one-dimensional isentropic flow of an ideal gas.

It is apparent from Eq. A-129 that for given values of the expansion ratio P/P^0 , specific heat ratio γ , and total temperature T^0 , the isentropic exhaust velocity u' depends directly upon the parameter $\sqrt{T^0/\bar{m}}$. For the same initial and final flow conditions, gases having small molecular weights give the larger values of the isentropic exhaust velocity u' , the latter is also termed the *isentropic discharge speed*.

The isentropic exhaust velocity u' is the highest speed which can be attained by expanding an ideal gas, under isentropic conditions, by discharging it through an exhaust nozzle. Since an actual flow through an exhaust nozzle is irreversible, the velocity u' cannot be obtained in a real flow expansion even when it is conducted under practically adiabatic conditions. Consequently, the adiabatic exhaust velocity u_e (see par. A-5.3) is always smaller than the isentropic exhaust velocity u' .

A-5.4.1 NOZZLE EFFICIENCY (η_n).

The efficiency of a nozzle is defined by

$$\eta_n \equiv \Delta h_t / \Delta h'_t = (u_e/u')^2 \quad (\text{A-131})$$

A-5.4.2 NOZZLE VELOCITY COEFFICIENT (ϕ)

By definition

$$\phi \equiv u_e/u = \sqrt{\eta_n} \quad (\text{A-132})$$

A-5.5 MAXIMUM ISENTROPIC SPEED (c_0)

Referring to Eqs. A-128 and A-129, one can show that the isentropic exhaust velocity attains

its maximum value when the expansion ratio P/P^0 is zero; i.e., when $Z_t = 1$. The value of u' corresponding to $Z_t = 1$ is called the maximum isentropic speed and is denoted by c_0 . Hence

$$\begin{aligned} c_0 = u_{\max} &= a^0 \sqrt{\frac{2}{\gamma-1}} = \sqrt{2 \left(\frac{\gamma}{\gamma-1} \right) RT^0} \\ &= \sqrt{2c_p T^0} \end{aligned} \quad (\text{A-133})$$

The speed $c_0 = u_{\max}$ is a *fictitious characteristic* quantity for a given flow. If T^0 is given then for a given gas, the speed c_0 is determined. Physically, the speed c_0 is that which would be attained by an ideal gas if all of its random kinetic energy were transformable into *directed kinetic energy*. Since $T = 0$ when $P = 0$, all real gases liquefy before the condition $T = 0$ can be attained.

The maximum isentropic speed c_0 is the maximum speed which can be obtained by the isoenergetic flow of an ideal gas from an infinite reservoir. It does *not* apply to the motion of a body in a gas, such as a missile moving through the atmosphere. The limitation on the maximum speed attainable by such a body is the difference between the available thrust and the drag of the body.

A-5.6 CONTINUITY EQUATION FOR STEADY ONE-DIMENSIONAL ISENTROPIC FLOW OF AN IDEAL GAS IN TERMS OF STAGNATION CONDITIONS

The mass rate of flow of a gas \dot{m} , assuming steady one-dimensional flow, is given by Eq. A-72 which is repeated for convenience. Thus

$$\dot{m} = APM \sqrt{\frac{\gamma}{RT}}$$

In terms of the stagnation temperature T^0 and the stagnation pressure P^0 , \dot{m} is given by

$$\begin{aligned} \dot{m} &= AM \frac{P^0}{\sqrt{T^0}} \sqrt{\frac{\gamma}{R}} \left[\frac{1}{1 + \left(\frac{\gamma-1}{2} \right) M^2} \right]^{\frac{\gamma+1}{2(\gamma-1)}} \\ &= \text{constant} \end{aligned} \quad (\text{A-134})$$

The flow density $G = \dot{m}/A = \rho u$ is accordingly given by¹

$$G = \frac{P^0 \gamma}{\sqrt{\gamma R T^0}} \sqrt{\frac{2}{\gamma-1}} \sqrt{\left(\frac{P}{P^0} \right)^{\frac{2}{\gamma}} - \left(\frac{P}{P^0} \right)^{\frac{\gamma+1}{\gamma}}} \quad (\text{A-135})$$

In Eq. A-135, when $P = P_e$ = the static pressure in the exit section of a propulsive nozzle having the cross-sectional area A_e , the mass rate of flow $\dot{m} = G_e A_e$.

Let $r_t = P/P^0$ = the expansion ratio. Then Eq. A-135 can be rewritten in the form

$$G = \rho u = \frac{P^0 \gamma}{\sqrt{\gamma R T^0}} \sqrt{\frac{2}{\gamma-1}} \left[r_t^{2/\gamma} - r_t^{(\gamma+1)/\gamma} \right] \quad (\text{A-135a})$$

Eq. A-135a can be rewritten in the form

$$G = \frac{P^0 \gamma}{a^0} \sqrt{\frac{2}{\gamma-1}} \sqrt{r_t^{2/\gamma} - r_t^{(\gamma+1)/\gamma}} \quad (\text{A-135b})$$

where

$$a^0 = \sqrt{\gamma R T^0} = \text{stagnation acoustic speed.}$$

Table B-5 presents values of functions of γ — such as $(\gamma + 1)/\gamma$, $1/\gamma$, etc. — as functions of γ . Table B-6 presents values of (P_c^0/P_e) as a function of γ . Hence

$$\frac{G_a^0}{P^0} = \gamma \sqrt{\frac{2}{\gamma - 1}} \sqrt{\left(\frac{P}{P^0}\right)^{2/\gamma} - \left(\frac{P}{P^0}\right)^{(\gamma+1)/\gamma}} \quad (\text{A-135c})$$

The ratio G_a^0/P^0 is often termed the *dimensionless flow density parameter*.

For a given gas flowing under prescribed conditions, all of the terms in Eq. A-135a are constants except the expression involving r_t . The equation for G shows that there is a particular value of $r_t = P/P^0$, termed the *critical expansion ratio* (denoted by r_t^*), that makes G a maximum. The *critical expansion ratio* $r_t^* = P^*/P^0$ is determined by differentiating the radical involving r_t in Eq. A-135a and setting the result equal to zero. The result is

$$r_t^* = \frac{P^*}{P^0} = \left(\frac{2}{\gamma + 1}\right)^{\gamma/(\gamma-1)} \quad (\text{A-136})$$

It will be seen in par. A-6.1.3 that when $r_t = r_t^*$ the Mach number in the flow area where $P = P^*$ has the value $M = 1$.

If the value of $r = P/P^0$ is reduced continuously from unity to $r = r^*$ the flow density G increases continuously. Reducing r below the value r^* does not increase the flow density G because u' increases to the value c_0 when $r_t = 0$, and the density ρ decreases and is zero when $r_t = 0$.

When $r_t = r_t^*$, the corresponding flow density is $G = G^*$ and is given by

$$G^* = \frac{P^0 \gamma}{\sqrt{\gamma R T^0}} \left(\frac{2}{\gamma + 1}\right)^{\frac{\gamma+1}{2(\gamma-1)}} \quad (\text{A-137})$$

Eq. A-137 applies to the steady, one-dimensional isentropic flow of an ideal gas.

It will be seen later that the maximum flow density for the isentropic flow in a nozzle occurs in the *throat* of the nozzle.

Table B-5 presents the parameters $\left(\frac{2}{\gamma + 1}\right)^{\frac{\gamma}{\gamma-1}}$ and $\left(\frac{2}{\gamma + 1}\right)^{\frac{\gamma+1}{2(\gamma-1)}}$ as functions of γ .

A-6 CRITICAL CONDITION FOR THE STEADY ONE-DIMENSIONAL ISENTROPIC FLOW OF AN IDEAL GAS

Assume that an ideal gas is discharged from an infinite reservoir wherein $u = 0$, $T = T^0$, $P = P^0$, and $\rho = \rho^0$; and that the gas expands *isentropically* ($ds = 0$) as it flows through a variable area one-dimensional discharge duct. Fig. A-8 illustrates schematically the physical situation due to the flow expansion of the gas.

The isentropic flow expansion causes the following physical changes in the properties of the gas as it flows through the variable area duct:

- The stagnation pressure P^0 and the total temperature T^0 remain constant throughout the flow path.
- The static pressure P of the fluid decreases in the direction of flow.
- The static temperature T of the fluid decreases.
- The isentropic velocity u' of the fluid increases.
- The local acoustic speed $a = \sqrt{\gamma R T}$ of the fluid decreases.
- The local Mach number $M = u'/a$ increases.

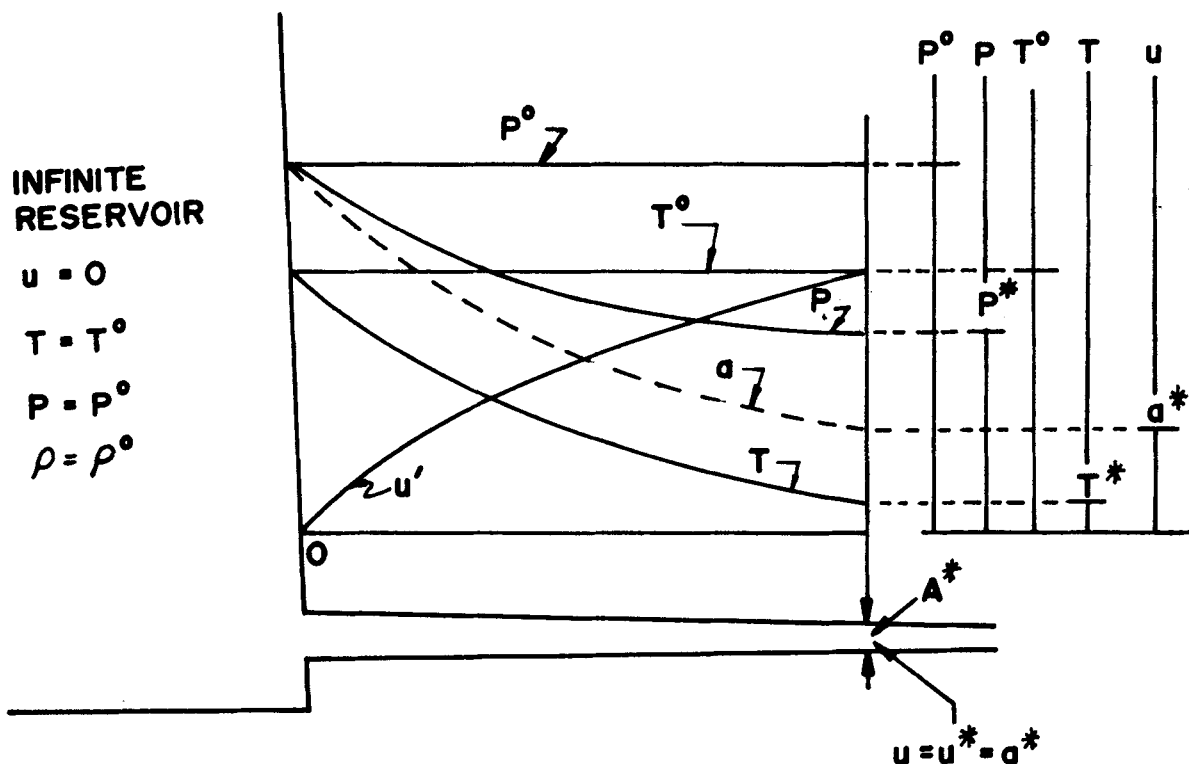


Figure A-8. Isentropic Flow Expansion of a Gas to the Critical Condition

- (g) At a particular cross-sectional area of the duct, denoted by A^* , the velocity u' is equal to the local acoustic speed, i.e., $M = u'/a = 1$.

The cross-sectional area A^* is called the *critical area* and the value of a in A^* is called the *critical acoustic speed* which is denoted by a^* , i.e., $u' = u^* = a^*$. The corresponding Mach number is unity. Thus

$$M_{A^*} = \left(\frac{u'}{a} \right)_{A^*} = \frac{a^*}{a^*} = 1$$

A-6.1 CRITICAL THERMODYNAMIC PROPERTIES FOR THE ISENTROPIC FLOW OF AN IDEAL GAS

It was shown in the foregoing that if an ideal gas is expanded isentropically in a steady one-dimensional flow, there is a critical area A^* where the gas velocity $u' = a^* =$ critical acoustic speed.

A-6.1.1 CRITICAL ACOUSTIC SPEED (a^*)

By definition

$$a^* \equiv \sqrt{\gamma R T^*} \quad (\text{A-138})$$

The critical acoustic speed a^* and the local acoustic speed at an arbitrary cross-sectional area A can be related by the following form of the energy equation for an isoenergetic flow:

$$\frac{u^2}{2} + \frac{a^2}{\gamma - 1} = \left[\frac{\gamma + 1}{2(\gamma - 1)} \right] (a^*)^2 = \text{constant} \quad (\text{A-139})$$

Eq. A-139 applies to the steady one-dimensional isentropic flow of an ideal gas. Since γ and R are constants for a given gas, the critical acoustic speed (see Eq. A-139) is a constant which can be employed as a reference velocity for the flow.

A-6.1.2 CRITICAL STATIC TEMPERATURE (T^*)

From Eqs. A-122, A-136, and A-138, it follows that

$$\frac{T^*}{T^0} = \frac{a^*}{a^0} = \frac{2}{\gamma + 1} \quad (\text{A-140})$$

or

$$T^* = T^0 \left(\frac{2}{\gamma + 1} \right)$$

A-6.1.3 CRITICAL EXPANSION RATIO (P^*/P^0)

For an isentropic process

$$\frac{P^*}{P^0} = \left(\frac{T^*}{T^0} \right)^{\gamma/(\gamma-1)} = \left(\frac{2}{\gamma + 1} \right)^{\gamma/(\gamma-1)} = r_t^* \quad (\text{A-141})$$

Eq. A-141 was presented earlier in par. A-5.6 and is the critical expansion ratio for the flow of an ideal gas.

A-6.1.4 CRITICAL DENSITY RATIO (ρ^*/ρ^0)

For an ideal gas which experiences an isentropic change of state

$$\frac{P}{\rho^\gamma} = \text{constant}$$

Hence

$$\frac{\rho^*}{\rho^0} = \frac{v^0}{v^*} = \left(\frac{P^*}{P^0} \right)^{1/\gamma} = \left(\frac{2}{\gamma + 1} \right)^{1/(\gamma-1)} \quad (\text{A-142})$$

Table B-5 presents the functions of γ that are equal to the ratios T^*/T^0 , P^*/P^0 , and ρ^*/ρ^0 as functions of the specific heat ratio γ .

A-6.1.5 DIMENSIONLESS VELOCITY ($M^* = u/a^*$)

The local Mach number $M = u/a$ suffers from the disadvantage that it is not proportional to the flow speed of a flowing fluid because the acoustic speed a varies with the temperature of the fluid. A so-called dimensionless velocity, denoted by M^* , is useful because it is proportional to the flow speed u . By definition

$$M^* \equiv \frac{u}{a^*} = \text{dimensionless velocity} \quad (\text{A-143})$$

The dimensionless velocity M^* can be related to the local Mach number¹. Thus

$$M^{*2} \equiv \left(\frac{u}{a^*} \right)^2 = \frac{\left(\frac{\gamma + 1}{2} \right) M^2}{1 + \left(\frac{\gamma - 1}{2} \right) M^2} \quad (\text{A-144})$$

Solving Eq. A-144 for M^2 , yields

$$M^2 = \frac{\left(\frac{2}{\gamma+1}\right) (M^*)^2}{1 - \left(\frac{\gamma-1}{\gamma+1}\right) (M^*)^2} \quad (\text{A-145})$$

Inspection of Eqs. A-144 and A-145 shows that

- (a) If $M = 0$, $M^* = 0$
- (b) $M = 1$, $M^* = 1$
- (c) $M \rightarrow \infty$, $M^* \rightarrow \sqrt{(\gamma+1)/(\gamma-1)}$

Table A-1 presents M^* as a function of M .

A-6.2 RELATIONSHIPS BETWEEN THE REFERENCE SPEEDS a^0 , a^* AND c_0

The critical acoustic speed a^* can be related to the stagnation acoustic speed a^0 and the maximum isentropic speed c_0 . Thus¹

$$a^0 = a^* \sqrt{\frac{\gamma+1}{2}} \quad (\text{A-146})$$

Also

$$c_0 = a^0 \sqrt{\frac{2}{\gamma-1}} = a^* \sqrt{\frac{\gamma+1}{\gamma-1}} \quad (\text{A-147})$$

A-6.2.1 RELATIVE VALUES OF REFERENCE SPEEDS FOR A GAS HAVING $\gamma = 1.40$

The reference speeds a^0 , c_0 , and a^* have the following relative values for an ideal gas having a specific heat ratio $\gamma = 1.40$:

$$a^0 = 1.095 a^*, \quad c_0 = 2.449 a^*$$

A-42

where

$$a^* = \sqrt{\gamma R T^*} \quad (\text{A-148})$$

A-6.2.2 ENERGY EQUATIONS IN TERMS OF THE REFERENCE SPEEDS a^0 AND c_0

The energy equation for the steady one-dimensional isentropic flow of an ideal gas in terms of a^* is given by Eq. A-139. The corresponding equations in terms of the stagnation acoustic speed a^0 and the maximum isentropic speed c_0 are as follows:

$$u^2 + \left(\frac{2}{\gamma-1}\right) a^2 = \frac{2}{\gamma-1} (a^0)^2 \quad (\text{A-149})$$

and

$$u^2 + \left(\frac{2}{\gamma-1}\right) a^2 = c_0^2 \quad (\text{A-150})$$

A-6.3 CRITICAL AREA RATIO FOR THE STEADY ONE-DIMENSIONAL ISENTROPIC FLOW OF AN IDEAL GAS

The general continuity equation for a steady one-dimensional flow is given by Eq. A-47 which is repeated here for convenience. Thus

$$\dot{m} = \rho u A = \text{constant}$$

If the flowing fluid is an ideal gas and the flow is isentropic, one may write

$$\dot{m} = \rho u A = \rho^* a^* A^* = \text{constant}$$

where A^* , the *critical flow area*, is the flow area where the gas speed $u = a^*$. The *critical flow density* G^* is introduced, which is defined by

$$G^* \equiv \dot{m}/A^* = \rho^* a^*$$

But

$$G \equiv \dot{m}/A = \rho a$$

Hence

$$\frac{A}{A^*} = \frac{G^*}{G} = \text{the critical area ratio} \quad (\text{A-151})$$

A-6.3.1 CRITICAL AREA RATIO (A/A^*)

The ratio A/A^* in terms of the ratio $r_t = P/P^0$ is given by¹

$$\frac{A}{A^*} = \frac{\left(\frac{2}{\gamma+1}\right)^{1/(\gamma-1)}}{\sqrt{\frac{\gamma+1}{\gamma-1}} \sqrt{\left(\frac{P}{P^0}\right)^{2/\gamma} - \left(\frac{P}{P^0}\right)^{(\gamma+1)/\gamma}}} \quad (\text{A-152})$$

Eq. A-152 relates the static pressure at a given flow cross-section to the area of that cross-section.

The critical area ratio can be expressed as function of the flow Mach number M by eliminating the ratio P/P^0 from Eq. A-152 by means of Eq. A-113 (see par. A-5.2.3). The result is

$$\frac{A}{A^*} = \frac{1}{M} \left[\frac{1 + \left(\frac{\gamma-1}{2}\right) M^2}{(\gamma+1)/2} \right]^{\frac{\gamma+1}{2(\gamma-1)}} \quad (\text{A-153})$$

Eq. A-153 relates the local Mach number to the location in a one-dimensional flow passage where the area ratio is A/A^* . For each value of A/A^* there are two values of M which satisfy Eq. A-153; one value is a subsonic flow ($M < 1$) and the other is a supersonic flow ($M > 1$). The value $M < 1$ corresponds to subsonic flow in a converging flow passage and the value $M > 1$ corresponds to flow in a diverging flow passage.

Table A-1 presents values of A/A^* as a function of the flow Mach number M .

A-6.3.2 MASS FLOW RATE (\dot{m}) AND CRITICAL AREA RATIO (A/A^*)

From Eq. A-134 (see par. A-5.6) and Eq. A-153 one obtains the following relationships between the mass flow rate \dot{m} and the critical area ratio A/A^* for a one-dimensional flow passage¹:

$$\dot{m} = \frac{P^0 A}{\sqrt{T^0}} \sqrt{\frac{\gamma}{R}} \sqrt{\left(\frac{2}{\gamma+1}\right)^{\frac{\gamma+1}{\gamma-1}} \left(\frac{1}{A/A^*}\right)} \quad (\text{A-154})$$

The advantage of Eq. A-154 is that Table A-1, which lists values of A/A^* as a function of Mach number for the steady one-dimensional isentropic flow of an ideal gas, can be employed for determining the flow Mach number directly, as is seen from the example which follows.

EXAMPLE A-3.

At a particular station in a converging passage the weight rate of flow of air at standard sea level is 25 lb per sec. The stagnation temperature and pressure of the air are 900°R and 30 psia, respectively. The cross-sectional

area is $A = 0.4$ sq ft and the flow is subsonic. Calculate the Mach number.

SOLUTION.

$$P^0 = 30 \text{ psia}; \quad T^0 = 900^\circ\text{R}; \quad \gamma = 1.40; \\ R = 53.35 \text{ ft-lb/}^\circ\text{R}.$$

Eq. A-154

$$\dot{w} = \dot{m}g_c = \frac{P^0 A}{\sqrt{T^0}} \sqrt{\frac{\gamma g_c}{R}} \sqrt{\left(\frac{2}{\gamma+1}\right)^{\frac{\gamma+1}{\gamma-1}}} \frac{1}{A/A^*} \\ = \frac{(30)A}{1.88\sqrt{900}} \left(\frac{1}{A/A^*}\right)$$

Hence

$$\frac{A}{A^*} = \frac{30 (144) (0.4)}{1.88\sqrt{900} (25)} = 1.225$$

From Table A-1, $M = 0.57$

A-6.4 FLOW AREA CHANGES FOR SUBSONIC AND SUPERSONIC ISENTROPIC FLOW

Eq. A-153 relates the critical area ratio A/A^* and the local Mach number M for a steady one-dimensional isentropic flow of an ideal gas. The relative change in flow cross-sectional area dA/A , the relative change in velocity du/u , and the relative change in the static pressure dP/P are related to the flow Mach number M . It can be shown that¹

$$\frac{dA}{A} = (M^2 - 1) \frac{du}{u} \quad (\text{A-155})$$

and

$$\frac{dA}{A} = \frac{1}{\gamma} \left(\frac{1}{M^2} - 1 \right) \frac{dP}{P} \quad (\text{A-156})$$

Eqs. A-155 and A-156 govern the manner in which the flow area A of a flow passage must be varied to accomplish either *nozzle action* (dP/P negative) or *diffuser actions* (dP/P positive) for either the subsonic ($M < 1$) or supersonic ($M > 1$) steady one-dimensional isentropic flow of an ideal gas.

Fig. A-9 illustrates the configurations of the flow passages for nozzle and diffuser actions.

From the consideration of Eqs. A-155 and A-156 one derives the following conclusions:

- A continuous flow passage for accelerating the isentropic one-dimensional flow of an ideal gas must comprise a converging passage followed by a diverging passage, as illustrated in Fig. A-10.
- A continuous flow passage for decelerating an ideal gas from an *initially supersonic flow* to a subsonic flow must comprise a converging passage followed by a diverging passage.
- The *back pressure* P^0 acting on the exit cross-sectional area A_e of the diverging flow passage determines whether that portion of complete flow passage accomplishes either nozzle or diffuser action.

A-6.5 DIMENSIONLESS THRUST FUNCTION (F/F^*)

The thrust function (see par. A-3.2.1) is defined by Eq. A-56, which is repeated here for convenience. Thus

$$F \equiv PA + \dot{M} = PA + \rho Au^2$$

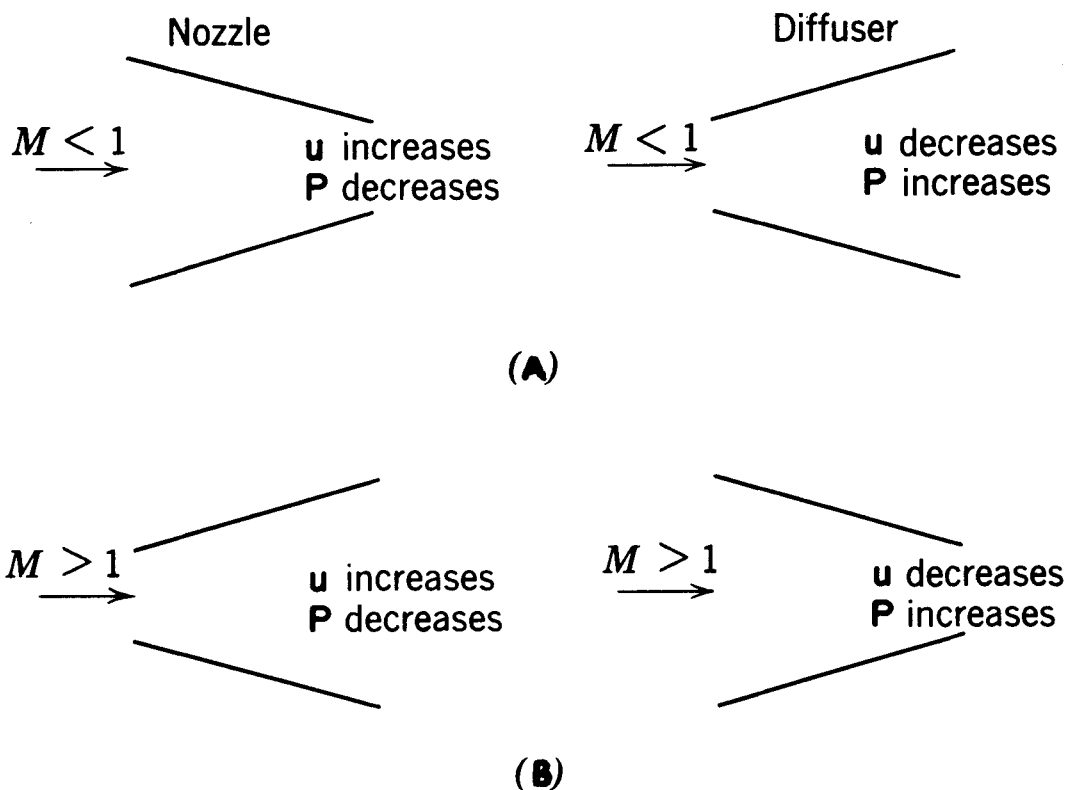


Figure A-9. Area Configuration for Nozzle or Diffuser Action, for the One-dimensional Flow of an Ideal Gas

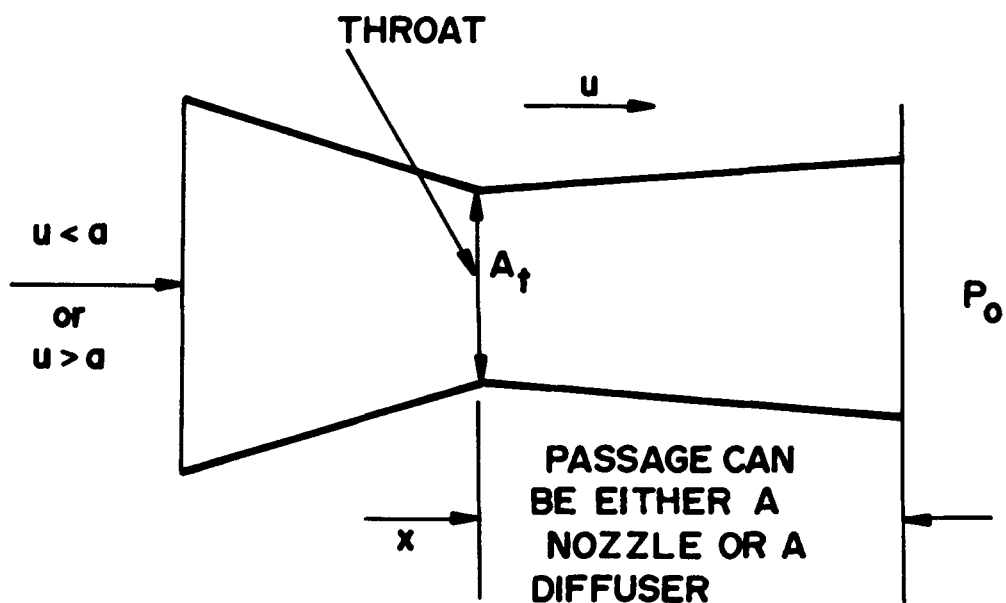


Figure A-10. Converging-diverging Flow Passage

For an ideal gas $a^2 = \gamma P/\rho$ and $M^2 = u^2/a^2$ so that

$$F = PA (1 + \gamma M^2) \quad (\text{A-157})$$

Eq. A-157 applies to the steady one-dimensional flow of an ideal gas. Let F^* be the value of the thrust function when it is evaluated for $M = 1$. Hence, the dimensionless thrust function F/F^* is given by

$$\frac{F}{F^*} = \left(\frac{P}{P^*}\right) \left(\frac{A}{A^*}\right) \left(\frac{1 + \gamma M^2}{1 + \gamma}\right) \quad (\text{A-158})$$

For P/P^* one may write

$$\frac{P}{P^*} = \left(\frac{P}{P^0}\right) \left(\frac{P^0}{P^*}\right)$$

Employing Eq. A-113 for P/P^0 , Eq. A-141 for P^0/P^* , and Eq. A-153 for A/A^* , one obtains

$$\frac{F}{F^*} = \frac{(1 + \gamma M^2)}{M \sqrt{2(\gamma + 1) \left[1 + \left(\frac{\gamma - 1}{2}\right) M^2\right]}} \quad (\text{A-159})$$

Eq. A-159 applies to the steady one-dimensional isentropic flow of an ideal gas.

For a steady one-dimensional *adiabatic* flow, the stagnation pressure ratio is given by Eqs. A-113 and A-116 (see par. A-5.2.4), and can be rewritten in the form

$$\frac{P}{P^0} = \exp \left[- (s^* - s)/c_p \right]$$

where s^* is the value of s where $M = 1$. Hence, if the flow is steady, one-dimensional, and adiabatic

$$\frac{F}{F^*} = \frac{(1 + \gamma M^2) \exp \left[- (s^* - s)/c_p \right]}{M \sqrt{2(\gamma + 1) \left[1 + \left(\frac{\gamma - 1}{2}\right) M^2\right]}} \quad (\text{A-160})$$

For solving some types of problems the product of the following ratios $(A/A^*)(P/P^0)$ is useful. It is tabulated as a function of M , for different values of the specific heat ratio γ in Table A-1. Multiplying Eq. A-153 by Eq. A-113, gives

$$\frac{A}{A^*} \left(\frac{P}{P^0}\right) = \frac{1}{M \sqrt{1 + \left(\frac{\gamma - 1}{2}\right) M^2}} \sqrt{\left(\frac{2}{\gamma + 1}\right)^{\frac{\gamma + 1}{\gamma - 1}}} \quad (\text{A-161})$$

A-7 FLOW OF AN IDEAL GAS IN A CONVERGING-DIVERGING ONE-DIMENSIONAL PASSAGE

Fig. A-11 illustrates schematically a converging-diverging flow passage through which an ideal gas flow isentropically. The continuity equation for a one-dimensional flow of an ideal gas (see par. A-4) is given by Eq. A-72 which is repeated here for convenience. Thus

$$\dot{m} = APM\sqrt{\gamma/RT}$$

The dimensionless flow density parameter Ga^0/P^0 is obtained from Eq. A-135c. Thus

$$\frac{Ga^0}{P^0} = \gamma \sqrt{\frac{2}{\gamma - 1}} \sqrt{r_t^{2/\gamma} - r_t^{(\gamma + 1)/\gamma}}$$

where the expansion ratio $r_t = P/P^0$.

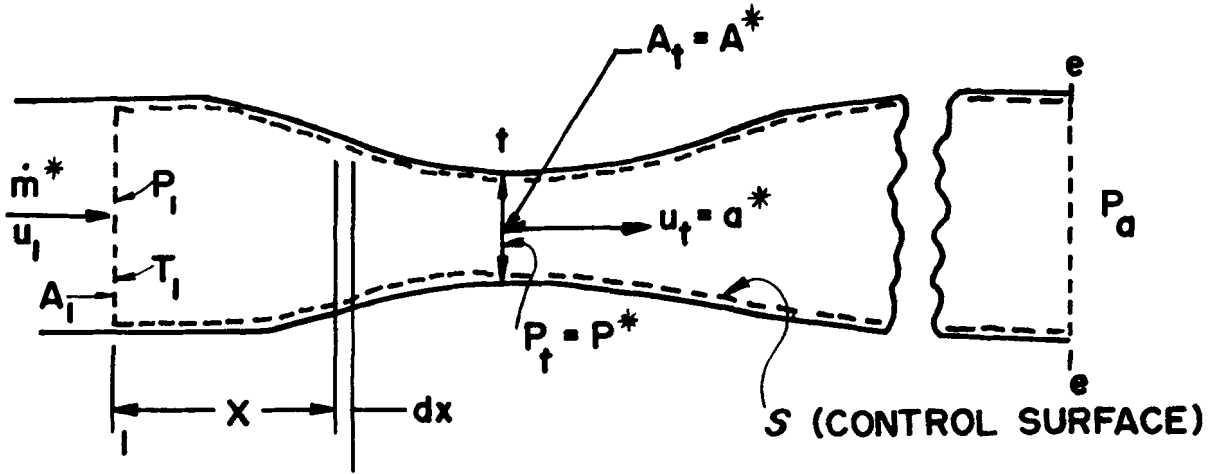


Figure A-11. Converging-diverging Flow Passage Which Passes the Critical Mass Flow Rate \dot{m}^*

The parameter Ga^0/P^0 vanishes for two conditions: (1) if the velocity $u = 0$, or (2) if the density $\rho = 0$. These two cases will now be examined.

Case 1. ($P/P^0 = 1$)

In this case $P^0 - P = 0$, so that $u = 0$ and $\rho = \rho^0$. Consequently $\dot{m} = 0$.

Case 2. ($P/P^0 = 0$)

In this case the gas expands into a vacuum, and since the flow is isentropic, the gas attains the maximum isentropic speed (see par. A-5.5). Hence

$$c_o = a^0 \sqrt{2/(\gamma - 1)}$$

Since $P = 0$ and $T = 0$, then for a perfect gas $\rho = 0$. Consequently, $G = \rho u = 0$ and $\dot{m} = 0$.

It would appear from the preceding that if G is plotted as a function of P/P^0 , then $G = 0$ when $P/P^0 = 0$ and when $P/P^0 = 1$. Consequently, G would have at least one maximum

point between the two aforementioned values of P/P^0 ; actually, there is a single maximum point.

A-7.1 MAXIMUM FLOW DENSITY

Fig. A-11 illustrates schematically the isentropic flow through a converging-diverging flow passage. Assume that the passage passes the *maximum mass flow rate* of an ideal gas, denoted by \dot{m}^* . Hence, one may write for any *arbitrary* cross-sectional area of the flow passage A that

$$\dot{m} = \dot{m}^* = \rho A u = \text{constant}$$

Logarithmic differentiation of the last equation with respect to x , the length of the converging-diverging flow passage, yields

$$\left(\frac{1}{A}\right) \frac{dA}{dx} + \left(\frac{1}{u}\right) \frac{du}{dx} + \left(\frac{1}{\rho}\right) \frac{d\rho}{dx} = 0 \quad (\text{A-162})$$

Fig. A-12 presents dA/dx as a function of x . It is evident that at the smallest cross-sectional area of the flow passage, called the *throat* and denoted by A_t , the derivative $(dA/dx)_t = 0$.

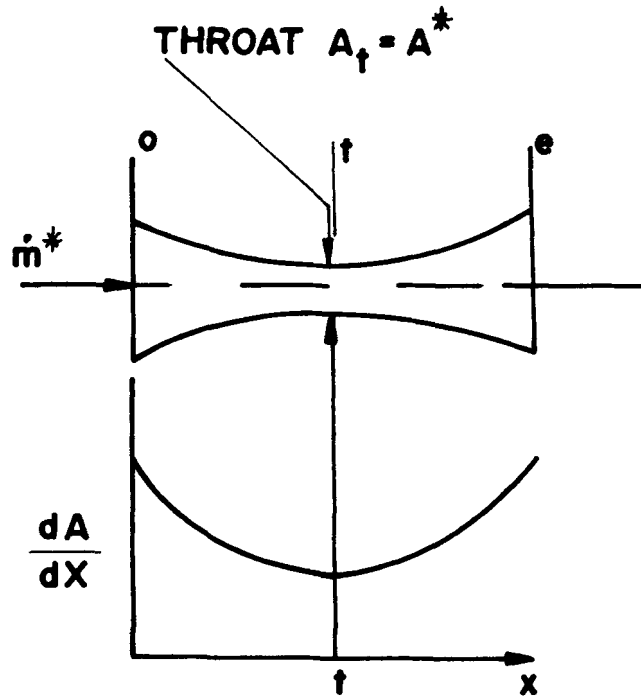


Figure A-12. Functional Relationship Between dA/dx and x for the Flow of an Ideal Gas in a Converging-diverging Flow Passage

Substituting $dA/dx = 0$ into Eq. A-151, one obtains

$$\left(\frac{du}{dx}\right)_t = -\frac{u_t}{\rho_t} \left(\frac{dp}{dx}\right)_s$$

where the subscript t refers to the throat section A_t , and the subscript s denotes that the expansion of the gas is isentropic. Because the flow is assumed to be isentropic, the momentum equation referred to the throat (see par. A-4.2.3) becomes

$$dP + \rho u du = 0$$

or

$$\left(\frac{du}{dx}\right)_t = -\left(\frac{1}{\rho u_t}\right) \left(\frac{dP}{dx}\right)_s$$

Equating the two expressions for $(du/dx)_t$ and solving for the velocity in the throat section A_t yields

$$u = u_t = \left(\frac{dP}{d\rho}\right)_s = (a^*)^2$$

The last equation demonstrates that when a converging-diverging passage passes the maximum flow rate \dot{m}^* , assuming isentropic flow, the fluid speed crossing the *throat* of the passage is equal to the local acoustic speed, i.e., $u = u_t = u^* = a^*$. Hence, in the case of the steady, one-dimensional, isentropic flow of an ideal gas if $\dot{m} = \dot{m}^*$; then $u_t = a^*$, $P_t = P^*$, $T_t = T^*$, and $M_t^* = u_t/a^* = 1$. Consequently,

$$A_t = A^* = \text{critical flow area}$$

INDEX

Index Terms

Links

A

Ablation cooling systems	10-17
Acoustic instability	
principal conclusions	8-18
solid propellant motors	8-17
suppression methods	8-18
Aerodynamic heating	
rocket motors	8-24
Aerazine	9-30
Afterburning	
turbofan engines	15-52
Air-augmented engines	11-1
Air-augmented rocket engine	12-8
Air-breathing engines	
classification	12-7
efficiency	12-23
overall propulsive efficiency	12-23
thermal propulsive efficiency	12-24
general comments	12-28
performance expressed terms	
of efficiencies	12-23
performance parameters	12-27
specific engine weight	12-27
factors affecting	12-28
specific fuel consumption	12-24
specific impulse	
air specific impulse	12-27
fuel specific impulse	12-27
thrust equations	12-18
specific air-breathing engines	12-20
terms of fuel-air ratio	12-19

Index Terms

Links

Air-breathing engines (*Cont.*)

turbine inlet temperature 12-28

Aircraft (Army) 15-2

Air-turborocket engines 11-1 12-8

Altitude

burnout 5-14

coasting 5-14

coasting after burnout 5-14

maximum drag-free 5-14

ramjet engine, effect on 14-10

Alumizine 9-31

Ammonia

and hydrazine mixtures 9-31

anhydrous 9-31

Area ratio

adiabatic nozzle 4-26

complete expansion of gas flow in a
converging-diverging nozzle 4-14

critical area ratio in terms of flow expansion
ratio 3-20

nozzle, for complete expansion 6-13

B

Ballistics 7-2

Ballistics

solid propellant rocket motors 8-3

Binders

composite propellants 7-4

raw materials of 7-9

Bipropellant liquid engines 10-2

Bipropellant rocket systems

fuels for 9-22

Borohydride fuels 9-24

Boundary layer

in a flow 13-1

Index Terms

Links

Burning rate

controllable linear 7-7

Burning surface

effect of shape 8-12

Burning time

rocket engine 5-2

Burnout velocity

rocket-propelled body 5-9 5-13

ideal 5-14

vacuum 5-14

C

Cavitation

turbopumps of liquid propelled missiles 9-3

Chemical jet propulsion systems

11-1

Chemical reactions

endothermic 6-5

exothermic 6-5

Chlorine trifluoride

9-16

Coburning

turbofan engines 15-52

Coefficients

divergence loss 4-31

gross thrust 14-8

mass flow 5-4

net thrust of ramjet engine 14-8

nozzle discharge 4-27

nozzle performance 4-27

nozzle velocity 4-27

propellant flow 6-11

thermal expansion 7-7

thrust 5-4 6-13

weight flow 5-4 6-11

Index Terms

Links

Cooling systems

ablation cooling	10-17
classification of thrust chambers	10-10
compound heat-sink/heat-bamer	
cooling	10-14
film	10-16
heat barriers in thrust chambers	10-11
heat sinks in thrust chambers	10-11
internal systems	10-16
nonregenerative systems	10-11
transpiration cooling	10-17

Compression shock

development of	3-37
----------------	------

Combustion chamber

hybrid engine	11-14
---------------	-------

Combustion products

reassociation into gas flow through a	
nozzle	4-28

Conductivity

thermal	7-7
---------	-----

Configurations

nozzle design	4-29	4-30
---------------	------	------

Continuity equation

steady one-dimensional flow	3-7
steady one-dimensional isentropic flow of	
an ideal gas	3-20
steady one-dimensional flow of an ideal	
gas	3-10
terms of stagnation conditions	3-21

Contour

potential wall	4-29
----------------	------

Control

flight control	5-8
----------------	-----

Index Terms

Links

Control surface

fictitious control surface	2-3
stationary control surface	2-3
transport of a fluid property across	2-3

Cordites	7-2
----------	-----

Counterflow heat exchanger	15-25
----------------------------	-------

Critical area

critical area ratio	3-20
critical area ratio in terms of flow expansion ratio	3-20
critical area ratio in terms of flow Mach number	3-20
definition of	3-18

Cryogenic fuels

liquid bipropellant systems	9-22
physical properties	9-23

D

Design

diffuser	13-11
hybrid rocket engines	11-12 11-16
nozzle design configuration	4-29
nozzle design principles	4-28

Design point charts	15-18
---------------------	-------

Density

critical mass flow density	3-21
impulse	6-23
propellant, density of	7-7
propellant loading, density of	5-8

Differential equation

solution of, for linear motion with drag and gravity	5-11
---	------

Diffuser

axisymmetrical diffuser system	13-9
compressible flow	13-1

Index Terms

Links

Diffuser (*Cont.*)

conical spike diffuser	13-11
additive drag of a conical spike	
diffuser	13-12
design of	13-11
drag	
additive drag of a conical-spike	
diffuser	13-12
external drag of the diffusion system	13-12
efficiency	
energy efficiency of a diffuser	13-6
isentropic diffuser efficiency	13-5
external-compression diffuser	
static pressure ratio	13-2
static temperature ratio	13-2
external shock diffusers, operating	
mode	13-11
isentropic diffuser efficiency	13-5
isentropic spike diffuser	13-13
normal shock diffuser	13-7
ram pressure	13-8
operation	
critical operation of a diffuser	13-11
subcritical operation of a diffuser	13-11
supercritical operation of a diffuser	13-11
performance	
characteristics	13-11
criteria	13-5
in a ramjet engine	14-14
stagnation pressure ratio as a criterion	
of	13-5
ramjet engine, diffuser performance in	14-14
ram pressure for normal shock diffuser	13-8
subsonic diffuser	13-1
subsonic external-compression diffuser	13-2
subsonic intake diffuser	13-2

Index Terms

Links

Diffuser (*Cont.*)

subsonic internal-compression diffuser	13-3
supersonic diffuser	13-1
external compression	13-9
reversed DeLaval nozzle	13-9
supersonic-inlet diffuser	13-7

Diethylenetriamine (DETA)	9-30
---------------------------	------

Dimazine	9-29
----------	------

Dimethylhydrazine (unsymmetrical)	9-29
-----------------------------------	------

Dissociation reactions	6-5
------------------------	-----

Dithekites	9-9	9-12
------------	-----	------

Divergence loss	6-11
-----------------	------

Drag

additive drag of a conical spike diffuser	13-12
aerodynamic drag	5-11
external drag in a diffusion system	13-12
linear motion with drag and gravity	5-9
nose drag	5-11
skin friction drag	5-11
tail drag	5-11
viscous drag	13-1

Dual-cycle engine	12-6
-------------------	------

Duct length

critical duct length for Fanno flow of ideal	
gas	3-27
for specified change in Mach number	3-27

E

Efficiency

engine weight efficiency	5-8
ideal propulsive efficiency	2-16
isentropic diffuser efficiency	13-5
nozzle efficiency	4-27
overall propulsion system efficiency	2-16
propulsive efficiency	2-16
thermal efficiency	2-16

<u>Index Terms</u>	<u>Links</u>
Elastomeric monomers	7-4
Electromagnetic signals	
attenuation of electromagnetic signals	7-8
Emulsions	
possible liquid propellants	9-33
Energy equation	
simple adiabatic flow	3-12
simple adiabatic flow of an ideal gas	3-13
steady one-dimensional flow	3-8 3-12
steady one-dimensional flow of an ideal gas	3-14
Engine	
characteristic velocity and performance of	
different rocket engines	5-5
engine weight efficiency	5-8
hybrid rocket engine	1-11
liquid bipropellant rocket engine	1-11
liquid monopropellant engine	1-11
liquid monopropellant rocket engine	1-11
specific engine weight	5-7
Enthanol	9-26
Equilibrium	
combustion pressure	6-5
combustion temperature	6-5
composition of a gas propellant	6-5
frozen equilibrium	6-4
thermochemical equilibrium	6-6
Erosive burning	
solid propellants	8-13
Ethyl alcohol	
ethyl alcohol as an organic fuel	9-29
Ethylene oxide	
ethylene oxide as a liquid propellant	9-12
Euler's equation of motion	3-8
Exhaust	
smoke in exhaust gases	7-8

Index Terms

Links

Expansion

thermal expansion ratio	7-7
overexpansion in a converging-diverging nozzle	4-20
underexpansion in a converging-diverging nozzle	4-21

F

Feed systems

liquid propellant rocket engines	10-20
----------------------------------	-------

Film cooling systems

10-16

Flight

flight control of a rocket-propelled vehicle	5-8
flight performance of a rocket-propelled vehicle	5-8
flight stability of a rocket-propelled vehicle	5-8

Flow

adiabatic flow	
energy equation for simple adiabatic flow	3-17
energy equation for simple adiabatic flow of an ideal gas	3-13
choked flow	6-11
compressible flow in nozzles	4-3
compression	13-1
cold flow through a shaped duct	14-1
critical area ratio in terms of flow expansion	3-20
critical flow density	3-21
critical flow parameters	3-18
external flow	2-7
equilibrium flow	4-34

Index Terms

Links

Flow (*Cont.*)

energy equation

simple adiabatic equation 3-12

simple adiabatic equation of an ideal

gas 3-13

steady one-dimensional flow 3-7

steady one-dimensional isentropic flow

of an ideal gas 3-14

expansion

critical area ratio in terms of 3-20

Fanno flow

characteristics of 3-23 3-24 3-25

equations for 3-23

ideal gases

characteristics of the Fanno flow of an

ideal gas 3-28

critical duct length for Fanno flow of

ideal gas 3-26

equation for computing Fanno flow

functions for ideal gases 3-28

example problem for computation of

Fanno flow functions for ideal gases 3-29

Fanno line equation

frozen flow 4-34 6-4

internal flow 2-7 2-11

isentropic flow

critical conditions for steady one-dimensional

isentropic flow of an ideal gas 3-18

critical thermodynamic properties for steady

isentropic flow of an ideal gas 3-18

energy equation for steady one-dimensional

isentropic flow of an ideal gas 3-14

functions for ideal gases 3-21 3-22

steady one-dimensional 3-13

isoenergetic flow 3-15

losses in a ramjet engine 14-13

Index Terms

Links

Fanno line equation (*Cont.*)

mass flow

coefficient	5-4
rate for ideal nozzle flow	4-8
rate for nozzle operating with adiabatic	
flow and wall friction	4-28
rate of propellant gas	6-11

momentum equation

steady one-dimensional flow of an ideal	
gas	3-12
steady one-dimensional reversible flow	3-8

perfect gas flow in a converging nozzle

(isentropic throat velocity)	4-5
------------------------------	-----

nozzle

ideal flow in a nozzle	4-3
ideal flow in a converging nozzle	4-5
ideal flow in a DeLaval nozzle	4-10
flow in real nozzles	4-26

Rayleigh flow

definition	3-29		
equations for	3-29	3-31	3-32
functions for ideal gases, equations for			
tables of	3-35		
ideal gases, equations for	3-34	3-35	
reversible flow			
Euler's equation of motion	3-8		
momentum equation for reversible, steady			
one-dimensional flow	3-12		
steady flow	2-4		
steady one-dimensional flow			
energy equation for steady one-			
dimensional flow	3-7		
ideal gas	3-10		
unsteady flow	2-4		
weight flow coefficient	6-11	5-4	

Index Terms

Links

Fluorine

fluorine monoxide	9-22	
liquid fluorine as a propellant	9-13	
oxidizers	9-17	9-20

Fluid compressibility

3-7

Forces

body force	2-6
drag force	
external drag force	2-7
internal drag force	2-7
external force on a flowing fluid	2-6
hydrostatic force	2-6
net component of force	2-7
net internal axial force	2-7
normal force	2-6
surface force	2-6
tangential force	2-6

Friction

friction coefficient	3-23
wall friction	
decelerating influence of wall friction	4-23
mass flow rate for a nozzle operating with adiabatic flow & wall friction	4-28

Fuel

consumption, rate of	2-15
fluorine and oxygen oxidizers, fuel	
performance with	11-6
hybrid fuels	11-6
hydrogen peroxide, chlorine oxidizers, fuel	
performance with	11-7
mixture ratio	2-13

Fuel-plasticizers

homogeneous propellants	7-2
-------------------------	-----

Index Terms

Links

G

Gas

calorically perfect gas	3-6	
flow in a converging-diverging nozzle, area ratio for complete expansion of	4-14	
gas dynamics	3-4	
assumptions in calculations	6-4	6-5
hot gas	15-25	
hot gas generators	1-3	
hybrid engine, gas characteristics	11-7	
ideal gas	3-5	3-7
acoustic or sonic speed	3-7	
adiabatic flow, energy equation for	3-13	
Fanno flow		
characteristics of	3-28	
critical duct length	3-27	
equations for computing Fanno flow		
for an ideal gas	3-28	
equations governing the Fanno flow	3-26	
example problem for computation of		
Fanno flow functions	3-29	
with ideal gases	3-26	
isentropic flow functions	3-21	3-22
isentropic flow, steady one-dimensional		
critical conditions for	3-18	
critical thermodynamic properties	3-18	
energy equation for	3-13	
pressure drop		
gas side pressure drop in a thrust chamber	10-8	
pressurization		
chemical gas	10-21	
stored inert	10-20	
steady one-dimensional flow	3-10	
momentum equations	3-12	

Index Terms

Links

Gas-turbine engines

combustion process	15-6
compressor	
pressure ratio parameter	15-4
temperature rise in air-compressor	15-4
compression process	15-4
conclusions about gas turbine engines	15-55
cycle of engine	
cycle losses	15-12
thermodynamic analysis	15-12
diffuser	
pressure ratio parameter	15-2
temperature	15-2
diffusion process	15-2
dimensionless heat parameter	15-6
efficiency	
burner	15-6
components' efficiency	15-2
isentropic diffuser	15-2
flow rate	
ideal fuel flow rate	15-6
jet engines	15-38 12-11
types	15-1
turbine	
expansion process	15-6
inlet temperature	15-7

Gels

thixotropic gels	9-32
------------------	------

Grain configuration

8-20

Gravity

differential equation for linear motion with	
drag and gravity, solution of	5-11
linear motion with drag and gravity	5-9

Index Terms

Links

H

Handbook

division of handbook	1-1
purpose and scope of handbook	1-1
units of measurements employed	1-11

Hazards

explosive hazards of propellants	7-8
----------------------------------	-----

Heat-barrier cooling	10-11
----------------------	-------

Heat-sink cooling	10-11
-------------------	-------

Heat transfer

liquid propellant thrust chambers	10-9
solid propellant rocket motors	8-23

Hybrid rocket engines

advantages of	11-4
afterburner chamber	11-16
afterburning conventional engine	11-3
burning rate	11-11
classification	11-1
combustion of propellants	11-8
definition	11-1
design considerations	11-12
exhaust nozzle design	11-14
gas characteristics	11-7
head-end injection	11-2 11-13
ignition injectors	11-14
internal ballistics	11-10
safety in handling propellants	11-4
simplicity	11-5
specific impulses	11-5
specific performance	11-9
thrust equation	11-11
thrust termination and restart	11-14
velocity	11-9

Index Terms

Links

Hydrazine

fuel in a bipropellant system	9-31
liquid propellant	9-9
mixtures of hydrazine and ammonia	9-31

Hydrocarbon fuels	9-27	9-29	9-30
-------------------	------	------	------

Hydrogen peroxide

liquid propellant	9-10
oxidizer	9-18
water solution of hydrogen peroxide	9-10

Hygroscopicity	7-7
----------------	-----

I

Ignition

hybrid rocket engines	11-14
propellant grain	8-19

Impulse

density impulse	6-23		
specific impulse	2-15	5-3	7-7
jet power	2-15		
reduced	6-20		
theoretical	6-20		
total impulse	5-5		
weight ratio for rocket engines	5-8		

Injectors, hybrid engines	11-14
---------------------------	-------

Insulation, rocket motor chamber	8-26
----------------------------------	------

J

Jet engines

air-breathing jet engines	1-4	1-16	2-17
chemical air-breathing jet engine	1-4		
nuclear air-breathing jet engine	1-4		
flow processes in jet propulsion engines	3-4		
gas-turbine jet engine	1-4		
propulsive duct jet engine	1-4		

Jet power	5-5
-----------	-----

Index Terms

Links

Jet propulsion systems

classification 1-3

performance parameters 2-15

Jetvator 8-31

JP fuels 9-29

M

Mach number 3-7

critical area ratio in terms of flow Mach

number 3-20

duct length for specified change in Mach

number 3-27

effect on thrust 15-46

Measurements

units employed in handbook 1-11

Methanol 9-12

Methyl nitrate 9-12

Mixture ratio 2-13

Momentum

equation 3-8

equation for reversible steady one-

dimensional flow of an ideal gas 3-12 3-8

equation for steady, one-dimensional,

reversible flow 3-8

fluid in a steady flow 2-7

theorem of fluid mechanics 2-3

theorem for propulsion systems 2-7

theorem for steady flow 2-7

Monopropellants (liquid)

classes 9-8 9-9

definition 9-8

Monopropellant runout 9-31

Index Terms

Links

Motion

Euler's equation of motion 3-8

linear motion

differential equation for linear motion

with drag and gravity, solution of 5-11

thrust of rocket engine with linear motion

of vehicle 5-9

with drag and gravity 5-9

Myrols 9-9 9-12

N

Nitric acid

use as an oxidizer 9-18

use as a propellant 9-12

Nitrobenzene

use as a propellant 9-12

Nitrogen

oxides of nitrogen

mixed oxides of nitrogen 9-19

physical properties of oxides of

nitrogen 9-21

nitrogen hydrides and derivatives 9-27 9-31

Nitromethane

use as a propellant 9-12

Nitroparaffins

use as an oxidizer 9-18

use as a propellant 9-12

Nitropropane

use as a propellant 9-12

Nozzles

adiabatic nozzle

area ratio 4-26

annular nozzle 4-3

area ratio for complete expansion 6-13

choked exhaust nozzle 14-9

complete nozzling 4-28 6-11

Index Terms

Links

Nozzles (*Cont.*)

compressible flow	4-3
conical nozzle	4-30
adequacy	4-32
thrust equation	4-31
contoured (bell-shaped) nozzle	4-34
initial expansion section	4-34
converging nozzle	
back pressure acting on	4-7
ideal flow	4-5
isentropic throat velocity	4-5
for the flow of a perfect gas	4-5

DeLaval nozzle

area ratio for complete expansion of gas	
flow	4-14
back pressure acting on	4-20
ideal flow	4-10
overexpansion	4-21
underexpansion	4-20
real nozzles	
flow in a real nozzle	4-26
losses in a real nozzle	4-26
self-adjusting nozzle	4-37
subsonic flow	
transition into supersonic flow	4-34
solid propellant rocket motors	8-27
swivel nozzle	8-22 8-33
thrust equation for conical nozzle	4-31
velocity coefficients	4-27

O

Off-design point	15-18
------------------	-------

Organic fuels

containing carbon, hydrogen and oxygen	9-24
containing carbon, hydrogen and nitrogen	9-24 9-29

Index Terms

Links

Oxidizer-plasticizers

for homogeneous propellants 7-2

Oxidizers

composite propellants 7-5

containing fluorine 9-17

containing fluorine and oxygen 9-19 9-22

containing oxygen 9-20

liquid oxidizers, physical properties 9-14 9-15

liquid propellant systems 9-12

materials of 7-9

Oxidizer tank, pressure requirements 11-13

Oxygen

liquid oxygen 9-16

bladders 11-13

injectors, hybrid engines 11-14

pressurization in hybrid engine 11-13

tank pressure requirements 11-13

oxygen bifluoride 9-22

oxidizers 9-17

Ozone

liquid ozone as an oxidizer 9-18

P

Parallel heat exchanger 15-25

Payload ratio 5-7

Perchlorylfluoride 9-21

Performance criteria

diffuser performance 13-5

flight performance 5-8

rocket performance criteria, thermodynamic
equations 6-6

vehicle performance 5-8

Piobert's law 8-5

Poisson's ratio 7-9

Post-combustion 12-13

Index Terms

Links

Power

definition for propulsive system	2-14	
exit loss	2-14	
jet power	2-15	5-5
limited systems	2-15	
propulsive power	2-14	
thrust power	2-14	

Pressure

back pressure		
modes of operation	47	423
varying on a converging nozzle	4-7	
varying on a converging-diverging nozzle	4-20	
equilibrium combustion pressure	6-5	
inlet total pressure of a nozzle, effect of varying	4-24	
static pressure inside a duct, support of	14-1	

Principles

jet propulsion principle	1-3	1-10
nozzle design principle	4-28	
reaction principle	1-3	

Propellants

ballistite propellants	7-2
composite propellant	
additive to composite propellants	7-6
binders for composite propellants	7-4
formulations	7-6
heterogeneous or composite propellants	7-4
oxidizers for composite propellants	7-5
cordite propellants	7-2
homogeneous (double-base) propellants	7-1
additives	7-2
applications	7-2
characteristics	7-2
fuel plasticizers	7-2
oxidizer-plasticizers	7-2
polymers for	7-2
properties of	7-3

Index Terms

Links

Propellants (*Cont.*)

hybrid, combustion	11-8		
liquid propellants			
availability	9-4		
boiling point	9-2		
chemical reactivity	9-2		
chemical stability	9-3		
chemical structures	9-2		
corrosivity	9-3		
cost	9-4	9-7	
density	9-2		
enthalpy of combustion	9-1		
freezing point	9-3		
gelled liquid propellants	9-32		
grains	7-2		
heterogeneous liquid propellants	9-32		
oxidizers	9-12		
selection of	9-1		
specific heat	9-3		
specific impulse	9-5	9-6	9-7
toxicity	9-4		
vapor pressure	9-2		
viscosity	9-3		
loading density	5-8		
mass flow rate of a propellant gas	6-11		
mass ratio	5-7		
mesa propellants	8-9		
plastic propellants, brittle temperature	7-11		
rocket engines			
bipropellant engines	10-2		
combustion chambers	10-5		
cooling systems	10-10		
feed systems	10-20		
heat transfer in thrust chambers	10-9		
injectors	10-3		
thrust chambers	10-3	10-6	

Index Terms

Links

Propellants

rocket engines (<i>Cont.</i>)	
variable thrust	10-24
safety in handling	11-4
solid propellants	
acoustic instability	8-14
ballistics, internal	8-3
burning	8-3
combustion pressure oscillations	8-14
compression strength	7-10
cost	7-9
creep	7-10
deformation at rupture in	
compression	7-10
density	7-7
elongation in tension	7-10
fabrication	7-9
modulus in compression	7-10
modulus in tension	7-10
process-control	7-9
properties of	7-9 11-5
Piobert's law	8-3
selection of	7-7
sensitivity	8-13
shear strength between propellant and	
chamber	7-11
storability	11-5
stress relaxation	7-10
stress-strain behavior	7-9
temperature effect	8-12
tensile strength	7-9
vehicles	8-29

Propulsion

jet propulsion differentiation from other	
propulsion methods	1-3
performance criteria for rocket propulsion	5-5

Index Terms

Links

Propulsion (*Cont.*)

rocket propulsion	1-10
scope of the field of propulsion	1-2

Propulsion engines

air-breathing jet engines	1-4
classification of	1-2
flow processes	3-4

Propulsion systems

high energy	11-5
ideal system	2-4
jet propulsion systems	
classification	1-3
subassemblies	1-3
thermodynamic	1-7
momentum theorem	2-7
performance parameters	2-15
readiness of	9-7
rocket propulsion systems	
chemical rocket propulsion systems	1-7
classification	1-5
rocket jet propulsion systems	1-5 2-17
volume limited propulsion systems	9-33 11-4
weight	5-6

Propulsive duct engine

heat addition to internal flow of a shaped duct	
duct	14-5
performance parameters	14-1
restriction of exit area of a shaped duct	14-1
static pressure	14-1
thrust developed by	14-1

Propulsive jet engine

definition of	1-3
exit velocity parameters	12-19

Index Terms

Links

R

Ramjet engine	12-8
altitude, effect on	14-10
choked exhaust nozzle	14-9
diffuser performance	14-14
drag (external)	14-7
efficiency	
burner efficiency	14-16
overall efficiency	14-16
fixed geometry ramjet engine	14-10
flowpasses (internal)	14-13
fuel-air ratio, effect	14-10
operation	
critical operation	14-13
modes of operation	14-10
subcritical operation	14-13
supercritical operation	14-13
thrust	
gross thrust	14-5
gross thrust coefficient	14-8
gross thrust specific fuel consumption	14-16
net thrust	14-7
net thrust coefficient	14-8
technology, definition of terms	
employed	14-5
thrust coefficients	12-20
thrust equations	12-20
variable ramjet engine	14-16
Ratios	
fuel-air ratio, effect on ramjet engine	14-10
impulse-weight ratio for rocket engine	5-8
payload ratio	5-7
propellant mass ratio	5-7
relationship with vehicle mass ratio	5-8

Index Terms

Links

Ratios (*Cont.*)

ram pressure ratio for normal shock	
diffuser	13-8
vehicle mass ratio	5-7
relationship with propellant mass ratio	5-8
weight and mass ratios	5-6
work ratio for regenerative turboshaft	
engine	15-24

Rayleigh line

characteristics (general)	3-32	
characteristics for the flow of an ideal gas	3-32	3-34

Reassociation reactions

6-6

Regeneration, cooling systems

10-14

Regenerative turboshaft engine

15-24

cycle analyses for regenerative turboshaft	
engine	15-28
heat supplied to	15-29
performance characteristics	15-30
regeneration process	15-25
regenerator	
effect of pressure drops	15-27
effectiveness	15-27
effectiveness, specific output loss as a	
function of	15-28
heat transfer surface area	15-28
temperature of air leaving air	
compressor	15-29
temperature of gas leaving turbine	15-29
specific output	15-29
thermal efficiency	15-30
work ratio	15-30

Regenerator

15-24

Rocket motors

air-augmented engines	11-1
air-turborocket engines	11-1
chamber insulation	8-26

Index Terms

Links

Rocket motors (*Cont.*)

heat transfer	8-23	
hybrid engines	11-1	
design considerations	8-25	
propellants		
liquid propellant	10-1	
solid propellant	8-1	
thrust vector control	8-28	10-22
vehicle range, control of	8-28	

S

Saint-Robert's Law	8-9	
SCRAMJET engine	12-10	
gross thrust	14-17	
gross thrust specific impulse	14-17	
inlet kinetic energy efficiency	14-18	
nozzle-thrust efficiency	14-18	
performance parameters	14-17	
Shock sensitivity	7-8	
Signals, attenuation of electromagnetic	7-8	
Signatures	7-8	
Slurry, thixotropic	9-33	
Specific heat	3-5	
constant pressure	3-6	
constant volume	3-6	
ratio	3-6	
relationships	3-6	
specific enthalpy	3-6	
Speed		
acoustic or sonic speed	3-7	3-17
critical acoustic speed	3-18	
isentropic speed	3-21	
stagnation acoustic speed	3-20	
Stability		
chemical stability	7-7	
flight stability	5-8	

Index Terms

Links

Stabilizers	7-2
Stagnation	
acoustic speed	3-17
conditions	3-15
continuity equations in terms of stagnation	
conditions	3-21
density	3-17
enthalpy	3-15
entropy, relationship with stagnation	
pressure	3-17
pressure	3-15
temperature	3-15
Stress, yielding	9-32

T

Tensile strength	
ultimate tensile strength of propellant	
grains	7-9
Thermochemical calculations, assumptions	6-4
Thermochemical equilibrium, conditions for	6-6
Thermodynamic equations for rocket perform-	
ance criteria	6-6
Thermodynamic properties	
critical thermodynamic properties for steady	
one-dimensional, isentropic flow of an	
ideal gas	3-18
flow of an ideal gas	3-18
Thermodynamic rocket engines	6-3
Thrust	
available thrust	2-7
chambers	
cooling systems	10-10
characteristic length	10-6
gas-side pressure drop	10-8
liquid propellants	10-3
coefficient	5-4 6-13

Index Terms

Links

Thrust (*Cont.*)

definition	1-3
equations	
air-breathing engines	12-18 12-19
conical nozzle	4-31
general	2-9
rocket propulsion	2-13
hybrid engines	11-5
jet propulsion system, calculation of	
thrust	2-9
liquid engines	10-24
power	2-14
propulsive duct engine	14-1
ramjet engine	14-5
rocket engine with linear motion of	
vehicle	14-1
specific thrust	2-15
time cure	5-4
vector control	
ablation	10-18
mechanical means	8-30
movable nozzles	8-32
secondary injection	8-32
Toxicity	7-8
Tribrid rocket engines	11-3
Turbofan engine	12-14
air specific impulse	15-55
burner fuel-air ratio	15-52
bypass ratio	15-49
compressor	15-51
definitions	15-49
diffusion for hot gas generator	15-51
duct burning turbofan engine	12-14
gas dynamic processes	15-51
isentropic efficiency	15-49
jet velocity (mean)	15-54

Index Terms

Links

Turbofan engine (*Cont.*)

nozzle expansion	15-53
for cold-air stream	15-54
for gas generator nozzle	15-54
performance parameters	15-54
pressure ratio parameter	15-49
turbine power	15-52
thrust equation	15-54

Turbojet

compressor pressure ratio	
effect on constant flight speed	15-44
effect on engine performance	15-46
cycle temperature ratio	
effect on constant flight speed	15-44
effect on dimensionless thrust	
parameter	15-46
dimensionless heat addition	15-41
dimensionless thrust parameter	15-43
flight Mach number, effect on dimensionless	
thrust parameter	15-46
flight speed, effect on engine performance	15-46
isentropic efficiency	15-8
machine efficiency	15-8
nozzle expansion process	15-8
overall efficiency	15-43
performance characteristics	15-44
thermal efficiency	15-43
turbine	
isentropic efficiency	15-8
pressure ratio	15-41
work	15-8

Turboprop engine

altitude, effect on	15-36
isentropic efficiency	15-8
jet thrust	12-17
machine efficiency	15-8 15-38

Index Terms

Links

Turboprop engine (*Cont.*)

nozzle expansion process	15-8		
operating characteristics	15-38		
performance characteristics	15-34		
propeller thrust	12-17		
propeller thrust horsepower	15-34		
total thrust horsepower	15-34		
turbine			
inlet temperature	15-36	15-38	
isentropic efficiency	15-8		
work	15-8		

Turboramjet engine 12-16

Turboshaft engine

air cycle efficiency	15-11		
air-rate	15-9	15-14	15-18
air ratio	15-9		
ambient air-temperature	15-19		
compression work	15-13		
cycle pressure ratio	15-15		
design criteria	15-9		
engine cycle, analysis of	15-12		
fixed shaft turboshaft engine	12-16		
free turbine turboshaft engine	12-16		
heat addition	15-13		
ideal turboshaft engine, thermal			
efficiency	15-10		
losses	15-12		
machine efficiency	15-8	15-18	
optimum pressure ratio	15-15		
modifications	15-21		
performance characteristics	15-15		
performance improvement	15-21		
pressure drops	15-20		
specific fuel consumption	15-15		
specific output	15-9		
thermal efficiency	15-9		

Index Terms

Links

Turboshaft engine (*Cont.*)

thermodynamic cycle	15-10	
turbine		
isentropic efficiency	15-8	
turbine work	15-7	
two-spool turboshaft engine	12-17	
work ratio	15-15	15-18

U

Unsymmetrical dimethylhydrazine	9-29
---------------------------------	------

V

Vector control, thrust	8-28	10-22		
Vehicle centroid	5-8			
Vehicle performance criteria	5-8			
adiabatic exhaust velocity	6-3	6-9		
burnout velocity	5-9	5-13		
ideal burnout velocity	5-14			
vacuum burnout velocity	5-14			
characteristic velocity				
calculation when lacking experimental				
data	6-18			
performance of different rocket				
engines	5-5			
dimensionless isentropic velocity	4-7			
effective absolute velocity	2-14			
effective jet (exhaust velocity)	2-12	5-2	6-13	14-7
exit velocity of the propulsive jet	2-13			
gradient in a boundary layer	13-1			
isentropic exhaust velocity	3-17			
isentropic exit velocity	6-7			
isentropic exit velocity for converging				
nozzle	4-5			
isentropic throat velocity for flow of a				
perfect gas in a converging nozzle	4-5			
jet velocity of a propulsive jet, calculation of	2-13			

This page has been reformatted by Knovel to provide easier navigation.

Index Terms

Links

Vehicle performance criteria (*Cont.*)

mass velocity	3-7
nozzle velocity coefficient	4-27

W

Weapons

rocket-propelled weapons	1-16
--------------------------	------

Weight

engine weight	5-7
engine weight efficiency	5-8
propulsion system weight	5-6
weight flow coefficient	6-11
weight and mass ratios	5-6